
Report No. FHWA-KS-09-5
FINAL REPORT

**DEVELOPMENT AND CONSTRUCTION OF
LOW-CRACKING HIGH-PERFORMANCE CONCRETE
(LC-HPC) BRIDGE DECKS: FREE SHRINKAGE,
MIXTURE OPTIMIZATION AND CONCRETE
PRODUCTION**

Will Lindquist
David Darwin, Ph.D., P.E.
JoAnn Browning, Ph.D., P.E.
The University of Kansas
Lawrence, Kansas

August 2009

KANSAS DEPARTMENT OF TRANSPORTATION

**Division of Operations
Bureau of Materials and Research**



1 Report No. FHWA-KS-09-5	2 Government Accession No.	3 Recipient Catalog No.	
4 Title and Subtitle Development and Construction of Low-Cracking High-Performance Concrete (LC-HPC) Bridge Decks: Free Shrinkage, Mixture Optimization and Concrete Production		5 Report Date August 2009	
		6 Performing Organization Code	
7 Author(s) Will Lindquist, David Darwin, Ph.D., P.E., JoAnn Browning, Ph.D., P.E.		8 Performing Organization Report No. SM Report No. 92	
9 Performing Organization Name and Address Office of Research and Graduate Studies The University of Kansas Youngberg Hall Lawrence, Kansas 66045		10 Work Unit No. (TRAIS)	
		11 Contract or Grant No. C1465	
12 Sponsoring Agency Name and Address Kansas Department of Transportation Bureau of Materials and Research 700 SW Harrison Street Topeka, Kansas 66603-3745		13 Type of Report and Period Covered Final Report June 2004 - June 2009	
		14 Sponsoring Agency Code RE-0388-01	
15 Supplementary Notes For more information write to address in block 9.			
16 Abstract <p>The development and evaluation of low-cracking high-performance concrete (LC-HPC) for use in bridge decks is described based on laboratory test results and experience gained during the construction of 14 bridges. This report emphasizes the material aspects of the construction process; a companion report will provide a detailed discussion of the construction, design, and environmental factors affecting the performance of LC-HPC bridge decks.</p> <p>The KU Mix design methodology for determining an optimized combined gradation uses the percent retained chart and the Modified Coarseness Factor Chart. The process begins by developing an ideal gradation followed by the determination of an optimum blend of user-selected aggregates. A Microsoft® Excel workbook enhanced with Visual Basic for Applications is available to perform the optimization process at www.iri.ku.edu.</p> <p>The second portion of the study involves evaluating the effect of paste content, water-cement (w/c) ratio, coarse aggregate type, mineral admixture type (silica fume, slag cement, and Class F fly ash each at two levels of replacement), cement type and fineness, a shrinkage reducing admixture, and the duration of curing on the free-shrinkage characteristics of concrete mixtures in the laboratory tested in accordance with ASTM C 157.</p> <p>The final portion of the study presents the specifications, construction experiences, and the preliminary evaluation of 14 LC-HPC bridge decks that have been built or are planned in Kansas. The techniques used to reduce cracking in these bridge decks are presented, and the field experiences for the 18 individual LC-HPC placements completed to date are presented. The results indicate that LC-HPC decks with an optimized aggregate gradation and design w/c ratios of 0.44 and 0.45 with cement contents of 317 and 320 kg/m³ (535 and 540 lb/yd³) have more than adequate workability, finishability, and pumpability, in addition to reduced cracking. A preliminary evaluation of these decks indicates that, on average, the LC-HPC decks are performing at a level approximately equal to or exceeding the best performing monolithic decks in Kansas surveyed over the past 15 years.</p>			
17 Key Words aggregates, aggregate optimization, bridge decks, cement fineness, concrete bridge construction, concrete mix design, cracking, durability, fly ash, free shrinkage, high-performance concrete, paste content, slag cement, silica fume		18 Distribution Statement No restrictions. This document is available to the public through the National Technical Information Service, Springfield, Virginia 22161	
19 Security Classification (of this report) Unclassified	20 Security Classification (of this page) Unclassified	21 No. of pages 546	22 Price

**DEVELOPMENT AND CONSTRUCTION OF
LOW-CRACKING HIGH-PERFORMANCE
CONCRETE (LC-HPC) BRIDGE DECKS: FREE
SHRINKAGE, MIXTURE OPTIMIZATION AND
CONCRETE PRODUCTION**

Final Report

Prepared by

Will Lindquist
David Darwin, Ph.D., P.E.
JoAnn Browning, Ph.D., P.E.

The University of Kansas
Lawrence, Kansas

A Report on Research Sponsored By

THE KANSAS DEPARTMENT OF TRANSPORTATION
TOPEKA, KANSAS

August 2009

© Copyright 2009, **Kansas Department of Transportation**

NOTICE

The authors and the state of Kansas do not endorse products or manufacturers. Trade and manufacturers' names appear herein solely because they are considered essential to the object of this report.

This information is available in alternative accessible formats. To obtain an alternative format, contact the Office of Transportation Information, Kansas Department of Transportation, 700 SW Harrison Street, Topeka, Kansas 66603-3745 or phone (785) 296-3585 (Voice) (TDD).

DISCLAIMER

The contents of this report reflect the views of the authors who are responsible for the facts and accuracy of the data presented herein. The contents do not necessarily reflect the views or the policies of the state of Kansas. This report does not constitute a standard, specification or regulation.

ABSTRACT

The development and evaluation of low-cracking high-performance concrete (LC-HPC) for use in bridge decks is described based on laboratory test results and experience gained during the construction of 14 bridges. The study is divided into three parts covering (1) the development of an aggregate optimization and concrete mixture design program entitled *KU Mix*, (2) free-shrinkage tests to evaluate potential LC-HPC mixtures developed for use in bridge decks, and (3) the construction and preliminary evaluation of LC-HPC bridge decks constructed in Kansas. This report emphasizes the material aspects of the construction process; a companion report will provide a detailed discussion of the construction, design, and environmental factors affecting the performance of LC-HPC bridge decks.

The *KU Mix* design methodology for determining an optimized combined gradation uses the percent retained chart and the Modified Coarseness Factor Chart. The process begins by developing an *ideal gradation* followed by the determination of an optimum blend of user-selected aggregates. A Microsoft® Excel workbook enhanced with Visual Basic for Applications is available to perform the optimization process at www.iri.ku.edu. Experiences with the *KU Mix* design methodology during the construction of several LC-HPC bridge decks indicate that the process is easily implemented and transferred to concrete suppliers and governing officials.

The second portion of the study involves evaluating the effect of paste content, water-cement (w/c) ratio, coarse aggregate type, mineral admixture type (silica fume, slag cement, and Class F fly ash each at two levels of replacement), cement type and fineness, a shrinkage reducing admixture, and the duration of curing on the free-shrinkage characteristics of concrete mixtures in the laboratory tested in accordance with ASTM C 157. The evaluation of shrinkage properties includes a total of 56 individual concrete batches. Both a high-absorption (2.5 to 3.0%) coarse

aggregate and a low-absorption (less than 0.7%) coarse aggregate are evaluated in many of the comparisons. The results indicate that a reduction in w/c ratio (achieved by reducing the water content), longer curing periods, and the addition of a shrinkage reducing admixture reduce concrete shrinkage. When cast with a high-absorption coarse aggregate, the addition of either silica fume or slag cement results in a reduction in shrinkage at all ages, while the addition of fly ash increases early-age shrinkage but has little or no effect on long-term shrinkage. For mixtures containing a low-absorption coarse aggregate, the addition of silica fume or slag cement results in increased early-age shrinkage if the specimens are cured for seven days. These mixtures exhibit reduced shrinkage at all ages when the curing period is increased to 14 days. The addition of fly ash increases shrinkage at all ages for either curing period. The high-absorption limestone used in the study provides internal curing water, which results in the shrinkage of mixtures containing slag cement or silica fume.

The final portion of the study presents the specifications, construction experiences, and the preliminary evaluation of 14 LC-HPC bridge decks that have been built or are planned in Kansas. The techniques used to reduce cracking in these bridge decks are presented, and the field experiences for the 18 individual LC-HPC placements completed to date are presented. The results indicate that LC-HPC decks with an optimized aggregate gradation and design w/c ratios of 0.44 and 0.45 with cement contents of 317 and 320 kg/m³ (535 and 540 lb/yd³) have more than adequate workability, finishability, and pumpability, in addition to reduced cracking. A preliminary evaluation of these decks indicates that, on average, the LC-HPC decks are performing at a level approximately equal to or exceeding the best performing monolithic decks in Kansas surveyed over the past 15 years.

ACKNOWLEDGEMENTS

This report is based on a thesis presented by Will Lindquist in partial fulfillment of the requirements for the Ph.D. degree from the University of Kansas. Funding for this research was provided by the Kansas Department of Transportation serving as the lead agency for the “Construction of Crack-Free Bridge Decks” Transportation Pooled Fund Study, Project No. TPF-5(051). The Federal Highway Administration (FHWA) of the U.S. Department of Transportation (DOT), Delaware DOT, Idaho Transportation Department, Indiana DOT, Michigan DOT, Minnesota DOT, Mississippi DOT, Missouri DOT, Montana DOT, New Hampshire DOT, North Dakota DOT, Oklahoma DOT, South Dakota DOT, Texas DOT, Wyoming DOT, and the City of Overland Park, KS provided funding to the pooled fund. Additional support was provided by the University of Kansas Transportation Research Institute. Representatives from each sponsor served on a Technical Advisory Committee that provided advice and oversight to the project.

LRM Industries, BASF Construction Chemicals, Holcim US, Fordyce Concrete, Grace Construction Products, Ash Grove Cement, and Lafarge North America provided concrete materials.

TABLE OF CONTENTS

ABSTRACT	ii
ACKNOWLEDGEMENTS	iv
LIST OF TABLES	xii
LIST OF FIGURES	xx
CHAPTER 1: INTRODUCTION	1
1.1 GENERAL.....	1
1.2 SIGNIFICANCE OF BRIDGE DECK CRACKING.....	2
1.3 CAUSES OF BRIDGE DECK CRACKING	3
1.3.1 Crack Classification Based on the Cause of Cracking.....	3
1.3.2 Crack Classification Based on Orientation.....	6
1.4 CONCRETE DRYING SHRINKAGE.....	7
1.4.1 Drying Shrinkage Mechanisms.....	7
1.4.2 Free-Shrinkage Significance.....	9
1.5 MINERAL ADMIXTURES	10
1.5.1 Silica Fume	11
1.5.2 Fly Ash.....	12
1.5.3 Slag Cement.....	13
1.6 OPTIMIZED AGGREGATE GRADATIONS.....	15
1.6.1 Modified Coarseness Factor Chart and Mortar Factor	17
1.6.2 Percent Retained Chart	21
1.6.3 Modified 0.45 Power Chart.....	22
1.7 PREVIOUS WORK.....	25
1.7.1 Effect of Cracking on Chloride Contents.....	26

1.7.2	Material Factors Affecting Bridge Deck Cracking.....	29
1.7.3	Material Factors Affecting Free Shrinkage.....	38
1.7.3.1	Effect of Paste Content and Water-Cementitious Material Ratio	39
1.7.3.2	Effect of Aggregate Type	44
1.7.3.3	Effect of Aggregate Size, Gradation, and Shape	50
1.7.3.4	Effect of Mineral Admixtures.....	51
1.7.3.5	Effect of Curing.....	65
1.7.4	Summary of Previous Work.....	66
1.8	OBJECTIVE AND SCOPE	68
CHAPTER 2: EXPERIMENTAL PROGRAM.....		69
2.1	GENERAL.....	69
2.2	CRACK SURVEY PROCEDURE.....	69
2.3	CRACK DENSITY DETERMINATION.....	70
2.4	LABORATORY WORK.....	71
2.4.1	ASTM C 157 Free-Shrinkage Specimens.....	72
2.4.2	Free-Shrinkage Measurements and Data Collection.....	73
2.4.3	Casting	74
2.4.4	Curing	74
2.4.5	Drying.....	75
2.5	MATERIALS.....	75
2.5.1	Cement.....	76
2.5.2	Fine Aggregate.....	77
2.5.3	Coarse Aggregate.....	77
2.5.8	Mineral Admixtures	78
2.6	MIX PROPORTIONING.....	79
2.7	MIXING.....	81

2.8	FREE SHRINKAGE TEST PROGRAMS	82
2.8.1	Program I (Paste Content, w/c Ratio, Curing Period).....	83
2.8.2	Program II (Paste Content, w/c Ratio Curing Period)	84
2.8.3	Program III (Coarse Aggregate Type)	86
2.8.4	Program IV (Shrinkage Reducing Admixture).....	87
2.8.5	Program V (Cement Type and Fineness).....	88
2.8.6	Program VI (Mineral Admixtures)	89
2.8.6.1	Sets 1 and 2 (Silica Fume).....	91
2.8.6.2	Sets 3 and 4 (Class F Fly Ash).....	92
2.8.6.3	Sets 5 through 8 (Slag Cement).....	93
2.8.6.4	Set 9 (Oven-Dry versus Saturated-Surface Dry Aggregate)	95
2.8.6.5	Set 10 (Ternary Mixtures).....	96
CHAPTER 3: AGGREGATE OPTIMIZATION USING THE KU MIX METHOD		98
3.1	GENERAL.....	98
3.1.1	Identification of Sieve Sizes and Definition of Gradation Fractions.....	99
3.1.2	Definition of Coarseness Factor CF and Workability Factor WF	100
3.2	DEVELOPING AN <i>IDEAL</i> GRADATION MODEL	102
3.2.1	General Equation for the <i>Ideal</i> Gradation.....	103
3.2.2	Determining the <i>Ideal</i> Gradation	105
3.2.3	Determining the CF_{ideal} and WF_{ideal}	108
3.2.4	Adjusting the <i>Ideal</i> Gradation to Account for Changes in the Cementitious Material Content.....	112
3.3	OPTIMIZING THE ACTUAL AGGREGATE BLEND	117
3.3.1	Least Squares Fit to Blended Gradation to the <i>Ideal</i> Gradation.....	118

3.3.2	Least Squares Fit of Blended CF and WF to CF_{ideal} and WF_{ideal}	118
3.3.3	Completing the Optimization Routine	119
3.3.4	Additional Constraints and Manuel Adjustments	121
3.4	CONCRETE MIXTURE PROPORTIONING	121
CHAPTER 4: FREE-SHRINKAGE RESULTS AND EVALUATION		123
4.1	GENERAL	123
4.2	STATISTICAL ANALYSIS	125
4.3	ADDITIONAL FREE SHRINKAGE TEST DETAILS	125
4.4	PROGRAM I (PASTE CONTENT, W/C RATIO, CURING PERIOD)	126
4.4.1	Program I Set 1 (Limestone Aggregate, Type I/II Portland Cement)	128
4.4.2	Program I Set 2 (Limestone Coarse Aggregate, Type II Portland Cement)	133
4.4.3	Program I Set 3 (Granite Coarse Aggregate, Type I/II Portland Cement)	137
4.4.4	Program I Comparison: Type I/II Cement Versus Type II Cement	139
4.4.5	Program I Study	146
4.5	PROGRAM II (W/C, PASTE CONTENT AND CURING PERIOD)	147
4.5.1	Program II Set 1 (w/c ratio)	148
4.5.2	Program II Set 2 (Paste Content and Curing Period)	152
4.5.3	Program II Summary	154
4.6	PROGRAM II (AGGREGATE TYPE)	156
4.6.1	Program III Specimens Cured for 7-Days	157
4.6.2	Program III Specimens Cured for 14-Days	160
4.6.3	Program III Summary	163
4.7	PROGRAM IV (SHRINKAGE REDUCING ADMIXTURE)	167
4.7.1	Program IV Summary	172

4.8	PROGRAM V (CEMENT TYPE AND FINENESS)	172
4.8.1	Program V Specimens Cured for 7 Days.....	174
4.8.2	Program V Specimens Cured for 14 Days.....	178
4.8.3	Program V Summary	181
4.9	PROGRAM VI (MINERAL ADMIXTURES)	186
4.9.1	Program VI Set 1 (Silica Fume and Limestone Coarse Aggregate).....	189
4.9.2	Program IV Set 2 (Silica Fume and Granite Coarse Aggregate).....	196
4.9.3	Program VI Set 3 (Class F Fly Ash and Limestone Coarse Aggregate).....	201
4.9.4	Program VI Set 4 (Class F Fly Ash and Granite Coarse Aggregate).....	209
4.9.5	Program VI Set 5 (Slag Cement and Limestone Coarse Aggregate).....	217
4.9.6	Program VI Set 6 (Grade 120 Slag Cement and Limestone or Quartzite Coarse Aggregate).....	226
4.9.7	Program VI Set 7 (Grade 100 Slag Cement and Limestone or Granite Coarse Aggregate)	231
4.9.8	Program VI Set 8 (Grade 100 Slag Cement and Granite Coarse Aggregate)	238
4.9.9	Program VI Set 9 (Oven-Dry versus Saturated-Surface Dry Aggregate and Grade 100 Slag).....	243
4.9.10	Program VI Set 10 (Ternary Mixtures).....	250
4.9.11	Program VI Summary	253
 CHAPTER 5: LOW-CRACKING HIGH PERFORMANCE CONCRETE (LC-HPC) BRIDGE DECKS		256
5.1	GENERAL.....	256
5.2	SPECIFICATIONS.....	257
5.2.1	Control Bridge Subdecks and Control Monolithic Decks	257
5.2.2	Silica-Fume Overlays.....	261

5.2.3	Low-Cracking High Performance Concrete (LC-HPC) Specifications	263
5.3	LC-HPC EXPERIENCES IN KANSAS	270
5.3.1	LC-HPC Bridges 1 and 2	272
5.3.2	LC-HPC-7: County Road 150 over US-75	281
5.3.3	LC-HPC Bridges 10 and 8: E 1800 Road and E 1350 Road over US-69	287
5.3.4	LC-HPC Bridge 11: K-96 over K&O Railway	294
5.3.5	LC-HPC Bridges 3 through 6: I-435 Project	299
5.3.6	LC-HPC Bridge 14: Metcalf over Indian Creek	317
5.3.7	LC-HPC Bridge 12: K-130 over Neosho River Unit 2	324
5.3.8	LC-HPC Bridge 13: Northbound US-69 over BNSF Railway	327
5.3.9	Summary of Lessons Learned	329
5.4	CRACK SURVEY RESULTS AND EVALUATION	334
5.4.1	Bridge Deck Cracking Versus Bridge Age	335
5.4.2	Individual LC-HPC Crack Density Results	338
5.4.2.1	LC-HPC-1 and 2 Crack Density Results	339
5.4.2.2	LC-HPC-3 through 6 Crack Density Results	342
5.4.2.3	LC-HPC-7 Crack Density Results	345
5.4.3	Influence of Bridge Deck Type	346
5.4.4	Influence of Material Properties	348
5.4.4.1	Water Content	349
5.4.4.2	Cement Content	351
5.4.4.3	Percent Volume of Water and Cement	353
5.4.4.4	Compressive Strength	355
5.4.4.5	Slump	357
5.5	LC-HPC COSTS	359

CHAPTER 6: SUMMARY, CONCLUSIONS, AND RECOMMENDATIONS	366
6.1 SUMMARY	366
6.2 CONCLUSIONS.....	369
6.2.1 Aggregate Optimization Using the KU Mix Method	369
6.2.2 Free Shrinkage of Potential LC-HPC Mixtures.....	369
6.2.3 Construction Experiences and Preliminary Evaluation of LC-HPC Bridge Decks.....	372
6.3 RECOMMENDATIONS.....	374
REFERENCES:	377
APPENDIX A: CONCRETE MIXTURE PROPORTIONS	384
APPENDIX B: AGGREGATE OPTIMIZATION EXAMPLE PROBLEM	408
B.1 GENERAL.....	408
B.2 EXAMPLE CONCRETE SPECIFICATIONS.....	408
B.3 MATERIALS SELECTED.....	409
B.4 CALCULATE THE <i>IDEAL</i> GRADATION.....	411
B.5 DETERMINE CF_{ideal} AND WF_{ideal}	417
B.6 ADJUSTING THE <i>IDEAL</i> GRADATION TO ACCOUNT FOR CHANGES IN THE CEMENTITIOUS MATERIAL CONTENT.....	420
B.7 OPTIMIZING THE ACTUAL AGGREGATE BLEND	426
B.8 COMPLETE MIX DESIGN.....	430
APPENDIX C: INDIVIDUAL FREE-SHRINKAGE CURVES	434
APPENDIX D: CONCRETE MIXTURE DATA AND TEST RESULTS FOR LC-HPC AND CONTROL BRIDGE DECKS	461

LIST OF TABLES

Table

1.1	Slag-Activity Index (ASTM C 989)	14
1.2	Mortar factors appropriate for various construction methods for normal-strength, air-entrained concrete (ACI Committee 211 2004)	21
2.1	Portland Cement Characteristics.....	76
2.2	Mineral admixtures used in Program VI Sets 1 through 10.....	79
2.3	Program I Test Matrix.....	85
2.4	Program II Test Matrix	86
2.5	Program III Test Matrix	87
2.6	Program IV Test Matrix.....	88
2.7	Program V Test Matrix	89
2.8	Program VI Test Matrix.....	91
2.9	Program VI Sets 1 and 2 Test Matrix	92
2.10	Program VI Sets 3 and 4 Test Matrix	94
2.11	Program VI Sets 5 through 8 Test Matrix.....	95
2.12	Program VI Set 9 Test Matrix.....	96
2.13	Program VI Set 10 Test Matrix.....	97
3.1	Identification of sieve sizes and designations, percent retained designations, and gradation fraction designations	100
3.2	Definitions for the <i>Cubic-Cubic Model</i> , using Eq. (3.9a) and (3.9b), and the <i>Ideal Gradation</i>	104
4.2	Program I Summary	128
4.3	Summary of Program I Set 1 Free-Shrinkage Data (in microstrain)	129
4.4	Student's t-test Results for Program I Set 1 30-Day Free-Shrinkage Data....	131
4.5	Student's t-test Results for Program I Set 1 365-Day Free Shrinkage Data	13

4.6	Summary of Program I Set 2 Free-Shrinkage Data (in microstrain)	134
4.7	Student's t-test Results for Program I Set 2 30-Day Free-Shrinkage Data....	135
4.8	Student's t-test Results for Program I Set 2 365-Day Free-Shrinkage Data	136
4.9	Summary of Program I Set 3 Free-Shrinkage Data (in microstrain)	137
4.10	Student's t-test Results for Program I Set 3 30-Day Free-Shrinkage Data....	139
4.11	Student's t-test Results for Program I Set 3 365-Day Free-Shrinkage Data	140
4.12	Student's t-test results for Program I Set 1 and 2 specimens cured for 7 days. 30-day comparison of free-shrinkage data	141
4.13	Student's t-test results for Program I Set 1 and 2 specimens cured for 7 days. 365-day comparison of free-shrinkage data	143
4.14	Student's t-test results for Program I Set 1 and 2 specimens cured for 14 days. 30-day comparison of free-shrinkage data	144
4.15	Student's t-tests results for Program I Set 1 and 2 specimens cured for 14 days. 365-day comparison of free-shrinkage data	146
4.16	Program II Summary.....	148
4.17	Summary of Program II Set 1 Free-Shrinkage Data (in microstrain).....	149
4.18	Student's t-test Results for Program II Set 1 30-Day Free-Shrinkage Data	150
4.19	Student's t-test Results for Program II Set 1 365-Day Free-Shrinkage Data	151
4.20	Summary of Program II Set 2 Free-Shrinkage Data (in microstrain).....	152
4.21	Student's t-test Results for Program II Set 2 30-Day Free-Shrinkage Data	153
4.22	Student's t-test Results for Program II Set 2 365-Day Free-Shrinkage Data	155
4.23	Program III Summary	156
4.24	Summary of 7-Day Program III Free-Shrinkage Data (in microstrain).....	157
4.25	Student's t-test results for Program III specimens cured for 7 days. 30- Day comparison of free-shrinkage data	159

4.26	Student's t-test results for Program III specimens cured for 7 days. 365-Day comparison of free-shrinkage data	160
4.27	Summary of Program III Specimens Cured for 14 Days	161
4.28a	Student's t-test results for Program III specimens cured for 14 days. 30-Day comparison of free-shrinkage data	162
4.28b	Student's t-test results for Program III specimens cured for 14 days. 9-Day comparison of free-shrinkage data	163
4.29	Student's t-test results for Program III specimens cured for 14 days. 365-Day comparison of free-shrinkage data	164
4.30	Student's t-test Results for Program III 30-Day Free-Shrinkage Data	165
4.31	Student's t-test Results for Program III 365-Day Free-Shrinkage Data	166
4.32	Program IV Summary	168
4.33	Summary of Program IV Free-Shrinkage Data (in microstrain)	169
4.34	Student's t-test Results for Program IV 30-Day Free-Shrinkage Data	170
4.35	Student's t-test Results for Program IV 365-Day Free-Shrinkage Data	172
4.36	Program V Summary	173
4.37	Summary of Free-Shrinkage Data for Program V (in microstrain)	174
4.38	Student's t-test results for Program V specimens cured for 7 days. 30-Day comparison of free-shrinkage data	176
4.39	Student's t-test results for Program V specimens cured for 7 days. 365-Day comparison of free-shrinkage data	177
4.40	Summary of Program V Free-Shrinkage Data (in microstrain)	178
4.41	Student's t-test results for Program V specimens cured for 14 days. 30-Day comparison of free-shrinkage data	179
4.42	Student's t-test results for Program V specimens cured for 14 days. 365-Day comparison of free-shrinkage data	181
4.43	Student's t-test Results for Program V 30-Day Free-Shrinkage Data	183
4.44	Student's t-test Results for Program V 365-Day Free-Shrinkage Data	183
4.45	Program VI Summary	187
4.46	Program VI Set I Summary	189

4.47	Summary of Free-Shrinkage Program VI Set 1a Data (in microstrain).....	190
4.48	Student's t-test Results for Program VI Set 1a 30-Day Free-Shrinkage Data.....	192
4.49	Student's t-test Results for Program VI Set 1a 365-Day Free-Shrinkage Data.....	193
4.50	Summary of Program VI Set 1b Free-Shrinkage Data (in microstrain)	194
4.51	Student's t-test Results for Program VI Set 1b 30-Day Free-Shrinkage Data.....	195
4.52	Student's t-test Results for Program VI Set 365-Day Free-Shrinkage Data.....	196
4.53	Program VI Set 2 Summary.....	197
4.54	Summary of Free-Shrinkage Program VI Set 2 Data (in microstrain)	198
4.55	Student's t-test Results for Program VI Set 2 30-Day Free-Shrinkage Data.....	199
4.56	Student's t-test Results for Program VI Set 2 365-Day Free-Shrinkage Data.....	201
4.57	Program VI Set 3 Summary.....	201
4.58	Summary of Program VI Set 3 Free-Shrinkage Data (in microstrain)	202
4.59	Student's t-test Results for Program IV Set 3 30-Day Free-Shrinkage Data.....	204
4.60	Student's t-test Results for Program VI Set 3 365-Day Free-Shrinkage Data.....	205
4.61	Summary of Program VI Set 3 Free-Shrinkage Data (in microstrain)	206
4.62	Student's t-test Results for Program VI Set 3 30-Day Free-Shrinkage Data.....	207
4.63	Student's t-test Results for Program VI Set 3 365-Day Free-Shrinkage Data.....	209
4.64	Program VI Set 4 Summary.....	210
4.65	Summary of Program VI Set 4 Free-Shrinkage Data (in microstrain)	210
4.66	Student's t-test Results for Program VI Set 4 Free-Shrinkage Data.....	212

4.67	Student's t-test Results for Program VI Set 4 365-Day Free-Shrinkage Data	213
4.68	Summary of Free-Shrinkage Data for Program VI Set 4 (in microstrain).....	214
4.69	Student's t-test Results for Program VI Set 4 30-Day Free-Shrinkage Data	216
4.70	Student's t-test Results for Program VI Set 4 365-Day Free-Shrinkage Data	217
4.71	Program VI Set 5 Summary	218
4.72	Summary of Free-Shrinkage Data for Program VI Set 5 (in microstrain).....	219
4.73	Student's t-test Results for Program VI Set 5 30-Day Free-Shrinkage Data	220
4.74	Student's t-test Results for Program VI Set 5 365-Day Free-Shrinkage Data	222
4.75	Summary of Program VI Set 5 Free-Shrinkage Data (in microstrain)	223
4.76	Student's t-test Results for Program VI Set 5 30-Day Free-Shrinkage Data	224
4.77	Student's t-test Results for Program VI Set 5 365-Day Free-Shrinkage Data	226
4.78	Program VI Set 6 Summary	226
4.79	Summary of Program VI Set 6 Free-Shrinkage Data (in microstrain)	227
4.80	Student's t-test Results for Program IV Set 6 30-Day Free-Shrinkage Data	229
4.81	Student's t-test Results for Program VI Set 6 365-Day Free-Shrinkage Data	230
4.82	Program VI Set 7 Summary	231
4.83	Summary of Program VI Set 7 Free-Shrinkage Data for Specimens Containing Limestone Coarse Aggregate (in microstrain)	232
4.84	Student's t-test Results for Program IV Set 7 30-Day Free-Shrinkage Data for Specimens Containing Limestone Coarse Aggregate.....	233
4.85	Student's t-test Results for Program IV Set 7 365-Day Free-Shrinkage Data for Specimens Containing Limestone Coarse Aggregate.....	235

4.86	Summary of Program VI Set 7 Free-Shrinkage Data for Specimens Containing Limestone or Granite Coarse Aggregate (in microstrain).....	236
4.87	Student's t-test Results for Program VI Set 7 30-Day Free-Shrinkage Data for Specimens Containing Limestone or Granite Coarse Aggregate	237
4.88	Student's t-test Results for Program VI Set 7 365-Day Free-Shrinkage Data for Specimens Containing Limestone or Granite Coarse Aggregate	238
4.89	Program VI 8 Summary	239
4.90	Summary of Free-Shrinkage Data for Program VI Set 8 (in microstrain).....	240
4.91	Student's t-test Results for Program VI Set 8 30-Day Free-Shrinkage Data	241
4.92	Student's t-test Results for Program VI Set 8 365-Day Free-Shrinkage Data	243
4.93	Program VI Set 9 Summary	244
4.94	Summary of Program VI Set 9 Free-Shrinkage Data (in microstrain)	244
4.95	Student's t-test Results for Program VI Set 9 30-Day Free-Shrinkage Data	249
4.96	Student's t-test Results for Program VI Set 9 365-Day Free-Shrinkage Data	249
4.97	Program VI Set 10 Summary	250
4.98	Summary of Program VI Set 10 Free-Shrinkage Data (in microstrain)	251
4.99	Student's t-test Results for Program VI Set 10 30-Day Free-Shrinkage Data	253
4.100	Student's t-test Results for Program VI Set 10 365-Day Free-Shrinkage Data	254
5.1	Fine and Coarse Aggregate Gradation Requirements for Bridge Deck Concrete	259
5.2	Maximum Concrete Placement Time	260
5.3	Gradation Requirements for Silica Fume Overlay Aggregate	262
5.4	LC-HPC Specifications-Special Provision Designations	264
5.5	Combined Aggregate Gradation Requirements for LC-HPC	266

5.6	Project let date, bridge contractor, ready-mix supplier, and construction date for the 14 Kansas LC-HPC bridge decks	271
5.7	Construction Dates for LC-HPC-1 and 2.....	273
5.8	Summary of Plastic Concrete Properties for LC-HPC-1	279
5.9	Summary of Plastic Concrete Properties for LC-HPC-2	280
5.10	Construction Dates for LC-HPC-7.....	282
5.11	Summary of Plastic Concrete Properties or LC-HPC-7	286
5.12	Construction Dates for LC-HPC-8 and 10.....	288
5.13	Summary of Plastic Concrete Properties for LC-HPC-10	291
5.14	Summary of Plastic Concrete Properties for LC-HPC-8	293
5.15	Construction Dates for LC-HPC-11.....	295
5.16	Summary of Plastic Concrete Properties for LC-HPC-11	298
5.17	Construction Dates for LC-HPC-3 through 6	300
5.18	Proposed Aggregate Blends for LC-HPC-3 through 6	301
5.19	Construction Dates for LC-HPC-3 through 6	304
5.20	Summary of Plastic Concrete Properties for the Qualification Batch of LC-HPC-3 through 6.....	306
5.21	Summary of Plastic Concrete Properties for the Qualification Slab of LC-HPC-3 through 6.....	307
5.22	Summary of Plastic Concrete Properties for LC-HPC-4 Placement 1	309
5.23	Summary of Plastic Concrete Properties for LC-HPC-4 Placement 2	311
5.24	Summary of Plastic Concrete Properties for LC-HPC-6	312
5.25	Summary of Plastic Concrete Properties for LC-HPC-3	314
5.26	Summary of Plastic Concrete Properties for LC-HPC-5	315
5.27	Construction Dates for LC-HPC-14.....	318
5.28	Summary of Plastic Concrete Properties for LC-HPC-14 Placement 1	321
5.29	Summary of Plastic Concrete Properties for LC-HPC-14 Placement 2	322
5.30	Summary of Plastic Concrete Properties for LC-HPC-14 Placement 3	324

5.31	Construction Dates for LC-HPC-12.....	325
5.32	Summary of Plastic Concrete Properties for LC-HPC-12	327
5.33	Construction Dates for LC-HPC-13.....	328
5.34	Summary of Plastic Concrete Properties for LC-HPC-13	329
5.35	Summary of Cracking Rates for Bridges Surveyed Multiple Times	337
5.36	LC-HPC and Corresponding Control Decks Surveyed to Date.....	339
5.37	Student's t-test for average crack density versus bridge deck type [both age-corrected and uncorrected data (Fig. 5.29)]	347
5.38	Student's t-test for mean age-corrected crack density versus water content (Fig. 5.30).....	350
5.39	Student's t-test for mean age-corrected crack density versus cement content (Fig. 5.31).....	352
5.40	Student's t-test for mean age-corrected crack density versus percent volume of water and cement (Fig. 5.32).....	354
5.41	Student's t-test for mean age-corrected crack density versus compressive strength (Fig. 5.33).....	356
5.42	Student's t-test for mean age-corrected crack density versus slump (Fig. 5.34)	358
A.1	Cement and mineral admixture chemical composition.....	384
A.2	Aggregate Gradations	387
A.3	Program I Set 1 mixture proportions and concrete properties	391
A.4	Program I Set 2 mixture proportions and concrete properties	392
A.5	Program I Set 3 mixture proportions and concrete properties	393
A.6	Program II Set 1 and 2 mixture proportions and concrete properties	394
A.7	Program III mixture proportions and concrete properties.....	395
A.8	Program IV mixture proportions and concrete properties	396
A.9	Program V mixture proportions and concrete properties.....	397
A.10	Program VI Set 1 mixture proportions and concrete properties	398
A.11	Program VI Set 2 mixture proportions and concrete properties	399

A.12	Program VI Set 3 mixture proportions and concrete properties	400
A.13	Program VI Set 4 mixture proportions and concrete properties	401
A.14	Program VI Set 5 mixture proportions and concrete properties	402
A.15	Program VI Set 6 mixture proportions and concrete properties	403
A.16	Program VI Set 7 mixture proportions and concrete properties	404
A.17	Program VI Set 8 mixture proportions and concrete properties	405
A.18	Program VI Set 9 mixture proportions and concrete properties	406
A.19	Program VI Set 10 mixture proportions and concrete properties	407
B.1	Low-cracking high-performance concrete (LC-HPC) specifications	408
B.2	LC-HPC slump requirements.....	408
B.3	Grading requirements for combined aggregates for LC-HPC	409
B.4	Cementitious material quantities selected based on the specifications.....	409
B.5	Aggregate Properties.....	410
B.6	Percent Retained on Each Sieve for the Trial Set of Aggregates	410
B.7	Sieve openings and related log calculations	412
B.8	Percents retained for both cubic equations and the <i>Cubic-Cubic Model</i> prior to optimizing the <i>CF</i> and <i>WF</i> using notation defined in Table 3.2.....	417
B.9	Percents retained for both cubic equations and the <i>Cubic-Cubic Model</i> with the optimized CF_{ideal} and WF_{ideal}	418
B.10	Blended Aggregate Gradation.....	421
B.11	Summary Results for <i>Steps 3</i> through <i>6</i>	423
B.12	Percents retained for both cubic equations and the <i>Ideal Gradation</i>	425
B.13	Results for the least squares fit to the <i>Ideal Gradation</i>	426
B.14	Results for the least squares fit of the <i>WF</i> and <i>CF</i> to the WF_{target} and CF_{target}	428
B.15	Final Optimized Aggregate Gradation.....	431
B.16	Final Mix Proportions.....	433

D.1	Low-Cracking High Performance Concrete (LC-HPC) Mix Design Information	461
D.2	LC-HPC Aggregate Gradations	463
D.3	Average Properties for the Low-Cracking High Performance Concrete (LC-HPC) Bridge Decks.....	467
D.4	Average Compressive Strength Results for LC-HPC Placements.....	468
D.5	Individual Plastic Concrete Test Results for LC-HPC Bridge Decks.....	469
D.6	Control Bridge Deck Mix Design Information.....	494
D.7	Average Properties for Control Bridge Decks	498
D.8	Crack Densities for Individual Bridge Placements.....	500
D.9	LC-HPC / Control Bridge Deck Bid Quantities and Costs.....	502

LIST OF FIGURES

Figure

1.1	Percent retained chart for combined aggregates with an optimized “haystack” gradation and a poor “peak–valley–peak” gradation	16
1.2	Modified Coarseness Factor Chart (MCFC).....	20
1.3	Modified 0.45 Power Chart with <i>ideal</i> combined gradations plotted for aggregates with different maximum sizes.....	23
1.4	<i>Ideal</i> gradations obtained from the Modified 0.45 Power Chart plotted on a Percent Retained Chart.....	24
1.5	Workability and Coarseness Factors for <i>ideal</i> gradations obtained from the Modified 0.45 Power Chart plotted on a Modified Coarseness Factor Chart..	25
1.6	Chloride content taken away from cracks interpolated at a depth of 76.2 mm (3.0 in.) versus placement age (Lindquist et al. 2006).....	27
1.7	Chloride content taken at cracks interpolated at a depth of 76.2 mm (3.0 in.) versus placement age (Lindquist et al. 2006).....	28
1.8	Free shrinkage plotted versus time through 365 days for concrete containing nominal paste contents between 20 and 40% with w/c ratios ranging from 0.40 to 0.50 [Adapted from Deshpande et al. (2007)].....	41
1.9	Free shrinkage plotted versus w/c ratio for concrete containing paste contents (V_p) between 20 and 50% [Adapted from Ödman (1968)].....	42
1.10	56-Day free shrinkage plotted versus paste content (V_p) for three percentages of Class F fly ash [Based on data reported by Symons and Fleming (1980)]	59
2.1	Minimum, maximum, and average percent retained on each sieve for the combined gradations of the 56 batches in this study	81
3.1	Modified Coarseness Factor Chart (MCFC).....	102
3.2	<i>Cubic-Cubic Model</i> of an <i>ideal</i> gradation with a 25-mm (1-in.) maximum size aggregate (MSA) plotted on a percent retained chart.....	105
3.3	Relationship between the coarseness factor and workability factor plotted on the Modified Coarseness Factor Chart (MCFC).....	109

3.4	Effect of minimizing Eq. (3.19), “After Optimization,” on the combined aggregate gradation for the <i>Cubic-Cubic Model</i> with 15% retained on the 12.5-mm (½-in.) sieve.....	112
3.5	General procedure to adjust the <i>ideal</i> gradation based on the cementitious material content of the concrete mixture	117
3.6	General Optimization and Iteration Process	120
4.1	Free-Shrinkage Test (ASTM C 157). Example average free-shrinkage curves with specimens demolded on day 1 and cured for and additional 6 or 13 days.....	127
4.2	Free-Shrinkage Test (ASTM C 157). Example average free-shrinkage curves showing drying time only	127
4.3	Free-Shrinkage Test (ASTM C 157). Program I Set 1. Average free-shrinkage versus time through 30 days (drying only).....	130
4.4	Free-Shrinkage Test (ASTM C 157). Program I Set 1. Average free-shrinkage versus time through 365 days (drying only).....	132
4.5	Free-Shrinkage Test (ASTM C 157). Program I Set 2. Average free-shrinkage versus time through 30 days (drying only).....	134
4.6	Free-Shrinkage Test (ASTM C 157). Program I Set 2. Average free-shrinkage versus time through 365 days (drying only).....	136
4.7	Free-Shrinkage Test (ASTM C 157). Program I Set 3. Average free-shrinkage versus time through 30 days (drying only).....	138
4.8	Free-Shrinkage Test (ASTM C 157). Program I Set 3. Average free-shrinkage versus time through 365 days (drying only).....	140
4.9	Free-Shrinkage Test (ASTM C 157). Program I Set 1 and Set 2 specimens cured for 7 days. Average free shrinkage versus time through 30 days (drying only).....	141
4.10	Free-Shrinkage Test (ASTM C 157). Program I Set 1 and Set 2 specimens cured for 7 days. Average free shrinkage versus time through 365 days (drying only).....	143
4.11	Free-Shrinkage Test (ASTM C 157). Program I Set 1 and Set 2 specimens cured for 14 days. Average free shrinkage versus time through 30 days (drying only).....	144
4.12	Free-Shrinkage Test (ASTM C 157). Program I Set 1 and Set 2 specimens cured for 14 days. Average free shrinkage versus time through 365 days (drying only).....	145

4.13	Free-Shrinkage Test (ASTM C 157). Program II Set 1. Average free shrinkage versus time through 30 days (drying only).....	150
4.14	Free-Shrinkage Test (ASTM C 157). Program II Set 1. Average free shrinkage versus time through 365 days (drying only).....	151
4.15	Free-Shrinkage Test (ASTM C 157). Program II Set 2. Average free shrinkage versus time through 30 days (drying only).....	153
4.16	Free-Shrinkage Test (ASTM C 157). Program II Set 2. Average free shrinkage versus time through 365 days (drying only).....	154
4.17	Free-Shrinkage Test (ASTM C 157). Program III specimens cured for 7 days. Average free shrinkage values time through 30 days (drying only)....	159
4.18	Free-Shrinkage Test (ASTM C 157). Program III specimens cured for 7 days. Average free shrinkage versus time through 365 days (drying only).....	160
4.19	Free-Shrinkage Test (ASTM C 157). Program III specimens cured for 14 days. Average free shrinkage versus time through 30 days (drying only).....	162
4.20	Free-Shrinkage Test (ASTM C 157). Program III specimens cured for 14 days. Average free shrinkage versus time through 365 days (drying only).....	164
4.21	Free-Shrinkage Test (ASTM C 157). Program III. Average free shrinkage versus time through 30 days (drying only).....	165
4.22	Free-Shrinkage Test (ASTM C 157). Program III. Average free shrinkage versus time through 365 days (drying only).....	166
4.23	Free-Shrinkage Test (ASTM C 157). Program IV. Average free shrinkage versus time through 30 days (drying only).....	170
4.24	Free-Shrinkage Test (ASTM C 157). Program IV. Average free-shrinkage versus time through 365 days (drying only).....	171
4.25	Free-Shrinkage Test (ASTM C 157). Program IV specimens cured for 7 days. Average free shrinkage versus time through 30 days (drying only)....	176
4.26	Free-Shrinkage Test (ASTM C 157). Program V specimens cured for 7 days. Average free shrinkage versus time through 365 days (drying only).....	177
4.27	Free-Shrinkage Test (ASTM C 157). Program V specimens cured for 14 days. Average free shrinkage versus time through 30 days (drying only)....	179

4.28	Free-Shrinkage Test (ASTM C 157). Program V specimens cured for 14 days. Average free shrinkage versus time through 365 days (drying only).....	180
4.29	Free-Shrinkage Test (ASTM C 157). Program V. Average free-shrinkage versus time through 30 days (drying only).....	184
4.30	Free-Shrinkage Test (ASTM C 157). Program V. Average free-shrinkage versus time through 30 days (drying only).....	185
4.31	Free-Shrinkage Test (ASTM C 157). Program VI Set 1a. Average free shrinkage versus time through 30 days (drying only).....	191
4.32	Free-Shrinkage Test (ASTM C 157). Program VI Set 1a. Average free shrinkage versus time through 365 days (drying only).....	193
4.33	Free-Shrinkage Test (ASTM C 157). Program VI Set 1b. Average free shrinkage versus time through 30 days (drying only).....	195
4.34	Free-Shrinkage Test (ASTM C 157). Program VI Set 1b. Average free shrinkage versus time through 365 days (drying only).....	196
4.35	Free-Shrinkage Test (ASTM C 157). Program VI Set 2. Average free shrinkage versus time through 30 days (drying only).....	199
4.36	Free-Shrinkage Test (ASTM C 157). Program VI Set 2. Average free shrinkage versus time through 365 days (drying only).....	200
4.37	Free-Shrinkage Test (ASTM C 157). Program VI Set 3. Average free shrinkage versus time through 30 days (drying only).....	203
4.38	Free-Shrinkage Test (ASTM C 157). Program VI Set 3. Average free shrinkage values time through 365 days (drying only).....	205
4.39	Free-Shrinkage Test (ASTM C 157). Program VI Set 3. Average free shrinkage versus time through 30 days (drying only).....	207
4.40	Free-Shrinkage Test (ASTM C 157). Program VI Set 3. Average free shrinkage versus time through 365 days (drying only).....	209
4.41	Free-Shrinkage Test (ASTM C 157). Program VI Set 4. Average free shrinkage versus time through 30 days (drying only).....	211
4.42	Free-Shrinkage Test (ASTM C 157). Program VI Set 4. Average free-shrinkage versus time through 365 days (drying only).....	213
4.43	Free Shrinkage Test (ASTM C 157). Program VI Set 4. Average free-shrinkage versus time through 30 days (drying only).....	215

4.44	Free Shrinkage Test (ASTM C 157). Program VI Set 4. Average free-shrinkage versus time through 30 days (drying only).....	217
4.45	Free Shrinkage Test (ASTM C 157). Program VI Set 5. Average free-shrinkage versus time through 30 days (drying only).....	220
4.46	Free Shrinkage Test (ASTM C 157). Program VI Set 5. Average free-shrinkage versus time through 365 days (drying only).....	222
4.47	Free Shrinkage Test (ASTM C 157). Program VI Set 5. Average free-shrinkage versus time through 30 days (drying only).....	224
4.48	Free Shrinkage Test (ASTM C 157). Program VI Set 5. Average free-shrinkage versus time through 365 days (drying only).....	225
4.49	Free Shrinkage Test (ASTM C 157). Program VI Set 6. Average free-shrinkage versus time through 30 days (drying only).....	228
4.50	Free Shrinkage Test (ASTM C 157). Program VI Set 6. Average free-shrinkage versus time through 365 days (drying only).....	230
4.51	Free Shrinkage Test (ASTM C 157). Program VI Set 7. Average free-shrinkage versus time through 30 days (drying only) for specimens containing limestone coarse aggregate.	233
4.52	Free Shrinkage Test (ASTM C 157). Program VI Set 7. Average free-shrinkage versus time through 365 days (drying only) for specimens containing limestone coarse aggregate	234
4.53	Free Shrinkage Test (ASTM C 157). Program VI Set 7. Average free-shrinkage versus time through 30 days (drying only) for specimens containing limestone or granite coarse aggregate.....	236
4.54	Free Shrinkage Test (ASTM C 157). Program VI Set 7. Average free-shrinkage versus time through 365 days (drying only) for specimens containing limestone or granite coarse aggregate.....	238
4.55	Free Shrinkage Test (ASTM C 157). Program VI Set 8. Average free-shrinkage versus time through 30 days (drying only).....	241
4.56	Free Shrinkage Test (ASTM C 157). Program VI Set 8. Average free-shrinkage versus time through 365 days (drying only).....	242
4.57	Free Shrinkage Test (ASTM C 157). Program VI Set 9. Average free-shrinkage versus time through 30 days (drying only).....	247
4.58	Free Shrinkage Test (ASTM C 157). Program VI Set 9. Average free-shrinkage versus time through 365 days (drying only).....	248

4.59	Free Shrinkage Test (ASTM C 157). Program VI Set 10. Average free-shrinkage versus time through 30 days (drying only).....	252
4.60	Free Shrinkage Test (ASTM C 157). Program VI Set 10. Average free-shrinkage versus time through 365 days (drying only).....	254
5.1	Locations of the Kansas LC-HPC Bridge Decks.....	272
5.2	Original approved design gradation used for the qualification batch and the first qualification slab and the actual gradation used for the second qualification slab and bridges LC-HPC-1 and 2.....	274
5.3	Modified Coarseness Factor Chart for the approved design gradation and the actual gradation used for the LC-HPC-1 and 2 placements.....	275
5.4	Example of a ramp used by ready-mix trucks to increase the chute angle and facilitate unloading the relatively low-slump LC-HPC	275
5.5	Bladder valve used to restrict and stop concrete flow through the concrete pump. The bladder valve works by compressing the discharge hose to restrict flow of the concrete.....	278
5.6	Typical scaling observed in the gutter areas of LC-HPC-2	281
5.7	Compressive Strengths for the qualification batch (QB), qualification slab (QS), and LC-HPC-1 (1a and 1b) and LC-HPC-2 (2) bridge placement.....	282
5.8	“S-Hook” fitted to the end of the pump discharge hose used to limit air loss through the pump.....	285
5.9	Cement paste volume and w/c ratio versus the cumulative volume of concrete delivered for LC-HPC-10. Each data point represents one ready-mix truck.....	290
5.10	Cement paste volume and w/c ratio versus the cumulative volume of concrete delivered for LC-HPC-8. Each data point represents one ready-mix truck.....	292
5.11	Compressive Strengths for the qualification batch (QB), qualification slabs (QS-8 and 10), and LC-HPC-10 (10) bridge placements.	294
5.12	Elbow fitted to the end of the pump hose to limit air lose through the pump	297
5.13	Example of a large coarse aggregate particle taken from the LC-HPC likely resulting in pumping difficulties.....	297
5.14	Typical conveyor drop for LC-HPC-11	299

5.15	Combined <i>Design</i> Gradation (used for the qualification batch and slab and Combined <i>Actual</i> Gradation (used for the LC-HPC bridges)).	302
5.16	Combined <i>Design</i> Gradation (used for the qualification batch and slab) and Combined <i>Actual</i> Gradation (used for the LC-HPC bridges).	303
5.17	Combined <i>Design</i> Gradation (used for the qualification batch and slab) and Combined <i>Actual</i> Gradation (used for the LC-HPC bridges).	303
5.18	Cement paste volume and <i>w/c</i> ration versus the cumulative volume of concrete delivered for LC-HPC-5. Each data point represents one ready-mix truck.	316
5.19	Compressive Strengths for LC-HPC-3 through 6	318
5.20	Twenty-eight day compressive strengths for all LC-HPC placements	332
5.21	Crack density of bridge decks versus bridge age for all LC-HPC and control decks included in the analysis. Data points connected by lines indicate the same bridge surveyed more than once	336
5.22	Crack density versus bridge age for the LC-HPC, control decks, and monolithic control decks surveyed by Lindquist et al. (2005). Observations connected by lines indicate the same bridge more than once	338
5.23	Crack density values for LC-HPC-1 and LC-HPC-1 placements	341
5.24	Age-corrected and uncorrected crack density values for LC-HPC-2	341
5.25	Age-corrected and uncorrected crack density values for Control- ½	342
5.26	Crack density values for LC-HPC-3 and Control-3	344
5.27	Crack density values for LC-HPC-4, Control 4, LC-HPC-5 and 6	344
5.28	Crack density results for LC-HPC-7 and Control-7	346
5.29	Age-corrected and uncorrected crack density values for the entire LC-HPC-1 deck and individual placements	347
5.30	Mean age-corrected and uncorrected crack density values versus water content	350
5.31	Mean age-corrected and uncorrected crack density values versus cement content for the monolithic placements	352
5.32	Mean age-corrected and uncorrected crack density values versus percent volume of water and cement for monolithic placements	354

5.33	Mean age-corrected and uncorrected crack density values versus measured air content for monolithic placements	356
5.34	Mean age-corrected and uncorrected crack density values versus slump for monolithic placements.....	358
5.35	Awarded concrete cost and range of non-winning bids for low-cracking high performance concrete and their associated concrete for control bridges built in the Kansas City metropolitan or Topeka areas (<i>urban</i> areas).....	361
5.36	Awarded concrete cost and range of non-winning bids for low-cracking high performance concrete and the associated concrete for control bridges built in <i>rural</i> areas.....	363
5.37	Unit costs of the qualification slab compared to the LC-HPC deck.....	364
5.38	Total costs of the qualification slab for each LC-HPC deck	365
B.1	Percents retained on each sieve for the trial set of aggregates.....	411
B.2	Percents retained for the initial <i>Cubic-Cubic Model</i> prior to optimizing <i>CF</i> and <i>WF</i> and the <i>Ideal</i> Gradation after optimizing <i>CF</i> and <i>WF</i>	419
B.3	Percent retained for the initial aggregate blend (based on the assumption that each aggregate is 33% of the total blend) and for the <i>ideal</i> gradation....	425
B.4	Percent Retained Chart of the aggregate blend (after a least squared fit) and the <i>ideal</i> gradation.....	427
B.5	MCFC for the <i>ideal</i> gradation and the actual aggregate gradation (after a least squared fit).....	427
B.6	Percent Retained Chart of the combined aggregate gradation (after a least squared fit of the <i>WFs</i> and <i>CFs</i>) and the <i>ideal</i> gradation	429
B.7	MCFC for the <i>ideal</i> gradation and the actual aggregate gradation (after a least squared fit of the <i>WFs</i> and <i>CFs</i>).....	429
B.8	Percent Retained Chart for the optimized combined gradation and for the <i>ideal</i> gradation – the gradation limits are identified in Table B.3	431
B.9	Modified Coarseness Factor Chart for the optimizing combined gradation and the <i>ideal</i> gradation.....	432
C.1a	Free Shrinkage, Batch 234. Program I Set 1. Type I/II Cement, Limestone CA, 0.41 <i>w/c</i> ratio, 7-day cure.....	434

C.1b	Free Shrinkage, Batch 234. Program I Set 1. Type I/II Cement, Limestone CA, 0.41 w/c ratio, 14-day cure	434
C.2a	Free Shrinkage, Batch 235. Program I Set 1. Type I/II Cement, Limestone CA, 0.43 w/c ratio, 7-day cure	434
C.2b	Free Shrinkage, Batch 235. Program I Set 1. Type I/II Cement, Limestone CA, 0.43 w/c ratio, 14-day cure	434
C.3a	Free Shrinkage, Batch 239. Program I Set 1. Type I/II Cement, Limestone CA, 0.45 w/c ratio, 7-day cure	435
C.3b	Free Shrinkage, Batch 239. Program I Set 1. Type I/II Cement, Limestone CA, 0.45 w/c ratio, 14-day cure	435
C.4a	Free Shrinkage, Batch 240. Program I Set 2. Type II Cement, Limestone CA, 0.41 w/c ratio, 7-day cure	435
C.4b	Free Shrinkage, Batch 240. Program I Set 2. Type II Cement, Limestone CA, 0.41 w/c ratio, 14-day cure	435
C.5a	Free Shrinkage, Batch 244. Program I Set 2. Type II Cement, Limestone CA, 0.43 w/c ratio, 7-day cure	436
C.5b	Free Shrinkage, Batch 244. Program I Set 2. Type II Cement, Limestone CA, 0.43 w/c ratio, 14-day cure	436
C.6a	Free Shrinkage, Batch 246. Program I Set 2. Type II Cement, Limestone CA, 0.45 w/c ratio, 7-day cure	436
C.6b	Free Shrinkage, Batch 246. Program I Set 2. Type II Cement, Limestone CA, 0.45 w/c ratio, 14-day cure	436
C.7a	Free Shrinkage, Batch 412. Program I Set 3. Type I/II Cement, Granite CA, 0.41 w/c ratio, 7-day cure	437
C.7b	Free Shrinkage, Batch 412. Program I Set 3. Type I/II Cement, Granite CA, 0.41 w/c ratio, 14-day cure	437
C.8a	Free Shrinkage, Batch 414. Program I Set 3. Type I/II Cement, Granite CA, 0.43 w/c ratio, 7-day cure	437
C.8b	Free Shrinkage, Batch 414. Program I Set 3. Type I/II Cement, Granite CA, 0.43 w/c ratio, 14-day cure	437
C.9a	Free Shrinkage, Batch 417. Program I Set 3. Type I/II Cement, Granite CA, 0.45 w/c ratio, 7-day cure	438

C.9b	Free Shrinkage, Batch 417. Program I Set 3. Type I/II Cement, Granite CA, 0.45 w/c ratio, 14-day cure	438
C.10a	Free Shrinkage, Batch 330 and 334. Program II Set 1. Type I/II Cement, Limestone CA, 14-day cure, 0.36 w/c ratio.....	438
C.10b	Free Shrinkage, Batch 330 and 334. Program II Set 1. Type I/II Cement, Limestone CA, 14-day cure, 0.38 w/c ratio.....	438
C.11a	Free Shrinkage, Batch 335 and 338. Program II Set 1 and 2. Type I/II Cement, Limestone CA, 14-day cure, 0.40 w/c ratio.....	439
C.11b	Free Shrinkage, Batch 335 and 338. Program II Set 1 and 2. Type I/II Cement, Limestone CA, 14-day cure, 0.42 w/c ratio.....	439
C.12	Free Shrinkage, Batch 338. Program II Set 2. Type I/II Cement, Limestone CA, 21-day cure, 0.42 w/c ratio	439
C.13a	Free Shrinkage, Batch 342. Program II Set 2 and Program III. Type I/II Cement, Limestone CA, 21.6% Paste, 0.42 w/c ratio, 7-day cure	440
C.13b	Free Shrinkage, Batch 342. Program II Set 2 and Program III. Type I/II Cement, Limestone CA, 21.6% Paste, 0.42 w/c ratio, 14-day cure	440
C.14a	Free Shrinkage, Batch 343. Program III. Type I/II Cement, Granite CA, 21.6% Paste, 0.42 w/c ratio, 7-day cure.....	440
C.14b	Free Shrinkage, Batch 343. Program III. Type I/II Cement, Granite CA, 21.6% Paste, 0.42 w/c ratio, 14-day cure.....	440
C.15a	Free Shrinkage, Batch 344. Program III. Type I/II Cement, Quartzite CA, 21.6% Paste, 0.42 w/c ratio, 7-day cure	441
C.15b	Free Shrinkage, Batch 343. Program III. Type I/II Cement, Quartzite CA, 21.6% Paste, 0.42 w/c ratio, 14-day cure	441
C.16a	Free Shrinkage, Batch 273. Program IV. Type I/II Cement, Limestone CA, 0% SRA, 0.42 w/c ratio, 7-day cure	441
C.16b	Free Shrinkage, Batch 273. Program IV. Type I/II Cement, Limestone CA, 0% SRA, 0.42 w/c ratio, 14-day cure.....	441
C.17a	Free Shrinkage, Batch 323. Program IV. Type I/II Cement, Limestone CA, 1% SRA, 0.42 w/c ratio, 7-day cure.....	442
C.17b	Free Shrinkage, Batch 323. Program IV. Type I/II Cement, Limestone CA, 1% SRA, 0.42 w/c ratio, 14-day cure.....	442

C.18a	Free Shrinkage, Batch 308. Program IV. Type I/II Cement, Limestone CA, 2% SRA, 0.42 w/c ratio, 7-day cure	442
C.18b	Free Shrinkage, Batch 308. Program IV. Type I/II Cement, Limestone CA, 2% SRA, 0.42 w/c ratio, 14-day cure	442
C.19a	Free Shrinkage, Batch 298. Program V. Type II Cement Sample 3, Limestone CA, 0.42 w/c ratio, 7-day cure	443
C.19b	Free Shrinkage, Batch 298. Program V. Type II Cement Sample 3, Limestone CA, 0.42 w/c ratio, 14-day cure	443
C.20a	Free Shrinkage, Batch 300. Program V. Type II Cement Sample 2, Limestone CA, 0.42 w/c ratio, 7-day cure	443
C.20b	Free Shrinkage, Batch 300. Program V. Type II Cement Sample 2, Limestone CA, 0.42 w/c ratio, 14-day cure	443
C.21a	Free Shrinkage, Batch 367. Program V. Type III Cement, Limestone CA, 0.42 w/c ratio, 7-day cure	444
C.21b	Free Shrinkage, Batch 367. Program V. Type III Cement, Limestone CA, 0.42 w/c ratio, 14-day cure	444
C.22a	Free Shrinkage, Batch 274. Program VI Set 1a. Type I/II Cement, Limestone CA, 0.42 w/c ratio, 3% SF Sample 1, 7-day cure	444
C.22b	Free Shrinkage, Batch 274. Program VI Set 1a. Type I/II Cement, Limestone CA, 0.42 w/c ratio, 3% SF Sample 1, 14-day cure	444
C.23a	Free Shrinkage, Batch 275. Program VI Set 1a. Type I/II Cement, Limestone CA, 0.42 w/c ratio, 6% SF Sample 1, 7-day cure	445
C.23b	Free Shrinkage, Batch 275. Program VI Set 1a. Type I/II Cement, Limestone CA, 0.42 w/c ratio, 6% SF Sample 1, 14-day cure	445
C.24a	Free Shrinkage, Batch 325. Program VI Set 1b. Type I/II Cement, Limestone CA, 0.42 w/c ratio, 3% SF Sample 2, 7-day cure	445
C.24b	Free Shrinkage, Batch 325. Program VI Set 1b. Type I/II Cement, Limestone CA, 0.42 w/c ratio, 3% SF Sample 2, 14-day cure	445
C.25a	Free Shrinkage, Batch 326. Program VI Set 1b. Type I/II Cement, Limestone CA, 0.42 w/c ratio, 6% SF Sample 2, 7-day cure	446
C.25b	Free Shrinkage, Batch 326. Program VI Set 1b. Type I/II Cement, Limestone CA, 0.42 w/c ratio, 6% SF Sample 2, 14-day cure	446

C.26a	Free Shrinkage, Batch 409. Program VI Set 2. Type I/II Cement, Granite CA, 0.42 w/c ratio, 0% SF Sample 2, 7-day cure	446
C.26b	Free Shrinkage, Batch 409. Program VI Set 2. Type I/II Cement, Granite CA, 0.42 w/c ratio, 0% SF Sample 2, 14-day cure	446
C.27a	Free Shrinkage, Batch 392. Program VI Set 2. Type I/II Cement, Granite CA, 0.42 w/c ratio, 3% SF Sample 2, 7-day cure	447
C.27b	Free Shrinkage, Batch 392. Program VI Set 2. Type I/II Cement, Granite CA, 0.42 w/c ratio, 3% SF Sample 2, 14-day cure	447
C.28a	Free Shrinkage, Batch 394. Program VI Set 2. Type I/II Cement, Granite CA, 0.42 w/c ratio, 6% SF Sample 2, 7-day cure	447
C.28b	Free Shrinkage, Batch 394. Program VI Set 2. Type I/II Cement, Granite CA, 0.42 w/c ratio, 6% SF Sample 2, 14-day cure	447
C.29a	Free Shrinkage, Batch 363. Program VI Set 3. Type I/II Cement, Limestone CA, 0.42 w/c ratio, 20% FA Sample 1, 7-day cure.....	448
C.29b	Free Shrinkage, Batch 363. Program VI Set 3. Type I/II Cement, Limestone CA, 0.42 w/c ratio, 20% FA Sample 1, 14-day cure.....	448
C.30a	Free Shrinkage, Batch 364. Program VI Set 3. Type I/II Cement, Limestone CA, 0.42 w/c ratio, 40% FA Sample 1, 7-day cure.....	448
C.30b	Free Shrinkage, Batch 364. Program VI Set 3. Type I/II Cement, Limestone CA, 0.42 w/c ratio, 40% FA Sample 1, 14-day cure.....	448
C.31a	Free Shrinkage, Batch 290. Program VI Set 3. Type I/II Cement, Limestone CA, 0.42 w/c ratio, 20% FA Sample 2, 7-day cure.....	449
C.31b	Free Shrinkage, Batch 290. Program VI Set 3. Type I/II Cement, Limestone CA, 0.42 w/c ratio, 20% FA Sample 2, 14-day cure.....	449
C.32a	Free Shrinkage, Batch 292. Program VI Set 3. Type I/II Cement, Limestone CA, 0.42 w/c ratio, 40% FA Sample 2, 7-day cure.....	449
C.32b	Free Shrinkage, Batch 292. Program VI Set 3. Type I/II Cement, Limestone CA, 0.42 w/c ratio, 40% FA Sample 2, 14-day cure.....	449
C.33a	Free Shrinkage, Batch 399. Program VI Set 4. Type I/II Cement, Granite CA, 0.42 w/c ratio, 20% FA Sample 2, 7-day cure.....	450
C.33b	Free Shrinkage, Batch 399. Program VI Set 4. Type I/II Cement, Granite CA, 0.42 w/c ratio, 20% FA Sample 2, 14-day cure.....	450

C.34a	Free Shrinkage, Batch 403. Program VI Set 4. Type I/II Cement, Granite CA, 0.42 w/c ratio, 40% FA Sample 2, 7-day cure.....	450
C.34b	Free Shrinkage, Batch 403. Program VI Set 4. Type I/II Cement, Granite CA, 0.42 w/c ratio, 40% FA Sample 2, 14-day cure.....	450
C.35a	Free Shrinkage, Batch 419. Program VI Set 4. Type I/II Cement, Granite CA, 0.42 w/c ratio, 20% FA Sample 3, 7-day cure.....	451
C.35b	Free Shrinkage, Batch 419. Program VI Set 4. Type I/II Cement, Granite CA, 0.42 w/c ratio, 20% FA Sample 3, 14-day cure.....	451
C.36a	Free Shrinkage, Batch 421. Program VI Set 4. Type I/II Cement, Granite CA, 0.42 w/c ratio, 40% FA Sample 3, 7-day cure.....	451
C.36b	Free Shrinkage, Batch 421. Program VI Set 4. Type I/II Cement, Granite CA, 0.42 w/c ratio, 40% FA Sample 3, 14-day cure.....	451
C.37a	Free Shrinkage, Batch 278. Program VI Set 5. Type I/II Cement, Limestone CA, 0.42 w/c ratio, 30% GGBFS Sample 1, 7-day cure.....	452
C.37b	Free Shrinkage, Batch 278. Program VI Set 5. Type I/II Cement, Limestone CA, 0.42 w/c ratio, 30% GGBFS Sample 1, 14-day cure.....	452
C.38a	Free Shrinkage, Batch 282. Program VI Set 5. Type I/II Cement, Limestone CA, 0.42 w/c ratio, 60% GGBFS Sample 1, 7-day cure.....	452
C.38b	Free Shrinkage, Batch 282. Program VI Set 5. Type I/II Cement, Limestone CA, 0.42 w/c ratio, 60% GGBFS Sample 1, 14-day cure.....	452
C.39a	Free Shrinkage, Batch 309. Program VI Set 5. Type I/II Cement, Limestone CA, 0.42 w/c ratio, 60% GGBFS Sample 2, 7-day cure.....	453
C.39b	Free Shrinkage, Batch 309. Program VI Set 5. Type I/II Cement, Limestone CA, 0.42 w/c ratio, 60% GGBFS Sample 2, 14-day cure.....	453
C.40a	Free Shrinkage, Batch 317. Program VI Set 5. Type I/II Cement, Limestone CA, 0.42 w/c ratio, 80% GGBFS Sample 2, 7-day cure.....	453
C.40b	Free Shrinkage, Batch 317. Program VI Set 5. Type I/II Cement, Limestone CA, 0.42 w/c ratio, 80% GGBFS Sample 2, 14-day cure.....	453
C.41a	Free Shrinkage, Batch 232. Program VI Set 6. Type I/II Cement, Limestone CA, 0.42 w/c ratio, 60% GGBFS Sample 2, 7-day cure.....	454
C.41b	Free Shrinkage, Batch 232. Program VI Set 6. Type I/II Cement, Limestone CA, 0.42 w/c ratio, 60% GGBFS Sample 2, 14-day cure.....	454

C.42a	Free Shrinkage, Batch 312. Program VI Set 6. Type I/II Cement, Quartzite CA, 0.42 w/c ratio, 60% GGBFS Sample 2, 7-day cure.....	454
C.42b	Free Shrinkage, Batch 312. Program VI Set 6. Type I/II Cement, Quartzite CA, 0.42 w/c ratio, 60% GGBFS Sample 2, 14-day cure.....	454
C.43a	Free Shrinkage, Batch 324. Program VI Set 6. Type I/II Cement, Quartzite CA, 0.42 w/c ratio, 60% GGBFS Sample 2, 7-day cure.....	455
C.43b	Free Shrinkage, Batch 324. Program VI Set 6. Type I/II Cement, Quartzite CA, 0.42 w/c ratio, 60% GGBFS Sample 2, 14-day cure.....	455
C.44	Free Shrinkage, Batch 328. Program VI Set 7. Type I/II Cement, Limestone CA, 0.42 w/c ratio, 60% GGBFS Sample 4, 14-day cure.....	455
C.45a	Free Shrinkage, Batch 340. Program VI Set 7. Type I/II Cement, Granite CA, 0.42 w/c ratio, 60% GGBFS Sample 4, 7-day cure.....	456
C.45b	Free Shrinkage, Batch 340. Program VI Set 7. Type I/II Cement, Granite CA, 0.42 w/c ratio, 60% GGBFS Sample 4, 14-day cure.....	456
C.46a	Free Shrinkage, Batch 407. Program VI Set 8. Type I/II Cement, Granite CA, 0.42 w/c ratio, 30% GGBFS Sample 3, 7-day cure.....	456
C.46b	Free Shrinkage, Batch 407. Program VI Set 8. Type I/II Cement, Granite CA, 0.42 w/c ratio, 30% GGBFS Sample 3, 14-day cure.....	456
C.47a	Free Shrinkage, Batch 408. Program VI Set 8. Type I/II Cement, Granite CA, 0.42 w/c ratio, 60% GGBFS Sample 3, 7-day cure.....	457
C.47b	Free Shrinkage, Batch 408. Program VI Set 8. Type I/II Cement, Granite CA, 0.42 w/c ratio, 60% GGBFS Sample 3, 14-day cure.....	457
C.48a	Free Shrinkage, Batch 368. Program VI Set 9. Type I/II Cement, OD Limestone CA, 0.42 w/c ratio, 60% GGBFS Sample 5, 7-day cure.....	457
C.48b	Free Shrinkage, Batch 368. Program VI Set 9. Type I/II Cement, OD Limestone CA, 0.42 w/c ratio, 60% GGBFS Sample 5, 14-day cure.....	457
C.49a	Free Shrinkage, Batch 369. Program VI Set 9. Type I/II Cement, SSD Limestone CA, 0.42 w/c ratio, 60% GGBFS Sample 5, 7-day cure.....	458
C.49b	Free Shrinkage, Batch 369. Program VI Set 9. Type I/II Cement, SSD Limestone CA, 0.42 w/c ratio, 60% GGBFS Sample 5, 14-day cure.....	458
C.50a	Free Shrinkage, Batch 373. Program VI Set 9. Type I/II Cement, SSD Limestone CA, 0.42 w/c ratio, 0% GGBFS, 7-day cure.....	458

C.50b	Free Shrinkage, Batch 373. Program VI Set 9. Type I/II Cement, SSD Limestone CA, 0.42 w/c ratio, 0% GGBFS, 14-day cure.....	458
C.51a	Free Shrinkage, Batch 427. Program VI Set 9. Type I/II Cement, OD Limestone CA, 0.42 w/c ratio, 0% GGBFS, 7-day cure.....	459
C.51b	Free Shrinkage, Batch 427. Program VI Set 9. Type I/II Cement, OD Limestone CA, 0.42 w/c ratio, 0% GGBFS, 14-day cure.....	459
C.52a	Free Shrinkage, Batch 351 and 354. Program VI Set 10. Type I/II Cement, Limestone CA, 497 CF, 60% GGBFS #2.....	459
C.52b	Free Shrinkage, Batch 351 and 354. Program VI Set 10. Type I/II Cement, Limestone CA, 497 CF, 60% GGBFS #2 and 6% SF #2.....	459
C.53a	Free Shrinkage, Batch 355 and 358. Program VI Set 10. Type I/II Cement, Limestone CA, 460 CF, 60% GGBFS #2 and 6% SF #2.....	460
C.53b	Free Shrinkage, Batch 355 and 358. Program VI Set 10. Type I/II Cement, Limestone CA, 460 CF, 80% GGBFS #2 and 6% SF #2.....	461

CHAPTER 1: INTRODUCTION

1.1 GENERAL

The corrosion of bridge deck reinforcing steel is a significant financial and potential safety problem that is greatly accelerated by bridge deck cracking and the application of corrosive deicing chemicals, primarily sodium chloride and calcium chloride. Alternatives to these corrosive deicers are available; however, their widespread use as a replacement for conventional deicers is unlikely due to their high cost and lower effectiveness (Committee on the Comparative Costs 1991). As a result, transportation agencies have devoted significant resources, beginning in the 1960s, to limit the extent of bridge deck cracking and subsequent corrosion and deck deterioration. Bridge deck cracking has, however, remained a significant problem warranting continued attention. Cracks provide the principal path for deicing chemicals to reach the reinforcing steel and accelerate freeze-thaw damage, and may extend through the full thickness of the deck and accelerate corrosion of the supporting members.

Since the middle 1970s, efforts to limit corrosion of reinforcing steel have included the use of epoxy coatings, increased reinforcing steel cover, and low-permeability concrete. Many regulating agencies now require the use of mineral admixtures to extend the life of bridge decks, as well as reduce their carbon footprint. These methods work by limiting the exposure of the reinforcing steel to oxygen, moisture, and deicers. While these methods have had measurable success in limiting corrosion, both damaged epoxy coatings and deck cracking regularly occur. In addition to these factors, the widespread use of deicing salts further compromises the reinforcing steel protection. In fact, chloride concentrations in bridge decks taken at crack locations often exceed the level required to initiate corrosion of conventional reinforcement after the first winter (Lindquist et al. 2006).

Experience with bridge deck cracking over the past 40 years has resulted in a number of changes to material and design specifications, more stringent weather limitations on concrete placement, and improved construction procedures. Cracking, however, remains a significant problem. In fact, bridge deck surveys in Kansas indicate that bridge decks cast between 1993 and 2003 exhibit more cracking than decks cast during the preceding 10 years. Experience indicates that drying shrinkage and thermal shrinkage dominate the cracking behavior of bridge deck concrete, while cracking related to design details, placement sequences, and construction activities generally play a less important role. Thermal shrinkage cracking in addition to the effects of construction procedures on cracking are discussed at greater length by McLeod, Darwin, and Browning (2009). Many other researchers have performed field and laboratory studies to evaluate the shrinkage and cracking potential of concrete. This chapter reviews significant aspects of their work and outlines an experimental study to evaluate materials and methods to minimize shrinkage. Subsequent chapters describe the development of low-cracking high-performance concrete (LC-HPC), LC-HPC specifications, an aggregate optimization technique for concrete mix design, the relation of optimized aggregates to the construction of LC-HPC bridge decks, and the performance of LC-HPC concrete in the field.

1.2 SIGNIFICANCE OF BRIDGE DECK CRACKING

Bridge deck cracking followed by reinforcing steel corrosion is a significant problem facing the country's infrastructure. A 2002 estimate places the direct cost associated with corrosion of highway bridges at \$8.3 billion annually, with indirect user costs as much as ten times that amount (Yunovich et al. 2002). Information gathered by the Federal Highway Administration (FHWA) in 2006 indicates that 12.4% (73,764 out of 596,842) of the country's bridges were classified as structurally deficient. In the 2005 Report Card for America's Infrastructure, the American Society of Civil Engineers (ASCE) gave the national bridge system a grade of *C* and

estimated that a \$9.4 billion investment per year would be required for the next 20 years to eliminate current bridge deficiencies. Local transportation agencies (the bridge owners) also recognize deck cracking as a significant problem. Krauss and Rogalla (1996) conducted a survey of transportation agencies and of the 52 respondents, 62% believed early-age transverse cracking was a significant problem, while the remaining respondents acknowledged the occurrence of transverse cracks but did not believe they posed a durability problem.

1.3 CAUSES OF BRIDGE DECK CRACKING

Bridge deck cracking is commonly classified based on the physical description of the cracks or based on the physical phenomenon that resulted in cracking. The following sections describe the principal processes that cause bridge deck cracking and a physical description of the types of cracks observed on bridge decks.

1.3.1 Crack Classification Based on the Cause of Cracking

Bridge deck cracking is the result of a complex interaction of multiple factors that are not fully understood. Cracks are typically categorized into two groups: cracks that occur while the concrete is still plastic and cracks that occur after the concrete has hardened. Plastic shrinkage cracking and settlement cracking have been identified and occur in plastic concrete, while shrinkage cracking and flexural cracking are believed to be the primary causes of cracking in hardened concrete. While cracks are classified into one of the two groups, it is important to note that they are not independent of each other and that cracking is a culmination of many factors.

The causes of and remedies for **plastic shrinkage cracking** are well known. If no preventative measures are taken, plastic shrinkage cracks occur in fresh concrete when the rate of surface evaporation exceeds the rate at which concrete bleed water reaches the surface. As water from the surface of the deck is removed by

evaporation, negative capillary pressures form and cause the paste to shrink. Since this occurs predominately at the surface of the deck, differential shrinkage between the top layer and the underlying layer create tensile stresses that are likely to create surface cracks. The concrete bleeding rate, a primary factor in plastic shrinkage cracking, can be reduced (thereby aggravating plastic shrinkage) for a number of different reasons, including the use of silica fume or finely-ground cements. In addition, increasing the rate of cement hydration, the use of entrained air, and a reduction of the water content of the concrete reduces bleeding and makes concrete more susceptible to plastic shrinkage cracking (Mindess, Young, and Darwin 2003). Many methods have been successfully employed to mitigate plastic shrinkage cracking during concrete placement. Admixtures that increase the bleeding rate, evaporation retarders, windbreaks, water fogging systems, curing compounds, cooling the concrete or its constituents, and the early application of wet burlap and polyethylene have all been used in various combinations to successfully eliminate plastic shrinkage cracking.

Settlement or **subsidence cracking** occurs as fresh concrete settles around reinforcing bars near the surface of the deck. Since these cracks occur directly above and parallel to the deck reinforcement, settlement cracks provide a direct path for deicing chemicals to reach the reinforcing steel. Settlement cracks are caused by a local tensile stress concentration resulting from fresh concrete subsiding on either side of the reinforcing steel. The probability of settlement cracks occurring increases with increasing bar size, increasing slump, and decreasing concrete cover (Dakhil, Cady, and Carrier 1975). In addition to forming visually observable cracks, weakened planes in the concrete above the reinforcing bars may also increase the probability of cracking after the concrete has hardened (Babaei and Fouladgar 1997). In addition to decreasing the top bar size, decreasing the concrete slump, and increasing the bar cover, the addition of polypropylene fibers has also been found to

reduce the probability of settlement cracking (Suprenant and Malisch 1999).

Thermal cracking in bridge decks results from thermally-induced shrinkage and restraint provided by girders, deck reinforcement, shear studs, and abutments. As concrete cures, hydration results in increasing concrete temperatures and expansion. This initial expansion during hydration causes little or no stress in the plastic concrete. The concrete hardens in a “stress-free” condition approximately at the same time the concrete reaches its peak temperature. As the concrete begins cooling to the ambient temperature, it shrinks; girders and other structural elements, however, restrict the shrinkage and induce tensile stresses. These tensile stresses can result in cracks or leave the deck more susceptible to cracking caused by other factors. Babaei and Purvis (1996) reported that the maximum temperature differential between the concrete and the girders must be limited to 12° C (22° F), corresponding to a thermal shrinkage of 121 $\mu\epsilon$, “for at least 24 hours after placement” to avoid thermally induced cracks. McLeod, Darwin, and Browning (2009) provide a more detailed examination and analysis of thermal shrinkage and its influence on bridge deck cracking.

Drying shrinkage results from the loss of water in the cement paste and can cause cracking in a manner similar to thermal shrinkage. An examination of drying and autogenous shrinkage (a special case of drying shrinkage) is presented in Section 1.4. Drying shrinkage by itself is not a problem, except that in bridge decks, the shrinkage is restrained. Drying shrinkage, however, occurs over a much longer period than other types of shrinkage and its effect can be reduced by concrete creep, which can alleviate a portion of the tensile stresses resulting from the restraint. Although many factors affect drying shrinkage, shrinkage caused by water loss from the cement paste constituent of concrete (more specifically the C–S–H gel) is the most significant. By maximizing the aggregate content (the concrete constituent that does not shrink) and minimizing the paste content, overall shrinkage can be reduced.

Other mix design factors, such as cement type and fineness, aggregate type, admixtures, and member geometry, also affect the amount of drying shrinkage (Mindess et al. 2003). Some of these factors are discussed at greater length in Section 1.7.3.

In addition to cracks caused by the restraint of volume changes and settlement of fresh concrete, directly applied loads are also responsible for bridge deck cracking. **Flexural cracks** can occur in negative moment regions as a result of dead and live loads. Finally, the placing sequence during construction can affect the tensile stresses induced in a bridge deck, both during and after construction.

1.3.2 Crack Classification Based on Orientation

In a 1970 study, the Portland Cement Association categorized bridge deck cracks into five groups: transverse, longitudinal, diagonal, pattern or map, and random cracking (*Durability* 1970). A sixth category, D-cracking, was defined but not found on any of the decks examined. The following observations and definitions were developed as part of that extensive study.

Transverse cracks are fairly straight and occur perpendicular to the roadway centerline. Transverse cracks have been the focus of many studies because they are generally recognized as both the most common and the most detrimental form of cracking (*Durability* 1970, Krauss and Rogalla 1996, Eppers and French 1998, Le and French 1998). Transverse cracks frequently occur directly above transverse reinforcement and can extend completely through the deck (*Durability* 1970).

Longitudinal cracking is primarily found in slab bridges. These cracks are typically straight and run parallel to the roadway centerline above the void tubes in hollow-slab bridges and above the longitudinal reinforcement in solid-slab bridges. Like transverse cracks, these cracks frequently occur before the bridge is open to traffic and can extend completely through the deck (*Durability* 1970, Eppers and French 1998). Longitudinal cracks are also observed in decks near abutments when

the deck slab is cast integrally with the abutment (Schmitt and Darwin 1995, Miller and Darwin 2000, Lindquist, Darwin, and Browning 2005).

Diagonal cracking typically occurs near the ends of skewed bridges and over single-column piers. Generally, these cracks are parallel and occur at an angle other than 90 degrees with respect to the roadway centerline (*Durability* 1970). Diagonal cracks are typically shallow in depth and do not follow any distinct pattern. The likely causes of these cracks are inadequate design details near abutments, resulting in flexural cracking and drying shrinkage induced cracking.

Pattern or map cracking consists of interconnected cracks of any size. They are generally shallow in depth and are not believed to significantly affect bridge performance (*Durability* 1970). Both drying shrinkage and plastic shrinkage are thought to be the primary causes. Finally, **random cracks** are irregularly shaped cracks that do not fit into any of the other classifications. These cracks occur frequently, but there is not always a clear relationship between their occurrence and bridge deck characteristics (*Durability* 1970).

1.4 CONCRETE DRYING SHRINKAGE

Cracking in concrete bridge decks is a complex process involving many factors, although drying shrinkage is a principal cause contributing to cracking. The mechanisms responsible for drying shrinkage and the significance of limiting shrinkage in bridge deck concrete are described next.

1.4.1 Drying Shrinkage Mechanisms

Drying and autogenous shrinkage are volumetric changes (generally expressed as a linear strain) that result from the movement and loss of water. Drying shrinkage occurs as the internal relative humidity of concrete equilibrates with the drying environment, resulting in water loss. Autogenous shrinkage is an internal phenomenon that occurs without the loss of water to the surrounding environment. In

terms of the potential to cause cracking, drying and autogenous shrinkage are generally measured together and called total or free shrinkage.

Autogenous shrinkage is a result of two processes: self desiccation caused by the hydration reaction's consumption of internal water, and chemical shrinkage resulting from the reduced volume of the hydration products. The most significant autogenous shrinkage is a result of self desiccation that occurs at low w/c ratios when there is not enough water available for complete hydration and the internal surfaces are no longer saturated. A w/c ratio of 0.42 is generally assumed to be the minimum required for complete hydration, although this value can vary slightly and depends on the assumed gel porosity (Mindess et al. 2003). Autogenous shrinkage was first described by Lynam (1934), but at that time it was not a problem for the construction industry because a high w/c ratio was generally required for adequate workability. The development of water-reducing admixtures, however, has permitted the regular use of low w/c concrete. For general construction, autogenous shrinkage is generally regarded to be relatively small (compared to drying shrinkage), although at an extremely low w/c of 0.17, Tazawa and Miyazawa (1993) reported an ultimate shrinkage under sealed conditions of 700 $\mu\epsilon$.

Drying shrinkage occurs as water contained in capillary pores, hardened calcium silicate gel (calcium silicate hydrate or C-S-H), and solid surfaces is lost to the environment. Drying shrinkage is caused by internal pressures that cause an increase in *capillary stresses, disjoining pressures, and surface free energy*. Capillary stresses (hydrostatic forces) result as the relative humidity (RH) drops and a meniscus forms that exerts compressive forces on the pore walls. Capillary stresses occur when the RH is between 45 and 95% and vary indirectly with the pore radius and directly with the water's surface tension and the natural logarithm of the RH. With a RH greater than 95%, only slight shrinkage is observed as the large capillaries are emptied first and only small capillary stresses are developed.

Disjoining pressure is a result of water adsorbed on the surfaces of C–S–H. It offsets the attractive van der Waals' forces that pull the C–S–H particles together. Disjoining pressure increases with an increase in the thickness of adsorbed water and is only significant down to a RH of 45%. Below 45% RH, capillary stresses and disjoining pressures are not significant and shrinkage results from changes in surface energy. When low RH conditions exist, a large increase in surface free energy occurs as the most strongly adsorbed water is removed from the C–S–H surfaces. The shrinkage pressure resulting from these changes increases with increases in the specific area of the solid. (Mindess et al. 2003)

1.4.2 Free Shrinkage Significance

Concrete shrinkage by itself does not cause cracking; when concrete shrinkage is restrained, however, tensile stresses develop that often result in cracking. In bridge decks, a relatively high amount of restraint is provided by the supporting girders, shear studs, reinforcing steel, and supports, which often results in significant levels of cracking. The development of these cracks is a complex process that depends on many factors including free shrinkage, shrinkage rate, tensile-strength development, creep, drying conditions, and the degree of restraint. Free shrinkage (and consequently shrinkage rate) measurements, such as specified in ASTM C 157, are often used to assess the cracking potential of different concrete mixtures even though additional factors influence the cracking potential. Another method that is commonly used to assess cracking potential is the restrained ring test. This test involves casting concrete around a steel ring and monitoring stresses in the steel due to restrained shrinkage of the concrete and the time at which cracking first occurs. Free shrinkage and restrained ring tests are excellent tools to evaluate the suitability of concrete mixtures for use in bridge decks, although there is no substitute for information and experience gathered from actual bridge decks.

The term “free shrinkage” is generally associated with a test that measures the total longitudinal shrinkage of concrete prisms allowed to dry in a controlled environment. These free shrinkage measurements include the combined effects of drying shrinkage and autogenous shrinkage and are taken at regular intervals, usually for a year or more. Free shrinkage measurements by themselves do not provide sufficient information to determine with certainty whether or not a particular concrete mixture will crack in the field, although there is a strong correlation between free shrinkage and cracking. Babaei and Purvis (1996) and Mokarem, Weyers, and Lane (2005) recommend limiting the 28-day shrinkage to 400 $\mu\epsilon$ to minimize the potential for cracking. Controlling long-term shrinkage is not nearly as critical to limit cracking as controlling early-age shrinkage because a beneficial reduction in stress due to creep can be expected to occur over time.

The standard test method (and the method employed in this study) for measuring free shrinkage is ASTM C 157, “Standard Test Method for Length Change of Hardened Hydraulic Cement Mortar and Concrete.” This relatively simple method uses a mechanical length comparator to measure the shrinkage of concrete prisms over time.

1.5 MINERAL ADMIXTURES

The use of mineral admixtures in bridge decks is being specified with increased regularity. Many current high-performance concrete specifications require one or more mineral admixtures with the goals of extending the life of the deck and reducing the need for costly repairs. The following sections provide an introduction to the three most commonly used mineral admixtures: silica fume, fly ash, and slag cement. The free-shrinkage characteristics of concrete containing these mineral admixtures are evaluated in this study. Previous work to characterize the influence of these mineral admixtures on free-shrinkage is treated separately in Section 1.7.3.4.

1.5.1 Silica Fume

Silica fume is often used as a partial replacement of portland cement to decrease the permeability and increase the durability of concrete. Silica fume is a by-product of the production of silicon metal or ferrosilicon alloys and consists of very small spherical particles, generally with a mean diameter between 0.1 and 0.3 μm (4 to 12 $\mu\text{in.}$) (Mindess et al. 2003). During cement hydration, silica fume reacts with calcium hydroxide (CH) and forms calcium-silicate hydrate (C-S-H) through the pozzolanic reaction. In addition to the supplementary C-S-H produced, the fine spherical particles act as filler between cement and aggregate particles and within the cement-paste matrix (Whiting and Detwiler 1998). The addition of silica fume in concrete results in a stronger, denser, and less permeable concrete. Research has shown that in hardened concrete, although the total porosity is not reduced, the number of large capillary pores is reduced, thus increasing the likelihood of a discontinuous pore system (ACI Committee 234 1996).

Although silica fume is associated with improved durability, high strength, high early-strength, and abrasion resistance, the primary use of silica fume in bridge decks is to provide improved corrosion protection based on the low permeability of the concrete. Silica fume is approximately 100 times finer than portland cement and has a correspondingly high surface area (Whiting and Detwiler 1998). This high surface area results in a cohesive mix with a substantially increased water demand. Typically, this increase in water demand is offset through the use of a high-range water reducer and selecting a target slump approximately 50 mm (2 in.) more than would be used for conventional concretes. The high surface area of silica-fume, however, reduces the total amount and rate of bleeding, leaving the concrete especially susceptible to plastic shrinkage cracking (ACI Committee 234 1996). There is reason to believe that the finer pore structure and higher solid surface area

may result in more drying shrinkage (due to an increase in capillary stresses and surface free energy).

1.5.2 Fly Ash

Fly ash is the most widely used mineral admixture and is produced as a by-product of burning powdered coal to generate electricity. While fly ash is a cheap substitute for cement (approximately half the cost of portland cement), there are many other beneficial reasons to use fly ash in concrete. Fly ash is spherical, with a mean particle diameter between 10 and 15 μm , similar to that of portland cement, but with a higher specific surface area (Mindess et al. 2003). Unlike silica fume and ground granulated blast furnace slag, which come from more controlled processes, the chemical and physical properties of fly ash vary considerably based on the source of the coal. For this reason, ASTM C 618 subdivides fly ash into two classes (F and C) depending on composition. Class F fly ashes are produced mainly from bituminous and anthracite coals, found east of the Mississippi River, in which the major acidic oxides ($\text{SiO}_2 + \text{Al}_2\text{O}_3 + \text{Fe}_2\text{O}_3$) content is greater than 70%. Class C fly ashes, also called high-lime ashes, are produced mainly from lignite coal found in western states, in which the major acidic oxides content is between 50 and 70%. These high-lime ashes generally contain more than 20% CaO, and as a result, the sum of the major acidic oxides is often less than the 70% minimum for Class F fly ashes. Fly ashes contain several other constituents (including SO_3 , MgO, Na_2O , and K_2O), and wide ranges exist in the chemical composition (ACI Committee 232 2002). In addition to the pozzolanic properties, Class C fly ashes also contain small amounts of cementitious materials (C_2S and crystalline C_3A) that increase early-age reactivity as compared to Class F fly ash (Papayianni 1987).

During cement hydration, the SiO_2 in fly ash reacts with calcium hydroxide (CH) and forms calcium-silicate hydrate (C–S–H) through the pozzolanic reaction. This reaction, however, does not occur as quickly as it does with silica fume and may

take as long as a week to begin (Fraay, Bijen, and de Haan 1989). As a consequence of this low reactivity, heat gain and early-age compressive strengths are reduced, and extended curing is required for continued pozzolanic activity. If adequate curing is provided, the long-term reaction of fly ash and CH reduces porosity and pore size, resulting in concrete with reduced permeability and increased long-term strength (Mindess et al. 2003). The spherical shape of fly ash generally reduces water demand by decreasing particle interference and allows the water content to be reduced for a given workability (Brown 1980).

1.5.3 Slag Cement

Slag cement, also called ground granulated blast-furnace slag, is being specified and used in bridge decks with increased regularity. Slag cement is produced as a by-product during the blast-furnace production of iron. The molten slag is cooled rapidly with water and the resulting calcium aluminosilicate glass granules are ground to a specified fineness. Slag is a cementitious material that reacts very slowly with water due to an impervious coating that forms on the slag particles early in the hydration process. Hydroxyl ions from the calcium hydroxide (CH) released during the hydration of portland cement break down the impervious coatings and initiate hydration. A portland cement content of only 10 to 20% is required to activate slag-cement blends. In addition to CH, other alkaline compounds, such as soluble sodium salts, can activate slag cement hydration. Slag cement that includes an alkali activator (other than portland cement) is referred to as alkali-activated slag (AAS). Because slag has a lower lime content than portland cement, the resulting C-S-H has a lower C/S ratio that is unstable and results in pozzolanic behavior as CH reacts with silica. (Mindess et al. 2003)

Slag cement is classified by ASTM C 989 into three grades (80, 100, and 120) based on a slag-activity index. The activity index is the ratio of compressive strengths of mortar cubes made with a 50:50 mixture of slag and portland cement and

mortar cubes made with portland cement only. The slag activity index is calculated at 7 and 28 days and increases for increasing grades as shown in Table 1. Increasing grades of slag cement are generally achieved by varying the fineness; Frigione (1986) found that as the Blaine fineness is increased from 0.25 to 0.50 m²/g the average compressive strength of mortar cubes is more than doubled. Due to the relatively slow hydration reaction of slag, however, extended curing and controlled temperature conditions are important to ensure proper hydration of the slag-cement blend. Fulton (1974) reports that concrete containing more than 30% slag is susceptible to significant strength loss if the curing period is terminated prematurely.

Table 1.1 – Slag-Activity Index (ASTM C 989)

Grade	Slag-activity index, minimum percent			
	7-day index		28-day index	
	Average [†]	Individual [‡]	Average [†]	Individual [‡]
80	--	--	75	70
100	75	70	95	90
120	95	90	115	110

[†]Average of last five consecutive samples

[‡]Any individual sample

If an adequate curing regime is used, the benefits of slag are well-documented. Concrete permeability is reduced due to a reduction in the porosity resulting from the reaction of slag cement with the CH and alkalis released during cement hydration (Bakker 1980). The rate of strength gain depends primarily on the slag-activity index, although long-term strengths (beyond 28 days) are generally higher for all grades (ACI Committee 233 2003) than a similar concrete containing 100% portland cement. The cost of slag cement is slightly less than the cost of Type I/II portland cement, and due to increased workability, paste contents can generally be reduced. Wimpenny, Ellis, and Higgins (1989) found that with a constant w/cm ratio, concrete slump increased significantly as the replacement of slag with portland cement increased. In addition to increased workability, the initially slow hydration reaction

generally results in some delay in setting time. Hogan and Meusel (1981) reported that with 50% slag and a concrete temperature of 23° C (73° F), setting time is increased by ½ to 1 hour, although no change is observed for temperatures above 29° C (85° F). The degree of retardation is a function of the concrete temperature, the level of slag replacement, the *w/cm* ratio, and the portland cement characteristics (Fulton 1974).

1.6 OPTIMIZED AGGREGATE GRADATIONS

While the combined aggregate gradation alone is not a primary factor affecting concrete shrinkage or cracking, there are several reasons that make the combined aggregate gradation important for quality concrete. Cement paste is the constituent of concrete that undergoes the most shrinkage, while aggregate provides restraint and limits shrinkage. For this reason, concrete mixtures containing a high volume of aggregate (and a low volume of cement paste) have both reduced shrinkage and cracking. An optimized combined aggregate gradation allows the volume of aggregate to be maximized while maintaining good plastic concrete characteristics. In addition to reduced shrinkage and cracking potential with the reduction of paste contents, concretes with well-graded aggregates exhibit less segregation, increased cohesiveness, and improved workability compared to concretes with poor combined gradations.

Many methods and procedures exist to obtain an optimized aggregate gradation, but the underlying premise behind each method is the same. A well-graded combined aggregate consists of all aggregate particle sizes and plots as a *haystack* shape on a percent retained chart, as shown in Fig. 1.1. In general, this requires the combination of a minimum of three differently sized aggregates to obtain an optimized gradation. Typically, however, concretes contain only two aggregates: a fine aggregate generally with a large percentage passing the 2.36-mm (No. 8) sieve, and a coarse aggregate with very few gradation-based restrictions. The combination

of these two aggregates is generally not well-graded due to a deficiency in intermediate sized particles. This deficiency has, in fact, become worse over the last several decades as fine aggregates have become increasingly finer and coarse aggregates have become increasingly coarser (ACI Committee 211 2004). An example of a poorly-graded combined particle distribution, also referred to as a *gap-graded* or *peak–valley–peak* gradation (ACI Committee 211 2004) is shown in Fig. 1.1. As a result of the poor combined gradation, increased paste or mortar contents are often needed to aid in concrete placement and finishing. It is important to point out that it is the combined aggregate gradation that is of interest – not the individual aggregate gradations.

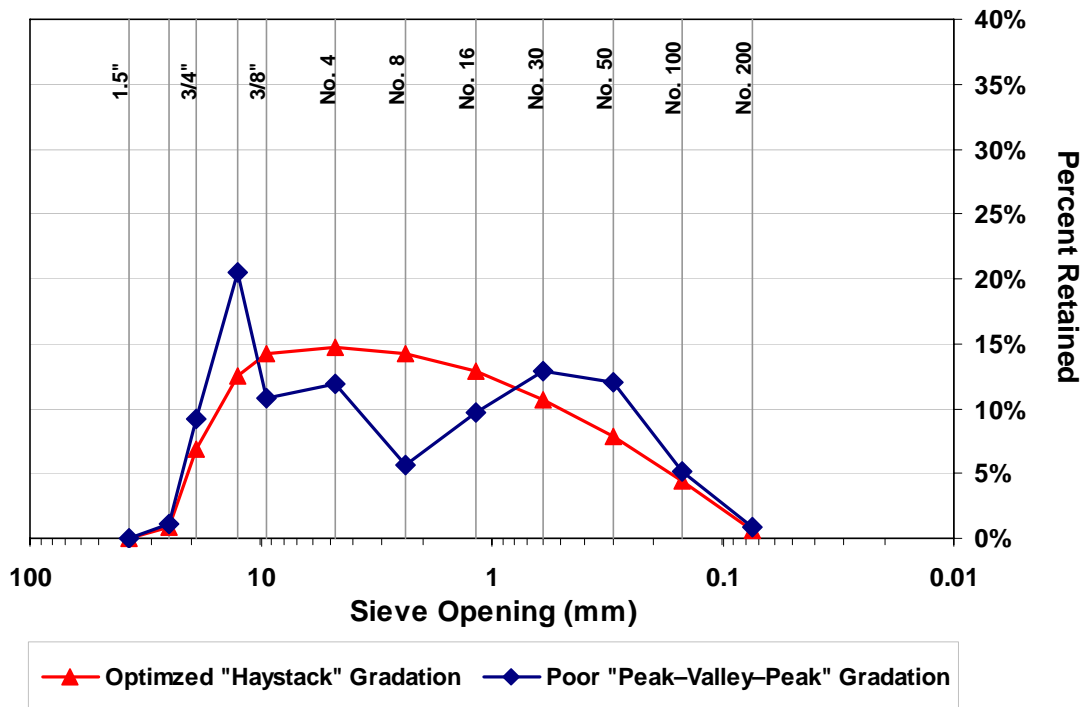


Fig. 1.1 – Percent retained chart for combined aggregates with an optimized “haystack” gradation and a poor “peak–valley–peak” gradation.

For concrete with a deficiency in intermediate aggregate particle sizes [particles retained on the 4.75 and 2.36-mm (No. 4 and No. 8) sieves], the resulting voids in the gradation must be filled by small aggregate particles and cement paste.

Cramer, Hall, and Parry (1995) found that for a constant cement content, optimized concrete mixtures (that is, concrete with a good representation of all aggregate particle sizes) require up to 15% less water, and thus, cement paste content, to maintain a constant slump. The increased paste demand of non-optimized mixtures results in higher material costs and increased life-cycle costs due to an increased incidence of shrinkage cracking.

A number of optimization techniques are available, although the most common techniques involve the Modified Coarseness Factor Chart, the Percent Retained Chart, and the Modified 0.45 Power Chart. Other techniques involve examining the combined fineness modulus of the aggregate blend (ACI Committee 211 2004) or using particle packing models to minimize voids with combinations of spheres of different sizes (Goltermann, Johansen, and Palbøl 1997). Most of these techniques use either linear or quadratic programming to optimize the aggregate blend so that it satisfies gradation limits, cost requirements, or other user-specified parameters (Easa and Can 1985, Kasperkiewicz 1994).

1.6.1 Modified Coarseness Factor Chart and Mortar Factor

Perhaps the most widely known aggregate optimization technique is based on empirical work by Shilstone (1990) using the Modified Coarseness Factor Chart (MCFC). The MCFC is used to evaluate and design concrete mixtures and is based on construction experience with various concrete mixtures. Shilstone (1990) identified three principal factors that affect concrete mixture optimization: (1) the relationship between the aggregate size fractions, (2) the quantity of cement, and fine aggregate, and (3) the combined aggregate particle distribution. The MCFC is a tool used to evaluate and develop optimized aggregate gradations based on the relationship between different aggregate sizes and the quantity of cement and fine aggregate.

The process begins by dividing aggregate particles into three categories based on size. The first category, quality (Q) particles, is defined as aggregate retained on or above the 9.5-mm ($\frac{3}{8}$ -in.) sieve. These larger particles are inert filler that have a small surface area to volume ratio and, thus, have a low cement paste demand. The second category, intermediate (I) particles, is defined as the percentage of material retained on the 4.75 and 2.36-mm (No. 4 and No. 8) sieves. These particle sizes are generally missing in coarse and fine aggregates today but are critical to filling the larger voids between quality particles. The last category, workability (W) particles, represents aggregate passing the 2.36-mm (No. 8) sieve. These particles, coupled with the cementitious materials, provide workability for the mixture, although too high a quantity of these particles will result in a high water demand due to their large surface area. The MCFC provides a method to evaluate and achieve an optimized balance of Q , I , and W particles.

The MCFC methodology is based on the interaction of two factors: the coarseness factor (CF) and the workability factor (WF), both of which are calculated using the percentage of aggregate in the three size categories. The CF defines a relationship between the Q and I particles and the WF quantifies the particles that provide workability to the mixture – the W particles with an adjustment to account for the quantity of cementitious material. The CF is defined as the ratio of Q particles to the sum of Q and I particles expressed as a percent.

$$CF = \frac{Q}{Q + I} \times 100 \quad (1.1)$$

where Q = Quality Particles – percent retained on or above the 9.5-mm ($\frac{3}{8}$ -in.) sieve.
 I = Intermediate Particles – percent retained on the 4.75 and 2.36-mm (No. 4 and No. 8) sieves.

The WF is defined as the percentage of W particles plus a correction factor to account for deviations in cementitious materials from a mix design containing 335

kg/m³ (564 lb/yd³) of cementitious material (this is referred to as a six-sack mix). The 2.5 multiplier is a volume correction to account for any deviations in the cementitious material content. The volume of a standard U.S. sack of cement is approximately equal to a variation of 2.5 percent in the W particles.

$$WF = \frac{W}{Q + I + W} \times 100 + 2.5 \left(\frac{W_c}{B} - 6 \right) \quad (1.2)$$

where W = Workability Particles – percent retained on sieves smaller than the 2.36-mm (No. 8) sieve.
 W_c = Mass (weight) of total cementitious material content in (kg/m³) lb/yd³.
 B = Weight of one U.S. sack of cement, 56 kg (94 lb).

The MCFC (presented in Fig. 1.2) is the tool used to evaluate combined aggregate gradations as a function of the WF and CF . The chart is divided into five zones that identify regions with similar characteristics based on field experience (ACI Committee 211 2004). The point (CF , WF) is plotted and the mixture is evaluated based on the position of the point in the chart. In addition to the five zones, a *trend bar* is included that represents a region where maximum aggregate density is achieved, although such mixtures have little workability and are only suitable for mass concrete placements. Combined aggregate gradations that plot in Zone I are gap-graded and, consequently, require more cement paste and will likely segregate during placement and consolidation due to a lack of intermediate-sized particles. Mixtures that plot in Zone II represent the optimum CF and WF combinations for mixtures with a maximum aggregate size between 19-mm ($\frac{3}{4}$ -in.) and 38-mm (1.5-in.). Field observations for mixtures that plot near the center of Zone II (60, 35) indicate these mixtures consistently have good characteristics (ACI Committee 211 2004). Zone III represents the optimum region for concrete mixtures with a maximum aggregate size smaller than 19-mm ($\frac{3}{4}$ -in.). Mixtures that plot in Zone IV

contain excessive fines and have a tendency to segregate, and mixtures that plot in Zone V are too coarse and may be difficult to place, consolidate, and finish.

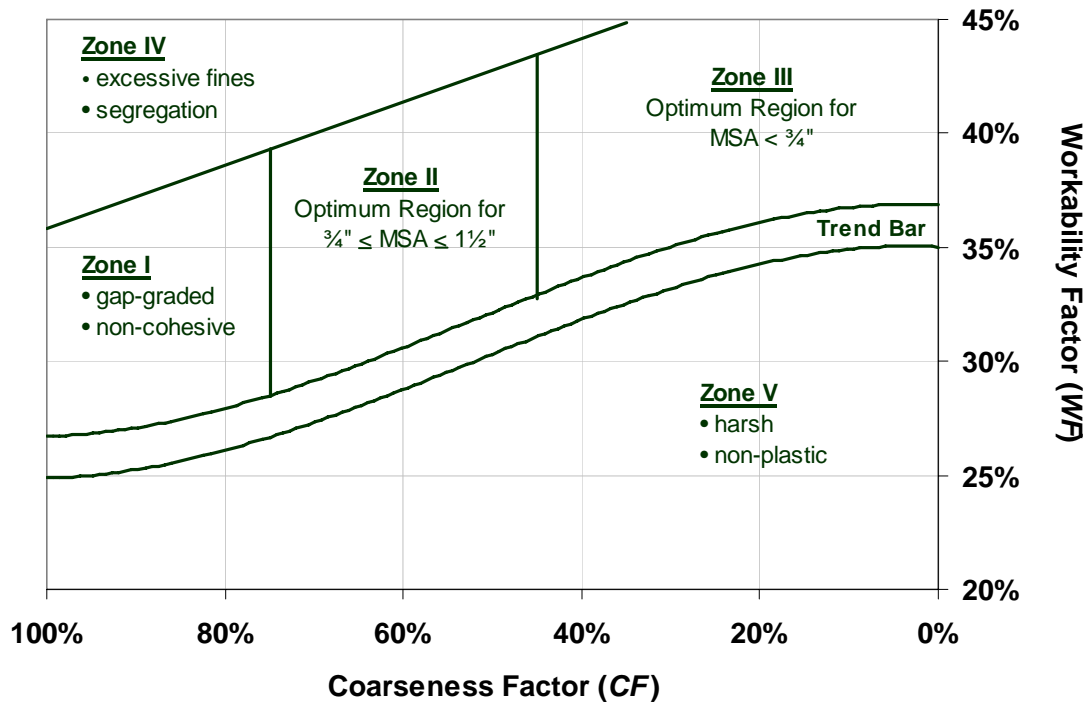


Fig. 1.2 – Modified Coarseness Factor Chart (MCFC)

In addition to the development of the MCFC, Shilstone (1990) introduced the *mortar factor* and provided guidance for its use based on different types of concrete construction. The mortar factor is defined as the percentage of fine sand [material passing the 2.36-mm (No. 8) sieve] and paste in a concrete mixture. The mortar factor is a mixture design variable that balances concrete durability and constructability. Mortar in excess of that required for construction can lead to increased shrinkage and subsequent cracking due to high paste contents, while insufficient mortar can cause workability, pumpability, placeability, and finishability problems during construction. Shilstone (1990) defined ten classes of concrete based on the type of placement and the approximate mortar demand for each. To simplify the process and remove ambiguity inherent with so many categories, the ten categories were reduced to five by ACI Committee 211 (2004) and are shown in

Table 1.2. These categories were expressly developed for normal-strength, air-entrained concrete containing a water reducer.

Table 1.2 – Mortar factors appropriate for various construction methods for normal-strength, air-entrained concrete (ACI Committee 211 2004)

Mortar Factor, %	Method of Construction
50 – 53	Placed by steep sided bucket, chute, or conveyor in an open space without heavy reinforcement.
53 – 55	Placed by bucket, chute, or a paving machine in lightly reinforced members.
55 – 57	Placed by a pump, chute, bucket, or conveyor for general concrete.
57 – 60	Placed in thin vertically cast members.
60 – 65	Placed by a 50-mm (2-in.) pump for thin toppings and overlays.

1.6.2 Percent Retained Chart

The percent retained chart, shown in Fig. 1.1, is commonly used as a tool to optimize aggregate blends through a trial-and-error process and to evaluate existing aggregate blends. The percent retained chart is a graphical representation of the particle distribution by sieve size. A perfect “haystack” shape (as shown in Fig. 1.1) is desirable but often unattainable and unnecessary for quality concrete. ACI Committee 211 (2004) provides some guidance to determine whether the aggregate gradation is acceptable based on a comparison with an ideal optimized well-graded aggregate, although it does not provide an ideal optimized gradation for comparison. A material deficiency on one sieve size is acceptable if an adjacent sieve has an excess of material to balance the deficiency. Likewise, a material deficiency on two consecutive sieves is acceptable if the two adjacent sieves on either side have excess material. A deficiency on three or four consecutive sieves (as shown for the “peak-valley-peak” gradation in Fig 1.1) is not acceptable and should be corrected (ACI Committee 211 2004).

1.6.3 Modified 0.45 Power Chart

As presented, the MCFC, mortar factor guidelines, and the percent retained chart are aggregate gradation evaluation tools. The modified 0.45 power chart, however, provides an “ideal” combined aggregate gradation for concrete with different sizes of aggregate. The chart was developed based on work completed by Fuller and Thompson (1907). The Federal Highway Administration adopted the 0.45 power chart in the 1960s for use in the asphalt industry (Roberts et al. 1996), and the chart was later adjusted for the concrete industry by reducing the optimum percentage of materials finer than the 2.36-mm (No. 8) sieve to account for the fine cementitious materials (Fig. 1.3). The *ideal* gradation using the 0.45 power chart for all particles of size d larger than the 2.36-mm (No. 8) sieve with a nominal maximum aggregate size (MSA) D is calculated using Eq. (1.3).

$$P_t = \left(\frac{d}{D} \right)^{0.45} \quad (1.3)$$

where P_t = fraction of total solids finer than size d
 D = Maximum nominal aggregate size

After the ideal gradation is calculated for aggregate larger than the 2.36-mm (No. 8) sieve, a straight line is drawn from zero percent passing the 0.075-mm (No. 200) sieve to the optimum percent passing the 2.36-mm (No. 8) sieve. Modified 0.45 power charts are presented in Fig. 1.3 for *ideal* aggregate gradations with nominal maximum sizes of 13, 19, 25, and 38-mm ($\frac{1}{2}$, $\frac{3}{4}$, 1, and 1½-in.).

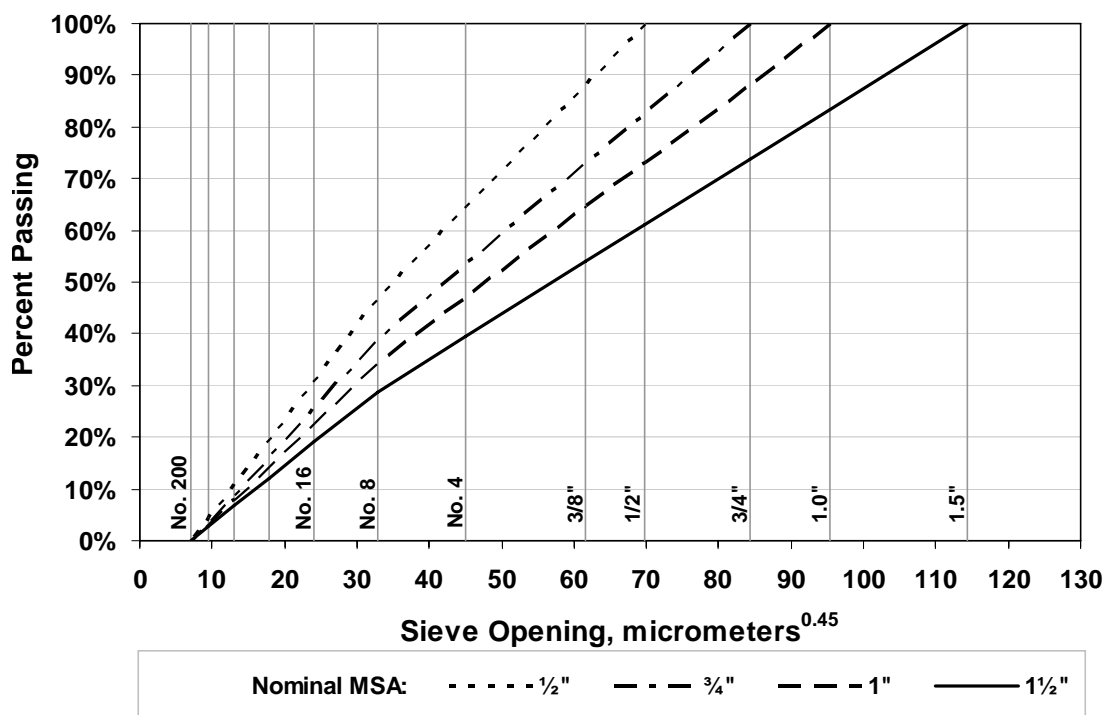


Fig. 1.3 – Modified 0.45 Power Chart with *ideal* combined gradations plotted for aggregates with different maximum sizes

The modified 0.45 power chart can be used to evaluate existing gradations, but more importantly, it is a tool that can be used in an optimization process to help select an appropriate aggregate blend. The *ideal* gradations presented in Fig. 1.3 are plotted on a percent retained chart in Fig. 1.4, and the coarseness factor and workability factors (assuming no adjustment based on deviations in the cementitious material content from a six-sack mixture) are plotted on a modified coarseness factor chart in Fig. 1.5. It is clear from both Figs. 1.4 and 1.5 that the *ideal* gradations produced from the modified 0.45 power chart do not always correspond to an acceptable gradation based on other methods. For example, the *ideal* gradation for a nominal MSA of 38-mm (1½-in.) is nearly gap-graded with a significant deficiency on the 9.5-mm (¾-in.) sieve (Fig. 1.4) and has a (*CF*, *WF*) point that plots below Zone II in the trend bar. The *ideal* gradation with a nominal MSA of 13 mm (½ in.) has more of a *haystack* shape (Fig. 1.4), but the (*CF*, *WF*) point plots above Zone III

(Fig. 1.5), indicating a high percentage of fine material. Based on these comparisons, it is clear that not all techniques result in an optimum gradation and that discretion must be exercised depending on the evaluation or optimization technique used.

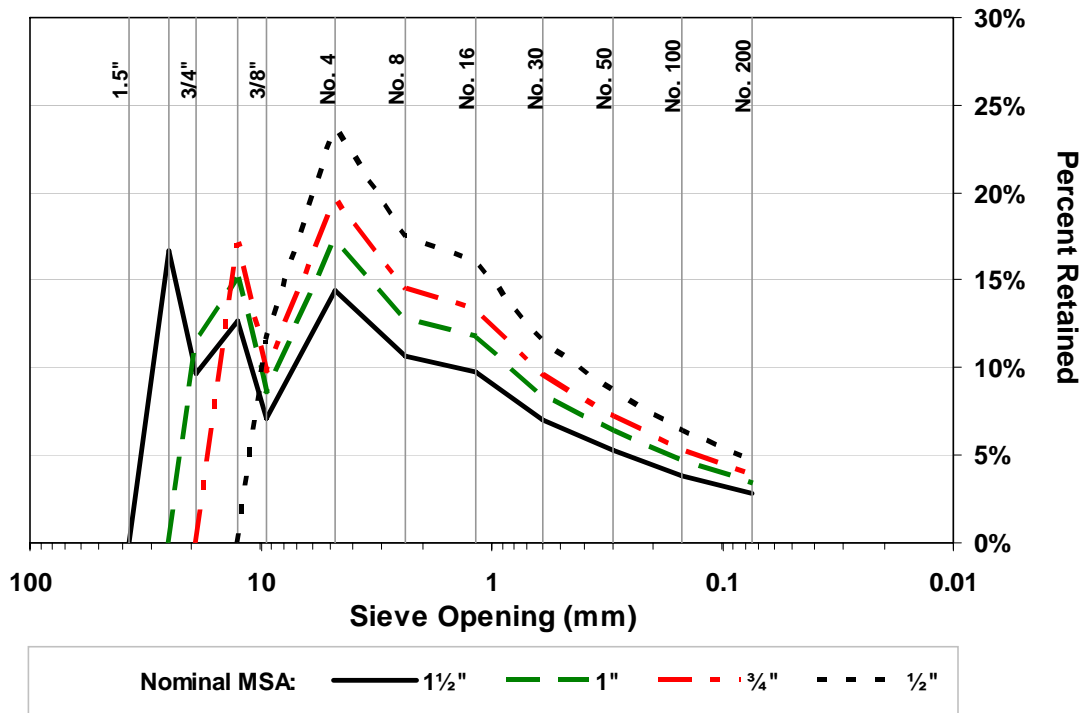


Fig. 1.4 – *Ideal* gradations obtained from the Modified 0.45 Power Chart plotted on a Percent Retained Chart.

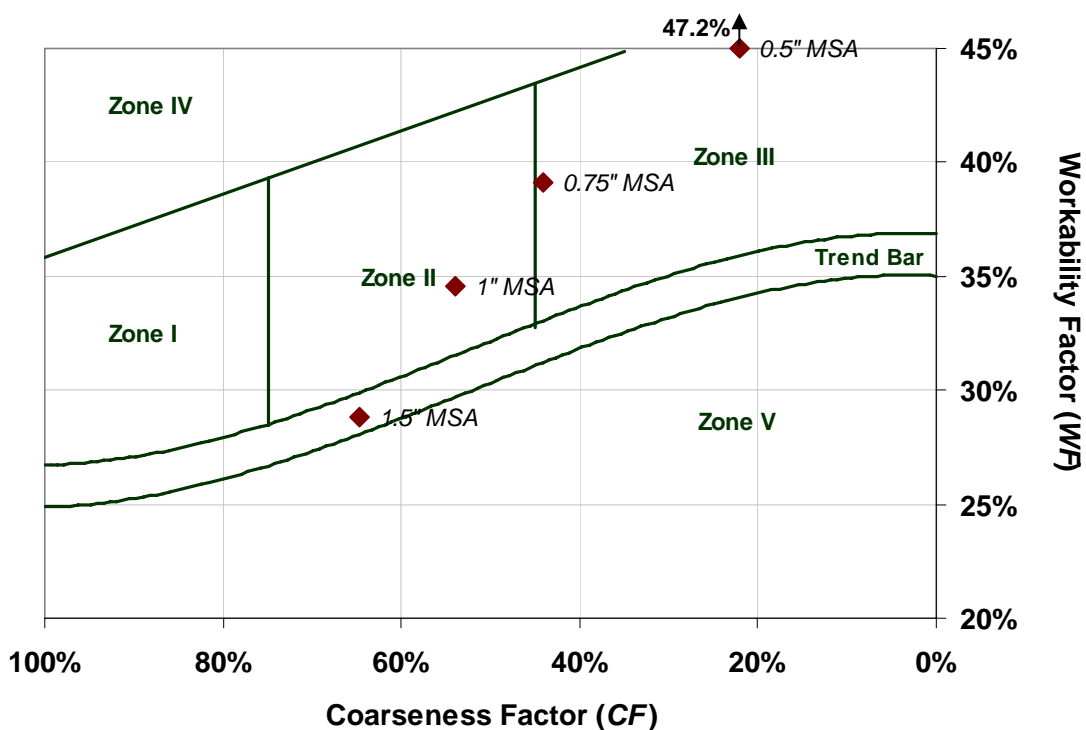


Fig. 1.5 – Workability and Coarseness Factors for *ideal* gradations obtained from the Modified 0.45 Power Chart plotted on a Modified Coarseness Factor Chart.

1.7 PREVIOUS WORK

Section 1.7 is divided into three parts. Each reflects a major portion of this research project. The first identifies the importance of limiting access of deicing salts to the reinforcing steel in bridge decks by examining two studies performed at the University of Kansas (Miller and Darwin 2000, Lindquist, Darwin, and Browning 2005, Lindquist et al. 2006). These unique studies evaluated the effect of cracking on chloride contents and provide the primary justification for this project. The second part summarizes four major studies to ascertain the principal causes and remedies for bridge deck cracking. Each study selected for review provides a unique perspective, substantial advance, or significant body of research on the causes and remedies of bridge deck cracking. Focus is given to the material aspects covered in these reports; the reader is directed to McLeod et al. (2009) for a detailed discussion of construction

and design factors that affect bridge deck cracking. The last part provides a review of the major material factors that affect concrete free shrinkage and provides background information for the laboratory portion of this study.

1.7.1 Effect of Cracking on Chloride Contents

To fully understand the influence of bridge deck cracking on deck deterioration, it is important to evaluate the effect that cracking has on chloride concentrations in reinforced concrete bridge decks. The susceptibility of reinforcing steel to corrosion is a separate issue that is not dealt with here. It is important to note, however, that the lower bound chloride threshold (the value required to initiate corrosion for conventional reinforcing steel) is generally agreed to equal a chloride concentration of 0.6 kg/m^3 (1.0 lb/ft^3).

Chloride contents were sampled as a part of two studies (Miller and Darwin 1998, Lindquist et al. 2005) performed at the University of Kansas and involved 57 bridges, 107 individual concrete placements, and 97 surveys. Three different types of bridge deck system were evaluated: decks with a conventional high-density low slump overlay, decks with a silica fume overlay (either a 5 or 7% replacement of cement with silica fume), and monolithic decks. To determine the chloride content, the concrete was sampled at three locations on cracks and three locations away from cracks for each concrete placement. Powdered concrete samples were obtained using a hammer drill fitted with a hollow 19 mm ($\frac{3}{4}$ in.) bit attached to a vacuum. Five powdered samples were taken in 19 mm ($\frac{3}{4}$ in.) increments at depths of 0–19 mm (0–0.75 in.), 19–38 mm (0.75–1.5 in.), 38–57 mm (1.5–2.25 in.), 57–76 mm (2.25–3 in.), and 76–95 mm (3–3.75 in.). For decks that were sampled on a second occasion as a part of both studies, the new samples were taken within 150 mm (6 in.) of the earlier sampling points. Figure 1.6 shows the individual chloride contents in uncracked concrete at a depth of 76 mm (3 in.), the standard cover depth used in Kansas bridge decks. The concentrations at 76 mm (3 in.) are interpolated from the last two samples

taken at each location, with the value for each sample assigned to the mid-height of the sampling region. In addition to the individual chloride values, Fig. 1.6 includes the best fit lines, along with upper and lower prediction intervals corresponding to 20% and 80% probabilities of exceedance. As expected, the chloride content increases with age, but does not differ as a function of bridge deck type. Through a period of twelve years, only four samples out of 514 exceed the corrosion threshold, and the average trend line does not reach 0.6 kg/m^3 until 20 years (Lindquist et al. 2006).

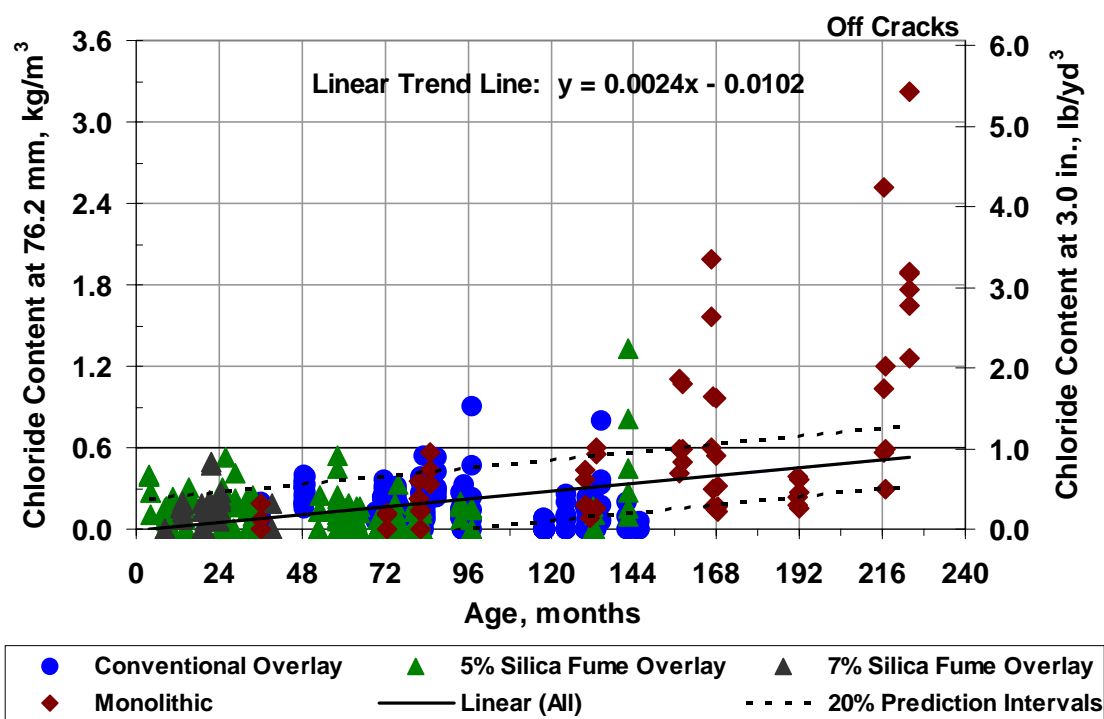


Fig. 1.6 – Chloride content taken away from cracks interpolated at a depth of 76.2 mm (3.0 in.) versus placement age (Lindquist et al. 2006).

The previous observations change significantly when chloride contents at crack locations are evaluated. Figure 1.7 shows the chloride contents at a depth of 76 mm (3 in.) for samples taken at crack locations, along with the best fit lines and the upper and lower prediction intervals. By the end of the first year, the chloride content exceeds the lower value for the chloride threshold, 0.6 kg/m^3 (1 lb/yd^3), in a number

of cases, and by the end of the second year, in over half of the samples. The chloride contents are even greater for bridges in the study that are subjected to higher traffic counts, and presumably higher salt treatments. For bridges with an AADT greater than 7500, the average chloride content reaches 3 kg/m^3 (5 lb/yd^3) in less than 12 years (Lindquist et al. 2006).

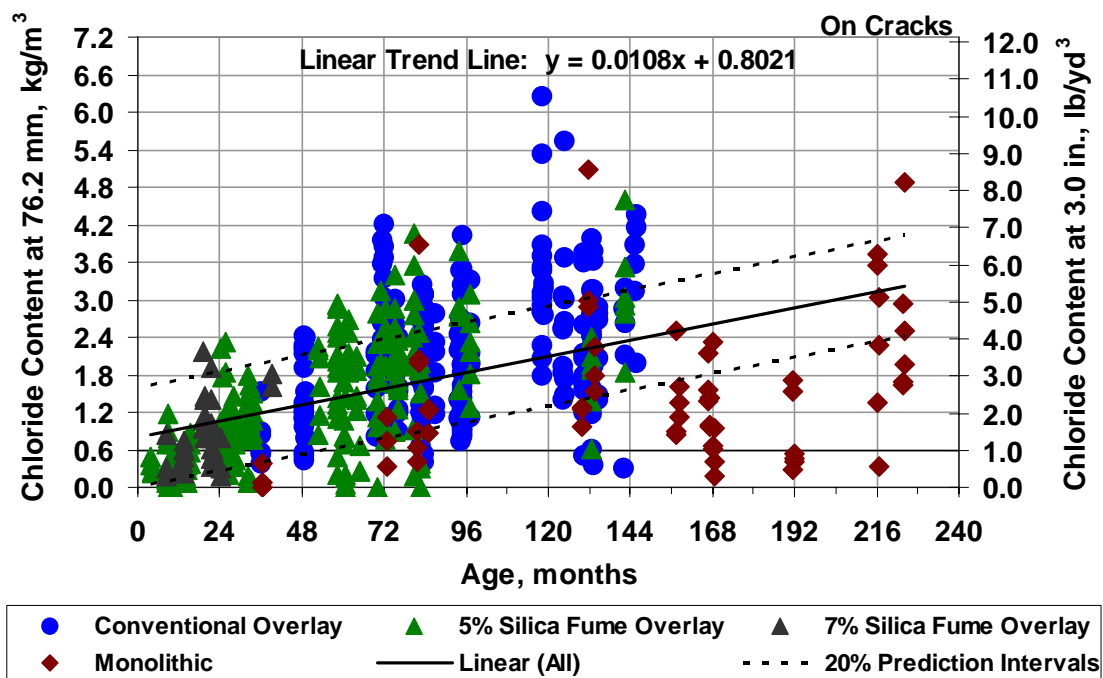


Fig. 1.7 – Chloride content taken at cracks interpolated at a depth of 76.2 mm (3.0 in.) versus placement age (Lindquist et al. 2006).

Lindquist et al. (2005, 2006) observed that chloride contents increase with the age of the bridge deck, regardless of deck type. In addition, concrete sampled in the same age range exhibit similar chloride contents for samples taken both at and away from cracks regardless of the bridge deck type. For bridges within the same age range, the average chloride concentration taken away from cracks at the level of the top transverse reinforcement rarely exceeds even the most conservative estimates of the corrosion threshold for conventional reinforcement. Chloride concentrations taken at crack locations, however, can exceed the corrosion threshold after the first winter. Based on these observations, it appears clear that attention should be focused

on minimizing bridge deck cracking rather than on concrete permeability. This change would represent a paradigm shift, as most agencies currently focus on concrete permeability. Because of the negative impact of cracking on chloride contents, Lindquist et al. (2006) concluded not only that corrosion protection systems are needed in bridge decks, but that protection is needed early in the life of the deck.

1.7.2 Material Factors Affecting Bridge Deck Cracking

Portland Cement Association 1970. The Portland Cement Association (PCA) completed one of the earliest studies, beginning in 1961, intended to both characterize and investigate the causes of bridge deck deterioration (*Durability 1970*). The study had four specific objectives: to determine the types and extent of bridge deck durability problems, to determine the causes of different types of deterioration, to improve the durability of future bridge decks, and to develop methods to mitigate the deterioration of existing bridge decks. To meet these objectives, the study included a detailed field investigation of 70 bridge decks in four states, random surveys of over 1000 bridge decks in eight states, and an analytical study of the vibration characteristics of 46 bridge decks. No correlation was found between the vibration characteristics of the deck and deterioration observed during the field investigations.

The random surveys of over 1000 bridges built from 1940 to 1962 included a summary of the deterioration observed with the primary purpose to determine the types and extent of deck deterioration. The types of deterioration observed included scaling, various types of cracking, rusting, surface spalls, joint spalls, and popouts. Data from the random surveys indicated that the most severe instances of scaling occurred in decks cast with non-air-entrained concrete. Cracking was observed in approximately two-thirds of the bridge decks, with transverse cracking being the most prevalent. Transverse cracking appeared to increase with age and span length and had a higher incidence for continuous spans and decks supported by steel girders.

The detailed investigations of 70 bridge decks included sketches of the deterioration, collection of concrete cores for evaluation in the laboratory, and an examination of available construction and design documentation. The 70 bridges included in the investigation represented a wide range of ages, locations, structure types, and degrees of deterioration. Several different types of bridge deck deterioration were observed and categorized into three groups: scaling, cracking, and surface spalling.

As with the results from the random surveys, in the detailed investigations, scaling was found to be most severe on bridge decks cast with non-air-entrained concrete, although some isolated areas of scaling were found on decks with air-entrained concrete. Based on laboratory measurements of the air content and air void distribution in these decks, scaling was found to be caused by localized deficiencies in entrained air. In addition to deficiencies in air content, scaling was also found on some decks with a high w/c ratio paste at the deck surface. Chloride tests performed on samples of air-entrained concrete showed no correlation with scaling.

The laboratory analysis of cores taken from cracked sections indicated that transverse cracks typically occurred directly above the reinforcing steel and were likely caused by subsiding plastic concrete. Steel girder bridges had transverse cracks at close regularly spaced intervals over the entire length of the deck. Diagonal cracking was observed less frequently and typically occurred at the corners of skewed bridges. Pattern cracking was generally found to be shallow and most likely caused by plastic shrinkage cracking. Surface spalling was often observed on decks with inadequate reinforcing steel cover. The spalling observed on these decks was caused by an increase in reinforcing steel volume due to corrosion, and pressure generated by freezing liquids in cracks around reinforcing bars.

Based primarily on the results of the detailed investigation, several recommendations were made with regard to concrete mix design and bridge design.

The authors recommended that the largest maximum size aggregate should be used to minimize the concrete's paste content. The maximum recommended slump was 75 mm (3 in.) to reduce the effects of excess bleeding, drying shrinkage (caused by an increase in the water content), and settlement cracking. Concrete cover should be at least 50 mm (2 in.) over the top reinforcement in areas where deicers are used and at least 38 mm (1.5 in.) in all other areas. In addition to the cover requirements, the report recommended that adequate deck drainage be emphasized during the design phase to reduce surface scaling in gutter areas.

Babaei and Purvis 1996. In a 1996 study by Babaei and Purvis for the Pennsylvania Department of Transportation (PennDOT), the causes and methods to mitigate premature cracking were investigated. A field investigation of bridge deck cracking was completed in two phases. The first phase included a "walk-by" survey of 111 Pennsylvania bridge decks and an in-depth study of 12 decks with the goal of determining the types, significance, and causes of premature cracking in bridge decks. The second phase consisted of field tests and the observation of eight bridge deck construction projects with the intent of identifying any construction or design procedures that may lead to cracking.

Of the 111 bridges surveyed, 51 were prestressed concrete girder bridges, 41 were prestressed concrete spread box-beam bridges, and 19 were steel girder bridges, all built within 5 years of the study. The surveys indicated that transverse cracking occurred more frequently than other types of cracking and occurred in both positive and negative moment regions. Simply-supported bridges were found to perform better than continuous span bridges, presumably because of the negative moments present in continuous bridges. The in-depth surveys of 12 simply-supported bridges included crack mapping, crack width measurements, top reinforcement cover and location measurements, and concrete coring.

Based on the data obtained from the in-depth surveys and comparisons with design and construction records, Babaei and Purvis observed that most of the transverse cracks were directly above the top transverse reinforcing bars and extended down at least to the level of the bars. In addition, based on concrete cores, the transverse cracks typically intersected the coarse aggregate particles, indicating that the cracks formed after the concrete had hardened. Thermal shrinkage and drying shrinkage were thought to largely control cracking in these decks.

Phase two of the study included field tests, and the observation of eight bridge decks under construction. During the construction of the eight bridge decks, concrete temperature was recorded throughout the curing process and concrete samples were taken to determine thermal and drying shrinkage, respectively. Based on observations of construction procedures, two practices were identified for their potential to cause cracking: delayed concrete curing in hot weather and increasing the water content of the mix after the truck had left the ready-mix plant.

Temperature measurements were taken at the construction site to estimate the amount of thermal shrinkage, and field samples were tested in the laboratory to measure the amount of drying shrinkage. Thermal shrinkage was estimated using the maximum difference between the concrete temperature during a period up to 8.5 hours after casting and the ambient air temperature. The ambient temperature was assumed to be the temperature of the underlying girders since no artificial heating was employed during the construction of the decks. The difference between the maximum concrete temperature and the corresponding ambient air temperature was assumed to contribute to thermal shrinkage at a rate of 9.9 microstrain per degree C (5.5 microstrain per degree F). Deck drying shrinkage was estimated from free-shrinkage specimens cured for 7 days, the same as the bridge decks, and measured for up to 112 days after casting. The drying shrinkage measured from the $76 \times 76 \times 254$ mm ($3 \times 3 \times 10$ in.) free-shrinkage specimens was divided by 2.5 to account for the

lower volume-to-surface area ratio of the specimens compared to the deck. The basis for determining 2.5 correction factor was not clearly described in the report. Thermal shrinkage ranged from 0 to 170 $\mu\epsilon$, and drying shrinkage measured in the laboratory ranged from 192 to 580 $\mu\epsilon$.

Based on analytical work, the authors found that a thermal shrinkage of 228 $\mu\epsilon$ may initiate cracking in only a few days. Unlike thermal shrinkage, drying shrinkage occurs over a much longer period, allowing concrete creep to help diminish stresses. The cracking threshold, based on the calculated average tensile strength and modulus of elasticity, was found to be 400 $\mu\epsilon$. An average crack spacing was calculated for each bridge deck based on the total long-term shrinkage displacement of the deck and an average crack width of 0.25 mm (0.01 in.). The results of the shrinkage study correlated very well with the observations in the field. The only four bridges that showed cracking were also predicted to crack based on the thermal and drying shrinkage results. The authors concluded that, to limit the average crack spacing to a minimum of 9 m (30 ft), two conditions had to be met: the 28-day drying shrinkage measured in the laboratory must be limited to 400 $\mu\epsilon$ (corresponding to a long-term shrinkage of 700 $\mu\epsilon$), and the maximum temperature differential between the concrete and the girders must be limited to 12° C (22° F), corresponding to a thermal shrinkage of 121 $\mu\epsilon$, “for at least 24 hours after placement.”

Krauss and Rogalla 1996. In 1996, Krauss and Rogalla also completed a multipart study to determine the major factors that contribute to early transverse cracking of bridge decks. The study included laboratory testing, bridge deck instrumentation, and an analytical study of the stresses resulting from different combinations of variables thought to influence bridge deck cracking. The primary focus of the project was to identify the factors thought to contribute to cracking from variables in three categories: bridge design, materials, and construction procedures.

A field study was performed that involved the instrumentation of the Portland-Columbia Bridge between Pennsylvania and New Jersey. A system was installed to monitor the strains and temperatures of the girders and deck, beginning during the deck replacement and continuing for several months after construction. Although the results obtained from this specific bridge could not be generalized to include all bridges, the results were helpful in confirming the theoretical analysis (described briefly next) and providing a general understanding of early transverse cracking.

A series of equations were derived in the analytical study to describe the stresses developed in a composite reinforced bridge deck subjected to temperature and shrinkage conditions. The stresses based on strains measured in the Portland-Columbia Bridge were very similar to the stresses predicted using the analytical equations. Shrinkage and thermal stresses were calculated for more than 18,000 combinations of bridge geometry and material properties. Shrinkage stresses were found to be affected primarily by material properties rather than design parameters. The most significant design factors influencing shrinkage stresses were girder depth, deck thickness, and narrow girder spacings. In addition, steel studs or channels and stay-in-place steel forms were found to increase deck stresses. In particular, stay-in-place forms were found to create non-uniform shrinkage that has the tendency to produce large tensile stresses at the deck surface.

Laboratory testing included the development of a restrained ring test to measure cracking tendency of different deck mixes. In addition, free-shrinkage specimens and strength cylinders were made to help relate cracking tendency with shrinkage, strength, modulus of elasticity, and creep characteristics. Thirty-nine concrete mixtures were investigated using the restrained ring test. The effects of w/c ratio, cement content, aggregate size and type, high-range water reducers, silica fume, set accelerators and retarders, air entrainment, freeze-thaw cycles, evaporation rate,

curing, and shrinkage-compensating cement were examined and ranked by importance.

Based on the laboratory study, several trends with respect to cracking tendency were observed. Cracking tendency was found to increase with increasing cement content and decreasing w/c ratios. Cracking tendency generally decreased the most with a low cement content mix. Silica fume was found to increase cracking tendency, while the addition of a high-range water reducer and Class F fly ash was found to slightly decrease the cracking tendency. Set accelerators were found to have a minimal effect on cracking tendency, and the addition of set retarders produced mixed results. While the use of set retarders may not have an effect on cracking tendency in the laboratory, retarded concrete is especially susceptible to plastic shrinkage and settlement cracking. The use of air entraining agents was not found to have an effect on cracking tendency. Both the diffusion properties and Poisson's ratio were found to only have a minor effect on cracking. Above all else, Krauss and Rogalla found that aggregate type had the most significant material-related effect on cracking. Restrained ring specimens with hard trap rock aggregate cracked relatively late, as did other angular aggregates when compared with round aggregates. Aggregate shrinkage characteristics were also found to be an important factor affecting cracking tendency.

Several recommendations were made with respect to material and environmental aspects to minimize cracking potential: Effort should be made to minimize paste contents and cements with a high heat of hydration. Lower cement contents should be specified in addition to 28-day compressive strengths between 21 and 28 MPa (3000 and 4000 psi). Krauss and Rogalla suggest a maximum cement content 306 kg/m^3 (517 lb/yd^3) used in conjunction with a 38 mm (1.5 in.) maximum size aggregate. In addition, they suggested that bridge deck concrete should be specified based on 56 or 90-day compressive strengths to encourage lower heat of

hydration concrete mixes. High water contents, although they result in higher paste contents, were not found to increase cracking tendency. This observation is in contrast to the field observations of Babaei and Purvis (1996) and Lindquist et al. (2005). Krauss and Rogalla suggest that the increased water content may result in increased creep and consequently decreased cracking tendency. Both the creep characteristics and the modulus of elasticity of the concrete were found to have a major effect on bridge deck cracking. The coefficient of thermal expansion, although limited in range, was found to have a moderate effect on cracking.

In an effort to reduce concrete temperatures and solar radiation effects, concrete should be cast in the late afternoon or evening, and cast with a temperature below 27° C (80° F). The decks should be protected with windbreaks and immediate water fogging when the evaporation rate exceeds 1.0 kg/m²/hr (0.2 lb/ft²/hr). Misting or the use of a monomolecular film immediately after screeding, applying two coats of a curing compound before the concrete surface dries, moist curing with wet burlap for at least 7 days, using a curing membrane following the wet cure, and grooving the deck after the curing period with a diamond saw to avoid delays caused by tining the fresh concrete should be required.

Lindquist, Darwin, and Browning 2005. In 2005, Lindquist et al. completed a follow-up study to two previous Kansas Department of Transportation research reports (Schmitt and Darwin 1995, 1999, Miller and Darwin 2000). This report represents a culmination of three studies with the overarching goal of identifying the principal factors contributing to bridge deck cracking. Material properties, design documents, construction practices, and environmental site conditions were compared with the performance of the reinforced concrete bridge decks as part of the evaluation. The study included two bridge deck types with silica fume overlays, one in which 5% of the cement was replaced by silica fume (19 bridges) and the other in which 7% of the cement was replaced by silica fume (11 bridges), in addition to

decks with conventional overlays (16 bridges) and monolithic bridge decks (13 bridges). For the overlay decks, comparisons were made based on both the overlay properties and the properties of the bridge subdecks.

Performance of the bridge decks was measured through field surveys performed on 59 steel girder bridges – bridges that are generally agreed to exhibit the greatest amount of bridge deck cracking. Of these bridge decks, 49 were surveyed in previous studies by Schmitt and Darwin (1995, 1999) or Miller and Darwin (2000) or both. The field surveys were performed to measure deck crack density and chloride ingress (described in Section 1.7.1). In total, 27 variables were evaluated, covering bridge age, construction practices, material properties, site conditions, bridge design, and traffic volume. The performance of silica fume overlay decks relative to that of conventional overlay and monolithic decks was of particular interest due to the widespread use of silica fume overlays in the State of Kansas.

The field surveys were performed by marking all of the cracks on the bridge deck and transferring these marks to a scale drawing of the deck. The drawings were scanned, and crack densities, in linear meters of crack per square meter of bridge deck, were calculated for each deck from the crack maps through the use of computer programs. In addition to the entire bridge deck, crack densities were also calculated for individual spans, individual placements, and the first and last 3 m (10 ft) of each bridge deck. Due to the inherent differences in the bridge deck types included in the study, most of the variables were analyzed separately for each deck type.

The study demonstrated that cracking increased with increases in the volume of cement paste and that neither higher compressive strengths nor higher concrete slumps were beneficial to bridge deck performance. Crack density was found to decrease with increasing amounts of entrained air, with significant decreases observed when the air content exceeded 6.0%. In addition, crack density was found to be higher in the end regions of decks that were integral with the abutments than

decks with pin-ended girders. The researchers also observed significant differences in bridge deck performance depending on the contractor responsible for deck construction. The results of the crack surveys indicated that cracking increased with age, although a large percentage of the cracking was established early in the life of the deck. Even with the increase in crack density over time, however, both monolithic and conventional overlay bridges cast in the 1980s exhibited less cracking than those cast in the 1990s. The differences were attributed to changes in material properties and construction procedures over the past 20 years. The trend in cracking for decks with silica fume overlays cast in the 1990s (containing 5% silica fume), however, was quite the opposite. A decrease in crack density was observed for 5% silica fume overlay decks, which appears to be the result of increased efforts to limit evaporation prior to the initiation of wet curing. The most recently constructed silica fume overlay decks (containing 7% silica fume), however, had an increased crack density, presumably due to the increased silica fume content.

In light of the observations made during the field surveys, conventional high-density overlays were recommended in lieu of silica fume overlays, and full-depth monolithic decks were recommended in lieu of either for new deck construction. The researchers recommended a maximum paste content of 27% and the use of the lowest slump that will allow for proper placement and consolidation. The final recommendation was to implement a contractor selection process based on the quality of previous work. It was clear based on the surveys that some contractors consistently constructed bridge decks with severe cracking, while others consistently produced bridges with low cracking.

1.7.3 Material Factors Affecting Free Shrinkage

Many factors influence free shrinkage, although there is a general consensus among researchers that the primary factor is the paste content or, alternatively, the aggregate volume fraction. This topic, plus the effects of water-cement ratio,

aggregate shape and gradation, mineral admixtures, and curing period on free-shrinkage, are discussed next.

1.7.3.1 Effect of Paste Content and Water-Cementitious Material Ratio

The amount of cement paste (cementitious materials and water) has long been recognized as a key factor affecting concrete shrinkage. In a 1956 study by Pickett, a theoretical formula using the theory of elasticity was derived to characterize the influence of aggregate content (and paste content) on concrete shrinkage. Pickett then performed a series of shrinkage tests to test the validity of the theoretical formula. The formula was derived by first examining the effect of one small spherical aggregate particle in a large spherical body of shrinking cement paste. The aggregate particle and cement paste were assumed to be elastic, and the formula was expressed in differential form and integrated to obtain the final formula [Eq. (1.4)] for concrete containing any percentage of aggregate.

$$S_c = S_p (1 - V_g)^\alpha \quad (1.4)$$

where

$$\alpha = \frac{3(1 - \mu)}{1 + \mu + 2(1 - 2\mu_g)E / E_g} \quad (1.5)$$

S_c, S_p = concrete shrinkage, paste shrinkage

V_g = aggregate volumetric fraction

α = material constant

μ, μ_g = Poisson's ratio for concrete, aggregate

E, E_g = elastic modulus for concrete, aggregate

If material specific information is not available, typical values suggested for α range from 1.2 to 1.7. It should also be noted that α is assumed to be independent of the w/c ratio and the aggregate volumetric fraction.

Pickett (1956) examined mortars with aggregate contents ranging from zero to 70% by volume to test the validity of Eq. (1.4). In addition to examining the aggregate volume fraction, three aggregate types (pulverized silica, standard Ottawa sand, and graded Elgin sand), two w/c ratios (0.35 and 0.50), and two cement types (normal and high-early-strength) were examined to determine their influence on shrinkage. Free-shrinkage specimens [$25 \times 22 \times 286$ mm ($1 \times \frac{7}{8} \times 11\frac{1}{4}$ in.) prisms] were cured in water for seven days and then stored at 24° C (76° F) and 50% relative humidity. All of the mixtures examined were non-air entrained. Mixtures containing 5% aggregate or less were “too wet” and mixtures containing 50% aggregate or more were “too dry” to adequately cast and consolidate the free-shrinkage prisms. The results of the laboratory investigation indicated that Eq. (1.4) represented the effect of aggregate content on shrinkage very well. As the aggregate volume was increased, shrinkage decreased, and at a given aggregate content, shrinkage increased with an increase in the w/c ratio. Pickett reported only small differences in shrinkage between mortars made with different aggregate and cement types.

Deshpande, Darwin, and Browning (2007) examined many factors thought to influence concrete shrinkage and found that shrinkage was primarily a function of paste content. The effects of paste content (nominally, 20, 30, and 40%), w/c ratio (0.40, 0.45, and 0.50), and cement type (Type I/II and Type II coarse ground) on concrete shrinkage were evaluated. Free-shrinkage specimens [$76 \times 76 \times 286$ mm ($3 \times 3 \times 11\frac{1}{4}$ in.)] were produced in triplicate and cast with saturated-surface-dry limestone coarse aggregate. Gage studs were placed on opposite ends of the specimens to facilitate measurements with a mechanical dial gage. The non-air-entrained specimens were cured in lime-saturated water for three days and then stored at 23° C (73° F) and 50% relative humidity.

The results for ages in excess of 150 days for concrete containing Type I/II cement (presented in Fig. 1.8) show that shrinkage increased by about $200 \mu\epsilon$ as the

paste content increased from 20 to 30% and by another $150 \mu\epsilon$ as the paste content was increased from 30 to 40%. For a constant paste volume, there was considerable variability in the relationship between w/c ratio and shrinkage, although there was some tendency towards decreased shrinkage for concrete mixtures with higher w/c ratios. This supports the work by Krauss and Rogalla (1996) who reported an increase in cracking tendency with an increase in cement content (and paste content) and decreasing w/c ratios. These results indicate that shrinkage is largely controlled by the paste content and not directly by the water content. Deshpande et al. (2007) observed a similar trend for concrete containing Type II coarse ground cement.

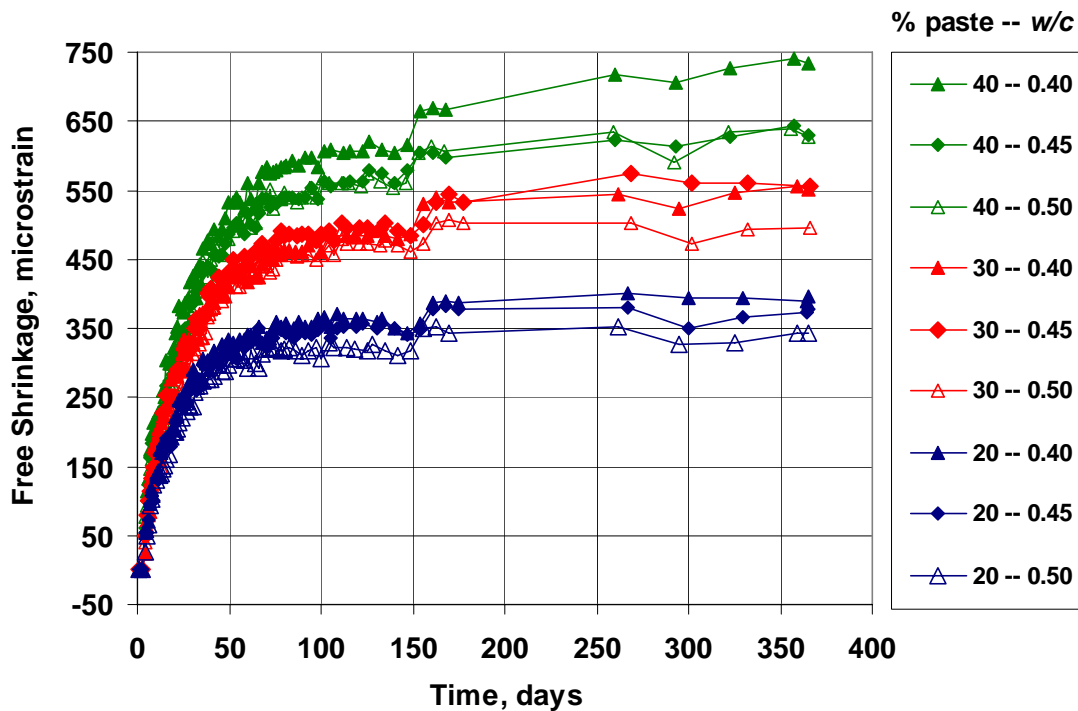


Fig. 1.8 – Free shrinkage plotted versus time through 365 days for concrete containing nominal paste contents between 20 and 40% with w/c ratios ranging from 0.40 to 0.50 [Adapted from Deshpande et al. (2007)].

Similar results were obtained by Ödman (1968), who reexamined work reported by Blanks, Vidal, Price, and Russell (1940) that addressed the effect of water content, cement content, and w/c ratio on concrete shrinkage and first concluded that shrinkage varied “almost” directly with water content. Ödman (1968) expressed the

combined effect of water content and cement content as the volumetric aggregate fraction (or paste content) and found that paste content, rather than water content, controlled free shrinkage. The w/c ratio was found to play a relatively minor role compared to the effect of paste content on shrinkage. For concretes with paste contents (20 to 30%) typically used for bridge deck construction (Fig. 1.9), shrinkage increases as the w/c ratio increases from 0.30 to 0.50, and then remains nearly constant from 0.50 to over 0.70.

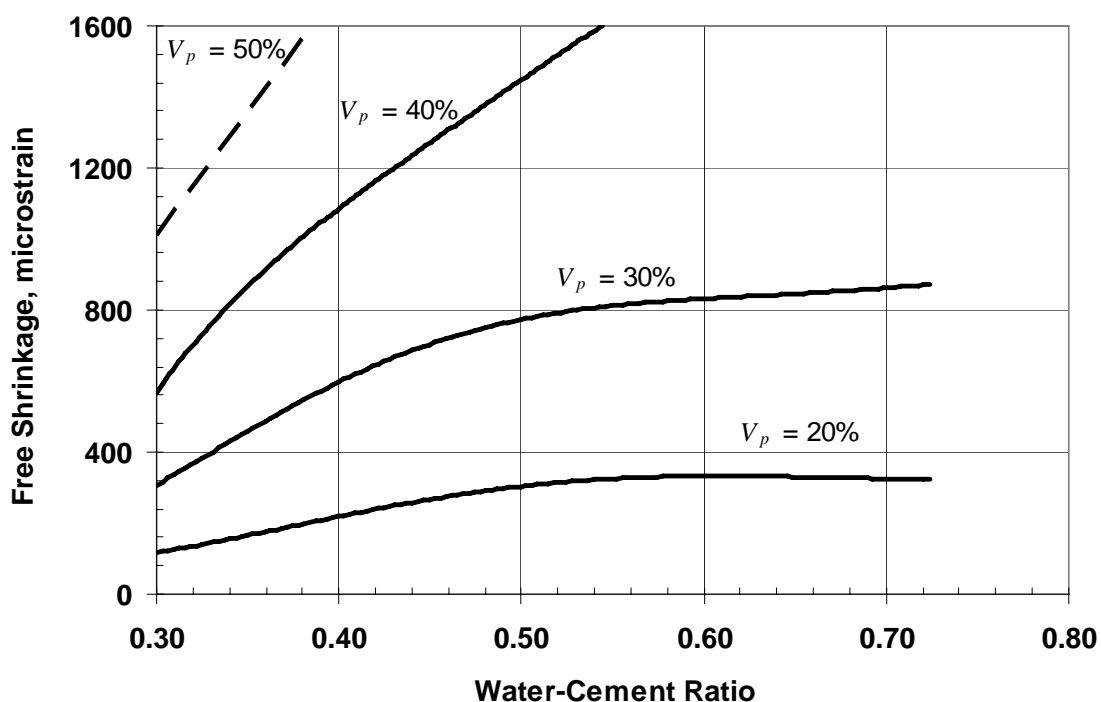


Fig. 1.9 – Free shrinkage plotted versus w/c ratio for concrete containing paste contents (V_p) between 20 and 50% [Adapted from Ödman (1968)].

Bissonnette, Pierre, and Pigeon (1999) examined the effect of paste content and w/c ratio on drying shrinkage using cement pastes, mortars, and concretes. Two sets of free-shrinkage specimens were produced: smaller $4 \times 8 \times 32$ mm ($0.16 \times 0.32 \times 1.28$ in.) prisms for pastes and mortars, and larger $50 \times 50 \times 400$ mm ($1.97 \times 1.97 \times 15.75$ in.) prisms for mortar and concrete. The smaller specimens were chosen to obtain approximately gradient-free shrinkage and to compare shrinkage results with

the larger specimens. Type I portland cement was used with granitic sand and crushed limestone with a maximum nominal size of 10 mm (0.39 in.). The mortar mixes contained aggregate/cement ratios of 1 or 2, and the concrete mixtures contained either 30 or 35% paste by volume. All specimens, produced in duplicate, were cured in lime-saturated water for 28 days and then stored at 23° C (73° F) with 48% relative humidity. Additional smaller specimens were also stored at 75 and 92% relative humidity to determine the influence of relative humidity on shrinkage.

Results for the small paste and mortar specimens (with a constant paste content) indicated that shrinkage was reduced by an average of 14% with a reduction in the w/c ratio from 0.50 to 0.35. A significant decrease in shrinkage was observed as the paste content was decreased. For specimens dried at 48% relative humidity for one year, shrinkage was reduced from approximately 3200 $\mu\epsilon$ for paste specimens to 1400 and 950 $\mu\epsilon$ for mortar specimens with aggregate/cement ratios of 1 and 2, respectively. Shrinkage was found to increase linearly with a decrease in relative humidity between 92 and 48%. For concrete specimens with constant paste contents, the effect of w/c ratio on shrinkage was slightly more pronounced but still only represented a small percentage (less than 4% for both paste contents examined) of the total shrinkage. The reduction in paste content from 35 to 30% resulted in a reduction in shrinkage from 640 to 540 $\mu\epsilon$ for mixtures with a w/c ratio of 0.50 and from 610 to 560 $\mu\epsilon$ for mixtures with a w/c ratio of 0.35 after one year of drying. Bissonnette et al. (1999) also compared shrinkage rates of mixtures cast using different specimen sizes in an effort to determine the effect of size on shrinkage characteristics. They observed that the shrinkage rate was strongly affected by the specimen size, with smaller specimens shrinking more rapidly, although the ultimate shrinkage did not differ significantly between specimen sizes.

1.7.3.2 Effect of Aggregate Type

Concrete used for standard construction generally contains between 50 and 80% aggregate (Hobbs 1974); so it comes as no surprise that both the aggregate volume fraction and aggregate mechanical characteristics are primary factors affecting concrete shrinkage. Aggregate particles (in addition to unhydrated cement and calcium hydroxide crystals) within the concrete restrain shrinkage of the cement paste. For this reason, concrete containing low-absorptive aggregates with a high modulus of elasticity generally exhibit lower shrinkage (Carlson 1938, Alexander 1996). This observation is not universal, however, and some researchers (Fujiwara 1984, Imamoto and Arai 2006) believe that the specific surface area of the aggregate influences shrinkage characteristics more than the modulus of elasticity.

Recent work indicates that concrete containing saturated porous aggregate can result in lower shrinkage due to internal curing resulting from the slow release of water from the aggregate pores (Collins and Sanjayan 1999).

The total volume (or volume fraction) of aggregate in a concrete mixture has the largest potential effect on shrinkage (ACI Committee 209 2005) and, thus, should be considered separately from the influence of aggregate mechanical properties. Several studies on the influence of the mechanical properties of aggregate on shrinkage are discussed next. The influence of aggregate volume (or cement paste volume) is discussed in Section 1.7.3.1.

Carlson (1938) performed one of the first studies to determine the effect of aggregate type on drying shrinkage. Concrete mixtures containing quartz, limestone, dolomite, granite, and feldspar, in addition to several types of natural sand and gravel, were evaluated. Water-cement ratios ranged from 0.62 to 0.87, with paste contents between 27 and 35%. The differences in w/c ratio and paste content were the result of changes in mix water to maintain a constant slump of 75 mm (3 in.) (the cement content was held constant). Because of these differences, Carlson normalized the

shrinkage results to a w/c ratio of 0.65 to allow for a comparison between mixes with different w/c ratios by adjusting shrinkage values by 1.75% for each one percent difference in water content.

Using the normalized data, Carlson (1938) observed that the compressibility of the aggregates had a significant influence on concrete shrinkage. At an age of six months, the highest shrinkage (870 $\mu\epsilon$) was observed for concrete containing crushed mixed gravel and the lowest (450 $\mu\epsilon$) was observed for concrete containing crushed quartz. Concrete mixtures containing natural sands and gravels generally had higher shrinkage than concrete mixtures containing crushed aggregates including quartzite, granite, and limestone. Among the crushed aggregates, shrinkage was higher for concrete mixtures containing aggregates with higher absorptions. Carlson noted that maximum aggregate size and aggregate gradation had little effect on concrete shrinkage directly, although these aggregate properties clearly influence the amount of water required to attain a given slump.

In an effort to determine the effect of aggregate type on the properties of hardened concrete, Alexander (1996) examined concrete containing 23 different aggregates and found that concrete elastic modulus, shrinkage, and creep can vary by as much as 100% depending on the aggregate used. The study included nine different types of aggregate, many of which were obtained from multiple sources. The aggregates examined (including the number of sources for each type) were andesite (2), dolerite (3), dolomite (2), felsite (2), granite (3), greywacke (1), siltstone (1), tillite (1), and quartzite (8). The study was divided into two series of tests: the first included concrete mixtures designed to obtain 28-day compressive strengths of 20, 30, 40, and 60 MPa (2900, 4350, 5800, and 8700 psi), and the second designed using mixtures with w/c ratios of 0.41, 0.51, 0.61, and 0.74. Free-shrinkage specimens [100 \times 100 \times 200 mm (4 \times 4 \times 8 in.) prisms with demountable mechanical gages placed on opposite faces with a 100 mm (4 in.) gage length] were produced in triplicate, cured

in lime-saturated water for 28 days, and then stored at 23° C (73° F) and 60% relative humidity.

Based on the test results, Alexander (1996) concluded that concrete shrinkage is affected primarily by two factors: the amount of water required to attain a workable mix, and the stiffness of the aggregate. The water demand was used to determine the cement content (and paste content) for each strength grade and w/c ratio examined. Although the basis for determining the water demand was not clear, slumps ranged from 20 to 95 mm (0.80 to 3.75 in.) and paste contents ranged from 26 to 30%. The water content (and paste content) was presumably adjusted to account for the angularity or elongation of different aggregate types until adequate workability was obtained. The results indicate that mixtures containing aggregates with a high water demand produce concretes with higher shrinkage due to increased cement paste.

In an effort to normalize the test results, Alexander attempted to eliminate the effect of different paste contents using a modified version of Pickett's equation, Eq. (1.4), to normalize the shrinkage results to the mean paste volume.

$$\frac{S_c}{S_{cm}} = \left(\frac{V_p}{V_{pm}} \right)^\alpha \quad (1.6)$$

where S_c, S_{cm} = concrete shrinkage, shrinkage corresponding to concrete with V_{pm}
 V_p, V_{pm} = cement paste volume, mean cement paste volume
 α = material constant assumed to be 1.5

After normalizing the shrinkage data to account for differences in paste content, the aggregate type was found to have a large effect on shrinkage. Concrete mixtures containing aggregates with higher elastic moduli tended to produce concrete with less shrinkage (although this was not always the case). Concretes containing dolomite (a carbonate rock similar to limestone with the highest elastic modulus) had

the least 28-day and six-month shrinkage, while concretes containing siltstone (a clastic rock derived from silt with the lowest elastic modulus) had the highest 28-day and six-month shrinkage. Among the remaining aggregates tested, there was considerable scatter in the shrinkage values, but concrete containing quartzite, siltstone, or tillite had higher shrinkage while concrete containing dolerite or dolomite had the least shrinkage.

Deshpande et al. (2007) examined the effect of three different types of coarse aggregate, limestone (2.9 to 3.0% absorption), granite (0.6% absorption), and quartzite (0.4% absorption) on concrete shrinkage. This portion of their study was divided into four sets of tests, all of which examined the effect of aggregate type. The first three sets included non-air-entrained concrete mixtures containing 30% paste at a 0.45 *w/c* ratio cast using limestone, quartzite, or granite. The fourth set consisted of air-entrained concrete mixes (7.4% air) containing these three aggregates with a *w/c* ratio of 0.45 and a paste content of 23.8%. Free-shrinkage specimens produced in triplicate were 76 × 76 × 286 mm (3 × 3 × 11¼ in.) with gage studs on opposite ends to facilitate measurements with a mechanical dial gage. Specimens were cured in lime-saturated water for three days and then stored at 23° C (73° F) with 50% relative humidity.

The results reported by Deshpande et al. (2007) for the first and fourth set supported the assertion that concrete made with dense aggregates exhibit less shrinkage than those containing more porous aggregates. The results for sets two and three contained mixed results. For the first set at an age of 30 days, the free-shrinkage was 227 µε for the concrete containing limestone and 173 µε for the concrete containing quartzite. At 365 days, the shrinkage increased to 407 µε for concrete containing limestone and 333 µε for concrete containing quartzite. The results for the fourth series were similar. At an age of 30 days, the least shrinkage was obtained for concrete containing granite (313 µε), followed by quartzite (347 µε)

and limestone (377 $\mu\epsilon$). At an age of 90 days (the last reported), the trend remained the same. The least shrinkage was obtained for concrete containing granite (447 $\mu\epsilon$), followed by quartzite (497 $\mu\epsilon$) and limestone (520 $\mu\epsilon$). The results for sets two and three were not as conclusive. Differences in shrinkage for set two were not statistically significant, and for the third set, the granite mixture exhibited significantly lower shrinkage than either the quartzite or limestone batch, while the mixture containing quartzite exhibited the highest shrinkage. The authors concluded that concrete containing denser aggregates exhibit less shrinkage than concrete containing porous aggregate, although the results for individual sets are not always consistent.

Carlson (1938), Alexander (1996), and Deshpande et al. (2007) found that soft aggregates, as indicated by the modulus of elasticity and absorption, tend to promote higher concrete shrinkage as compared to concrete containing stiff aggregates with a low absorption. In a further effort to determine the influence of aggregate type on shrinkage, Imamoto and Arai (2006) related the specific surface area (total surface area per unit of mass) of different aggregates to concrete drying shrinkage. The coarse aggregate specific surface area was measured using the B.E.T. (Brunauer, Emmett and Teller 1938) method with water as the adsorbate. The aggregates examined consisted of two samples of hardened sandstone (0.73 and 0.96% absorption), two samples of limestone (0.33 and 0.41% absorption), gravel (1.07% absorption), and artificial lightweight aggregate (27.20% absorption). Values of the aggregate modulus of elasticity were not reported. The concrete mixtures were cast with a 0.50 w/c ratio and contained 29.4% cement paste. A polycarboxylic-based superplasticizer was added to each mixture to maintain the slump between 165 and 195 mm (6.5 and 7.75 in.).

Imamoto and Arai (2006) used free-shrinkage specimens [$100 \times 100 \times 400$ mm ($4 \times 4 \times 15\frac{3}{4}$ in.)] that were cured in water for 7 days and then dried at 20° C

(68° F) and 60% relative humidity. The drying shrinkage at one year ranged from 700 to greater than 1000 $\mu\epsilon$. Concrete made using the hardened sandstone (0.96% absorption) had the most shrinkage followed by concrete made with artificial lightweight aggregate (27.20% absorption), gravel (1.07% absorption), hardened sandstone (0.73% absorption), limestone (0.33% absorption), and finally the least with limestone (0.41%). With the exception of the artificial lightweight aggregate, concrete made using hardened sandstone or gravel exhibited the most shrinkage, and concrete made using limestone exhibited the least shrinkage. When drying shrinkage was compared with the specific surface area of all the coarse aggregate types, however, a strong correlation was observed with all aggregate types. The authors reasoned that changes in the surface energy due to drying resulted in aggregate shrinkage and that the specific surface area was directly related to the surface energy. This may explain why concrete containing the artificial lightweight aggregate with a high absorption (27.2%) but relatively low specific surface area did not have the highest shrinkage. Another explanation for the reduction in shrinkage that the authors did not address is the ability of the porous aggregate to absorb water and provide internal curing to the concrete. Thus, the lightweight aggregate acted as a water reservoir and supplied water for extended internal curing.

Collins and Sanjayan (1999) studied the influence of a saturated porous coarse aggregate on the drying shrinkage of alkali-activated slag (AAS) concrete. A powdered sodium silicate activator and gypsum were added to slag cement. The study included three concrete mixtures containing a 0, 50, or 100% replacement of portland cement with AAS by weight that were cast with a 0.50 *w/c* ratio and contained 29.4, 29.9, and 30.4% cement paste. The concrete mixtures cast with 0 and 50% AAS were cast with a basalt coarse aggregate (1.2% absorption and 2.95 specific gravity) and the mixture containing 100% AAS was cast with a blast furnace slag (BFS) coarse aggregate (4.4% absorption and 2.71 specific gravity). All

aggregate was prepared and cast in the saturated-surface dry condition. The free-shrinkage specimens, produced in triplicate, were $75 \times 75 \times 285$ mm ($3 \times 3 \times 11.2$ in.) prisms. Three sets of specimens were cast for each series, with each set subjected to different exposure conditions. The types of exposure included drying [23° C (73° F) and 50% relative humidity] after one day of curing in lime-saturated water, sealed, and cured in lime-saturated water for 7 days and then exposed to drying conditions. Shrinkage measurements were taken for 56 days.

Collins and Sanjayan (1999) found that concrete mixtures cured for 7 days containing basalt as the coarse aggregate cast without AAS had significantly less shrinkage than similar concrete containing 50% AAS at all ages. At 56 days, the shrinkage was approximately $400 \mu\epsilon$ for the control mixture (no AAS and basalt coarse aggregate) and $925 \mu\epsilon$ for the 50% AAS mixture. The shrinkage of the concrete mixture cast with 100% AAS containing saturated BFS was slightly higher than the control mixture ($450 \mu\epsilon$ at 56 days). A similar trend was observed for specimens subjected to drying conditions after only one day of curing. At 56 days, the shrinkage was $1000 \mu\epsilon$ for the 50% AAS mixture, $575 \mu\epsilon$ for the 100% AAS mixture, and $450 \mu\epsilon$ for the control mixture. The final set of sealed specimens showed much less shrinkage since moisture loss to the environment was eliminated. In this case, the two mixtures containing AAS had similar shrinkage (approximately $575 \mu\epsilon$ at 56 days), while the control mixture had the least amount of shrinkage ($275 \mu\epsilon$). While not representing a full factorial test, these results suggest that gradually released internal curing water provided by the saturated BFS during drying can lead to a significant reduction in shrinkage. The importance of curing as it pertains to mineral admixtures is discussed in Section 1.7.3.4.

1.7.3.3 Effect of Aggregate Size, Gradation, and Shape

The volume of aggregate in a concrete mixture is the most important factor affecting potential shrinkage, but aggregate shape and gradation do not directly have

any effect (Alexander 1964). For practical purposes, however, these latter characteristics effect shrinkage by influencing the volume of paste required for concrete cohesiveness, workability, and finishability. As the maximum aggregate size is increased, a higher aggregate volume may be incorporated into the mixture for a given level of workability. These particles require less cement paste to coat the surface due to the reduced surface area-to-volume ratio of the larger particles. Likewise, an optimized aggregate gradation (described in Section 1.6) requires less cement paste than a gap-graded aggregate, and round aggregate, as opposed to angular aggregate, will result in a lower cement paste demand for a given level of workability.

Ibragimov (1989) evaluated the effect of the maximum aggregate size on concrete properties. The author found that as the maximum aggregate size increased from 40 to 80 mm (1.6 to 3.1 in.), the paste content, as a percentage of concrete volume, required to maintain a slump between 40 and 80 mm (1.6 to 3.1 in.) decreased by an average of 2.1% for concretes with a w/c ratio between 0.40 and 0.68. Cramer, Hall, and Parry (1999) compared differences in performance for concrete mixtures containing gap-graded aggregates and those with optimized gradations. The optimized gradations were obtained using the Modified Coarseness Factor Chart. The evaluation showed that optimized mixtures required up to 15% less water to attain the same workability, resulting in an increase in strength of between 10 to 20%. The authors also found that optimized mixtures segregated less during extended vibration.

1.7.3.4 Effect of Mineral Admixtures

Many different types of mineral admixtures are available to improve the properties of plastic and hardened concrete. Metakaolin and rice husk ash are being used with more frequency, but silica fume, fly ash, and slag cement (ground granulated blast furnace slag) are currently the most frequently and widely available

mineral admixtures. The effect of these mineral admixtures on free shrinkage is not fully understood, and research in this area has produced mixed results. Several research programs are next examined to determine the effects that silica fume, fly ash, and slag cement have on free shrinkage.

Silica fume has been used successfully in concrete, primarily to reduce permeability and to increase early and long-term compressive strengths. Deshpande et al. (2007) examined concrete with 0 and 10% replacements of cement with silica fume. Replacements were made on a volume basis (30 cement paste for all batches), and as a result, the w/cm ratio increased from 0.45 for the control mixes to 0.47 for the silica fume batches due to the lower specific gravity of the silica fume. In addition to comparing mixtures that were cast with different w/cm ratios, specimens were only cured for three days, the slump was not monitored, and the mixtures containing dry-densified silica fume were mixed by hand prior to casting, in all likelihood resulting in a non-uniform distribution of silica fume. The results indicated a slight tendency towards decreased shrinkage with the use of silica fume, although these results were not always consistent and more testing was recommended.

In a study completed in 1998, Whiting and Detwiler examined silica fume for use in concrete bridge decks. Two primary mixes were developed: an “overlay” mix and a “full-depth” mix. Mixtures for each of these applications were made with a number of silica fume contents and w/cm ratios. Both the full-depth and overlay mixes were tested for drying shrinkage and their ability to resist chloride ingress.

Cracking tendency and drying shrinkage were used to evaluate full-depth mixes with a cementitious material content of approximately 370 kg/m^3 (620 lb/yd^3) and overlay mixes with a cementitious material content of approximately 415 kg/m^3 (700 lb/yd^3). The w/cm ratio varied from 0.35 to 0.45 for full-depth mixes and from 0.30 to 0.40 for overlay mixes. The silica fume content varied from 0 to 12% by

mass of total cementitious material. The slump for both mixtures was greater than 75 mm (3 in.), obtained through the use of a high-range water reducer, and the air contents of full-depth and overlay mixes were $6\% \pm 1.5\%$ and $7.5\% \pm 1.5\%$, respectively. Unrestrained drying shrinkage (free shrinkage) specimens were $75 \times 75 \times 254$ mm ($3 \times 3 \times 10$ in.); restrained ring test specimens, developed by Krauss and Rogalla (1996), measured 150 mm (5.9 in.) high and 75 mm (3 in.) thick and were cast around a 19 mm (0.75 in.) thick steel ring with an outside diameter of 300 mm (11.8 in.). Before testing began, the specimens made from the full-depth mix and the specimens made with the overlay mix were cured in lime-saturated water for 7 and 3 days, respectively. These curing times were selected to simulate typical best practices for full-depth decks and deck overlays. Following the curing period, the specimens were stored at 23°C (73°F) with 50% relative humidity.

The drying shrinkage results, measured over a period of 64 weeks, indicated that both the overlay and full-depth mixes with the lower w/cm ratios (and lower paste contents) exhibited the least shrinkage. Drying shrinkage for the overlay mixes was generally larger, even with the lower w/cm ratios, presumably due to higher paste contents, shorter moist curing periods, and autogenous shrinkage. The drying shrinkage of mixtures containing approximately 6 to 12% silica fume increased significantly as the w/cm ratio (and paste content) increased. For a fixed w/cm ratio, the researchers found that total shrinkage increased with increases in silica fume content, primarily at the extremes of the w/cm ratio range (0.35 and 0.45 for full-depth mixes and 0.30 and 0.40 for overlay mixes). Mixes with w/cm ratios near the median (0.40 for full-depth mixes and 0.35 for overlay mixes) exhibited virtually no change in long-term drying shrinkage as the silica fume content increased, even to 12%. The authors offered no explanation for the insensitivity to silica fume content for the median w/cm ratio mixes. The tests indicated that during the early stages of

drying (four days), the rate of shrinkage increased significantly as silica fume contents increased for all w/cm ratios.

The results of the restrained shrinkage tests, reported in terms of time-to-cracking, revealed that cracking tendency was highly dependent on the length of the curing period. Curing periods of 1 and 7 days were used for the full-depth mixes to determine the effect of curing on cracking tendency. An increased quantity of silica fume was found to increase cracking when the concrete was cured for only 1 day, while, that same amount of silica fume had little effect on cracking when the concrete was moist cured for 7 days. Additionally, the mixes that contained higher cementitious material contents were found to have an increased tendency to crack, although the increase was not as great as that resulting from a decrease in the curing period from 7 to 1 day.

Based on all aspects of the study, the authors recommended a silica fume content of between 6 and 8% by mass of cementitious materials. Additional silica fume did not provide significant additional protection to the reinforcing steel given the high cost. The authors also recommended a moist curing period of at least seven days to limit both free shrinkage and cracking tendency.

Ding and Li (2002) also examined the effect of silica fume on restrained and unrestrained shrinkage. The authors examined three replacements of portland cement with silica fume (0, 5, 10, and 15% by weight) at a constant w/cm ratio of 0.35. The paste content increased from 30.9 to 31.5% as the silica fume replacement was increased from 0 to 15% of total cementitious material. For the shrinkage tests, concrete rings [35 mm (1.4 in.) thick, 140 mm (5.5 in.) in height, and an outside diameter of 305 mm (12.0 in.)] were cast around 25 mm (1.0 in.) thick steel rings for the restrained test and removable forms for the unrestrained test. The specimens were cured for one day and then stored at 23° C (73° F) with 40% relative humidity. Only drying from the outer circumferential surface was permitted, and all other surfaces

were sealed with an epoxy resin. Measurements were taken with a dial-gage extensometer mounted along the top of the specimens in the circumferential direction.

The researchers found that as the silica fume content increased from 0 to 15%, drying shrinkage decreased by 33% at 28 days. This conflicts with the results obtained by Whiting and Detwiler (1998) who reported a significant increase in early-age shrinkage with the addition of silica fume. While Ding and Li (2002) reported a reduction in free-shrinkage, restrained shrinkage specimens cast with silica fume cracked earlier than the control mixture containing only portland cement. This matches the results of Whiting and Detwiler (1998) who found that specimens containing silica fume cracked earlier than the control specimens when cured for only one day, highlighting the importance of longer curing periods for concrete mixtures containing mineral admixtures.

Fly ash has long been used in concrete, primarily to reduce cost and reduce concrete permeability, and to help control maximum concrete temperatures. There are different opinions, however, concerning the effect of fly ash on drying shrinkage. Atiş (2003) completed a study to evaluate the strength and shrinkage of high-volume fly ash (HVFA) concrete containing a 50 or 70% weight replacement of portland cement with Class F fly ash (ASTM C 618). A control mixture without fly ash and two HVFA mixtures were developed with zero slump to obtain maximum compactability using the vibrating slump test (Cabrera and Atiş 1999). These batches were then repeated and made flowable using a carboxylic superplasticizer until a spread of between 560 and 600 mm (22.0 and 23.6 in.) was obtained. Due to the compactability optimization and differences in specific gravities of the cementitious materials, w/cm ratios ranged from between 0.28 and 0.34 and paste contents ranged from between 25.5 and 27.9%. Free-shrinkage specimens were produced in duplicate and measured $50 \times 50 \times 200$ mm ($2 \times 2 \times 7.9$ in.). Specimens were demolded after

one day and then stored at 20° C (68° F) and 65% relative humidity. Shrinkage was measured using a mechanical dial gage, and the tests continued for six months.

Atiş (2003) observed significantly lower shrinkage for the HVFA concrete than for the control mixture at all ages. For the mixtures cast without a superplasticizer, the 28-day shrinkage was the lowest, 163 and 169 $\mu\epsilon$, for concretes containing 70 and 50% fly ash, respectively, while the highest shrinkage (265 $\mu\epsilon$) was observed for the control mixture. At an age of six months, drying shrinkage increased to 263, 294, and 385 $\mu\epsilon$ for the mixtures containing 70, 50, and 0% fly ash, respectively. Atiş concluded that an increase in fly ash resulted in decreased shrinkage, although other mix design factors that were not considered may have affected the results. For example, the w/cm ratios ranged from 0.29 for the 70% fly ash mixture up to 0.32 for the control mixture and less superplasticizer was needed for mixtures containing fly ash. For the flowable mixtures cast with a superplasticizer, shrinkage increased by approximately 50% at all ages compared to the mixtures cast with zero slump. It should be noted that a direct comparison is not possible because the zero slump control and 50% fly ash mixtures had slightly lower w/cm ratios (0.32 and 0.30 compared to 0.34 and 0.33) and paste contents (25.5 and 26.7% compared to 26.3 and 27.9%) than the superplasticized mixtures. The zero slump 70% fly ash mixture had a slightly higher w/cm ratio (0.29 compared to 0.28) and paste content (27.1 compared to 26.3%) than the superplasticized mixture. Atiş (1999) reported that the compressive and tensile strengths for HVFA concrete mixtures were similar or slightly higher than the control (all portland cement) concretes, although the comparison did not take into account the considerable variation in w/cm ratios.

Deshpande et al. (2007) examined concrete with and without a 30% replacement of cement with Class C fly ash (ASTM C 618). These replacements were made on a volume basis while holding the aggregate and water contents

constant, and as a result, the w/cm ratio increased from 0.45 for the portland cement only control mixes to 0.47 for the fly ash batches due to difference in the specific gravity of the two materials. The paste volume was maintained at 30%. Three free-shrinkage specimens were cast for each batch, and cured for three days in lime-saturated water, and then stored at 23° C (73° F) and 50% relative humidity for one year. Two sets of specimens were cast using the same fly ash and source of cement. For both sets, the addition of fly ash to concrete mixtures increased shrinkage at all ages. During the first 30 days, the difference between the fly ash and the control mixture was 34 $\mu\epsilon$ for the first set and 54 $\mu\epsilon$ for the second set. At 180 days, the difference increased to 76 $\mu\epsilon$ for the first set and decreased slightly to 50 $\mu\epsilon$ for the second set. Deshpande et al. (2007) concluded that concrete containing Class C fly ash shrinks more than concrete containing only portland cement.

Symons and Fleming (1980) observed a decrease in shrinkage with a partial replacement of cement with Class F fly ash (ASTM C 618), although they used much higher paste contents and w/cm ratios than Atiş (1999). The work consisted of four test programs, each with a constant weight of cementitious materials. The first three programs were carried out on mixtures with cementitious material contents of 285, 345, and 405 kg/m^3 (480, 581, and 683 lb/yd^3). Drying shrinkage was measured for control mixtures with 100% ordinary portland cement and mixtures with a 20 or 30% replacement of cement with an equal weight of fly ash. The fourth program incorporated high-early strength portland cement and a total cementitious material content of 500 kg/m^3 (843 lb/yd^3). Drying shrinkage was measured for control mixtures and mixtures with a 25, 35, or 40% replacement of cement with an equal weight of fly ash. The mixtures were produced in triplicate with four 75 × 75 × 285 mm (3.0 × 3.0 × 11.2 in.) shrinkage prisms prepared for each batch (for a total of 12 shrinkage specimens for each mixture). The specimens were cured for three days and then stored at 23° C (75° F) and 50% relative humidity.

For each test program, Symons and Fleming (1980) designed and batched several mixtures for a range of slumps between 25 and 150 mm (1 and 5.9 in.) for each mixture and replacement of fly ash. The mixes did not contain a superplasticizer and the target slump was obtained by adjusting the water content, and consequently the w/cm ratio and paste content. The relatively high paste contents varied from 27.6 to 41.9%, and the w/cm ratios varied from 0.42 to 0.86. This test program allows for the determination of the effect of fly ash on workability, although the differences in the w/cm ratios and especially the paste contents clearly influence the free-shrinkage results. Based on the mixture design information and shrinkage data provided by Symons and Fleming (1980), it is possible to calculate the paste content for many of the batches reported.

The results for concrete cast with ordinary portland cement (presented in Fig. 1.10) indicate that the 56-day shrinkage increased as the paste content increased for mixtures both with and without fly ash. In all but one case, the addition of fly ash reduced the 56-day shrinkage for the range of paste contents examined, although no discernable difference is observed between mixtures containing a 20 or 30% replacement of cement with fly ash. When compared on an equal slump basis, the addition of 20% fly ash resulted in an average water reduction of 4.4% (1.1% reduction in paste) and the addition of 30% fly ash resulted in an average water reduction of 3.1% (0.8% reduction in paste) over the range of slumps examined.

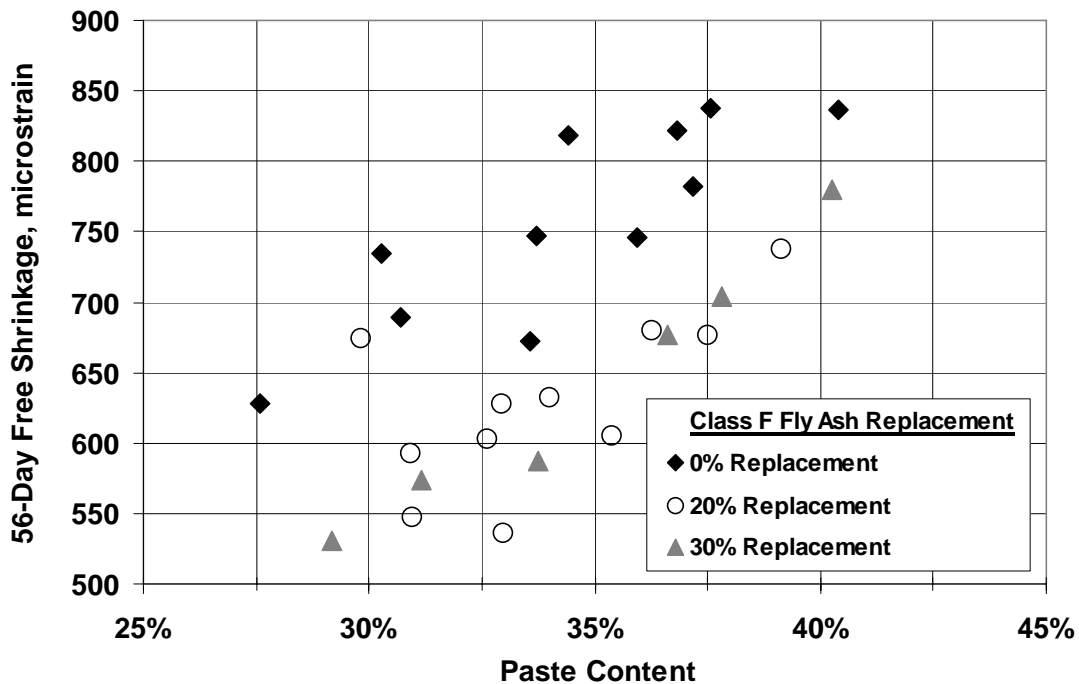


Fig. 1.10 – 56-Day free shrinkage plotted versus paste content (V_p) for three percentages of Class F fly ash [Based on data reported by Symons and Fleming (1980)].

Slag cement is used as a partial replacement for cement to improve durability, decrease cementitious material costs, and to reuse a waste material. Jardine and Wolhuter (1977) evaluated the shrinkage and creep characteristics of mortars containing between 50 and 80% slag by weight of cementitious materials. Three w/cm ratios (0.40, 0.50, and 0.60), three levels of slag replacement (50, 65, and 80%), and three paste contents (50, 40, and 30%) were evaluated in a full-factorial test program. Six $50 \times 50 \times 100$ mm ($2.0 \times 2.0 \times 3.9$ in.) shrinkage prisms with demountable mechanical gages placed on opposite faces were prepared for each of the 27 mortars examined. Following the 28-day curing period, the specimens were stored in humidity tents with a temperature of between 22° and 25° C (72° and 77° F). Half of the specimens were stored at a relative humidity of 60%, while the remaining specimens were stored at a relative humidity of 40%. Jardine and

Wolhuter (1977) reported the relative 98-day free shrinkage of the mixtures. The relative shrinkage was expressed as a percentage of the shrinkage of a mortar with the same w/c ratio and volumetric paste content cast without slag cement. With the addition of 50% slag, the relative shrinkage increased by 34% for a w/cm ratio of 0.40 and by 54% for w/cm ratios of 0.50 or 0.60. With the addition of 80% slag, the relative shrinkage increased by 66% for a 0.40 w/cm ratio and by 105% for w/cm ratios of 0.50 and 0.60 compared to the control specimens. The relative shrinkage was found to be independent of the relative humidity under which the specimens were stored.

The results obtained by Jardine and Wolhunter (1977) that indicate significantly increased shrinkage with the addition of slag are generally not supported by other researchers. Deshpande et al. (2007) examined concrete with and without a 30% volume replacement of cement with slag cement. Because the slag replacement was done on a volume basis, the w/cm ratio increased from 0.45 for the portland cement only control mixture to 0.47 for the batches containing slag. The paste volume was maintained at 30%. Three free-shrinkage specimens were cast for each batch and were cured for three days in lime-saturated water and then stored at 23° C (73° F) and 50% relative humidity for one year. Two sets of specimens were cast using the same slag cement. For both sets of specimens, the addition of slag to concrete mixtures slightly increased shrinkage up to an age of 180 days and then similar shrinkage was observed. After the first 30 days of drying, the shrinkage for the control mixture was 303 $\mu\epsilon$ compared to 333 $\mu\epsilon$ for the slag mixture. The difference between the slag and control mixture was smaller for the second set where the control mixture shrinkage was 293 $\mu\epsilon$ compared to 313 $\mu\epsilon$ for the slag mixture. After one year of drying, the relative shrinkage remained nearly the same for the first set (402 $\mu\epsilon$ for the control mixture and 435 $\mu\epsilon$ for the slag mixture), while the slag mixture for the second set exhibited slightly less shrinkage than the control mixture

(497 $\mu\epsilon$ compared to 503 $\mu\epsilon$). Deshpande et al. (2007) concluded that slag does not appear to affect ultimate shrinkage, although early-age shrinkage may be affected.

Tazawa, Yonekura, and Tanaka (1989) also reported that early-age drying shrinkage was increased while the ultimate shrinkage was reduced by the addition of slag as a partial replacement of cement. They evaluated the effect of slag content on drying shrinkage in addition to the influence of w/cm ratio, slag fineness, and the length of curing period. Slag was used at three levels of replacement: 0, 35, and 55% by weight. For slag replacements of 0 and 35%, the w/cm ratios examined were 0.51, 0.59, and 0.70. For the 55% slag mixtures, a w/cm ratio of 0.40 was also used. The water content was 190 kg/m^3 (320 lb/yd^3) for all of the mixtures, resulting in relatively high paste contents, ranging from 27.6 to 34.8%. Three slags with specific surface areas of 4410, 5680, and 7860 cm^2/g were used in the study. Free-shrinkage specimens measured 100 \times 100 \times 400 mm (3.9 \times 3.9 \times 15.7 in.). The specimens were cured for 7 or 28 days in water and then stored in air at 20° C (68° F) and 50% relative humidity. Shrinkage was measured using contact gages mounted at the ends of the specimens.

Tazawa et al. (1989) reported that drying shrinkage was reduced with an increase in the specific surface area of the slag and increased length of curing. The early-age drying shrinkage (through 28 days) of concrete containing slag was approximately equal to the early-age drying shrinkage of the control mixture, but the long-term shrinkage (300 days) was reduced with the addition of slag. The shrinkage reduction increased as the percentage of slag increased from 35 to 55% and as the curing period was increased from 7 to 28 days. The largest reduction in shrinkage occurred for specimens cured for only 7 days. The authors suggested that the decrease in shrinkage resulted from an increased compressive strength and stiffness of the cement-paste matrix.

Two mineral admixtures, such as slag and silica fume, in combination with portland cement (called *ternary mixtures*) are being used with increased regularity to take advantage of the benefits accorded by each admixture. Silica fume is often combined with slag or fly ash to increase the early age strength or to decrease permeability and to provide increased workability and cohesion. Slag and fly ash are generally used to reduce the heat of hydration and the rate of strength gain and to decrease permeability. Departments of Transportation in Iowa, Minnesota, Ohio, and Wisconsin use ternary systems regularly, and this practice appears to be becoming more common (ACI Committee 233 2003).

Khatri and Sirivivatnanon (1995) examined seven concrete mixtures with a w/cm ratio of 0.35 and a cementitious material content of 430 kg/m^3 (725 lb/yd^3) using different percentages of fly ash, slag, and silica fume. The mixtures included a control mix with portland cement only, and mixes with 10% silica fume cast with and without fly ash or slag. The fly ash mixtures contained a 15 or 25% replacement of cement by weight, and the slag mixtures contained a 35 or 65% replacement. Mixtures cast with mineral admixtures contained 1 to 1.6% more paste than the control mixture (28.3% paste) due to the lower mineral admixture specific gravities. The mixtures were cast without an air entraining agent and all contained a superplasticizer to achieve a slump in the range of 120 to 210 mm (4.7 to 8.3 in.). Free-shrinkage specimens were cast in triplicate and measured $75 \times 75 \times 285 \text{ mm}$ ($3.0 \times 3.0 \times 11.2 \text{ in.}$). The specimens were cured for 7 days in lime-saturated water and then stored in air at 23° C (73° F) and 50% relative humidity for the duration of the test.

The results indicate that the addition of silica fume increased early-age (28 days) shrinkage by approximately 8% compared to the control mix, although the long-term (365 days) shrinkage was reduced by an average of approximately 9%. For mixtures containing slag, drying shrinkage at all ages was higher than the control

mixture, although the addition of silica fume partially offset the increase in long-term shrinkage. The mixture containing 65% slag had only slightly higher shrinkage than the mixture containing 35% slag. The drying shrinkage of ternary systems containing fly ash and silica fume also showed higher drying shrinkage than the control mixture, and the amount of fly ash (15 or 25%) did not have an effect on the amount of shrinkage. As mentioned previously, the mixtures containing mineral admixtures had higher paste contents, which could have contributed to the increased shrinkage.

Saric-Coric and Aïtcin (2003) performed a study to determine the influence of curing conditions on ternary systems containing 20, 30, 50, or 80% slag and 5% silica fume by weight. The mixtures had a w/cm ratio of 0.35 and a cementitious material content of 450 kg/m^3 (758 lb/yd^3). A reference concrete, cast with 100% portland cement, was included for comparison. As with most of the studies examined, the concrete mixtures cast with mineral admixtures contained 1 to 1.6% more paste than the control mixture (28.3% paste). Free-shrinkage specimens were cast in triplicate and measured $100 \times 100 \times 400 \text{ mm}$ ($3.9 \times 3.9 \times 15.7 \text{ in.}$). The effect of three different curing methods on shrinkage was evaluated in the study. *Method 1* – The samples were placed under water at 22° C (72° F) three to four hours after casting and remained under water for 280 days. *Method 2* – The samples were sealed in plastic bags immediately after mixing and then wrapped in adhesive aluminum tape after demolding. These specimens were stored in air at 22° C (72° F) for 280 days. *Method 3* – The specimens were wet cured for seven days and then were sealed with aluminum tape for 21 days. At an age of 28 days, the tape was removed and the samples were stored in air at 22° C (72° F) and 50% relative humidity for one year.

The specimens cured continuously underwater (*Method 1*) swelled throughout the 280 days during which readings were taken. At an age of 280 days, concrete cast without slag swelled the most ($260 \mu\epsilon$), while concretes cast with slag swelled significantly less ($160 \mu\epsilon$). Most of the swelling occurred during the first 18 to 20

hours, and the 280-day swelling of concretes cast with slag was independent of the amount of slag. Specimens cured using *Method 2* were sealed and not allowed to absorb any water from an external source, and therefore were only subjected to autogenous shrinkage. The concrete containing 80% slag had the highest autogenous shrinkage at 280 days (360 $\mu\epsilon$), while the reference concrete cast without slag had the least shrinkage (110 $\mu\epsilon$). Concrete cast with 30 and 50% slag had autogenous shrinkage equal to 250 $\mu\epsilon$. The authors suggested that the increased autogenous shrinkage observed for slag-blended cement was a result of a much finer pore structure inherent to concrete containing slag. Specimens cured using *Method 3* were cured under water for 7 days and then sealed (allowing autogenous shrinkage only) for 21 days. Through 7 days of water curing, the swelling results were similar to those obtained in *Method 1*. The greatest swelling was observed for the reference concrete (100 $\mu\epsilon$ at 7 days); the concretes containing slag swelled less (between 56 and 62 $\mu\epsilon$). An additional set of specimens containing only 5% silica fume was added to this series to determine the effect of silica fume on swelling and autogenous shrinkage. After less than one day of underwater curing, the binary mixture containing 5% silica fume and no slag began to shrink, and after 7 days of water curing, the had a net shrinkage of 30 $\mu\epsilon$. After the initial underwater curing period, the specimens were sealed for 21 days and autogenous shrinkage developed at a nearly identical rate for all of the mixtures examined. Following the sealed curing period, the specimens were subjected to drying for one year. The highest total shrinkage at all ages was attained with the 5% silica fume mixture followed by the reference mixture. When the effect of swelling and autogenous shrinkage were removed leaving only drying shrinkage, the reference concrete had the greatest shrinkage, while the 5% silica fume reference mixture had the least shrinkage. The effect of slag content on the total shrinkage and drying shrinkage was small.

Saric-Coric and Aïtcin (2003) concluded that concrete containing only portland cement swelled as long as the specimen was underwater. Conversely, specimens containing 5% silica fume begin to shrink after only a few days. Ternary mixtures presented an intermediate behavior that resulted in slight swelling after 7 days. After the curing period, drying shrinkage was found to develop more rapidly in silica fume and plain portland cement concretes, although after one year of drying, the total shrinkage was nearly identical. Finally, the authors suggested that water curing should begin as soon as possible before initial setting to help reduce the development of autogenous shrinkage and, thus, total shrinkage.

1.7.3.5 Effect of Curing

The effect of curing on concrete shrinkage is often overlooked. In fact, in 1959 Powers stated that the length of curing period was a relatively unimportant factor affecting concrete volume changes. Powers suggested that a reduction in unhydrated cement particles, resulting from an increased curing period, will tend to increase shrinkage since unhydrated cement helps to restrain paste shrinkage. At the same time, Powers stated that this shrinkage is partially offset due to the formation of internal cracks that relieve compressive stresses around aggregate particles caused by prolonged curing. Typical bridge decks are rarely cured for more than seven days, and even in those cases the intent of “extending” the curing period is to increase compressive strength or reduce permeability.

Deshpande et al. (2007) examined the effect of curing on free-shrinkage specimens containing 100% Type I/II portland cement. The specimens were air-entrained (4.75 to 5.5% air) and had a *w/c* ratio of 0.45 and an aggregate content of 70%. The specimens were cured for 3, 7, 14, or 28 days. Free-shrinkage specimens produced in triplicate were 76 × 76 × 286 mm (3 × 3 × 11.25 in.), cured in lime-saturated water, and then stored at 23° C (73° F) and 50% relative humidity. Deshpande et al. (2007) observed a considerable decrease in shrinkage as the curing

period was increased from 3 to 28 days. After 30 days of drying, the largest reduction in shrinkage, from 500 to 367 $\mu\epsilon$, occurred as the curing period increased from 3 to 7 days. Shrinkage decreased from 367 to 343 and finally to 275 $\mu\epsilon$ as the curing period was increased from 7 to 14, and then again from 14 to 28 days. Considerable differences in shrinkage were also observed at the end of the drying period (300 days). Long-term shrinkage decreased from 695 to 519 $\mu\epsilon$ as the curing period was increased from 3 to 7 days and from 519 to 440 $\mu\epsilon$ as the curing period was increased from 7 to 28 days.

The results by Deshpande et al. (2007) indicate that the degree of hydration clearly influences shrinkage. As the curing period is increased, more water is chemically combined and unavailable to evaporate during drying. This appears to offset the effect of the reduction in pore size (and increase in capillary stresses) that accompanies an increase in the degree of hydration. Extending the curing period is especially important for mixtures containing mineral admixtures. Studies indicating a reduction in shrinkage with an increase in the curing period for mixtures containing silica fume, fly ash, and slag are presented in Section 1.7.3.4.

1.7.4 Summary of Previous Work

Bridge deck cracking is the result of a complex interaction of variables. Many studies of bridge deck cracking have been performed, although many questions regarding the causes of cracking remain. There is little question, however, that bridge deck cracking is a significant problem requiring continued attention. In Kansas, chloride concentrations taken at crack locations often exceed the corrosion threshold after the first winter. Conversely, chloride concentrations taken away from cracks rarely exceed the corrosion threshold. Based on this information, it is clear that attention should be focused on the development of materials and construction practices to minimize bridge deck cracking.

In an effort to characterize the primary factors contributing to bridge deck cracking, several field studies, beginning in the 1960s, have been performed to evaluate existing bridge decks. These evaluations have resulted in a number of observations and recommendations to minimize cracking. In general, factors that increase drying (or thermal) shrinkage or increase the degree of restraint also increase cracking. An increase in the volume of cement paste (cement and water), and the use of fine cements correlate with increased bridge deck cracking. Other material factors that have been found to increase cracking include low air contents (less than 6%), unnecessarily high compressive strengths, a high modulus of elasticity, low creep, and the addition of some mineral admixtures.

The importance of limiting drying shrinkage is well-understood, and as a result, many studies have been performed to determine the principal factors affecting drying shrinkage. Paste content is generally regarded as the primary factor. Similarly, individual increases in the cement content or water content also result in an increase in shrinkage. Most studies indicate that an increase in the w/c ratio results in only a small increase in shrinkage. Given the importance of paste content, it comes as no surprise that aggregate properties also play an important role in shrinkage and cracking. Stiff aggregates tend to provide more restraint to the shrinking paste. Lower stiffness, saturated porous aggregates, however, provide an internal supply of water for curing, which will reduce shrinkage at early ages. While some researchers dismiss the influence of curing on free shrinkage, most studies have found that increased curing results in reduced concrete shrinkage. This is especially true for mixtures containing mineral admixtures that react more slowly than mixes containing only portland cement. The effect of mineral admixtures on shrinkage (aside from curing conditions) is not well understood, and many opinions exist regarding their use in bridge decks. An in-depth examination is provided as a part of this study.

1.8 OBJECTIVE AND SCOPE

Bridge deck cracking is a well-documented and well-studied problem, and while there is much agreement on practices that contribute to cracking, there are still many questions that exist, especially with regard to the implementation of techniques to reduce cracking in the field. This study bridges that gap through the development and implementation of techniques to construct low-cracking high-performance concrete (LC-HPC) bridge decks.

This objective will be achieved by:

1. Evaluating the effect of aggregate type, length of curing period, binary and ternary mixtures, cement type, cement fineness, paste content, w/cm ratio, and shrinkage reducing admixtures on the free-shrinkage characteristics of concrete mixtures in the laboratory using the “Standard Test Method for Length Change of Hardened Hydraulic Cement Mortar and Concrete,” ASTM C 157.
2. Developing an aggregate optimization and mix design procedure and implementing that procedure using Microsoft Excel and Visual Basic for Applications to help ensure that ready mix suppliers and transportation officials have the technical tools necessary to produce LC-HPC using a clearly defined and proven process.
3. Evaluating LC-HPC candidate mixtures for cohesiveness, workability, finishability, and pumpability in both the laboratory and the field. This includes the development of LC-HPC specifications, in addition to working with contractors, ready-mix suppliers, and transportation officials to ensure successful construction of LC-HPC bridge decks.
4. Evaluating the performance of bridge decks constructed with LC-HPC by performing crack surveys of the deck surface.

CHAPTER 2: EXPERIMENTAL PROGRAM

2.1 GENERAL

The experimental program described in this chapter involves both laboratory and field work. The laboratory work consisted of six free shrinkage test programs, involving 56 individual concrete batches, to measure free shrinkage and gage relative performance as a function of paste content, water-cementitious material (w/cm) ratio, aggregate type, mineral admixture content, cement type and fineness, the use of shrinkage reducing admixture, and the duration of curing. With the exception of one batch in Program II, three shrinkage specimens were cured in lime-saturated water for 7 days and three for 14 days for each batch. Following the curing period, specimens were moved to a controlled drying environment and measurements were taken over a period of one year in accordance with ASTM C 157.

The field work involved the construction and evaluation of 14 low-cracking high-performance concrete (LC-HPC) bridge decks. The selection of these decks, development of specifications and LC-HPC, construction experiences, and their performance, measured in terms of linear meters of crack per square meter (crack density) of bridge deck, is covered in Chapter 5. The crack survey procedure and the procedure to calculate the crack density of a bridge deck is covered next in Sections 2.3 and 2.4.

2.2 CRACK SURVEY PROCEDURE

An on-site survey was performed for each of the LC-HPC and control bridge decks approximately every 6 to 18 months. Prior to arriving at a bridge, a plan drawing of the bridge deck, including all boundary areas, was made at a scale of 1 inch equals 10 feet (the required scale for the image analysis programs). Several guidelines were followed for each survey with the intent of minimizing any

differences that may result from changing personnel. Three to six inspectors performed each survey on days that were at least partly sunny with a minimum temperature of 16° C (60° F). In addition, the entire deck surface was required to be completely dry before beginning the survey. Traffic control was maintained to ensure that at least one lane was clear of traffic and available to the surveyors. Prior to identifying and marking cracks, a 5 × 5 ft (1.52 × 1.52 m) grid was marked on the available surface of the deck. Inspectors then began to mark cracks that were visible while bending at the waist. Once a crack was identified, the entire crack was marked, even if parts of the crack were not initially visible while bending at the waist. The cracks were marked with lumber crayons and then transferred to the scale drawing using the grids on the deck and the drawing as a guide. Lindquist, Darwin, and Browning (2005) provide a draft specification describing the crack survey techniques.

2.3 CRACK DENSITY DETERMINATION

The crack density, in linear meters of crack per square meter of bridge deck, was determined directly from field surveys. To do this, several steps were required to prepare the field crack maps for crack analysis. The first step was to digitally scan the crack maps at 100 dots per inch (dpi) as grayscale tagged image file format (TIFF) files with 256 shades of gray. Since the ultimate goal was to calculate crack lengths from scaled drawings, it was important that the crack map scale and scanned image resolution be exactly 1 in. equals 10 ft and 100 dpi, respectively. Equally as important, if the crack map included more than one page (which was often the case), the individual scanned files were combined into one TIFF image of the entire uninterrupted bridge deck surface; every effort was made to accurately align the images. A black line one pixel in width was added from the top edge of the image down to the top left corner of the bridge deck. This line indicated the starting point for the program to begin looking for cracks. All other boundary lines and other markings or notes that did not represent cracks were removed from the image to

ensure that extraneous lines were not counted as cracks. Finally, any cracks that bent by more than 15° or that intersected other cracks were separated into single straight lines by converting a “dark” pixel to a white pixel at the intersection or bend. This ensures that the program accurately calculates the straight-line distance between crack end points. The file was then saved as an uncompressed TIFF image.

The TIFF images were then converted to ASCII files containing image data using two programs created at the Information and Telecommunication Technology Center at the University of Kansas. These programs are available on UNIX platforms and are used to create an ASCII file with the gray-scale color of each pixel recorded as a number between zero and 255 (zero for black and 255 for white). After removing unrelated header and footer information from the beginning and end of each ASCII file, the files were ready for analysis. In three previous studies, Schmitt and Darwin (1995), Miller and Darwin (2000), and Lindquist, Darwin, and Browning (2005) used a FORTRAN program to calculate crack lengths from the ASCII file. The FORTRAN program groups “dark” pixels together and, by finding the end points of the groups, calculates the distance between those points.

Any pixels that were darker than a gray level of 200 were classified as “dark” and were assumed to represent part of a crack. These “dark” pixels were grouped together and the straight-line distance between the end points was calculated. Finally, the crack density was calculated as the sum of all crack lengths (m) divided by the appropriate deck surface area (m^2). In addition, it was also possible to calculate the total length of cracks with a specified angle or within a specified range of angles. A listing of the current crack measurement program is provided by Lindquist, Darwin, and Browning (2005).

2.4 LABORATORY WORK

The free-shrinkage test, performed in accordance with ASTM C 157, provides a relatively simple and quick method to determine both long and short-term free

shrinkage of concrete prisms. The test specimens, free-shrinkage measurements and data collection, specimen casting procedure, curing, and drying environment are described in the following sections. Concrete mixture proportioning and mixing procedures are described in Sections 2.7 and 2.8, respectively.

In addition to ASTM C 157 free-shrinkage specimens, a minimum of two 100 × 200 mm (4 × 8 in.) cylinders were cast and tested for compressive strength in accordance with ASTM C 39. The cylinder curing regime, number of cylinders tested and the age of the cylinder at the time of testing is provided in Sections 2.9.1 through 2.9.6, and the results are provided in Appendix A.

2.4.1 ASTM C 157 Free-Shrinkage Specimens

The free-shrinkage specimens were cast in cold-rolled steel molds purchased from Humboldt Manufacturing Co. (Fig. 2.1). The molds produced 76 × 76 × 286 mm (3 × 3 × 11¼ in.) prisms, as specified in ASTM C 157. Gage studs were embedded in both ends of the prism providing a gage length of 254 mm (10 in.) (Fig. 2.2).

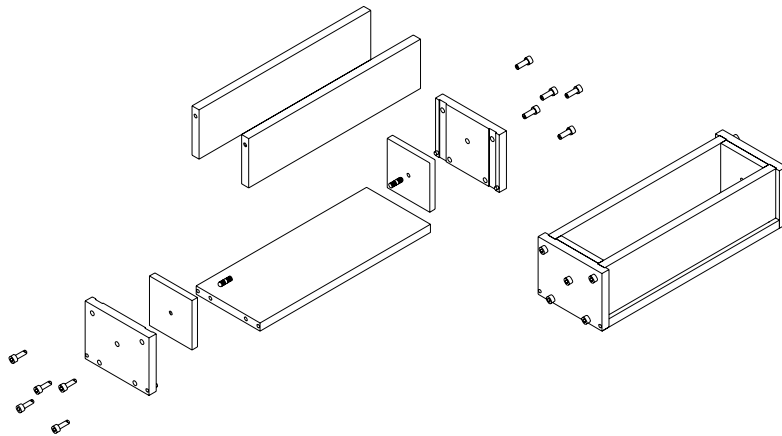


Fig. 2.1 – Free Shrinkage Molds (Tritsch 2005)

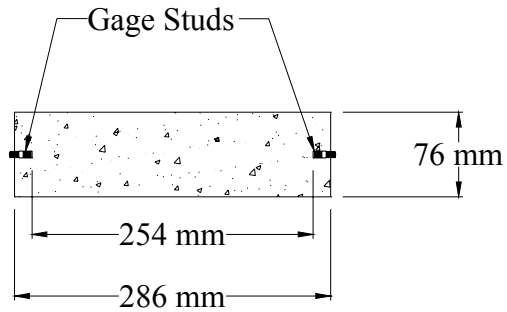


Fig. 2.2 – Free Shrinkage Specimens (Tritsch 2005)

2.4.2 Free-Shrinkage Measurements and Data Collection

Free-shrinkage measurements were made with a mechanical dial gage length comparator from Humboldt Manufacturing Co. with a least count of 0.00254 mm (0.0001 in.) and a total range of 10 mm (0.4 in.). The length comparator was zeroed prior to taking free-shrinkage readings using a calibration bar in accordance with ASTM C 157. A measurement of the calibration bar with the length comparator was taken daily and used to establish a reference reading. Subsequent reference readings were taken after every nine individual specimen readings. Care was taken to ensure that both the specimens and the calibration bar were always oriented in the same position. Readings were taken by slowly spinning the calibration bar or specimens in the clockwise direction and recording the minimum value indicated on the length comparator.

The initial comparator reading difference (CRD), calculated as the difference between the comparator reading of a specimen and the calibration bar, was recorded immediately after demolding ($23\frac{1}{2} \pm \frac{1}{2}$ hours after casting). The cumulative change in length for each specimen on any day thereafter was calculated by subtracting the initial CRD from the daily CRD. The shrinkage strains, reported in microstrain, were calculated by dividing the change in length by the gage length [254 mm (10 in.)]. The strains reported in Chapter 4 represent the average of three specimens.

Specimen readings were taken more frequently than prescribed by ASTM C 157, which only requires eight readings over a period of 64 weeks (448 days). After the specified curing period (7 or 14 days for specimens in this study), readings were taken daily for the first 30 days of drying. Following the first 30 days, readings were taken every other day between 30 and 90 days, once a week between 90 and 180 days, and once a month between 180 and 365 days. The specimens were discarded after 365 days of drying.

2.4.3 Casting

Specimens were cast immediately following completion of slump and air content tests. The molds were coated with mineral oil just prior to casting the specimens. The concrete was placed in the molds in two layers of approximately equal depth and consolidated on a vibrating table with an amplitude of 0.15 mm (0.006 in.) and a frequency of 60 Hz for 20 to 30 seconds per layer. The upper surface of the specimens was struck off using a 50 × 135 mm (2 × 5½ in.) steel strike-off screed. Following consolidation, the specimen molds were cleaned and moved to the lab floor for initial curing. In most cases, six specimens were cast simultaneously (three cured for seven days and three cured for fourteen days).

2.4.4 Curing

Initial curing, performed next to the vibrating table, consisted of covering the top surface of each specimen with 152 µm (6 mil) Marlex[®] strips. The top and sides of each mold were covered with 89 µm (3.5 mil) plastic sheets secured by rubber bands. The specimens were grouped into sets of three and covered again with a 12.7 mm (½ in.) thick piece of Plexiglas[®] held in place with four 152 × 305 mm (6 × 12 in.) concrete cylinders. The specimens were demolded 23½ ± ½ hours (in accordance with ASTM C 157) and immediately wrapped with water-saturated towels to prevent moisture loss. Initial shrinkage measurements (to determine the initial comparator

reading difference) were taken immediately and then the specimens were cured in lime-saturated water prepared in accordance with ASTM C 511. The specimens remained in the lime tank for a period of 6 or 13 days (making the total curing period 7 or 14 days). Following this curing period, the specimens were removed from the lime tank, measured, and placed into an environmental room for drying (described in Section 2.5.5).

2.4.5 Drying

The free shrinkage specimens were placed in a $3.7 \times 3.7 \times 2.1$ m ($12 \times 12 \times 6.8$ ft) environmental room fabricated with structural lumber and $89 \mu\text{m}$ (3.5 mil) plastic sheeting. This room was located in a larger temperature and humidity controlled laboratory and maintained at $23^\circ \pm 2^\circ$ C ($73^\circ \pm 3^\circ$ F) and $50\% \pm 4\%$ relative humidity. Seasonal temperature and humidity variations in the laboratory were compensated in the environmental room with a humidifier (primarily used during the winter) and a dehumidifier (primarily used during the summer). The specimens were stored on wooden racks and allowed to dry on all sides with a minimum clearance of 25 mm (1 in.) to allow proper air circulation. The specimens were not removed from the environmental room during the 365 day drying period.

2.5 MATERIALS

The test programs reported in this study were cast over a nearly two-year period. In many cases, no change in the material source was reported, but the physical or chemical properties did change frequently. Each time a new sample of cement was obtained, even if it was from a previously used source, a new chemical analysis was performed. Similarly, sieve analyses and specific gravity tests were performed each time a sample of aggregate was obtained. The following sections describe the different types and samples of cement, fine aggregate, coarse aggregate, and mineral admixtures used in this study.

2.5.1 Cement

Three types of cement were used in this study: Type I/II (meets the specification for ASTM C 150 Type I normal portland cement and Type II modified portland cement), coarse-ground Type II, and Type III portland cements. The Type I/II portland cement used in this study was obtained in five samples over a period of nearly two years. The cement was produced by Ashgrove in Chanute, KS and had a specific gravity of either 3.15 or 3.20. The Blaine fineness varied from 360 to 380 m²/kg, with an average fineness of 372 m²/kg. The coarse-ground Type II portland cement was obtained in two different samples both produced by Lafarge North America in Seattle, WA. The Type II cement also had a specific gravity of 3.15 or 3.20 and an average Blaine fineness of 330 m²/kg. The Type III cement, produced by Lone Star Industries (now Buzzi Unicem) in Greencastle, IN, had a Blaine fineness of 549 m²/kg and a specific gravity of 3.15. The Bogue composition, Blaine fineness, and specific gravity for the eight cement samples are given in Table 2.1. The chemical composition of each sample, along with the individual concrete batches containing those samples, is provided in Table A.1.

Table 2.1 – Portland Cement Characteristics

	Percentages								
	Portland Cement Type								
	I/II					II			III
Sample No.	1	2	3	4	5	1(a)	1(b)	2	1
C₃S	53	52	53	37	47	65	61	61	42
C₂S	21	22	20	34	24	11	13	15	27
C₃A	7	6	7	7	7	7	7	6	10
C₄AF	10	11	11	10	10	11	11	11	7
Blaine (m²/kg)	367	380	379	360	373	335	333	323	549
Specific Gravity (SSD)	3.15	3.15	3.20	3.20	3.20	3.15	3.15	3.20	3.15

2.5.2 Fine Aggregate

Kansas River sand from the Victory Sand and Gravel Company in Topeka, KS was used in all mixtures as the fine aggregate. The specific gravity [saturated surface dry (SSD)] was 2.63 and the absorption (dry) was 0.35%. Pea gravel (a coarse sand) was used to fill in the middle sieve sizes [4.75-mm (No. 4) and 2.36-mm (No. 8) sieves] and ensure that the combined aggregate gradation was optimized. The pea gravel was Kansas Department of Transportation (KDOT) classification UD-1 obtained from Midwest Concrete Materials in Manhattan, KS. The pea gravel used in this study had the same maximum size as the Kansas River sand [4.75-mm (No. 4)], but the pea gravel contained a larger quantity of coarse particles. The specific gravity (SSD) was 2.62 and the absorption (dry) was 0.70%.

Five different samples of Kansas River sand and pea gravel (each with a different gradation) were used for the six free-shrinkage test programs. The combined gradations were adjusted for each batch depending on the individual gradations to provide an optimum combined gradation as defined in Chapter 3. The individual aggregate gradations, along with the concrete batches that contain those aggregates, are provided in Table A.2.

2.5.3 Coarse Aggregate

Three coarse aggregates, all with a maximum size of 19 mm ($\frac{3}{4}$ in.), were evaluated. The coarse aggregates included granite, limestone, and quartzite. The granite had a specific gravity (SSD) of 2.63 and an absorption (dry) of 0.56% and was obtained from Granite Mountain Quarries in Little Rock, AR. The limestone had a specific gravity (SSD) of 2.57 and an absorption (dry) between 2.5 and 3.0% and was obtained from Hunts Midwest Mining in De Soto, KS. The quartzite had a specific gravity (SSD) of 2.64 and an absorption (dry) of 0.44% and was obtained from L. G. Everist Inc. in Dell Rapids, SD.

To obtain an optimized combined gradation, all three of the coarse aggregates were divided on the 9.5-mm ($\frac{3}{8}$ -in.) sieve and recombined during the mixing. Two samples of granite, six samples of limestone, and one sample of quartzite were used for the six test programs. The first limestone sample was the only coarse aggregate sample that was not split using the 9.5-mm ($\frac{3}{8}$ -in.). The individual aggregate gradations (including the gradations for the split aggregates) and the batches that contain those particular gradations are provided in Table A.2.

2.5.4 Mineral Admixtures

Five types of mineral admixture were used as a partial replacement of portland cement in Program VI, Sets 1 through 10, three Class F fly ashes, two Grade 120 (G120) and three Grade 100 (G100) slag cements (labeled 1 through 5), and two silica fumes. Class F fly ash No. 1 (Coal Creek fly ash) from Headwaters Resources in Underwood, ND had a specific gravity of 2.55. Class F fly ash No. 2 from Lafarge North America in Chicago, IL had a specific gravity of 2.40. Class F fly ash No. 3 (trade name Durapoz[®] F) from Ashgrove in Louisville, NE had a specific gravity of 2.87. Ashgrove adds gypsum (SO_3) to Durapoz[®] F in an effort to limit shrinkage. The measured SO_3 content of the three Class F fly ashes was 0.66, 0.25, and 2.83% for samples 1, 2, and 3, respectively. The G100 slag cement (trade name GranCem[®]) had a specific gravity of 2.86 and was obtained from Holcim in Theodore, AL (samples 1 and 3) and Chicago, IL (sample 2). The G120 slag cement (trade name NewCem[®]) had a specific gravity of 2.90 and was obtained from Lafarge in Chicago, IL. Densified silica fume was obtained from W.R. Grace (trade name Force 10,000[®] D) and Euclid (trade name Eucon MSA), and both samples had a specific gravity of 2.20. The mineral admixtures used in this study are summarized in Table 2.2.

Table 2.2 – Mineral admixtures used in Program VI Sets 1 through 10

Material	Sample Number(s)	Producer	Trade Name	Specific Gravity
Class F Fly Ash	1	Headwaters	Coal Creek	2.55
	2	Lafarge	--	2.40
	3	Ashgrove	Durapoz [®] F	2.87
Grade 120 Slag Cement	1, 2	Lafarge	NewCem [®]	2.90
Grade 100 Slag Cement	3, 4, 5	Holcim	GranCem [®]	2.86
Densified Silica Fume	1	W.R. Grace	Force 10,000 [®] D	2.20
	2	Euclid	Eucon MSA	2.20

2.6 MIX PROPORTIONING

The mixture designs presented in this study have two primary goals: To facilitate the determination of the effect that different variables have on concrete shrinkage, but also, to develop mixtures that, at least in the laboratory, appear suitable for use in the field. Careful consideration was given to the cohesiveness, workability, finishability, and apparent constructability prior to casting any specimens in the laboratory. The completed mixture designs, all of which meet these two requirements, are presented in Appendix A, Tables A.3 through A.19. All of the mixtures have paste volumes less than 24.4% and a design air content of 8%.

It is well understood that cement paste is the constituent of concrete that undergoes the most shrinkage, and for this reason, the first step in developing a low-shrinkage mixture is to select the volume of cement paste. This is most often accomplished simply by specifying the cement content and water-cement (w/c) or water-cementitious material (w/cm) ratio. For mixtures containing a mineral admixture, the percentage replacement of cement (by volume) is also required. The following equations are solved simultaneously to determine the quantities of cementitious materials and water given a known paste volume V_{paste} , w/cm , and percentage (by volume of cementitious materials) of each mineral admixture P_1 , P_2 ,

..., P_p . Equation (2.3) is repeated for each mineral admixture incorporated into the mixture.

$$V_{paste} = \frac{M_c}{SG_c \times UW_w} + \sum_p \left(\frac{M_p}{SG_p \times UW_w} \right) + \left[\left(M_c + \sum_p M_p \right) \times w/cm \right] / UW_w \quad (2.1)$$

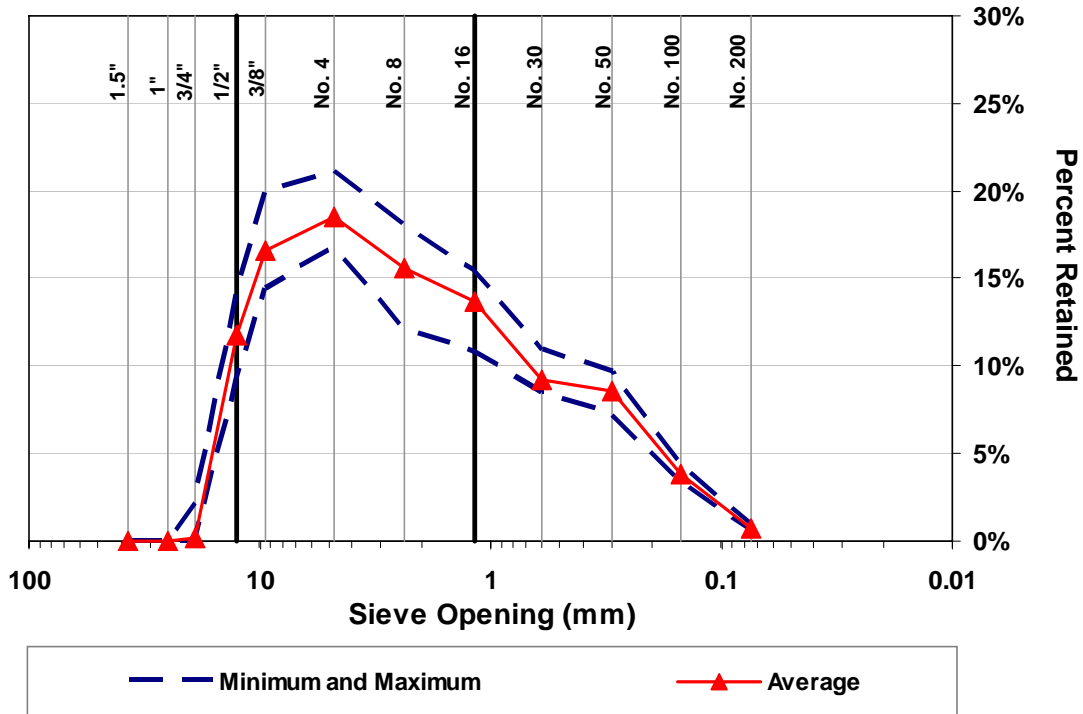
$$w/cm = \frac{M_w}{M_c + \sum_p M_p} \quad (2.2)$$

$$P_p = \left[\begin{array}{c} P_1 \\ P_2 \\ \vdots \\ P_p \end{array} \right] = \sum_p \left(\frac{M_p}{SG_p \times UW_w} \right) / \left[\sum_p \left(\frac{M_p}{SG_p \times UW_w} \right) + \frac{M_c}{SG_c \times UW_w} \right] \times 100 \quad (2.3)$$

where V_{paste} = known volume of paste in m^3 (ft^3)
 $M_c, M_p,$
 M_w = mass (weight) of cement, mineral admixture p , or water in kg (lb)
 SG_c, SG_p = specific gravity of cement or mineral admixture p
 UW_w = unit weight of water, 1000 kg/m^3 (62.4 lb/ft^3)
 w/cm = known water-cementitious material (water-cement) ratio
 P_p = known percentage (by volume of cementitious materials) of each mineral admixture p , denoted P_1, P_2, \dots, P_p

All of the mixtures in this study have a well-graded combined aggregate obtained by selecting a blend of aggregates (coarse aggregate, pea gravel, and sand) that consists of all aggregate particle sizes, plots as a *haystack* shape on the percent retained chart, and falls in the center of the optimum region on the Modified Coarseness Factor Chart (MCFC). Details regarding the percent retained chart and the MCFC are provided in Section 1.6, and the aggregate optimization methodology, entitled KU Mix, is the subject of Chapter 3. The minimum, maximum, and average percentages retained on each sieve of the combined gradation for the 56 batches cast in this study are presented in Fig. 2.1. Very little difference between the minimum

and maximum percentages exists (less than 6% for all sieve sizes) on the 19-mm ($\frac{3}{4}$ -in.), 12.5-mm ($\frac{1}{2}$ -in.), 0.60-mm (No. 30), 0.30-mm (No. 50), 0.15-mm (No. 100), and 0.075-mm (No. 200) sieves. Slightly larger differences exist for the middle sized sieves (4 to 6%) although even these differences are not large enough to create a gap-graded or peak-valley-peak combined gradation.



the effects of internal curing. The coarse aggregate was batched in the oven-dry condition for these batches.

All mixtures were batched using the following procedure adapted from the Silica Fume User Manual (Holland 2005) developed primarily to ensure that the densified silica fume is properly dispersed. The mixing procedure is as follows: First, dampen the interior surface of the mixer and add the coarse aggregate and 80% of the batch water. Slowly add in the densified silica fume (if any is used) with the mixer running and mix for 1½ minutes. Next, slowly add the cement and any additional mineral admixtures, mix for 1½ minutes, and then add in the fine aggregate. After another minute of mixing, add the plasticizing admixture mixed with 10% of the batch water and mix for one minute. Add the air entraining agent mixed with the remaining 10% batch water and mix for an additional minute. Finally, the shrinkage reducing admixture (if any is used) is added and then mixed for five minutes followed by a five minute rest period. Mix the concrete for three additional minutes, and, when necessary, add liquid nitrogen directly to the mixture while mixing to lower the temperature to approximately 21° C (70° F). If a shrinkage reducing admixture is used, an additional 30 minute rest period followed by 1 minute additional minute of mixing is added to allow the air content to stabilize.

2.8 FREE SHRINKAGE TEST PROGRAMS

A total of six programs are included in the free shrinkage evaluation of concretes considered for possible use in LC-HPC bridge decks. Several variables are examined within each program, although each program has a particular focus. Program I evaluates the effect of reducing the water content (and consequently reducing the w/c ratio and paste content) on free shrinkage, and Program II evaluates the effect of reducing the w/c ratio while maintaining a constant paste content. Program III evaluates the effect of coarse aggregate type on free shrinkage. Program IV addresses the use of a shrinkage reducing admixture and its effect on the

properties of both plastic and hardened concrete. The effect of cement type and fineness on free shrinkage is evaluated in Program V, and mineral admixtures are examined in Program VI. A summary of each program is provided next.

The prototypical LC-HPC mixture [317 kg/m^3 (535 lb/yd^3) of cement with a 0.42 w/c ratio] was often used as the control batch. The air entraining agent for all 56 batches was Micro Air[®] produced by BASF Admixtures, Inc. Micro Air[®] conforms to the requirements of ASTM C 260 and contains 13% solids and has a specific gravity of 1.01. Glenium[®] 3000 NS, also produced by BASF Admixtures, Inc., was used to maintain adequate workability. Glenium[®] 3000 NS conforms to the requirements of ASTM C 494 as a Type A and a Type F admixture. The solids content ranges from 27 to 33%, and the specific gravity is 1.08. Admixture dosages were obtained through trial batches.

2.8.1 Program I (Paste Content, w/c Ratio, Curing Period)

Program I included three sets of mixtures examining the effects of paste content, w/c ratio, cement type (fineness of cement) and curing period on free shrinkage. Each set contained three batches (for a total of nine batches) with w/c ratios of 0.45, 0.43, and 0.41 evaluated in conjunction with 7 and 14 day curing periods. All of the mixtures contained 317 kg/m^3 (535 lb/yd^3) of cement. In this program, a reduction in the w/c ratio was obtained by reducing the water content and replacing the water with an equal volume of aggregate. This approach also resulted in a reduction in the cement-paste volume from 24.4 to 23.1% for Sets 1 and 2 and 24.2 to 22.9% for Set 3 (the discrepancy in paste volumes between Sets 1 and 2 and Set 3 resulted from an increase in the specific gravity of the cement from 3.15 to 3.20). Differences between the three sets were limited to the type of cement and coarse aggregate. Set 1 batches contained a relatively porous limestone coarse aggregate (with an absorption between 2.5 and 3.0%) and Type I/II portland cement. Set 2 mixtures contained porous limestone and Type II coarse-ground cement, while

Set 3 contained granite coarse aggregate (with an absorption below 0.7%) and Type I/II cement. The same source of Type I/II cement was used for Sets 1 and 3; however, the samples were obtained nearly two years apart and had different chemical compositions. Sets 1 and 2 were mixed using the revolving drum mixer, and the batch volume was 0.131 m³ (0.171 yd³). Set 3 was mixed using the counter-current pan mixer with a batch volume of 0.027 m³ (0.035 yd³). Each mixture in this program was cast with a slump between 60 and 90 mm (2.25 to 3.5 in.) and a measured air content between 7.9 and 8.65%.

Set 1 batches containing limestone and Type I/II cement with *w/c* ratios of 0.45, 0.43, and 0.41 include batches 234, 235, and 239, respectively. Set 2 batches containing limestone and Type II coarse-ground with *w/c* ratios of 0.45, 0.43, and 0.41 include 240, 244, and 246, respectively. Sets 1 and 2 have companion permeability specimens that are reported by McLeod, Darwin, and Browning (2009). Set 3 batches containing granite and Type I/II cement also with *w/c* ratios of 0.45, 0.43, and 0.41 include 412, 414, and 417. For Sets 1 and 2, three compressive strength cylinders were cured for 3, 7, 14, or 28 days (for a total of 12 cylinders) in lime-saturated water, transferred to a drying tent [22° C (73° F) and 50% RH], and all tested at an age of 28 days. For Set 3, three cylinders were cured for 7 or 28 days in lime-saturated water and tested immediately following the curing period. The complete Program I test matrix is presented in Table 2.3, and mixture proportions, plastic properties, and average compressive strengths are given in Tables A.3 through A.5.

2.8.2 Program II (Paste Content, *w/c* Ratio, Curing Period)

The effects of paste content, *w/c* ratio, and curing period were evaluated in Program II. A total of seven batches were cast and divided into two sets. All batches were cast with limestone coarse aggregate and Type I/II portland cement. Set 1 examined four *w/c* ratios (0.36, 0.38, 0.40, and 0.42) while maintaining a constant

Table 2.3 – Program I Test Matrix[†]

Set Number	w/c Ratio	Coarse Aggregate	Paste Content	Cement Type	Batch Number
1	0.41	limestone	23.1%	I/II	234*
	0.43		23.7%		235*
	0.45		24.4%		239*
2	0.41	limestone	23.1%	II	240*
	0.43		23.7%		244*
	0.45		24.4%		246*
3	0.45	granite	22.9%	I/II	412
	0.43		23.3%		414
	0.41		24.2%		417

[†]The batches in Program I contain free shrinkage specimens cured for both 7 and 14 days.

*The results of companion permeability specimens are reported by McLeod, Darwin, and Browning (2009).

paste content of 23.3% and a curing period of 14 days. Set 2 included mixtures with a constant w/c ratio of 0.42, a paste content of either 23.3% or 21.6%, and a curing period of either 7, 14, or 21 days. Two different mixture designs were included in Set 2. The 23.3% paste mixtures had a cement content of 317 kg/m³ (535 lb/yd³), and the 21.6% paste mixtures had a cement content of 295 kg/m³ (497 lb/yd³). The 23.3% paste specimens were cured for either 14 or 21 days, and the 21.6% paste specimens were cured for 7 or 14 days. The batches in Program II were mixed using a counter-current pan mixer with batch volumes of 0.050 m³ (0.066 yd³). Each mixture in this program was cast with a slump of 50 to 95 mm (2 to 3.75 in.) and a measured air content of 8.15 to 8.65%.

Set 1 includes batches 330, 334, 335, and 338 (with w/c ratios of 0.36, 0.38, 0.40, and 0.42, respectively), and Set 2 includes batches 338 and 342. The Program II batches have companion permeability specimens that are reported by McLeod, Darwin, and Browning (2009). For Set 1, two compressive strength cylinders were cured for 7 or 28 days in lime-saturated water and tested immediately following the curing period. Set 2 included three compressive strength specimens for each curing

period instead of only two. The Program II test matrix is presented in Table 2.4, and mixture proportions, plastic properties, and average compressive strengths are given in Table A.6.

Table 2.4 – Program II Test Matrix[†]

Set Number	w/c	Paste Volume	Curing Period	Batch Number
1	0.36	23.3%	14	330*
1	0.38	23.3%	14	334*
1	0.40	23.3%	14	335*
1 and 2	0.42	23.3%	14	338*
2	0.42	23.3%	21	338*
2	0.42	21.6%	7	342*
2	0.42	21.6%	14	342*

[†]The batches in Program II contain Type I/II portland cement and limestone coarse aggregate.

*The results of companion permeability specimens are reported by McLeod, Darwin, and Browning (2009).

2.8.3 Program III (Coarse Aggregate Type)

The influence of three coarse aggregate types on free shrinkage was examined in Program III. The coarse aggregates evaluated were granite, quartzite, and limestone. Each mixture had a w/c ratio of 0.42, a paste content of 21.6% [295 kg/m³ (497 lb/yd³) of Type I/II portland cement], and include specimens cured for 7 and 14 days. The combined aggregate gradation for each mixture was optimized using the KU Mix method (described in Chapter 3), and as a result, the volume of coarse aggregate was similar, but not identical, for each of the mixtures evaluated. The coarse aggregate content varied slightly from 34.7 to 35.3% by volume. Program III batches were mixed using the counter-current pan mixer with a batch volume of 0.031 m³ (0.040 yd³). Each mixture in this program was cast with a slump of 70 to 95 mm (2.75 to 3.75 in.) and a measured air content of 7.9 to 8.4%.

Program III includes batches 342 through 344. Batch 342 containing limestone is also included in Program II Set 2. Three compressive strength cylinders were cured for 7 or 28 days in lime-saturated water and tested immediately following the curing period for Program III. The Program III test matrix is presented in Table 2.5, and mixture proportions, plastic properties, and average compressive strengths are given in Table A.7.

Table 2.5 – Program III Test Matrix[†]

Coarse Aggregate Type	Coarse Aggregate Content	Batch Number
limestone	34.7%	342 [‡]
granite	35.1%	343
quartzite	35.3%	344

[†]The batches in Program III contain Type I/II portland cement, a paste content of 21.6%, a *w/c* ratio of 0.42, and are cured for 7 and 14 days.

[‡]Batch 342 is also included in Program II Set 2.

2.8.4 Program IV (Shrinkage Reducing Admixture)

Program IV examined the effect of a shrinkage reducing admixture (SRA) on free shrinkage in conjunction with 7 and 14 day curing periods. Two SRA dosages, 1 and 2% by mass (weight) of cement, were used to determine both the effect on free shrinkage and plastic concrete properties. The batches in this series contained limestone coarse aggregate, a *w/c* ratio of 0.42, a paste content of 23.3% [equivalent to 317 kg/m³ (535 lb/yd³) of cement], and contained Type I/II portland cement. The mixtures containing an SRA were mixed and allowed to rest for 30 minutes prior to being remixed for one minute and tested for slump and air content (as described in Section 2.8). This additional rest period allowed the air-void system to stabilize before the concrete was cast and helped to gage the potential suitability of this concrete for use in the field. The 30-minute rest period was established by testing the air content of the 2% SRA mixture every five minutes until the change in the air content from one test to another was less than 1%. The manufacturer recommends

truck trial batches with a simulated haul time of at least 20 minutes to assess air content stability. Program IV batches were mixed using a counter-current pan mixer with batch volumes of 0.031 m³ (0.040 yd³). The mixtures in this program were cast with a slump between 50 and 75 mm (2 and 3 in.) and a measured air content between 7.9 and 8.65%.

Three compressive strength cylinders were cured for 7 or 28 days in lime-saturated water and tested immediately following the curing period for Program IV. The Program IV test matrix is presented in Table 2.6, and mixture proportions, plastic properties, and average compressive strengths are given in Table A.8. Batch 273 is the control (0% SRA) for batches 323 (2% SRA) and 308 (1% SRA). The control batch also serves as the control for Program V and VI Sets 1, 3, and 5.

Table 2.6 – Program IV Test Matrix[†]

Dosage by Weight of Cement	SRA Dosage mL/m³ (gal/yd³)	Batch Number
Control (0%)	--	273
1%	3165 (0.64)	323
2%	6330 (1.28)	308

[†]The batches in Program IV contain Type I/II portland cement, a paste content of 23.3%, a w/c ratio of 0.42, and are cured for 7 and 14 days.

2.8.5 Program V (Cement Type and Fineness)

The influence of cement type and fineness on free shrinkage was examined in Program V. Four portland cements (one Type I/II, two Type II, and one Type III) with values of Blaine fineness ranging from 323 to 549 m²/g were included in the comparison. The two samples of Type II cement had values of Blaine fineness of 323 and 334 m²/g, and the Type I/II and Type III cement samples had Blaine fineness values of 379 and 549 m²/g, respectively. The batches in this series contained limestone coarse aggregate, a w/c ratio of 0.42 and a paste content of 23.3% [equivalent to 317 kg/m³ (535 lb/yd³) of cement]. The batches in Program II were

mixed using a counter-current pan mixer with batch volumes of 0.031 m³ (0.040 yd³). Each mixture in this program was cast with a slump between 60 and 100 mm (2.25 and 4 in.) and a measured air content of between 8.65 and 8.9%.

Program V includes two Type II cement batches (298 and 300), one Type I/II batch (273), and one Type III batch (367). Three compressive strength cylinders were cured for 7 or 28 days in lime-saturated water and tested immediately following the curing period for specimens in Program V. The complete Program V test matrix is presented in Table 2.7, and mixture proportions and concrete properties are given in Table A.9. The Type I/II cement batch (No. 273) serves as the control batch for Program IV and Program VI Sets 1, 3, and 5.

Table 2.7 – Program V Test Matrix[†]

Blaine Fineness m²/g	Cement Type	Cement Sample No.	Batch Number
323	II	2	298
334	II	1(a) and 1(b)	300 [‡]
379	I/II	3	273 [*]
549	III	1	367

[†]All batches in Program IV have a paste content of 23.3%, a w/c ratio of 0.42, and are cured for 7 or 14 days.

[‡]Batch 300 was cast with the same cement as the specimens in Program I Set 2.

^{*}Batch 273 also serves as the control for Program IV and VI Sets 1, 3, and 5.

2.8.6 Program VI (Mineral Admixtures)

Three mineral admixtures were used as a partial replacement for Type I/II portland cement to determine their influence on free shrinkage in Program VI. The mineral admixtures evaluated include silica fume, Class F fly ash, and Grade 100 and 120 slag cement. A minimum of two sources and two replacement levels were evaluated for each mineral admixture. The mineral admixtures were evaluated in conjunction with different aggregate types and curing periods. Six specimens were

cast for each of the 38 batches – three cured for 7 days and 14 days. The 38 batches were cast and divided into 10 sets of specimens.

A summary of the 10 sets included in Program VI is shown in Table 2.8. The mineral admixture trade names are provided in Table 2.2 and their chemical composition is listed in Table A.1. Sets 1 and 2 compare the free shrinkage of mixtures containing 0, 3, or 6% volume replacements of cement with densified silica fume. The Set 1 batches contain limestone coarse aggregate, and Set 2 batches contain granite. Sets 3 and 4 compare the free-shrinkage performance of concrete containing 0, 20, or 40% volume replacements of cement with Class F Fly Ash. Set 3 batches contain limestone coarse aggregate, and Set 4 batches contain granite. Sets 5 through 9 compare the shrinkage performance of concrete containing Grade 100 or Grade 120 slag cement. Set 5 evaluates the relative shrinkage of mixtures containing limestone and 0, 30, 60, or 80% volume replacements of cement with Grade 120 slag cement, while Set 6 evaluates mixtures containing quartzite and 60% Grade 120 slag. Sets 7 and 8 evaluate mixtures containing limestone or granite and 0, 30, or 60% volume replacements of cement with Grade 100 slag cement. Set 9 compares the free shrinkage of specimens cast with limestone coarse aggregate in the saturated-surface-dry (SSD) condition and specimens cast with oven-dried aggregate to determine the ability of limestone to provide internal curing. Set 9 includes batches containing 0 and 60% volume replacements of cement with Grade 100 slag cement (which are particularly sensitive to the length of the curing period). Set 10 includes ternary mixtures containing a 6% volume replacement of cement with silica fume and 60 or 80% volume replacements of cement with Grade 120 slag cement. Mixtures containing 0 and 6% silica fume are included in Set 10 as control mixtures.

Three compressive strength cylinders were cured for 7 or 28 days in lime-saturated water and tested immediately following the curing period for all concrete mixtures included in Program VI. Additional details for each set are provided in

Sections 2.9.6.1 through 2.9.6.5 and mixture proportions, plastic concrete properties, and average compressive strengths are provided in Tables A.10 through A.19.

Table 2.8 – Program VI Test Matrix

Set Number	Mineral Admixture	Coarse Aggregate	Replacement Level [†]
1	Silica Fume	Limestone	0, 3, and 6%
2	Silica Fume	Granite	0, 3, and 6%
3	Class F Fly Ash	Limestone	0, 20, and 40%
4	Class F Fly Ash	Granite	0, 20, and 40%
5	Grade 120 Slag	Limestone	0, 30, 60, and 80%
6	Grade 120 Slag	Limestone Quartzite	60%
7	Grade 100 Slag	Limestone Granite	60%
8	Grade 100 Slag	Granite	0, 30, and 60%
9 [‡]	Grade 100 Slag	Limestone	0 and 60%
10	Grade 120 Slag Silica Fume	Limestone	0, 60, and 80% 0 and 6%

[†]All mineral admixture replacements are reported by volume of total cementitious materials.

[‡]Set 9 compares free shrinkage of specimens cast with coarse aggregate in the saturated-surface-dry (SSD) condition and specimens cast with oven-dried aggregate.

2.8.6.1 Sets 1 and 2 (Silica Fume)

Sets 1 and 2 compared the free shrinkage of mixtures containing 0, 3, or 6% volume replacements of cement with densified silica fume. They consisted of 8 batches, each with a w/cm ratio of 0.42 and a paste content of 23.3% [equivalent to 317 kg/m³ (535 lb/yd³) of cement and a 0.42 w/c ratio]. The Set 1 batches contained limestone coarse aggregate, while the Set 2 batches contained granite. The limestone batches were repeated with an additional silica fume source to verify the results with a different source. The batches in Sets 1 and 2 were mixed using the counter-current pan mixer with batch volumes of 0.031 m³ (0.040 yd³) and 0.027 m³ (0.035 yd³), respectively. The mixtures in these sets were cast with slumps between 50 and 100 mm (2 and 4 in.) and measured air contents between 7.9 and 8.9%.

The test matrix for Program VI Sets 1 and 2 is presented in Table 2.9, and the mixture proportions, plastic concrete properties, and average compressive strengths are given in Tables A.10 and A.11. Batch 273 is the control (0% silica fume) for batches 274 and 325 with 3% silica fume and batches 275 and 326 with 6% silica fume. For the Set 2 batches containing granite, batch 409 is the control for batches 392 and 394 containing 3 and 6% silica fume, respectively.

Table 2.9 – Program VI Sets 1 and 2 Test Matrix[†]

Set Number	Silica Fume Content [‡]	Silica Fume Sample No.	Coarse Aggregate	Batch Number
1	0% (control)	--	Limestone	273
1	3%	1	Limestone	274
1	6%	1	Limestone	275
1	3%	2	Limestone	325
1	6%	2	Limestone	326
2	0% (control)	--	Granite	409
2	3%	2	Granite	392
2	6%	2	Granite	394

[†]The batches in Program VI Sets 1 and 2 have a paste content of 23.3%, a w/cm ratio of 0.42, and are cured for 7 and 14 days.

[‡]The silica fume contents are reported by volume of cementitious materials.

2.8.6.2 Sets 3 and 4 (Class F Fly Ash)

Program VI Sets 3 and 4 compare the free shrinkage of mixtures containing 0, 20, or 40% volume replacements of cement with Class F fly ash. A total of 11 batches were cast, each with a w/cm ratio of 0.42 and a paste content of 23.3% [equivalent to 317 kg/m³ (535 lb/yd³) of cement at a 0.42 w/c ratio]. In total, three sources of Class F fly ash were examined in conjunction with either limestone or granite coarse aggregate. Set 3 batches contain limestone coarse aggregate, and Set 4 batches contain granite coarse aggregate. The batches in Sets 3 and 4 were mixed using the counter-current pan mixer with batch volumes of 0.031 m³ (0.040 yd³) and

0.027 m³ (0.035 yd³), respectively. These mixtures were cast with a slump of between 55 and 100 mm (2.25 and 4 in.) and had air contents between 7.9 and 8.9%.

The test matrix for Sets 3 and 4 is presented in Table 2.10, and the mixture proportions, concrete properties, and average compressive strengths are given in Tables A.12 and A.13. For the Set 3 batches containing limestone, batch 338 is the control (0% fly ash) for batches 363 (20% fly ash) and 364 (40% fly ash) containing Coal Creek Fly Ash (sample 1) and batch 273 is the control for batches 290 (20% fly ash) and 292 (40% fly ash) cast with Class F fly ash from Lafarge (sample 2). Set 4 batches contain granite coarse aggregate. Two different fly ashes are included in Set 4 with batch 409 serving as the control. Batches 399 and 403 contain Lafarge Class F fly ash (sample 2) and batches 419 and 421 contain Durapoz[®] F from Ashgrove (sample 3), each at replacement levels of 20 and 40%, respectively.

2.8.6.3 Sets 5 Through 8 (Slag Cement)

Sets 5 through 8 compare the free shrinkage of mixtures containing 0, 30, 60, or 80% volume replacements of cement with Grade 100 (G100) or Grade 120 (G120) slag cement. A total of 13 batches were cast – each with a 0.42 *w/cm* ratio and a paste content of 23.3% [equivalent to 317 kg/m³ (535 lb/yd³) of cement at a 0.42 *w/c* ratio]. Five different samples of slag cement were examined (three G100 and two G120) in conjunction with limestone, quartzite, or granite coarse aggregate. All of the batches in Sets 5 through 8 were mixed using the counter-current pan mixer with batch volumes between 0.027 m³ (0.035 yd³) and 0.031 m³ (0.040 yd³). These mixtures were cast with slumps between 55 and 80 mm (2.25 and 3.25 in.) and measured air contents between 7.9 and 8.9%.

The test matrix for Sets 5 through 8 is presented in Table 2.11, and the mixture proportions, plastic concrete properties, and average compressive strengths are given in Tables A.14 through A.17. For the Set 5 batches cast with limestone

Table 2.10 – Program VI Sets 3 and 4 Test Matrix[†]

Set Number	Fly Ash Content[‡]	Class F Fly Ash Sample No.	Coarse Aggregate	Batch Number
3	0% (control)	--	Limestone	338
3	20%	1	Limestone	363
3	40%	1	Limestone	364
3	0% (control)	--	Limestone	273
3	20%	2	Limestone	290
3	40%	2	Limestone	292
4	0% (control)	--	Granite	409
4	20%	2	Granite	399
4	40%	2	Granite	403
4	20%	3	Granite	419
4	40%	3	Granite	421

[†]The batches in Program VI Sets 1 and 2 have a paste content of 23.3%, a *w/cm* ratio of 0.42, and are cured for 7 and 14 days.

[‡]The fly ash contents are reported by volume of cementitious materials.

coarse aggregate, batch 273 is the control (0% slag) for batches 278, 282, 309, and 317. Batches 278 and 282 contain 30 and 60% volume replacements of cement with NewCem[®] G120 slag cement from Lafarge (sample 1), and batches 309 and 317 contain 60 and 80% G120 slag cement from Lafarge (sample 2). Batch 309 with limestone coarse aggregate was repeated in Batch 322 and compared with batches 312 and 324 both containing quartzite rather than limestone. Sets 7 and 8 contain GranCem[®] G100 slag cement from Holcim Ltd. Batch 338 contains limestone coarse aggregate and is the control (0% slag cement) for Set 7, and batch 409 contains granite and is the control for Set 8. Batches 328 and 340 contain 60% G100 slag cement (sample 4) and limestone and granite coarse aggregate, respectively. Batches 408 and 409 in Set 8 contain granite and 30 and 60% replacement of cement with G100 slag.

Table 2.11 – Program VI Sets 5 through 8 Test Matrix[†]

Set Number	Slag Cement Content [‡]	Slag Cement Sample No.	Coarse Aggregate	Batch Number
5	0% (control)	--	Limestone	273
5	G120 30%	1	Limestone	278
5	G120 60%	1	Limestone	282
5	G120 60%	2	Limestone	309
5	G120 80%	2	Limestone	317
6	G120 60%	2	Limestone	322
6	G120 60%	2	Quartzite	312
6	G120 60%	2	Quartzite	324
7	G100 60%	4	Limestone	328
7	0% (control)	--	Limestone	338
7	G100 60%	4	Granite	340
8	G100 30%	3	Granite	407
8	G100 60%	3	Granite	408
8	0% (control)	--	Granite	409

[†]The batches in Program VI Sets 1 and 2 have a paste content of 23.3%, a w/cm ratio of 0.42, and are cured for 7 and 14 days.

[‡]The slag cement contents [either Grade 100 (G100) or Grade 120 (G120)] are reported by volume of cementitious materials.

2.8.6.4 Set 9 (Oven-Dry versus Saturated-Surface Dry Aggregate)

Program VI Sets 1 through 8 and Set 10 compare the performance of free-shrinkage specimens in which the coarse aggregate moisture content at the time of batching is saturated-surface-dry (SSD). This represents the aggregate condition in concrete that neither adds nor subtracts water from the cement paste during the batching and mixing process. Water held within the pores of SSD aggregate is available to provide additional internal curing, and the quantity of this water is especially high when used in conjunction with the relatively porous limestone coarse aggregate. Set 9 is used to evaluate the effect of internal curing by comparing mixtures cast with limestone that is either in an SSD or oven-dry condition on mixtures containing 60% G100 slag cement (sample 5) and cured for 7 or 14 days. A

total of 4 batches were cast, each with a w/cm ratio of 0.42 and a paste content of 23.3% [equivalent to 317 kg/m^3 (535 lb/yd^3) of cement at a 0.42 w/c ratio]. The Set 9 batches were mixed using the counter-current pan mixer with batch volumes of either 0.040 m^3 (0.066 yd^3) or 0.027 m^3 (0.035 yd^3). These mixtures were cast with slumps between 65 and 90 mm (2.5 and 3.5 in.) and an air contents of 8.15 or 8.4%.

The test matrix for Set 9 is presented in Table 2.12, and the mixture proportions and concrete properties are given in Table A.18. Control batches (0% slag cement) were cast with limestone in both the SSD (batch 373) and the oven-dry condition (batch 427). Batch 368 was cast with 60% G100 slag and oven-dry limestone, while batch 369 was cast with 60% G100 slag and SSD limestone.

Table 2.12 – Program VI Set 9 Test Matrix[†]

Slag Cement Content [‡]	Slag Cement Sample No.	Aggregate Condition [*]	Batch Number
G100 60%	5	Oven Dry	368
G100 60%	5	SSD	369
control (0%)	--	SSD	373
control (0%)	--	Oven Dry	427

[†]The batches in Program VI Set 9 have a paste content of 23.3%, a w/c ratio of 0.42, and are cured for 7 and 14 days.

[‡]The slag cement contents [either Grade 100 (G100) or Grade 120 (G120)] are reported by volume of cementitious materials.

^{*}Set 9 compares free shrinkage of specimens cast with coarse aggregate in the saturated-surface-dry (SSD) condition and specimens cast with oven-dried aggregate.

2.8.6.5 Set 10 (Ternary Mixtures)

Program VI Set 10 compares the free-shrinkage of mixtures containing silica fume and G120 slag cement at reduced paste contents. A total of 5 batches were cast with w/cm ratios of 0.42 at two paste contents – 21.6% [equivalent to 295 kg/m^3 (497 lb/yd^3) of cement with a 0.42 w/c ratio] and 20.0% [equivalent to 272 kg/m^3 (460 lb/yd^3) of cement with a 0.42 w/c]. Set 10 includes mixtures containing 0 or 6% volume replacements of cement with densified silica fume and 0, 60, or 80% volume

replacements of cement with G120 slag cement in conjunction with limestone coarse aggregate and a 14 day curing period. A full-factorial test matrix was not possible because at the lowest paste content it was necessary to have at least 60% slag cement and 6% silica fume to maintain adequate finishability and cohesiveness of the mixture. Set 10 batches were mixed using a counter-current pan mixer with batch volumes of 0.040 m³ (0.066 yd³). These mixtures were cast with slumps between 55 and 90 mm (2.25 and 3.5 in.) and measured air contents between 8.25 and 8.9%.

The test matrix for Set 10 is presented in Table 2.13, and the mixture proportions and concrete properties are given in Table A.19. A single control batch (0% silica fume and slag cement) was cast with a paste content of 21.6% (batch 342). It does not appear that further reductions in the paste content will be possible without the use of silica fume and slag cement. Batch 351 contains 60% G120 slag cement and batch 354 contains 6% silica fume and 60% slag cement both with 21.6% paste and a *w/cm* ratio of 0.42. The paste content was further reduced to 20.0% for batches 355 (containing 6% silica fume and 60% slag cement) and batch 358 (containing 6% silica fume and 80% slag cement).

Table 2.13 – Program VI Set 10 test matrix[†]

Paste Content	Silica Fume Content[‡]	G120 Slag Cement Content[*]	Batch Number
21.6	0%	0%	342
21.6	0%	60%	351
21.6	6%	60%	354
20.0	6%	60%	355
20.0	6%	80%	358

[†]The batches in Program VI Set 10 have a *w/c* ratio of 0.42, limestone coarse aggregate, and are cured for 14 days.

[‡]The dry densified silica fume content in Program VI Set 10 (Sample 2) is reported by volume of cementitious materials.

^{*}The slag cement in Program VI Set 10 is Grade 120 (Sample 2) and is reported by volume of cementitious materials.

CHAPTER 3: AGGREGATE OPTIMIZATION USING THE KU MIX METHOD

3.1 GENERAL

The combined aggregate gradation by itself is not a primary factor affecting concrete shrinkage or cracking, but there are several reasons that make the combined aggregate gradation important for quality concrete. Cement paste is the constituent of concrete that undergoes the most shrinkage, while aggregate provides restraint and, thereby, helps limit shrinkage. For this reason, concrete mixtures containing a high volume of aggregate (and a low volume of cement paste) have both reduced shrinkage and cracking. An optimized combined aggregate gradation allows the volume of aggregate to be maximized while maintaining good characteristics in the plastic concrete. In addition to reduced shrinkage and cracking potential with the reduction of paste contents, concretes with optimized aggregate gradations exhibit less segregation, increased cohesiveness, and improved workability compared to concretes with poor combined gradations.

This chapter describes the KU Mix design methodology for determining an optimized combined gradation for selected aggregates using the percent retained chart and the Modified Coarseness Factor Chart (MCFC). The process begins by developing an *ideal gradation* that plots as a “haystack” on the percent retained chart and falls in the center of the optimum region on the MCFC. The optimum blend of a particular set of aggregates is then determined by performing a series of least-squared minimization routines using the *ideal gradation* as a model for the actual blended gradation.

The balance of this section provides the definitions that are used in the optimization process. Additional details and background information regarding the methods used by KU Mix are provided in Section 1.6, and an example illustrating the

calculations is provided in Appendix B. A Microsoft Excel spreadsheet enhanced with Visual Basic for Applications designed to perform the KU Mix optimization is available for download at www.iri.ku.edu.

3.1.1 Identification of Sieve Sizes and Definition of Gradation Fractions

The KU Mix design methodology uses the percent retained chart and the MCFC. The sieve sizes and designations, notation used to identify sieve sizes, the percent retained on each sieve, and the gradation fractions used in conjunction with the MCFC are identified in Table 3.1. The sieves run from 37.5-mm (1½-in.) to 0.075-mm (No. 200), plus the pan, and are designated as a through l for the sieves and m for the pan. The size (in millimeters) for each sieve is denoted as x_n , and the percent retained on each sieve is designated as R_n , where n corresponds to the sieves a through l and the pan. Aggregate retained on the individual sieves is categorized in one of three gradation fractions. The first category or gradation fraction, the quality Q particles, is defined as aggregate retained on or above the 9.5-mm (¾-in.) sieve. The second category, intermediate I particles, is defined as the percentage of material retained on the 4.75 and 2.36-mm (No. 4 and No. 8) sieves, and the third category, workability W particles, represents aggregate passing the 2.36-mm (No. 8) sieve.

Using the notation in Table 3.1, the three gradation fractions are defined as

$$Q = R_a + R_b + R_c + R_d + R_e \quad (3.1)$$

$$I = R_f + R_g \quad (3.2)$$

$$W = R_h + R_i + R_j + R_k + R_l + R_m \quad (3.3)$$

The sum of the three gradation fractions must equal 100 percent.

$$Q + I + W = 100 \quad (3.4)$$

Table 3.1 – Identification of sieve sizes and designations, percent retained designations, and gradation fraction designations

Sieve	Sieve Designation, n	Sieve Size Designation (mm), x_n	Percent Retained Designation, R_n	Gradation Fraction Designation
37.5-mm (1½-in.)	a	x_a	R_a	Quality Particles, Q
25-mm (1-in.)	b	x_b	R_b	
19-mm (¾-in.)	c	x_c	R_c	
12.5-mm (½-in.)	d	x_d	R_d	
9.5-mm (⅜-in.)	e	x_e	R_e	
4.75-mm (No. 4)	f	x_f	R_f	Intermediate Particles, I
2.36-mm (No. 8)	g	x_g	R_g	
1.18-mm (No. 16)	h	x_h	R_h	Workability Particles, W
0.60-mm (No. 30)	i	x_i	R_i	
0.30-mm (No. 50)	j	x_j	R_j	
0.15-mm (No. 100)	k	x_k	R_k	
0.075-mm (No. 200)	l	x_l	R_l	
Pan	m	--	R_{pan}	

3.1.2 Definition of Coarseness Factor CF and Workability Factor WF

The MCFC provides a means to achieve an optimized balance of the Q , I , and W particles based on the values of two factors: the coarseness factor CF and the workability factor WF , both of which are calculated using the percentage of aggregate in the three gradation fractions. The CF defines a relationship between the Q and I particles and the WF quantifies the particles that provide workability to the mixture – the W particles with an adjustment to account for the quantity of cementitious material.

The coarseness factor CF is defined as the ratio of Q particles to the sum of Q and I particles, expressed as a percent.

$$CF = \frac{Q}{Q+I} \times 100 \quad (3.5)$$

Using the notation defined in Table 3.1, Eq. (3.5) can be expressed as

$$CF = \frac{R_a + R_b + R_c + R_d + R_e}{R_a + R_b + R_c + R_d + R_e + R_f + R_g} \times 100 \quad (3.6)$$

The workability factor WF is defined as the percentage of W particles plus a correction factor to account for deviations in cementitious materials from a mix design containing 335 kg/m^3 (564 lb/yd^3) of cement (this is referred to as a six-sack mix). As discussed in Section 1.6.1, implementation of the MCFC has typically involved the use of an approximate multiplier, equal to 2.5, per sack of cement to account for any deviations in the cementitious material content from a six-sack mix. In contrast to this earlier approach, the KU Mix design method treats deviations from a six-sack mix as changes in the quantity of W particles, rather than as a direct change in WF . The process for adjusting the quantity of W particles based on the cementitious material in the concrete mixture is described in Section 3.2.4. The workability factor, without the correction factor for cement content introduced by Shilstone (1990), is defined as

$$WF = \frac{W}{Q+I+W} \times 100 \quad (3.7)$$

Using the notation in Table 3.1, Eq. (3.7) can be expressed as

$$WF = \frac{R_h + R_i + R_j + R_k + R_l + R_m}{R_a + R_b + \dots + R_m} \times 100 \quad (3.8)$$

The MCFC, shown in Fig. 3.1, is the tool used to evaluate the combined aggregate gradation based on the position of the point (CF , WF) in the chart. The chart is based on field experience and has five zones that identify regions that correspond to concrete with similar characteristics (ACI Committee 211 2004). In

addition to the five zones, a *trend bar* is included that represents a region where maximum aggregate density is achieved, although such mixtures have little workability and are only suitable for mass concrete placements. The characteristics of each zone are listed in Fig. 3.1; additional details are provided in Section 1.6.1.

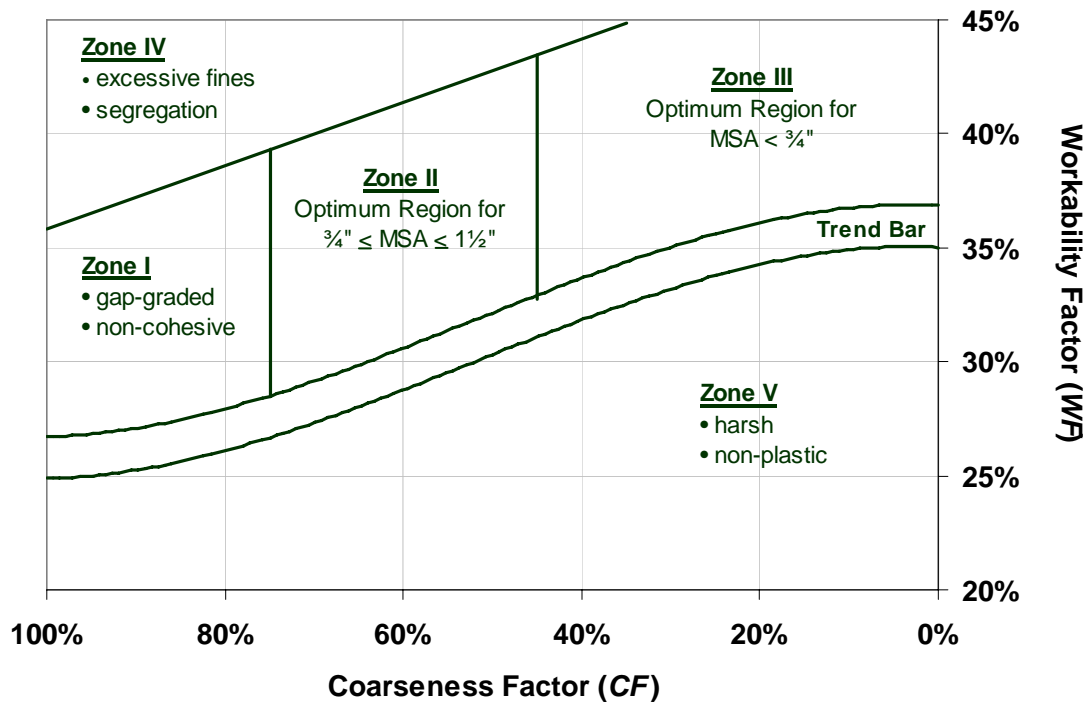


Fig. 3.1 – Modified Coarseness Factor Chart (MCFC)

3.2 DEVELOPING AN *IDEAL* GRADATION MODEL

An *ideal* gradation provides the basis for the KU Mix Optimization process by serving as the model and target for the actual blended gradation. The percent retained chart and the modified coarseness factor chart (MCFC) are used together to develop the *ideal* gradation. Development of this model gradation has four goals: produce an *ideal* gradation with a specified *CF* and *WF*, account for differences in workability resulting from variations in the cementitious material content, produce a percent retained gradation plot that is continuous (no abrupt changes or gaps) and in the shape of a haystack when plotted on a log scale, and finally, be easily adaptable and

versatile when used to establish optimized gradations for a wide range of commonly used aggregate sizes and gradations. The process is iterative and depends on a number of factors, including the gradations of the available aggregates, the optimized combined gradation produced using those aggregates, and the cementitious material content of the concrete mixture. The *ideal* gradation is produced simultaneously with the determination of the quantities of the available aggregate that are used to obtain the optimized combined aggregate gradation.

3.2.1 General Equation for the *Ideal* Gradation

Cubic equations are used to mathematically model the *ideal* gradation on a percent retained chart. The representation, entitled the *Cubic-Cubic Model*, consists of two overlapping cubic polynomial equations that are defined for specific sieves. The two equations and notation are as follows

$$y(x_n) = A(\log x_n)^3 + B(\log x_n)^2 + C(\log x_n) + D \quad (3.9a)$$

$$z(x_n) = A'(\log x_n)^3 + B'(\log x_n)^2 + C'(\log x_n) + D' \quad (3.9b)$$

where $y(x_n)$ and $z(x_n)$ = percent of total aggregate retained on a sieve with opening size x_n , in millimeters
 $\log x_n$ = sieve opening plotted on a logarithmic scale
 A through D' = coefficients that define the two cubic equations

Equation (3.9a) describes the percent retained on the quality Q and intermediate I gradation fractions [37.5-mm (1½-in.), 25.0-mm (1.0-in.), 19.0-mm (¾-in.), 12.5-mm (½-in.), 9.5-mm (⅜-in.), 4.75-mm (No. 4), 2.36-mm (No. 8)], while Eq. (3.9b) describes the intermediate I and workability W gradation fractions [4.75-mm (No. 4), 2.36-mm (No. 8), 1.18-mm (No. 16), 0.60-mm (No. 30), 0.30-mm (No. 50), 0.15-mm (No. 100), 0.075-mm (No. 200)] in addition to the percent retained on the 9.5-mm (⅜-in.) sieve. The two cubic equations are defined such that the percents retained on the 9.5-mm (⅜-in.) sieve and the intermediate sieves [4.75-mm (No. 4)

and 2.36-mm (No. 8)] are the same for both cubic equations. The *ideal* gradation, denoted \bar{R}_n , is defined as the combination of $y(x_n)$ and $z(x_n)$ as shown in Table 3.2. The percent retained on the pan \bar{R}_{pan} cannot be plotted on a logarithmic scale and must be handled separately (see Section 3.2.2). Note the difference in notation between the percent retained on each sieve of the *ideal* gradation, denoted \bar{R}_n , and the actual percentage of aggregate retained on each sieve, denoted R_n and defined in Table 3.1.

Table 3.2 – Definitions for the *Cubic-Cubic Model*, using Eq. (3.9a) and (3.9b), and the *Ideal Gradation*

Sieve	Percent Retained on Each Sieve		
	Eq. (3.9a), $y(x_n)$	Eq. (3.9b), $z(x_n)$	<i>Ideal</i> Gradation, \bar{R}_n
37.5-mm (1½-in.)	$y(x_a)$	--	\bar{R}_a
25-mm (1-in.)	$y(x_b)$	--	\bar{R}_b
19-mm (¾-in.)	$y(x_c)$	--	\bar{R}_c
12.5-mm (½-in.)	$y(x_d)$	--	\bar{R}_d
9.5-mm (⅜-in.)	$y(x_e)$	= $z(x_e)$	\bar{R}_e
4.75-mm (No. 4)	$y(x_f)$	= $z(x_f)$	\bar{R}_f
2.36-mm (No. 8)	$y(x_g)$	= $z(x_g)$	\bar{R}_g
1.18-mm (No. 16)	--	$z(x_h)$	\bar{R}_h
0.60-mm (No. 30)	--	$z(x_i)$	\bar{R}_i
0.30-mm (No. 50)	--	$z(x_j)$	\bar{R}_j
0.15-mm (No. 100)	--	$z(x_k)$	\bar{R}_k
0.075-mm (No. 200)	--	$z(x_l)$	\bar{R}_l
Pan	--	--	\bar{R}_{pan}

An example of an *ideal* gradation, determined using the *Cubic-Cubic Model*, for a combined gradation with a maximum size of 25-mm (1.0-in.) is presented in Fig. 3.2.

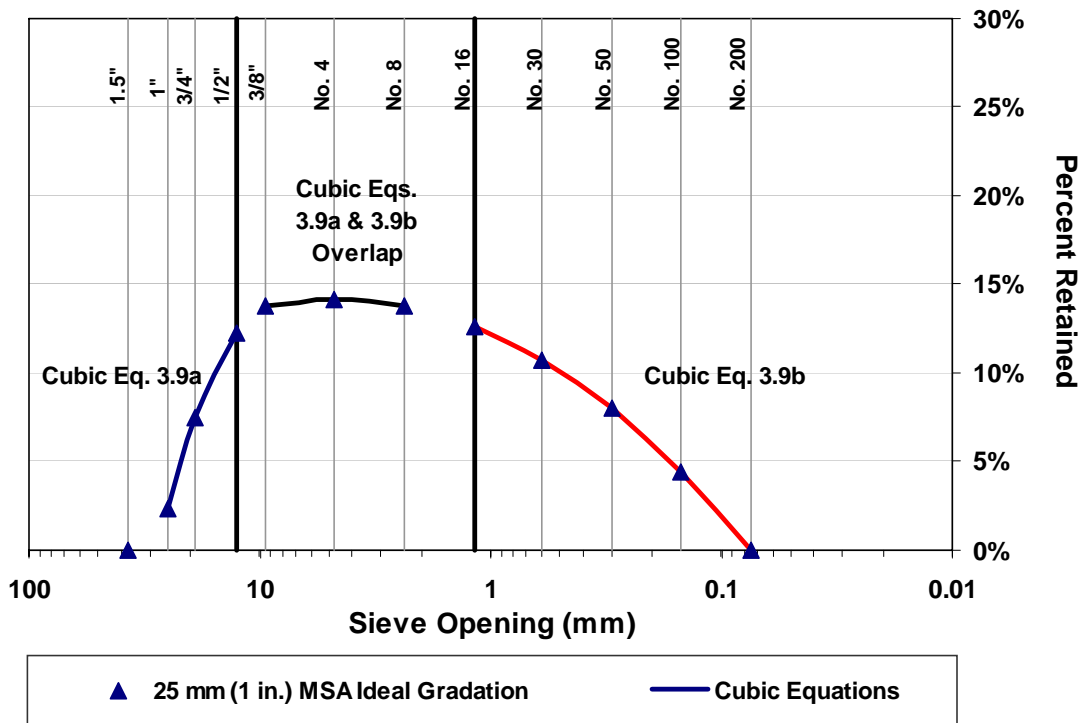


Fig. 3.2 – *Cubic-Cubic Model* of an ideal gradation with a 25-mm (1-in.) maximum size aggregate (MSA) plotted on a percent retained chart

3.2.2 Determining the *Ideal* Gradation

To solve for the eight coefficients in Eq. (3.9a) and (3.9b) (four for each cubic equation) that define the *Cubic-Cubic Model*, eight equations must be defined and solved simultaneously. The solution to the eight equations depends in part on the optimized combined gradation of the actual aggregates (which is initially unknown). This requires an iterative solution, with each iteration producing both an updated *ideal* gradation and an updated optimized gradation. The solution process is described in Section 3.3. Each of the eight equations is based on one of eight criteria that are used to define the model. These criteria are discussed next.

Criterion 1. The percentage of aggregate retained on the top sieve for the *ideal* gradation model is equal to the quantity retained on the top sieve of the final optimized aggregate gradation, and thus, the top sieve for the *ideal* gradation is controlled by the size of the actual aggregates available. For the *Cubic-Cubic Model*,

the top sieve size must be larger than or equal to 12.5-mm (½-in.) [because of the unique sieves that define the first cubic equation, Eq. (3.8a)]. It is not possible to determine the percent retained on the top sieve in the *ideal* gradation prior to optimizing the aggregate blend for the first time. For this reason, the user is required to select a range of percentages for the top sieve (defined by the desired minimum and maximum percents retained on the top sieve that are commonly specified in aggregate specifications). The midpoint of the range is used for the first iteration. The percentage retained on the top sieve of the *ideal* gradation is updated along with the percentage retained on the top sieve of the optimized gradation after an iteration is completed. This requirement ensures that the *ideal* gradation accurately represents the maximum size of the optimized combined gradation. When it is not possible for the percent retained on the top sieve to fall within the user-selected range using the actual aggregate gradations, [*e.g.*, the user selects a MSA of 25-mm (1.0-in.) but does not provide material that is retained on the 25-mm (1.0-in. sieve)], the maximum or minimum percentage is used to define the percent retained on the top sieve of the *ideal* gradation. The following relationship defines *Criterion 1*.

$$\bar{R}_{TS} = A(\log x_{TS})^3 + B(\log x_{TS})^2 + C(\log x_{TS}) + D \quad (3.10)$$

where x_{TS} = sieve opening size (mm) for the top sieve retaining aggregate
[must be larger than or equal to 12.5-mm (½-in.)]
 \bar{R}_{TS} = percent retained on the top sieve of the *ideal* gradation

Criterion 2. The quantity retained on the 0.075-mm (No. 200) sieve of the *ideal* gradation is set equal to the quantity retained on the 0.075-mm (No. 200) sieve of the optimized gradation. The value for the percent retained on the 0.075-mm (No. 200) sieve \bar{R}_i is initially unknown and assumed to be 2% by weight of the combined aggregate gradation. This value, in addition to the percent retained on the top sieve, is updated with the completion of each iteration. *Criterion 2* is shown in Eq. (3.11) using the notation presented in Tables 3.1 and 3.2.

$$\bar{R}_l = A'(\log x_l)^3 + B'(\log x_l)^2 + C'(\log x_l) + D' \quad (3.11)$$

Criteria 3 – 5. For both cubic equations that define the *ideal* gradation [Eq. (3.9a) and Eq. (3.9b)], the quantity retained on the 2.36-mm (No. 8), 4.75-mm (No. 4), and 9.5-mm ($\frac{3}{8}$ -in.) sieves must be equal. This requirement ensures both continuity and a smooth transition between the two cubic equations, as shown in Fig. 3.2. The equations resulting from these criteria are

$$\begin{aligned} A(\log x_g)^3 + B(\log x_g)^2 + C(\log x_g) + D &= \\ A'(\log x_g)^3 + B'(\log x_g)^2 + C'(\log x_g) + D' & \end{aligned} \quad (3.12)$$

$$\begin{aligned} A(\log x_f)^3 + B(\log x_f)^2 + C(\log x_f) + D &= \\ A'(\log x_f)^3 + B'(\log x_f)^2 + C'(\log x_f) + D' & \end{aligned} \quad (3.13)$$

$$\begin{aligned} A(\log x_e)^3 + B(\log x_e)^2 + C(\log x_e) + D &= \\ A'(\log x_e)^3 + B'(\log x_e)^2 + C'(\log x_e) + D' & \end{aligned} \quad (3.14)$$

Criteria 6 – 8. The *ideal* gradation is associated with target values of CF and WF (denoted CF_{ideal} and WF_{ideal}) that depend, in part, on the maximum size of the available aggregates and the percentage of aggregate retained on the top sieve (*Criterion 1*). The final three criteria required to solve for the eight coefficients that define the *Cubic-Cubic Model* are based on CF_{ideal} and WF_{ideal} . Initial values for CF_{ideal} and WF_{ideal} , 60 and 35, respectively, in the middle of Zone II in the MCFC, are selected for the first iteration, and subsequent values of CF_{ideal} and WF_{ideal} are selected using a process that is described in Section 3.2.3. Because $Q + I + W = 100\%$, specific values of CF and WF uniquely define Q , I , and W . Thus, CF_{ideal} and WF_{ideal} uniquely define Q_{ideal} , I_{ideal} , and W_{ideal} . Although not plotted directly on the percent retained chart, the percent passing the 0.075-mm (No. 200) sieve and retained on the pan is included in the W particles and in the *ideal* gradation model. As with the percent retained on the top sieve and the 0.075-mm (No. 200)

sieve, the percent retained on the pan of the *ideal* gradation is set equal to the percent retained on the optimized gradation. The initial percent retained on the pan for the *ideal* gradation model \bar{R}_{pan} is assumed to be 2% by weight of the combined aggregate gradation. Equations (3.15) through (3.17) are used to formulate the final three equations required to solve for the coefficients in the *Cubic-Cubic Model*.

$$Q_{ideal} = \sum_{n=TS}^e [A(\log x_n)^3 + B(\log x_n)^2 + C(\log x_n) + D] \quad (3.15)$$

$$I_{ideal} = \frac{A[(\log x_f)^3 + (\log x_g)^3] + B[(\log x_f)^2 + (\log x_g)^2]}{C[\log x_f + \log x_g] + 2D} \quad (3.16)$$

$$W_{ideal} - \bar{R}_{pan} = \frac{A'[(\log x_h)^3 + (\log x_i)^3 + (\log x_j)^3 + (\log x_k)^3 + (\log x_l)^3] + B'[(\log x_h)^2 + (\log x_i)^2 + (\log x_j)^2 + (\log x_k)^2 + (\log x_l)^2]}{C'[\log x_h + \log x_i + \log x_j + \log x_k + \log x_l] + 5D'} \quad (3.17)$$

3.2.3 Determining the CF_{ideal} and WF_{ideal}

There are an infinite number of combinations of CF and WF that plot within Zone II or Zone III on the Modified Coarseness Factor Chart and result in acceptable combined aggregate gradations. It is recognized, however, that mixtures plotting near the center of Zone II ($CF=60$, $WF=35$) with maximum size aggregates (MSA) ranging from 19-mm ($\frac{3}{4}$ -in.) to 37.5-mm ($1\frac{1}{2}$ -in.) consistently have good characteristics (ACI Committee 211 2004). It is also known that as either the MSA or the percentage retained on the top sieve for a given MSA decreases, the values of CF and WF providing these characteristics move closer to Zone III, the optimum region for concrete with a MSA smaller than 19-mm ($\frac{3}{4}$ -in.).

With this understanding, the *ideal* gradation is defined so that the locus of points (CF , WF) for the target values passes through the point (60, 35) and runs

parallel to the trend bar (theoretically optimum mixes) up through Zone III. This helps to ensure consistent aggregate gradations with desirable characteristics regardless of the MSA and percentage of the MSA. This relationship couples the values of CF and WF , thereby simplifying the calculation process and resulting in an *ideal* gradation that produces values of CF and WF that plot near the mid-height of Zone II or III. The locus of points (CF , WF) or *parallel line* that defines the relationship is plotted on the Modified Coarseness Factor Chart (ACI Committee 211 2004) in Fig. 3.3 and is represented by

$$WF(CF) = 2.17 \times 10^{-5} \cdot CF^3 - 0.00340 \cdot CF^2 + 0.0216 \cdot CF + 41.3 \quad (3.18)$$

where $WF(CF)$ is the workability factor as a function of the coarseness factor.

The coefficients for Eq. (3.18) are obtained by fitting a curve to data points taken from Shilstone's Coarseness Factor Chart (1990).

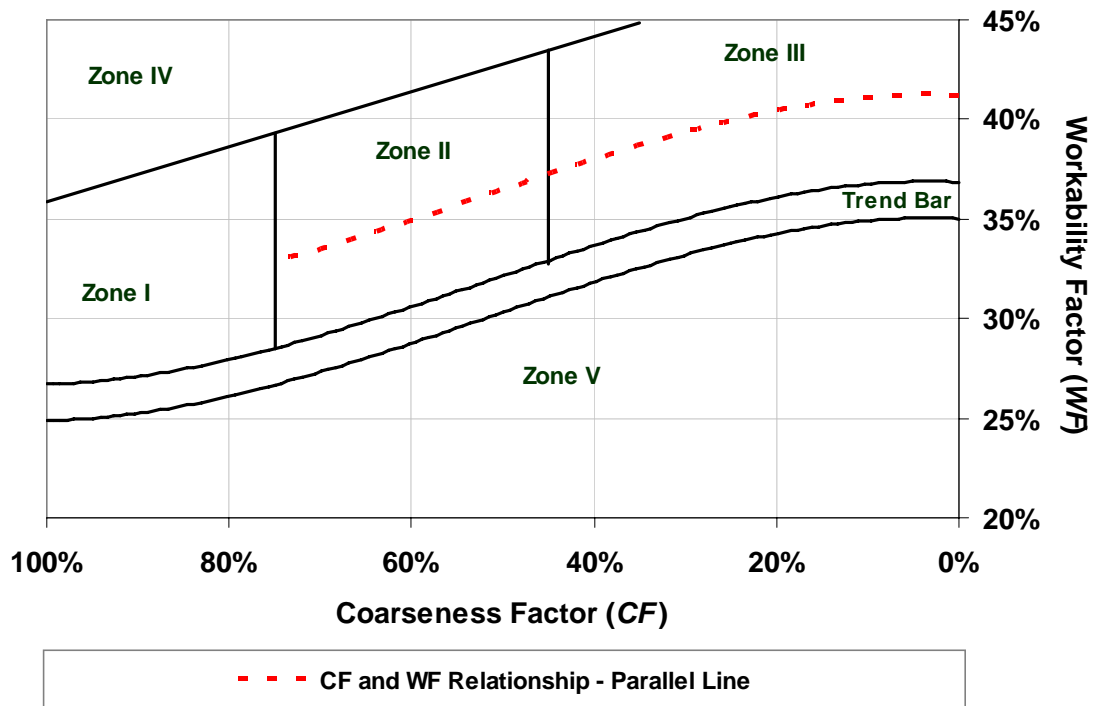


Fig. 3.3 – Relationship between the coarseness factor and workability factor plotted on the Modified Coarseness Factor Chart (MCFC)

It should also be noted that while specifying CF and WF using Eq. (3.18) is appropriate for most concrete, this relationship does not take into consideration the effect of aggregate particle shape on the properties of plastic concrete. Elongated, flat, or angular particles increase particle interference, and therefore, reduce concrete workability. For this reason, it may be necessary to adjust the *parallel line* upwards, so that for a given CF , the WF is higher. Likewise, natural round aggregate, such as river gravel, often has a lower paste demand than angular aggregate and a lower WF may be appropriate. The *parallel line* can be adjusted by changing the y-intercept from the value of 41.3 used in Eq. (3.18) [shown as $WF(0)=41.3\%$ in Fig. 3.3 and Eq. (3.18)].

In addition to defining an *ideal* gradation with CF and WF (Fig. 3.3) on the *parallel line* in Zone II or III, it is equally important to ensure that the *ideal* gradation plots as a haystack (or mound shape) on the percent retained chart (see Fig. 3.2). Simply solving for the eight coefficients that define the *Cubic-Cubic Model* (described in Section 3.2.2) using $CF=60$ and $WF=35$ will not necessarily ensure a properly-shaped *ideal* gradation. To achieve a properly-shaped *ideal* gradation using KU Mix, the sum of the absolute differences between the percents retained on the 2.36-mm (No. 8), 4.75-mm (No. 4), and 9.5-mm ($\frac{3}{8}$ in.) sieves is minimized by moving along the *parallel line* (changing CF_{ideal} and WF_{ideal}) on the MCFC (Fig. 3.3). This step couples the *ideal* gradation to both the quantity and the size of the largest aggregate particles by forcing the top of the haystack to occur over the intermediate particle sizes and the 9.5-mm ($\frac{3}{8}$ in.) sieve, thereby ensuring that the *ideal* gradation will be in the shape of a haystack. As either the MSA or the percentage retained on the top sieve for a given MSA decreases, CF_{ideal} and WF_{ideal} move towards Zone III, where a smaller percentage of Quality particles are required, further ensuring a haystack shape. The step to minimize the sum of the differences is summarized in Eq. (3.19) (using notation defined in Table 3.2).

$$\text{Minimize } \left\{ \left| \bar{R}_f - \bar{R}_g \right| + \left| \bar{R}_e - \bar{R}_f \right| + \left| \bar{R}_e - \bar{R}_g \right| \right\} \text{ by changing the } CF \text{ [Eq. (3.18)]} \quad (3.19)$$

A spreadsheet solver routine can easily be used to determine the values of CF and WF on the parallel line that fulfill this criterion. The process is further simplified because WF for the *ideal* gradation is a function of the CF , as defined by Eq. (3.18).

An example illustrating the importance of adjusting the CF and WF based on the quantity and size of the largest aggregate particles is shown in Fig. 3.4 for a combined aggregate gradation with 15% retained on the 12.5-mm ($\frac{1}{2}$ -in.) sieve both before and after minimizing Eq. (3.19). Prior to minimizing Eq. (3.19), the initial values for the CF_{ideal} and WF_{ideal} are 60 and 35, respectively. This point is in the middle of Zone II, the optimum region for concrete with a MSA between 19-mm ($\frac{3}{4}$ -in.) and 37.5-mm ($1\frac{1}{2}$ -in.), and provides a good starting point for the optimization process. It is clear, however, that $CF=60$ and $WF=35$ are not appropriate for all mixtures and that it does not always produce the desirable haystack shape, as shown in Fig. 3.4. Prior to minimization, CF is too high (and WF is slightly low), resulting in an unusual and undesirable shape with excess material on the 9.5-mm ($\frac{3}{8}$ -in.) sieve (due to a high CF) and deficiencies on the 4.75-mm (No. 4) through 0.60-mm (No. 30) sieves. When Eq. (3.19) is minimized by adjusting the CF_{ideal} and WF_{ideal} to 48.9 and 36.7, respectively, (moving towards Zone III along the *parallel line* on the MCFC), a well-defined haystack shape is attained with the 9.5-mm ($\frac{3}{8}$ -in.), 4.75-mm (No. 4), and 2.36-mm (No. 8) sieves retaining the greatest quantity of aggregate.

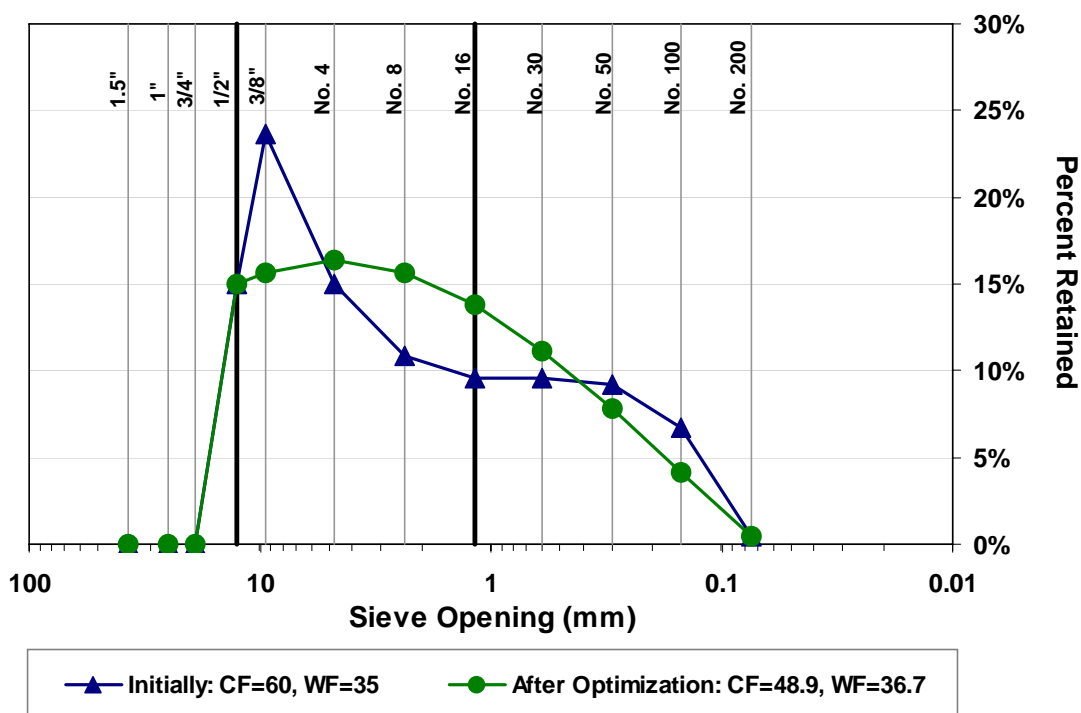


Fig. 3.4 – Effect of minimizing Eq. (3.19), “After Optimization,” on the combined aggregate gradation for the *Cubic-Cubic Model* with 15% retained on the 12.5-mm ($\frac{1}{2}$ -in.) sieve

3.2.4 Adjusting the *Ideal Gradation* to Account for Changes in the Cementitious Material Content

The modified coarseness factor chart developed by Shilstone (1990) is based on a U.S. six-sack mix [335 kg/m^3 (564 lb/yd^3) of portland cement] and any deviations must be accounted for by adjusting WF or W . The process for adjusting WF has typically been implemented by adjusting WF_{ideal} using a correction factor to account for deviations from a six-sack mix [shown in Eq. (1.2) and described in Section 1.6.1]. This correction does not adequately account for mineral admixtures, which have a different specific gravity than cement, and thus, affect workability differently when compared to cement on a weight basis.

The KU Mix approach involves calculating the volume of all cementitious materials and determining the deviation (by volume) from a U.S. six-sack mix. This

deviation is converted to an equivalent mass (weight) of fine aggregate (based on volume) that is added to the mass (weight) retained on the pan of the combined aggregate gradation. This procedure allows deviations in cementitious materials to be treated as changes in the quantity of W particles, ensuring that CF_{ideal} and WF_{ideal} always fall on the *parallel line* running through the center of Zone II and III, regardless of the cementitious material content. The procedure is outlined in the following eight steps.

Step 1. Calculate the total volume of the cementitious materials and subtract the volume of cement in a U.S. six-sack mix [335 kg/m^3 (564 lb/yd^3)] to determine the deviation (by volume) from a six-sack mix. A negative number indicates a deficiency in cementitious material (compared to a six-sack mix) and a positive number indicates excess cementitious materials. The equation used to perform this calculation is

$$V_{dev} = \frac{M_C}{SG_C \times UW_W} + \sum_p \left(\frac{M_p}{SG_p \times UW_W} \right) - \frac{6 \cdot S}{SG_C \times UW_W} \quad (3.20)$$

where

- V_{dev} = deviation (by volume) of cementitious material from a U.S. six-sack mix [335 kg/m^3 (564 lb/yd^3)]
- M_C, M_p = mass (weight) of cement or cementitious material p in kg (lb)
- SG_C, SG_p = specific gravity of cement or cementitious material
- UW_W = unit weight of water, 1000 kg/m^3 (62.4 lb/ft^3)
- S = mass (weight) of one U.S. sack of cement, 56 kg (94 lb)

Step 2. Convert V_{dev} to an equivalent mass (weight) of fine aggregate using Eq. (3.21). The mass (weight) of fine aggregate M_{dev} represents the mass (weight) of sand with a volume that is equal to V_{dev} . In cases where two or more “fine aggregates” are being considered, SG_{FA} corresponds to the aggregate with the lowest fineness modulus.

$$M_{dev} = V_{dev} \times SG_{FA} \times UW_W \quad (3.21)$$

where M_{dev} = mass (weight) of fine aggregate with a volume equal to V_{dev}
 SG_{FA} = specific gravity of the fine aggregate (aggregate with the lowest fineness modulus)

Step 3. Calculate the percent retained on each sieve for the combined aggregate gradation. This step requires the selection of possible aggregates, designated 1, 2 ... t , each with an assumed mass (weight) fraction of the total aggregate, expressed as $MF_1, MF_2 \dots MF_t$ (and collectively called the aggregate blend). Section 3.3 provides recommendations for the selection of the trial aggregate set to be considered in the optimization process. At this stage in the optimization process the optimum aggregate blend is unknown, and it may be assumed that each aggregate has an equal weight fraction (*e.g.*, if four aggregates are being considered, $MF_1=MF_2=MF_3=MF_4=25\%$) for the first iteration. The actual process for determining the optimum aggregate blend is discussed in Section 3.3. The combined percent retained on each sieve is calculated as

$$R_n = \frac{\sum^t MF_t \times r_{n,t}}{100} \quad (3.22)$$

where R_n = percent of total aggregate mass (weight) retained on sieve n for the combined gradation
 t = aggregate identification number
 MF_t = aggregate mass (weight) fraction in percent for aggregate t ($\sum MF_t = 100\%$)
 $r_{n,t}$ = percent retained on n sieve for aggregate t

Step 4. Convert the percent retained on each sieve R_n to an aggregate mass (weight) retained [on a per m^3 (yd^3) basis] on each sieve. This conversion requires the calculation of the total volume of aggregate V_{agg} . The volume of aggregate is calculated by determining the volume of the other constituents, cement paste and air. The volume of the cement paste and air are typically governed by the construction requirements or specifications. The volume of aggregate V_{agg} in the concrete mixture is

$$V_{agg} = UV - V_{paste} - V_{air} \quad (3.23)$$

where V_{agg} , V_{paste} , V_{air} = volume of aggregate, paste, and air in m^3 , (ft^3)
 UV = unit volume of concrete being designed, $1 m^3$ [$1 yd^3$ ($27 ft^3$)]

Details on handling chemical admixtures are provided in Section 3.4.

After the total volume of aggregate for the mixture has been calculated, the total mass (weight) of aggregate can be determined using the mass (weight) fractions MF_i [used in Eq. (3.22)] and the effective specific gravity SG_{Eff} of the combined aggregate. The effective specific gravity SG_{Eff} of the combined aggregate is calculated using Eq. (3.24), after which the total mass (weight) of aggregate is calculated using Eq. (3.25).

$$SG_{Eff} = \frac{100}{\frac{MF_1}{SG_1} + \frac{MF_2}{SG_2} + \dots + \frac{MF_t}{SG_t}} \quad (3.24)$$

$$M_{agg} = V_{agg} \times SG_{Eff} \times UW_w \quad (3.25)$$

Finally, the mass (weight) of the combined aggregate retained on each sieve M_n is calculated by multiplying the total mass (weight) of aggregate M_{agg} by the aggregate mass (weight) fractions retained on each sieve R_n [calculated in Eq. (3.22)].

$$M_n = M_{agg} \times R_n \quad (3.26)$$

Step 5. Add M_{dev} (calculated in Step 2) to the mass (weight) retained on the pan M_{pan} of the combined aggregate gradation [calculated using Eq. (3.26) in Step 4]. It should be noted that the new weight retained on the pan may be negative if there is a significant deficiency in cementitious materials compared to a U.S. six-sack mix. The new mass (weight) retained on each sieve is denoted M'_n for clarity, although the only difference between M_n and M'_n is the mass (weight) retained on the pan.

Step 6. Recalculate the percent retained on each sieve for the combined gradation including the addition of M_{dev} to the pan (*Step 5*) using Eq. (3.27). This new adjusted combined gradation R'_n now includes the effect of an excess or deficiency in cementitious materials.

$$R'_n = \frac{M'_n}{M_{agg} + M_{dev}} \quad (3.27)$$

Step 7. Calculate the sum of the workability particles W_{adj} for the adjusted combined gradation calculated in *Step 6*. The change in the workability particles ΔW resulting from a deviation in cementitious material from a U.S. six-sack mix is calculated as

$$\Delta W = W_{adj} - W \quad (3.28)$$

where ΔW = change in the workability particles resulting from a deviation (by volume) from a U.S. six-sack mix [335 kg/m³ (564 lb/yd³)]

W_{adj} = sum of the percents retained for the Workability particles of the adjusted combined gradation (*Step 6*)

W = sum of the percents retained for the Workability particles of the combined gradation before any adjustment (*Step 3*)

This change ΔW is subtracted from the workability particles of the *ideal* gradation W_{ideal} .

$$W'_{ideal} = W_{ideal} - \Delta W \quad (3.29)$$

where W'_{ideal} = sum of the percents retained for the Workability particles of the adjusted *ideal* gradation

This process ensures that the W particles for the *ideal* gradation will be adjusted to reflect the cementitious material of the actual mixture design.

Step 8. Calculate the new Quality particles Q'_{ideal} and Intermediate particles I'_{ideal} for the *ideal* gradation using CF_{ideal} , WF_{ideal} , and W'_{ideal} using Eqs. (3.5) and (3.7). Finally, recalculate the new *ideal* gradation using the *Cubic-Cubic Model*.

This process for adjusting the *ideal* gradation based on the cementitious material content of the concrete mixture must be performed for each iteration because the process depends on the updated CF_{ideal} and WF_{ideal} and, thus, the actual aggregate blend. Figure 3.5 summarizes the process.

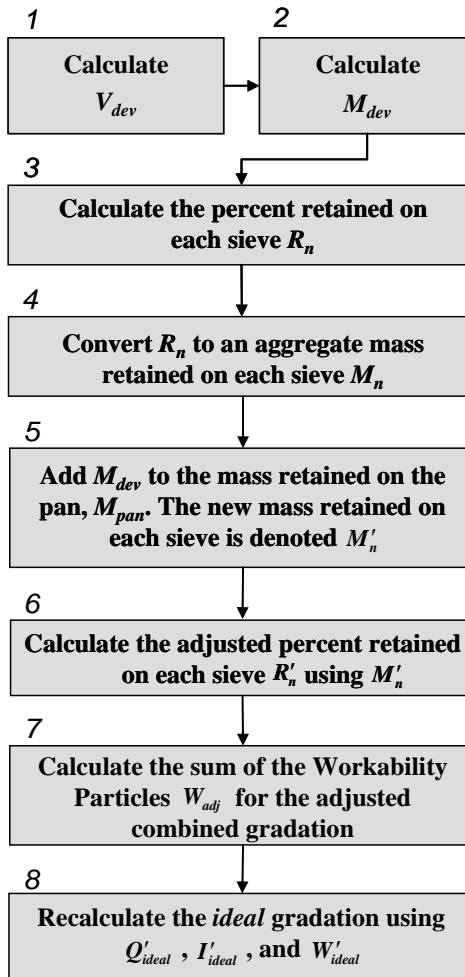


Fig. 3.5 – General procedure to adjust the *ideal* gradation based on the cementitious material content of the concrete mixture

3.3 OPTIMIZING THE ACTUAL AGGREGATE BLEND

The optimization process for selecting the combination, or blend, of aggregates requires that a trial set of aggregates be selected from those available for making the concrete. These aggregates should include at least one aggregate that

contains material retained on the desired maximum size sieve, and the remaining aggregates should contain material retained on all of the other size fractions. An iterative procedure based on a least squares fit is then performed to determine the combination of the trial aggregates that first, most closely matches the *ideal* gradation, and second, most closely matches WF_{ideal} and CF_{ideal} , which as explained in Section 3.2 depend, in turn, on the blend of aggregates (the combined gradation). This optimization process is described next.

3.3.1 Least Squares Fit of Blended Gradation to the *Ideal* Gradation

The first step is to perform a least squares fit of the potential gradations to the *ideal* gradation (obtained as described in Section 3.2). The least squares fit is performed to obtain the values of MF_t [the aggregate mass (weight) fractions in percent for each trial aggregate t] that provide the closest overall match between the percents of total aggregate mass (weight) R_n retained on all of the sieves for the *ideal* and combined gradations, \bar{R}_n and R_n , respectively [see Eq. (3.22) for R_n]. To perform a least squares fit, the sum of the squared differences between the percents retained for the combined and *ideal* gradations is minimized.

$$\text{Sum of Squares} = \sum (\bar{R}_n - R_n)^2 \quad (3.30)$$

A spreadsheet solver routine can easily be programmed to determine the values of MF_t that fulfill this criterion. The combination of aggregates produced by the minimization process represents the closest match to the *ideal* gradation for the aggregate set, but does not represent the completed optimized aggregate blend. Instead, this step provides initial values of MF_t for the least squares fit of the CF and WF described next.

3.3.2 Least Squares Fit of Blended CF and WF to CF_{ideal} and WF_{ideal}

The second step in the optimization process is to perform a least squares fit of the CF and WF for the combined gradations to the CF_{ideal} and WF_{ideal} (obtained as

described in Section 3.2.2) by modifying the values of MF_t obtained initially in Eq. (3.30).

$$\text{Sum of Squares} = (CF - CF_{ideal})^2 + (WF - WF_{ideal})^2 \quad (3.31)$$

The values of MF_t that minimize the squared difference between the combined gradation and the *ideal* gradation (determined in Section 3.3.1) are used as the initial values of MF_t to minimize the sum of the squares in Eq. (3.31). In many cases, more than one aggregate blend exists that will satisfy CF_{ideal} and WF_{ideal} . The use of these initial values MF_t ensures that minimizing Eq. (3.31) will always result in the same final values of MF_t since in some cases multiple solutions are possible. A spreadsheet solver routine, similar to the routine described in Section 3.3.1, can be programmed to determine the values of MF_t that minimize Eq. (3.31). This combination of aggregates represents the optimum gradation for the aggregate set, although additional iterations may still be required to obtain the final *ideal* gradation, as described in Section 3.3.3. The process for determining when the optimization process is complete is presented next.

3.3.3 Completing the Optimization Routine

The process of determining the optimized combination of aggregates, or optimized aggregate blend, is dependent on the *ideal* gradation, which also, in turn, depends on the percentages of aggregate retained on the pan, 0.075-mm (No. 200) sieve, and the top sieve of the actual combined aggregate gradation. These percentages for the *ideal* gradation are required to equal (within selected tolerances) the quantities retained on the corresponding sieves of the combined gradation. Because these percentages are initially unknown, they must be assumed for the first iteration and then updated for successive iterations.

The solution process, shown in Fig. 3.6, begins with the calculation of an initial *ideal* gradation and corresponding CF_{ideal} and WF_{ideal} (Section 3.2.2). Following the determination of the initial *ideal* gradation, a least squares fit of the

blended gradation to the *ideal* gradation is performed (Section 3.3.1) and immediately followed by a least squares fit to the WF_{ideal} and CF_{ideal} (Section 3.3.2). A new *ideal* gradation is next established by setting the percents retained on the pan, 0.075-mm (No. 200) sieve, and the top sieve of the *ideal* gradation equal to the quantities retained on the corresponding sieves of the combined gradation, and the process is repeated as necessary until the sum of the absolute differences between the percents retained on the pan, 0.075-mm (No. 200) sieve, and the top sieve for the combined and *ideal* gradations is less than 0.1%. If the percentage retained on the top sieve is outside the desired range (described in Section 3.2.2), then the percent retained on the top sieve for the *ideal* gradation is set to the minimum or maximum of the range and the difference is excluded from the calculation.

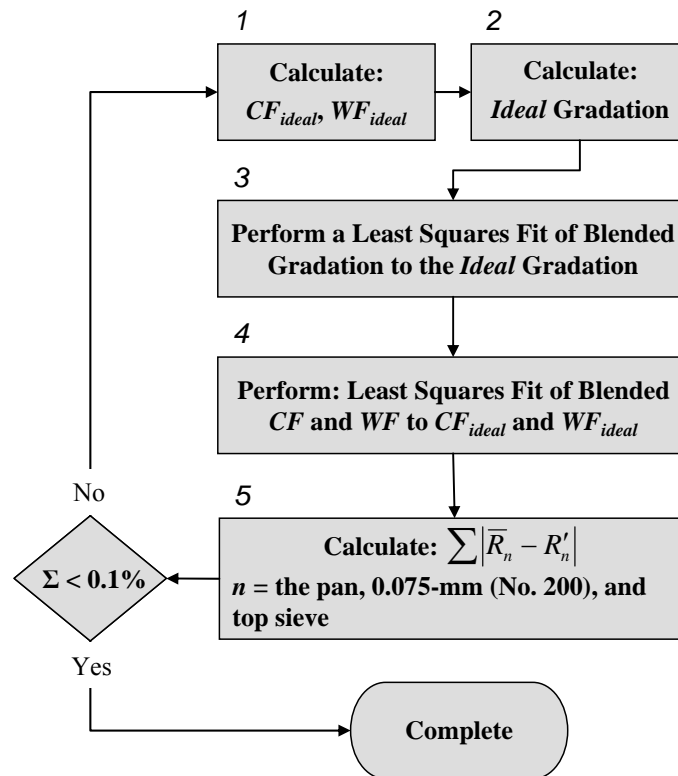


Fig. 3.6 – General Optimization and Iteration Procedure

3.3.4 Additional Constraints and Manual Adjustments

In some circumstances, it may be necessary to set a minimum or maximum limit on the weight fraction of a particular aggregate. For example, the user may limit the quantity of an aggregate to a specific percentage because of concerns with the alkali-aggregate reaction or simply to limit the quantity of a particular aggregate. These additional constraints can easily be added to the optimization routine, but doing so may limit the ability to obtain an optimized gradation.

The optimization routine emphasizes obtaining CF_{ideal} and WF_{ideal} , and as a result, the optimized combined gradation may have deficiencies or abundances on individual sieves compared to the *ideal* gradation. It may be possible to manually adjust the aggregate blend to minimize the deficiencies while maintaining “acceptable” values for CF and WF . Likewise, the optimization procedure does not ensure that the combined gradation will meet specifications for the percent retained on individual sieves, and so it may also be necessary to manually adjust the aggregate blend to meet these requirements.

3.4 CONCRETE MIXTURE PROPORTIONING

Completing the mixture proportioning is the final step. Several of the quantities have already been selected, calculated, or are known as the result of the aggregate optimization process. These quantities include: the mass (weight) of each cementitious material and the corresponding specific gravities, the water content, the total aggregate content and the effective specific gravity of the combined aggregates, and the air content. Only the individual mass (weight) of each aggregate and the contribution of the chemical admixtures to the water content of the mixture design remain to be calculated.

The individual mass (weight) of each aggregate is calculated by multiplying the aggregate mass (weight) fraction by the total mass (weight) of aggregate.

$$M_t = \frac{MF_t}{100} \times M_{agg} \quad (3.32)$$

where M_t = mass (weight) of aggregate t

Admixture dosage rates are generally based on manufacturer recommendations or trial batch experience. These dosages generally represent a small percentage of the volume of the concrete mixture, and as a result, are often neglected during mix design and added to the already complete mixture design. This practice neglects the contribution of the admixtures to the water content of the mixture, which may significantly affect the w/cm ratio, especially when water reducers or shrinkage reducing admixtures are used. Equation (3.33) is used to calculate the contribution of the chemical admixtures to the water content of the mixture. To do this, the amount of water [by mass (weight)] added to the mixture by the chemical admixtures is approximated as

$$M_{a-w} = \sum \left[V_{C_k} \times SG_{C_k} \times UW_W \times \left(1 - \frac{PS_{C_k}}{100} \right) \right] \quad (3.33)$$

where M_{a-w} = mass (weight) water contribution from chemical admixtures
 C_k = chemical admixture identification number
 V_k = admixture C_k dosage rate (by volume)
 UW_W = unit weight of water, 1000 kg/m³ (62.4 lb/yd³)
 PS_{C_k} = percent solids of admixture C_k

The contribution of water from the admixtures M_{a-w} is then subtracted from the design water content of the mixture.

As with other mixture design techniques, trial batches must be completed using the selected aggregates, cementitious materials, and chemical admixtures to ensure that the concrete has adequate workability, finishability, and cohesiveness and that the chemical admixtures have the desired effect on the properties of the plastic concrete.

CHAPTER 4: FREE-SHRINKAGE RESULTS AND EVALUATION

4.1 GENERAL

This chapter presents the results of six free-shrinkage test programs used to measure the relative performance of concrete mixtures as a function of paste content, water-cementitious (w/cm) material ratio, aggregate type, mineral admixture type and content, cement type and fineness, shrinkage reducing admixture, and the duration of curing. Performance is evaluated over a one-year period with special attention given to the early-age shrinkage that occurs during the first 30 days of drying. Early-age shrinkage is of special importance for bridge decks since the tensile stresses induced by long-term shrinkage are generally decreased due to the effects of tensile creep. The free-shrinkage measurements were taken in accordance with ASTM C 157.

The mixture designs evaluated in this chapter have two primary goals: First, to determine the effect of different variables on concrete shrinkage, but also, to develop mixtures that are suitable for use in the field. Careful consideration was given to the aggregate gradations, cohesiveness, workability, finishability, and apparent constructability prior to casting the laboratory specimens. All of the mixtures evaluated in this study have an optimized aggregate gradation, paste volumes less than 24.4%, a design air content of 8%, and a target slump of 75 ± 25 mm (3 ± 1 in.). Actual values for air content ranged from 7.9 to 8.9% and slump values ranged from 50 to 100 mm (2 to 4 in.).

The evaluation includes a total of 56 individual concrete batches that are divided into six test programs. Program I evaluates mixtures with w/c ratios ranging from 0.41 to 0.45 containing either a relatively porous limestone coarse aggregate (with an absorption between 2.5 and 3.0%) or granite coarse aggregate (with an absorption below 0.7%). In addition, concrete containing with limestone coarse aggregate are made with both Type I/II and coarse-ground Type II cement. For this

program, a reduction in the w/c ratio is obtained by reducing the water content (and paste volume) and replacing the water with an equal volume of aggregate while maintaining workability using a high-range water reducer. The effects of paste content, w/c ratio, and curing period are evaluated in Program II. The first set in this series includes four mixtures with w/c ratios of 0.36, 0.38, 0.40, and 0.42. Unlike the specimens cast in Program I with variable paste contents, these mixtures all have a paste content of 23.3%. A second set includes mixtures with a w/c ratio of 0.42, a paste content of either 23.3% or 21.6%, and a curing period of either 7, 14, or 21 days. Program III evaluates three coarse aggregates (granite, quartzite, and limestone) to determine their effect on free shrinkage, and Program IV examines the effect of a shrinkage reducing admixture on free shrinkage. The influence of cement type and fineness on free shrinkage is examined in Program V. Four portland cements (one Type I/II, two Type II, and one Type III) with Blaine fineness values ranging from 323 to 549 m^2/g are included in the Program V evaluation. The final test program evaluates three mineral admixtures as partial replacements for Type I/II cement. The mineral admixtures (and volume replacements examined) include silica fume (3 and 6% volume replacement), Class F fly ash (20 and 40%), and Grade 100 and 120 slag cement (30 and 60%). A minimum of two sources and two coarse aggregate types are included in the evaluation for each mineral admixture.

Unless noted, the free-shrinkage values reported in this chapter represent the average of three specimens that were cast for each mixture and curing period. The individual specimen free-shrinkage curves are presented in Appendix C in Figs. C.1 through C.113. Mixture proportions, plastic properties, and compressive strengths for the 56 individual concrete batches included in the comparisons are provided in Appendix A in Tables A.3 through A.20. The following section briefly describes the Student's t -test, which is used to determine if observed differences between two free-shrinkage samples represent statistically significant differences between populations.

4.2 STATISTICAL ANALYSIS

In many cases, the sample sizes and the differences between the means of categories are small. The Student's t-test is used to determine whether the differences between two samples represent significant differences between the corresponding populations. The Student's t-test is a parametric test that is frequently used when samples are small and the true population characteristics are unknown. The t-test relies on the means of the two sample groups, the size of the samples, and the standard deviation of each group to determine statistical significance. Specifically, the test is used to determine whether differences in the sample means, X_1 and X_2 , represent differences in the population means, μ_1 and μ_2 , at a specified level of significance α . For example, $\alpha = 0.05$ indicates a 5% chance that the test will incorrectly identify (or a 95% chance that the test will correctly identify) a statistically significant difference in sample means when, in fact, there is no difference (there is a difference). A two-sided test is used in the analyses, meaning that there is a probability of $\alpha/2$ of identifying that $\mu_1 > \mu_2$ and a probability of $\alpha/2$ of identifying that $\mu_1 < \mu_2$ when in fact, μ_1 and μ_2 are equal. The results of the Student's t-test are presented in tables that follow a standard format. A "Y" indicates that the difference being considered is statistically significant at $\alpha = 0.02$ (98% certainty that the difference is in fact significant), while an "N" indicates that the difference between samples is not statistically significant at the lowest confidence level considered, $\alpha = 0.2$ (80%). Statistically significant differences at confidence levels of least $\alpha = 0.2$, $\alpha = 0.1$, and $\alpha = 0.05$ are indicated by "80", "90", and "95", respectively.

4.3 ADDITIONAL FREE SHRINKAGE TEST DETAILS

Several steps have been taken to ensure that the comparisons provided in this chapter represent the actual relative shrinkage behavior that should be expected in the field. With the exception of Program V, which examines the effect of cement type

and fineness on free shrinkage, comparisons are only made between mixtures containing the same sample of cement. The reason is that considerable differences may exist between cement samples obtained at different times – even when they are from the same source. Additionally, all mixtures compared within a series were cast within two months, thereby helping to minimize any changes resulting from seasonal differences either with respect to the materials or the laboratory conditions. These restrictions limit some of the comparisons in Program I and Program VI.

All of the specimens were cast and protected against moisture loss for $23\frac{1}{2} \pm \frac{1}{2}$ hours (in accordance with ASTM C 157), demolded, and the initial length reading was recorded. The specimens were then cured in lime-saturated water for 6 or 13 additional days (making the total curing period 7 or 14 days). Following the specified curing period, the specimens were removed from the lime tank, measured, placed into the controlled drying environment, and then measured regularly over the course of one year. An example plot illustrating these readings is shown in Fig. 4.1, where day zero indicates the specimens were cast, and day one indicates they were demolded. Additional free-shrinkage measurements were taken during the curing period. When presented in this fashion, it is difficult to make worthwhile comparisons at a given age due to differences in the length of the drying period. For this reason, all of the comparisons presented in this chapter are based on the total drying time, as shown in Fig. 4.2, where the shrinkage reading on day zero indicates the average strain measured immediately after the specimens are removed from the curing tank.

4.4 PROGRAM I (PASTE CONTENT, W/C RATIO, CURING PERIOD)

Program I involved three sets of concrete mixtures examining the combined effects of paste content, w/c ratio, and curing period on free shrinkage. Three w/c ratios (0.41, 0.43, and 0.45) were examined for each set in conjunction with 7 and 14 day curing periods. Each mixture had a cement content of 317 kg/m^3 (535 lb/yd^3). A reduction in the w/c ratio from 0.45 to 0.41 was obtained by reducing the water

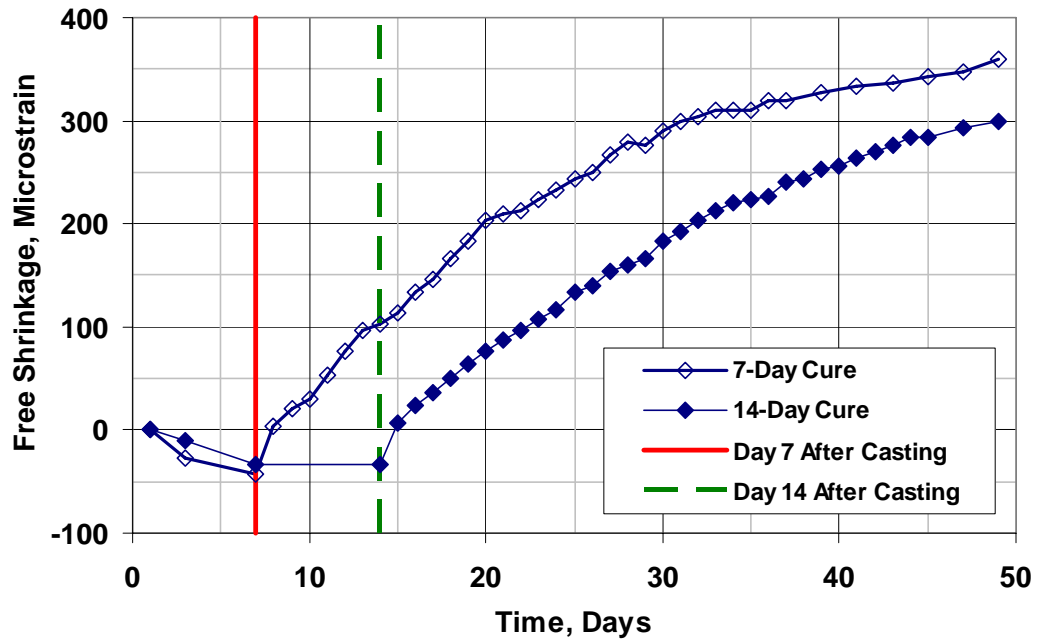


Fig. 4.1 – Free-Shrinkage Test (ASTM C 157). Example average free-shrinkage curves with specimens demolded on day 1 and cured for an additional 6 or 13 days.

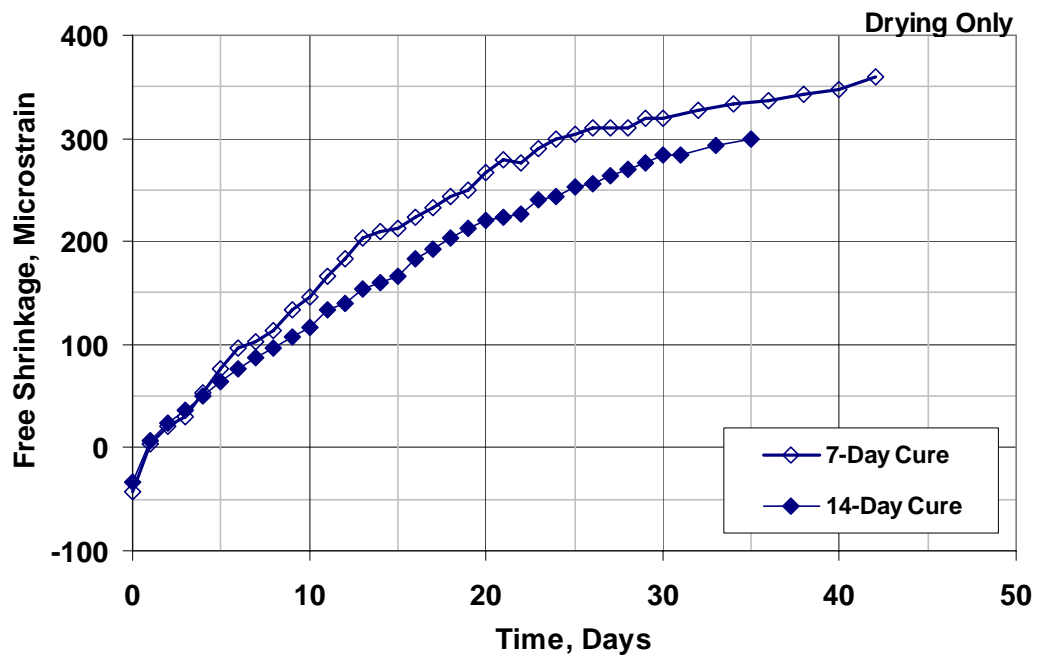


Fig. 4.2 – Free-Shrinkage Test (ASTM C 157). Example average free-shrinkage curves showing drying time only.

content and replacing the water with an equal volume of aggregate. Reducing the w/c ratio from 0.45 to 0.41 resulted in a 1.3% reduction in the paste content. Additional Program I details are provided in Section 2.9.1, and mixture designs, plastic concrete properties, and compressive strengths are provided in Tables A.3 through A.5 in Appendix A.

A summary of Program I is provided in Table 4.2. Sets 1 and 3 contain Type I/II cement, while Set 2 contains Type II cement. The average Blaine fineness for the Type I/II cement used in Sets 1 and 3 is $377 \text{ m}^2/\text{kg}$ compared to $334 \text{ m}^2/\text{kg}$ for the Type II cement. Sets 1 and 2 contain a relatively porous limestone coarse aggregate (with an absorption between 2.5 and 3.0%), and Set 3 contains granite coarse aggregate (0.60% absorption).

Table 4.2 – Program I Summary

Program I Set Number	Coarse Aggregate Type	Portland Cement Type
1	Limestone	Type I/II
2	Limestone	Type II
3	Granite	Type I/II

Many researchers have observed that a reduction in the cement paste content leads to a reduction in shrinkage (Pickett 1956, Ödman 1968, Bissonnette et al. 1999, Deshpande et al. 2007). Of particular interest here, however, are observations from previous studies that the use of high-range water reducers [used in this program to reduce the paste content while maintaining a slump between 60 and 90 mm (2.25 to 3.5 in.)] may lead to increased shrinkage (Ghosh and Malhotra 1979, Feldman and Swenson 1975). This observation is contrary to the behavior observed in this study.

4.4.1 Program I Set 1 (Limestone Aggregate, Type I/II Portland Cement)

The average free-shrinkage data for Set 1 after 0, 30, 90, 180, and 365 days of drying are presented in Table 4.3, and the corresponding individual free-shrinkage

curves are presented in Figs. C.1 through C.3 in Appendix C. Expansion (indicated as negative strain in Table 4.3) measured at the end of the curing period varied from 10 to 23 $\mu\epsilon$, and no clear relationship was observed as functions of w/c ratio or curing period. For each w/c ratio, an increase in the curing period from 7 to 14 days decreases shrinkage at all ages. Shrinkage is further reduced as the w/c ratio (and paste content) is reduced from 0.45 to 0.41, and thus, the greatest shrinkage is observed for the 0.45 w/c ratio specimens cured for 7 days, and the least shrinkage is observed for the 0.41 w/c ratio specimens cured for 14 days.

Table 4.3 – Summary of Program I Set 1 Free-Shrinkage Data (in microstrain)

Days of Drying	0.45 w/c		0.43 w/c		0.41 w/c	
	7-Day Cure	14-Day Cure	7-Day Cure	14-Day Cure	7-Day Cure	14-Day Cure
0	-20	-17	-13	-23	-10	-23
30	343	317	323	290	280	263
90	507	493	450	433	400	387
180	530	503	470	457	437	423
365	560	547	487	477	440	433

The average free-shrinkage curves for each mixture through the first 30 days of drying are presented in Fig. 4.3. The results show that the extra quantity of high-range water reducer (HRWR) added to offset the reduction in water content and maintain a constant slump did not result in an increase in shrinkage. Instead, shrinkage decreased as a result of a decrease in the w/c ratio (and paste content) obtained by reducing the water content. This trend is established after only a few days of drying. An increase in the curing period from 7 to 14 days also resulted in a reduction in shrinkage for each w/c ratio. After only 30 days of drying, increasing the curing period reduced shrinkage by 26, 33, and 17 $\mu\epsilon$ for the 0.45, 0.43, and 0.41 w/c ratio mixtures, respectively. The effect of curing was more pronounced during the first 30 days than for any other time during the test. While these differences due to curing are consistent for each w/c ratio, only the difference observed for the 0.41 w/c

ratio mixture is statistically significant ($\alpha = 0.1$) (Table 4.4). As the w/c ratio is reduced from 0.45 to 0.43, shrinkage decreases from 343 to 323 $\mu\epsilon$ for the specimens cured for 7 days and from 317 to 290 $\mu\epsilon$ for the 14-day specimens. The only statistically significant difference between these two mixtures occurred between the 7-day 0.45 w/c ratio mix and the 14-day 0.43 w/c ratio mix ($\alpha = 0.2$) (Table 4.4). Shrinkage decreases further to 280 $\mu\epsilon$ for the 7-day 0.41 w/c ratio mix and 263 $\mu\epsilon$ for the 14-day 0.41 w/c ratio mix. All of the differences observed between the 0.45 and 0.41 w/c ratio mixtures are statistically significant in addition to the differences observed between the 7-day 0.43 w/c ratio mix and the 0.41 w/c ratio mix (Table 4.4).

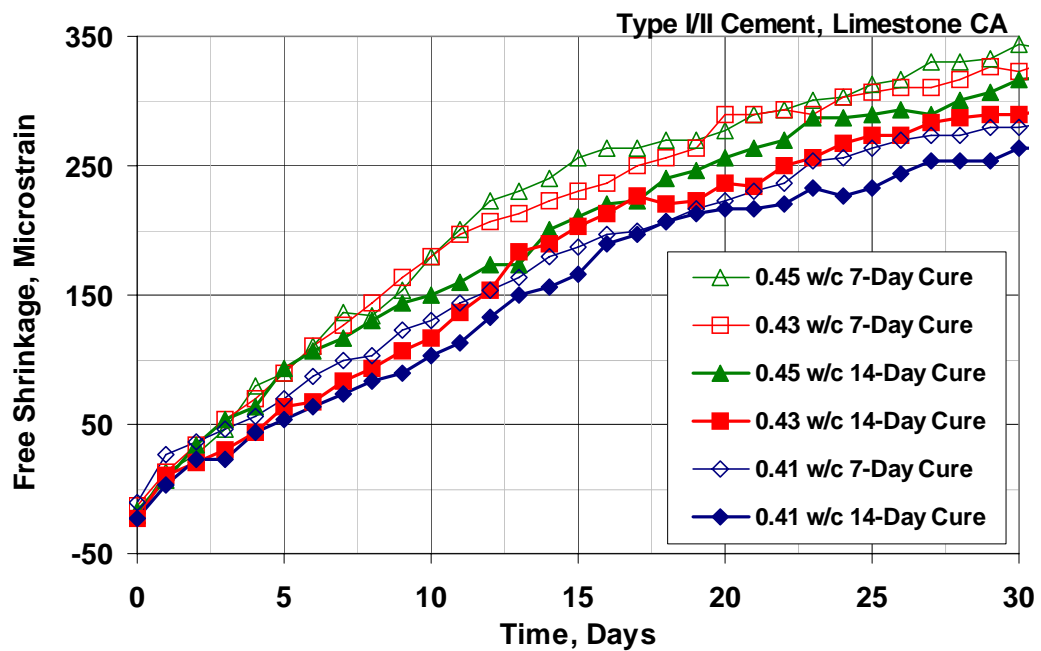


Fig. 4.3 – Free-Shrinkage Test (ASTM C 157). Program I Set 1. Average free shrinkage versus time through 30 days (drying only).

Table 4.4 – Student’s t-test Results for Program I Set 1 30-Day Free-Shrinkage Data

		30-Day Free Shrinkage ($\mu\epsilon$)	0.45 w/c		0.43 w/c		0.41 w/c	
			7-Day	14-Day	7-Day	14-Day	7-Day	14-Day
0.45 w/c	7-Day	343		N	N	80	Y	Y
	14-Day	317			N	N	80	95
0.43 w/c	7-Day	323				N	90	95
	14-Day	290					N	N
0.41 w/c	7-Day	280						90
	14-Day	263						

Note: For the results of the Student’s t-tests, “Y” indicates a statistical difference between the two samples at a confidence level of $\alpha = 0.02$ (98%). “N” indicates that there is no statistical difference at the lowest confidence level, $\alpha = 0.2$ (80%). Statistical differences at confidence levels at, but not exceeding $\alpha = 0.2, 0.1,$ and 0.05 are indicated by “80”, “90”, and “95”.

The average free-shrinkage curves for each mixture throughout the one-year drying period are presented in Fig. 4.4. After 90 days of drying, the effect of reducing the w/c ratio from 0.45 to 0.41 (and paste content) is easily observed. Average shrinkage decreases by about $60 \mu\epsilon$ as the w/c ratio is reduced from 0.45 to 0.43, and a similar decrease is observed with a further reduction in the w/c ratio to 0.41. During this period, increasing the curing time from 7 to 14 days resulted in an average reduction in shrinkage of only $14 \mu\epsilon$ with none of the differences being statistically significant at 365 days (Table 4.5). The 0.41 w/c ratio mixes exhibited the least shrinkage ($440 \mu\epsilon$ for the specimens cured for 7 days and $433 \mu\epsilon$ for the specimens cured for 14 days), followed by the 0.43 w/c ratio mixes (487 and $477 \mu\epsilon$, respectively) and the 0.45 w/c ratio mixes (560 and $547 \mu\epsilon$, respectively). All of the differences in shrinkage observed between the 0.41 and 0.45 w/c ratio mixes are statistically significant at $\alpha = 0.02$, and the differences between the 0.43 and 0.45 w/c ratio mixes are significant at least at $\alpha = 0.20$. The differences observed between the 14-day 0.41 w/c ratio mix and the 0.43 w/c ratio mixes are significant at $\alpha = 0.20$, although as shown in Table 4.5, the differences observed between the 7-day 0.41 w/c ratio mix and the 0.43 w/c ratio mixes are not significant.

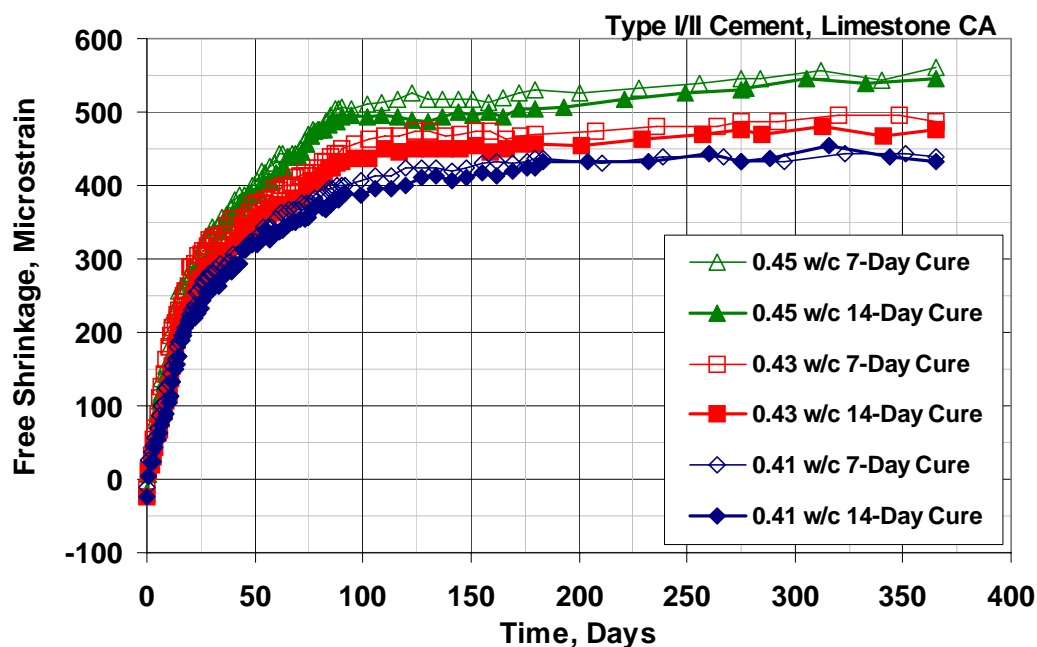


Fig. 4.4 – Free-Shrinkage Test (ASTM C 157). Program I Set 1. Average free shrinkage versus time through 365 days (drying only).

Table 4.5 – Student’s t-test Results for Program I Set 1 365-Day Free-Shrinkage Data

		365-Day Free Shrinkage ($\mu\epsilon$)	0.45 w/c		0.43 w/c		0.41 w/c	
			7-Day	14-Day	7-Day	14-Day	7-Day	14-Day
0.45 w/c	7-Day	560		N	95	Y	Y	Y
	14-Day	547			80	90	Y	Y
0.43 w/c	7-Day	487				N	N	80
	14-Day	477					N	80
0.41 w/c	7-Day	440						N
	14-Day	433						

Note: See the Table 4.4 note for an explanation of the terms “N”, “80”, “90”, “95”, and “Y”.

4.4.2 Program I Set 2 (Limestone Coarse Aggregate, Type II Portland Cement)

The effect of curing period, paste content, and w/c ratio on shrinkage is further illustrated in Set 2 using Type II portland cement rather than Type I/II. The average Blaine fineness of the cement in Set 2 is 334 m²/kg compared to 377 m²/kg for Set 1.

Chariton and Weiss (2002) and Deshpande et al. (2007) found that concrete cast with coarser cements shrink less than concrete containing fine cements. Lower shrinkage is associated with coarse cements for two reasons: First, the unhydrated portion of the large cement particles act as aggregate and restrain the shrinking paste, and second, the coarser pore structure results in lower capillary stresses, and thus, lower shrinkage. Those two studies, however, compared a much broader range of cement finenesses than the current study.

The following section compares the performance of concrete containing only Type II portland cement; a direct comparison of the shrinkage performance of concrete containing Type I/II and Type II cement is presented in Section 4.4.4. The average free-shrinkage data for Set 2 after 0, 30, 90, 180, and 365 days of drying are presented in Table 4.6. The individual free-shrinkage curves for each specimen are presented in Figs. C.4 through C.6 in Appendix C. The results indicate that the free-shrinkage specimens cast with Type II cement are more sensitive to the curing period than specimens cast with Type I/II cement, particularly for mixes with a high w/c ratio. The overall trend remains the same: a reduction in the w/c ratio (and paste content) and an increase in the curing period reduces shrinkage.

Figure 4.5 shows the average free-shrinkage strain versus time for each mixture during the first 30 days of drying. All of the specimens expanded slightly during the curing period (13 to 23 $\mu\epsilon$). After 30 days of drying, the 7-day 0.45 w/c ratio mix had the greatest shrinkage (340 $\mu\epsilon$), while the 14-day 0.41 w/c ratio mix had the least shrinkage (253 $\mu\epsilon$). The 7-day 0.43 w/c ratio mix cured for 7 days had the second highest shrinkage (313 $\mu\epsilon$), followed by the 14-day 0.45 w/c ratio mix (297 $\mu\epsilon$), the 7-day 0.41 w/c ratio mix (287 $\mu\epsilon$), and the 0.43 and 0.41 w/c ratio mixes both cured for 14 days (270 and 253 $\mu\epsilon$, respectively). The results of the Student's t-test for Program II Set 2 after 30 days of drying are presented in Table 4.7. Increasing the curing period from 7 to 14 days resulted in a reduction of 43, 43, 34 $\mu\epsilon$ for the 0.45,

Table 4.6 – Summary of Program I Set 2 Free-Shrinkage Data (in microstrain)

Days of Drying	0.45 w/c		0.43 w/c		0.41 w/c	
	7-Day Cure	14-Day Cure	7-Day Cure	14-Day Cure	7-Day Cure	14-Day Cure
0	-17	-13	-13	-20	-23	-20
30	340	297	313	270	287	253
90	497	447	470	407	437	407
180	513	483	510	450	450	430
365	553	517	533	470	477	450

0.43, and 0.41 w/c ratio mixtures, respectively. The differences observed for the 0.45 and 0.43 w/c ratio mixtures are statistically significant at the highest level, while the difference observed for the 0.41 w/c ratio mix is not significant.

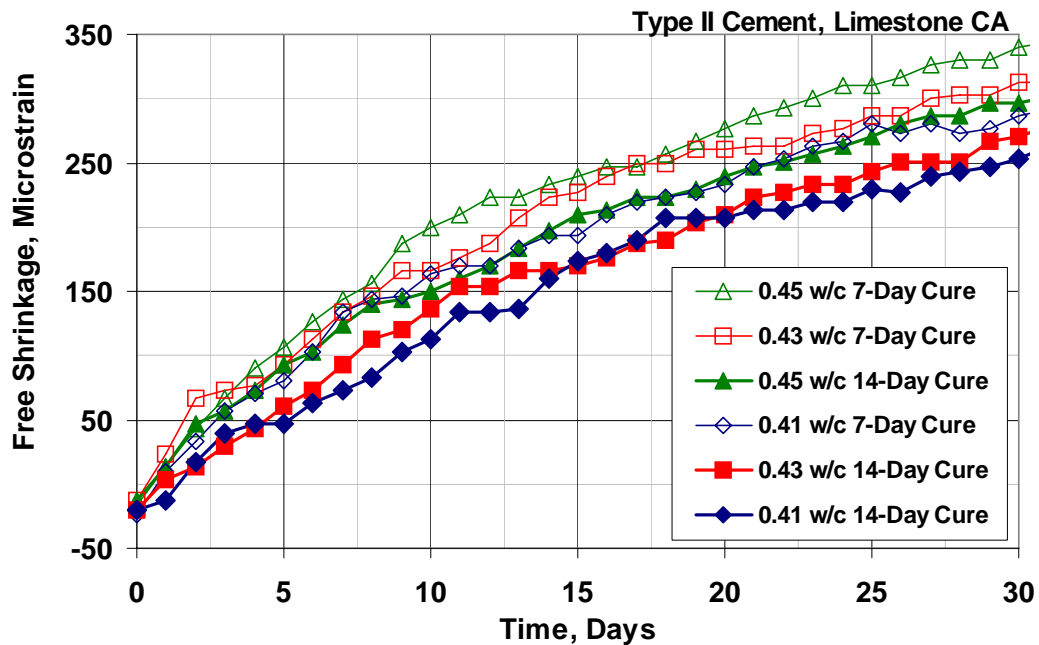


Fig. 4.5 – Free-Shrinkage Test (ASTM C 157). Program I Set 2. Average free shrinkage versus time through 30 days (drying only).

Table 4.7 – Student’s t-test Results for Program I Set 2 30-Day Free-Shrinkage Data

		30-Day Free Shrinkage ($\mu\epsilon$)	0.45 <i>w/c</i>		0.43 <i>w/c</i>		0.41 <i>w/c</i>	
			7-Day	14-Day	7-Day	14-Day	7-Day	14-Day
0.45 <i>w/c</i>	7-Day	340		Y	Y	Y	90	Y
	14-Day	297			95	Y	N	90
0.43 <i>w/c</i>	7-Day	313				Y	N	95
	14-Day	270					N	N
0.41 <i>w/c</i>	7-Day	287						N
	14-Day	253						

Note: See the Table 4.4 note for an explanation of the terms “N”, “80”, “90”, “95”, and “Y”.

Figure 4.6 presents the average free-shrinkage curves throughout the one-year drying period. The results of the Student’s t-test are presented in Table 4.8. Unlike the results for the Type I/II cement mixes (Program I Set 1), all of the differences in shrinkage resulting from increasing the curing period from 7 to 14 days (for a given *w/c* ratio) are statistically significant. This further emphasizes the sensitivity of the Type II cement to the length of the curing period. The relatively small surface area of the cement particles results in a slower hydration reaction, making the concrete more sensitive to the length of the curing period. Shrinkage is reduced by 36 $\mu\epsilon$ for the 0.45 *w/c* ratio mix, 63 $\mu\epsilon$ for the 0.43 *w/c* ratio mix, and 27 $\mu\epsilon$ for the 0.45 *w/c* ratio mix as the curing period is increased from 7 to 14 days. For the 7-day specimens, shrinkage decreased by 20 $\mu\epsilon$ as the *w/c* ratio is reduced from 0.45 to 0.43. This small difference is not statistically significant, although a much larger (and statistically significant) decrease in free-shrinkage (approximately 70 $\mu\epsilon$) is observed as the *w/c* ratio is reduced further to 0.41. The specimens cured for 14 days exhibit a similar trend. Free shrinkage decreased by 47 $\mu\epsilon$ as the *w/c* ratio is reduced from 0.45 to 0.43 and by 20 $\mu\epsilon$ as the *w/c* ratio is reduced further to 0.41. The difference observed between the 14-day 0.45 and 0.43 *w/c* ratio mixes is statistically significant at $\alpha = 0.05$, but the difference between the 0.43 and 0.41 *w/c* ratio mix is not

significant. The 67 $\mu\epsilon$ reduction as the w/c ratio is decreased from 0.45 to 0.41 w/c ratio is statistically significant at $\alpha = 0.05$ (Table 4.8).

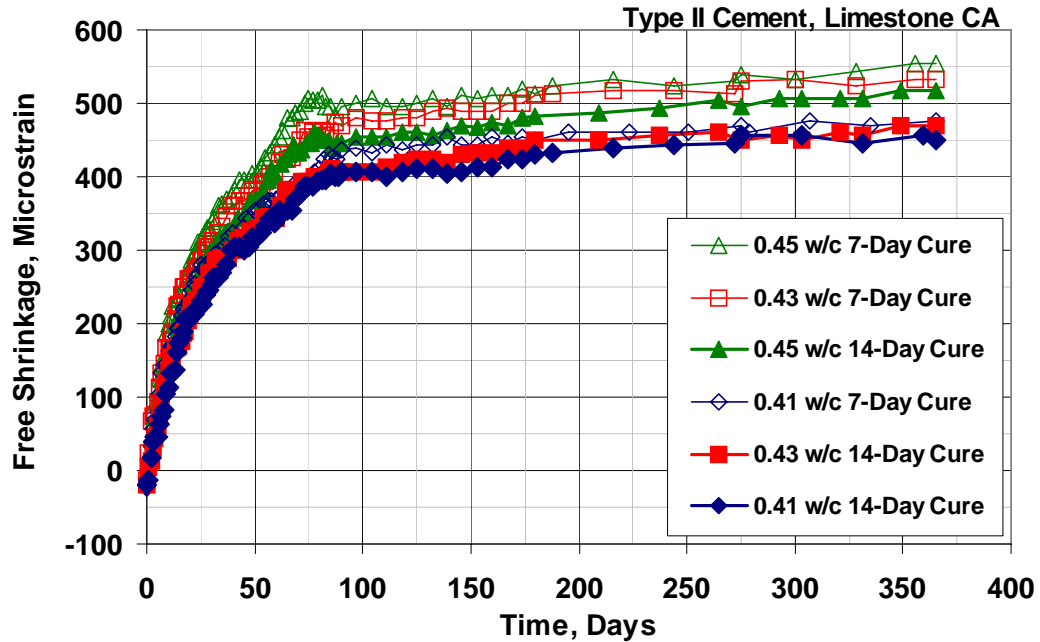


Fig. 4.6 – Free-Shrinkage Test (ASTM C 157). Program I Set 2. Average free shrinkage versus time through 365 days (drying only).

Table 4.8 – Student’s t-test Results for Program I Set 2 365-Day Free-Shrinkage Data

		365-Day Free Shrinkage ($\mu\epsilon$)	0.45 w/c		0.43 w/c		0.41 w/c	
			7-Day	14-Day	7-Day	14-Day	7-Day	14-Day
0.45 w/c	7-Day	553		90	N	Y	Y	80
	14-Day	517			N	95	95	95
0.43 w/c	7-Day	533				Y	Y	Y
	14-Day	470					N	N
0.41 w/c	7-Day	477						80
	14-Day	450						

Note: See the Table 4.4 note for an explanation of the terms “N”, “80”, “90”, “95”, and “Y”.

4.4.3 Program I Set 3 (Granite Coarse Aggregate, Type I/II Portland Cement)

Program I Set 3 again examines the effect of curing period, paste content, and w/c ratio on shrinkage; however, granite is used as the coarse aggregate (rather than limestone) for this set. Aggregate particles restrain shrinkage, and for this reason, concrete containing low-absorptive aggregates with a high modulus of elasticity generally exhibit lower shrinkage (Carlson 1938, Alexander 1996). Recent work also indicates, however, that concrete containing saturated porous aggregate can result in lower shrinkage due to internal curing provided by the slow release of water from the aggregate pores (Collins and Sanjayan 1999). The objective of Set 3 is to determine whether the reductions in shrinkage observed with a reduction in w/c ratio (and paste content) in Sets 1 and 2 are dependent on the type of aggregate.

The Set 3 average free-shrinkage data after 0, 30, 90, 180, and 365 days of drying are presented in Table 4.9. Individual free-shrinkage curves are presented in Figs. C.7 through C.9 in Appendix C. The basic conclusions for Set 3 remains the same as for Sets 1 and 2 – for a given w/c ratio, an increase in the curing period from 7 to 14 days decreases shrinkage, and further reductions in shrinkage are observed as the w/c ratio is reduced from 0.45 to 0.41. Expansion at the end of the curing period ranged from 47 to 90 $\mu\epsilon$, which, on average, is more than three times higher than the expansion observed for the limestone mixtures in Sets 1 and 2.

Table 4.9 – Summary of Program I Set 3 Free-Shrinkage Data (in microstrain)

Days of Drying	0.45 w/c		0.43 w/c		0.41 w/c	
	7-Day Cure	14-Day Cure	7-Day Cure	14-Day Cure	7-Day Cure	14-Day Cure
0	-90	-53	-57	-50	-67	-47
30	287	283	300	267	270	250
90	397	370	377	347	333	310
180	443	393	427	403	363	353
365	487	470	460	440	400	367

The average free-shrinkage curves through the first 30 days of drying are presented in Fig. 4.7. After 30 days of drying, the greatest shrinkage (300 $\mu\epsilon$) is observed for the specimens with a w/c ratio of 0.43 cured for 7 days, followed by the 0.45 w/c ratio mixtures cured for 7 and 14 days with shrinkage strains of 287 and 283 $\mu\epsilon$, respectively. None of the differences in shrinkage between these mixtures are statistically significant (Table 4.10). The least shrinkage is observed for the 0.41 and 0.43 w/c ratio mixtures cured for 14 days, with shrinkage strains of 250 and 267 $\mu\epsilon$, respectively. An increase in the curing period from 7 to 14 days resulted in modest reductions in shrinkage of 4, 33, and 20 $\mu\epsilon$ for the 0.45, 0.43, and 0.41 w/c ratio mixtures, respectively. Only the reduction in shrinkage for the 0.43 w/c ratio mixture is statistically significant (at $\alpha = 0.10$). In general, the trend is similar to that obtained in Sets 1 and 2, although the differences are less pronounced with a total range of only 50 $\mu\epsilon$ compared to 80 $\mu\epsilon$ for the Set 1 specimens and 87 $\mu\epsilon$ for the Set 2 specimens.

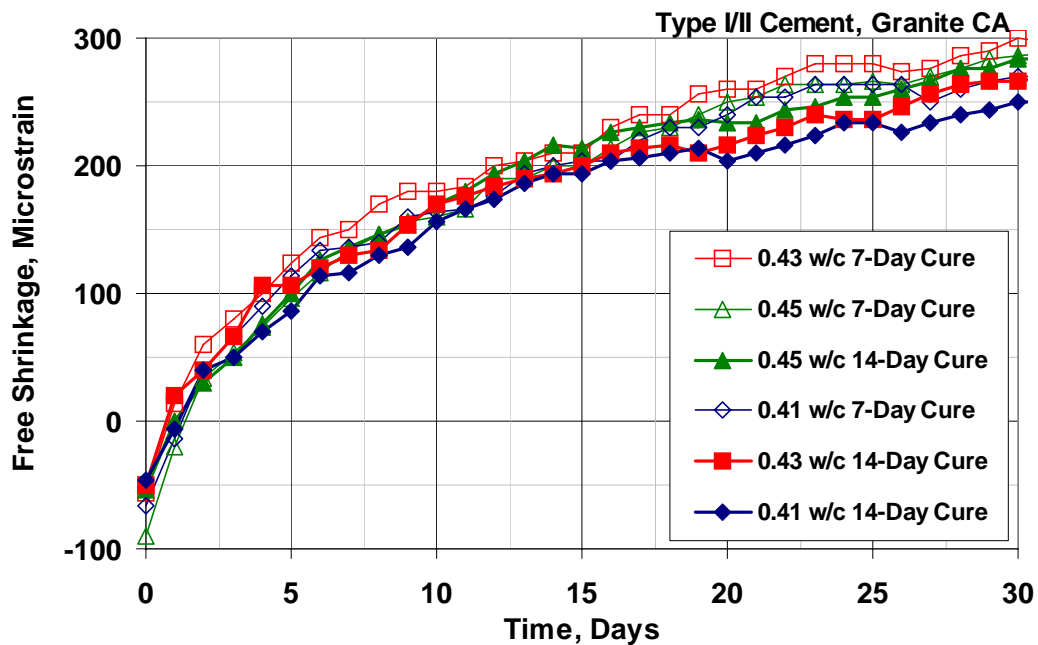


Fig. 4.7 – Free-Shrinkage Test (ASTM C 157). Program I Set 3. Average free shrinkage versus time through 30 days (drying only).

Table 4.10 – Student’s t-test Results for Program I Set 3 30-Day Free-Shrinkage Data

		30-Day Free Shrinkage ($\mu\epsilon$)	0.45 w/c		0.43 w/c		0.41 w/c	
			7-Day	14-Day	7-Day	14-Day	7-Day	14-Day
0.45 w/c	7-Day	287		N	N	80	80	80
	14-Day	283			N	N	N	N
0.43 w/c	7-Day	300				90	90	90
	14-Day	267					N	N
0.41 w/c	7-Day	270						N
	14-Day	250						

Note: See the Table 4.4 note for an explanation of the terms “N”, “80”, “90”, “95”, and “Y”.

The average free-shrinkage curves through 365 days of drying are shown in Fig. 4.8. The trend established during the first 30 days of drying remains essentially unchanged throughout the remainder of the test. At 365 days, the 0.45 w/c ratio mixture cured for 7 days exhibited the most shrinkage (487 $\mu\epsilon$), and the 0.41 w/c ratio mixture cured for 14 days exhibited the least (367 $\mu\epsilon$). For periods greater than 200 days, the 0.45 w/c ratio mixture cured for 14 days exhibited similar shrinkage as the 0.43 w/c ratio mixture cured for 7 days. At 365 days, the shrinkage of these mixtures was 470 and 460 $\mu\epsilon$, respectively. The 0.43 w/c ratio mixture cured for 14 days exhibited slightly less shrinkage at 365 days (440 $\mu\epsilon$). The differences in shrinkage between the 0.43 w/c ratio mixture cured for 14 days and both of the 0.45 w/c mixtures are statistically significant at $\alpha = 0.2$ (Table 4.11). An increase in the curing period from 7 to 14 days resulted in a reduction in shrinkage for each of the w/c ratios examined, although none of the differences were statistically significant at 365 days.

4.4.4 Program I Comparison: Type I/II Cement Versus Type II Cement

The relative difference in shrinkage properties of concrete containing Type I/II and Type II cement is of particular interest and is presented next. The results of Program I Sets 1 and 2 are compared in Figs. 4.9 and 4.10 for specimens cured for 7 days. Figure 4.9 shows the average free-shrinkage strain versus time for the Set 1

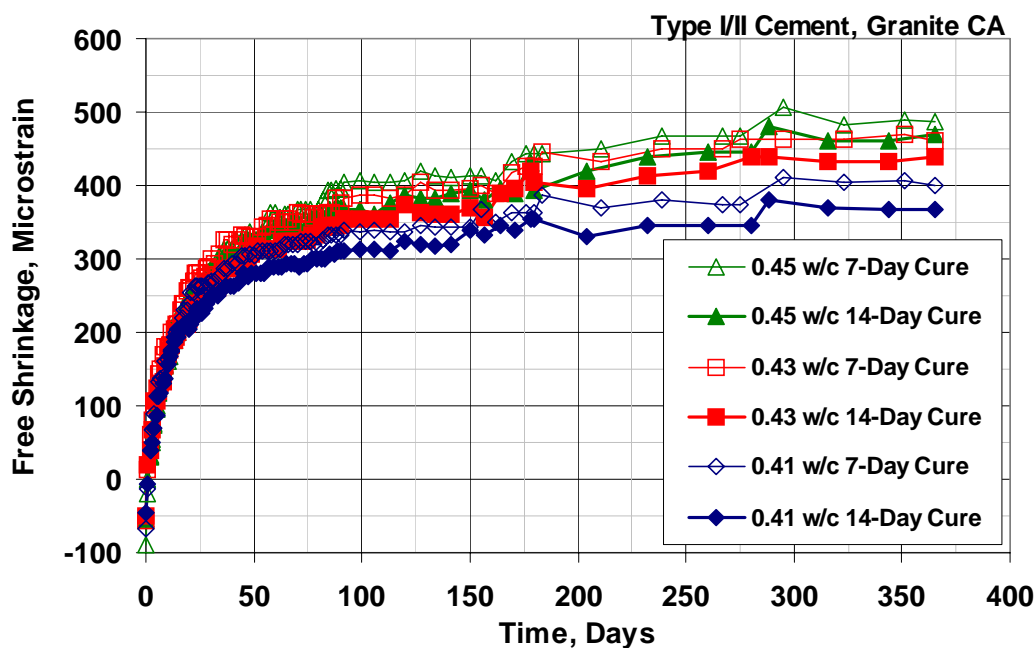


Fig. 4.8 – Free Shrinkage Test (ASTM C 157). Program I Set 3. Average free-shrinkage versus time through 365 days (drying only).

Table 4.11 – Student’s t-test Results for Program I Set 3 365-Day Free-Shrinkage Data

		365-Day Free Shrinkage ($\mu\epsilon$)	0.45 w/c		0.43 w/c		0.41 w/c	
			7-Day	14-Day	7-Day	14-Day	7-Day	14-Day
0.45 w/c	7-Day	487		N	N	80	95	Y
	14-Day	470			Y	80	Y	Y
0.43 w/c	7-Day	460				N	Y	Y
	14-Day	440					80	95
0.41 w/c	7-Day	400						N
	14-Day	367						

Note: See the Table 4.4 note for an explanation of the terms “N”, “80”, “90”, “95”, and “Y”.

mixtures (containing Type I/II cement) and the Set 2 mixtures (containing Type II cement) cured for 7 days during the first 30 days of drying. The results of the Student’s t-test are shown in Table 4.12. For a given w/c ratio, the behavior of

concrete cast with Type I/II and Type II cement is very similar. The results of the Student’s t-test confirm this observation (Table 4.12).

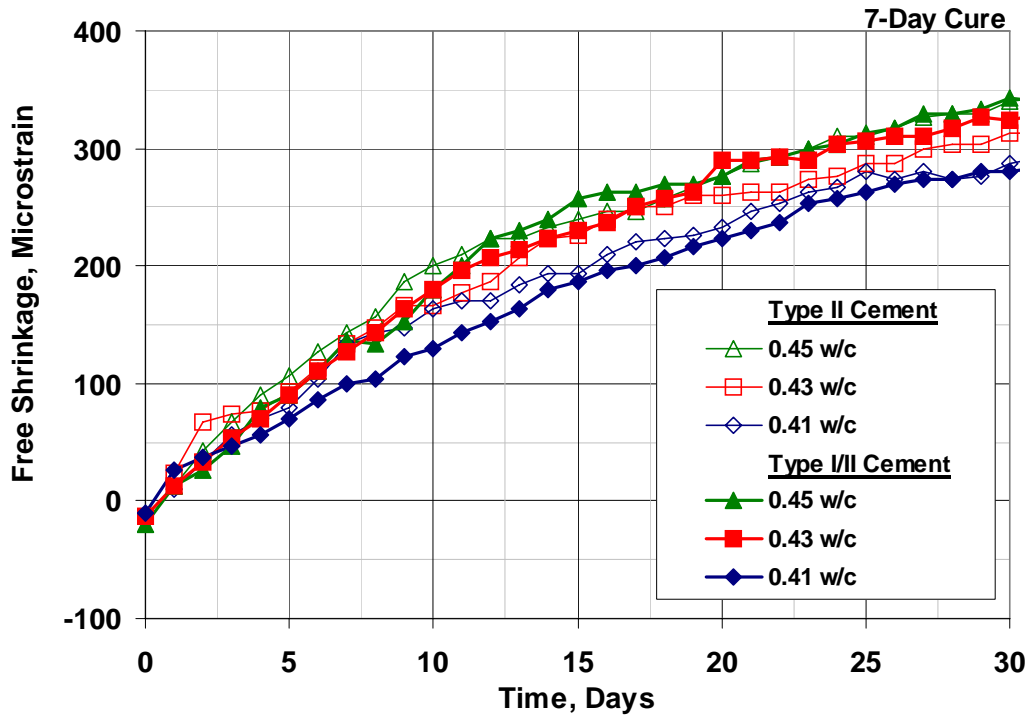


Fig. 4.9 – Free-Shrinkage Test (ASTM C 157). Program I Set 1 and Set 2 specimens cured for 7 days. Average free shrinkage versus time through 30 days (drying only).

Table 4.12 – Student’s t-test results for Program I Set 1 and 2 specimens cured for 7 days. 30-day comparison of free-shrinkage data

		30-Day Free Shrinkage (µε)	0.45 w/c		0.43 w/c		0.41 w/c	
			I/II	II	I/II	II	I/II	II
0.45 w/c	I/II	343		N	N	Y	Y	95
	II	340			N	Y	Y	90
0.43 w/c	I/II	323				N	90	N
	II	313					Y	N
0.41 w/c	I/II	280						N
	II	287						

Note: See the Table 4.4 note for an explanation of the terms “N”, “80”, “90”, “95”, and “Y”.

The effect of cement type on long-term shrinkage is illustrated in Fig. 4.10 for specimens cured for 7 days. The mixtures with a 0.45 w/c ratio exhibited similar shrinkage behavior throughout the entire drying period, and the difference at 365 days is not statistically significant (Table 4.13). The 0.43 and 0.41 w/c ratio mixtures, however, began to show differences after approximately 90 days of drying, and contrary to the expected behavior, the concrete containing Type II cement exhibited increased shrinkage compared to the Type I/II cement mixtures. For periods greater than 90 days, the difference in shrinkage between the 0.43 w/c ratio mixtures is approximately $20 \mu\epsilon$, increasing to $46 \mu\epsilon$ at 365 days (a statistically significant difference at $\alpha = 0.2$) (Table 4.13). The difference in shrinkage between the 0.41 w/c ratio mixtures is at least $13 \mu\epsilon$ for periods greater than 90 days, increasing to $37 \mu\epsilon$ at 365 days (a statistically significant difference at $\alpha = 0.2$) (Table 4.13). The higher shrinkage of the Type II mixes is contrary to the results obtained by Chariton and Weiss (2002) and Deshpande et al. (2007), but may be the result of natural variations in the mixtures and the relatively narrow difference in fineness.

The results for specimens cured for 14 days are shown in Figs. 4.11 and 4.12, and the corresponding Student's t -test results are shown in Tables 4.14 and 4.15, respectively. As shown in Fig. 4.11, the results through 30 days are qualitatively similar to the results obtained for the specimens cured for only 7 days. The free-shrinkage curves for the mixtures containing Type I/II or Type II cement with a w/c ratio of 0.41 are nearly indistinguishable through the first 30 days of drying. For w/c ratios of 0.43 and 0.45, there is a slight bias towards increased shrinkage for mixtures containing Type I/II cement. Neither of these small differences is statistically significant, however, precluding any conclusions with regard to the relative early-age shrinkage behavior of these concretes.

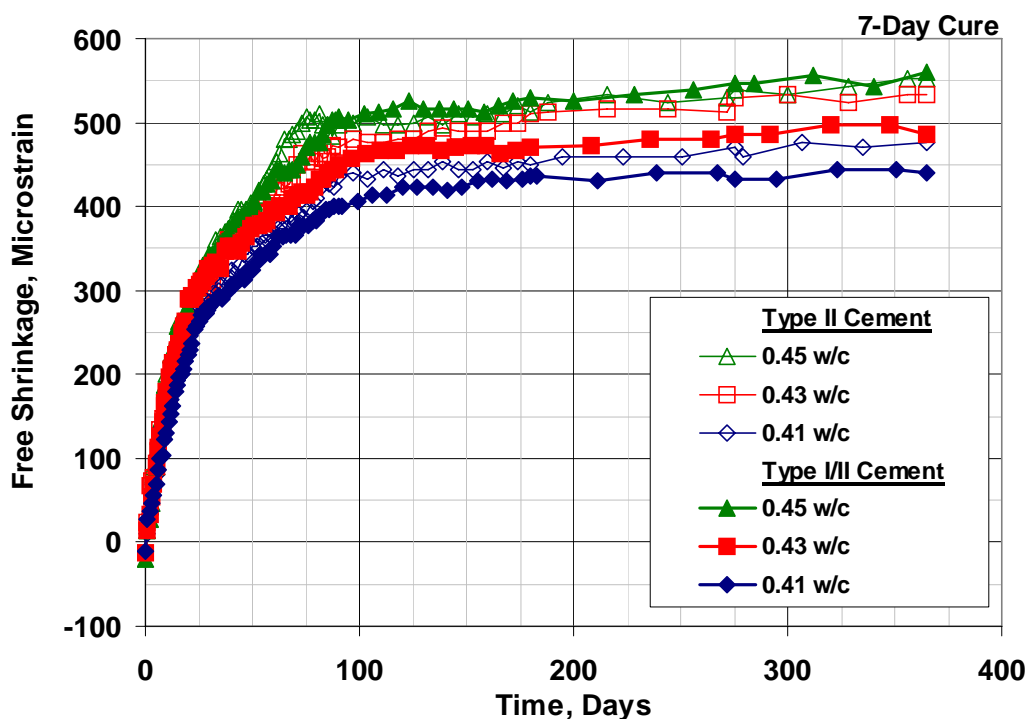


Fig. 4.10 – Free-Shrinkage Test (ASTM C 157). Program I Set 1 and Set 2 specimens cured for 7 days. Average free shrinkage versus time through 365 days (drying only).

Table 4.13 – Student’s t-test results for Program I Set 1 and 2 specimens cured for 7 days. 365-day comparison of free-shrinkage data

		365-Day Free Shrinkage ($\mu\epsilon$)	0.45 w/c		0.43 w/c		0.41 w/c	
			I/II	II	I/II	II	I/II	II
0.45 w/c	I/II	560		N	95	90	Y	Y
	II	553			90	N	Y	Y
0.43 w/c	I/II	487				80	N	N
	II	533					Y	Y
0.41 w/c	I/II	440						80
	II	477						

Note: See the Table 4.4 note for an explanation of the terms “N”, “80”, “90”, “95”, and “Y”.

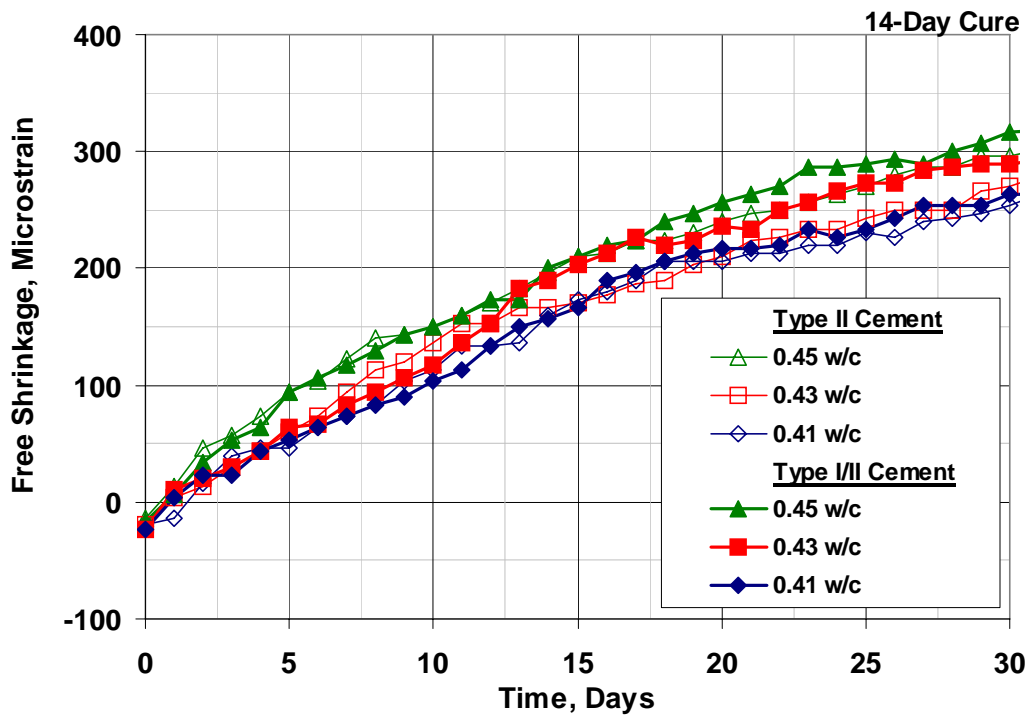


Fig. 4.11 – Free-Shrinkage Test (ASTM C 157). Program I Set 1 and Set 2 specimens cured for 14 days. Average free shrinkage versus time through 30 days (drying only).

Table 4.14 – Student’s t-test results for Program I Set 1 and 2 specimens cured for 14 days. 30-day comparison of free-shrinkage data

		30-Day Free Shrinkage ($\mu\epsilon$)	0.45 w/c		0.43 w/c		0.41 w/c	
			I/II	II	I/II	II	I/II	II
0.45 w/c	I/II	317		N	N	90	95	90
	II	297			N	Y	Y	90
0.43 w/c	I/II	290				N	N	N
	II	270					N	N
0.41 w/c	I/II	263						N
	II	253						

Note: See the Table 4.4 note for an explanation of the terms “N”, “80”, “90”, “95”, and “Y”.

The effect of cement type on long-term shrinkage is illustrated in Fig. 4.12 for specimens cured for 14 days. With the exception of the 0.41 w/c ratio mixtures, there

is a slight tendency for concrete containing Type I/II cement to shrink more than concrete containing Type II for periods greater than approximately 75 days. While this trend appears to coincide with previous observations, none of these differences are statistically significant, making it impossible to draw firm conclusions (Table 4.15). As with the results for previous comparisons, the 0.41 w/c ratio mixtures exhibited similar shrinkage behavior throughout the drying period.

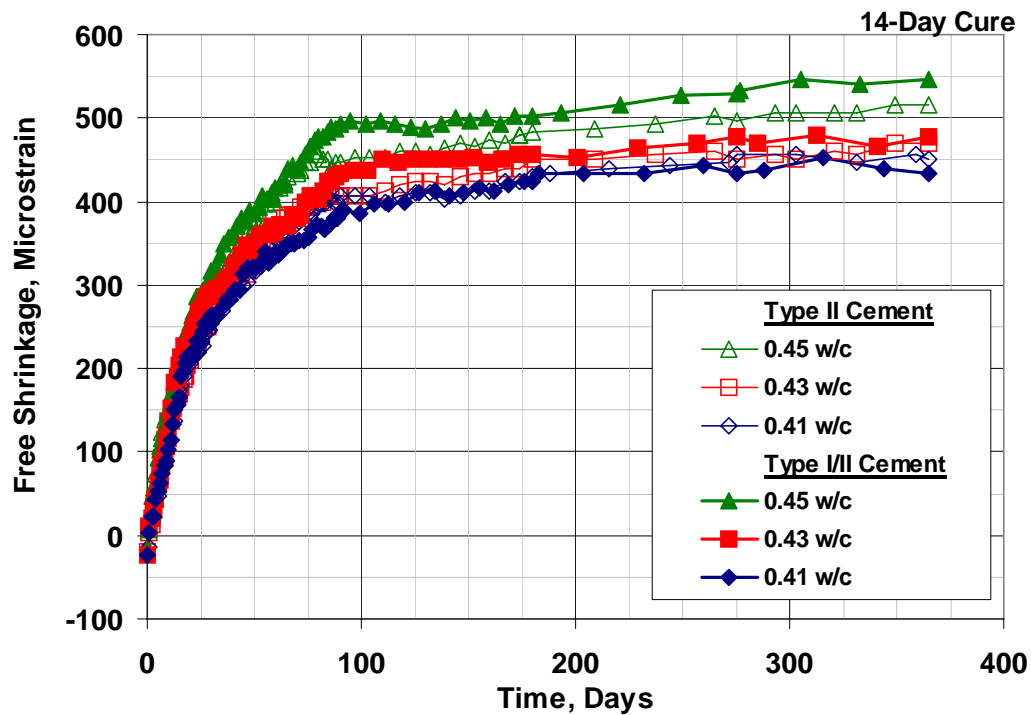


Fig. 4.12 – Free-Shrinkage Test (ASTM C 157). Program I Set 1 and Set 2 specimens cured for 14 days. Average free shrinkage versus time through 365 days (drying only).

Table 4.15 – Student’s t-test results for Program I Set 1 and 2 specimens cured for 14 days. 365-Day comparison of free-shrinkage data

		365-Day Free Shrinkage ($\mu\epsilon$)	0.45 w/c		0.43 w/c		0.41 w/c	
			I/II	II	I/II	II	I/II	II
0.45 w/c	I/II	547		N	90	Y	Y	Y
	II	517			80	90	Y	95
0.43 w/c	I/II	477				N	80	N
	II	470					95	N
0.41 w/c	I/II	433						N
	II	450						

Note: See the Table 4.4 note for an explanation of the terms “N”, “80”, “90”, “95”, and “Y”.

4.4.5 Program I Summary

The results of Program I indicate that a reduction in the w/c ratio (and paste content) obtained by reducing the water content and replacing the water with an equal volume of aggregate and using a high-range water reducer (HRWR) to maintain workability did not result in an increase in shrinkage. Observations from previous studies indicate that the use of HRWRs to maintain consistent workability in such cases may lead to increased shrinkage (Ghosh and Malhotra 1979, Feldman and Swenson 1975). These earlier observations are contrary to the behavior observed in this study. Shrinkage decreased as a result of a decrease in the w/c ratio (and paste content), and increasing the curing period from 7 to 14 days resulted in at least a slight reduction in shrinkage at all ages.

The evaluation in Program I included three sets of specimens. Sets 1 and 3 contain Type I/II cement and Set 2 contained a coarser Type II cement. In addition, two different aggregates were evaluated: a relatively porous limestone coarse aggregate in Sets 1 and 2, and granite coarse aggregate in Set 3. The individual results for each of the sets indicate that for a given w/c ratio, an increase in the curing period from 7 to 14 days decreases shrinkage at all ages. This reduction in shrinkage

is measurable, but it is generally small and tends to decrease over time. Shrinkage is further reduced as the w/c ratio (and paste content) is reduced from 0.45 to 0.41, and thus, the greatest shrinkage is generally observed for the 0.45 w/c ratio mixtures cured for only 7 days, and the least shrinkage is observed for the 0.41 w/c ratio mixtures cured for 14 days.

A direct comparison between the shrinkage of concretes containing these Type I/II and Type II cements indicates very little, if any, difference in free shrinkage for a given w/c ratio and curing period. This behavior contradicts previous findings that indicate concrete cast with coarse cements shrink less than concrete containing fine cements. This difference may be due to the relatively small range of cement finenesses examined in this study. The results do indicate, however, that the free-shrinkage specimens cast with Type II cement were more sensitive to the curing period than specimens cast with Type I/II cement, particularly for mixes with a high w/c ratio. A direct comparison between concrete containing limestone coarse aggregate and granite coarse aggregate was not possible due to differences in the cement samples and an extended period of time between casting dates. A direct comparison between concrete cast with different aggregate types is the subject of Program III.

4.5 PROGRAM II (W/C, PASTE CONTENT AND CURING PERIOD)

Program II involves two sets of mixtures examining the effect of w/c ratio and the combined effect of paste content and curing period on free shrinkage. Set 1 examines mixtures with w/c ratios of 0.42, 0.40, 0.38, and 0.36, all with a paste content of 23.3%. To maintain a constant paste content, the cement content varied from 317 to 346 kg/m^3 (535 to 583 lb/yd^3) as the w/c ratio was reduced from 0.42 to 0.36. Set 2 includes mixtures with a w/c ratio of 0.42 and a paste content of 23.3% or 21.6%. The 23.3% cement-paste mixtures have a cement content of 317 kg/m^3 (535 lb/yd^3), and the 21.6% cement-paste mixtures have a cement content of 295 kg/m^3

(497 lb/yd³). Specimens in both Sets 1 and 2 contain porous limestone coarse aggregate (with an absorption between 2.5 and 3.0%). Program II Sets 1 and 2 are summarized in Table 4.16 with additional details provided in Section 2.9.2. Mixture proportions, plastic concrete properties, and compressive strengths are provided in Table A.6 in Appendix A.

Table 4.16 – Program II Summary

Series	w/c Ratio	Paste Volume	Curing Period
1	0.36	23.26%	14
1	0.38	23.26%	14
1	0.40	23.26%	14
1 and 2	0.42	23.26%	14
2	0.42	23.26%	21
2	0.42	21.61%	7
2	0.42	21.61%	14

4.5.1 Program II Set 1 (w/c ratio)

The average free-shrinkage data for Set 1 after 0, 30, 90, 180, and 365 days of drying are presented in Table 4.17. Individual free-shrinkage specimen curves are presented in Figs. C.10 and C.11 in Appendix C. Expansion occurring during the curing period varied from 13 to 27 $\mu\epsilon$ – similar to the expansion observed in the Program I Sets cast with limestone coarse aggregate. In general, the results presented in Table 4.17 indicate a moderate reduction in shrinkage as the w/c ratio is reduced. The greatest difference occurs after only 30 days of drying when a reduction in the w/c ratio from 0.42 to 0.36 results in an 80 $\mu\epsilon$ reduction in shrinkage. After one year of drying that difference is reduced to only 33 $\mu\epsilon$.

The effect of w/c ratio on early-age shrinkage is illustrated in Fig. 4.13 where no discernable difference in shrinkage is observed through the first 15 days of drying. The 30-day shrinkage results, however, demonstrate that a reduction in the w/c ratio

Table 4.17 – Summary of Program II Set 1 Free-Shrinkage Data (in microstrain)

Days of Drying	<i>w/c</i> ratio			
	0.42	0.40	0.38	0.36
0	-17	-13	-27	-10
30	317	283	273	237
90	417	410	397	380
180	453	443	423	403
365	443	433	437	410

from 0.42 to 0.36 decreases free shrinkage from 317 to 237 $\mu\epsilon$. This reduction in shrinkage of 80 $\mu\epsilon$ is statistically significant at $\alpha = 0.02$ (Table 4.18). A reduction in the *w/c* ratio from 0.42 to 0.40 results in a 34 $\mu\epsilon$ reduction in shrinkage, and a further reduction in the *w/c* ratio to 0.38 reduces shrinkage by an additional 10 $\mu\epsilon$. All of the differences in shrinkage observed are statistically significant, except for the 10 $\mu\epsilon$ difference between the 0.40 and 0.38 *w/c* ratio mixtures (Table 4.18).

These results represent the performance of mixtures in which the aggregate moisture content at the time of batching is at least saturated-surface-dry (SSD). As a result, the relatively porous limestone may provide internal curing water and extending the hydration reaction longer than might be expected otherwise. For this reason, these shrinkage results should not be extended to concrete mixtures containing a low-absorption aggregate (that does not have internal curing water available) due to the possibility of autogenous shrinkage for mixtures with *w/c* ratios below 0.42.

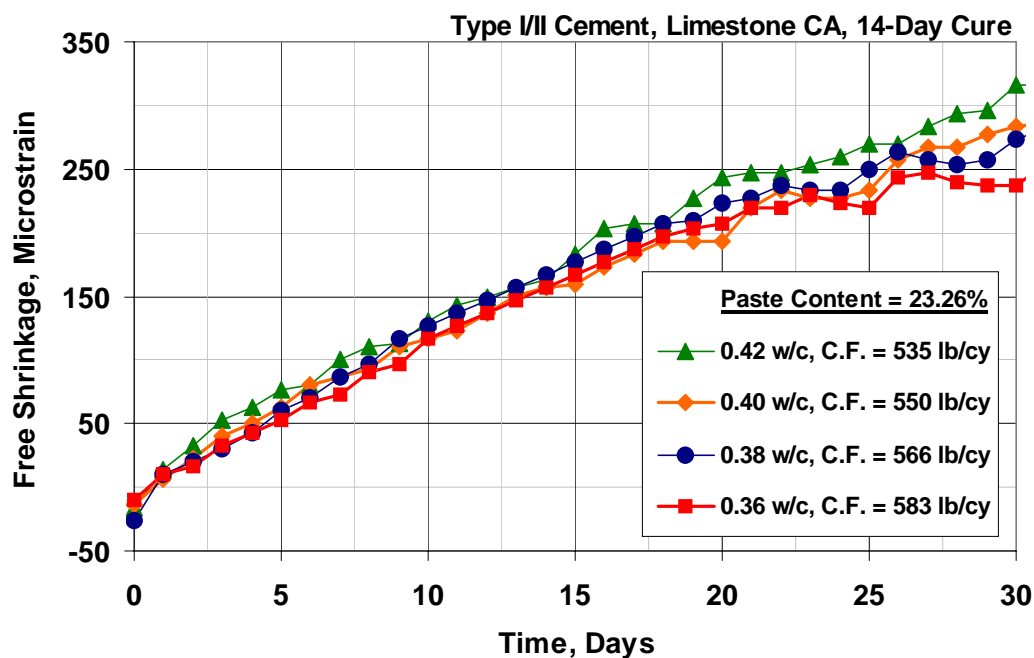


Fig. 4.13 – Free-Shrinkage Test (ASTM C 157). Program II Set 1. Average free shrinkage versus time through 30 days (drying only).

Table 4.18 – Student’s t-test Results for Program II Set 1 30-Day Free-Shrinkage Data

		30-Day Free Shrinkage ($\mu\epsilon$)	w/c ratio			
			0.42	0.40	0.38	0.36
w/c ratio	0.42	317		80	95	Y
	0.40	283			N	95
	0.38	273				90
	0.36	237				

Note: See the Table 4.4 note for an explanation of the terms “N”, “80”, “90”, “95”, and “Y”.

The effect of reducing the w/c ratio from 0.42 to 0.36 (while maintaining a constant paste content) on long-term shrinkage is illustrated in Fig. 4.14. After approximately 150 days, there is no discernable difference in shrinkage for mixtures with w/c ratios of 0.38, 0.40, and 0.42. After one year, shrinkage values range from only 433 to 443 $\mu\epsilon$. A further reduction in the w/c ratio to 0.36 did, however, result in an average reduction in shrinkage of 28 $\mu\epsilon$ at the end of the testing period. The

differences in shrinkage observed between the 0.36 *w/c* ratio mixture and the 0.38, 0.40, and 0.42 *w/c* ratio mixtures are statistically significant at confidence levels of $\alpha = 0.1, 0.2,$ and $0.1,$ respectively (Table 4.19). The effect of working with reduced *w/c* ratios in the field will be discussed in Chapter 5.

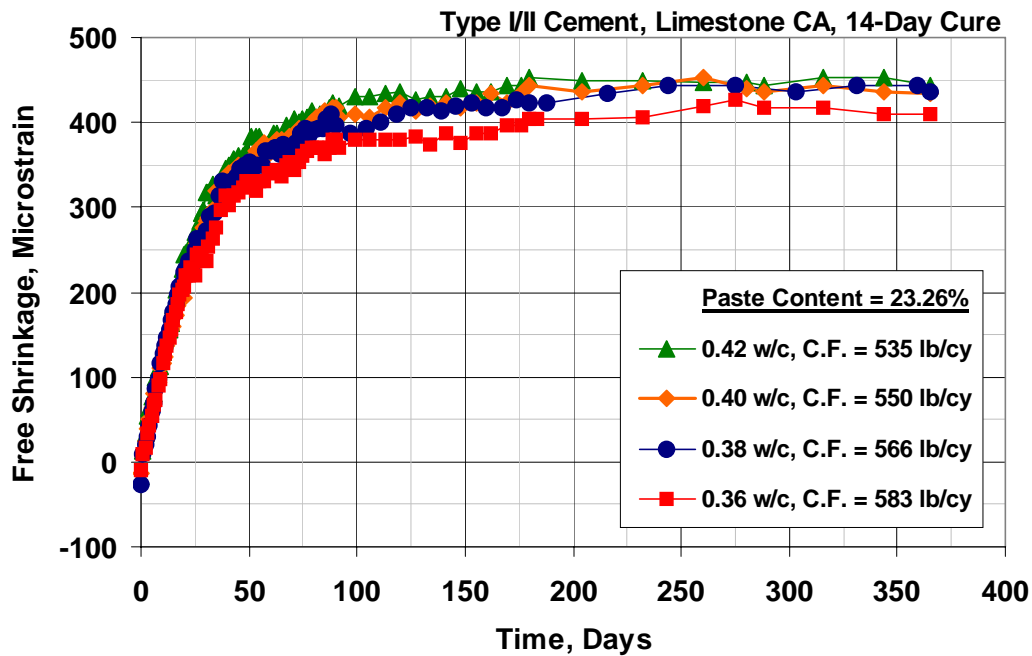


Fig. 4.14 – Free-Shrinkage Test (ASTM C 157). Program II Set 1. Average free shrinkage versus time through 365 days (drying only).

Table 4.19 – Student’s t-test Results for Program II Set 1 365-Day Free-Shrinkage Data

		365-Day Free Shrinkage (µε)	<i>w/c</i> Ratio			
			0.42	0.40	0.38	0.36
<i>w/c</i> Ratio	0.42	443		N	N	90
	0.40	433			N	80
	0.38	437				90
	0.36	410				

Note: See the Table 4.4 note for an explanation of the terms “N”, “80”, “90”, “95”, and “Y”.

4.5.2 Program II Set 2 (Paste Content and Curing Period)

The average free-shrinkage data for Set 2 after 0, 30, 90, 180, and 365 days of drying are presented in Table 4.20. Individual free-shrinkage specimen curves are presented in Figs. C.11 through C.13 in Appendix C. Expansion occurring during the curing period varied from 10 to 20 $\mu\epsilon$. As expected, and consistent with the results of Program I, shrinkage is reduced as the curing period is increased from 7 to 14 days for the 21.6% paste specimens or from 14 to 21 days for the 23.3% paste specimens.

Table 4.20 – Summary of Program II Set 2 Free-Shrinkage Data (in microstrain)

Days of Drying	21.6% Paste		23.3% Paste	
	7-Day Cure	14-Day Cure	14-Day Cure	21-Day Cure
0	-10	-10	-17	-20
30	323	290	317	267
90	427	383	410	370
180	450	407	453	420
365	467	420	443	420

The free-shrinkage results through the first 30 days of drying are presented in Fig. 4.15. The mixture containing 21.6% paste cured for 7 days exhibited the most shrinkage (323 $\mu\epsilon$), followed by the mixture containing 23.3% paste cured for 14 days (317 $\mu\epsilon$), the 21.6% paste mixture cured for 14 days (290 $\mu\epsilon$), and finally, the 23.3% paste mixture cured for 21 days (267 $\mu\epsilon$). Through the first 30 days of drying, the mixtures containing 21.6% and 23.3% paste cured for 14 days exhibited similar shrinkage with a difference of only 27 $\mu\epsilon$ (this difference increases to 46 $\mu\epsilon$ after 180 days of drying) that is not statistically significant. The 23.3% paste specimens cured for 21 days exhibited the least shrinkage, and all of the differences between this batch and the others were statistically significant at least at $\alpha = 0.2$ (Table 4.21). These results clearly highlight the importance of extended curing periods – even compared to reducing the paste content from 23.3 to 21.6%.

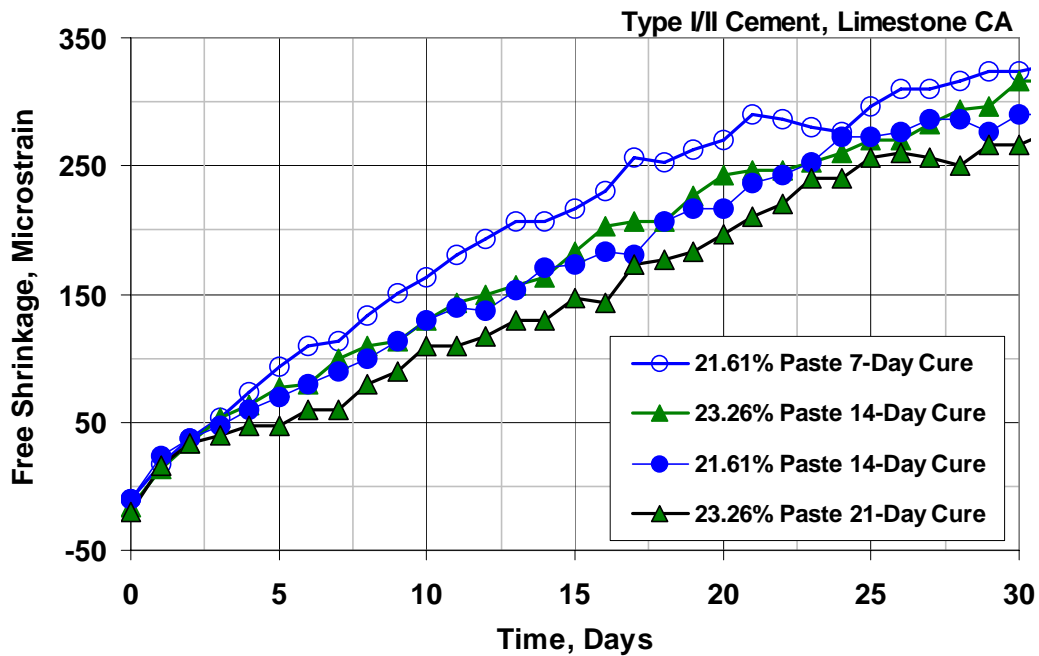


Fig. 4.15 – Free-Shrinkage Test (ASTM C 157). Program II Set 2. Average free shrinkage versus time through 30 days (drying only).

Table 4.21 – Student’s t-test Results for Program II Set 2 30-Day Free-Shrinkage Data.

		30-Day Free Shrinkage (μϵ)	21.6% Paste		23.3% Paste	
			7-Day Cure (7D)	14-Day Cure (14D)	14-Day Cure (14D)	21-Day Cure (21D)
21.6% Paste	7D	323		90	N	Y
	14D	290			N	80
23.3% Paste	14D	317				95
	21D	267				

Note: See the Table 4.4 note for an explanation of the terms “N”, “80”, “90”, “95”, and “Y”.

The free-shrinkage results after one year of drying are shown in Fig. 4.16. The mixture containing 21.6% paste cured for 7 days exhibited the most shrinkage (467 μϵ), while the mixture containing 23.3% paste cured for 21 days and the mixture containing 21.6% paste cured for 14 days exhibited the least shrinkage (both with 420 μϵ). After approximately 90 days of drying, the 23.3% paste mixture cured for 14

days exhibited slightly less shrinkage (between 0 and 24 $\mu\epsilon$) than the 21.6% paste mixture cured for 7 days, and the 21.6% paste mixture cured for 14 days exhibited similar shrinkage as the 23.3% paste mixture cured for 21 days. These results indicate that for periods greater than 90 days, increasing the curing period from 7 to 14 days or from 14 to 21 days has approximately the same influence on shrinkage as reducing the paste content from 23.3% to 21.6%. The Student's t-test results are shown in Table 4.22. At 365 days, all of the differences in shrinkage are statistically significant at least at a confidence level of $\alpha = 0.2$ (no difference in shrinkage was observed between the 14-day 21.6% paste and 21-day 23.3% paste specimens).

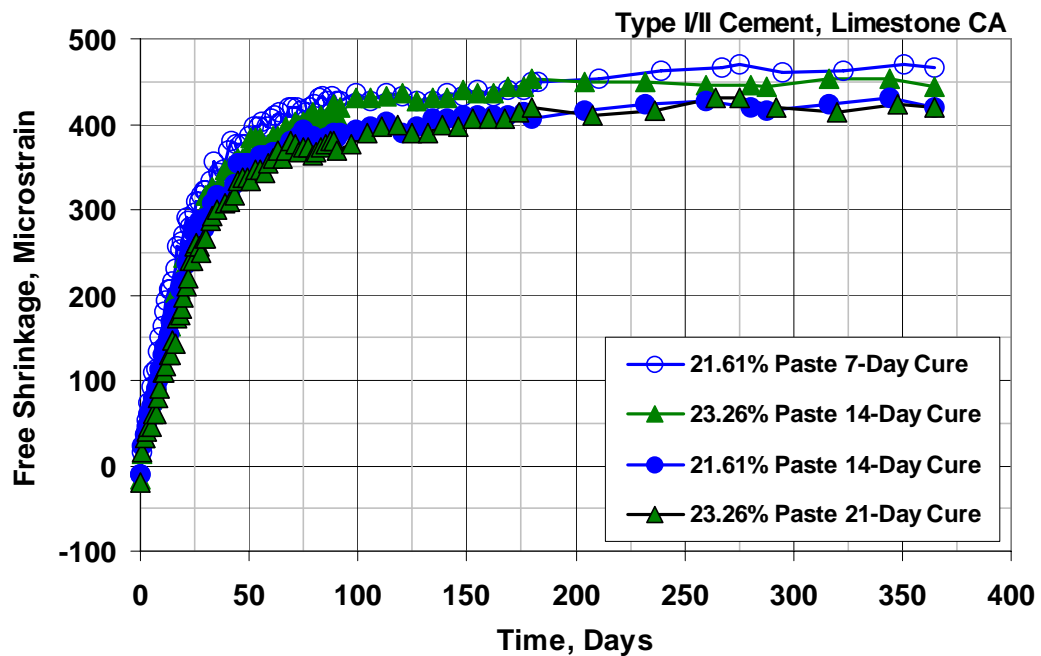


Fig. 4.16 – Free-Shrinkage Test (ASTM C 157). Program II Set 2. Average free shrinkage versus time through 365 days (drying only).

4.5.3 Program II Summary

The results of Program II Set 1 support observations by Ödman (1968) and Bissonnette et al. (1999) in which the w/c ratio was also reported to have a small, but measurable, influence on long-term shrinkage. Deshpande et al. (2007) examined

Table 4.22 – Student’s t-test Results for Program II Set 2 365-Day Free-Shrinkage Data

		365-Day Free Shrinkage ($\mu\epsilon$)	21.6% Paste		23.3% Paste	
			7-Day Cure (7D)	14-Day Cure (14D)	14-Day Cure (14D)	21-Day Cure (21D)
21.6% Paste	7D	467		95	80	95
	14D	420			90	N
23.3% Paste	14D	443				80
	21D	420				

Note: See the Table 4.4 note for an explanation of the terms “N”, “80”, “90”, “95”, and “Y”.

slightly higher w/c ratios (0.40, 0.45, and 0.50) and observed the opposite, concluding that for a given paste content, concrete with a higher w/c ratio exhibits less shrinkage than concrete with a lower w/c ratio. In all three studies, however, the results indicate that shrinkage is largely controlled by the paste content, and any differences resulting from changes in the w/c ratio are small in comparison. Specifically, the results of this program indicate that a reduction in the w/c ratio from 0.42 to 0.36 will decrease both the short-term shrinkage, and to a lesser extent, the long-term shrinkage. This reduction in shrinkage may or may not result in a reduction in cracking due to the reduced tensile creep capacity associated with higher strength concrete. A more direct measure of cracking tendency, such as the restrained ring test, is required to fully assess concrete with reduced w/c ratios.

The results of Program II Set 2 indicate clearly that while shrinkage is influenced by the paste content, the curing period can play just as important of a role – specifically when comparing two mixtures with a low paste contents (23.3 and 21.6%). A more comprehensive examination of free shrinkage and curing time is recommended to determine the relative importance of the two for a broader range of mixtures.

4.6 PROGRAM III (AGGREGATE TYPE)

The influence of three different coarse aggregates on free shrinkage is evaluated in Program III. Concrete containing granite, quartzite, and limestone and cured for either 7 or 14 days are included in the evaluation. Each mixture has a w/c ratio of 0.42 and a paste content of 21.6% [corresponding to a cement content 295 kg/m³ (497 lb/yd³)]. A reduced paste content was chosen to maximize the volume of coarse aggregate while maintaining adequate concrete workability. The combined aggregate gradation for each mixture was optimized using the KU Mix method (described in Chapter 3), and as a result, the volume of coarse aggregate was similar, but not identical, for each of the mixtures evaluated. A summary of Program III is presented in Table 4.23, and additional details are provided in Section 2.9.3. Individual mixture designs, plastic concrete properties, and compressive strengths are provided in Table A.7 in Appendix A. Individual specimen free-shrinkage curves are presented in Figs. C.13 through C.15 in Appendix C.

Table 4.23 – Program III Summary

Aggregate Type	w/c ratio	Percent Volume of Cement Paste	Percent Volume of Coarse Aggregate
Limestone	0.42	21.6	34.7
Granite	0.42	21.6	35.1
Quartzite	0.42	21.6	35.3

Aggregate particles (in addition to unhydrated cement and calcium hydroxide crystals) within the concrete restrain shrinkage of the cement paste, and for this reason, soft aggregates, as indicated by the modulus of elasticity and absorption, tend to promote higher concrete shrinkage as compared to concrete containing stiff aggregates with a low absorption. Thus, concrete containing low-absorptive aggregates with a high modulus of elasticity generally exhibit lower shrinkage (Carlson 1938, Alexander 1996, Deshpande et al. 2007). This observation is consistent with the results obtained in Program I, specifically with regard to long-

term shrinkage, but some more recent work suggests that porous aggregate may provide internal curing, thereby reducing shrinkage (Collins and Sanjayan 1999, Imamoto and Arai 2006). The results of Program III are clearly dependent on the length of the curing period, and as such, the results are discussed based on the length of the curing period. Sections 4.6.1 and 4.6.2 describe specimens cured for 7 and 14 days, respectively. Section 4.6.3 provides a brief comparison and summary of all specimens.

4.6.1 Program III Specimens Cured for 7-Days

The average free-shrinkage data for Program III specimens cured for 7-days after 0, 30, 90, 180, and 365 days of drying are presented in Table 4.24. Figures 4.17 and 4.18 compare the shrinkage results after 30 and 365 days of drying, respectively. Expansion values range from 10 $\mu\epsilon$ for the concrete containing limestone to 23 $\mu\epsilon$ for both the concrete containing granite and quartzite. As shown in Table 4.24, after 30 days of drying, the free shrinkage values begin to separate, and after 90 days of drying, concrete containing quartzite has the least shrinkage (340 $\mu\epsilon$) followed by the granite mixture (377 $\mu\epsilon$), and finally, the limestone mixture (427 $\mu\epsilon$). Similar differences are maintained throughout the remainder of the drying period. At 365 days, shrinkage increases to 373, 407, and 467 $\mu\epsilon$ for the quartzite, granite, and limestone batches, respectively, with the quartzite batch exhibiting a slight decrease in shrinkage from 377 to 373 $\mu\epsilon$ between 180 and 365 days.

Table 4.24 – Summary of 7-Day Program III Free-Shrinkage Data (in microstrain)

Days of Drying	Limestone	Granite	Quartzite
	7-Day Cure	7-Day Cure	7-Day Cure
0	-10	-23	-23
30	323	300	270
90	427	377	340
180	450	400	377
365	467	407	373

The early-age shrinkage results through 30 days of drying are shown in Fig. 4.17. The quartzite specimens have the least shrinkage at 30 days (270 $\mu\epsilon$), followed by the concrete containing granite (300 $\mu\epsilon$), and finally, limestone (323 $\mu\epsilon$). The 23 $\mu\epsilon$ difference in shrinkage between the limestone and granite batches is not statistically significant, but the differences between the limestone and quartzite batches (53 $\mu\epsilon$) and the granite and quartzite batches (30 $\mu\epsilon$) are significant at $\alpha = 0.02$ and $\alpha = 0.2$, respectively (Table 4.25). The results taken at 30 days, however, do not fully explain the early-age shrinkage behavior of these three mixtures. Through at least 10 days after the end of the curing period, the limestone batch exhibits the least amount of shrinkage. The shrinkage curve for the concrete containing quartzite exceeds the limestone batch as late as day 10 and then drops below for the remainder of the one-year drying period. The free-shrinkage curve for the concrete containing granite behaves in a similar fashion, in this case falling below the limestone curve on day 16. These results appear to indicate that the restraint provided by stiff aggregates (granite and quartzite) lead to reduced long-term shrinkage, although initially, the water held within the pores of the limestone extends the hydration reaction and slows internal drying, resulting in lower early-age shrinkage.

The effect of aggregate type on long-term shrinkage is illustrated in Fig. 4.18, where it can be seen that the relative order of shrinkage at 365 days is the same as the 30-day shrinkage. The quartzite batch is observed to have the least shrinkage (373 $\mu\epsilon$), followed by the granite (300 $\mu\epsilon$) and limestone (323 $\mu\epsilon$) batches. All of the differences observed are statistically significant at least at $\alpha = 0.10$ (Table 4.26). These long-term shrinkage results are consistent with previous observations that aggregates with a higher modulus of elasticity tend to reduce shrinkage. It is clear, however, that curing (both internal and external) plays an important role in determining the extent of this shrinkage reduction. Specimens cured for 14-days are discussed next in Section 4.6.2.

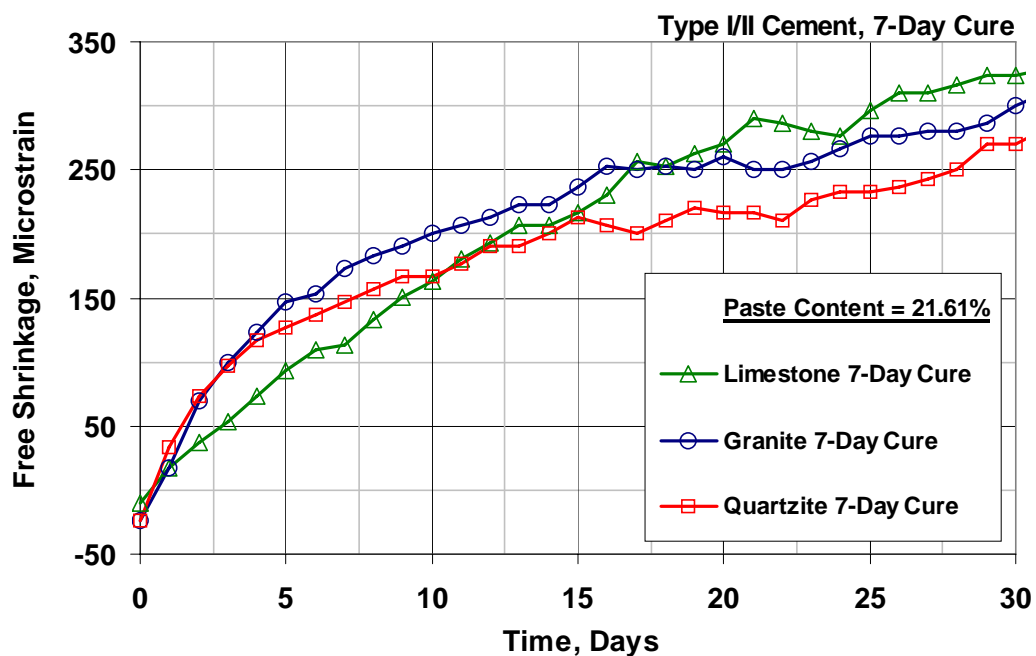


Fig. 4.17 – Free-Shrinkage Test (ASTM C 157). Program III specimens cured for 7 days. Average free shrinkage versus time through 30 days (drying only).

Table 4.25 – Student’s t-test results for Program III specimens cured for 7 days. 30-Day comparison of free-shrinkage data

	30-Day Free Shrinkage ($\mu\epsilon$)	Limestone	Granite	Quartzite
Limestone	323		N	Y
Granite	300			80
Quartzite	270			

Note: See the Table 4.4 note for an explanation of the terms “N”, “80”, “90”, “95”, and “Y”.

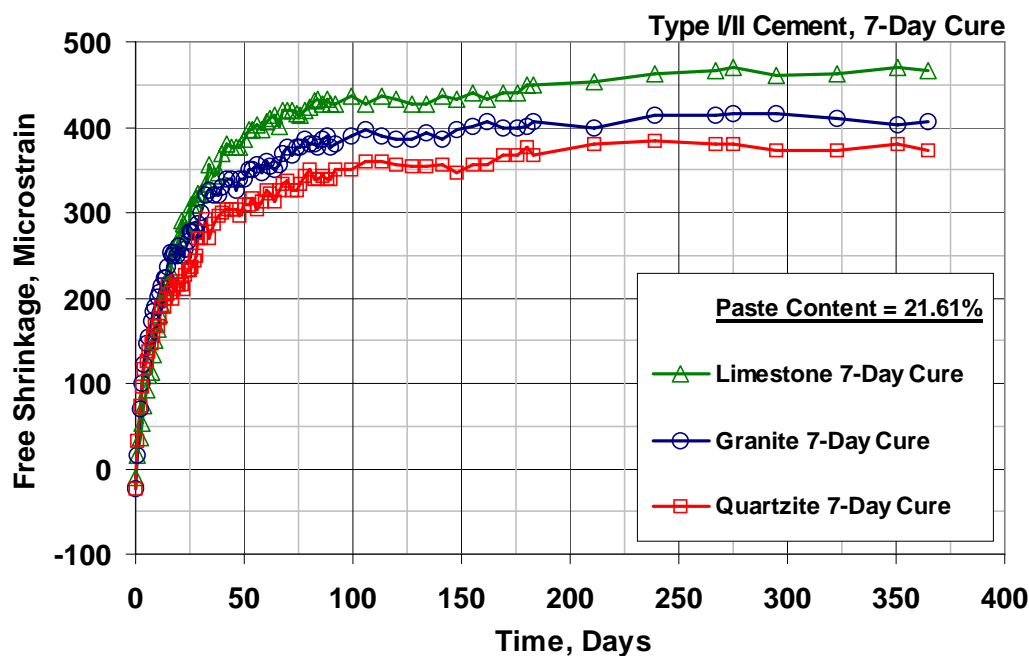


Fig. 4.18 – Free-Shrinkage Test (ASTM C 157). Program III specimens cured for 7 days. Average free shrinkage versus time through 365 days (drying only).

Table 4.26 – Student’s t-test results for Program III specimens cured for 7 days. 365-Day comparison of free-shrinkage data

	365-Day Free Shrinkage (μϵ)	Limestone	Granite	Quartzite
Limestone	467		95	Y
Granite	407			90
Quartzite	373			

Note: See Table 4.4 for an explanation of the terms “N”, “80”, “90”, “95”, and “Y”.

4.6.2 Program III Specimens Cured for 14-Days

The average free-shrinkage data for Program III specimens cured for 14-days after 0, 30, 90, 180, and 365 days of drying are presented in Table 4.27. Only relatively small differences in shrinkage compared to the specimens cured for 7 days are observed between the three mixtures, although the concrete containing quartzite has the least shrinkage throughout most of the testing period. After 30 days of drying, the specimens containing quartzite exhibit the least shrinkage (283 μϵ),

followed by the limestone mixture (290 $\mu\epsilon$), and the granite mixture (293 $\mu\epsilon$). At the conclusion of the test, free shrinkage increases to 380, 413, and 420 $\mu\epsilon$ for the concrete containing quartzite, granite, and limestone, respectively. The results for specimens cured for 14 days, however, are qualitatively very similar to the results obtained for the specimens cured for only 7 days.

Table 4.27 – Summary of Program III Specimens Cured for 14 Days

Days of Drying	Limestone	Granite	Quartzite
	14-Day Cure	14-Day Cure	14-Day Cure
0	-10	-27	-23
30	290	293	283
90	383	370	353
180	407	410	383
365	420	413	380

The specimens cured for 14 days are shown through the first 30 days of drying in Fig. 4.19 where shrinkage ranges from only 283 to 293 $\mu\epsilon$. Similar to the results shown in Fig. 4.17, however, the concretes containing quartzite and granite behave quite differently than the limestone batch prior to day 30. The free-shrinkage curves for the concrete containing quartzite and granite exhibit shrinkage during the first 30 days that exceed the limestone batch by as much as 77 $\mu\epsilon$. The maximum difference occurs on day 8 and day 9 for the quartzite and granite batches, respectively, but slowly decreases until day 24 when the average shrinkage for all three batches is equal. The results of the Student's t-test after 30 days of drying are shown in Table 4.28a, and an additional analysis after only 9 days of drying is shown in Table 4.28b. As expected, none of the differences in shrinkage at 30 days are statistically significant, but after 9 days of drying, the shrinkage of the batches containing low-absorption aggregate is significantly higher (at $\alpha = 0.02$) than the shrinkage of the concrete containing limestone. This behavior, observed through the first 24 days of

drying, is similar to the behavior observed for the specimens cured for 7 days, although it is more pronounced for the specimens cured for 14 days.

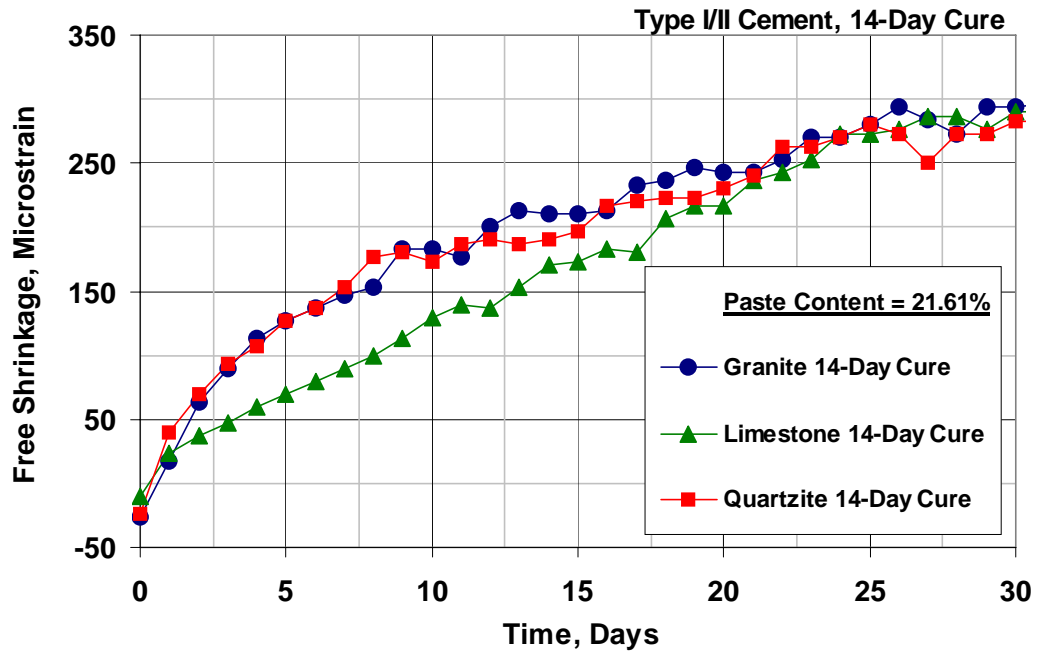


Fig. 4.19 – Free-Shrinkage Test (ASTM C 157). Program III specimens cured for 14 days. Average free shrinkage versus time through 30 days (drying only).

Table 4.28a – Student’s t-test results for Program III specimens cured for 14 days. 30-Day comparison of free-shrinkage data

	30-Day Free Shrinkage (µε)	Limestone	Granite	Quartzite
Limestone	290		N	N
Granite	293			N
Quartzite	283			

Note: See the Table 4.4 note for an explanation of the terms “N”, “80”, “90”, “95”, and “Y”.

The free-shrinkage curves after one year of drying are presented in Fig. 4.20, and the results of the Student’s t-test at 365 days are shown in Table 4.29. After the initial differences in shrinkage observed during the first 24 days of drying, very little difference is observed between the specimens cast with limestone and those cast with granite. This difference is not statistically significant after 365 days of drying (Table

Table 4.28b – Student’s t-test results for Program III specimens cured for 14 days. 9-Day comparison of free-shrinkage data

	9-Day Free Shrinkage ($\mu\epsilon$)	Limestone	Granite	Quartzite
Limestone	113		Y	Y
Granite	183			N
Quartzite	180			

Note: See the Table 4.4 note for an explanation of the terms “N”, “80”, “90”, “95”, and “Y”.

4.29). The quartzite free-shrinkage curve equals and then drops below the other two curves on day 43 and exhibits the least shrinkage for the balance of the testing period. Both the differences between the specimens containing quartzite and limestone and quartzite and granite are statistically significant at least at $\alpha = 0.10$ (Table 4.29). The average shrinkage after one year of drying for the limestone, granite, and quartzite specimens are 420, 413, and 380 $\mu\epsilon$, respectively. The total difference in shrinkage of only 40 $\mu\epsilon$, compared to 94 $\mu\epsilon$ for the specimens cured for 7 days, results almost entirely from the 47 $\mu\epsilon$ reduction in shrinkage of the limestone batch as the curing time is increased from 7 to 14 days.

4.6.3 Program III Summary

The combined effect of curing and aggregate type on shrinkage is shown in Figs. 4.21 and 4.22. The results through 30-days of drying are presented in Fig. 4.21 and indicate that increasing the curing time from 7 to 14 days has very little effect on the shrinkage of concrete containing quartzite or granite. In fact, none of the small differences between the 7 and 14-day specimens are statistically significant (Table 4.30). This is not the observation for the limestone mixtures, where increasing the curing period from 7 to 14 days reduced shrinkage by 33 $\mu\epsilon$, a difference that is statistically significant at a confidence level of $\alpha = 0.1$ (Table 4.30). In general, the trends remain the same after one-year of drying (Fig. 4.22). Concretes containing quartzite or granite shrink less than concrete containing limestone, and increasing the

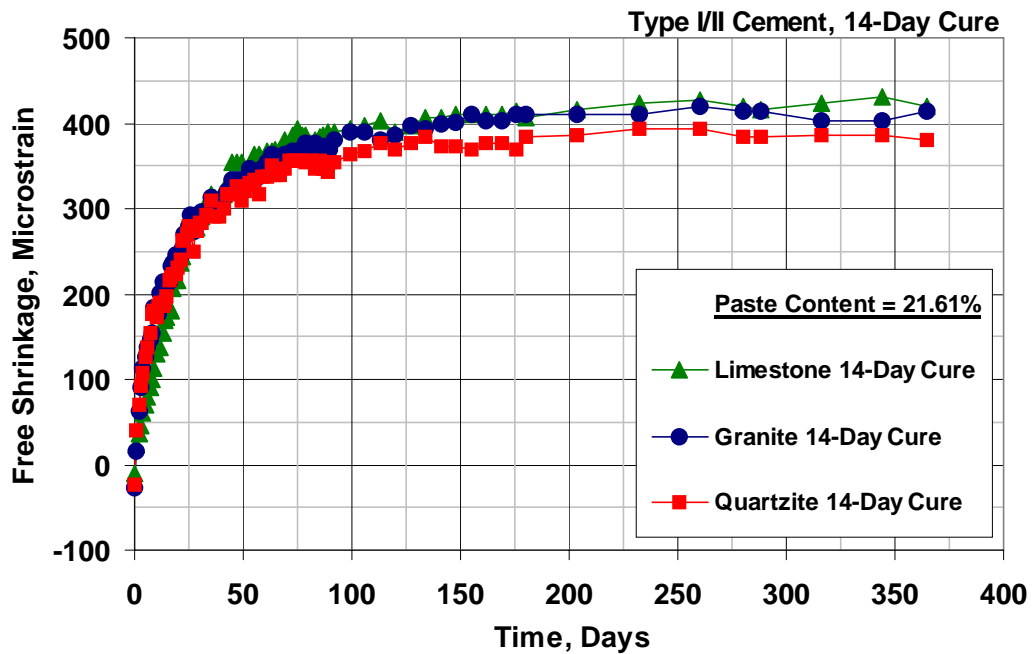


Fig. 4.20 – Free-Shrinkage Test (ASTM C 157). Program III specimens cured for 14 days. Average free shrinkage versus time through 365 days (drying only).

Table 4.29 – Student’s t-test results for Program III specimens cured for 14 days. 365-Day comparison of free-shrinkage data

	365-Day Free Shrinkage (µε)	Limestone	Granite	Quartzite
Limestone	420		N	Y
Granite	413			90
Quartzite	380			

Note: See the Table 4.4 note for an explanation of the terms “N”, “80”, “90”, “95”, and “Y”.

curing period from 7 to 14 days results in a significant reduction in shrinkage for concrete containing limestone (Table 4.31). Finally, increasing the curing period from 7 to 14 days has little impact on the shrinkage behavior of concrete containing quartzite or granite in this series.

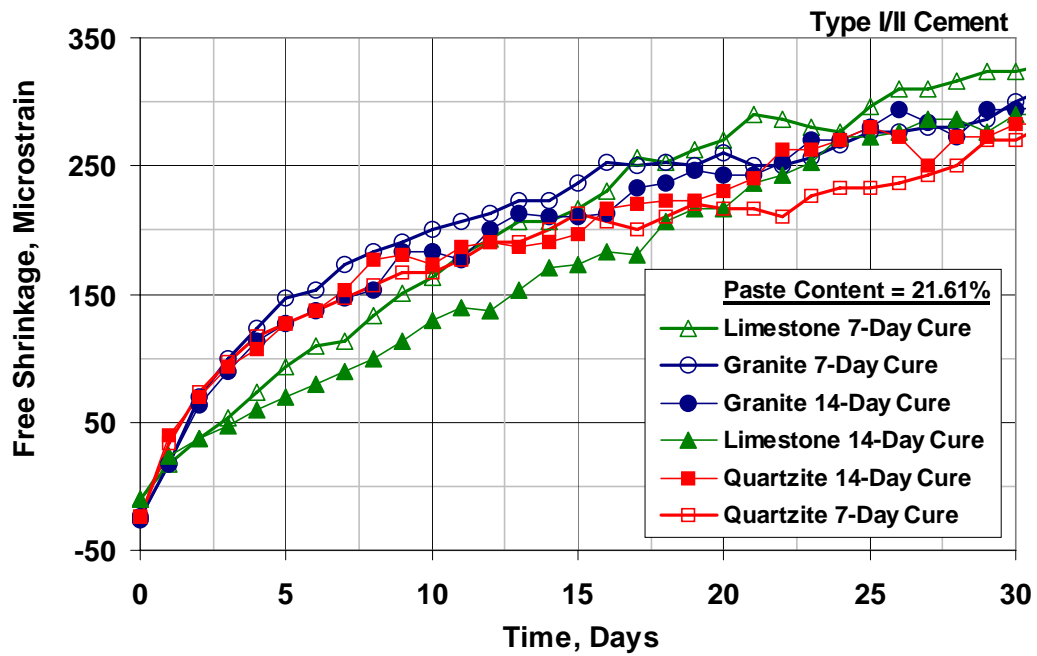


Fig. 4.21 – Free-Shrinkage Test (ASTM C 157). Program III. Average free shrinkage versus time through 30 days (drying only).

Table 4.30 – Student’s t-test Results for Program III 30-Day Free-Shrinkage Data

		30-Day Free Shrinkage ($\mu\epsilon$)	Limestone (LS)		Granite (G)		Quartzite (Q)	
			7-Day	14-Day	7-Day	14-Day	7-Day	14-Day
LS	7-Day	323		90	N	90	Y	95
	14-Day	290			N	N	80	N
G	7-Day	300				N	80	N
	14-Day	293					90	N
Q	7-Day	270						N
	14-Day	283						

Note: See the Table 4.4 note for an explanation of the terms “N”, “80”, “90”, “95”, and “Y”.

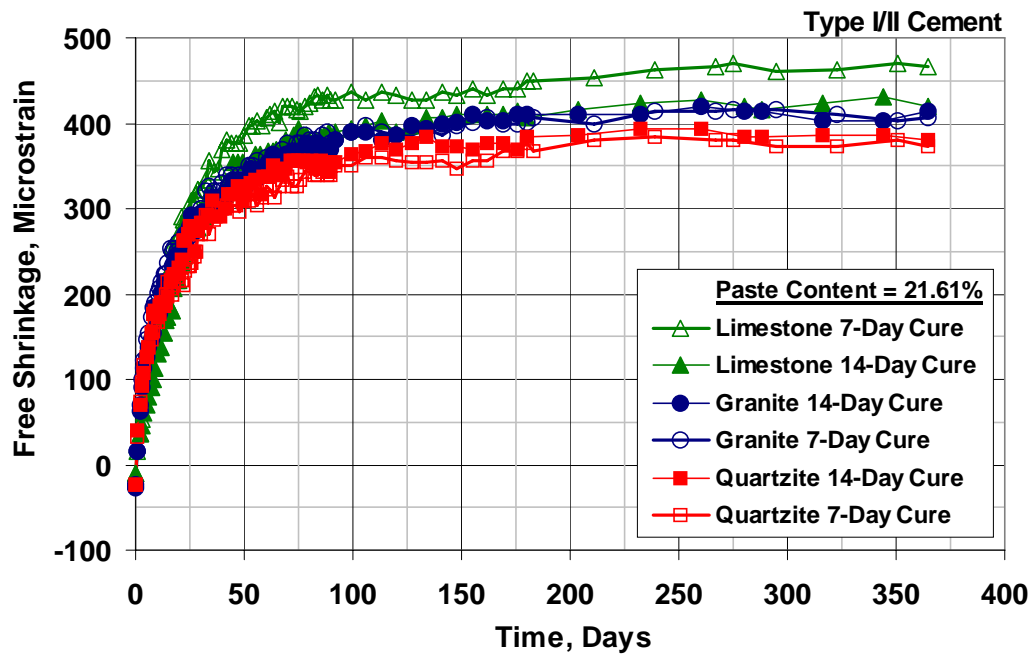


Fig. 4.22 – Free-Shrinkage Test (ASTM C 157). Program III. Average free shrinkage versus time through 365 days (drying only).

Table 4.31 – Student’s t-test Results for Program III 365-Day Free-Shrinkage Data

		365-Day Free Shrinkage ($\mu\epsilon$)	Limestone (LS)		Granite (G)		Quartzite (Q)	
			7-Day	14-Day	7-Day	14-Day	7-Day	14-Day
LS	7-Day	467		95	95	95	Y	Y
	14-Day	420			N	N	Y	Y
G	7-Day	407				N	90	80
	14-Day	413					95	90
Q	7-Day	373						N
	14-Day	380						

Note: See the Table 4.4 note for an explanation of the terms “N”, “80”, “90”, “95”, and “Y”.

In general, the Program III results reinforce the results obtained in Program I and indicate, as expected, that concrete containing aggregate with a higher modulus of elasticity will shrink less than concrete with a lower modulus. Both the results from Program I and Program III also indicate that increasing the curing period from 7

to 14 days will consistently reduce both the short and long-term shrinkage of concrete containing limestone, granite, or quartzite. The reductions in shrinkage obtained as the curing period is increased from 7 to 14 days for concrete containing limestone are in each case statistically significant, and while the reductions in shrinkage for concrete containing granite or quartzite are measurable, they are generally small and not statistically significant. Internal curing provided by the saturated porous limestone results initially in a slower shrinkage rate for the limestone specimens compared to the granite and quartzite specimens through the first 10 to 25 days of drying. After this initial drying period that appears to be dominated by the slow release of water within the pores of the aggregate, the concretes containing stiffer aggregates exhibit less shrinkage than the concrete containing porous limestone.

4.7 PROGRAM IV (SHRINKAGE REDUCING ADMIXTURE)

The effect of a shrinkage reducing admixture (SRA) [0, 1, and 2% dosage by mass (weight) of cement] on free shrinkage is evaluated in Program IV in conjunction with 7 and 14 day curing periods. The batches in this program contain limestone coarse aggregate, a w/c ratio of 0.42, and a paste content of 23.3% [corresponding to a cement content 317 kg/m^3 (535 lb/yd^3)]. For each of the batches containing an SRA, the water content is adjusted to account for the volume of SRA and ensure that the void content of the hardened concrete is the same for each mixture. A summary of Program IV is presented in Table 4.32. Individual mixture proportions, plastic concrete properties, and compressive strengths are presented in Table A.8 in Appendix A, and individual free-shrinkage curves are presented in Figs. C.16 through C.18 in Appendix C.

Shrinkage reducing admixtures have been available commercially since 1985, and are now being used with increased regularity – especially for non-air-entrained concrete applications. Shrinkage reducing admixtures reduce drying shrinkage by

Table 4.32 – Program IV Summary

Dosage by Weight of Cement	Percent Paste	w/c Ratio	SRA Dosage mL/m³ (gal/yd³)
Control (0%)	23.3	0.42	--
1%	23.3	0.42	3165 (0.64)
2%	23.3	0.42	6330 (1.28)

decreasing the surface tension of pore water. The capillary stresses that result in drying shrinkage occur when the internal relative humidity is between 45 and 95% and vary directly with the surface tension of water. Reducing the surface tension of water reduces capillary stresses, but also leads to difficulties in maintaining a stable air-void system, and as a result, special precautions must be made to ensure that the desired air content is achieved. Details of the mixing procedure used in Program IV are provided in Section 2.9.4.

The average free-shrinkage data for Program IV specimens cured after 0, 30, 90, 180, and 365 days of drying are presented in Table 4.33. Figures 4.23 and 4.24 compare the shrinkage results after 30 and 365 days, respectively. Expansion values range from 20 $\mu\epsilon$ for the 1% SRA dosage mixture cured for 7 days to 43 $\mu\epsilon$ for the control specimens cured for 7 days. No apparent trend exists between the SRA dosage or the curing period and the amount of expansion that occurs during the curing period. The results indicate that as the SRA dosage is increased, shrinkage is reduced. In addition, a slight, but measurable, reduction in shrinkage is observed as the curing period is increased from 7 to 14 days.

The shrinkage results through 30 days of drying are shown in Fig. 4.23. Increasing the SRA dosage from 0 to 2% results in a reduction in shrinkage at all ages, although the largest reduction in shrinkage is obtained with an increase in the dosage from 0 to 1%. For mixtures cured for 14 days, an increase in the dosage from 0 to 1% reduced the early-age shrinkage from 283 to 180 $\mu\epsilon$. A further reduction in shrinkage of 67 $\mu\epsilon$ is obtained as the SRA dosage is doubled to 2%. The results of

Table 4.33 – Summary of Program IV Free-Shrinkage Data (in microstrain)

Days of Drying	1% SRA		2% SRA		Control (0% SRA)	
	7-Day Cure	14-Day Cure	7-Day Cure	14-Day Cure	7-Day Cure	14-Day Cure
0	-20	-23	-40	-27	-43	-33
30	197	180	127	113	320	283
90	313	313	263	253	413	387
180	360	340	327	313	453	420
365	363	357	350	330	483	460

the Student's t-test are shown in Table 4.34 and indicate that these differences are statistically significant at the highest level of confidence. Similar reductions in shrinkage are obtained for the specimens cured for only 7 days where an increase in the SRA dosage from 0 to 2% reduces shrinkage by a total 197 $\mu\epsilon$ at 30 days. Increasing the curing period from 7 to 14 days does not have a significant effect on the early-age shrinkage of mixtures containing an SRA. Increasing the curing period from 7 to 14 days reduced the shrinkage of the control mixture (0% SRA dosage) from 320 to 283 $\mu\epsilon$ at 30 days. This reduction in shrinkage is statistically significant at $\alpha = 0.1$ (Table 4.34).

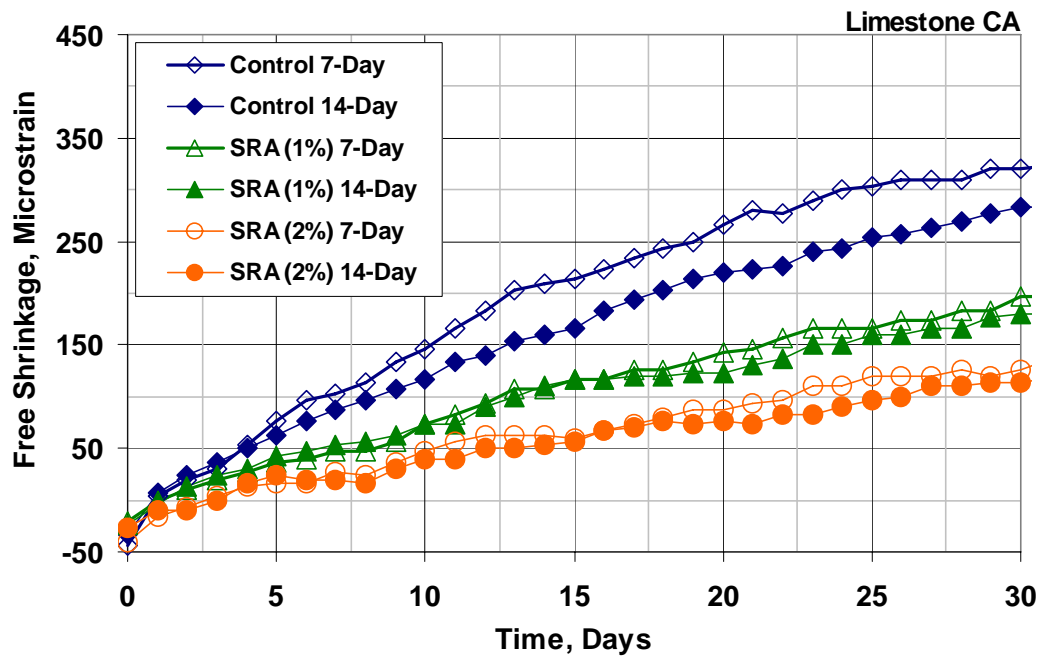


Fig. 4.23 – Free-Shrinkage Test (ASTM C 157). Program IV. Average free shrinkage versus time through 30 days (drying only).

Table 4.34 – Student’s t-test Results for Program IV 30-Day Free-Shrinkage Data

		30-Day Free Shrinkage (µε)	1% SRA		2% SRA		Control (0% SRA)	
			7-Day	14-Day	7-Day	14-Day	7-Day	14-Day
1%	7-Day	197		90	Y	Y	Y	Y
	14-Day	180			Y	Y	Y	Y
2%	7-Day	127				N	Y	Y
	14-Day	113					Y	Y
0%	7-Day	320						90
	14-Day	283						

Note: See the Table 4.4 note for an explanation of the terms “N”, “80”, “90”, “95”, and “Y”.

The free-shrinkage results through the one-year drying period are illustrated in Fig. 4.24. The relative order of long-term shrinkage is identical to that of the early-age shrinkage shown in Fig. 4.23 and demonstrates clearly that the addition of an SRA significantly reduces shrinkage. For mixtures cured for 14 days, an increase in

the dosage from 0 to 1% resulted in a decrease in shrinkage of $74 \mu\epsilon$ after 90 days of drying. The difference increased to $103 \mu\epsilon$ after 365 days of drying – a statistically significant difference at the highest level of confidence (Table 4.35). An additional reduction in shrinkage of $60 \mu\epsilon$ at 90 days and $27 \mu\epsilon$ at 365 days is obtained as the SRA dosage is increased further from 1 to 2%. The shrinkage reduction at 365 days, however, is not statistically significant (Table 4.35). A similar reduction in shrinkage is obtained as the SRA dosage is increased from 0 to 2% for the specimens cured for only 7 days. Throughout most of the drying period, specimens cured for 7 days exhibited more shrinkage than those cured for 14 days. After 365 days of drying, the reduction in shrinkage is $23 \mu\epsilon$ for the control batch, $20 \mu\epsilon$ for the 2% SRA batch, and $6 \mu\epsilon$ for the 1% SRA batch, although none of these differences are statistically significant (Table 4.35).

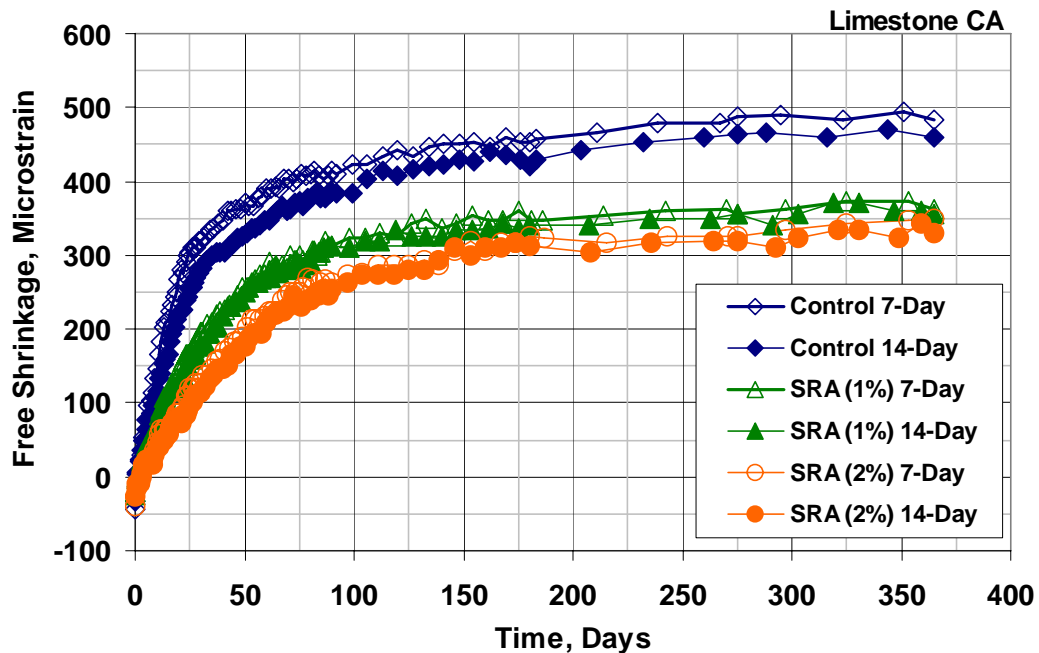


Fig. 4.24 – Free-Shrinkage Test (ASTM C 157). Program IV. Average free shrinkage versus time through 365 days (drying only).

Table 4.35 – Student’s t-test Results for Program IV 365-Day Free-Shrinkage Data

		365-Day Free Shrinkage ($\mu\epsilon$)	1% SRA		2% SRA		Control (0% SRA)	
			7-Day	14-Day	7-Day	14-Day	7-Day	14-Day
1%	7-Day	363		N	N	80	Y	Y
	14-Day	357			N	N	Y	Y
2%	7-Day	350				N	Y	Y
	14-Day	330					Y	Y
0%	7-Day	483						N
	14-Day	460						

Note: See the Table 4.4 note for an explanation of the terms “N”, “80”, “90”, “95”, and “Y”.

4.7.1 Program IV Summary

The addition of an SRA to concrete mixtures results in significantly less early-age and long-term drying shrinkage as the SRA dosage is increased from 0 to 2%. Increasing the curing period from 7 to 14 days does not have a significant effect on the free shrinkage of mixtures containing an SRA. Before these promising mixtures are implemented into the field, careful consideration must be given to the interaction of the chemical admixtures, the mixing procedures, and the placing techniques to ensure that a stable air-void system is achieved. The relatively large reduction in shrinkage obtained with the 1% SRA dosage, combined with the greater ease in maintaining the air content compared to the 2% dosage rate indicates that useable mixes can be developed that provide desired concrete properties in both the plastic and hardened state. Additional details regarding the mixing procedures are provided in Section 2.9.4.

4.8 PROGRAM V (CEMENT TYPE AND FINENESS)

The influence of cement type and fineness on free shrinkage is examined in Program V, representing an expansion of the comparisons included in Program I. This evaluation includes four mixtures, each cast with a different sample of portland

cement (one Type I/II, two Type II, and one Type III) and cured for either 7 or 14 days. Blaine fineness values for the samples range from 323 to 549 m²/kg, and a summary of Program V is provided in Table 4.36. The coarse Type II cement with a Blaine fineness of 323 m²/kg is designated as Type II (C) while the finer Type II cement, with a Blaine fineness of 334 m²/kg, is simply designated as Type II. Each mixture has a *w/c* ratio of 0.42 and a cement content of 317 kg/m³ (535 lb/yd³), corresponding to a paste content of 23.3%. Mixture proportions, plastic concrete properties, and compressive strengths are provided in Table A.9 in Appendix A, and individual free-shrinkage curves are presented in Figs. C.16 and C.19 through C.21 in Appendix C.

Table 4.36 – Program V Summary

Blaine Fineness m²/kg	Cement Type	Sample No.[†]
323	II (C)	2
334	II	1(a) and 1(b)
379	I/II	3
549	III	1

[†]The sample number corresponds to the cement designation provided in Tables 2.1 and A.1.

Previous observations by Bennett and Loat (1970), Chariton and Weiss (2002), and Deshpande et al. (2007) indicate that concretes cast with coarse cements shrink less than concretes containing fine cements. Lower shrinkage is generally associated with coarse cements for two reasons: First, the unhydrated portion of the large cement particles act as aggregate and restrain the shrinking paste, and second, the coarser pore structure results in lower capillary stresses, and thus, lower shrinkage. At the same time, the reduction in shrinkage may be partially offset due to a reduction in the stiffness of the cement-paste matrix resulting from the coarse pore structure. Additionally, the relatively small surface area of the coarse cement particles means less water is chemically combined during hydration compared to fine cements. The results of Program I, which compared the shrinkage performance of

concrete cast with Type II cement compared to Type I/II cement, indicated that the coarser Type II cement provides no special advantage, and when only cured for 7 days as compared to 14 days, led to increased shrinkage. Program V includes two additional cements [Type II (C) and Type III] and provides a basis for determining the suitability of three commercially available cements. The results of Program V are discussed based on the length of the curing period. Sections 4.8.1 and 4.8.2 describe specimens cured for 7 and 14 days, respectively. Section 4.8.3 provides a brief comparison and summary of all specimens.

4.8.1 Program V Specimens Cured for 7 Days

The average free-shrinkage data for Program V specimens cured for 7-days after 0, 30, 90, 180, and 365 days of drying are presented in Table 4.37. After the 7-day curing period, average shrinkage strains range from $-43 \mu\epsilon$ (indicating expansion) for the Type I/II cement mixture to $30 \mu\epsilon$ (indicating shrinkage) for the Type III cement mixture. The results shown in Table 4.37 indicate only small differences in shrinkage between the concrete containing Type I/II or either Type II cement, but the concrete containing Type III cement has increased shrinkage throughout the drying period. After 365 days of drying, shrinkage strains of 477, 483, 513, and 533 $\mu\epsilon$ are obtained for the concrete cast, respectively, with Type II (C), Type I/II, Type II, and Type III portland cement.

Table 4.37 – Summary of Free-Shrinkage Data for Program V (in microstrain)

Days of Drying	Cement Type and Blaine Fineness (m^2/kg)			
	II (C) - 323	II - 334	I/II - 379	III - 549
0	-23	-30	-43	30
30	300	323	320	400
90	423	443	413	473
180	460	487	453	523
365	477	513	483	533

The early-age shrinkage of the Program V specimens cured for 7 days is illustrated in Fig. 4.25. The 73 $\mu\epsilon$ difference in shrinkage between the mixtures containing Type I/II and Type III cement established during the curing period increases slightly to 80 $\mu\epsilon$ at 30 days, but the largest difference of 100 $\mu\epsilon$ occurs between the Type III cement mixture and the Type II (C) mixture at 30 days. Through the first 30 days, the Type I/II and Type II cement mixtures exhibited similar shrinkage. After approximately 10 days of drying, the shrinkage for the batch containing Type II (C) cement dropped slightly below that of the other batches and remained there for the duration of the test. The concretes containing Type II (C), Type II, Type I/II, and Type III cement had 30-day shrinkage strains of 300, 323, 320, and 400 $\mu\epsilon$, respectively. The results of the statistical analysis (Table 4.38) show that, at 30 days, the difference in shrinkage of concrete containing Type III cement and those containing Type I/II and both Type II cements is significant at the highest level of confidence. The small difference between the Type I/II and Type II cement mixtures is not statistically significant, but the differences between the between the Type II (C) cement mixture and the Type II and Type I/II cement mixtures are significant at $\alpha = 0.1$ and $\alpha = 0.2$ confidence levels, respectively (Table 4.38).

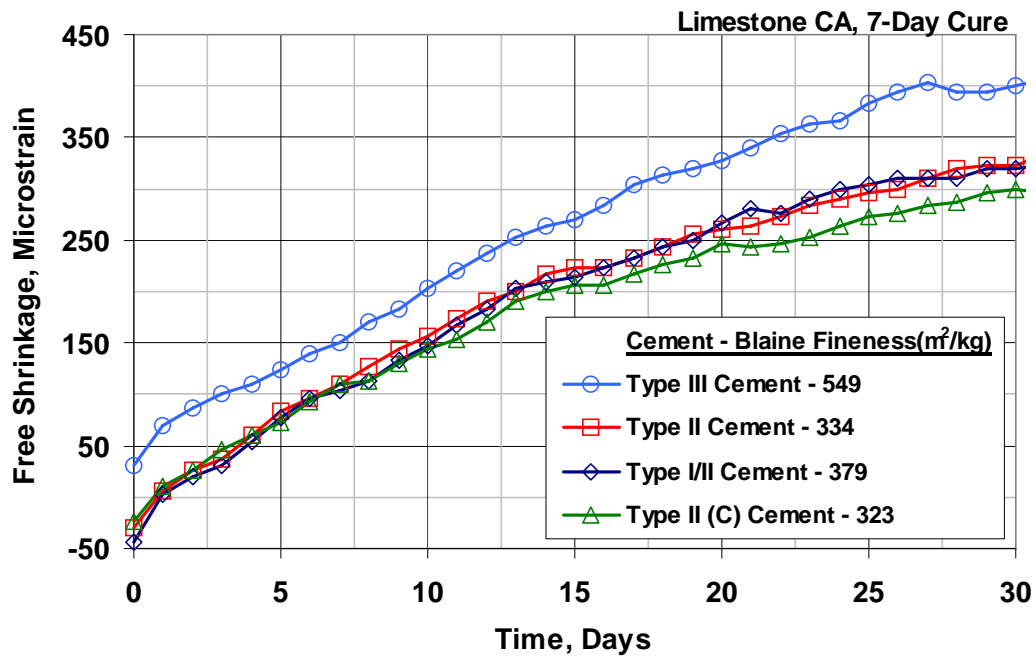


Fig. 4.25 – Free-Shrinkage Test (ASTM C 157). Program IV specimens cured for 7 days. Average free shrinkage versus time through 30 days (drying only).

Table 4.38 – Student’s t-test results for Program V specimens cured for 7 days. 30-Day comparison of free-shrinkage data

	30-Day Free Shrinkage ($\mu\epsilon$)	Cement Type and Blaine Fineness (m^2/kg)			
		II (C) – 323	II – 334	I/II – 379	III – 549
II (C) – 323	300		90	80	Y
II – 334	323			N	Y
I/II – 379	320				Y
III – 549	400				

Note: See the Table 4.4 note for an explanation of the terms “N”, “80”, “90”, “95”, and “Y”.

The effect of cement type on long-term shrinkage is shown in Fig. 4.26 where the results after 365 days of drying are very similar to those observed after only 30 days. The concrete containing Type III cement exhibits the most shrinkage throughout the drying period, while the remaining concrete mixtures exhibit similar behavior. At the conclusion of the test, the concretes containing Type II (C) cement and Type I/II cement exhibited shrinkage strains of 477 and 483 $\mu\epsilon$, respectively,

followed by the concretes containing Type II cement (513 $\mu\epsilon$) and Type III cement (533 $\mu\epsilon$). All of these shrinkage differences are statistically significant, with the exception of the 6 $\mu\epsilon$ difference between the shrinkage of concrete containing Type II and Type I/II cement (Table 4.39).

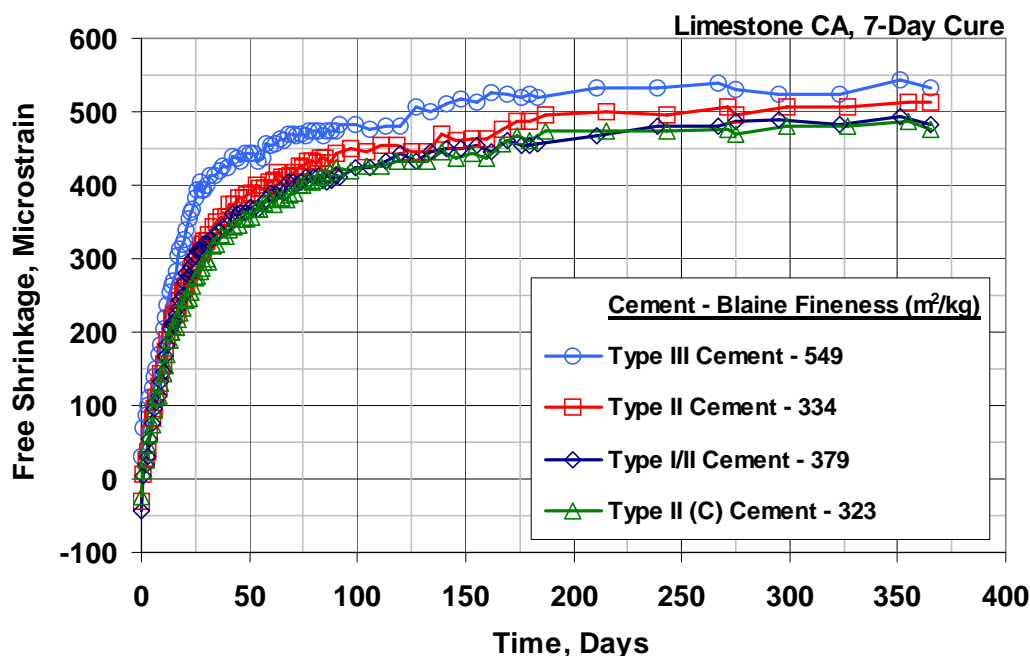


Fig. 4.26 – Free-Shrinkage Test (ASTM C 157). Program V specimens cured for 7 days. Average free shrinkage versus time through 365 days (drying only).

Table 4.39 – Student’s t-test results for Program V specimens cured for 7 days. 365-Day comparison of free-shrinkage data

	365-Day Free Shrinkage ($\mu\epsilon$)	Cement Type and Blaine Fineness (m^2/kg)			
		II (C) – 323	II – 334	I/II – 379	III – 549
II (C) – 323	477		95	N	Y
II – 334	513			80	90
I/II – 379	483				95
III – 549	533				

Note: See the Table 4.4 note for an explanation of the terms “N”, “80”, “90”, “95”, and “Y”.

4.8.2 Program V Specimens Cured for 14 Days

Average free shrinkage values for 0, 30, 90, 180, and 365 days are tabulated in Table 4.40 based on cement type and fineness for specimens cured for 14 days. The concrete cast with Type III cement exhibits increased shrinkage through most of the drying period, but this increase begins to decrease after approximately 180 days, and at the end of the testing period no apparent trend with respect to cement type or fineness is apparent. After one year of drying, concrete containing Type II cement had the most shrinkage (490 $\mu\epsilon$), followed by concrete containing Type III cement (477 $\mu\epsilon$), and finally concrete containing Type II (C) or Type I/II cements (460 $\mu\epsilon$).

Table 4.40 – Summary of Program V Free-Shrinkage Data (in microstrain)

Days of Drying	Portland Cement Type and Blaine Fineness (m^2/kg)			
	II (C) – 323	II – 334	I/II – 379	III – 549
0	-33	-37	-33	17
30	283	307	287	360
90	387	397	387	447
180	420	460	443	470
365	460	490	460	477

Figure 4.27 compares the early-age shrinkage results for concrete containing Type I/II, Type II, or Type III cement and cured for 14 days. After 30 days of drying, the two Type II and Type I/II cement mixtures exhibit similar shrinkage, while the Type III cement mixture exhibits increased shrinkage. The majority of this difference is established during the curing period prior to the onset of drying. On day zero (corresponding to the last day in the curing period), the Type III mixture exhibited an average shrinkage strain of 17 $\mu\epsilon$, while each of the other mixtures exhibited expansion values of 33 or 37 $\mu\epsilon$. The resulting difference of approximately 50 $\mu\epsilon$ accounts for most, if not all, of the difference in shrinkage observed for the Type III mixture through the first 30 days. Thirty days after drying began, the concretes containing Type II (C), Type II, Type I/II, and Type III cement exhibit average

shrinkage strains of 307, 287, 283, and 360 $\mu\epsilon$, respectively. The differences in shrinkage between the Type II (C) cement mixture and the Type II and Type I/II mixtures are significant at confidence levels of $\alpha = 0.2$ and $\alpha = 0.1$, respectively. Differences between the Type III cement mixture and those containing Type I/II or Type II cement are statistically significant at confidence levels of at $\alpha = 0.02$ (Table 4.41).

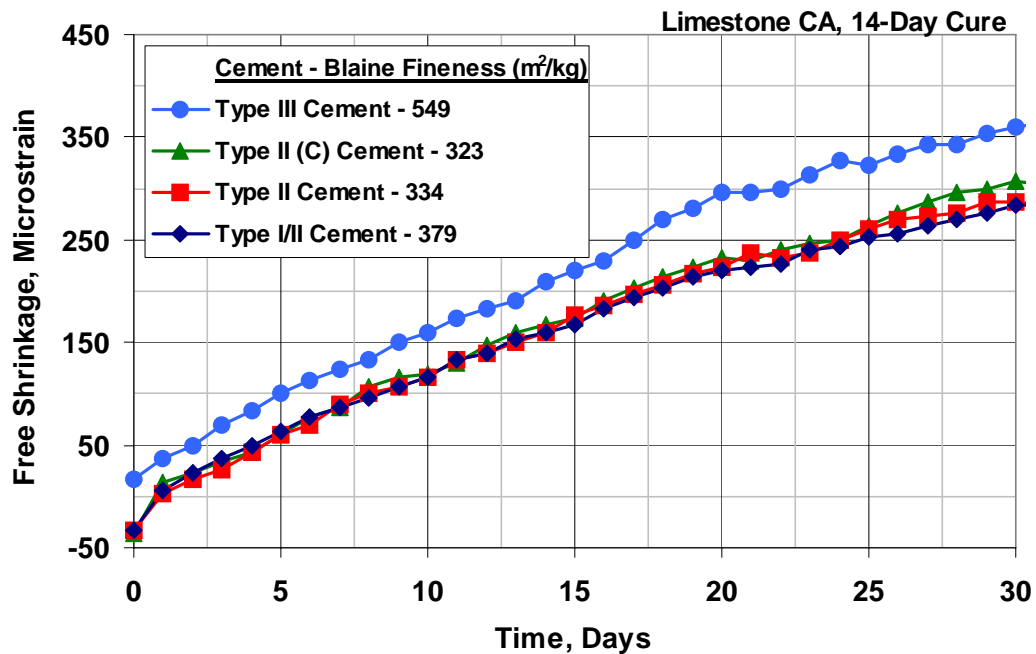


Fig. 4.27 – Free Shrinkage Test (ASTM C 157). Program V specimens cured for 14 days. Average free-shrinkage versus time through 30 days (drying only).

Table 4.41 – Student’s t-test results for Program V specimens cured for 14 days. 30-Day comparison of free-shrinkage data

	30-Day Free Shrinkage ($\mu\epsilon$)	Cement Type and Blaine Fineness (m^2/kg)			
		II (C) – 323	II – 334	I/II – 379	III – 549
II (C) – 323	307		80	90	Y
II – 334	287			N	Y
I/II – 379	283				Y
III – 549	360				

Note: See the Table 4.4 note for an explanation of the terms “N”, “80”, “90”, “95”, and “Y”.

The free-shrinkage curves through one year are presented in Fig. 4.28, and the results of the Student's t-test for the results after 365 days of drying are presented in Table 4.42. At the conclusion of the test period, there is no apparent effect of cement type on long-term shrinkage of concrete cured for 14 days. The concrete containing Type III portland cement exhibits increased shrinkage for periods up to 180 days of drying, but by the end of the testing period, the Type III cement mixture exhibits less shrinkage than the concrete containing Type II cement. Shrinkage values range from 460 $\mu\epsilon$ for the concrete cast with Type II (C) and Type I/II cement to 490 $\mu\epsilon$ for the concrete containing Type II cement. The differences in shrinkage between these specimens and the specimen cast with Type III cement are significant at $\alpha = 0.2$ (Table 4.42).

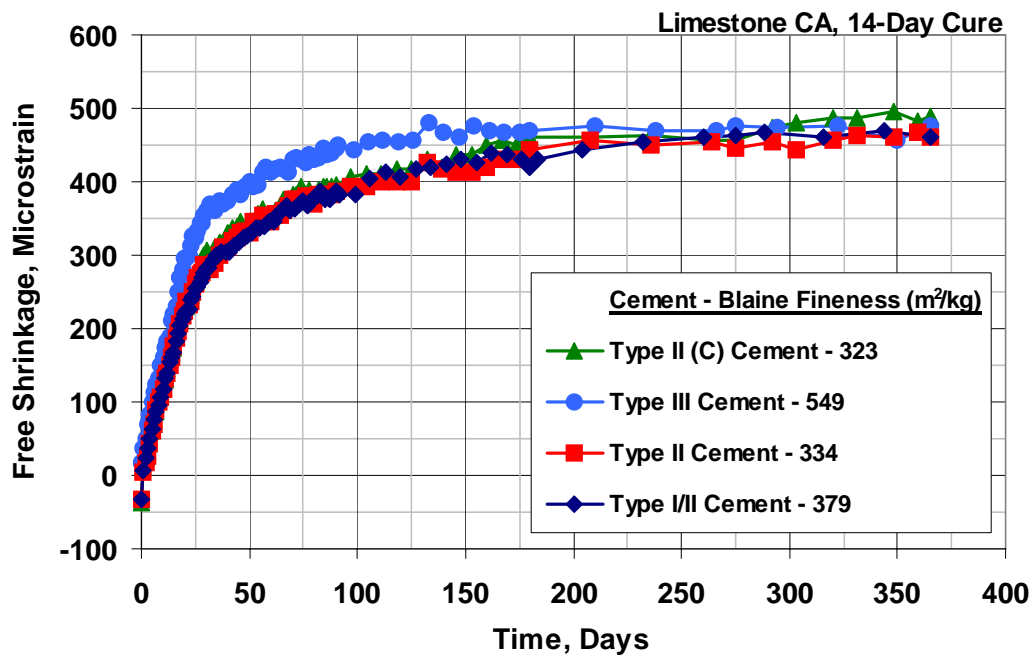


Fig. 4.28 – Free-Shrinkage Test (ASTM C 157). Program V specimens cured for 14 days. Average free shrinkage versus time through 365 days (drying only).

Table 4.42 – Student’s t-test results for Program V specimens cured for 14 days. 365-Day comparison of free-shrinkage data

	365-Day Free Shrinkage ($\mu\epsilon$)	Cement Type and Blaine Fineness (m^2/kg)			
		II (C) – 323	II – 334	I/II – 379	III – 549
II (C) – 323	460		80	N	80
II – 334	490			N	N
I/II – 379	460				80
III – 549	477				

Note: See the Table 4.4 note for an explanation of the terms “N”, “80”, “90”, “95”, and “Y”.

4.8.3 Program V Summary

The effect of increasing the curing period from 7 to 14 days on the shrinkage of the Program V specimens is presented in Figs. 4.29 and 4.30. With the exception of the concrete containing Type II (C) cement, increased curing reduces shrinkage. For the concrete containing Type II (C) cement, there was no statistically significant difference in shrinkage between specimens cured for 7 days and those cured for 14 days at either 30 or 365 days (Table 4.43 and 4.44). This finding for the Type II (C) is inconsistent with the results of Program I and previous work by Deshpande et al. (2007) that found a significant reduction in shrinkage as the curing time was increased from 7 to 14 days for coarse-ground cement. After only 30 days of drying, increasing the curing period from 7 to 14 days reduced average shrinkage strains by 36, 37, and 40 $\mu\epsilon$ for concrete containing Type II, Type I/II, and Type III cement, respectively. All of these reductions in shrinkage are statistically significant at least at $\alpha = 0.1$ (Table 4.43). After 365 days of drying, these differences increase to 53 and 56 $\mu\epsilon$ for the concrete containing Type II and Type III cement (differences that are statistically significant at $\alpha = 0.05$ and $\alpha = 0.02$, respectively), and decrease from 37 to 23 $\mu\epsilon$ for the concrete containing Type I/II cement (Fig. 4.30). With few exceptions, increasing the moist curing period from 7 to 14 days can be used to help control concrete shrinkage and limit cracking in bridge decks.

The use of Type III cement resulted in a significant increase in shrinkage compared to the control mixture (containing Type I/II cement) at 30 days, but only a slight increase in shrinkage after one year for specimens cured for 14 days. Only small differences in shrinkage are observed between the control mixture and specimens containing either of the Type II cements cured for 14 days. For the specimens cured for 7 days, the Type II (C) cement had the least shrinkage at both 30 and 365 days, but in many cases, the difference in shrinkage between this mixture and the mixtures containing Type II or Type I/II cement were not statistically significant. These results do not necessarily contradict previous work by Deshpande et al. (2007) that reported significant reductions in shrinkage with the use of a coarse-ground Type II cement. The Type II cements in this study had higher fineness values (323 and 334 m^2/kg) than the cement evaluated by Deshpande et al. (2007) (Blaine fineness = 306 m^2/kg), and thus, smaller differences in shrinkage should be expected.

Table 4.43 – Student’s t-test Results for Program V 30-Day Free-Shrinkage Data

		30-Day Free Shrinkage ($\mu\epsilon$)	Cement Type and Blaine Fineness (m^2/kg)							
			II (C) – 323		II – 334		I/II – 379		III – 549	
			7-Day	14-Day	7-Day	14-Day	7-Day	14-Day	7-Day	14-Day
II (C)	7-Day	300		N	90	N	80	80	Y	Y
	14-Day	307			80	80	N	90	Y	Y
II	7-Day	323				95	N	95	Y	90
	14-Day	287					90	N	Y	Y
I/II	7-Day	320						90	Y	90
	14-Day	283							Y	Y
III	7-Day	400								90
	14-Day	360								

Table 4.44 – Student’s t-test Results for Program V 365-Day Free-Shrinkage Data

		365-Day Free Shrinkage ($\mu\epsilon$)	Cement Type and Blaine Fineness (m^2/kg)							
			II (C) – 323		II – 334		I/II – 379		III – 549	
			7-Day	14-Day	7-Day	14-Day	7-Day	14-Day	7-Day	14-Day
II (C)	7-Day	477		N	95	N	N	80	Y	N
	14-Day	490			95	80	N	80	Y	N
II	7-Day	513				95	80	Y	90	Y
	14-Day	460					N	N	Y	N
I/II	7-Day	483						N	95	N
	14-Day	460							Y	80
III	7-Day	533								Y
	14-Day	477								

Note: See the Table 4.4 note for an explanation of the terms “N”, “80”, “90”, “95”, and “Y”.

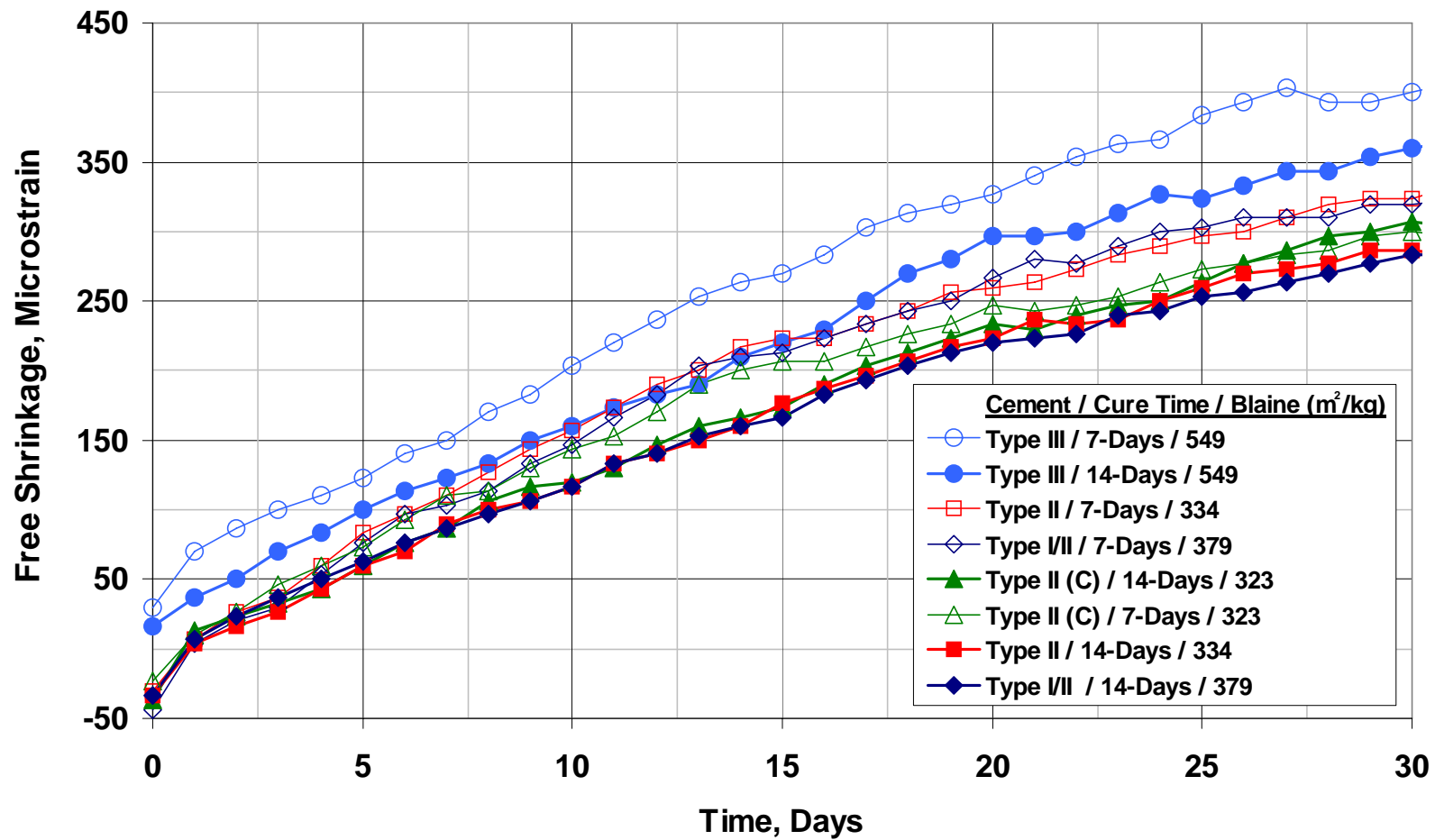


Fig. 4.29 – Free-Shrinkage Test (ASTM C 157). Program V. Average free shrinkage versus time through 30 days (drying only).

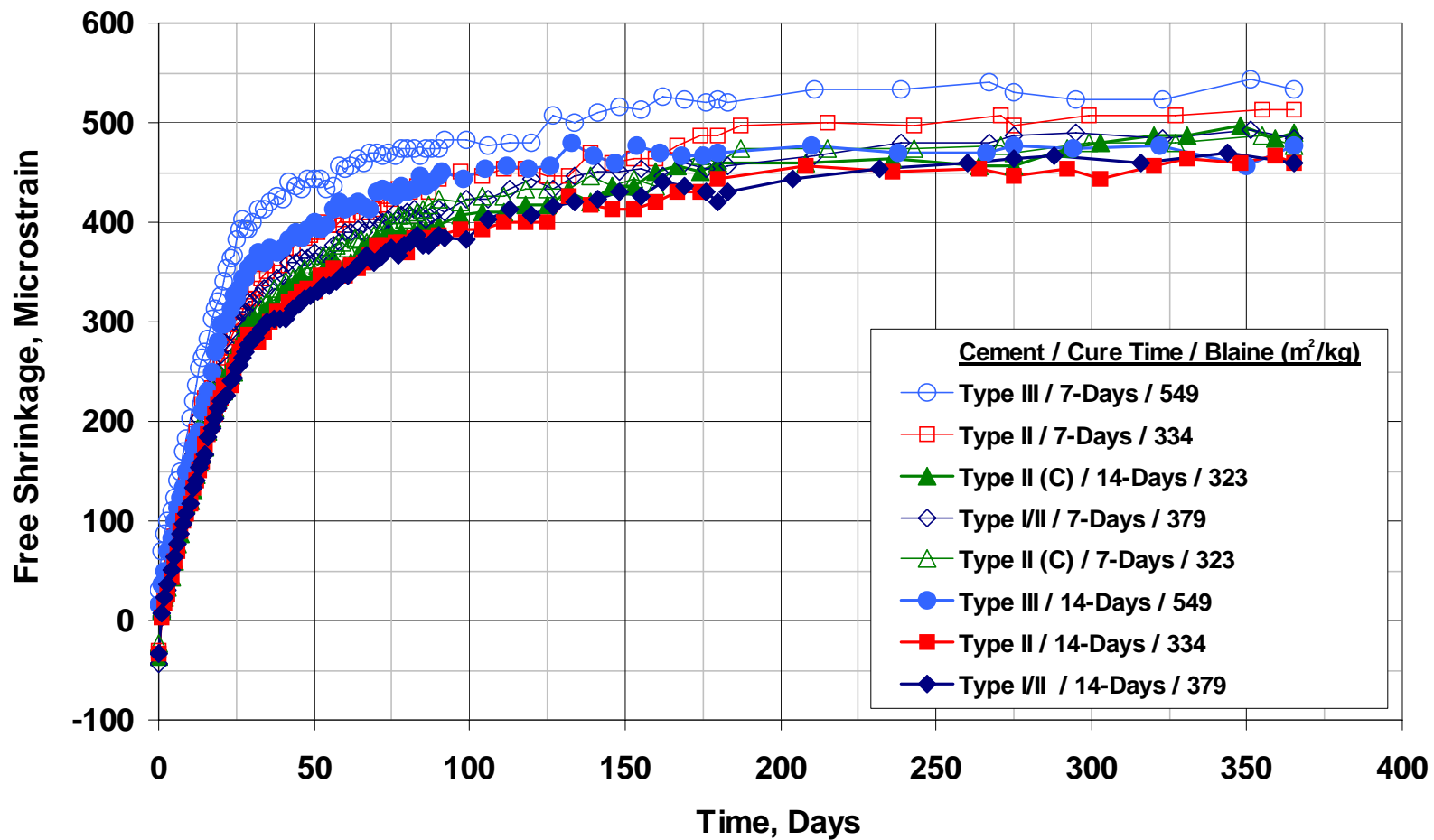


Fig. 4.30 – Free-Shrinkage Test (ASTM C 157). Program V. Average free shrinkage versus time through 365 days (drying only).

4.9 PROGRAM VI (MINERAL ADMIXTURES)

Silica fume, Class F fly ash, and Grade 100 and 120 slag cement were evaluated as partial replacements for Type I/II portland cement to determine their influence on free shrinkage in Program VI. A minimum of two sources, two replacement levels, and two aggregate types were evaluated for each mixture in conjunction with 7 and 14 day curing periods. With the exception of the three batches evaluating ternary mixtures in Set 10, all of the batches in Program VI have a paste content of 23.3% and w/cm ratio of 0.42 [equivalent to a 100% portland cement mixture with a cement content of 317 kg/m^3 (535 lb/yd^3) and a w/c ratio of 0.42)]. Details regarding Program VI mix proportioning are provided in Section 2.7, and mixture designs, plastic concrete properties, and compressive strengths are provided in Appendix A.

Program VI contains 38 batches that are divided into 10 different sets. The batches in Sets 1 and 2 contain densified silica fume as a partial replacement of cement with either limestone (Set 1) or granite (Set 2) coarse aggregate. Sets 3 and 4 are used to evaluate the shrinkage performance of concretes containing Class F fly ash with limestone (Set 3) or granite (Set 4) coarse aggregate. Sets 5 through 9 consist of mixtures containing either Grade 100 or Grade 120 slag cement. Mixtures in Sets 5 and 6 contain Grade 120 slag cast with limestone (Set 5) or quartzite (Set 6) coarse aggregate, while mixtures in Sets 7 and 8 contain Grade 100 slag cast with limestone (Set 7) or granite (Set 8). Set 9 is used to evaluate the free shrinkage of specimens cast with limestone coarse aggregate in the saturated-surface-dry (SSD) condition with that of specimens cast with oven-dried aggregate to determine the ability of the limestone to provide internal curing. The Set 9 mixtures include specimens cast with and without Grade 100 slag cement. Set 10 includes ternary mixtures containing silica fume and Grade 120 slag cement in addition to binary

control mixtures. A summary of these sets is provided in Table 4.45 and Section 2.9.6.

Table 4.45 – Program VI Summary

Set Number	Mineral Admixture	Coarse Aggregate	Replacement Level [†]
1	Silica Fume	Limestone	0, 3, and 6%
2	Silica Fume	Granite	0, 3, and 6%
3	Class F Fly Ash	Limestone	0, 20, and 40%
4	Class F Fly Ash	Granite	0, 20, and 40%
5	Grade 120 Slag	Limestone	0, 30, 60, and 80%
6	Grade 120 Slag	Limestone Quartzite	60%
7	Grade 100 Slag	Limestone Granite	60%
8	Grade 100 Slag	Granite	0, 30, and 60%
9*	Grade 100 Slag	Limestone	0 and 60%
10	Grade 120 Slag Silica Fume	Limestone	0, 60, and 80% 0 and 6%

[†]All mineral admixture replacements are reported by volume of total cementitious materials.

^{*}Set 9 compares free shrinkage of specimens cast with coarse aggregate in the saturated-surface-dry (SSD) condition and specimens cast with oven-dried aggregate.

Silica fume is primarily used in concrete to reduce permeability and to increase early and long-term compressive strengths, and as such, relatively few studies have been performed to assess the shrinkage characteristics of concrete containing silica fume. Interestingly, the results of the few studies that are available are often times conflicting or inconclusive. Whiting and Detwiler (1998) reported an increase in both the early and long-term shrinkage of concrete with a 6 to 12% replacement of cement with silica fume, while Ding and Li (2002) reported a significant reduction in shrinkage with a 15% replacement of cement with silica fume. The results reported by Deshpande et al. (2007) were inconclusive. Much of the confusion and inconsistencies in the earlier studies is likely attributable to differences in the paste content, w/cm ratio, or both, between control and silica fume

mixtures resulting from differences in the specific gravities of the cement and silica fume. Short moist curing periods may also be a factor contributing to differences between researchers due to the relative sensitivity of mineral admixtures to the length of the curing period.

Fly ash is commonly used in concrete to help reduce cost, reduce permeability, and control maximum concrete temperatures. Several studies have been performed to assess the shrinkage characteristics of concrete containing fly ash, but similar to the findings for silica fume, they have generally been inconsistent. Symons and Fleming (1980) and Atiş (2003) observed reductions in shrinkage with a partial replacement of cement with Class F fly ash, while Deshpande et al. (2007) reported an increase in shrinkage at all ages for concrete containing Class C fly ash. Khatri and Sirivivatnanon (1995) examined ternary mixtures containing silica fume and Class F fly ash and also reported that the addition of fly ash resulted in an increase drying shrinkage compared to a control mixture containing only silica fume. The chemical and physical properties of fly ash vary considerably depending on their source, and so it comes as no surprise that the results of various comparisons differ.

Slag cement is often used as a partial replacement for cement to improve durability, decrease cementitious material costs, and reuse a waste material. Again, previous research on the shrinkage performance of mixtures containing slag cement has been generally inconsistent, and not unlike silica fume and fly ash, these results appear to be heavily dependent on the mixture proportioning method and the length of the curing period. Jardine and Wolhunter (1977) reported significantly increased shrinkage after nearly 100 days of drying, while Deshpande et al. (2007) concluded that slag does not appear to affect ultimate shrinkage (after one year) but may increase early-age shrinkage (30 days). Tazawa et al. (1989) reported that the addition of slag did not have an effect on early-age shrinkage, but that ultimate shrinkage was reduced.

The different findings provided by various authors indicate the importance of evaluating different sources for each mineral admixture, various levels of replacement, different coarse aggregate types, and different curing period lengths. The results of the mineral admixture free-shrinkage evaluation are presented next.

4.9.1 Program VI Set 1 (Silica Fume and Limestone Coarse Aggregate)

Program VI Set 1 compares the free shrinkage of mixtures containing 0, 3, or 6% volume replacements of cement with densified silica fume. Limestone coarse aggregate is evaluated with silica fume in Set 1, while granite coarse aggregate is evaluated in Set 2 (Section 4.9.2). The Set 1 batches were repeated with an additional silica fume source to verify the results. The test matrix for Program VI Set 1 is presented in Table 4.46. Individual mixture proportions, plastic concrete properties, and compressive strengths are presented in Tables A.8 and A.10 in Appendix A. Individual free-shrinkage curves are presented in Figs. C.16 and C.22 through C.25 in Appendix C.

Table 4.46 – Program VI Set 1 Summary

Set Number	Silica Fume Content [†]	Silica Fume Sample No.	Coarse Aggregate
1	0% (control)	--	Limestone
1a	3%	1	Limestone
1a	6%	1	Limestone
1b	3%	2	Limestone
1b	6%	2	Limestone

[†]The silica fume contents are reported by volume of cementitious materials.

The average free-shrinkage data for the first series of Program VI Set 1 specimens after 0, 30, 90, 180, and 365 days of drying are presented in Table 4.47, and the average free shrinkage curves are presented in Figs. 4.31 and 4.32. The results of the Student's t-test are presented in Tables 4.48 and 4.49. Expansion occurring during the curing period ranged from 43 $\mu\epsilon$ for the control mixture (0%

silica fume) cured for 7 days to 20 $\mu\epsilon$ for both the 6% silica fume mixtures cured for 7 and 14 days. In general, the results indicate that shrinkage is reduced as the percentage replacement of silica fume and the curing period are increased. Hence, the most shrinkage is exhibited by the control mixture cured for 7 days, and the least shrinkage is exhibited by the 6% silica fume mixture cured for 14 days.

Table 4.47 – Summary of Free-Shrinkage Program VI Set 1a Data (in microstrain)

Days of Drying	Control (0% SF)		3% SF #1		6% SF #1	
	7-Day Cure	14-Day Cure	7-Day Cure	14-Day Cure	7-Day Cure	14-Day Cure
0	-43	-33	-23	-40	-20	-20
30	320	283	317	253	293	203
90	413	387	423	367	370	307
180	453	420	460	400	417	340
365	483	460	487	443	443	387

Figure 4.31 compares the shrinkage results for concrete containing 0, 3, or 6% volume replacements of cement with densified silica fume through the first 30 days of drying. For specimens cured for 14 days, an increase in the silica fume content from 0 to 3% resulted in a decrease in shrinkage by 30 $\mu\epsilon$ at 30 days. An additional 50 $\mu\epsilon$ reduction in shrinkage is obtained as the silica fume content is increased further from 3 to 6%. The reductions that occur as the silica fume content is increased from 0 to 3%, and from 3 to 6%, are statistically significant at $\alpha = 0.2$ and 0.05, respectively (Table 4.48). The 80 $\mu\epsilon$ difference in shrinkage between the 0 and 6% silica fume mixtures is significant at the highest level of confidence (Table 4.48).

Specimens cured for only 7 days exhibited greater shrinkage than those cured for 14 days. The control mixture (0% silica fume) cured for 7 days exhibited similar shrinkage to the 3% silica fume mixture cured for 7 days, both of which were approximately 25 $\mu\epsilon$ higher than the 6% silica fume mixture also cured for 7 days. None of these differences is statistically significant at 30 days (Table 4.48). As the curing period is increased from 7 to 14 days, shrinkage is reduced by 90 $\mu\epsilon$ for the

6% silica fume mixture, $64 \mu\epsilon$ for the 3% silica fume mixture, and $37 \mu\epsilon$ for the control mixture. These differences are statistically significant at confidence levels of $\alpha = 0.05, 0.02,$ and 0.1 (Table 4.48). A comparison of the effect of the curing period length shows the importance of increased curing (to obtain reduced shrinkage at early ages) as the quantity of silica fume increases and that silica fume has little effect on short-term shrinkage of concrete cured for 7 days.

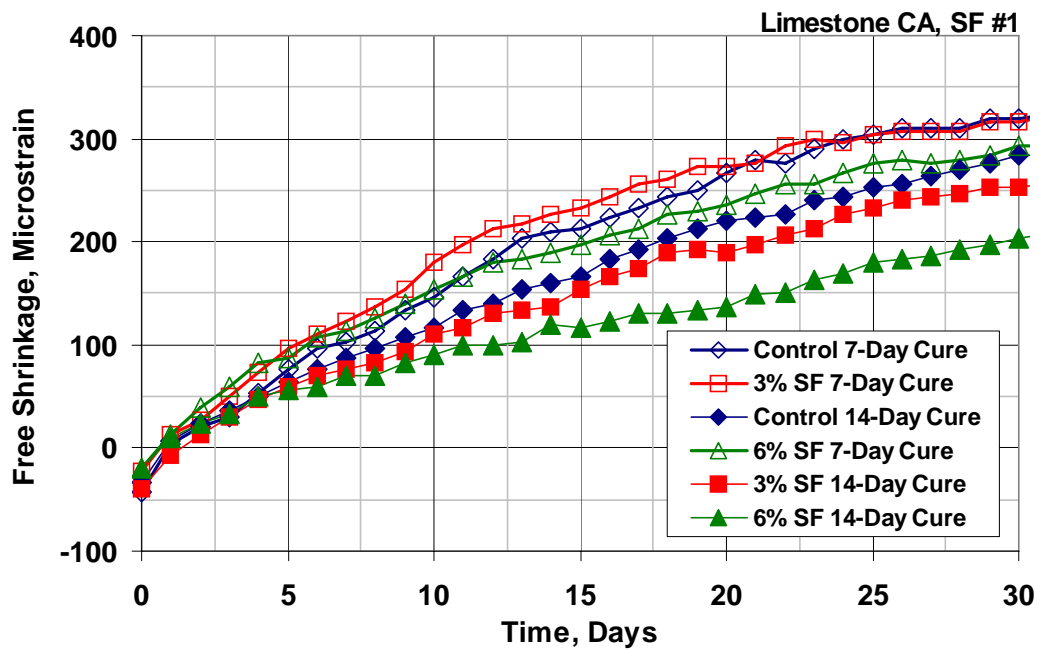


Fig. 4.31 – Free-Shrinkage Test (ASTM C 157). Program VI Set 1a. Average free shrinkage versus time through 30 days (drying only).

Figure 4.32 compares the long-term shrinkage results for concrete containing densified silica fume. These results are qualitatively very similar to the results obtained after only 30 days of drying (Fig. 4.31). For mixtures cured for 14 days, an increase in the silica fume content from 0 to 3% resulted in a decrease in shrinkage by approximately $30 \mu\epsilon$ for periods greater than 90 days. An even greater reduction in shrinkage (about $60 \mu\epsilon$ for periods of 90 days and longer) is obtained with an increase in the silica fume content from 3 to 6%. After one year of drying, these reductions are statistically significant at $\alpha = 0.2$ and $\alpha = 0.05$, respectively (Table 4.49). The

Table 4.48 – Student’s t-test Results for Program VI Set 1a 30-Day Free-Shrinkage Data

		30-Day Free Shrinkage ($\mu\epsilon$)	Control (0% SF #1)		3% SF #1		6% SF #1	
			7-Day	14-Day	7-Day	14-Day	7-Day	14-Day
0%	7-Day	320		90	N	Y	N	Y
	14-Day	283			90	80	N	Y
3%	7-Day	317				Y	N	Y
	14-Day	253					90	95
6%	7-Day	293						95
	14-Day	203						

Note: See the Table 4.4 note for an explanation of the terms “N”, “80”, “90”, “95”, and “Y”.

difference between the control mixture (0% silica fume) and the 6% silica fume mixture is statistically significant at the highest level of confidence as indicated in Table 4.49.

As indicated previously for the 30-day results, specimens cured for 7 days exhibit greater shrinkage than those cured for 14 days. Throughout the drying period, the 3% silica fume mixture cured for 7 days exhibited the same shrinkage as the control mixture (0% silica fume) cured for 7 days, while the 6% silica fume mixture cured for 7 days exhibited the same shrinkage as the 3% silica fume mixture cured for 14 days. As the curing period is increased from 7 to 14 days, shrinkage is reduced by 23, 44, and 56 $\mu\epsilon$ for the control (0% silica fume), 3% silica fume, and 6% silica fume mixtures, respectively, at the conclusion of the drying period. The differences in shrinkage for the mixtures containing silica fume are statistically significant at $\alpha = 0.02$ and $\alpha = 0.05$ for the 3% and 6% silica fume mixtures, respectively. The difference in shrinkage between the control mixtures cured for 7 days and 14 days is not significant (Table 4.32).

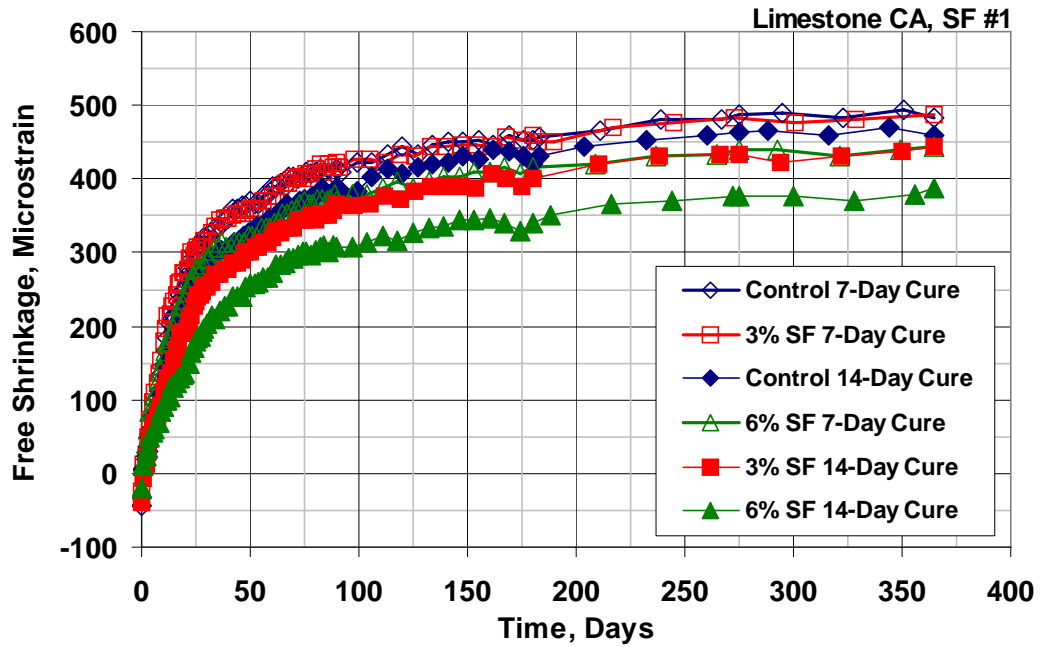


Fig. 4.32 – Free-Shrinkage Test (ASTM C 157). Program VI Set 1a. Average free shrinkage versus time through 365 days (drying only).

Table 4.49 – Student’s t-test Results for Program VI Set 1a 365-Day Free-Shrinkage Data

		365-Day Free Shrinkage ($\mu\epsilon$)	Control (0% SF #1)		3% SF #1		6% SF #1	
			7-Day	14-Day	7-Day	14-Day	7-Day	14-Day
0%	7-Day	483		N	N	90	80	Y
	14-Day	460			Y	80	N	Y
3%	7-Day	487				Y	95	Y
	14-Day	443					N	95
6%	7-Day	443						95
	14-Day	387						

Note: See the Table 4.4 note for an explanation of the terms “N”, “80”, “90”, “95”, and “Y”.

To verify the results obtained in the first series of specimens, a second series was cast using the same materials except for the silica fume. For these specimens, an alternate source of silica fume was obtained and tested (designated sample #2 compared to sample #1 used in the first series). A comparison of the chemical

analyses for the samples (provided in Table A.1) indicates only small differences in the chemical composition, and as a result, the shrinkage results are very similar. The average free-shrinkage data for these mixtures after 0, 30, 60, 90, 180, and 365 days are provided in Table 4.50. The results presented in Table 4.50 reinforce the previous observations that shrinkage decreases with increases in both the silica fume content and the curing period (in this case from 7 to 14 days).

Table 4.50 – Summary of Program VI Set 1b Free-Shrinkage Data (in microstrain)

Days of Drying	Control (0% SF)		3% SF #2		6% SF #2	
	7-Day Cure	14-Day Cure	7-Day Cure	14-Day Cure	7-Day Cure	14-Day Cure
0	-43	-33	-17	-40	-3	0
30	320	283	320	260	307	207
90	413	387	410	370	373	323
180	453	420	430	397	390	340
365	483	460	457	430	403	353

The average free shrinkage curves for Program VI Set 1 mixtures containing the second silica fume sample are presented in Figs. 4.33 and 4.34, and the results for the Student's t-tests at 30 and 365 days are presented in Tables 4.51 and 4.52. The relative order of shrinkage after 30 days of drying (shown in Fig. 4.33) is the same as that for concrete containing the first silica fume sample shown in Fig. 4.31. In fact, the shrinkage between concrete cast with the first sample and the second sample differ by no more than 14 $\mu\epsilon$ at 30 days.

The long-term shrinkage results shown in Fig. 4.34 are also similar to those presented in Fig. 4.32, although the mixtures containing silica fume exhibited even lower shrinkage strains compared to the control mixture. In this case, the 3% silica fume mixture cured for 14 days exhibited similar shrinkage to the 6% silica fume mixture cured for 7 days. In addition, the 3% silica fume mixture cured for 7 days exhibited similar shrinkage to the control mixture cured for 14 days for periods greater than 90 days. These results tend to indicate that for periods greater than 90

days, increasing the silica fume content by 3% has approximately the same effect on shrinkage as increasing the curing period from 7 to 14 days.

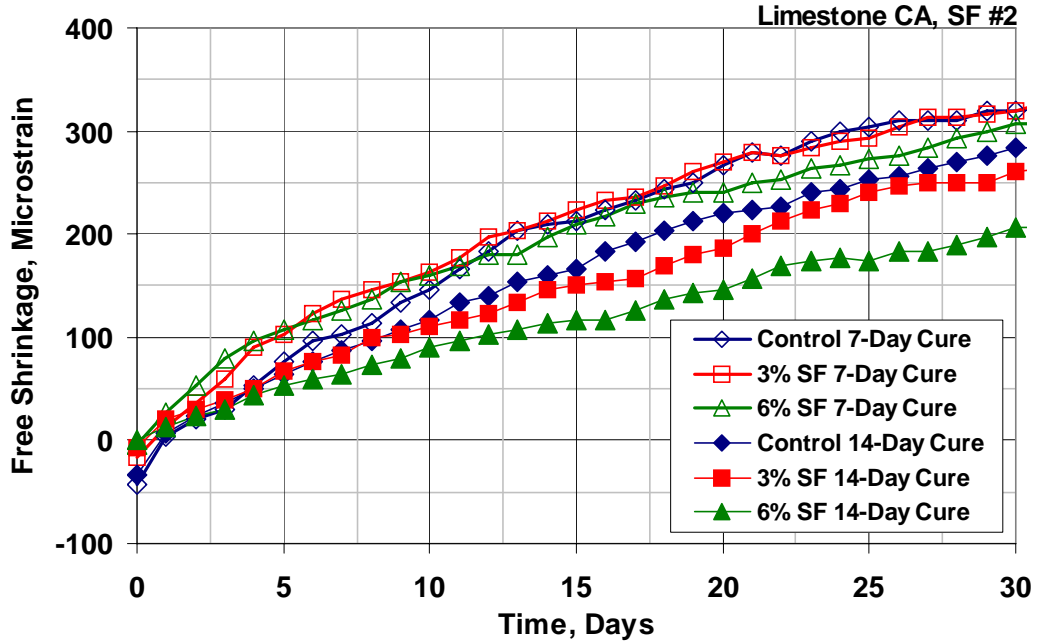


Fig. 4.33 – Free-Shrinkage Test (ASTM C 157). Program VI Set 1b. Average free shrinkage versus time through 30 days (drying only).

Table 4.51 – Student’s t-test Results for Program VI Set 1b 30-Day Free-Shrinkage Data

		30-Day Free Shrinkage (µε)	Control (0% SF)		3% SF #2		6% SF #2	
			7-Day	14-Day	7-Day	14-Day	7-Day	14-Day
0%	7-Day	320		90	N	Y	N	Y
	14-Day	283			80	90	95	Y
3%	7-Day	320				Y	N	Y
	14-Day	260					Y	Y
6%	7-Day	307						Y
	14-Day	207						

Note: See the Table 4.4 note for an explanation of the terms “N”, “80”, “90”, “95”, and “Y”.

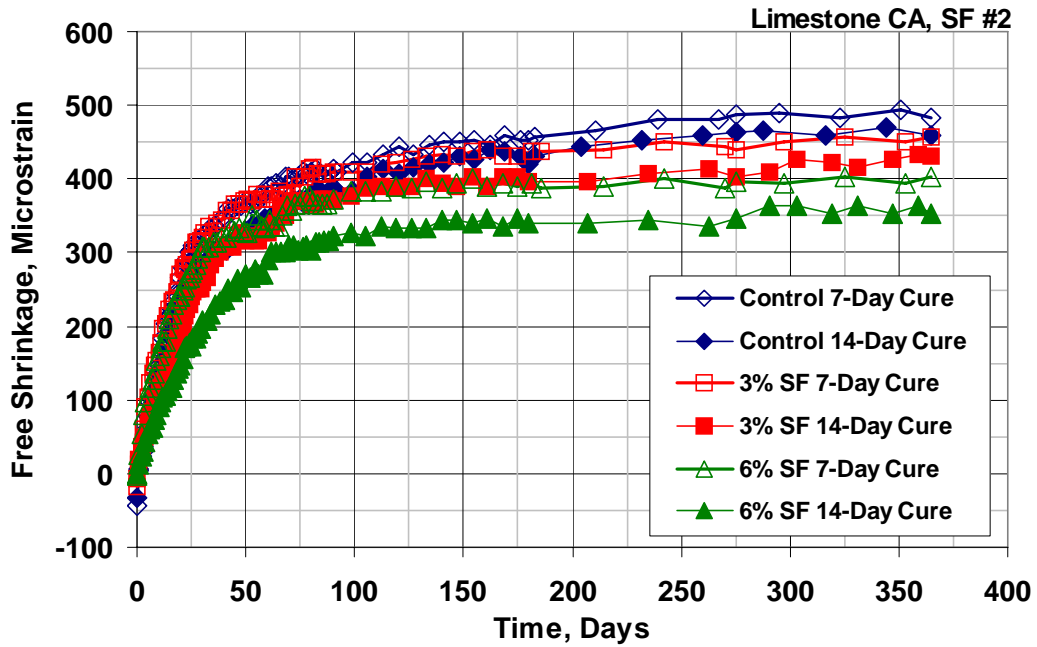


Fig. 4.34 – Free-Shrinkage Test (ASTM C 157). Program VI Set 1b. Average free shrinkage versus time through 365 days (drying only).

Table 4.52 – Student’s t-test Results for Program VI Set 1b 365-Day Free-Shrinkage Data

		365-Day Free Shrinkage ($\mu\epsilon$)	Control (0% SF)		3% SF #2		3% SF #2	
			7-Day	14-Day	7-Day	14-Day	7-Day	14-Day
0%	7-Day	483		N	N	95	95	Y
	14-Day	460			Y	95	95	Y
3%	7-Day	457				80	90	Y
	14-Day	430					N	Y
6%	7-Day	403						90
	14-Day	353						

Note: See the Table 4.4 note for an explanation of the terms “N”, “80”, “90”, “95”, and “Y”.

4.9.2 Program VI Set 2 (Silica Fume and Granite Coarse Aggregate)

The results of Program VI Set 2, which compares the free shrinkage results for concrete containing 0, 3, or 6% volume replacements of cement with densified silica

fume and granite coarse aggregate, are presented next. A summary of the comparisons for Program VI Set 2 is presented in Table 4.53. Individual mixture proportions, plastic concrete properties, and compressive strengths are presented in Table A.11 in Appendix A. Individual free-shrinkage curves are presented in Figs. C.26 through C.28 in Appendix C.

Table 4.53 – Program VI Set 2 Summary

Set Number	Silica Fume Content [†]	Silica Fume Sample No.	Coarse Aggregate
2	0% (control)	--	Granite
2	3%	2	Granite
2	6%	2	Granite

[†]The silica fume contents are reported by volume of cementitious materials.

The average free-shrinkage data for Program VI Set 2 specimens after 0, 30, 90, 180, and 365 days of drying are presented in Table 4.54. Initial swelling strains, measured immediately after the curing period, range from 33 $\mu\epsilon$ to 63 $\mu\epsilon$. These strains are 20 to 50 $\mu\epsilon$ greater than the swelling observed for the batches containing limestone (shown in Tables 4.47 and 4.50), making direct comparisons between concrete cast with limestone and granite difficult. The results of this set indicate that the addition of silica fume decreases shrinkage at all ages provided that the specimens are cured for 14 days. When only cured for 7 days, however, the addition of 3 or 6% silica fume resulted in an increase in early-age shrinkage that likely occurs before the concrete has a chance to creep, thereby increasing the probability of shrinkage cracking.

Figure 4.35 compares the free shrinkage of concrete containing granite and densified silica fume through 30 days of drying. Unlike the results obtained for the specimens containing limestone coarse aggregate, the addition of silica fume results in increased early-age shrinkage compared to the control mixture when the concrete is cured for only 7 days; for these specimens, the addition of 3 or 6% silica fume

Table 4.54 – Summary of Free-Shrinkage Program VI Set 2 Data (in microstrain)

Days of Drying	Control (0% SF)		3% SF #2		6% SF #2	
	7-Day Cure	14-Day Cure	7-Day Cure	14-Day Cure	7-Day Cure	14-Day Cure
0	-63	-57	-50	-60	-33	-50
30	277	260	303	267	297	237
90	347	323	340	287	317	250
180	360	343	390	330	340	267
365	430	420	405	367	355	313

increased shrinkage by an average of 23 $\mu\epsilon$ compared to the control mixture at 30 days. In both cases, this increase in shrinkage is statistically significant at least at $\alpha = 0.1$ (Table 4.55). The results change significantly when specimens are allowed to cure for 14 days. For these specimens, an increase in the silica fume content from 0 to 3% resulted in only a slight (but statistically insignificant) increase in shrinkage compared to the control mixture. As the silica fume content is increased again to 6%, a small reduction in shrinkage of 23 $\mu\epsilon$ occurs at 30 days. This reduction in shrinkage is statistically significant at $\alpha = 0.1$ (Table 4.55). These results indicate the sensitivity of mixtures containing silica fume when cast with low-absorption coarse aggregates. As the curing period is increased from 7 to 14 days, shrinkage is reduced by 60 $\mu\epsilon$ for the 6% silica fume mixture, 36 $\mu\epsilon$ for the 3% silica fume mixture, and 17 $\mu\epsilon$ for the control mixture. These differences are statistically significant at the highest level of confidence for the silica fume mixtures and at $\alpha = 0.1$ for the control mixture (Table 4.55).

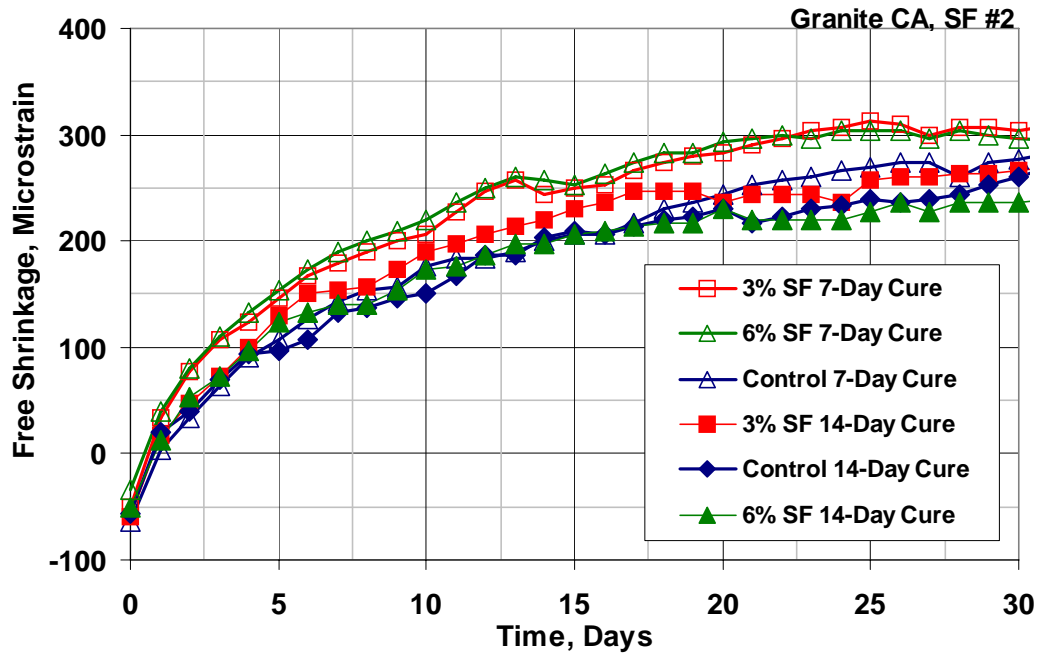


Fig. 4.35 – Free-Shrinkage Test (ASTM C 157). Program VI Set 2. Average free shrinkage versus time through 30 days (drying only).

Table 4.55 – Student’s t-test Results for Program VI Set 2 30-Day Free Shrinkage Data

		30-Day Free Shrinkage (µε)	Control (0% SF)		3% SF #2		6% SF #2	
			7-Day	14-Day	7-Day	14-Day	7-Day	14-Day
0%	7-Day	277		90	Y	80	90	Y
	14-Day	260			Y	N	Y	90
3%	7-Day	303				Y	N	Y
	14-Day	267					Y	95
6%	7-Day	297						Y
	14-Day	237						

Note: See the Table 4.4 note for an explanation of the terms “N”, “80”, “90”, “95”, and “Y”.

Figure 4.35 compares the free shrinkage of concrete containing granite and densified silica fume through the entire 365-day drying period. In this case, the results are qualitatively very similar to the results obtained for the silica fume mixtures containing limestone coarse aggregate. For specimens cured for 14 days, an

increase in the silica fume content from 0 to 3% resulted in a decrease in shrinkage of between 10 and 50 $\mu\epsilon$ for periods greater than 90 days. At 365 days, the difference is 53 $\mu\epsilon$ and is statistically significant at $\alpha = 0.05$ (Table 4.56). A further increase in the silica fume content from 3 to 6% results in an even greater reduction in shrinkage (a 37 $\mu\epsilon$ reduction in shrinkage after 90 days increasing to 54 $\mu\epsilon$ at 365 days). At 365 days, this reduction in shrinkage is statistically significant at the highest level of confidence (Table 4.56). Specimens cured for only 7 days exhibit a similar trend as the silica fume content is increased from 0 to 6%.

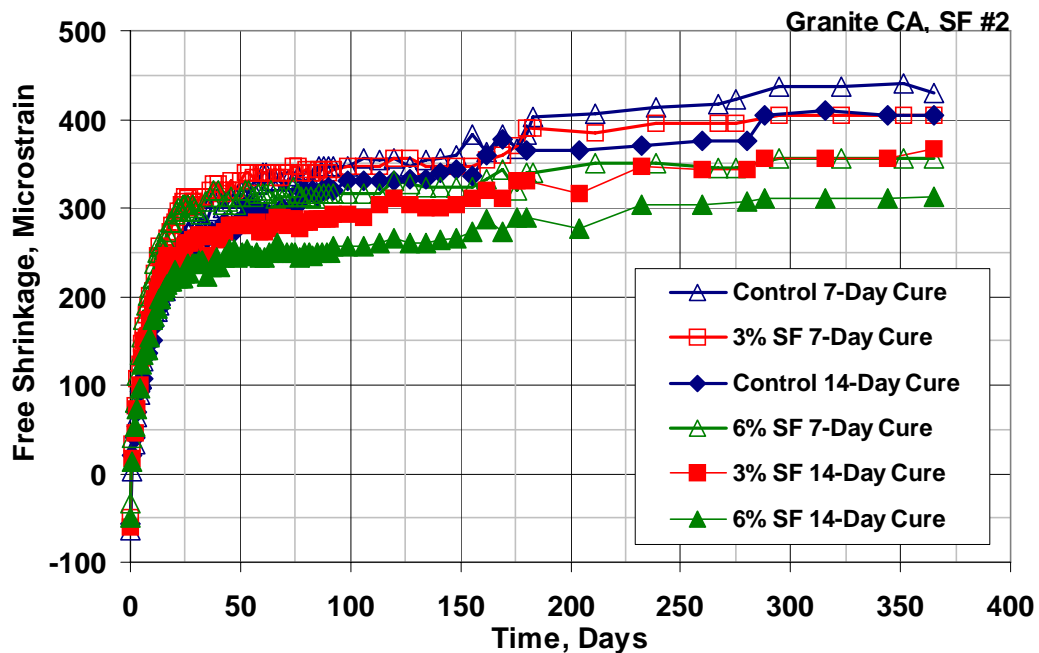


Fig. 4.36 – Free-Shrinkage Test (ASTM C 157). Program VI Set 2. Average free shrinkage versus time through 365 days (drying only).

Table 4.56 – Student’s t-test Results for Program VI Set 2 365-Day Free-Shrinkage Data

		365-Day Free Shrinkage ($\mu\epsilon$)	Control (0% SF)		3% SF #2		3% SF #2	
			7-Day	14-Day	7-Day	14-Day	7-Day	14-Day
0%	7-Day	430		N	90	Y	Y	Y
	14-Day	420			N	95	95	Y
3%	7-Day	405				95	Y	Y
	14-Day	367					N	Y
6%	7-Day	355						95
	14-Day	313						

Note: See the Table 4.4 note for an explanation of the terms “N”, “80”, “90”, “95”, and “Y”.

4.9.3 Program VI Set 3 (Class F Fly Ash and Limestone Coarse Aggregate)

Program VI Set 3 compares the free shrinkage of mixtures containing 0, 20, or 40% volume replacements of cement with Class F fly ash. Two Class F fly ashes are evaluated in Set 3 in conjunction with limestone coarse aggregate. A summary of the test matrix for this set is presented in Table 4.57. Individual mixture proportions, plastic concrete properties, and compressive strengths are given in Tables A.6, A.8, and A.12 in Appendix A. Individual specimen free-shrinkage curves are presented in Figs. C.11 and C.29 through C.32 in Appendix C.

Table 4.57 – Program VI Set 3 Summary

Set Number	Fly Ash Content [†]	Class F Fly Ash Sample No.	Coarse Aggregate
3	0% (control)	--	Limestone
3	20%	1	Limestone
3	40%	1	Limestone
3	0% (control)	--	Limestone
3	20%	2	Limestone
3	40%	2	Limestone

[†]The fly ash contents are reported by volume of cementitious materials.

The average free-shrinkage data for the Program VI Set 3 specimens after 0, 30, 90, 180, and 365 days of drying are presented in Table 4.58 for fly ash No. 1 obtained from Headwaters Resources in Underwood, ND, and the average free-shrinkage curves are presented in Figs. 4.37 and 4.38. For this comparison, the control specimens cured for 7-days were mishandled during the curing period, and as a result, shrinkage strains were not measured. As shown in Table 4.58, all of the mixtures in this series containing fly ash shrank between 15 and 30 $\mu\epsilon$ during the curing period. This is unlike the mixtures cast with silica fume and limestone which expanded during curing. The control mixture, cast during the same period of time as the fly ash mixtures, expanded during curing. The results shown in Table 4.58 indicate that shrinkage increases as the fly ash content is increased from 0 to 40%, and that an increase in the curing period from 7 to 14 days reduces shrinkage.

Table 4.58 – Summary of Program VI Set 3 Free-Shrinkage Data (in microstrain)

Days of Drying	Control (0% FA)		20% Class F FA #1		40% Class F FA #1	
	7-Day Cure	14-Day Cure	7-Day Cure	14-Day Cure	7-Day Cure	14-Day Cure
0	--	-25	17	23	30	15
30	--	310	407	360	450	370
90	--	410	473	437	500	425
180	--	450	503	470	537	440
365	--	445	520	497	543	490

Figure 4.37 compares the shrinkage of concretes containing 0, 20, or 40% volume replacements of cement with Class F fly ash through the first 30 days of drying. The addition of fly ash at either the 20 or 40% replacement level significantly increases the early-age shrinkage compared to the control mixture (0% fly ash). For specimens cured for 14 days, an increase in the fly ash content from 0 to 20% increased shrinkage by 50 $\mu\epsilon$ at 30 days. A similar increase in shrinkage (60 $\mu\epsilon$ at 30 days) occurs as the fly ash content is increased from 0 to 40%. These increases in shrinkage compared to the control mixture are statistically significant at $\alpha = 0.05$ and

$\alpha = 0.1$, respectively (Table 4.59). In each case, the specimens cured for only 7 days exhibited greater shrinkage than those cured for 14 days. For the 40% fly ash mixture, as the curing period is increased from 7 to 14 days, shrinkage is reduced by $90 \mu\epsilon$ at 10 days and $47 \mu\epsilon$ at 30 days. The 20% fly ash mixture is not as sensitive to the curing period as the 40% fly ash mixture, but an increase in the curing period from 7 to 14 days does result in a decrease in shrinkage of approximately $40 \mu\epsilon$ for periods greater than 10 days. After 30 days of drying, these reductions are statistically significant at least at $\alpha = 0.2$ (Table 4.59).

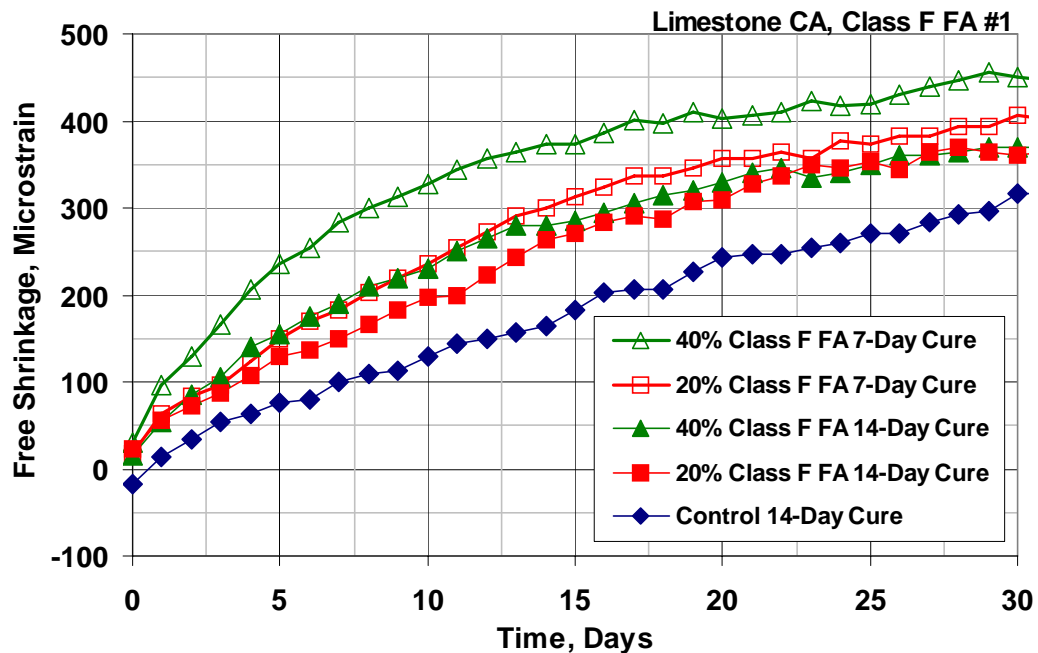


Fig. 4.37 – Free-Shrinkage Test (ASTM C 157). Program VI Set 3. Average free shrinkage versus time through 30 days (drying only).

Table 4.59 – Student’s t-test Results for Program IV Set 3 30-Day Free-Shrinkage Data

		30-Day Free Shrinkage ($\mu\epsilon$)	Control (0% FA)		20% Class F FA #1		40% Class F FA #1	
			7-Day	14-Day	7-Day	14-Day	7-Day	14-Day
0%	7-Day	--		--	--	--	--	--
	14-Day	310			Y	95	Y	90
20%	7-Day	407				Y	95	90
	14-Day	360					Y	Y
40%	7-Day	450						80
	14-Day	370						

Note: See the Table 4.4 note for an explanation of the terms “N”, “80”, “90”, “95”, and “Y”.

The free-shrinkage results after one year of drying are presented in Fig. 4.38 where it can be seen that the relative order of long-term shrinkage is the same as for the early-age shrinkage shown in Fig. 4.37. As with the earlier observations, longer curing periods coincide with lower free shrinkage. All of the differences observed after 365 days of drying are statistically significant at least at $\alpha = 0.2$ (Table 4.60) with the exception of the 20 and 40% fly ash mixtures cured for 14 days, which exhibit similar shrinkage throughout the entire drying period.

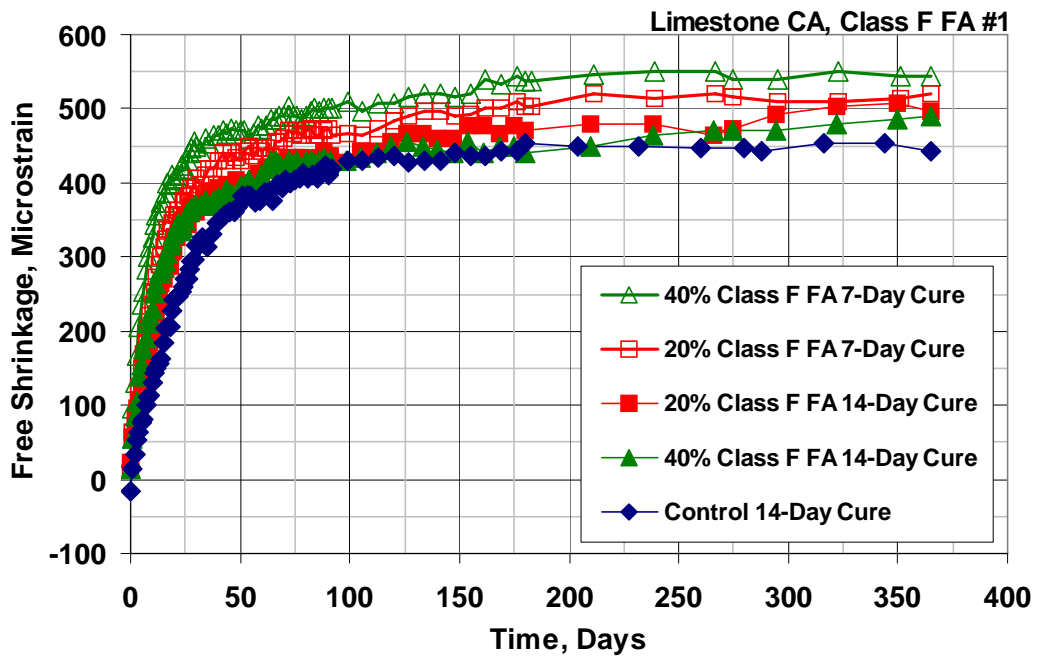


Fig. 4.38 – Free-Shrinkage Test (ASTM C 157). Program VI Set 3. Average free shrinkage versus time through 365 days (drying only).

Table 4.60 – Student’s t-test Results for Program VI Set 3 365-Day Free-Shrinkage Data

		365-Day Free Shrinkage ($\mu\epsilon$)	Control (0% FA)		20% Class F FA #1		40% Class F FA #1	
			7-Day	14-Day	7-Day	14-Day	7-Day	14-Day
0%	7-Day	--		--	--	--	--	--
	14-Day	445			90	Y	Y	95
20%	7-Day	520				90	90	80
	14-Day	497					Y	N
40%	7-Day	543						Y
	14-Day	490						

Note: See the Table 4.4 note for an explanation of the terms “N”, “80”, “90”, “95”, and “Y”.

A second sample of Class F fly ash, obtained from Lafarge North America in Chicago, IL, is also evaluated in Program VI Set 3 to verify the previous results, and to help determine the sensitivity of shrinkage properties of concrete cast with Class F fly ash obtained from different sources. Concrete containing 0, 20, or 40% volume

replacements of cement with a Class F fly ash are shown in Figs. 4.39 and 4.40 and tabulated in Table 4.61. The results again indicate that higher percentage replacements of fly ash result in increased shrinkage at all ages compared to the control mixture (0% fly ash), and that longer curing periods coincide with lower free shrinkage.

Table 4.61 – Summary of Program VI Set 3 Free-Shrinkage Data (in microstrain)

Days of Drying	Control (0% FA)		20% Class F FA #2		40% Class F FA #2	
	7-Day Cure	14-Day Cure	7-Day Cure	14-Day Cure	7-Day Cure	14-Day Cure
0	-43	-33	-27	-43	-27	-30
30	320	283	337	297	357	347
90	413	387	430	397	450	437
180	453	420	460	433	470	460
365	483	460	500	463	510	493

The relative order of short-term shrinkage (through 30 days) for the fly ash mixtures is shown in Fig. 4.39, which again demonstrates that the addition of fly ash provides no special advantage, and in fact, increases shrinkage for all mixtures. This increase is exacerbated by reduced curing periods. Thus, the lowest shrinkage through 30 days is attained by the control mixture (0% fly ash) cured for 14 days, and the highest shrinkage occurs for the 40% fly ash mixture cured for 7 days. The total difference between these specimens is $74 \mu\epsilon$ at 30 days and is statistically significant at $\alpha = 0.2$ (Table 4.62). An increase in the curing period from 7 to 14 days resulted in reductions in shrinkage of $37 \mu\epsilon$ for the control mix, $40 \mu\epsilon$ for the 20% fly ash mixture, and only $10 \mu\epsilon$ for the 40% fly ash mixture. The reduction in shrinkage for the 40% fly ash mixture is not significant, but the differences for the control mixture and the 20% fly ash mixtures are significant at $\alpha = 0.1$ and $\alpha = 0.02$, respectively (Table 4.62).

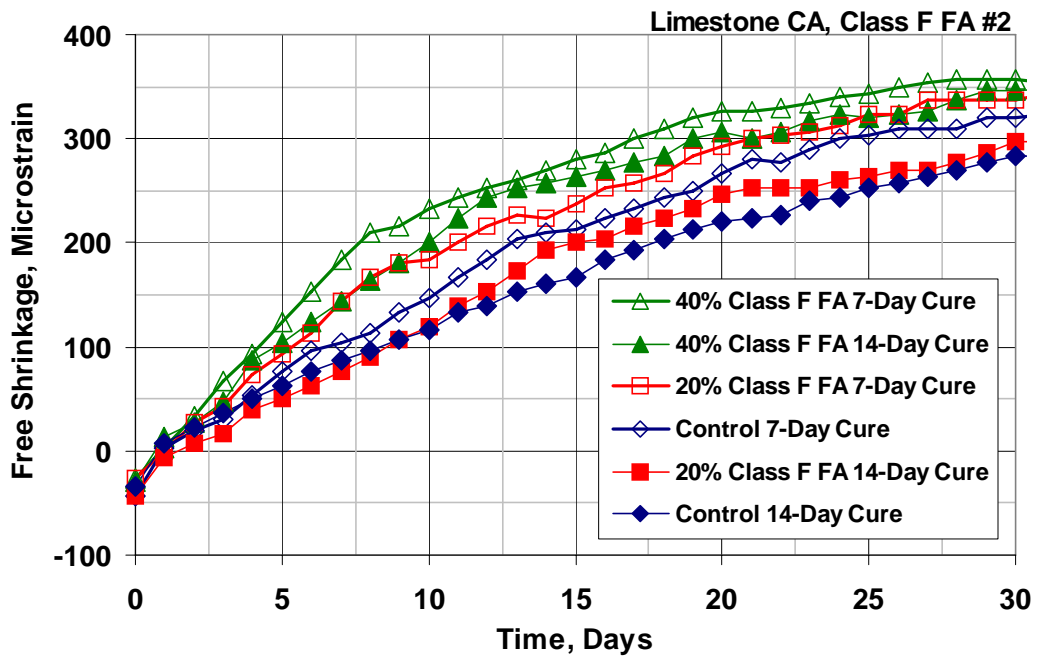


Fig. 4.39 – Free-Shrinkage Test (ASTM C 157). Program VI Set 3. Average free shrinkage versus time through 30 days (drying only).

Table 4.62 – Student’s t-test Results for Program VI Set 3 30-Day Free-Shrinkage Data

		30-Day Free Shrinkage (µε)	Control (0% FA)		20% Class F FA #2		40% Class F FA #2	
			7-Day	14-Day	7-Day	14-Day	7-Day	14-Day
0%	7-Day	320		90	N	80	90	80
	14-Day	283			Y	N	Y	Y
20%	7-Day	337				Y	80	N
	14-Day	297					Y	Y
40%	7-Day	357						N
	14-Day	347						

Note: See the Table 4.4 note for an explanation of the terms “N”, “80”, “90”, “95”, and “Y”.

The long-term (through one year) free-shrinkage results for the second series of concrete containing Class F fly ash are shown in Fig. 4.40. The differences in shrinkage for concrete containing this sample of fly ash are not as large as the differences observed for the first sample (shown in Fig. 4.38). The general trend for

concrete containing fly ash still remains, however, as the lowest shrinkage occurs for the control specimen cured for 14 days, and the greatest shrinkage occurs for the 40% fly ash mixture cured for 7 days. The difference in shrinkage between these specimens decreased from 74 $\mu\epsilon$ at 30 days to 50 $\mu\epsilon$ at one year. At 365 days, an increase in the curing period from 7 to 14 days reduces shrinkage by 23, 17, and 37 $\mu\epsilon$ for the control mixture, 20% fly ash mixture, and 40% fly ash mixture, respectively. The reductions in shrinkage for the 20% and 40% fly ash mixtures are statistically significant at $\alpha = 0.1$ (Table 4.63).

For specimens cured for 14 days, an increase in the fly ash content from 0 to 20% did not result in a statistically significant increase in shrinkage. This is not the case for concrete containing the first sample of Class F fly ash, as shown in Figs. 4.37 and 4.38. A further increase in the fly ash content from 20 to 40% resulted in an increase in shrinkage of about 30 $\mu\epsilon$ for periods greater than 90 days. At 365 days, this increase in shrinkage compared to both the control mixture and the 20% fly ash mixture is significant at $\alpha = 0.02$ and $\alpha = 0.2$, respectively (Table 4.63). Similar increases in shrinkage are observed for the specimens cured for 7 days as the fly ash replacement level is increased from 0 to 40%. The results of Program VI Set 3 clearly indicate that the addition of fly ash results in increased free shrinkage at all ages.

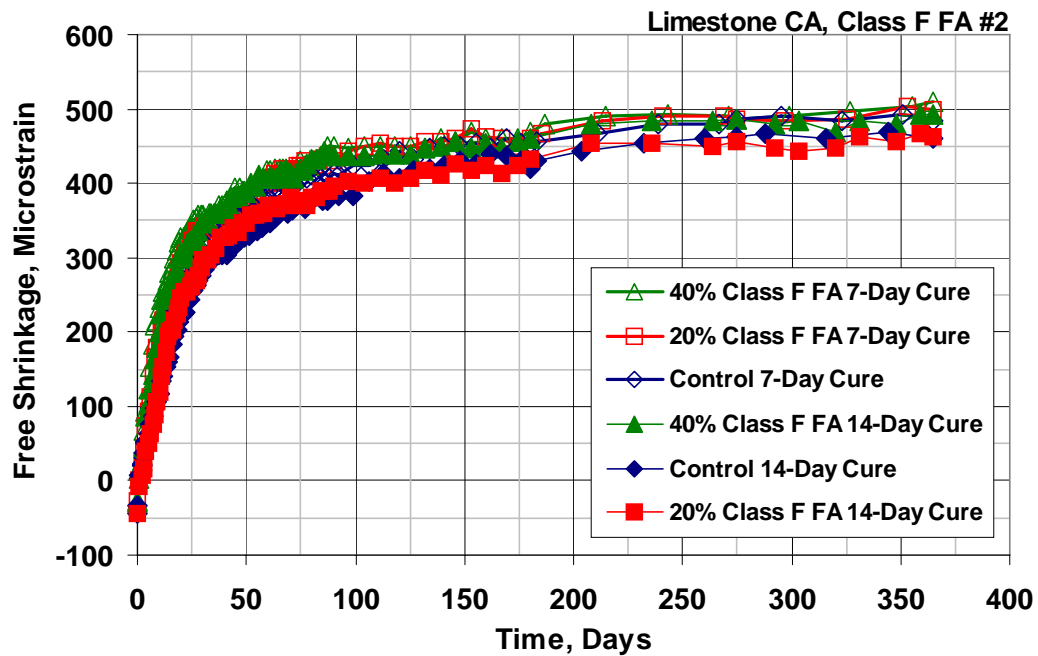


Fig. 4.40 – Free-Shrinkage Test (ASTM C 157). Program VI Set 3. Average free shrinkage versus time through 365 days (drying only).

Table 4.63 – Student’s t-test Results for Program VI Set 3 365-Day Free Shrinkage Data

		365-Day Free Shrinkage ($\mu\epsilon$)	Control (0% FA)		20% Class F FA #2		20% Class F FA #2	
			7-Day	14-Day	7-Day	14-Day	7-Day	14-Day
0%	7-Day	483		N	N	N	80	N
	14-Day	460			Y	N	Y	Y
20%	7-Day	500				90	80	80
	14-Day	463					95	80
40%	7-Day	510						90
	14-Day	493						

Note: See the Table 4.4 note for an explanation of the terms “N”, “80”, “90”, “95”, and “Y”.

4.9.4 Program VI Set 4 (Class F Fly Ash and Granite Coarse Aggregate)

Program VI Set 4 compares the free shrinkage of mixtures containing 0, 20, or 40% volume replacements of cement with Class F fly ash. The evaluation includes

two samples of Class F fly ash evaluated in conjunction with granite coarse aggregate. A summary of Program VI Set 4 mixtures is presented in Table 4.64. Individual mixture proportions, plastic concrete properties, and compressive strengths are given in Tables A.11 and A.13 in Appendix A. Individual specimen free-shrinkage curves are presented in Figs. C.26 and C.33 through C.36 in Appendix C.

Table 4.64 – Program VI Set 4 Summary

Set Number	Fly Ash Content [†]	Class F Fly Ash Sample No.	Coarse Aggregate
4	0% (control)	--	Granite
4	20%	2	Granite
4	40%	2	Granite
4	20%	3	Granite
4	40%	3	Granite

[†]The fly ash contents are reported by volume of cementitious materials.

The average free-shrinkage data for Program VI Set 4 specimens after 0, 30, 90, 180, and 365 days of drying are presented in Table 4.65. Initial expansion strains varied between 57 and 67 $\mu\epsilon$ for the 20% fly ash mixture and the control mixture (0% fly ash), but significantly higher expansion strains of 90 and 80 $\mu\epsilon$ were obtained for the 40% fly ash mixtures cured for 7 and 14 days, respectively. Despite this large initial expansion, the results demonstrate that the addition of fly ash in conjunction with granite coarse aggregate provides no advantage in terms of reducing free shrinkage.

Table 4.65 – Summary of Program VI Set 4 Free-Shrinkage Data (in microstrain)

Days of Drying	Control (0% FA)		20% Class F FA #2		40% Class F FA #2	
	7-Day Cure	14-Day Cure	7-Day Cure	14-Day Cure	7-Day Cure	14-Day Cure
0	-63	-57	-57	-67	-90	-80
30	277	260	343	323	307	287
90	347	323	383	353	343	330
180	383	380	420	377	353	357
365	430	405	453	410	400	403

The relative order of short-term shrinkage (through 30 days) for the Program VI Set 4 fly ash mixtures is shown in Fig. 4.41. For this comparison, the highest early-age shrinkage occurs for the 20% fly ash mixture cured for 7 days and the least shrinkage is exhibited by the control mixture (0% fly ash) cured for 14 days. The total difference in shrinkage for this set is 83 $\mu\epsilon$ at 30 days compared to 74 $\mu\epsilon$ for the Set 3 specimens containing the same fly ash sample and limestone coarse aggregate. As with the earlier observations, longer curing periods coincide with lower free shrinkage strains. These reductions, however, are not as large as the reductions observed for the fly ash mixtures cast with limestone coarse aggregate. An increase in the curing period from 7 to 14 days resulted in shrinkage reductions of 20 and 16 $\mu\epsilon$ for the mixtures containing 20 and 40% fly ash, respectively, and 17 $\mu\epsilon$ for the control mixture. Only the 17 $\mu\epsilon$ reduction observed for the control mixture is statistically significant (Table 4.66).

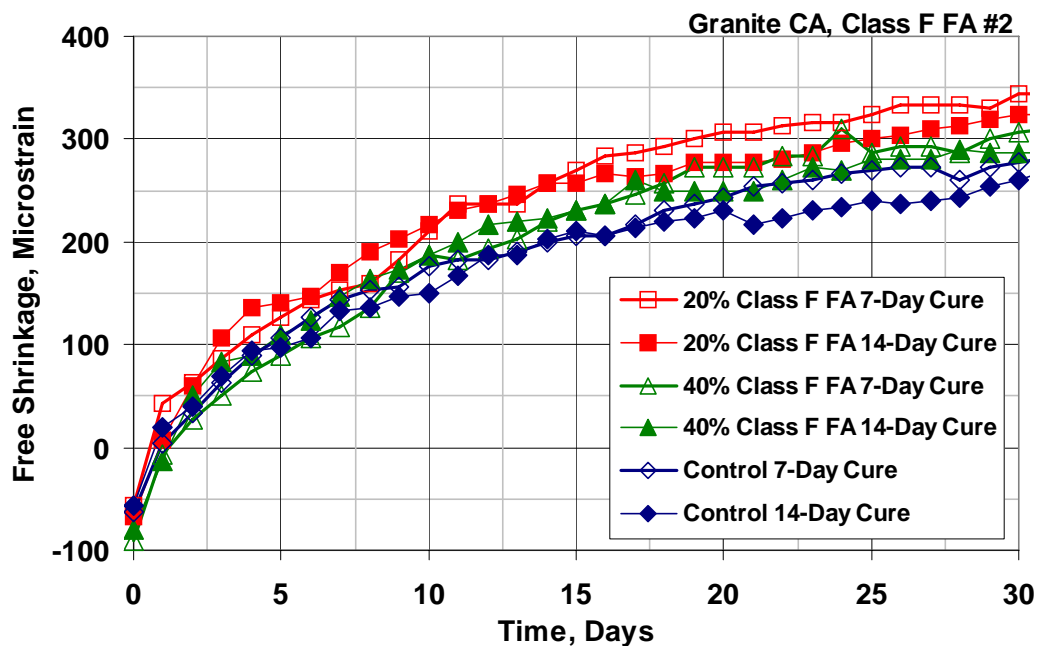


Fig. 4.41 – Free-Shrinkage Test (ASTM C 157). Program VI Set 4. Average free shrinkage versus time through 30 days (drying only).

Table 4.66 – Student’s t-test Results for Program VI Set 4 Free-Shrinkage Data

		30-Day Free Shrinkage ($\mu\epsilon$)	Control (0% FA)		20% Class F FA #2		40% Class F FA #2	
			7-Day	14-Day	7-Day	14-Day	7-Day	14-Day
0%	7-Day	277		90	Y	90	N	80
	14-Day	260			Y	95	90	Y
20%	7-Day	343				N	N	Y
	14-Day	323					N	80
40%	7-Day	307						N
	14-Day	287						

Note: See the Table 4.4 note for an explanation of the terms “N”, “80”, “90”, “95”, and “Y”.

Long-term shrinkage results for concrete containing 0, 20, or 40% volume replacements of cement with Class F fly ash are shown in Fig. 4.42. As with the early-age shrinkage results, the highest long-term shrinkage occurred for specimens containing a 20% replacement of cement with fly ash and cured for 7 days. For this comparison, the least shrinkage occurred for the 40% fly ash specimens cured for 7 days followed closely by the 40% fly ash specimens cured for 14 days. These results initially appear inconsistent with previous observations, but when the large initial expansion of the 40% fly ash specimens is considered, the relative order of shrinkage is appropriate.

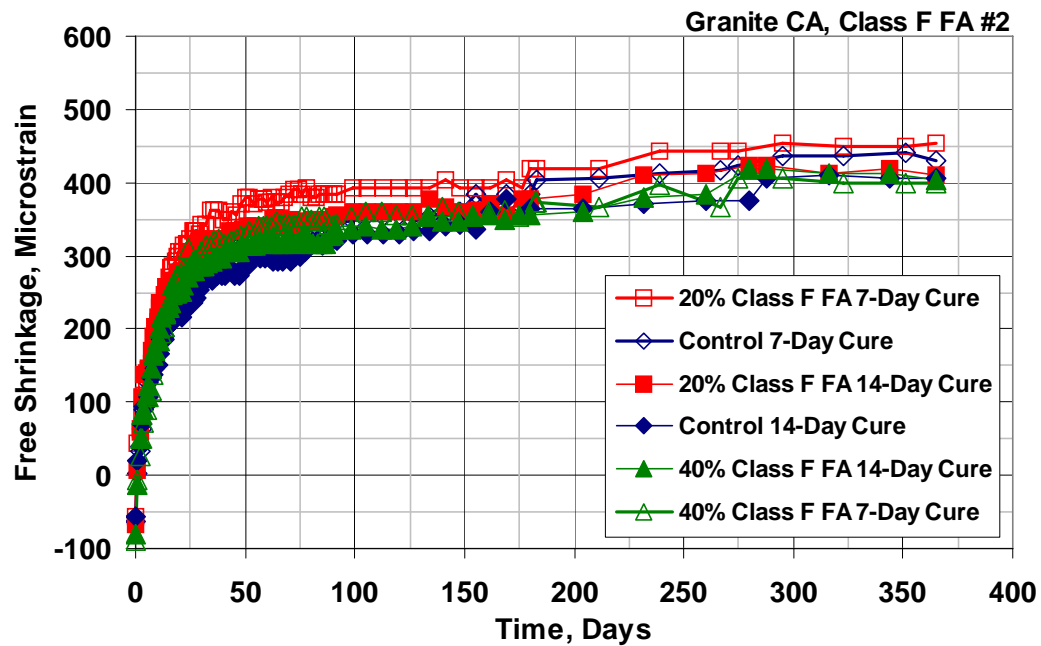


Fig. 4.42 – Free Shrinkage Test (ASTM C 157). Program VI Set 4. Average free-shrinkage versus time through 365 days (drying only).

Table 4.67 – Student’s t-test Results for Program VI Set 4 365-Day Free-Shrinkage Data

		365-Day Free Shrinkage ($\mu\epsilon$)	Control (0% FA)		20% Class F FA #2		40% Class F FA #2	
			7-Day	14-Day	7-Day	14-Day	7-Day	14-Day
0%	7-Day	430		N	N	N	N	80
	14-Day	405			80	N	N	N
20%	7-Day	453				N	80	90
	14-Day	410					N	N
40%	7-Day	400						N
	14-Day	403						

Note: See the Table 4.4 note for an explanation of the terms “N”, “80”, “90”, “95”, and “Y”.

In light of the inconsistent results obtained for the previous comparison, an additional series of free-shrinkage specimens containing a 0, 20, or 40% volume replacement of cement with Class F fly ash was added to the test program. Concrete for these specimens contained granite coarse aggregate and a third source of Class F

fly ash obtained from Headwaters Resources in Underwood, ND. The average free-shrinkage data for specimens in this series after 0, 30, 90, 180, and 365 days of drying are presented in Table 4.68, and the average free-shrinkage curves are presented in Figs. 4.43 and 4.44. The results of the Student's t-test are presented in Tables 4.69 and 4.70. The expansion that occurred for this series of specimens varied from 33 to 63 $\mu\epsilon$. The results for this series are similar to results obtained in Set 3 for concrete containing fly ash and limestone coarse aggregate, and indicate that shrinkage at all ages is increased with increases in the fly ash content and decreases as the curing period is increased from 7 to 14 days.

Table 4.68 – Summary of Free-Shrinkage Data for Program VI Set 4 (in microstrain)

Days of Drying	Control (0% FA)		20% Class F FA #3		40% Class F FA #3	
	7-Day Cure	14-Day Cure	7-Day Cure	14-Day Cure	7-Day Cure	14-Day Cure
0	-63	-57	-50	-53	-33	-57
30	277	260	313	300	347	333
90	347	323	390	373	423	417
180	383	380	417	413	473	500
365	430	420	483	467	497	530

Figure 4.43 compares the shrinkage results for concrete containing 0, 20, or 40% volume replacements of cement with Class F fly ash through the first 30 days of drying. As shown in Fig. 4.43, decreasing the curing period from 14 to 7 days results in only a small increase in shrinkage compared to increasing the fly ash content from 0 to 20% (or from 20 to 40%). For specimens cured for 14 days, an increase in the fly ash content from 0 to 20% resulted in an increase in shrinkage of 40 $\mu\epsilon$ at 30 days. Shrinkage increases by another 33 $\mu\epsilon$ as the fly ash content is increased further from 20 to 40%. These differences are statistically significant at $\alpha = 0.1$ and $\alpha = 0.2$, and the 73 $\mu\epsilon$ difference in shrinkage between the control mixture (0% fly ash) and the 40% fly ash mixture is statistically significant at the highest level of confidence (Table 4.69). Specimens cured for 7 days exhibited similar increases in shrinkage as

the fly ash content is increased from 0 to 40%. As the curing period is increased from 7 to 14 days, shrinkage is reduced by 13 $\mu\epsilon$ for the 40% fly ash mixture, 14 $\mu\epsilon$ for the 20% fly ash mixture, and 17 $\mu\epsilon$ for the control mixture after 30 days of drying. Although consistent, only the 17 $\mu\epsilon$ difference in shrinkage is statistically significant ($\alpha = 0.1$).

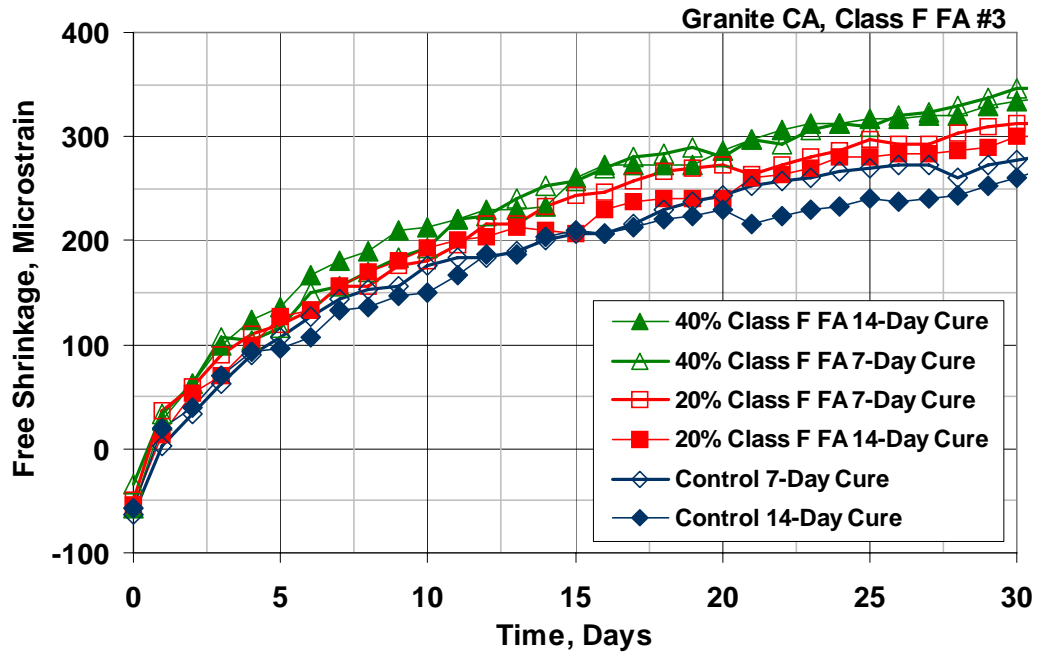


Fig. 4.43 – Free Shrinkage Test (ASTM C 157). Program VI Set 4. Average free-shrinkage versus time through 30 days (drying only).

Table 4.69 – Student’s t-test Results for Program VI Set 4 30-Day Free-Shrinkage Data

		30-Day Free Shrinkage ($\mu\epsilon$)	Control (0% FA)		20% Class F FA #3		40% Class F FA #3	
			7-Day	14-Day	7-Day	14-Day	7-Day	14-Day
0%	7-Day	277		90	Y	N	Y	Y
	14-Day	260			Y	90	Y	Y
20%	7-Day	313				N	90	N
	14-Day	300					90	80
40%	7-Day	347						Y
	14-Day	333						

Note: See the Table 4.4 note for an explanation of the terms “N”, “80”, “90”, “95”, and “Y”.

Figure 4.44 compares the long-term shrinkage results of concrete containing Class F fly ash. The results obtained after one year of drying are qualitatively similar to the early-age shrinkage results shown in Fig. 4.43. The addition of fly ash increases shrinkage at all ages, and increasing the curing period from 7 to 14 days has very little effect on the shrinkage behavior as none of these differences are statistically significant (Table 4.70). For this series, the greatest shrinkage is observed for the 40% fly ash mixture cured for 14 days, and the least shrinkage is observed for the control mixture 14 days (for a total difference in shrinkage of 110 $\mu\epsilon$). For specimens cured for 14 days, an increase in the fly ash content from 0 to 20% resulted in a 47 $\mu\epsilon$ increase in shrinkage at 365 days. A further increase in the fly ash content from 20 to 40% resulted in an additional 63 $\mu\epsilon$ increase in shrinkage. These differences are statistically significant at $\alpha = 0.2$ (Table 4.70). An increase in the fly ash content from 0 to 20% and from 20 to 40% resulted in shrinkage increases of 53 and 14 $\mu\epsilon$ for the specimens cured for 7 days. The 53 $\mu\epsilon$ increase in shrinkage as the fly ash content is increased from 0 to 20% is statistically significant at $\alpha = 0.1$.

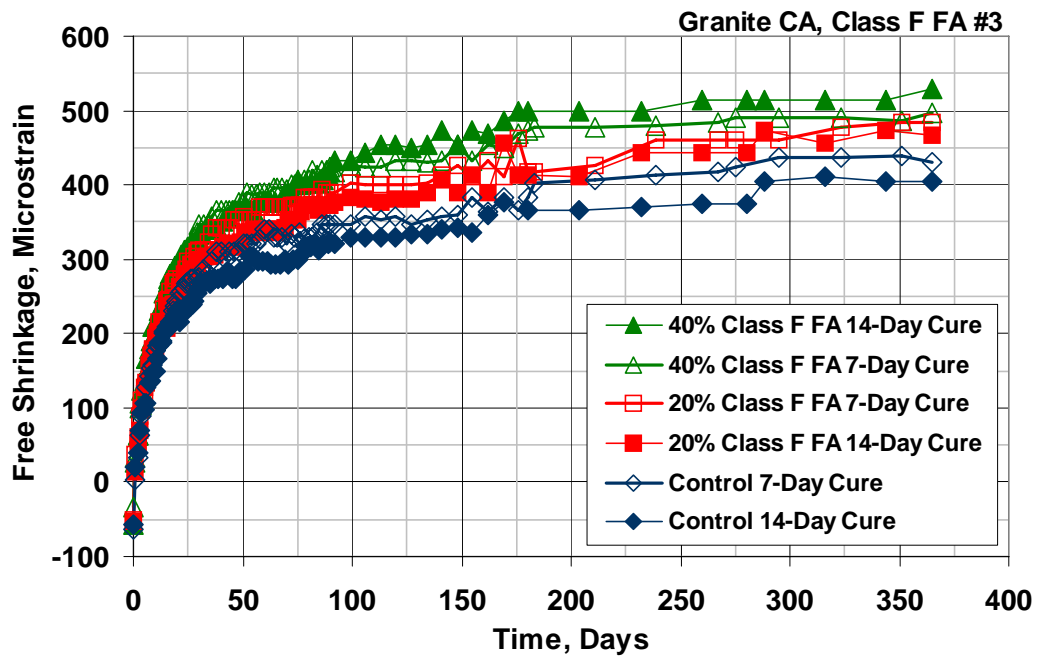


Fig. 4.44 – Free Shrinkage Test (ASTM C 157). Program VI Set 4. Average free-shrinkage versus time through 30 days (drying only).

Table 4.70 – Student’s t-test Results for Program VI Set 4 365-Day Free Shrinkage Data

		365-Day Free Shrinkage ($\mu\epsilon$)	Control (0% FA)		20% Class F FA #3		40% Class F FA #3	
			7-Day	14-Day	7-Day	14-Day	7-Day	14-Day
0%	7-Day	430		N	90	80	95	95
	14-Day	420			90	80	95	95
20%	7-Day	483				N	N	N
	14-Day	467					N	80
40%	7-Day	497						N
	14-Day	530						

Note: See the Table 4.4 note for an explanation of the terms “N”, “80”, “90”, “95”, and “Y”.

4.9.5 Program VI Set 5 (Slag Cement and Limestone Coarse Aggregate)

Program VI Set 5 compares the free shrinkage of mixtures containing 0, 30, 60, or 80% volume replacements of cement with Grade 120 slag cement (ground

granulated blast furnace slag). The Set 5 evaluation includes two samples of Grade 120 slag obtained from Lafarge North America in Chicago, IL cast with limestone coarse aggregate. Set 5 is divided into two different series. The first includes mixtures containing with slag contents of 0, 30, and 60%, and the second includes mixtures with 0, 60, and 80% slag contents. A summary of Program VI Set 5 is presented in Table 4.71. Individual mixture proportions, plastic concrete properties, and compressive strengths are given in Tables A.8 and A.14 in Appendix A. Individual specimen free-shrinkage curves are presented in Figs. C.16 and C.37 through C.40 in Appendix C.

Table 4.71 – Program VI Set 5 Summary

Set Number	Slag Cement Content[†]	Slag Cement Sample No.	Coarse Aggregate
5	0% (control)	--	Limestone
5	G120 30%	1	Limestone
5	G120 60%	1	Limestone
5	G120 60%	2	Limestone
5	G120 80%	2	Limestone

[†]The slag cement contents are reported by volume of cementitious materials.

The average free-shrinkage data for Program VI Set 5 specimens containing the first slag cement sample are presented in Table 4.72. Figures 4.45 and 4.46 compare the shrinkage results after 30 and 365 days of drying, respectively. As shown in Table 4.72, the partial replacement of cement with slag cement results in significantly less shrinkage at all ages. Shrinkage is reduced as the percentage replacement of slag is increased and as the curing period is increased. Thus, the greatest shrinkage is obtained for the control mixture (0% slag) cured for 7 days and the least shrinkage is obtained for the 60% slag mixture cured for 14 days. This trend remains consistent throughout the drying period, and is qualitatively similar to the results obtained for concrete containing silica fume and limestone coarse aggregate.

Table 4.72 – Summary of Free-Shrinkage Data for Program VI Set 5 (in microstrain)

Days of Drying	Control (0% Slag Cement)		30% G120 Slag Cement #1		60% G120 Slag Cement #1	
	7-Day Cure	14-Day Cure	7-Day Cure	14-Day Cure	7-Day Cure	14-Day Cure
0	-43	-33	-40	-20	-47	-47
30	320	283	317	233	280	183
90	413	387	407	353	383	337
180	453	420	450	407	423	383
365	483	460	507	443	477	433

The use of high-volume percentage replacements of cement with Grade 120 slag cement greatly reduces the early-age shrinkage of concrete, as shown in Fig. 4.45. At 30 days, shrinkage ranges from 183 $\mu\epsilon$ for the 60% volume replacement mixture cured for 14 days, to 320 $\mu\epsilon$ for the control (0% slag cement) cured for 7 days. The 30% slag mixture cured for 7 days exhibited the same shrinkage as the control mixture cured for 7 days, but the 60% slag mixture cured for 7 days exhibited the same shrinkage as the control mixture cured for 14 days. Significant reductions in shrinkage are obtained as the curing period is increased from 7 to 14 days. For the specimens cured for 14 days, an increase in the slag content from 0 to 30% reduces shrinkage by 50 $\mu\epsilon$ at 30 days. This reduction in shrinkage is statistically significant at $\alpha = 0.05$ (Table 4.73). A further increase in the slag content from 30 to 60% reduces shrinkage by an additional 50 $\mu\epsilon$ – making the total difference in shrinkage between the control mixture and the 60% slag mixture 100 $\mu\epsilon$ at 30 days. These differences in shrinkage between the control mixture and the 60% slag mixtures and between the 30 and 60% slag mixtures are statistically significant at the highest level of confidence (Table 4.73).

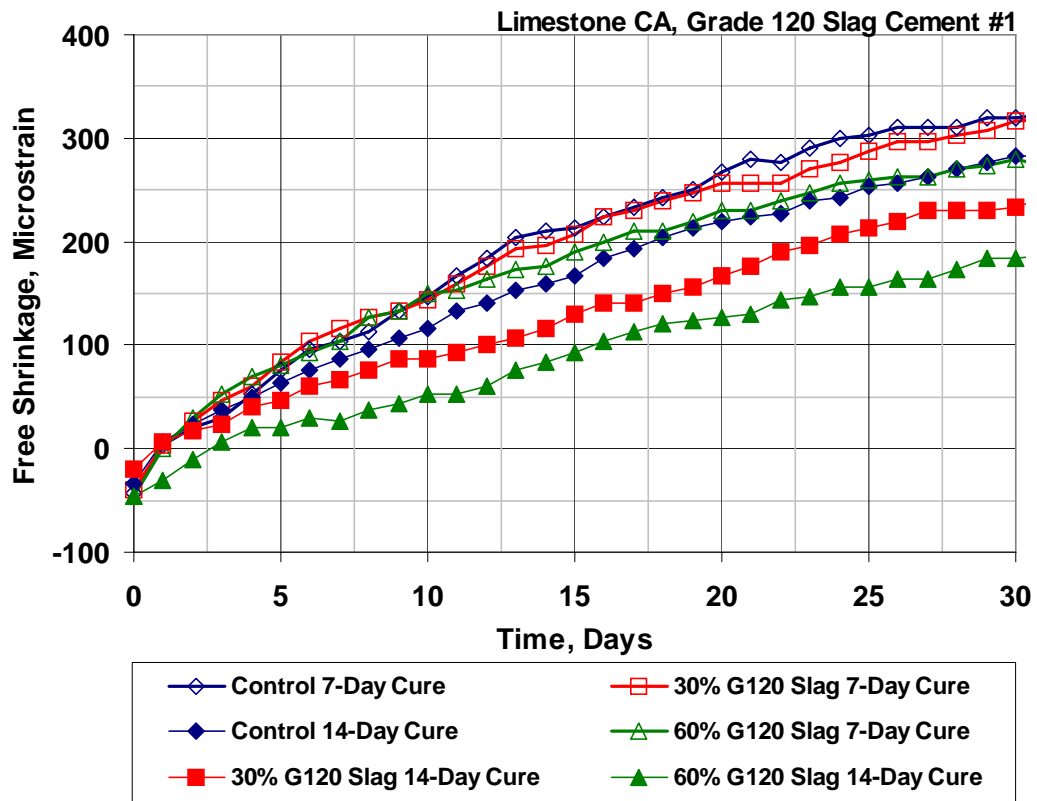


Fig. 4.45 – Free Shrinkage Test (ASTM C 157). Program VI Set 5. Average free-shrinkage versus time through 30 days (drying only).

Table 4.73 – Student’s t-test Results for Program VI Set 5 30-Day Free-Shrinkage Data

		30-Day Free Shrinkage (µε)	Control (0% Slag)		30% G120 Slag #1		60% G120 Slag #1	
			7-Day	14-Day	7-Day	14-Day	7-Day	14-Day
0%	7-Day	320		90	N	Y	90	Y
	14-Day	283			95	95	N	Y
30%	7-Day	317				Y	95	Y
	14-Day	233					95	95
60%	7-Day	280						Y
	14-Day	183						

Note: See the Table 4.4 note for an explanation of the terms “N”, “80”, “90”, “95”, and “Y”.

Figure 4.46 compares the long-term shrinkage results for concrete with limestone coarse aggregate containing 0, 30, or 60% volume replacements of cement with Grade 120 slag cement. For mixtures cured for 14 days, an increase in the slag content from 0 to 30% results in a decrease in shrinkage of about $20 \mu\epsilon$ for periods greater than 90 days. A similar reduction in shrinkage is obtained with a further increase in the slag content from 30 to 60%. After 365 days of drying, shrinkage strains of 460, 443, and 433 $\mu\epsilon$ are obtained for the concrete containing 0, 30, and 60% volume replacements of cement with Grade 120 slag cement. The 27 $\mu\epsilon$ difference in shrinkage between the control concrete and the 60% slag concrete is significant at $\alpha = 0.1$; the remaining differences, however, are not significant (Table 4.71).

Specimens cured for 7 days exhibited greater shrinkage than those cured for 14 days for each of the mixtures examined and throughout the drying period. After 365 days of drying, shrinkage strains of 483, 507, and 477 $\mu\epsilon$ are obtained for the concrete containing 0, 30, and 60% replacements of cement with slag. Only the difference in shrinkage between the two slag mixtures is statistically significant (at $\alpha = 0.2$) (Table 4.74). Shrinkage strains of 460, 443, and 433 are obtained for the mixtures containing 0, 30, and 60% slag for specimens cured for 14 days. In this case, only the difference in shrinkage between the control mixture (0% slag cement) and the mixture containing 60% slag is statistically significant ($\alpha = 0.1$) (Table 4.74). Increasing the curing period from 7 to 14 days has a much more significant effect on the mixtures containing slag than for the control mixture. Reductions in shrinkage of 64 and 44 $\mu\epsilon$ at 365 days are obtained for the mixtures containing 30 and 60% slag, respectively, compared to only 23 $\mu\epsilon$ for the control mixture. The differences in shrinkage resulting from an increase in the curing period from 7 to 14 days for the slag mixtures are statistically significant at $\alpha = 0.1$, but the difference observed for the control mixture is not significant (Table 4.74).

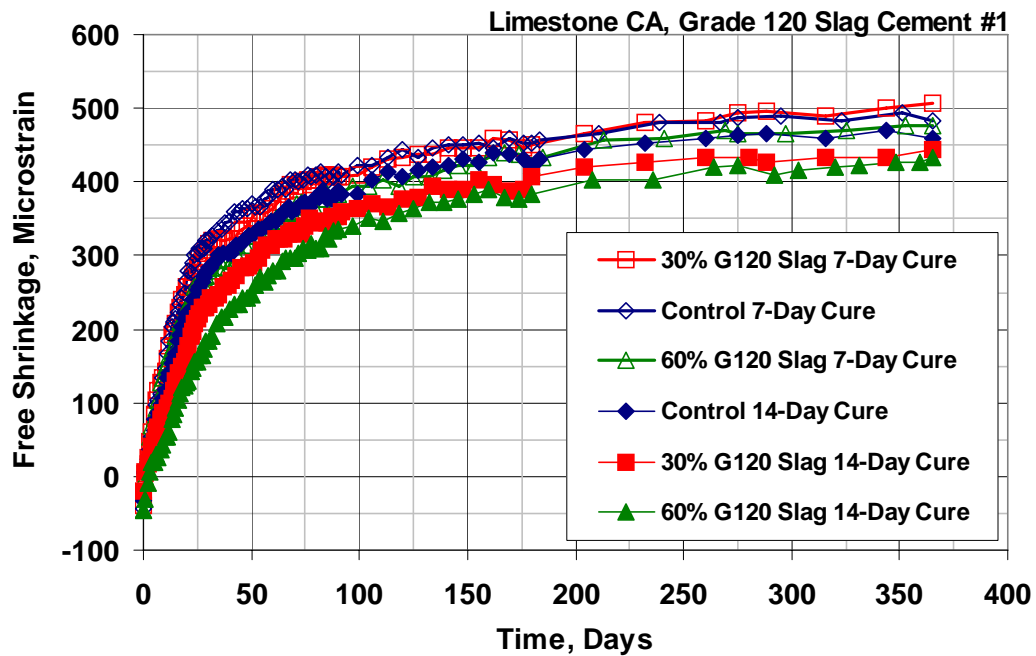


Fig. 4.46 – Free Shrinkage Test (ASTM C 157). Program VI Set 5. Average free-shrinkage versus time through 365 days (drying only).

Table 4.74 – Student’s t-test Results for Program VI Set 5 365-Day Free-Shrinkage Data

		365-Day Free Shrinkage ($\mu\epsilon$)	Control (0% Slag)		30% G120 Slag #1		60% G120 Slag #1	
			7-Day	14-Day	7-Day	14-Day	7-Day	14-Day
0%	7-Day	483		N	N	80	N	95
	14-Day	460			Y	N	N	90
30%	7-Day	507				95	80	Y
	14-Day	443					80	N
60%	7-Day	477						95
	14-Day	433						

Note: See the Table 4.4 note for an explanation of the terms “N”, “80”, “90”, “95”, and “Y”.

The significant reductions in shrinkage observed for first set of specimens containing a partial replacement of cement with slag cement, especially at early ages, prompted an additional comparison with 0, 60, and 80% volume replacements of cement with a second sample of Grade 120 slag also from Lafarge North America.

Average free-shrinkage data for these specimens throughout the entire drying period are shown in Table 4.75. The results for this series are even more striking than for the first as significant reductions in shrinkage are obtained with a high-volume replacement of cement with slag cement. As in the first series, the differences are greatest at early ages.

Table 4.75 – Summary of Program VI Set 5 Free-Shrinkage Data (in microstrain)

Days of Drying	Control (0% Slag Cement)		60% G120 Slag Cement #2		80% G120 Slag Cement #2	
	7-Day Cure	14-Day Cure	7-Day Cure	14-Day Cure	7-Day Cure	14-Day Cure
0	-43	-33	-57	-57	-63	-80
30	320	283	193	163	73	47
90	413	387	323	320	283	227
180	453	420	387	377	370	333
365	483	460	413	393	390	383

The free-shrinkage results through 30 days of drying for concrete with 0, 60, and 80% volume replacements of cement with slag cement are shown in Fig. 4.47. Increasing the percentage replacement of cement with slag, and to a somewhat lesser extent, increasing the curing period from 7 to 14 days reduces shrinkage. For mixtures cured for 14 days, an increase in the slag content from 0 to 60% results in a decrease in shrinkage of 120 $\mu\epsilon$ at 30 days (compared to 100 $\mu\epsilon$ at 30 days for the specimens shown in Fig. 4.45). As the slag content is increased further from 60 to 80%, shrinkage decreases by an additional 116 $\mu\epsilon$. Similar decreases in shrinkage are observed for the specimens cured for 7 days. For this series, increasing the curing period from 7 to 14 days resulted in a reduction in shrinkage of 30 $\mu\epsilon$ at 30 days (compared to 97 $\mu\epsilon$ for the specimens shown in Fig. 4.45) for the mixture containing 60% slag cement and a reduction in shrinkage of 26 $\mu\epsilon$ for the 80% mixture. Increasing the curing period resulted in a 37 $\mu\epsilon$ reduction in shrinkage for the control mixture. With the exception of these relatively small differences in shrinkage, all of

the remaining differences are statistically significant at the highest level of confidence (Table 4.76).

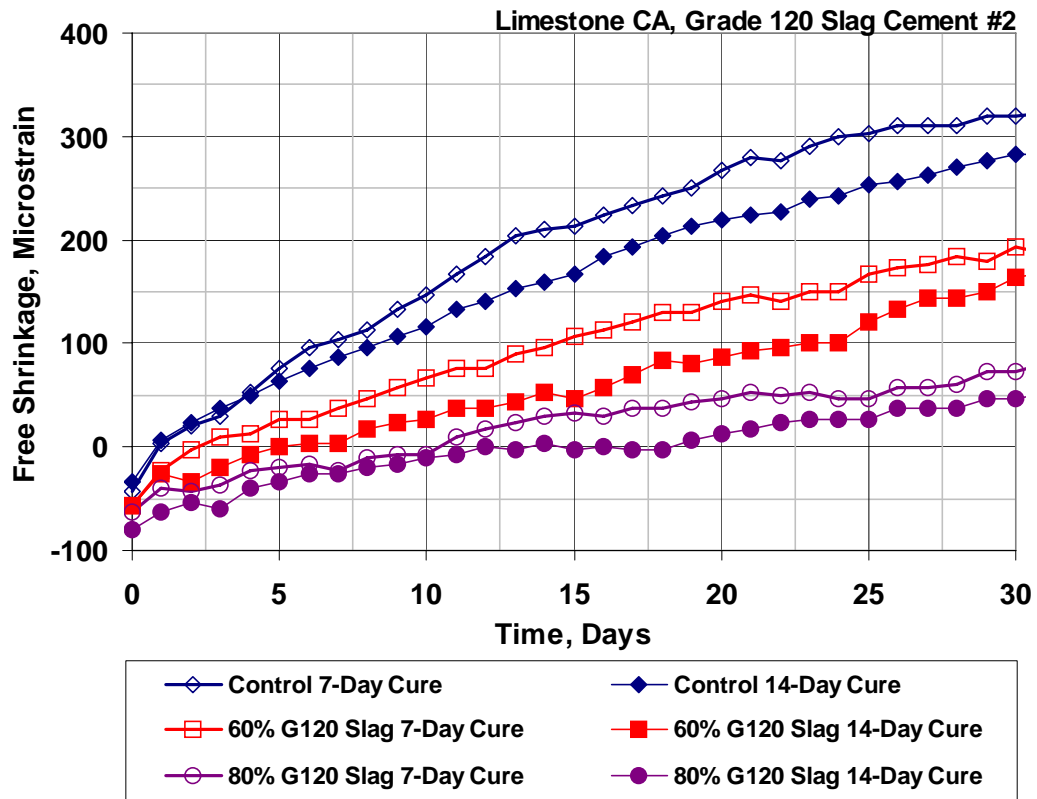


Fig. 4.47 – Free Shrinkage Test (ASTM C 157). Program VI Set 5. Average free-shrinkage versus time through 30 days (drying only).

Table 4.76 – Student’s t-test Results for Program VI Set 5 30-Day Free-Shrinkage Data

		30-Day Free Shrinkage (µε)	Control (0% Slag)		60% G120 Slag #2		80% G120 Slag #2	
			7-Day	14-Day	7-Day	14-Day	7-Day	14-Day
0%	7-Day	320		90	Y	Y	Y	Y
	14-Day	283			Y	Y	Y	Y
60%	7-Day	193				N	Y	Y
	14-Day	163					Y	Y
80%	7-Day	73						80
	14-Day	47						

Note: See the Table 4.4 note for an explanation of the terms “N”, “80”, “90”, “95”, and “Y”.

The free-shrinkage results after 365 days of drying are shown in Fig. 4.48. For periods greater than 200 days, there is very little difference in shrinkage between concrete containing either replacement level of slag cement. After 365 days of drying, shrinkage values of 413 and 393 $\mu\epsilon$ were obtained for the 60% slag mixtures cured for 7 and 14 days, respectively. Increasing the replacement level to 80% resulted in shrinkage values of 390 and 383 $\mu\epsilon$. None of the differences resulting from increasing the curing period from 7 to 14 days are statistically significant (Table 4.77). The differences in shrinkage between the slag mixtures and the control mixture, however, are statistically significant at the highest level for all of the specimens cured for either 7 or 14 days.

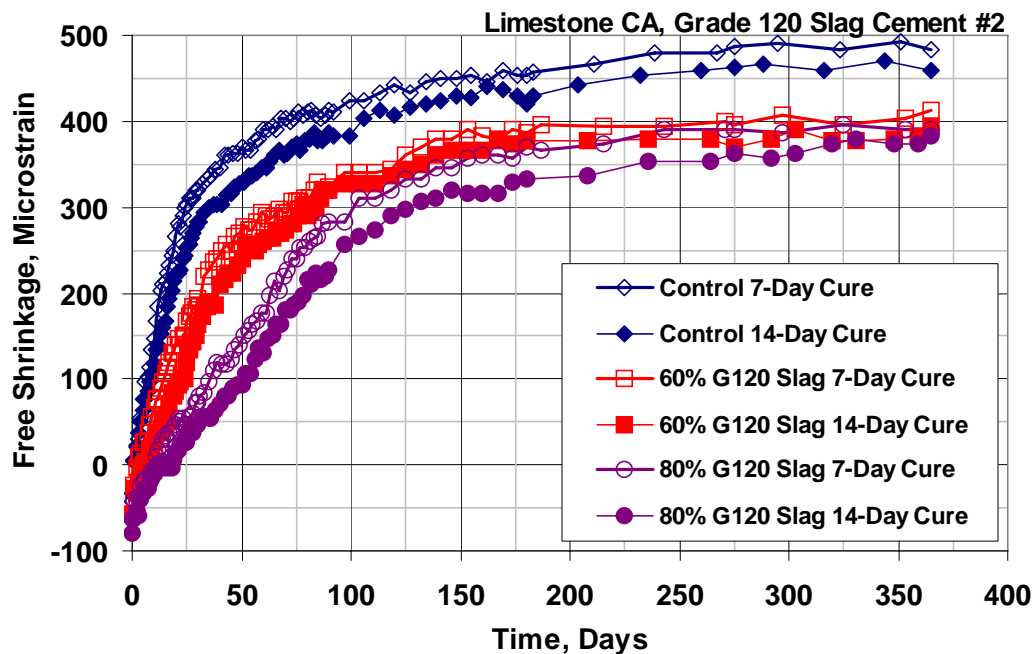


Fig. 4.48 – Free Shrinkage Test (ASTM C 157). Program VI Set 5. Average free-shrinkage versus time through 365 days (drying only).

Table 4.77 – Student’s t-test Results for Program VI Set 5 365-Day Free-Shrinkage Data

		365-Day Free Shrinkage ($\mu\epsilon$)	Control (0% Slag)		60% G120 Slag #2		80% G120 Slag #2	
			7-Day	14-Day	7-Day	14-Day	7-Day	14-Day
0%	7-Day	483		N	Y	Y	Y	Y
	14-Day	460			Y	Y	Y	Y
60%	7-Day	413				N	90	95
	14-Day	393					N	N
80%	7-Day	390						N
	14-Day	383						

Note: See the Table 4.4 note for an explanation of the terms “N”, “80”, “90”, “95”, and “Y”.

4.9.6 Program VI Set 6 (Grade 120 Slag Cement and Limestone or Quartzite Coarse Aggregate)

In the sixth set, two coarse aggregates, limestone and quartzite, were used in conjunction with a 60% replacement of cement with Grade 120 slag cement. A summary of Program VI Set 6 is presented in Table 4.78. The two batches containing quartzite coarse aggregate have the same mixture proportions and the batch containing limestone is also included in the previous set. Individual mixture proportions, plastic concrete properties, and compressive strengths are given in Table A.15 in Appendix A. Individual specimen free-shrinkage curves are presented in Figs. C.41 through C.43 in Appendix C.

Table 4.78 – Program VI Set 6 Summary

Set Number	Slag Cement Content [†]	Slag Cement Sample No.	Coarse Aggregate
6	G120 60%	2	Limestone
6	G120 60%	2	Quartzite
6	G120 60%	2	Quartzite

[†]The slag cement contents are reported by volume of cementitious materials.

The average free-shrinkage data for Program VI Set 6 specimens after 0, 30, 90, 180, and 365 days of drying are presented in Table 4.79. Initial expansion strains varied between 37 and 60 $\mu\epsilon$ with no trend apparent between the amount of expansion and the length of the curing period or the coarse aggregate type. The results shown in Table 4.79 indicate significantly increased early-age shrinkage for the concrete containing quartzite compared to that containing limestone, although this large initial difference is not maintained through the entire drying period. These shrinkage results are qualitatively similar to the results obtained for specimens containing granite and silica fume and supports the hypothesis that porous coarse aggregate provides internal curing leading to reduced shrinkage.

Table 4.79 – Summary of Program VI Set 6 Free-Shrinkage Data (in microstrain)

Days of Drying	60% G120 Slag #2 Limestone CA		60% G120 Slag #2 Quartzite CA		60% G120 Slag #2 Quartzite CA - R	
	7-Day Cure	14-Day Cure	7-Day Cure	14-Day Cure	7-Day Cure	14-Day Cure
0	-57	-57	-37	-53	-60	-53
30	193	163	330	247	307	247
90	323	320	377	320	393	333
180	387	377	410	367	407	360
365	413	393	437	373	420	377

The free-shrinkage results through the first 30 days of drying are presented in Fig. 4.49 and the Student's t-test results at 30 days are presented in Table 4.80. As expected, the free-shrinkage curves for the two quartzite batches are very similar, and the small differences at 30 days are not statistically significant (Table 4.80). Immediately upon drying, these batches began shrinking rapidly, and after only 5 days, the shrinkage of the mixtures containing quartzite and cured for 7 days exceed the limestone batch cured for 7 days by about 175 $\mu\epsilon$. This difference decreases to about 125 $\mu\epsilon$ at 30 days. For the specimens cured for 14 days, the largest difference of 150 $\mu\epsilon$ occurs on day 15 and decreases to about 80 $\mu\epsilon$ at 30 days. For a given

curing period, all of the differences observed between the limestone batch and the quartzite batches are statistically significant at the highest level of confidence. Increasing the curing period from 7 to 14 days reduced the 30-day shrinkage from 193 to 160 $\mu\epsilon$ for the limestone batch and from 330 to 247 $\mu\epsilon$ and 307 to 247 $\mu\epsilon$ for the two batches containing quartzite.

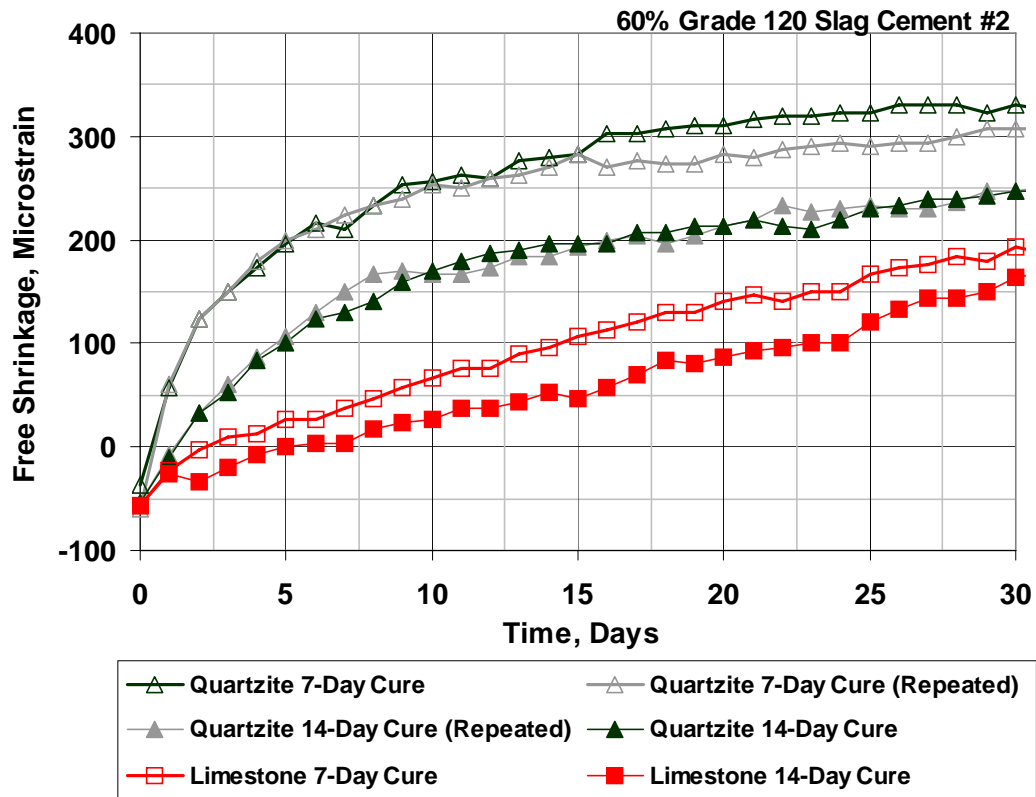


Fig. 4.49 – Free Shrinkage Test (ASTM C 157). Program VI Set 6. Average free-shrinkage versus time through 30 days (drying only).

Table 4.80 – Student’s t-test Results for Program IV Set 6 30-Day Free-Shrinkage Data

		30-Day Free Shrinkage ($\mu\epsilon$)	Control (0% Slag) Quartzite - R		60% G120 Slag #2 Quartzite		60% G120 Slag #2 Limestone	
			7-Day	14-Day	7-Day	14-Day	7-Day	14-Day
Q Repeat	7-Day	307		90	N	90	Y	Y
	14-Day	247			Y	N	Y	Y
Q	7-Day	330				N	Y	Y
	14-Day	247					95	Y
LS	7-Day	193						Y
	14-Day	163						

Note: See the Table 4.4 note for an explanation of the terms “N”, “80”, “90”, “95”, and “Y”.

The free-shrinkage curves after one year of drying are presented in Fig. 4.50, and the results of the Student’s t-test at 365 days are shown in Table 4.81. For periods greater than approximately 125 days, the free-shrinkage curves for the limestone mixtures (specimens cured for both 7 and 14 days) exceed the free-shrinkage curves for the mixtures containing quartzite. The average shrinkage values after one year of drying for the limestone mixtures are 413 and 393 $\mu\epsilon$ for the specimens cured for 7 and 14 days, respectively. This difference is not statistically significant (Table 4.81). The free shrinkage of the two mixtures containing quartzite and cured for 14 days is 373 and 377 $\mu\epsilon$ at 365 days compared to 437 and 420 $\mu\epsilon$ for the specimens cured for 7 days.

These results are also qualitatively very similar to the results from Program III where the use of a low-absorption coarse aggregate (i.e. quartzite or granite) led to increased early-age shrinkage compared to concrete containing the relatively porous limestone coarse aggregate. In this program, however, the difference in shrinkage is much larger and is maintained throughout most of the test period. These results are likely a result of the increased sensitivity of the slag mixtures to the length of the curing period. This behavior is examined further in Section 4.9.9.

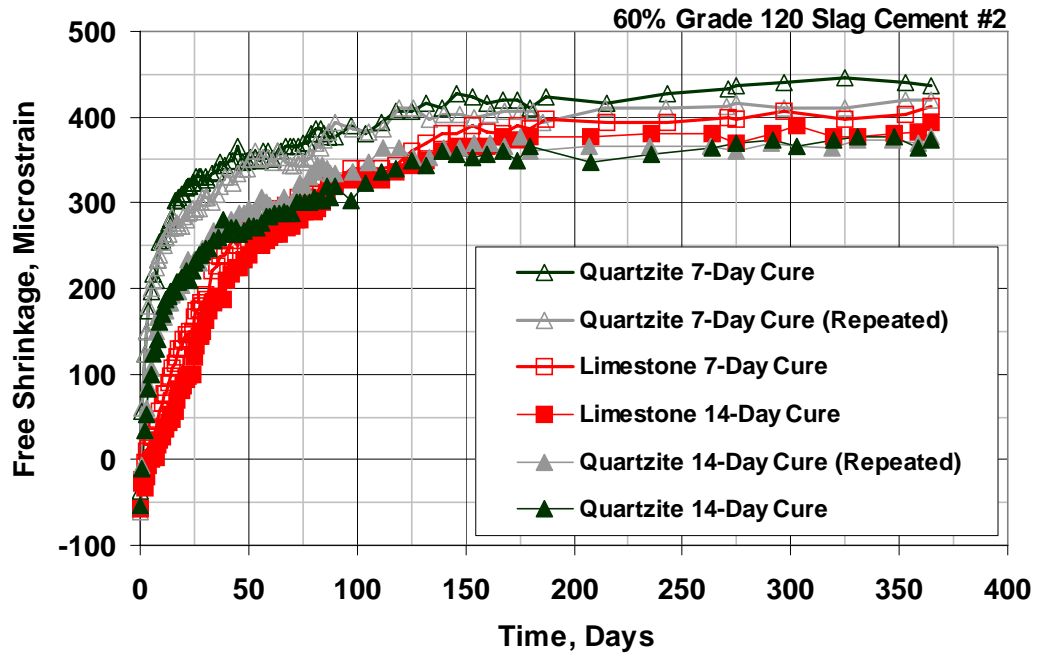


Fig. 4.50 – Free Shrinkage Test (ASTM C 157). Program VI Set 6. Average free-shrinkage versus time through 365 days (drying only).

Table 4.81 – Student’s t-test Results for Program VI Set 6 365-Day Free-Shrinkage Data

		365-Day Free Shrinkage (μϵ)	Control (0% Slag) Quartzite - R		60% G120 Slag #2 Quartzite		60% G120 Slag #2 Limestone	
			7-Day	14-Day	7-Day	14-Day	7-Day	14-Day
Q Repeat	7-Day	420		N	N	N	N	N
	14-Day	377			Y	N	Y	N
Q	7-Day	437				Y	80	80
	14-Day	373					Y	N
LS	7-Day	413						N
	14-Day	393						

Note: See the Table 4.4 note for an explanation of the terms “N”, “80”, “90”, “95”, and “Y”.

4.9.7 Program VI Set 7 (Grade 100 Slag Cement and Limestone or Granite Coarse Aggregate)

Additional free-shrinkage testing with a second low absorption aggregate in conjunction with slag cement is performed in Set 7 to verify the results obtained in Set 6. For this set, two series of mixtures containing a 60% volume replacement of cement with Grade 100 slag obtained from Holcim in Chicago, IL are evaluated. Mixtures with limestone coarse aggregate are evaluated first and then compared to mixture containing granite coarse aggregate. A summary of Program VI Set 7 is shown in Table 4.82, and additional details are provided in Section 2.9.6.3. Individual mixture designs, plastic concrete properties, and compressive strengths are provided in Tables A.6 and A.16 in Appendix A. Individual specimen free-shrinkage curves are presented in Figs. C.11, C.44, and C.45 in Appendix C.

Table 4.82 – Program VI Set 7 Summary

Set Number	Slag Cement Content [†]	Slag Cement Sample No.	Coarse Aggregate
7	0% (control)	--	Limestone
7	G100 60%	4	Limestone
7	G100 60%	4	Granite

[†]The slag cement contents are reported by volume of cementitious materials.

The average free-shrinkage data for the first series (limestone) of Program VI Set 7 specimens after 0, 30, 90, 180, and 365 days are summarized in Table 4.83. Expansion strains range from 13 to 43 $\mu\epsilon$, and just as in the previous observations, no apparent trend exists between the expansion values and the slag content or curing time. The results for Sets 5 and 6 are qualitatively very similar to the results obtained in Set 7. The addition of 60% slag cement results in a significant reduction in shrinkage. In this case, however, increasing the curing period from 7 to 14 days also results in even higher shrinkage reductions compared to the reductions observed for the batches containing Grade 120 slag.

Table 4.83 – Summary of Program VI Set 7 Free-Shrinkage Data for Specimens Containing Limestone Coarse Aggregate (in microstrain)

Days of Drying	Control (0% Slag)		60% G100 Slag #4	
	7-Day Cure	14-Day Cure	7-Day Cure	14-Day Cure
0	-43	-33	-13	-37
30	320	283	183	100
90	413	387	347	290
180	453	420	387	363
365	483	460	430	407

The early-age shrinkage results through 30 days of drying for the concretes containing limestone are shown in Fig. 4.51. The control mixtures (0% slag cement) have the most shrinkage throughout most of the drying period. The control mixture cured for 7 days had a 30-day free shrinkage value of 320 $\mu\epsilon$, and increasing the curing period from 7 to 14 days resulted in a 37 $\mu\epsilon$ reduction in shrinkage to 283 $\mu\epsilon$. This reduction in shrinkage is statistically significant at $\alpha = 0.1$ (Table 4.84). For all but the first few days, the free-shrinkage curve for the 60% slag mixture cured for 7 days is below both of the control shrinkage curves. At 30 days, the shrinkage for this mixture is 183 $\mu\epsilon$. Increasing the curing period from 7 to 14 days results in a further reduction in shrinkage, and after 30 days, the shrinkage strain for the 60% slag mixture cured for 14 days is only 100 $\mu\epsilon$. The difference in shrinkage resulting from this increase in the curing period is statistically significant at the highest level of confidence. All of the differences observed between the shrinkage of the control mixtures and the slag cement mixtures are also statistically significant at this level.

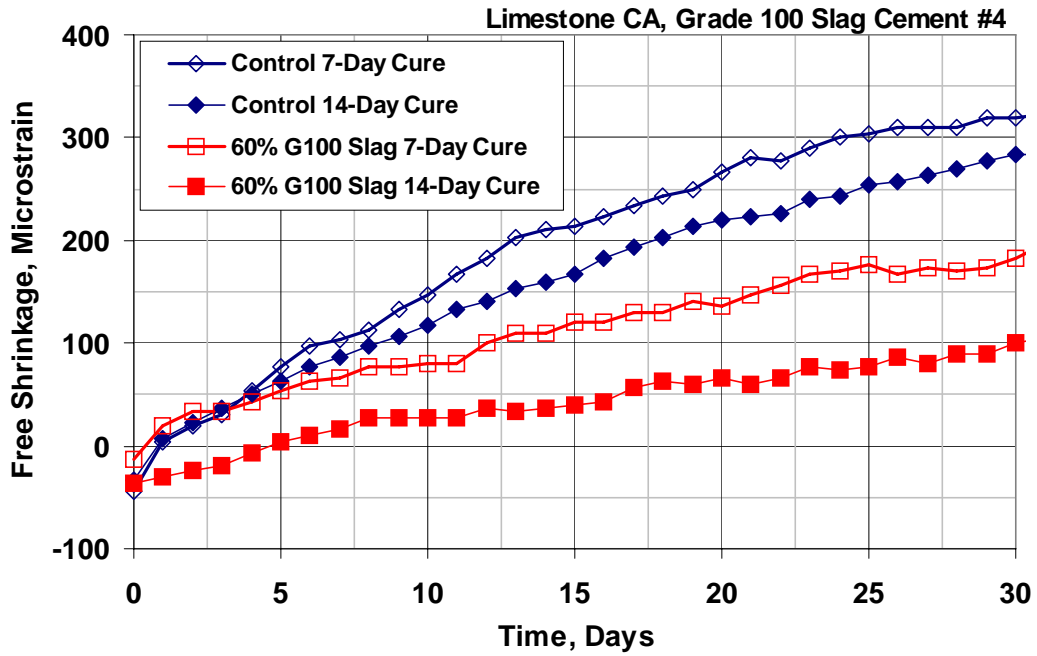


Fig. 4.51 – Free Shrinkage Test (ASTM C 157). Program VI Set 7. Average free-shrinkage versus time through 30 days (drying only) for specimens containing limestone coarse aggregate.

Table 4.84 – Student’s t-test Results for Program IV Set 7 30-Day Free-Shrinkage Data for Specimens Containing Limestone Coarse Aggregate

		30-Day Free Shrinkage (µε)	Control (0% Slag)		60% G100 Slag #4	
			7-Day	14-Day	7-Day	14-Day
0%	7-Day	320		90	Y	Y
	14-Day	283			Y	Y
60%	7-Day	183				Y
	14-Day	100				

Note: See the Table 4.4 note for an explanation of the terms “N”, “80”, “90”, “95”, and “Y”.

The effect of incorporating a 60% volume replacement of cement with Grade 100 slag cement on long-term shrinkage of concrete with limestone coarse aggregate is shown in Fig. 4.52, where it can be seen that the relative order of shrinkage remains the same as the order after 30 days of drying. For periods greater than approximately 150 days, a 60% slag replacement reduces shrinkage by approximately 60 µε for a

given curing period. The control mixtures cured for 7 and 14 days exhibited free-shrinkage values of 483 and 460 $\mu\epsilon$, respectively at 365 days. For this same period, the concrete containing a 60% replacement of cement with slag cement cured for 7 and 14 days exhibited shrinkage values of 430 and 407 $\mu\epsilon$, respectively. Although the trend is consistent, neither of these differences observed by increasing the curing period from 7 to 14 days are statistically significant (Table 4.85). The remaining differences in shrinkage between the control mixtures and the 60% slag mixtures are significant at least at $\alpha = 0.1$.

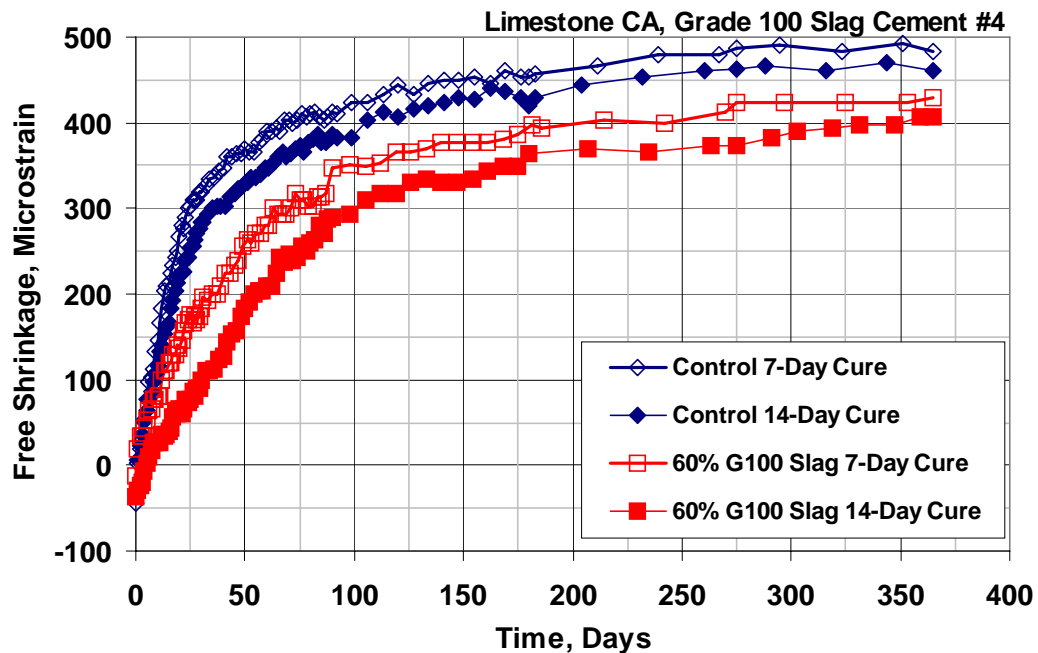


Fig. 4.52 – Free Shrinkage Test (ASTM C 157). Program VI Set 7. Average free-shrinkage versus time through 365 days (drying only) for specimens containing limestone coarse aggregate.

Additional testing with granite, which has a significantly lower absorption than the limestone (0.6% compared to between 2.5 and 3.0%), continues to indicate that a portion of the reduced shrinkage observed in Sets 5 through 7 for the mixtures containing slag may be due to the availability of water within the limestone pores, which provides internal curing. Three additional batches were cast comparing a

Table 4.85 – Student’s t-test Results for Program IV Set 7 365-Day Free-Shrinkage Data for Specimens Containing Limestone Coarse Aggregate

		365-Day Free Shrinkage ($\mu\epsilon$)	Control (0% Slag)		60% G100 Slag #4	
			7-Day	14-Day	7-Day	14-Day
0%	7-Day	430		N	95	95
	14-Day	407			Y	90
60%	7-Day	483				N
	14-Day	460				

Note: See the Table 4.4 note for an explanation of the terms “N”, “80”, “90”, “95”, and “Y”.

limestone control mixture (0% slag cement) with granite and limestone mixtures containing a 60% Grade 100 slag cement replacement of cement. All of the batches in this series were cured for 14 days and the same sample of Grade 100 slag was used (sample number 4).

The average free-shrinkage data for this second series of Program VI Set 7 specimens after 0, 30, 90, 180, and 365 days are summarized in Table 4.86. The limestone mixture with 60% Grade 100 slag cement has the least shrinkage throughout the drying period followed by the granite mixture with 60% slag cement, and finally, the limestone control mixture. These results further support the observation that the differences observed between mixtures containing limestone and granite (or quartzite) are directly related to the ability of the porous aggregate to provide internal curing.

The early-age shrinkage results for this series are shown in Fig. 4.53. The least shrinkage throughout the drying period is for the limestone mixture with 60% Grade 100 slag cement. At 16 days, the shrinkage of the granite mixture with 60% Grade 100 slag cement equals and then drops below the shrinkage exhibited by the limestone control mix. After 30 days of drying, the shrinkage of the limestone mixture with 60% slag cement is the least (87 $\mu\epsilon$), followed by the granite mixture containing 60% slag cement (267 $\mu\epsilon$), and finally, the limestone control mixture with

Table 4.86 – Summary of Program VI Set 7 Free-Shrinkage Data for Specimens Containing Limestone or Granite Coarse Aggregate (in microstrain)

Days of Drying	Control (0% Slag) Limestone CA	60% G120 Slag #4 Limestone CA	60% G100 Slag #4 Granite CA
	14-Day Cure	14-Day Cure	14-Day Cure
0	-17	-77	-43
30	317	87	267
90	410	273	360
180	453	327	380
365	443	340	390

100% portland cement ($317 \mu\epsilon$). The difference in shrinkage between the limestone control mixture and the granite mixture is statistically significant at $\alpha = 0.05$, but the remaining differences are statistically significant at the highest level of confidence (Table 4.87).

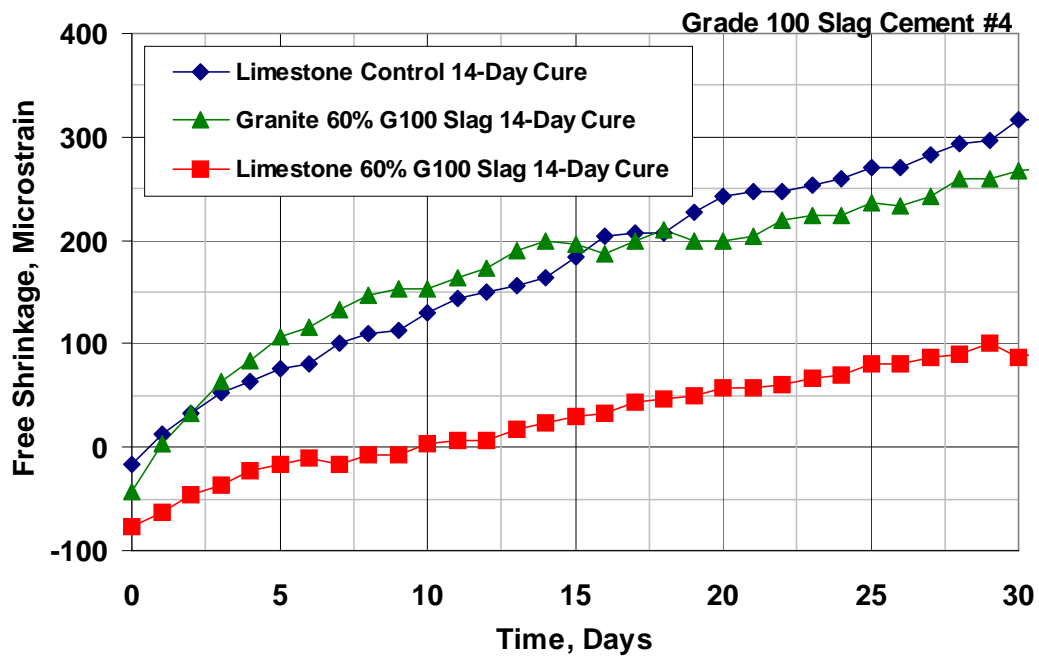


Fig. 4.53 – Free Shrinkage Test (ASTM C 157). Program VI Set 7. Average free-shrinkage versus time through 30 days (drying only) for specimens containing limestone or granite coarse aggregate.

Table 4.87 – Student’s t-test Results for Program VI Set 7 30-Day Free-Shrinkage Data for Specimens Containing Limestone or Granite Coarse Aggregate

	30-Day Free Shrinkage ($\mu\epsilon$)	Control (0% Slag) Limestone (LS)	60% G100 Slag #4 Limestone (LS)	60% G100 Slag #4 Granite (G)
0% (LS)	317		Y	95
60% (LS)	87			Y
60% (G)	267			

Note: See the Table 4.4 note for an explanation of the terms “N”, “80”, “90”, “95”, and “Y”.

The long-term shrinkage results through one year of drying are shown in Fig. 4.54, and the results of the statistical analysis are shown in Table 4.88. The limestone control mixture has the highest shrinkage after 16 days, and for periods greater than 100 days, the difference in shrinkage between the control mixture and the granite mixture containing 60% slag cement is about 50 $\mu\epsilon$. A further reduction of about 50 $\mu\epsilon$ for the same time period is obtained for the limestone mixture containing 60% slag cement. The ultimate shrinkage values for these mixtures are 443, 390, and 340 $\mu\epsilon$ for the limestone control and the granite and limestone mixtures containing 60% slag, respectively. All of the differences observed at 365 days are statistically significant at $\alpha = 0.02$ (Table 4.88). Interestingly, the shrinkage for the mixture containing granite appears to be stable after approximately 100 days, while the limestone mixture containing 60% slag cement exhibits continued shrinkage through about 200 days. These results are consistent with previous observations described in Section 4.9.6.

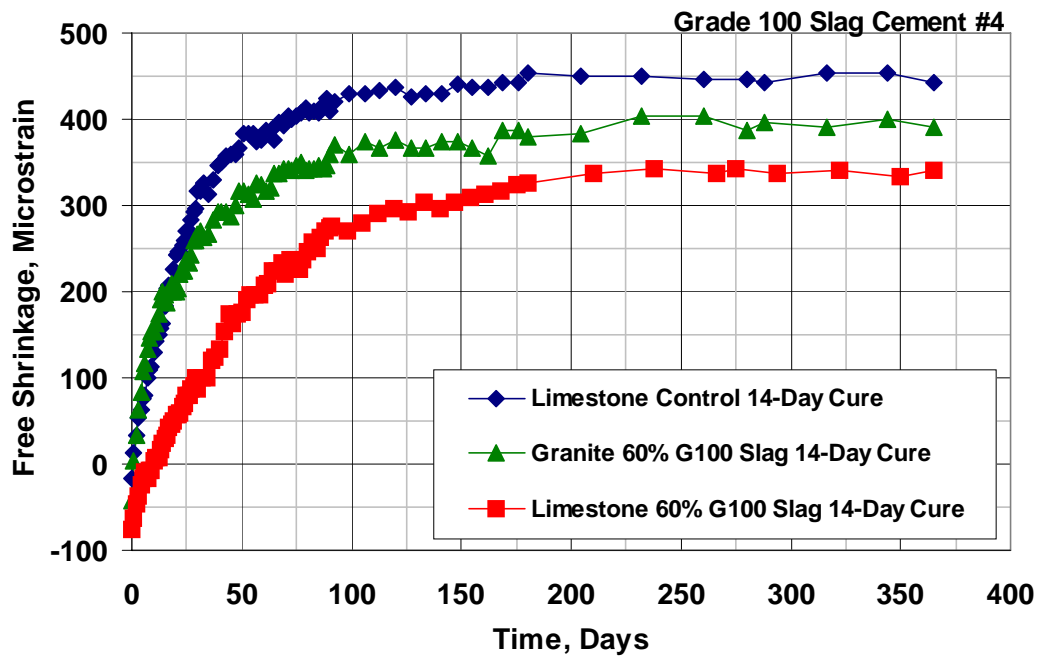


Fig. 4.54 – Free Shrinkage Test (ASTM C 157). Program VI Set 7. Average free-shrinkage versus time through 365 days (drying only) for specimens containing limestone or granite coarse aggregate.

Table 4.88 – Student’s t-test Results for Program VI Set 7 365-Day Free-Shrinkage Data for Specimens Containing Limestone or Granite Coarse Aggregate

	365-Day Free Shrinkage (µε)	Control (0% Slag) Limestone (LS)	60% G100 Slag #4 Limestone (LS)	60% G100 Slag #4 Granite (G)
0% (LS)	443		Y	Y
60% (LS)	340			Y
60% (G)	390			

Note: See the Table 4.4 note for an explanation of the terms “N”, “80”, “90”, “95”, and “Y”.

4.9.8 Program VI Set 8 (Grade 100 Slag Cement and Granite Coarse Aggregate)

Program VI Set 8 compares the shrinkage results for concrete with granite and 0, 30, or 60% volume replacements of cement with Grade 100 slag cement in conjunction with curing periods of 7 and 14 days. The slag cement sample used in

this set is from Holcim in Theodore, AL and is identified as slag sample number three in Table 2.2. A summary of Set 8 is presented in Table 4.89. Individual mixture proportions, plastic concrete properties, and compressive strengths are given in Table A.18 in Appendix A. Individual specimen free-shrinkage curves are presented in Figs. C.26, C.46, and C.47 in Appendix C.

Table 4.89 – Program VI 8 Summary

Set Number	Slag Cement Content [†]	Slag Cement Sample No.	Coarse Aggregate
8	0% (control)	--	Granite
8	G100 30%	3	Granite
8	G100 60%	3	Granite

[†]The slag cement contents are reported by volume of cementitious materials.

The average free-shrinkage data for the Program VI Set 8 specimens after 0, 30, 90, 180, and 365 days of drying are presented in Table 4.90. These mixtures exhibited significant expansion during the curing period. The 30% slag mixtures and the control mixture exhibited similar expansion values ranging only from 57 to 67 $\mu\epsilon$, but the 60% slag mixtures had expansion strains of 113 and 107 $\mu\epsilon$ for the specimens cured for 7 and 14 days, respectively. As shown in Table 4.90, the addition of slag results in a reduction in shrinkage at all ages provided that the specimens are cured for 14 days. The addition of either 30 or 60% results in increased shrinkage compared to the control mixture (0% slag cement) when they are only cured for 7 days.

Figure 4.55 presents the average free-shrinkage curves for the mixtures containing granite coarse aggregate and slag cement through the first 30 days of drying. At 30 days, shrinkage ranges from 190 $\mu\epsilon$ for the 60% volume replacement mixture cured for 14 days, to 303 $\mu\epsilon$ for the 30% slag cement mixture cured for 7 days. Unlike the comparisons for mixtures containing limestone and slag described in Set 5, when only cured for 7 days, the addition of slag (at either level of

Table 4.90 – Summary of Free-Shrinkage Data for Program VI Set 8 (in microstrain)

Days of Drying	Control (0% Slag Cement)		30% G100 Slag Cement #3		60% G100 Slag Cement #3	
	7-Day Cure	14-Day Cure	7-Day Cure	14-Day Cure	7-Day Cure	14-Day Cure
0	-63	-57	-60	-67	-113	-107
30	277	260	303	230	287	190
90	347	323	333	303	317	263
180	383	380	353	330	347	313
365	430	420	403	377	383	347

replacement) to granite mixtures results in increased shrinkage at 30 days compared to the control mixture. The 30 and 60% slag mixture cured for only 7 days exhibited similar shrinkage behavior through the first 30 days ending with shrinkage values of 303 and 287 $\mu\epsilon$, respectively. When cured for 14 days, however, high-volume percentage replacements of cement with slag cement can greatly reduce shrinkage, especially at early ages when the majority of shrinkage occurs. For specimens cured for 14 days, an increase in the slag cement content from 0 to 30% reduced shrinkage 30 $\mu\epsilon$ from 260 to 230 $\mu\epsilon$ at 30 days. A further increase in the slag content from 30 to 60% results in an additional 40 $\mu\epsilon$ reduction in shrinkage. As shown in Table 4.91, these differences in shrinkage are statistically significant at $\alpha = 0.1$ and 0.05, respectively. The difference in shrinkage between the control mixture and the 60% slag cement mixture is significant at the highest level of confidence.

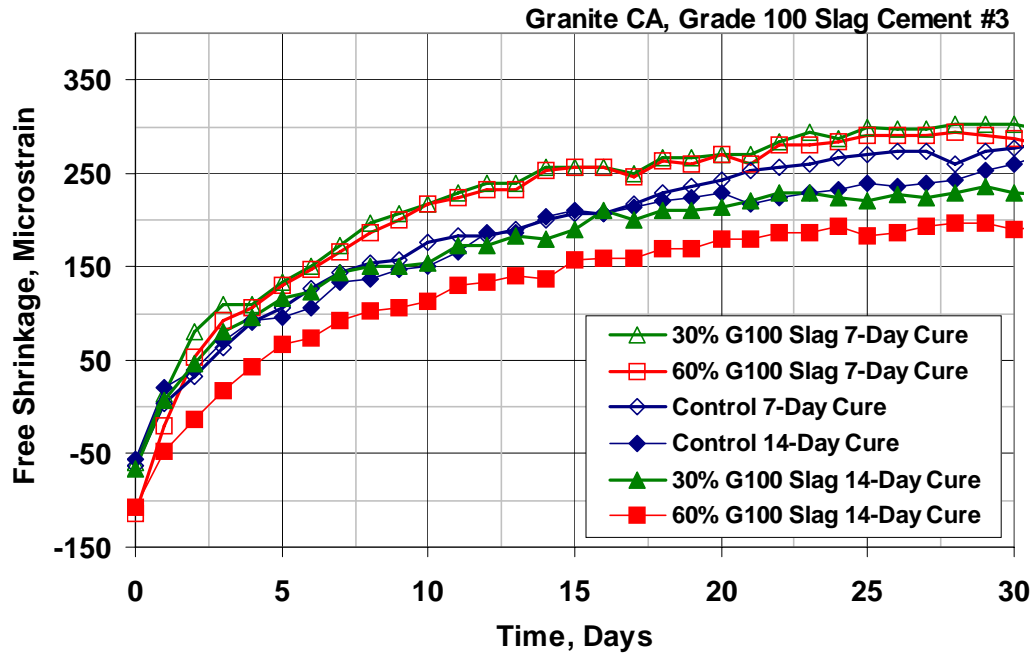


Fig. 4.55 – Free Shrinkage Test (ASTM C 157). Program VI Set 8. Average free-shrinkage versus time through 30 days (drying only).

Table 4.91 – Student’s t-test Results for Program VI Set 8 30-Day Free-Shrinkage Data

		30-Day Free Shrinkage (µε)	Control (0% Slag)		30% G100 Slag #3		60% G100 Slag #3	
			7-Day	14-Day	7-Day	14-Day	7-Day	14-Day
0%	7-Day	277		N	Y	Y	N	Y
	14-Day	260			Y	90	95	Y
30%	7-Day	303				Y	90	Y
	14-Day	230					Y	95
60%	7-Day	287						Y
	14-Day	190						

Note: See the Table 4.4 note for an explanation of the terms “N”, “80”, “90”, “95”, and “Y”.

The long-term shrinkage results are shown in Fig. 4.56. Although there is some scatter in the data, it is clear that the long-term shrinkage results are not as sensitive to the curing period as the early-age results for the concrete containing slag cement. After about 80 days of drying, the shrinkage of the control mixture cured for

7 days equals and then exceeds the shrinkage of both slag cement mixtures cured for 7 days. After 365 days, the control mixture cured for 7 days has the greatest shrinkage (430 $\mu\epsilon$) followed closely by the control mixture cured for 14 days (420 $\mu\epsilon$). This small difference is not statistically significant (Table 4.92). The 60% slag mixture cured for 14 days has the least shrinkage throughout the drying period with a free-shrinkage value of 347 $\mu\epsilon$ at 365 days. Reducing the curing period from 14 to 7 days results in a 36 $\mu\epsilon$ increase in shrinkage to 383 $\mu\epsilon$ at 365 days. This increase in shrinkage is statistically significant at $\alpha = 0.2$ (Table 4.92). A similar increase in shrinkage of 26 $\mu\epsilon$ (significant at $\alpha = 0.1$) occurs as the curing period is decreased from 14 to 7 days for the mixture containing a 30% replacement of cement with slag.

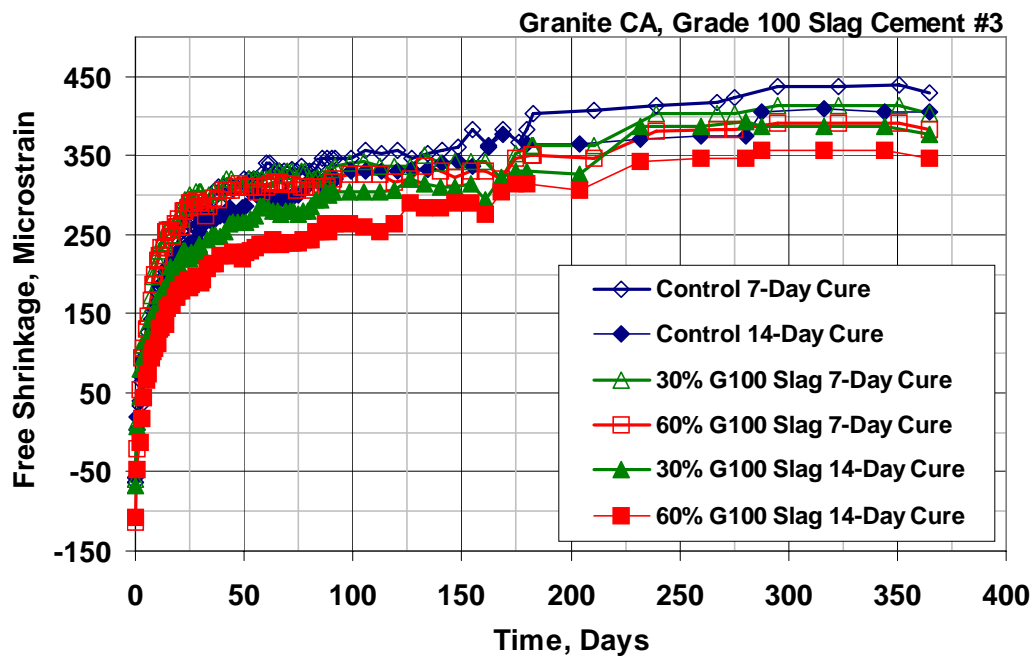


Fig. 4.56 – Free Shrinkage Test (ASTM C 157). Program VI Set 8. Average free-shrinkage versus time through 365 days (drying only).

Table 4.92 – Student’s t-test Results for Program VI Set 8 365-Day Free-Shrinkage Data

		365-Day Free Shrinkage ($\mu\epsilon$)	Control (0% Slag)		30% G100 Slag #3		60% G100 Slag #3	
			7-Day	14-Day	7-Day	14-Day	7-Day	14-Day
0%	7-Day	430		N	Y	Y	95	Y
	14-Day	420			N	90	80	95
30%	7-Day	403				90	80	Y
	14-Day	377					N	80
60%	7-Day	383						80
	14-Day	347						

Note: See the Table 4.4 note for an explanation of the terms “N”, “80”, “90”, “95”, and “Y”.

4.9.9 Program VI Set 9 (Oven-Dry versus Saturated-Surface Dry Aggregate and Grade 100 Slag)

Program VI Sets 1 through 8 and Set 10 mixtures compare the free-shrinkage behavior of mixtures in which the coarse aggregate moisture content at the time of batching is saturated-surface-dry (SSD). The effect of internal curing is evaluated in this set by comparing mixtures containing limestone that is either in an SSD or oven-dry (OD) condition. For the mixtures cast with oven-dry coarse aggregate, the total water content was adjusted to account for the absorption of the aggregate. Mixtures containing 0 or 30% volume replacements of cement with Grade 100 slag cement in conjunction with curing periods of 7 and 14 days are included in the evaluation. The slag cement sample used in this set is from Holcim in Theodore, AL and is identified as sample number 5 in Table 2.2. A summary of Program 9 is presented in Table 4.93. Individual mixture proportions, plastic concrete properties, and compressive strengths are given in Table A.19 in Appendix A. Individual specimen free-shrinkage curves are presented in Figs. C.48 through C.51 in Appendix C.

The average free-shrinkage data for the Program VI Set 9 specimens after 0, 30, 90, 180, and 365 days of drying is shown in Table 4.94. Expansion values ranged

Table 4.93 – Program VI Set 9 Summary

Slag Cement Content [†]	Slag Cement Sample No.	Aggregate Condition*
G100 60%	5	Oven Dry
G100 60%	5	SSD
control (0%)	--	SSD
control (0%)	--	Oven Dry

[†]The slag cement contents are reported by volume of cementitious materials.

*Set 9 compares free shrinkage of specimens cast with coarse aggregate in the saturated-surface-dry (SSD) condition and specimens cast with oven-dried aggregate.

from 15 to 97 $\mu\epsilon$ at the conclusion of the curing period. The results indicate that for mixtures containing 60% Grade 100 slag, the use of oven-dry limestone leads to slightly increased shrinkage compared to mixtures cast with SSD limestone. A similar behavior occurs for the control batches when the difference in initial expansion is considered in the evaluation.

Table 4.94 – Summary of Program VI Set 9 Free-Shrinkage Data (in microstrain)

Days of Drying	Control (0% Slag Cement)				60% Grade 100 Slag Cement Sample No. 5			
	SSD Coarse Aggregate		Oven-Dry Coarse Aggregate		SSD Coarse Aggregate		Oven-Dry Coarse Aggregate	
	7-Day	14-Day	7-Day	14-Day	7-Day	14-Day	7-Day	14-Day
0	-15	-20	-87	-97	-47	-80	-47	-80
30	335	277	300	237	157	95	213	117
90	490	423	390	317	337	285	377	330
180	500	430	463	367	377	330	423	363
365	500	447	497	397	390	355	447	387

The effect of internal curing on shrinkage is shown in Figs. 4.57 and 4.58, where control mixes, cured for 7 and 14 days, are compared with mixtures cast with limestone that was either in an SSD or oven-dry condition at the time of casting. The Student's t-test results are presented in Tables 4.95 and 4.96. As shown in Fig. 4.57, through 30 days, the mixtures cast with SSD limestone containing 60% Grade 100 slag cement exhibit less shrinkage than the corresponding mixtures cast with oven-

dried limestone. At this point, the difference is 56 $\mu\epsilon$ for the mixtures cured for 7 days and 22 $\mu\epsilon$ for the mixtures cured for 14 days. These differences in shrinkage are statistically significant at a confidence levels of $\alpha = 0.02$ and 0.20, respectively (Table 4.95). Presumably the oven-dry limestone absorbed some water during the mixing process, allowing a portion of that water to be available for internal curing once the concrete hardened. All of the water added to bring the oven-dry aggregate to an SSD condition, however, was probably not absorbed, resulting in an increased paste content and w/cm , as well as less water available for internal curing compared to the mixtures cast with SSD aggregate. These factors translated into slightly increased shrinkage. Longer curing results in lower shrinkage in all cases, and as expected based on previous sets, the control mixtures (0% slag cement) exhibited greater shrinkage than the corresponding mixtures containing 60% slag cement.

The control mixtures (0% slag cement) exhibited somewhat similar behavior through the first 30 days. In this case, however, the mixtures containing oven-dry limestone had slightly lower shrinkage than the corresponding mixtures containing SSD limestone. At 30 days, the differences in shrinkage were 35 $\mu\epsilon$ for the mixtures cured for 7 days, and 40 $\mu\epsilon$ for the specimens cured for 14 days. These differences should be tempered by the fact that the control mixtures containing SSD limestone had relatively very little initial expansion. Immediately following the curing period, the differences in expansion were 72 and 77 $\mu\epsilon$ for the specimens cured for 7 and 14 days, respectively. This large difference in expansion makes up for the differences in behavior observed between the control mixtures and the 60% slag mixtures throughout the drying period. Some scatter exists in the data for the control mixture containing oven-dry limestone, although in general, the same shrinkage behavior that is observed after 30 days of drying is observed at the conclusion of the test.

After 365 days of drying, the mixtures cast with SSD limestone and 60% Grade 100 slag continue to exhibit less shrinkage than the corresponding mixtures cast with oven-dried limestone. At 365 days, the differences in shrinkage are 57 and 32 $\mu\epsilon$ for the mixtures cured for 7 and 14 days, respectively. The difference in shrinkage for the 7-day specimens is statistically significant at $\alpha = 0.02$, but the difference observed between the specimens cured for 14 day is not significant (Table 4.56). The control mixtures cured exhibited a somewhat different behavior at 365 days, although as noted previously, these differences are primarily due to the large initial expansions observed for the control specimens containing oven-dried limestone. The control mixtures cured for 7 days exhibited the same shrinkage, but for the mixtures cured for 14 days, the difference is 50 $\mu\epsilon$ (statistically significant at $\alpha = 0.2$). In general, the control mixtures exhibited less shrinkage than the corresponding mixtures containing 60% slag cement (with the exception of the mixture containing oven-dried limestone cured for 14 days), and longer curing results in lower shrinkage.

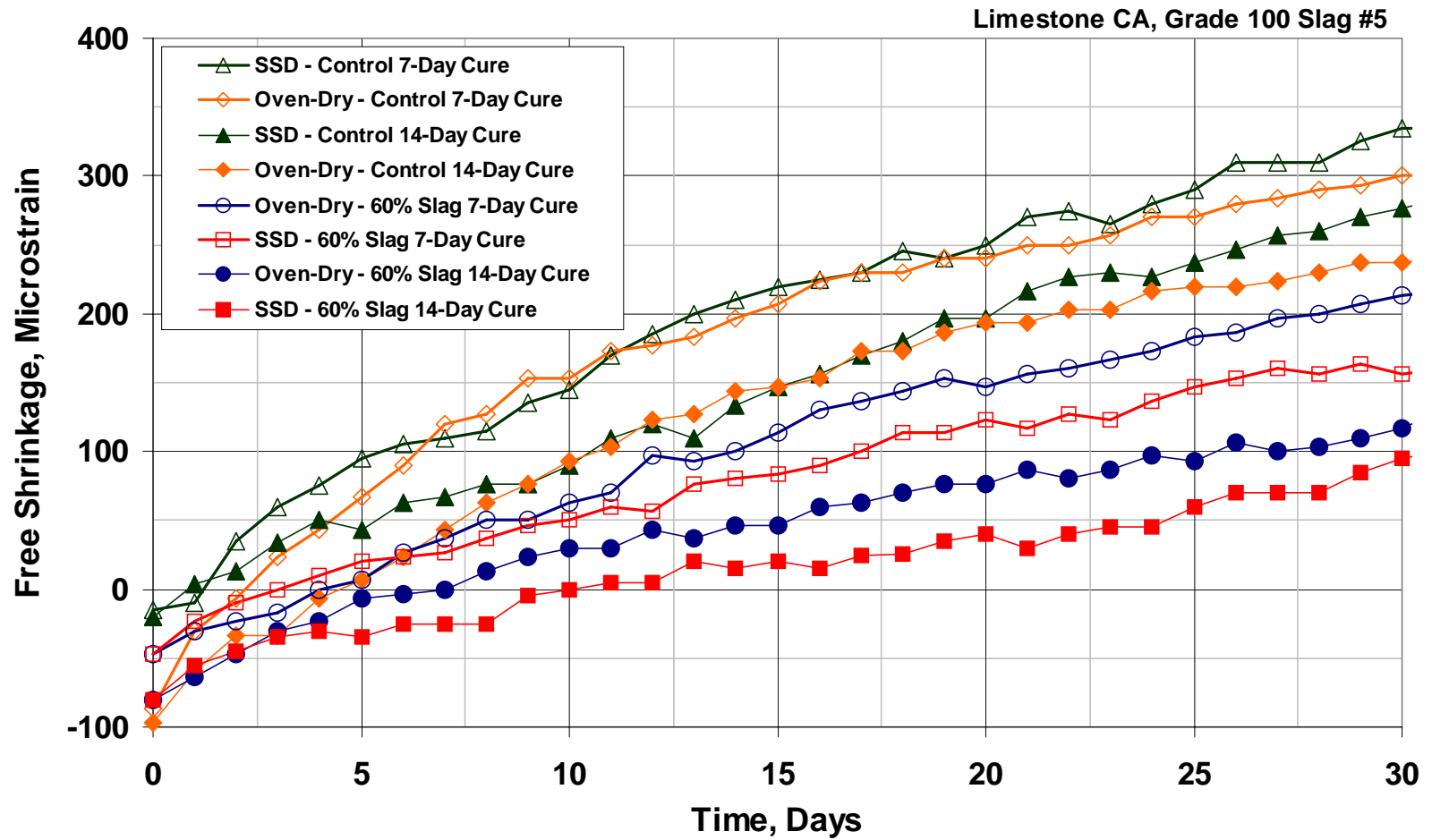


Fig. 4.57 – Free Shrinkage Test (ASTM C 157). Program VI Set 9. Average free-shrinkage versus time through 30 days (drying only).

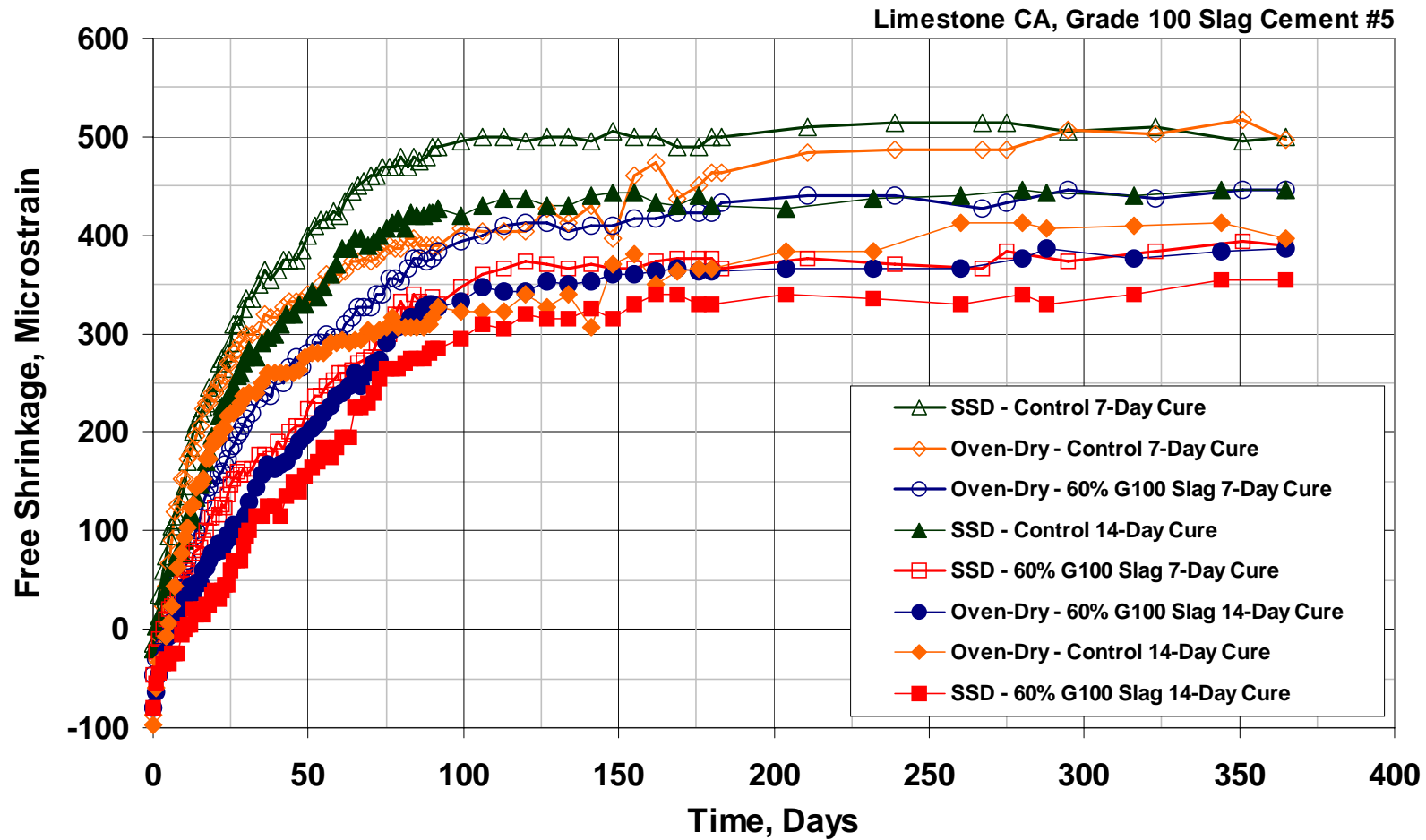


Fig. 4.58 – Free Shrinkage Test (ASTM C 157). Program VI Set 9. Average free-shrinkage versus time through 365 days (drying only).

Table 4.95 – Student’s t-test Results for Program VI Set 9 30-Day Free-Shrinkage Data

		30-Day Free Shrinkage ($\mu\epsilon$)	Control (0% Slag Cement)				60% G100 Slag Cement Control			
			SSD Aggregate		OD Aggregate		SSD Aggregate		OD Aggregate	
			7-Day	14-Day	7-Day	14-Day	7-Day	14-Day	7-Day	14-Day
0% Slag SSD	7-Day	335		80	N	95	Y	Y	Y	Y
	14-Day	277			N	80	Y	Y	95	Y
0% Slag OD	7-Day	300				Y	Y	Y	Y	Y
	14-Day	237					Y	Y	80	Y
60% Slag SSD	7-Day	157						Y	Y	95
	14-Day	95							Y	80
60% Slag OD	7-Day	213								Y
	14-Day	117								

Table 4.96 – Student’s t-test Results for Program VI Set 9 365-Day Free-Shrinkage Data

		365-Day Free Shrinkage ($\mu\epsilon$)	Control (0% Slag Cement)				60% G100 Slag Cement			
			SSD Aggregate		OD Aggregate		SSD Aggregate		OD Aggregate	
			7-Day	14-Day	7-Day	14-Day	7-Day	14-Day	7-Day	14-Day
0% Slag SSD	7-Day	500		N	N	90	95	N	80	90
	14-Day	447			80	80	90	95	N	90
0% Slag OD	7-Day	497				Y	Y	Y	Y	Y
	14-Day	397					N	N	90	N
60% Slag SSD	7-Day	390						90	Y	N
	14-Day	355							Y	N
60% Slag OD	7-Day	447								95
	14-Day	387								

Note: See the Table 4.4 note for an explanation of the terms “N”, “80”, “90”, “95”, and “Y”.

4.9.10 Program VI Set 10 (Ternary Mixtures)

Program VI Set 10 compares the free-shrinkage of mixtures containing silica fume and G120 slag cement at reduced paste contents. This set includes a total of five batches, each with a w/cm ratio of 0.42 and a paste content of either 21.6% [equivalent to 295 kg/m³ (497 lb/yd³) of cement at a w/c ratio of 0.42] or 20.0% [equivalent to 272 kg/m³ (460 lb/yd³) of cement at a w/c ratio of 0.42]. Set 10 includes mixtures containing 0 or 6% volume replacements of cement with densified silica fume and 0, 60, or 80% volume replacements of cement with Grade 120 slag cement, all with limestone coarse aggregate and cured for 14 days. The Grade 120 slag cement was from Lafarge North America in Chicago, IL, and the densified silica fume was obtained from Euclid Chemical Company. Both the silica fume and slag are identified as sample number two. A summary of Program VI Set 10 is presented in Table 4.97, and additional details are provided in Section 2.9.6.5. Individual mixture designs, plastic concrete properties, and compressive strengths are provided in Table A.7 and A.20 in Appendix A. Individual specimen free-shrinkage curves are shown in Figs. C.52 and C.53 in Appendix C.

Table 4.97 – Program VI Set 10 Summary

Paste Content	w/cm Ratio	Silica Fume Content[†]	G120 Slag Cement Content
21.6	0.42	0%	0%
21.6	0.42	0%	60%
21.6	0.42	6%	60%
20.0	0.42	6%	60%
20.0	0.42	6%	80%

[†]The dry densified silica fume content in Program VI Set 10 (Sample 2) is reported by volume of cementitious materials.

[‡]The slag cement in Program VI Set 10 is Grade 120 (Sample 2) and is reported by volume of cementitious materials.

The average free-shrinkage data for Program VI Set 10 specimens cured for 14 days after 0, 30, 90, 180, and 365 days of drying are summarized in Table 4.98. The five mixtures listed in Table 4.98 are identified by their equivalent cement content (497 or 460 lb/yd³) and by the volume replacements of cement with Grade 120 slag or silica fume or both. The control mixture contains 100% Type I/II portland cement. The results of Set 10 confirm previous observations regarding the effect of paste content, slag cement, and silica fume on free shrinkage. Shrinkage is reduced as the paste content is reduced from 21.6 to 20.0%, and additions of slag cement and silica fume (or both) reduce shrinkage. For this program, however, the shrinkage behavior is more closely related to the paste content than to the mineral admixture content. It should be noted that it was necessary to have at least 60% slag cement and 6% silica fume at these lower paste content in order to maintain adequate finishability and cohesiveness.

Table 4.98 – Summary of Program VI Set 10 Free-Shrinkage Data (in microstrain)

Days of Drying	497 Control	497 60% G120 Slag	497 60% G120 Slag, 6% SF	460 60% G120 Slag, 6% SF	460 80% G120 Slag, 6% SF
0	-10	-53	-50	-70	-27
30	290	123	140	90	93
90	383	297	303	237	250
180	407	370	360	280	323
365	420	397	397	313	353

Average free-shrinkage curves for each of the concrete mixtures through the first 30 days are presented in Fig. 4.59. At 30 days, the control mix had a free-shrinkage of 290 $\mu\epsilon$ (150 $\mu\epsilon$ more than the next closest mixture). The remaining mixtures exhibited similar shrinkage behavior, although at 30 days, there is a slight indication that the results for mixtures containing the mineral admixtures are beginning to separate based on paste content. This trend becomes clearer for periods

greater than about 40 days. The shrinkage values of the 21.6% paste (497) mixtures at 30 days were 123 and 140 $\mu\epsilon$ for the 60% slag cement mixture and the ternary mixture, respectively. The 20.0% paste mixtures (460) exhibited the least shrinkage, with values of only 90 and 93 $\mu\epsilon$ after 30 days. With the exception of this small difference, all of the other differences in shrinkage for these five batches are statistically significant at least at $\alpha = 0.2$ (Table 4.99).

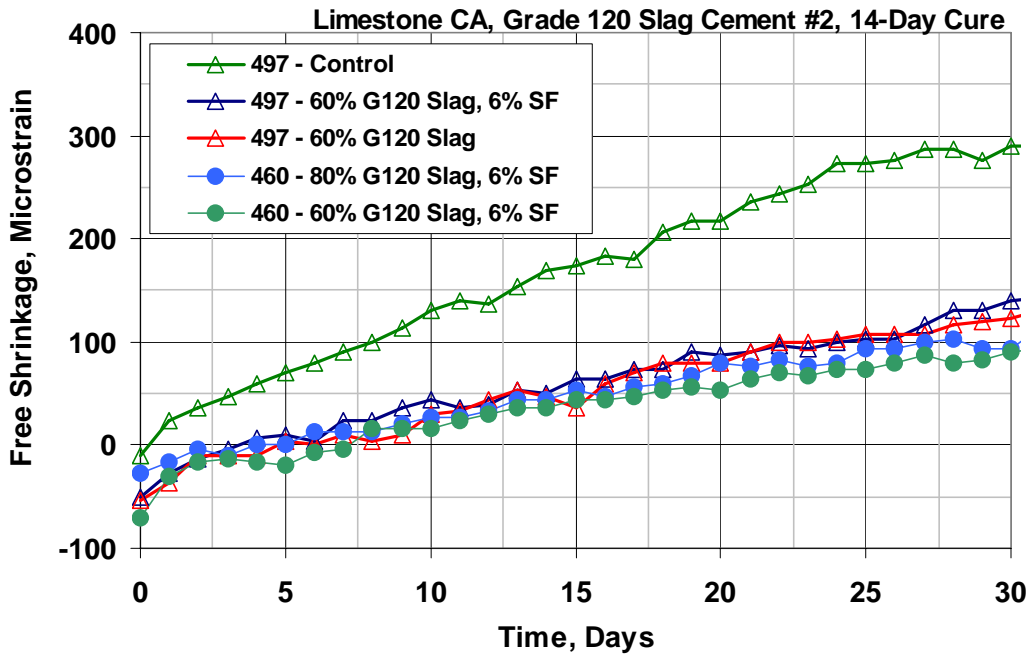


Fig. 4.59 – Free Shrinkage Test (ASTM C 157). Program VI Set 10. Average free-shrinkage versus time through 30 days (drying only).

The average free-shrinkage curves after one year of drying are shown in Fig. 4.60. The 460 ternary mixture containing 60% slag cement and 6% silica fume exhibited the lowest long-term shrinkage (313 $\mu\epsilon$ at 365 days). Increasing the slag content to 80% while maintaining a paste content of 20.0% and a silica fume content of 6% resulted in an increase in shrinkage of 40 $\mu\epsilon$ for periods greater than about 175 days. This observation is contrary to the behavior observed in Set 5, where increasing the slag content from 60 to 80% resulted in an additional reduction in shrinkage. At 365 days, the control mixture had the greatest free shrinkage of 420 $\mu\epsilon$ (only 23 $\mu\epsilon$

Table 4.99 – Student’s t-test Results for Program VI Set 10 30-Day Free-Shrinkage Data

	30-Day Free Shrinkage ($\mu\epsilon$)	497 Control	497 60% G120 Slag	497 60% G120 Slag, 6% SF	460 60% G120 Slag, 6% SF	460 80% G120 Slag, 6% SF
497 – Control	290		Y	Y	Y	Y
497 – 60% G120 Slag	123			80	Y	95
497 – 60% G120 Slag, 6% SF	140				Y	Y
460 – 60% G120 Slag, 6% SF	90					N
460 – 80% G120 Slag, 6% SF	93					

Note: See the Table 4.4 note for an explanation of the terms “N”, “80”, “90”, “95”, and “Y”.

greater than the other mixtures containing 21.6% cement paste, compared to the 150 $\mu\epsilon$ difference observed at 30 days). The 21.6% paste (497) mixtures containing mineral admixtures exhibited similar shrinkage throughout the entire drying period, and at the conclusion of the test, both mixtures had shrinkage values of 397 $\mu\epsilon$ at 365 days. The Student’s t-test results for the 365-day free-shrinkage data are presented in Table 4.100, where it can be seen that the difference in shrinkage between the control mixture and the 21.6% paste mixture containing 60% slag cement is statistically significant at $\alpha = 0.2$. The remaining differences between the five mixtures are significant at $\alpha = 0.05$ or 0.02.

4.9.11 Program VI Summary

Silica fume, Class F fly ash, and Grade 100 and Grade 120 slag cement at two levels of replacement were evaluated in Program VI with limestone (2.5 to 3.0% absorption), granite, and quartzite coarse aggregates (both with absorptions less than 0.6%). A total of ten sets examining two samples of silica fume, two samples of Grade 120 slag, three sources of Grade 100 slag, and three samples of Class F fly ash were used in conjunction with curing periods of 7 and 14 days.

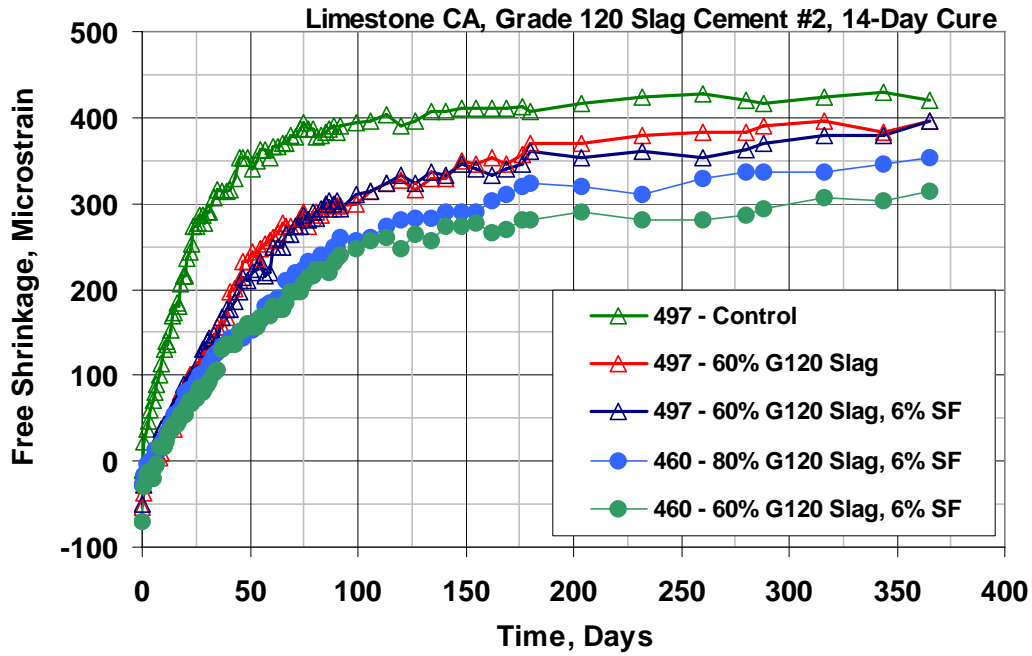


Fig. 4.60 – Free Shrinkage Test (ASTM C 157). Program VI Set 10. Average free-shrinkage versus time through 365 days (drying only).

Table 4.100 – Student’s t-test Results for Program VI Set 10 365-Day Free-Shrinkage Data

	365-Day Free Shrinkage ($\mu\epsilon$)	497 Control	497 60% G120 Slag	497 60% G120 Slag, 6% SF	460 60% G120 Slag, 6% SF	460 80% G120 Slag, 6% SF
497 – Control	420		80	95	Y	Y
497 – 60% G120 Slag	397			N	Y	95
497 – 60% G120 Slag, 6% SF	397				Y	Y
460 – 60% G120 Slag, 6% SF	313					95
460 – 80% G120 Slag, 6% SF	353					

Note: See the Table 4.4 note for an explanation of the terms “N”, “80”, “90”, “95”, and “Y”.

The results of these comparisons indicate that when cast with a high-absorption coarse aggregate, such as limestone, increasing the silica fume content from 0 to 3% results in very little change in the shrinkage behavior for specimens

cured for 7 days. These mixtures exhibit reduced shrinkage at all ages when the curing period is increased from 7 to 14 days or when the silica fume content is doubled from 3 to 6%. For mixtures containing a low-absorption coarse aggregate, such as granite, the addition of either 3 or 6% silica fume increases early-age shrinkage if the specimens are only cured for 7 days but results in a moderate reduction in long-term shrinkage. These specimens exhibit no statistically significant change in early-age shrinkage and similar or only slightly reduced long-term shrinkage when the curing period is increased from 7 to 14 days.

The addition of Class F fly ash results in increased early-age shrinkage compared to the control mixtures for concrete cast with either a low or high-absorption coarse aggregate and cured for either 7 or 14 days. The long-term shrinkage results are somewhat inconsistent, but in no case did the addition of fly ash reduce long-term shrinkage. Interestingly, an increase in the curing period from 7 to 14 days only had a small influence on the shrinkage behavior of the mixtures containing fly ash. Work is currently underway at the University of Kansas to determine the effect of even long curing periods on the free-shrinkage behavior of concrete containing Class C and Class F fly ash.

The results for concrete containing either Grade 100 or Grade 120 slag cement are qualitatively very similar to the results obtained for the silica fume mixtures. When cast with a high-absorption coarse aggregate, increasing the slag content from 0 to 30% did not affect the shrinkage behavior when cured for 7 days. For this mixture, significant reductions in both the short-term and long-term shrinkage are obtained when the curing period is increased to 14 days. Increasing the slag content further from 30 to 60 or even 80% results in a reduction in shrinkage at all ages, regardless of the curing period length. For mixtures containing a low-absorption coarse aggregate, the addition of 30 or 60% slag increased early-age shrinkage if the specimens are cured for 7 days. These same mixtures exhibit slightly reduced long-term shrinkage, and when they are cured for 14 days, both the early-age and long-term shrinkage is reduced.

CHAPTER 5: LOW-CRACKING HIGH-PERFORMANCE CONCRETE (LC-HPC) BRIDGE DECKS

5.1 GENERAL

This chapter details the development, construction, and preliminary performance of the 14 low-cracking high-performance concrete (LC-HPC) bridge decks built or planned in Kansas. The chapter is divided into four sections covering (1) the specifications used for construction, (2) experiences with LC-HPC bridge decks, (3) the crack density results based on initial crack surveys, and (4) the cost of LC-HPC. The construction experiences and crack density evaluations presented in this chapter is primarily limited to a discussion of the LC-HPC itself. A complete discussion of the bridge design and construction experiences is presented by McLeod et al. (2009).

The performance of the LC-HPC bridge decks is evaluated, in part, based on comparisons with *control* decks that are similar to the bridges with LC-HPC decks. Most of the control decks consist of two courses, a conventional subdeck covered with a thin overlay containing 7% silica fume, and represent a non-low-cracking high-performance deck that has been in use in Kansas for about ten years. In addition to the silica-fume overlay decks, two single-course (monolithic) control decks are included in the comparisons. To aid in the crack density and cost comparisons, detailed descriptions of the specifications used to construct both the control and LC-HPC decks are presented in Section 5.2. The experiences and lessons gained with these specifications based on the construction of 13 LC-HPC decks, presented in Section 5.3, indicate that the LC-HPC specifications can be readily implemented by concrete suppliers and bridge contractors. The initial crack surveys indicate that the LC-HPC decks exhibit significantly less cracking than the high-performance silica-fume overlay decks used in Kansas.

5.2 SPECIFICATIONS

One of the primary factors affecting the performance of both the control decks and the low-cracking high-performance concrete (LC-HPC) decks are the specifications that govern their construction. These specifications, which are the focus of this section, direct the development of mixture designs and dictate construction practices. The specifications are working documents that are changed with some regularity to address everything from unanticipated difficulties to emerging technologies. The balance of this section outlines the significant aspects and changes to the specifications used for both the control decks and the LC-HPC decks. Section 5.2.1 describes the requirements for subdecks and monolithic decks, and Section 5.2.2 describes the requirements for silica fume overlays. The applicable LC-HPC specifications are summarized in Section 5.2.3.

5.2.1 Control Bridge Subdecks and Control Monolithic Decks

The applicable concrete specifications for the control bridge subdecks and monolithic decks in this study (let between September 24, 2004 and January 17, 2007) are Special Provisions 90M(P)-156-R5, R7, R8, and R9 and 90M(P)-91-R15. These specifications cover a broad range of concrete applications with a wide range of required compressive strengths. Out of that range, two grades of concrete were specified for the bridges in this study: Grades 28 and 31 (Grade 4.0 and 4.5) [Grade 31 (4.5) was originally named Grade 30 (4.4)]. The maximum w/cm ratio for Grade 28 (4.0) concrete is 0.44, and the maximum w/cm ratio for Grade 31 (4.5) concrete is 0.40. The required design air content is $6.5 \pm 1.5\%$, and the maximum allowable slump is 75 mm (3 in.) without the use of a water reducer and 175 mm (7 in.) with the use of a water reducer.

The specifications allow the use of Types II, IP, I(PM), IS, and I(SM) portland cement. Type I portland cement is allowed for bridge subdecks but not for bridge

wearing surfaces. The minimum cement content for the 100% portland cement concrete mixes in this study is 357 kg/m^3 (602 lb/yd^3), corresponding to paste contents of 27.1% and 25.6% for the Grade 28 (4.0) and Grade 31 (4.5) concretes, respectively. Fly ash was not allowed for bridge decks constructed under 90M(P)-156-R5 but that option was added in the seventh revision (R7) of the special provisions. Class C fly ash is limited to 10% by weight of cement and Class F fly ash is limited to 25% by weight of cement. Slag cement may be substituted for as much as 35% (by weight) of the cement content, and beginning with 90M(P)-156-R8, Type IS and Type I(SM) cements may also contain a partial replacement of fly ash.

Several requirements for the coarse, fine, and combined aggregates are specified to provide a durable bridge deck. The individual gradation requirements for four different sizes of coarse aggregate, in addition to the requirements for fine aggregate, are shown in Table 5.1. The coarse aggregate, must have a minimum soundness of 0.90, a maximum degradation of 40%, and a maximum absorption of 2.0%. The coarse-aggregate soundness is determined using AASHTO T 103 Procedure C, except that the aggregate is soaked for a period of 24 ± 4 hours rather than being saturated in a vacuum. Coarse aggregate degradation is determined with the Los Angeles Abrasion Test (AASHTO T 96). Deleterious substances are limited for both the fine and coarse aggregate.

In addition to the requirements for individual aggregates, the combined aggregate must also meet specific soundness, degradation, and alkali-silica reactivity requirements. The combined gradation must have a minimum soundness of 0.90 and a maximum degradation of 50%. In addition, a wetting and drying test (KDOT KTMR-23) is also required to determine the alkali-silica reactivity of the combined gradation. The test consists of measuring concrete prisms as they are subjected to alternating cycles of wetting and drying over a period of one year. The maximum allowable expansion after 180 and 365 days is 0.050% and 0.070%, respectively. The

Table 5.1 – Fine and Coarse Aggregate Gradation Requirements for Bridge Deck Concrete

Type	Cumulative Percent Retained Square-Mesh Sieves [†]						
	25.0 mm (1")	19.0 mm (3/4")	12.5 mm (1/2")	9.5 mm (3/8")	4.75 mm (No. 4)	2.39 mm (No. 8)	600 µm (No. 30)
CA-3 Chat	0-5	-	-	-	55-75	87-97	95-100
CA-4 Siliceous Gravel or Crushed Stone	0	0	0-35	30-70	75-100	95-100	-
CA-5 Siliceous Gravel or Crushed Stone	0	0-20	-	40-70	-	95-100	-
CA-6 Siliceous Gravel, Chat, or Crushed Stone	0	0-20	-	-	-	95-100	-
	9.5 mm (3/8")	4.75 mm (No. 4)	2.39 mm (No. 8)	1.18 mm (No. 16)	600 µm (No. 30)	300 µm (No. 50)	150 µm (No. 100)
FA-A Fine Aggregate	0	0-10	0-27	15-55	40-77	70-93	90-100

[†]The maximum allowable percentage passing the 75 µm (No. 200) is 2.5% for the coarse aggregate and 2.0% for the fine aggregate.

coarse aggregate to fine aggregate ratio is specified as 50:50 by weight although adjustments to this ratio or the addition of other aggregates may be necessary to meet the soundness, degradation, and wetting and drying requirements.

Some projects have additional *project-specific specifications* that are used to either tighten the standard specifications or comply with local municipalities. Five of the control bridges (numbers 3 through 7) in this study have an additional *project-specific specification* (90M-7218) that required the coarse aggregate to meet requirements set by the Kansas City Metro Materials Board. This project specification reduced the maximum degradation determined using the Los Angeles abrasion test to 30%, down from 40%, and reduced the maximum absorption to 0.7%, down from 2.0%. These requirements necessitated the use of imported granite or quartzite rather than the locally available limestone.

The placement requirements defined in the applicable revisions of 90M(P)-156 and 90M(P)-91 are the same for all of the control bridges in this study. These specifications require fogging for all bridge deck placements immediately behind the

ting operation. The maximum estimated evaporation rate during placement is 1.0 kg/m²/hr (0.2 lb/ft²/hr); additional measures such as fogging, windbreaks, or cooling the concrete or its constituents must be used to maintain a satisfactory evaporation rate during the entire placement operation. In addition to specifying the maximum allowable evaporation rate, the time between mixing and placing the concrete is limited to between one and one-and-a-half hours depending on the ambient air temperature (shown in Table 5.2). Placement operations during cold weather must be discontinued when the descending ambient air temperature reaches 4° C (40° F) and may not resume until the ascending air temperature reaches 2° C (35° F). Alternatively, placement operations may continue if the ambient air temperature is greater than -7° C (20° F) and the concrete temperature is between 10° C (50° F) and 32° C (90° F).

Table 5.2 – Maximum Concrete Placement Time

Ambient Air Temperature, T °C (°F) [†]	Maximum Concrete Placement Time (hours)	Set Retarder
T < 24° (75°)	1.5	No
24° (75°) ≤ T < 32° (90°)	1	No
24° (75°) ≤ T < 32° (90°)	1.5	Yes
T ≥ 32° (90°)	1	No

[†]If the concrete temperature exceeds 32° C (90° F), placement must occur within 45 minutes.

Concrete consolidation is achieved using gang-mounted internal vibrators identical to those specified for the LC-HPC decks (described in Section 5.2.3), but the type of finisher (e.g., vibrating screed, single-drum roller, double-drum roller) is not specified. The final surface texture is achieved by tining 3-mm (1/8-in.) wide grooves into the fresh concrete. Initial curing for the full-depth (monolithic) bridge is achieved by applying a Type 1-D liquid membrane immediately following the tining operation – liquid membranes are not allowed for bridge subdecks. Final curing is

achieved with wet burlap and polyethylene sheeting for a period of seven days. If the ambient air temperature is expected to fall below 4° C (40° F) at any point during the seven-day curing period, the bridge surface must be covered with additional burlap, blankets, straw, or covered and heated so that the temperature of the deck surface is between 4° C (40° F) and 32° C (90° F).

5.2.2 Silica-Fume Overlays

The silica-fume overlay specifications applicable to the control bridges in this study are Special Provisions 90M(P)-158-R10 and R11. No substantive differences exist between these two special provision revisions. These provisions require a maximum *w/cm* ratio of 0.37 and Type I/II, IP, or II portland cement with a minimum cement content of 346 kg/m³ (581 lb/yd³). The minimum silica fume content is 26 kg/m³ (44 lb/yd³), equal to 7% by weight of cementitious materials. The required air content is 6.5 ± 1.5%, and the designated target slump must be between 50 and 125 mm (2 and 5 in.). The resultant mix design has an approximate paste volume of 25.9% and requires the use of a high-range water reducer.

The maximum aggregate size is 12.5 mm (½ in.), and the coarse aggregate to fine aggregate ratio is specified as 50:50 by weight. The coarse aggregate must have a minimum soundness of 0.95 and a maximum degradation of 40% using the Los Angeles Abrasion test (AASHTO T 96). There is no absorption requirement for coarse aggregate, and the fine aggregate requirements only limit deleterious substances. The fine aggregate (FA-A) gradation requirements are shown in Table 5.1, and the coarse aggregate (CA-7) requirements are provided in Table 5.3. The *project-specific specifications* (90M-7218) for control bridges numbers 3 through 7 reduce the maximum degradation determined with the Los Angeles abrasion test to 30%, down from 40%, and introduce a maximum absorption of 0.7% for the CA-7.

Table 5.3 – Gradation Requirements for Silica Fume Overlay Aggregate

Type	Cumulative Percent Retained Square-Mesh Sieves [†]						
	25.0 mm (1")	19.0 mm (3/4")	12.5 mm (1/2")	9.5 mm (3/8")	4.75 mm (No. 4)	2.39 mm (No. 8)	1.18 mm (No. 16)
CA-7 Coarse Aggregate	-	0	0-10	15-50	85-100	-	-

[†]The maximum allowable percentage passing the 75 μm (No. 200) is 2.5% for the CA-7.

The finishing and curing requirements for the silica-fume overlays have changed significantly since the first Kansas silica-fume overlays were placed in 1990 when no special precautions were taken. Under current specifications, overlay placement may commence only if the evaporation rate is below 1.0 kg/m²/hr (0.2 lb/ft²/hr). This evaporation rate must be maintained during the entire placement, or additional measures, such as fogging, windbreaks, or cooling the concrete or its constituents, must be used to create and maintain a satisfactory evaporation rate. After the concrete has been placed on the subdeck, the surface must be struck-off with an oscillating or vibrating drum-roller screed within ten minutes. The final surface texture is achieved by tining 3-mm (1/8-in.) grooves into the fresh concrete.

Fogging and the application of a precure material are required immediately following strike-off and during the tining operation. Intermittent fogging is required when the estimated evaporation rate is below 1.0 kg/m²/hr (0.2 lb/ft²/hr), and continuous fogging is required when the estimated evaporation rate exceeds that level. After the final surface texture is achieved, a Type 1-D liquid membrane must be applied followed by wet burlap and polyethylene sheeting. Fogging must continue until the wet burlap and polyethylene sheeting can be placed without damaging the surface and must be kept continuously wet and in place for a period of seven days.

The weather limitations for silica fume overlays are similar to the requirements for bridge subdecks. In cold weather, placement operations must stop when the descending air temperature falls below 7° C (45° F). Placement operations may not start or resume until the ascending air temperature reaches 5° C (40° F) and

the nighttime temperatures are expected to exceed 2° C (35° F). The hot-weather limitations for silica-fume overlays are the same as indicated for bridge subdecks and monolithic decks in Section 5.2.1.

5.2.3 Low-Cracking High-Performance Concrete (LC-HPC) Specifications

The LC-HPC specifications are divided into three individual documents covering the concrete, aggregate, and construction requirements. These specifications are based on the Kansas Department of Transportation (KDOT) specifications for bridge decks described in Section 5.2.1 with several significant changes. The LC-HPC specifications have been modified a number of times during the course of the project to improve the bridge decks based on experiences in the field, and to a lesser extent, findings in the laboratory. In addition to these modifications, some deviations from the specifications were allowed or required during construction of the decks. These deviations are discussed individually for each bridge deck in Section 5.3.

The applicable specification numbers are provided for each LC-HPC bridge deck in Table 5.4. The fourteenth bridge (denoted LC-HPC-14) is a City of Overland Park, KS project with specifications nearly identical to those listed for LC-HPC-13. The balance of this section provides a summary of the specifications. Additional recommended changes to the concrete and aggregate specifications based on lessons learned during construction are presented in Section 5.3.9.

Seven different revisions were made to the concrete specification during the course of the project, but the majority of these revisions were minor. In fact, the only major change was to reduce the cement content and w/c ratio. For the first two revisions, the cement content was limited to between 310 and 334 kg/m³ (522 and 563 lb/yd³), and the maximum specified w/c ratio was 0.45. It is important to point out, however, that the maximum cement content used by the ready-mix suppliers for the bridges constructed with this specification was 320 kg/m³ (540 lb/yd³). For subsequent revisions of the specification (beginning with 90M-7295), the allowable

Table 5.4 – LC-HPC Specifications – Special Provision Designations

LC-HPC Bridge Number	Concrete Specification	Aggregate Specification	Construction Specification
1	90M-7181	90M-7182	90M-7190
2	90M-7181	90M-7182	90M-7190
3	90M-7275	90M-7182	90M-7276
4	90M-7275	90M-7182	90M-7276
5	90M-7275	90M-7182	90M-7276
6	90M-7275	90M-7182	90M-7276
7	90M-7275	90M-7182	90M-7276
8	90M-7295	90M-7326	90M-7296
9	90M-7295	90M-7326	90M-7296
10	90M-7295	90M-7326	90M-7296
11	90M-7338	90M-7339	90M-7332
12	90P-5095	90P-5085	90M-5097
13	90M-7360	90M-7359	90M-7361
14 [†]	LCHPC-1	LCHPC-2	LCHPC-3

[†]LC-HPC-14 is a City of Overland Park, KS project.

cement content range was reduced to between 300 and 317 kg/m³ (500 and 535 lb/yd³), and the maximum *w/c* ratio was reduced to 0.42. These reductions were mandated to reduce concrete shrinkage (and cracking) through a reduction in the cement-paste volume. This reduction resulted in some difficulties pumping the concrete, and as a result, the *w/c* ratio was increased up to 0.44 or 0.45 for some of the bridges. Individual details for each bridge are provided in Section 5.3.

The specifications for slump, air content, and concrete temperature have, for the most part, remained unchanged. The designated slump is 36 to 75 mm (1½ to 3 in.) with a maximum allowable slump of 100 mm (4 in.). Slump control in the field is accomplished by withholding up to 10 L/m³ (2 gal/yd³) from the approved mixture

design or by redosing the concrete with a water reducer. On Bridge 13, however, the concrete supplier was required to add all of the water at the batch plant. The designated air content is $8.0 \pm 1.0\%$ with a minimum and maximum allowable air content of 6.5 and 9.5%, respectively. The plastic concrete temperature was initially limited to between 10° and 24° C (50° and 75° F), but the limits were changed (beginning with 90M-7295) to match the format of the slump and air content requirements. The new designated concrete temperature is 13° and 21° C (55° and 70° F) which may be up to 3° C (5° F) above or below this range with the approval of the construction engineer. This encourages the ready-mix supplier to avoid consistently supplying concrete at the limits of the allowable range.

Before the contractor is given permission to place concrete, a qualification batch of at least 5 m^3 (6 yd^3) is required to demonstrate that the concrete supplier is capable of producing concrete that meets the specified plastic concrete properties. The same ready-mix plant, equipment, and mixture design that are planned for the bridge deck should be used for the qualification batch. The qualification batch must meet the plastic concrete requirements and have adequate workability for use in the bridge deck. To ensure that adequate time is available to make any necessary changes to the mixture, the qualification batch must be successfully completed at least 35 days prior to placement of the bridge deck.

The aggregate specification for the LC-HPC decks has undergone only small revisions since the first version (90M-7182), and only consists of a few key differences with current KDOT aggregate specifications (described in Section 5.3.1). These differences are limited to combined gradation requirements and the maximum allowable coarse aggregate absorption. The requirements for soundness, degradation, limits on deleterious substances, and alkali-silica reactivity are unchanged. The maximum coarse aggregate absorption is reduced from 2.0% to 0.7% – equaling the

maximum coarse aggregate absorption required by the Kansas City Metro Materials Board.

The largest difference between the aggregate requirements for LC-HPC decks and standard KDOT decks involves the combined aggregate gradation limits and the requirement to optimize the combined gradation. For typical KDOT bridge decks, the coarse aggregate to fine aggregate ratio is specified as 50:50 by weight, the maximum sized aggregate (MSA) is 19 mm ($\frac{3}{4}$ in.), and each aggregate has individual gradation requirements (shown in Tables 5.1 and 5.3). The aggregate requirements for LC-HPC decks represent an entirely different approach. For these decks, the combined aggregate gradation must be optimized (as discussed in Chapter 3) with a MSA of 25 mm (1 in.). While special attention is given to the combined aggregate gradation, the specifications place no requirements on the individual aggregate gradations. The current combined aggregate gradation limits for LC-HPC bridge decks and corral rails are shown in Table 5.5. The combined aggregate gradation for the corral rails has a MSA of 19 mm ($\frac{3}{4}$ in.) to allow for the limited reinforcing steel cover. These limits have undergone some minor changes since the first aggregate specification (90M-7182).

Table 5.5 – Combined Aggregate Gradation Requirements for LC-HPC

Usage	Percent Retained on Individual Sieves – Square Mesh Sieves [†]									
	25.0 mm (1")	19.0 mm (3/4")	12.5 mm (1/2")	9.5 mm (3/8")	4.75 mm (No. 4)	2.39 mm (No. 8)	1.18 mm (No. 16)	600 μm (No. 30)	300 μm (No. 50)	150 μm (No. 100)
Bridge Decks	2-6	5-18	8-18	8-18	8-18	8-18	8-18	8-15	5-15	0-5
Corral Rails	0	2-6	8-20	8-20	8-20	8-20	8-20	5-15	5-15	0-6

[†]The maximum allowable percentage passing the 75 μm (No. 200) is 2.5%.

The LC-HPC construction specification covers the concrete placement, finishing, and curing requirements. The maximum estimated evaporation rate is limited to 1.0 kg/m²/hr (0.2 lb/ft²/hr), which must be monitored hourly. Adequate

fogging is encouraged for any unanticipated delays, but is not considered in the evaporation rate calculation. Additional measures, such as windbreaks, cooling of the concrete or its constituents, or alternate placement times, must be used to maintain satisfactory evaporation rates during the entire placement. The construction specifications listed in Table 5.4 require fogging for all placements; however, this requirement has been dropped for future revisions of the specifications due to an inability of contractors to properly fog the air above the concrete. In most cases, water from the fogging apparatus dripped onto the surface and was subsequently worked into the concrete surface.

Temperature limitations for concrete placements are divided into cold and hot-weather provisions. Placement operations during cold weather must be discontinued when the descending ambient air temperature reaches 4° C (40° F) and may not resume until the ascending air temperature reaches 2° C (35° F). Additionally, placement operations may not begin if there is a chance that air temperatures will be more than 25° C (14° F) below the temperature of the concrete during the first 24 hours. In hot weather when the ambient temperature is above 32° C (90° F), the forms, reinforcing steel, and any other contact surfaces must be cooled to below 32° C (90° F). In all cases, the concrete temperature must be maintained between 13° and 21° C (55° and 70° F) throughout the placement. With approval of the construction engineer, the temperature of the concrete may be up to 3° C (5° F) above or below these limits.

The first version of the construction specifications required placement with a conveyor belt or concrete bucket and restricted placement with a pump to limited circumstances. This requirement was amended for subsequent versions of the specification (beginning with 90M-7296). For these revisions, placement using a pump is acceptable if the contractor demonstrates that the approved concrete mixture can be pumped at least 15 days prior to placing the deck. As an alternative, the

contractor may demonstrate pump adequacy during the qualification slab (described below). Upcoming construction specifications will explicitly require the same type and size of pump for both the pump test and the actual bridge placement.

Concrete consolidation is achieved using gang-mounted internal vibrators identical to those used for standard bridge deck placements. The surface should be finished with a vibrating screed or a single-drum roller followed by a metal pan, burlap drag, or both. If necessary, a bullfloat or fresno trowel may be used to remove any local surface irregularities. Surface variations exceeding 3 mm ($\frac{1}{8}$ in.) in 3 m (10 ft) on the deck after it has hardened must be corrected using a surface grinder to achieve a plane surface after the curing period. The final surface texture is achieved by grooving the hardened surface. Some versions of the construction specifications required the entire surface ground regardless of surface variations although this requirement was not always enforced for properly-finished surfaces.

Curing is achieved using two layers of wet burlap covered by soaker hoses and polyethylene sheeting. The first layer of presoaked burlap must be applied within 10 minutes after strike-off, followed by a second layer within five minutes. The burlap and concrete surface must be kept continuously wet for the entire 14-day curing period. For the first two versions of the specification, the polyethylene sheeting placement was required on the evening after the day of placement. This provision was changed to require the sheeting to be placed within 12 hours of concrete placement. The upcoming construction specification will also require that the burlap to be pre-soaked for a minimum of 12 hours prior to placement on the fresh concrete. This will ensure that all of the burlap is completely saturated prior to placement on the deck.

Special precautions must be taken during the curing period when concrete is placed in cold weather. Two conditions can trigger the cold weather curing procedures. The first condition occurs if the ambient air temperature is expected to

fall below 4° C (40° F) at any point during the fourteen-day curing period, and the second condition occurs if the ambient air temperature is expected to fall more than 14° C (25° F) below the temperature of the concrete during the first 24 hours after placement. These provisions require additional measures to be taken to ensure that both the concrete and girder temperatures, as measured on the upper and lower surfaces, are maintained between 13° and 24° C (55° and 75° F). This requires the area underneath the deck to be enclosed and artificially heated during the cold weather. Following the cold weather curing, the protective measures must be removed such that the temperature of the concrete does not fall more than 14° C (25° F) in 24 hours.

At the conclusion of the 14-day curing period, the polyethylene sheeting, soaker hoses, and burlap are removed, and two coats of a curing membrane must be applied to the concrete surface within 30 minutes. The curing membrane must be protected for a period of 7 days, which allows the surface to dry slowly.

Before the contractor is given permission to place the LC-HPC bridge deck, a qualification slab must be constructed to demonstrate that both the concrete supplier and the contractor are able to adequately produce, place, finish, and cure the concrete. The qualification slab should only be completed after the qualification batch is accepted and between 15 and 45 days prior to placing the deck. The qualification slab is 10 m (33 ft) long and has a width equal to the bridge deck. The slab serves as a “dress rehearsal” for the actual placement. The same personnel, methods, ready-mix plant, concrete mixture design, and equipment that are planned for use on the deck must be used for the qualification slab. Acceptance of the qualification slab is contingent upon demonstrating that the requirements for placement, consolidation, finishing, curing, and concrete properties are satisfied. Consolidation is checked by examining four cores taken from the slab shortly after construction.

5.3 LC-HPC EXPERIENCES IN KANSAS

The project let date, bridge contractor, ready-mix supplier, and construction date are shown in Table 5.6 for the 14 low-cracking high-performance (LC-HPC) bridge decks in Kansas. These LC-HPC decks are concentrated in northeast Kansas, as shown in Fig. 5.1. The individual bridge numbers are assigned and listed in the order they were let. Twelve of these decks have been built, and the remaining two are scheduled for spring 2009. As indicated in Table 5.6, the ninth LC-HPC bridge (denoted LC-HPC-9) and the second phase of LC-HPC-12 are not complete (the deck in Phase I of LC-HPC-12 was cast on 4/4/2008). The balance of this section describes the experiences and lessons learned during construction of the qualification batches, qualification slabs, and LC-HPC bridge decks. These experiences are specifically related to LC-HPC and are presented in the order of construction, although bridges let in multiple bridge contracts are presented together. McLeod et al. (2009) presents a detailed description of the LC-HPC bridges specifically related to the construction experiences. The results of the crack surveys for the bridges surveyed to date are provided in Section 5.4.

Table 5.6 – Project let date, bridge contractor, ready-mix supplier, and construction date for the 14 Kansas LC-HPC bridge decks.

LC-HPC Bridge Number	Project Let Date	Bridge Contractor	Ready Mix Supplier	Construction Date
1	9/15/2004	Clarkson	Fordyce	11/2/2005
2	9/15/2004	Clarkson	Fordyce	9/13/2006
3	8/17/2005	Clarkson	Fordyce	11/13/2007
4	8/17/2005	Clarkson	Fordyce	10/2/2007
5	8/17/2005	Clarkson	Fordyce	11/14/2007
6	8/17/2005	Clarkson	Fordyce	11/3/2007
7	10/19/2005	Capital	CST	6/24/2006
8	7/19/2006	AM Cohron	O'Brien	10/3/2007
9	7/19/2006	United	O'Brien	--
10	7/19/2006	AM Cohron	O'Brien	5/17/2007
11	8/16/2006	King	Mid-America Redi-Mix	6/9/2007
12	11/15/2006	AM Cohron	Builder's Choice	Phase I of II 4/4/2008
13	1/17/2007	Beachner	O'Brien	4/29/2008
14	3/26/2007	Pyramid	Fordyce	5/31/08

concrete mixture designs, aggregate gradations, plastic concrete test results, and compressive strength test results are provided in Appendix D.

Table 5.7 – Construction Dates for LC-HPC-1 and 2

Item Constructed	Date Completed
Qualification Batch (Trial Batch)	6/20/05
Qualification Slab (Trial Slab) for LC-HPC-1 Attempt 1	7/29/05
Qualification Slab (Trial Slab) for LC-HPC-1 Attempt 2	9/8/05
LC-HPC-1 Placement 1	10/14/05
LC-HPC-1 Placement 2	11/2/05
Qualification Slab (Trial Slab) for LC-HPC-2	5/24/06
LC-HPC-2	9/13/06

The concrete for LC-HPC-1 and 2 was designed with a cement content of 320 kg/m³ (540 lb/yd³) and a *w/c* ratio of 0.45. The corresponding paste content for this mixture was 24.6%, well below the 27% maximum recommended by Lindquist et al. (2005). A Type A/F mid-range water reducer (lignosulfonate-based) was selected to obtain the desired workability. Three granite coarse aggregates and natural Kansas River sand were selected to meet the combined aggregate gradation specified in Section 5.2.3. The approved combined gradation (used for both the qualification batch and the LC-HPC-1 qualification slab) is shown in Fig. 5.2. Following successful completion of the qualification slab, the ready-mix supplier reordered additional aggregate to complete the project. These gradations differed from the original gradations and when they were combined using the same blend, they did not meet the specification (as shown in Fig. 5.2), although the coarseness and workability factors plotted on the modified coarseness factor chart for the approved gradation and the actual gradation are both near the center of Zone II (Fig. 5.3). Based on the aggregate specification, the combined aggregate gradation should have been re-

optimized to account for the “as-delivered” gradations. This small difference in the combined gradation, however, did not appear to affect the ability of the contractor to place or finish the concrete.

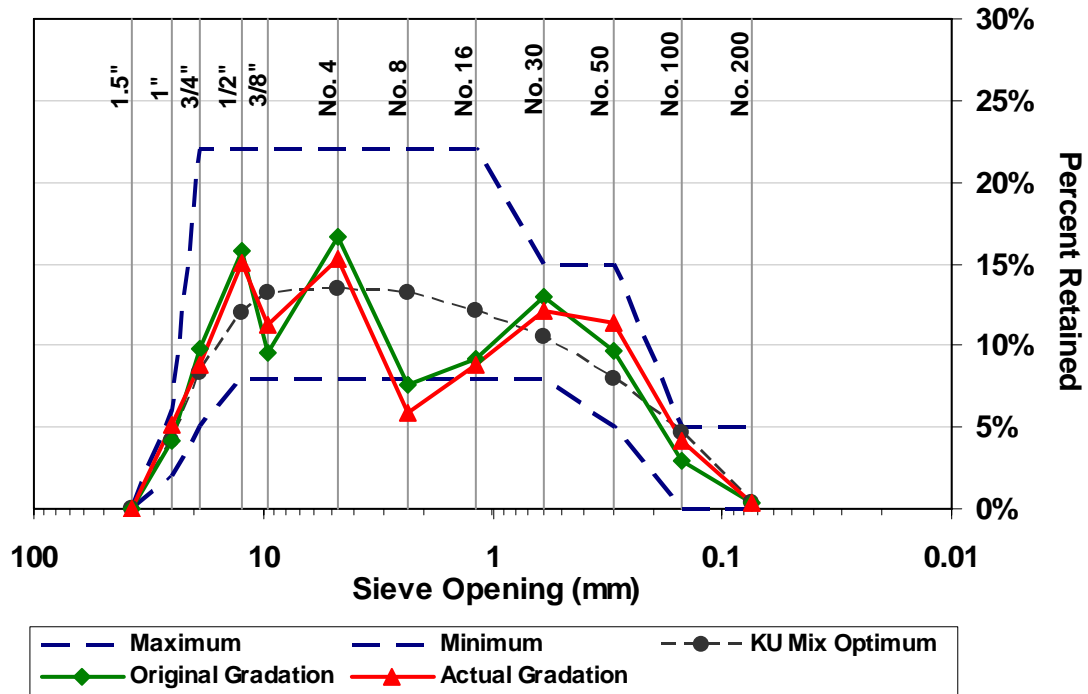


Fig. 5.2 – Original approved design gradation used for the qualification batch and the first qualification slab and the actual gradation used for the second qualification slab and bridges LC-HPC-1 and 2.

Compared with the optimum gradation (calculated using KU Mix), both the originally approved gradation and the actual gradation appear slightly gap-graded with significant deficiencies on the 2.36-mm and 1.18-mm (No. 8 and No. 16) sieves. Despite this fact, both of the mixtures pumped easily – at one point with a slump as low as 25 mm (1 in.). The only difficulty encountered for this concrete was getting the concrete from the ready-mix truck into the pump hopper. As a result, the contractor built a dirt ramp, similar to the steel and timber ramp shown in Fig. 5.4, which made the chute angle steeper and allowed the concrete to flow easily from the ready mix truck to the pump. The balance of this section outlines the concrete-related

experiences for the qualification batch, qualification slabs, and the LC-HPC bridge decks.

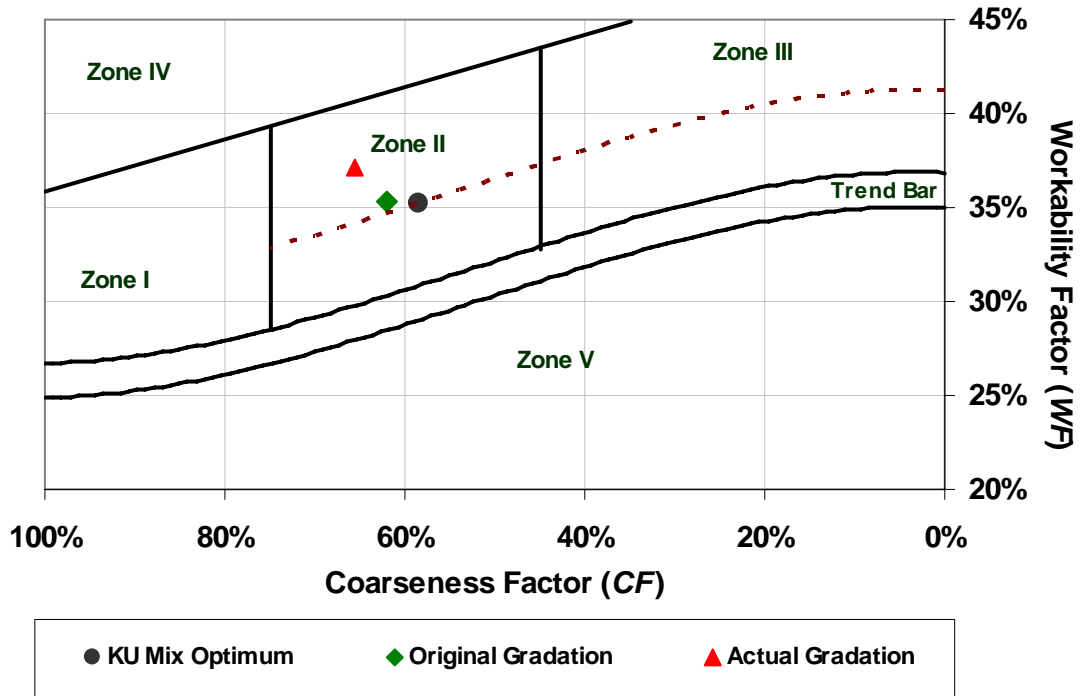


Fig. 5.3 – Modified Coarseness Factor Chart for the approved design gradation and the actual gradation used for the LC-HPC-1 and 2 placements.



Fig. 5.4 – Example of a ramp used by ready-mix trucks to increase the chute angle and facilitate unloading the relatively low-slump LC-HPC.

Qualification Batch – The qualification batch (originally called a trial batch) for LC-HPC-1 was performed on June 20, 2005 without KU personnel onsite. The plastic properties met the specifications for slump and air content [63 mm (2.5 in.) and 6.5%, respectively], but no measures were taken to control the concrete temperature. As a result, the temperature was 32° C (89° F), well above the maximum allowable temperature of 24° C (75° F). Despite the high concrete temperature, the out-of-specification concrete was accepted after a brief discussion of the temperature requirements.

Qualification Slab for LC-HPC-1 – The first qualification slab was attempted in late July when daytime temperatures regularly exceeded 32° C (90° F). Chilled water was used to control the concrete temperature, but the supplier was unable to lower the temperature below 26° C (78° F), and the placement was canceled after the rejection of two ready-mix trucks. This experience came at a considerable cost to the contractor and reinforced the importance of successfully completing all of requirements for the qualification batch prior to placing the qualification slab. It is reasonable to assume that concrete temperatures would not have been an issue had the supplier been required to address this issue at the qualification batch.

The qualification slab was completed successfully on the second attempt in early September when chilled water was sufficient to control concrete temperatures. A telescopic belt conveyor was used to place the concrete due to the low paste content of the LC-HPC mixture and, more importantly, the lack of previous experience with the mixture. Concrete was tested from the truck prior to placement by the conveyor. The four ready-mix trucks required to complete the placement had an average air content of 8.3% and a slump of 95 mm (3.75 in.). The concrete temperatures ranged from 19.4° C (67° F) to 21.7° C (71° F). The burlap placement rate was slow although in general, the placement went smoothly.

The specifications require concrete placement using a conveyor or bucket unless the contractor demonstrates prior to the deck construction that the mixture is pumpable. After working with the LC-HPC during the qualification slab, the contractor successfully test pumped 0.75 m³ (1.0 yd³) of LC-HPC on September 30, 2005. While this small demonstration worked for these two bridge decks, it does not ensure that any pump would capably handle the volume of concrete required for an entire placement. Three factors should be simulated during the test: First, the pump should be positioned and tested with the steepest boom angle expected on the bridge deck. Second, the concrete should be tested before and after the pump to establish the amount of air loss expected through the pump, and finally, the same pump and discharge hose fixtures that are tested should be used on the bridge deck. It is unclear and unlikely that these factors were considered during this test.

LC-HPC-1 – The first bridge (LC-HPC-1) consisted of two full-length partial-width placements due to the considerable width of the deck. The placements occurred in mid-October and early November and did not require chilled water or ice to control concrete temperatures. For both placements, concrete testing was performed at the point of deposit on the bridge deck after placement through the pump. Air loss was minimized using a bladder valve (Fig. 5.5) for the first placement, although the amount of air lost through the pump was not established during the placement of LC-HPC-1 or 2.

The LC-HPC pumped and finished well throughout the two placements. For the first placement, not all of the burlap was not initially saturated, and the placement rate was slow at times, mostly due to delays in the finishing operation. Some of the delays early in the placement resulted from difficulties in finishing the surface with a metal-pan finisher attached to the back of the single-drum roller screed. At times, the pan tore the surface requiring the use of a bullfloat to correct the surface irregularities. The pan was removed and the surface was finished exclusively with



Fig. 5.5 – Bladder valve used to restrict and stop concrete flow through the concrete pump. The bladder valve works by compressing the discharge hose to restrict flow of the concrete.

the single-drum roller screed and bullfloat. Burlap placement was generally within approximately 3 m (9.8 ft) of the finishing operation.

A summary of the plastic concrete properties for both LC-HPC-1 placements are shown in Table 5.8. For the first placement, the air content varied from 6.0% to 11.5% with an average of 7.9%, and concrete slump values ranged from 65 to 165 mm (2.5 to 6.5 in.) with an average of 95 mm (3.75 in.). For the second placement, slump values ranged from 65 to 110 mm (2.5 to 4.25 in.) with an average of 85 mm (3.25 in.), and air contents ranged from a low of 3.0 to a high of 9.0% with an average of 7.8%. No measures were taken to control concrete temperatures, which ranged from 16.0° to 22.0° C (61° to 72° F) for the first placement and from 19.0° to 21.0° C (66° to 70° F) for the second placement. Following the second placement, the bridge superintendent opined that he preferred working with optimized concrete with a cement content of 320 kg/m³ (540 lb/yd³) compared to the traditional mixture with a cement content of 357 kg/m³ (602 lb/yd³).

Table 5.8 – Summary of Plastic Concrete Properties for LC-HPC-1

Bridge			Plastic Property			
			Temperature, °C (°F)	Air Content, %	Slump, mm (in.)	Unit Weight, kg/m ³ (lb/ft ³)
105-304	LC-HPC-1	Average	19.8° (68°)	7.9	95 (3.75)	2251 (140.5)
	First (South) Placement	Minimum	16.0° (61°)	6.0	65 (2.5)	2188 (136.6)
		Maximum	22.0° (72°)	11.5	165 (6.5)	2276 (142.1)
105-304	LC-HPC-1	Average	20.1° (68°)	7.8	85 (3.25)	2238 (139.7)
	Second (North) Placement	Minimum	19.0° (66°)	3.0	65 (2.5)	2193 (136.9)
		Maximum	21.0° (70°)	9.0	110 (4.25)	2354 (146.9)

Qualification Slab for LC-HPC-2 – The qualification slab for LC-HPC-2 was placed on May 24, 2006 again using a pump. The concrete placement and finishing went smoothly, and the burlap placement was within 10 minutes after the deck was struck off and within 3 m (9.8 ft) of the roller screed. Concrete temperature was controlled using chilled water and ice which limited the concrete temperatures to between 19° C (66° F) and 22° C (72° F). The water content for the first ready-mix truck was not adjusted to account for the ice and was subsequently rejected. The three remaining trucks met the specifications for air content, but the slump ranged from 100 to 140 mm (4 to 5.5 in.) with an average of 115 mm (4.5 in.) measured after the pump. The pump used for this placement was not fitted with a bladder valve (shown in Fig. 5.5) or any other means of limiting air loss, but for this placement, no difficulties were encountered maintaining adequate and stable air contents.

LC-HPC-2 – The second bridge constructed (LC-HPC-2) and final bridge in this contract was completed on September 13, 2006. A summary of the plastic concrete properties for LC-HPC-2 is shown in Table 5.9. Air loss for this placement was limited with a bladder valve attached to the discharge hose (Fig. 5.5). Chilled water and a 17% replacement of mix water with bagged ice [24 kg/m³ (40 lb/yd³)] was used to control concrete temperatures, which ranged from 16.1° C (61° F) to 20.6° C (69° F). Slump values ranged from 35 to 100 mm (3 to 4 in.) with and

average of 75 mm (3 in.), and air contents ranged from 7.0 to 8.5% with an average of 7.7%. Placement and finishing operations went well throughout the placement with only minor adjustments required for the burlap positioning. This experience clearly highlighted the importance of experience for the contractor. The placement and finishing operations improved with each successive placement.

Table 5.9 – Summary of Plastic Concrete Properties for LC-HPC- 2

Bridge			Plastic Property			
			Temperature, °C (°F)	Air Content, %	Slump, mm (in.)	Unit Weight, kg/m ³ (lb/ft ³)
105-310	LC-HPC-2	Average	19.2° (67°)	7.7	75 (3.0)	--
Deck		Minimum	16.1° (61°)	7.0	35 (1.25)	--
		Maximum	20.6° (69°)	8.5	100 (4.0)	--

A significant amount of surface scaling was observed in both the north and south gutters of LC-HPC-2 approximately 7 months after construction. The scaling (ASTM C 672 Rating 2 and shown in Fig. 5.6) occurred over approximately two 0.5 m (1.6 ft) wide strips running the length of the bridge. Some aggregate was exposed, but the depth of the scaling did not exceed 2 mm (0.08 in.). A small amount of scaling next to a traffic signal base was also observed in control-1/2. It is difficult to identify the exact cause, but it is possible that runoff curing water in the gutters or excessive hand finishing may have contributed. In some cases in the Kansas City area, this type of scaling, known as “mortar flaking,” has been observed for concretes containing granite coarse aggregate. The defects are aesthetic in nature and do not represent a significant threat to long-term durability. Scaling of this magnitude has not been observed on any of the other LC-HPC decks.

Summary – The LC-HPC pumped and finished well despite not fully meeting the combined aggregate gradation specification, and the ready-mix supplier was able to consistently produce and supply LC-HPC that met the requirements for concrete

temperature, slump, and air content. Several issues were addressed prior to construction of the decks during the qualification batch and qualification slab further



Fig. 5.6 – Typical scaling observed in the gutter areas of LC-HPC-2

proving their value. The compressive strengths for the LC-HPC-1 and 2 placements are shown in Fig. 5.7.

The same mixture design was used for each placement [320 kg/m³ (540 lb/yd³) of cement with a *w/c* ratio of 0.45], but considerable variation exists between the strengths of these placements. The compressive strength of the bridge deck placements varied from 31.7 to 35.9 MPa (4600 to 5210 psi) for the lab-cured specimens and from 27.8 to 33.8 MPa (4030 to 4900 psi) for the field-cured specimens.

5.3.2 LC-HPC-7: County Road 150 over US-75

The seventh LC-HPC bridge let and the second LC-HPC bridge constructed is located north of Topeka, KS on County Road 150 over US-75. Koss Construction was awarded the project and subcontracted to Capital Construction to construct the bridge. Concrete Supply of Topeka, located 30.6 km (19.0 mi) south of the bridge, provided the concrete. The completion dates for the qualification batch, qualification

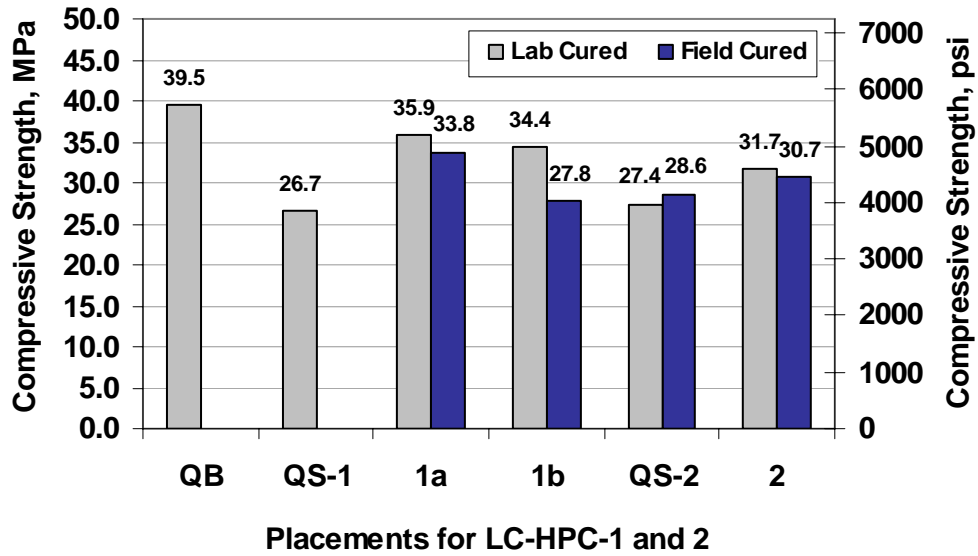


Fig. 5.7 – Compressive Strengths for the qualification batch (QB), qualification slab (QS), and LC-HPC-1 (1a and 1b) and LC-HPC-2 (2) bridge placements.

slab, and LC-HPC-7 are shown in Table 5.10, and the concrete mixture designs, aggregate gradations, plastic concrete test results, and compressive strength test results are provided in Appendix D.

Table 5.10 – Construction Dates for LC-HPC-7

Item Constructed	Date Completed
Qualification Batch (Trial Batch)	5/31/06
Qualification Slab (Trial Slab)	6/8/06
Bridge Deck	6/24/06

The concrete mixture design for this project was based on the design used for LC-HPC-1 with two notable differences. First, a water reducer was not required to obtain the desired slump [between 35 and 100 mm (1.5 and 4 in.)], and second, only three aggregates (compared to four) were required to meet the gradation limits described in Section 5.2.3. The aggregates were selected and combined using KU Mix and included two granite coarse aggregates and natural Kansas River sand. The

cement content was held constant at 320 kg/m³ (540 lb/yd³), but three different *w/c* ratios (and water contents) were used during the course of the project in order to adjust the mixture workability. The *w/c* ratios were 0.45, 0.43, and 0.41. A reduction in the *w/c* ratio was obtained by reducing the water content and replacing the water with an equal volume of aggregate. In addition to a reduction in the slump, this approach resulted in a reduction in the cement-paste volume from 24.6% to 23.3% as the *w/c* ratio was reduced from 0.45 to 0.41.

The qualification batch and qualification slab were used by the ready-mix supplier to practice techniques rather than to demonstrate proficiency. Instead of trial batching prior to qualifying the mixture on May 31, 2006, the supplier used the qualification batch to practice and qualify the mixture simultaneously. Separating the two processes requires the supplier to produce LC-HPC that meets the specifications a minimum of two times prior to construction of the qualification slab. Originally, the qualification batch and qualification slab were called the trial batch and trial slab. To help avoid ambiguity, these names were changed to qualification batch and qualification slab for future lettings as a result of this experience. The name change did not affect the intent or the purpose of these placements, but it did serve to remind the contractor and ready-mix supplier of their importance.

Qualification Batch – Three consecutive qualification batches were performed by the ready-mix supplier before the slump, air content, and temperature met the concrete specifications. The third batch had a slump of 95 mm (3.75 in.), an air content of 6.5%, and a concrete temperature of 23° C (73° F). This mixture, with a *w/c* ratio of 0.45, did not require the use of a water reducer or superplasticizer to obtain the desired slump. This raised some concern regarding the actual water content of the mixture, but further investigation into the proportions did not reveal any inconsistencies. A comparison of the compressive strengths gives some indication that the actual *w/c* ratio may be higher than 0.45 (a brief summary of the

compressive strengths obtained for this project is provided at the end of this section). Concrete temperature was controlled using a 37% replacement of mix water with bagged ice [47 kg/m^3 (80 lb/yd^3)] added manually to the ready-mix trucks.

The qualification batch met the minimum requirements set forth in the specifications and the experience was quite useful to both the ready-mix supplier and the inspectors. As mentioned previously, however, the supplier used the qualification batch both to develop and to qualify the mixture simultaneously. The intent of the specification is to qualify the batch by demonstrating the ability to produce LC-HPC based on previous trial batches. This ensures that the supplier has produced LC-HPC a minimum of two times and minimizes the chances that out-of-specification concrete will affect the contractor's ability to finish and complete the qualification slab.

Qualification Slab – The concrete delivered for the qualification slab met the plastic concrete specifications and pumped well, but the delivery was often delayed. This impeded the contractor's ability to place, cover, and finish the concrete in a timely fashion. The delays were primarily a result of two factors: First, the ready-mix supplier changed the w/c ratio from 0.45 to 0.41 and then back to 0.43 to make slump adjustments and provide flexibility if additional water was needed to increase the slump at the construction site. In addition, the supplier only had enough ice on hand to complete the slab if none of the trucks were rejected. As a result, only one truck was sent at a time after acceptance testing was performed on the previous truck. Despite these delays, both the contractor and supplier made significant progress that would have otherwise had to be accomplished on the bridge deck. The KDOT project manager agreed by saying "This proves the value of the [qualification] slab. You can see how much the contractor learned from the beginning to the end of the slab."

The practice of withholding water and using reduced w/c ratios is allowed, if not encouraged, by specifications that allow water to be withheld at the ready-mix plant [up to 10 L/m^3 (2 gal/yd^3) in this case] and set a maximum (and no minimum)

w/c ratio. In this particular case, the supplier withheld as much as 13 L/m^3 (2.6 gal/yd^3) of water resulting in a w/c ratio of 0.41. The ability to adjust the water content provides flexibility to the contractor but defeats the purpose of qualifying a specific concrete mixture. In addition, reduced w/c ratios may lead to increased cracking due to the reduced tensile creep capacity associated with higher strength concrete. The upcoming specifications do not allow any water to be withheld and specify both a minimum and maximum w/c ratio.

It should be added that no problems were encountered maintaining consistent or adequate air contents during concrete placement. An “S-Hook” attached to the end of the pump hose (shown in Fig. 5.8) confined the plastic concrete and prevented significant air loss as the concrete was pumped. A 1.0% loss in air was observed from one truck that was sampled and tested both before and after being pumped.



Fig. 5.8 – “S-Hook” fitted to the end of the pump discharge hose used to limit air loss through the pump.

LC-HPC Bridge Deck – Many of the problems that resulted in delays during the qualification slab were addressed prior to construction of the bridge deck. The w/c ratio was increased permanently to 0.45 to match the qualified batch, and the

supplier ordered plenty of ice to complete the entire deck. A summary of the plastic concrete test results from samples taken on the deck following placement is given in Table 5.11. The air contents measured varied from 6.5% to 10.5% with an average of 8.0%. Only one sample, with an air content of 10.5%, was outside of the specified range (6.5 to 9.5%), but fortunately, this concrete was placed in the west abutment and not the deck. Concrete slump values were consistently high throughout the placement. Eleven of the 23 samples had a slump greater than 75 mm (3 in.), and five of the samples exceeded the specified limit of 100 mm (4 in.). The slump varied from 55 mm (2.25 in.) to 150 mm (6 in.) with an average of 95 mm (3.75 in.). Concrete temperatures dropped throughout the deck placement from a high of 24° C (75° F) to a low of 20° C (68° F). A 37% replacement of mix water with ice [47 kg/m³ (80 lb/yd³)] was used throughout the placement to maintain satisfactory concrete temperatures.

Table 5.11 – Summary of Plastic Concrete Properties for LC-HPC-7

Bridge		Plastic Property [†]			
		Temperature, °C (°F)	Air Content, %	Slump, mm (in.)	Unit Weight, kg/m ³ (lb/ft ³)
43-33 LC-HPC-7	Average	21.9° (71°)	8.0	95 (3.75)	2221 (138.6)
Entire Deck	Minimum	20° (68°)	6.5	55 (2.25)	2148 (134.1)
	Maximum	24° (75°)	10.5	150 (6)	2292 (143.1)

[†]Test results are from samples taken directly from the bridge deck following placement by pump.

With the exception of the first four trucks, all of the test samples were taken from the deck after the concrete was placed. This method ensures that the test results accurately represent the as-placed concrete, but it does not prevent out-of-specification concrete from being placed in the deck. This problem can be addressed by visually inspecting the concrete from each truck as it is placed into the pump hopper from each ready-mix truck and holding back any trucks that do not appear to meet the specifications.

The average 28-day compressive strength for lab-cured specimens is 26.1 MPa (3790 psi) compared to an average of 35.1 and 31.7 MPa (5090 and 4600 psi) for the LC-HPC-1 and LC-HPC-2 placements, respectively. Part of this difference is due to the absence of a water reducer in the LC-HPC-7 mixture (which typically increases strength), but may also indicate that LC-HPC-7 was cast with a w/c ratio greater than 0.45.

5.3.3 LC-HPC Bridges 10 and 8: E 1800 Road and E 1350 Road over US-69

The eighth, ninth, and tenth LC-HPC bridges let are located along US-69 in Linn County, KS. Unlike the other Kansas LC-HPC bridges, which have steel girders, LC-HPC-8 and 10 have prestressed girders. These two bridges were constructed in mid to late 2007, but the last bridge (LC-HPC-9), a steel-girder bridge, is not scheduled for completion until the spring of 2009. Bridges 8 and 10 are located north of Pleasanton, KS on East 1350 Road and East 1800 Road over US-69, respectively. Koss Construction was awarded the project and subcontracted A.M. Cohron for the bridges. O'Brien Ready-Mix provided the concrete using a mobile ready-mix plant located 8.2 km (5.1 mi) from LC-HPC-8 and 16.9 km (10.5 mi) from LC-HPC-10. The dates for the qualification batch, qualification slabs, and LC-HPC bridge placements are shown in Table 5.12, and the concrete mixture designs, aggregate gradations, plastic concrete test results, and compressive strength test results are provided in Appendix D.

LC-HPC-8 and 10 were the first bridges cast with concrete under new specifications that contained a lower paste content than LC-HPC-1, 2, and 7. This concrete had a w/c ratio of 0.42, down from 0.45, and a cement content of 317 kg/m³ (535 lb/yd³), down from 320 kg/m³ (540 lb/yd³). These changes resulted in a reduction in the cement-paste volume from 24.6 (used on the first LC-HPC bridges) to 23.3%. KU Mix was used to optimize the combined gradation using a total of four

Table 5.12 – Construction Dates for LC-HPC-8 and 10

Item Constructed	Date Completed
Qualification Batch	4/11/07
Qualification Slab for LC-HPC-10	4/26/07
LC-HPC-10	5/17/07
Qualification Slab for LC-HPC-8	9/26/07
LC-HPC-8	10/3/07

aggregates: two granite coarse aggregates and two natural sands. In addition, these decks have corral railings, as opposed to jersey barriers, which require a maximum sized aggregate (MSA) of 19.0 mm (¾-in.) instead of the 25.0 mm (1-in.) MSA used for the deck. The ready-mix supplier carefully selected four aggregates for the bridge deck and used the three smallest for the corral rails. The ready-mix supplier used ice to control the concrete temperature for the bridge placements and a Type A water-reducer (lignosulfonate-based) to maintain adequate workability.

Qualification Batch – The qualification batch was completed on April 11, 2007, over one month prior to the construction of LC-HPC-10. This batch successfully met the specifications and was qualified without any adjustments or additional batches. In this case, the ready-mix supplier prepared for the qualification batch by trial batching. The slump, air content, and concrete temperature for the qualified batch were 40 mm (1.50 in.), 8.6%, and 18° C (65° F), respectively. A total of 5.0 L/m³ (1.0 gal/yd³) of water was withheld from the original mixture design to obtain the desired slump. For the remaining placements, the supplier planned to increase the water-reducer dosage and continue to withhold a portion of the mix water. The supplier planned to add a portion of the withheld water in the field and hold the water-reducer dosage constant. No measures were required to control the

temperature of the qualification batch, but the supplier anticipated the need for a partial replacement of mix water with ice for the bridge placement.

Qualification Slab for LC-HPC-10 – The concrete delivered for the LC-HPC-10 qualification slab met the plastic concrete specifications and pumped adequately. The reduced paste content mixture appeared slightly more difficult to pump than the concrete used for LC-HPC-1, 2, and 7. Delivery of the four trucks required to complete the placement was slow because the ready-mix supplier first tested each truck at the batch plant, and a new load was only batched after the previous load was accepted at the site. This practice resulted in delays of between 18 and 36 minutes between each truck that unnecessarily slowed down the contractor's ability to place concrete.

Three of the four trucks were placed smoothly. An "S-Hook" similar to the one shown in Fig. 5.8 was used to control air loss. For one of the trucks, additional water reducer was added at the site at the request of the pump operator, which increased the slump from 70 mm (2.75 in.) to 130 mm (5 in.). The average slump, air content, and concrete temperature for the as-placed concrete was 90 mm (3.50 in.), 8.7%, and 20.8° C (70° F), respectively.

LC-HPC-10 – Adequate preparation by the material supplier leading up to the deck placement played an important role in the successful delivery of LC-HPC, but construction of the deck was plagued with significant delays finishing and covering the plastic concrete. Concrete from the first truck was tested for slump and temperature at the truck discharge, but the air content was measured at the point of deposit on the bridge deck. The slump and air met the specification with values of 70 mm (2.75 in.) and 16° C (61° F), respectively, but the air content was low (5.5%). By this time, the second truck had been batched and sent to the site with the same admixture dosages, producing a measured air content of only 4.9%. Additional air entraining agent was added at the site, but the air content increased to only 5.1% and

further delayed placement. Based on the results from these two trucks, the admixture dosages were adjusted, and concrete from the third truck arrived with an air content of 11.1% and a slump of 125 mm (5.0 in.). The air content was retested at 8% and placed in the deck after approximately 20 minutes. The majority of the remaining trucks met the specifications for slump and air content.

The qualified mixture was designed with a w/c ratio of 0.42, but the specifications allow as much as 10 L/m^3 (2 gal/yd^3) to be withheld and added back as necessary. For this placement, the water content was adjusted for nearly every truck delivered to the site. This practice resulted in some differences between the design and actual w/c ratio and paste content for the bridge deck. The w/c ratio ranged from 0.40 to 0.42 with an average of 0.41, and the cement-paste volume ranged from 23.0 to 23.4% with an average of 23.2%. These changes in the w/c ratio and paste volume are shown in Fig. 5.9.

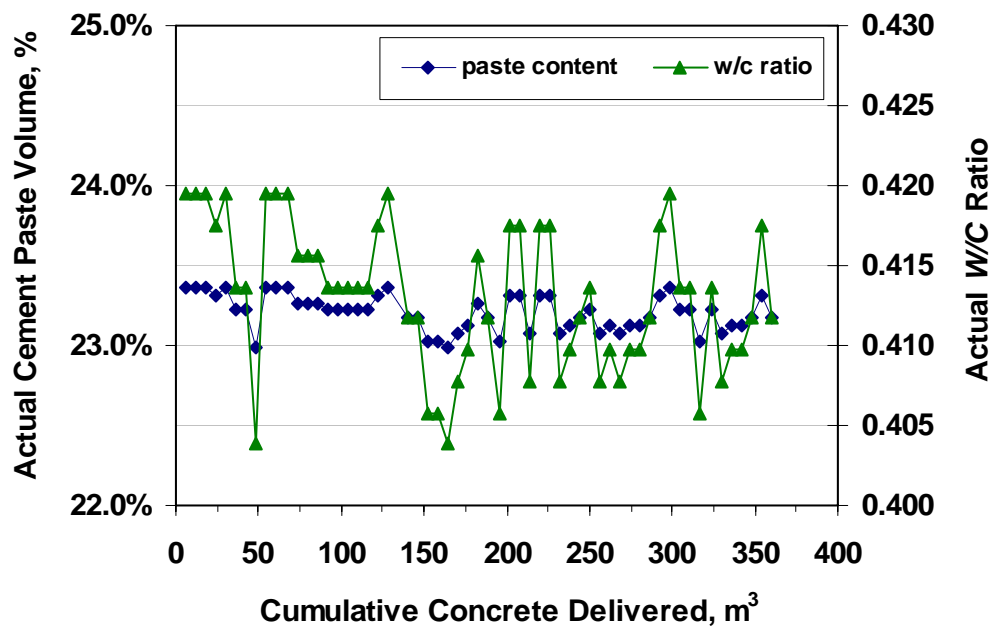


Fig. 5.9 – Cement paste volume and w/c ratio versus the cumulative volume of concrete delivered for LC-HPC-10. Each data point represents one ready-mix truck.

A summary of the plastic concrete test results from samples taken on the deck following placement is given in Table 5.13. Air contents varied from 5.1% to 9.2% with an average of 7.3%, and slumps varied from 45 mm (1.75 in.) to 125 mm (5 in.) with an average of 80 mm (3.25 in.). Three samples out of 19 had air contents lower than 6.5%, although two of these were placed in the east abutment, and only two of the 32 samples for slump exceeded the 100 mm (4 in.) maximum. Concrete temperatures increased through the placement from 15.6° C (60° F) to 22.2° C (72° F). The first four ready-mix trucks contained a 27% replacement of water with ice [36 kg/m³ (60 lb/yd³)], which was reduced to 20% [27 kg/m³ (45 lb/yd³)] for the remainder of the deck.

Table 5.13 –Summary of Plastic Concrete Properties for LC-HPC-10

Bridge			Plastic Property [†]			
			Temperature, C (F)	Air Content, %	Slump, mm (in.)	Unit Weight, kg/m ³ (lb/ft ³)
54-60	LC-HPC-10	Average	18.6° (66°)	7.3	80 (3.25)	2212 (138.1)
Deck		Minimum	15.6° (60°)	5.1	45 (1.75)	2149 (134.2)
		Maximum	22.2° (72°)	9.2	125 (5)	2276 (142.1)

[†]Test results are from samples taken directly from the point of discharge on the deck.

Qualification Slab for LC-HPC-8 – A second qualification slab was required prior to the construction of LC-HPC-8 due to the construction delays that occurred during the placement of LC-HPC-10. These delays were related to finishing and covering the deck rather than the LC-HPC, and as a result, a second qualification batch was not required. For this placement, samples were taken before and after the pump, which indicated an air loss of 1%. The average slump, air content, and temperature measured after the pump were 45 mm (1.75 in.), 7.0%, and 18.7° C (66° F), respectively.

LC-HPC-8 – By the time of this bridge placement, the ready-mix supplier had satisfactorily produced LC-HPC on four occasions and the contractor was

preparing for the fourth placement. The ready-mix supplier continued to initially withhold water from each truck and then add a portion of the water back at the jobsite to increase workability. The ready-mix supplier held out between 10 L/m^3 (2 gal/yd^3) and 2.5 L/m^3 (0.5 gal/yd^3). As a result, the w/c ratio varied between 0.39 to 0.41 with an average of 0.40, and the paste content varied between 22.6 and 23.2% with an average of 22.9%. The w/c ratios and paste contents for each ready-mix truck are plotted in Fig. 5.10. The ready-mix supplier was able to produce concrete that met the specifications, but for some of the batches, the w/c ratio was much lower than intended by the specification. For future versions of the concrete specification, none of the design water content may be withheld from the mixture.

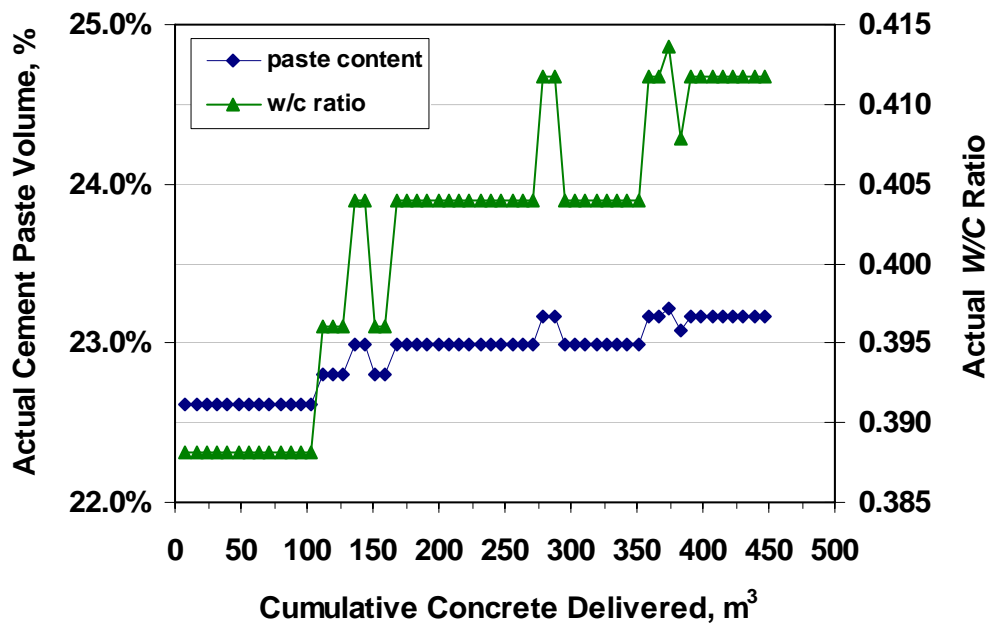


Fig. 5.10 – Cement paste volume and w/c ratio versus the cumulative volume of concrete delivered for LC-HPC-8. Each data point represents one ready-mix truck.

A summary of the plastic concrete test results from samples taken following placement through the pump is shown in Table 5.14. Air contents varied from 5.7% to 10.2% with an average of 7.9%, and slumps varied from 25 mm (1 in.) to 75 mm (3 in.) with an average of 50 mm (2 in.). The first truck was tested before and after

placement on the deck and the air loss (limited using an “S-Hook”) was 0.6%. Ice was used to control concrete temperatures, which increased throughout the placement from 15.0° C (59° F) to a high of 22.8° C (73° F). The first 16 trucks contained a 27% replacement of water with ice [36 kg/m³ (60 lb/yd³)], which was increased first to 36% [47 kg/m³ (80 lb/yd³)] and then again to 45% [59 kg/m³ (100 lb/yd³)].

Table 5.14 –Summary of Plastic Concrete Properties for LC-HPC-8

Bridge			Plastic Property [†]			
			Temperature, C (F)	Air Content, %	Slump, mm (in.)	Unit Weight, kg/m ³ (lb/ft ³)
54-53	LC-HPC-8	Average	19.5° (67°)	7.9	50 (2)	2264 (141.3)
Deck		Minimum	15.0° (59°)	5.7	25 (1)	2194 (137.0)
		Maximum	22.8° (73°)	10.2	75 (3)	2321 (144.9)

[†]Test results are from samples taken directly from the point of discharge on the deck.

Summary –The ready-mix supplier was able to provide concrete that met the specifications by first withholding water and then adding a portion of that water back. This required a significant amount of work at the jobsite and, at times, unnecessarily reduced the *w/c* ratio. The pump seized on one occasion, but for the most part, the concrete pumped adequately. Air lost through the pump was limited to between 0.6 and 1.0% using an “S-Hook”. The contractor had a difficult time finishing and covering the plastic concrete with wet burlap during the placement of LC-HPC-10, but made significantly improvement during the construction of LC-HPC-8.

The compressive strengths for these placements are shown in Fig. 5.11. Compressive strengths measured at 28 days ranged from 28.2 MPa (4090 psi) to 32.6 MPa (4730 psi) for the lab-cured specimens and from 29.9 to 31.6 MPa (4340 and 4590 psi) for the field-cured specimens.

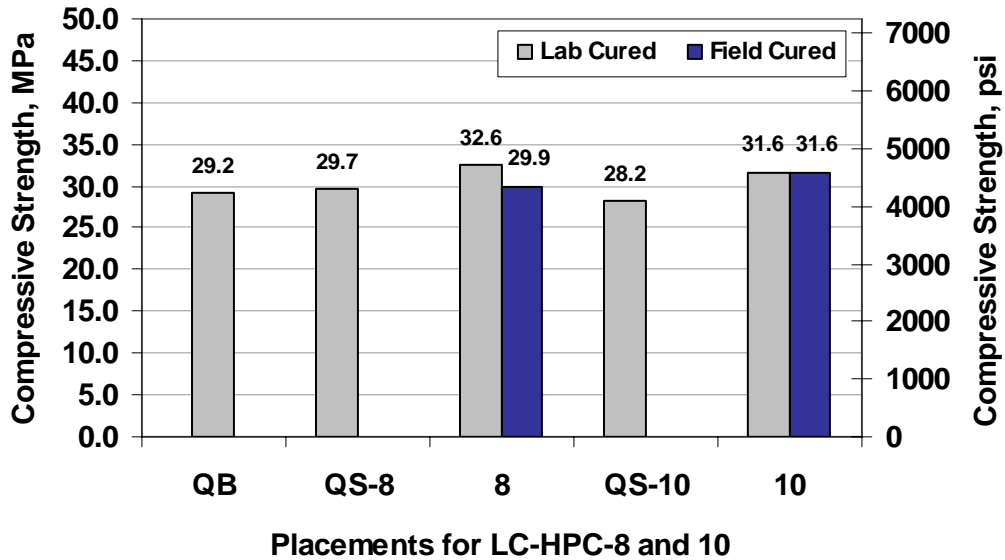


Fig. 5.11 – Compressive Strengths for the qualification batch (QB), qualification slabs (QS-8 and 10), and LC-HPC-8 (8) and LC-HPC-10 (10) bridge placements.

5.3.4 LC-HPC Bridge 11: K-96 over K&O Railway

The eleventh LC-HPC bridge let and the fifth LC-HPC bridge constructed is located in Hutchinson, KS on US-50 just east of K-96 over the K&O railroad tracks. Koss Construction was awarded the project and King Construction was subcontracted to construct the bridge. Mid-America Redi-Mix, located only 6.0 km (3.7 mi) from the bridge, provided the LC-HPC. The concrete mix design, individual aggregate gradations, combined gradation, plastic concrete test results, and compressive strength test results are provided in Appendix D. A summary of the dates for the qualification batches, qualification slab, and bridge construction are given in Table 5.15. A total of four qualification batches were required prior to the bridge placement before the contractor was allowed to proceed with the bridge deck placement.

A summary of the qualification batches, qualification slab, and bridge deck placement are provided next. For this bridge, however, it is important to first discuss the working relationships between the ready-mix supplier and Kansas Department of Transportation (KDOT) officials. Unlike any of the other LC-HPC bridges, KDOT

Table 5.15 – Construction Dates for LC-HPC-11

Item Constructed	Date Completed
Qualification Batch 1	5/22/07
Qualification Batch 2	5/23/07
Qualification Slab	5/25/07
Qualification Batch 3	6/6/07
Qualification Batch 4	6/7/07
Bridge Deck	6/9/07

representatives took ownership and control over the LC-HPC mixture design. The mixture design required four aggregates to meet the combined aggregate gradation specification and had a w/c ratio of 0.42, cement content of 317 kg/m^3 (535 lb/yd^3), and included a Type A/F mid-range water reducer (lignosulfonate-based). This arrangement worked well due to the inexperience of the ready-mix producer in working with optimized aggregate gradations.

Qualification Batch – The first qualification batch served as a trial batch to determine the proper admixture dosage rates. The slump and air content were out-of-specification, although adequate temperature control was maintained using a partial replacement of mix water with ice. For the second batch, the admixture dosages were adjusted to obtain an adequate slump and air content, but no temperature control measures were taken and the concrete temperature exceeded 24° C (75° F). The placement of the qualification slab was allowed to proceed despite the first two unsuccessful qualification batch attempts.

Qualification Slab – Several issues were encountered with the LC-HPC during the qualification slab, further reinforcing the importance of only qualifying a batch that meets all of the specification requirements. Temperature control was obtained by replacing 36% of the mix water with ice [47 kg/m^3 (80 lb/yd^3)]. Only

one out of the six trucks arrived with concrete that met the specifications for concrete temperature, slump, and air content, and despite the short haul time, the inconsistent and often out-of-specification concrete made construction of the slab disjointed. The relatively short qualification slab requires a consistent supply of concrete for the contractor to gain quality experience placing, finishing, and covering the concrete in a timely fashion. Following the qualification slab, two additional qualification batches were required to give the ready-mix supplier additional experience consistently producing LC-HPC that meets the concrete specification.

In addition to delays resulting from out-of-specification concrete, large coarse aggregate particles and excessive air loss through the pump contributed to difficulties. The contractor initially began pumping the concrete without any means to limit air loss through the pump, which resulted in a 4.5% loss in air as the concrete was pumped. The contractor fitted the hose end with an elbow (shown in Fig. 5.12), which reduced the air loss to a much more manageable level of only 1%. In addition, large coarse aggregate particles (an example of which is shown in Fig. 5.13) caused difficulties pumping the concrete. As a result of these large aggregate particles and the favorable access to the deck, the decision was made to use a conveyor for the actual bridge placement.



Fig. 5.12 – Elbow fitted to the end of the pump hose to limit air lose through the pump.



Fig. 5.13 – Example of a large coarse aggregate particle taken from the LC-HPC likely resulting in pumping difficulties.

LC-HPC Bridge Deck – A summary of the plastic concrete test results is shown in Table 5.16. With the exception of one truck, the concrete samples for testing were taken prior to placement on the deck. As mentioned previously, a conveyor was used to place the concrete. The conveyor was positioned with about a

3.7 m (12 ft) drop through an elephant trunk to the bridge deck (shown in Fig. 5.14). The trunk provided little, if any, confinement to the concrete and the resulting air loss was 2.4%. Air contents for samples taken at the ready-mix truck varied from 6.0 to 9.2% with an average of 7.8%. Using the average air content and assuming a uniform loss of 2.4% air, the average air content for the deck was only 5.4%. The slump varied from 55 to 100 mm (2.25 to 4 in.) with an average of 80 mm (3 in.). Ice was used to limit concrete temperatures, which increased slightly from 14.7° C (59° F) to 18.0° C (64° F) as the ambient temperature increased during the placement. Finally, the average 27-day compressive strength was 32.3 MPa (4680 psi).

Table 5.16 –Summary of Plastic Concrete Properties for LC-HPC-11

Bridge			Plastic Property [†]			
			Temperature, °C (°F)	Air Content, %	Slump, mm (in.)	Unit Weight, kg/m ³ (lb/ft ³)
78-119	LC-HPC-11	Average	15.8° (60°)	7.8	80 (3)	2278 (142.2)
	Deck	Minimum	14.7° (59°)	6.0	55 (2.25)	2235 (139.5)
		Maximum	18.0° (64°)	9.2	100 (4)	2317 (144.6)

[†]Test results are from samples taken directly from the ready-mix truck prior to placement on the deck. One load was tested before and after placement and a 2.4% reduction in the air content was observed. The average air content is reduced to 5.4% with this reduction included.

As with LC-HPC-1 and 7, this bridge emphasizes that the contractor should not be permitted to proceed with the qualification slab before producing a qualification batch that meets all of the specified plastic concrete properties. In addition, concrete test samples should be taken from the point of deposit on the bridge deck, or if that is not possible, comparative samples taken before and after placement should be used at the beginning of the placement to establish the air loss. To help minimize these losses, concrete should not be allowed to free-fall more than 1.5 m (5 ft) and concrete pump discharge hoses should be fitted with a bladder valve, elbow, or S-Hook attached to the end of the hose.



Fig. 5.14 – Typical conveyor drop for LC-HPC-11

5.3.5 LC-HPC Bridges 3 through 6: I-435 Project

The second contract group, containing four LC-HPC bridges, was awarded to Clarkson Construction Company, and Fordyce Concrete, located approximately 27 km (16.8 mi) from the project, was contracted to provide the concrete. Clarkson and Fordyce successfully completed LC-HPC-1 and 2 in late 2005 and 2006. Due to the success of these placements, only one qualification batch and one qualification slab were scheduled for the four bridges. Four placements were included in the original contract, but three were removed at the request of the contractor prior to the placement of any concrete. The construction of these bridges occurred over a two-month period, from the end of September to the middle of November, 2007. A complete listing of these dates is provided in Table 5.17.

The concrete mixture design proposed for this project was based on the mixture previously used by Fordyce for LC-HPC-1 and 2 with three important distinctions: First, the cement content was reduced from 320 to 317 kg/m³ (540 to 535 lb/yd³), and second, the *w/c* ratio was reduced from 0.45 to 0.42. These two changes reduced the paste content from 24.6% to 23.4% and represented the most

Table 5.17 – Construction Dates for LC-HPC-3 through 6

Item Constructed	Date Completed
Qualification Batch	6/7/07
Qualification Slab	9/14/07
LC-HPC-4 Placement 1	9/29/07
LC-HPC-4 Placement 2	10/2/07
LC-HPC-6	11/3/07
LC-HPC-3	11/13/07
LC-HPC-5	11/14/07

recent laboratory findings to reduce concrete shrinkage (see Section 4.4). In addition, these changes were already used successfully for LC-HPC-8, 10, and 11. It should be noted that these two changes were made voluntarily by the supplier and were not required (at the time) by the concrete specification. The last change centered on adjusting the combined aggregate gradation to meet the aggregate specification for each sieve. As discussed in Section 5.3.1, the combined aggregate gradation for LC-HPC-1 and 2 was gap-graded and did not have a minimum of 8% percent retained on the 2.36-mm (No. 8) sieve. Ensuring that gradation satisfied this criterion was deemed critical due to the further reduction in the paste content for these bridges compared to the first two LC-HPC bridges.

Two aggregate blends incorporating the same four aggregates were proposed as alternatives to the blend utilized in LC-HPC-1 and 2. The four aggregates included: two granite coarse aggregates, coarse manufactured sand, and natural river sand. The manufactured sand (crushed granite) was selected to fill in the missing intermediate sieves [2.36-mm and 1.18-mm (No. 8 and No. 16)] because comparable natural coarse sands were either unavailable or uneconomical. Manufactured sand was not used on LC-HPC-1 and 2. The first mixture, designed using KU Mix,

incorporated 33.1% (by weight) manufactured sand, compared to 13.0% for the alternate mixture designed by the ready-mix supplier. The complete blends for both mixtures are provided in Table 5.18. There were some concerns that the manufactured sand may result in difficulties pumping and finishing the concrete due to the angular nature of the sand. As a result of these discussions, both of the mixtures were used (and evaluated) for the qualification batch and qualification slab.

Table 5.18 – Proposed Aggregate Blends for LC-HPC-3 through 6

Aggregate Name	KU Mix Blend	Alternate Mix Blend
Granite – 25 mm (1.0 in.) Maximum Aggregate Size	23.9%	22.0%
Granite – 19 mm (¾ in.) Maximum Aggregate Size	25.6%	29.0%
Manufactured (crushed granite) Coarse Sand	33.1%	13.0%
Natural River Sand	17.4%	36.0%

The combined aggregate gradations for the two proposed mixtures, titled KU Mix and alternate mix, are shown in Figs. 5.15 and 5.16, and the modified coarseness factor chart (MCFC) is shown in Fig. 5.17. The optimum gradations (calculated using KU Mix), approved *design* gradations, and the *actual* as-delivered gradations are shown for both mixtures. The approved *design* gradations are based on gradations provided by the supplier to qualify the mixture. The supplier only had enough material stockpiled to complete the qualification batch and qualification slab so additional aggregate was ordered prior to the construction of the first bridge deck, LC-HPC-4. The newly delivered aggregate arrived with different gradations, but was combined using the originally approved blends. With the new aggregate gradations, the *actual* combined gradations were significantly finer than the *design* gradations and nearly shifted into Zone IV of the MCFC. The *actual* KU Mix gradation had excess material retained on both the 0.15-mm (No. 100) sieve and the pan, and the *actual* alternate gradation had excess material retained on the 0.15-mm (No. 100)

sieve. Despite this fact, placement proceeded without accounting for the “as-delivered” gradations.

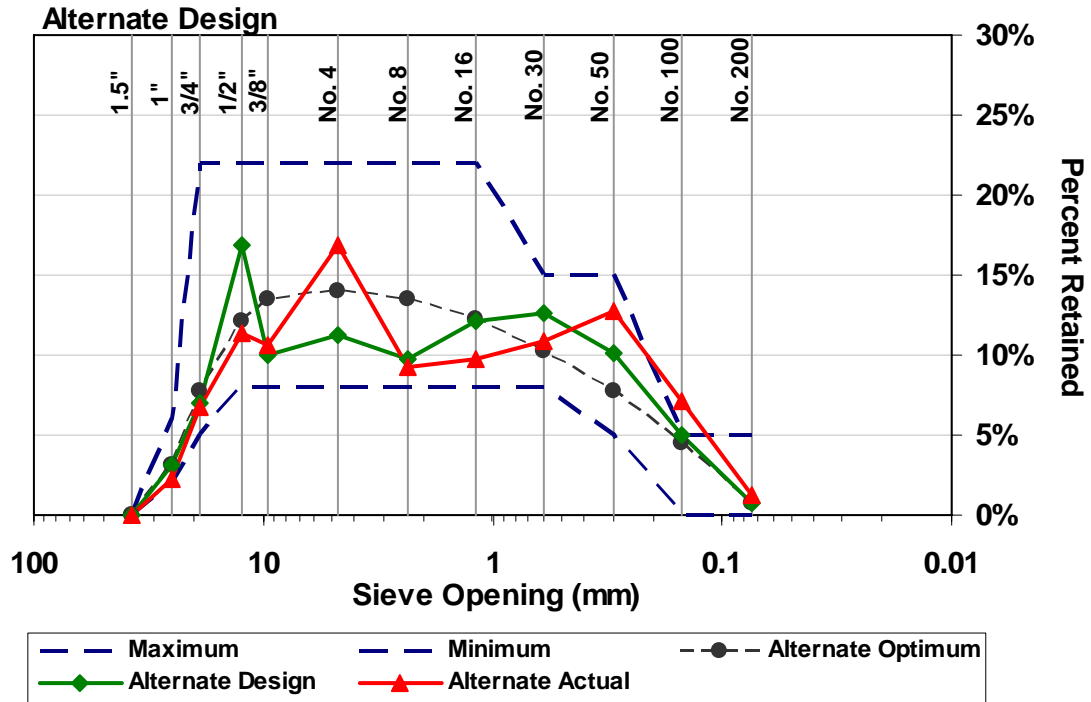


Fig. 5.15 – Combined *Design* Gradation (used for the qualification batch and slab) and Combined *Actual* Gradation (used for the LC-HPC bridges).

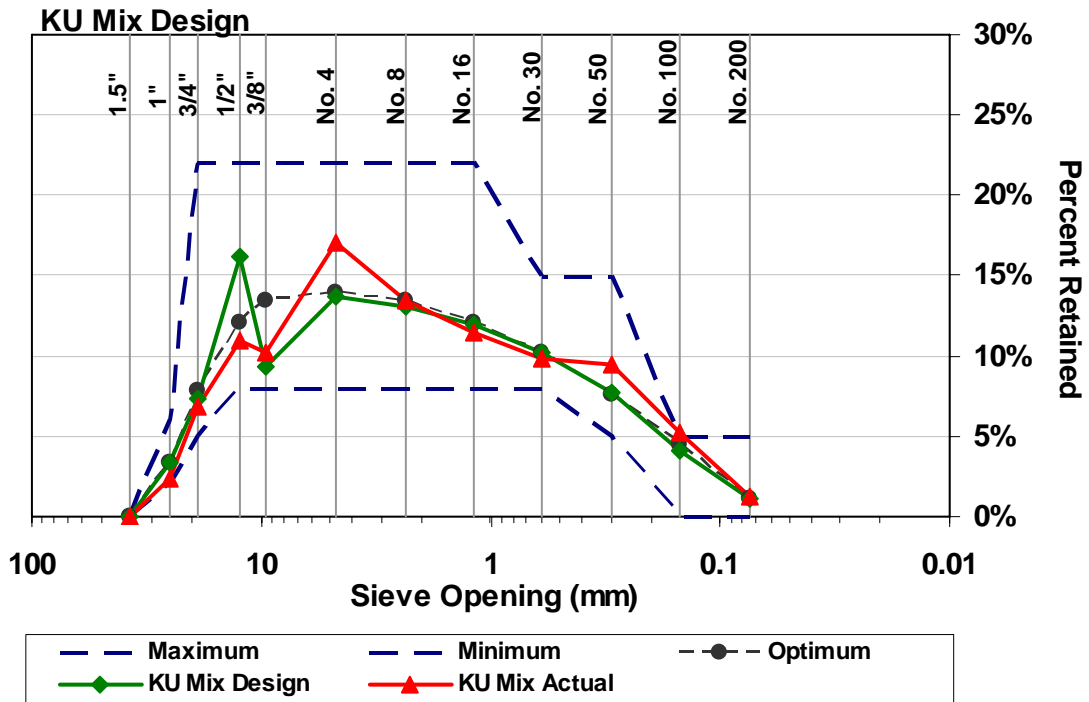


Fig. 5.16 – Combined *Design* Gradation (used for the qualification batch and slab) and Combined *Actual* Gradation (used for the LC-HPC bridges).

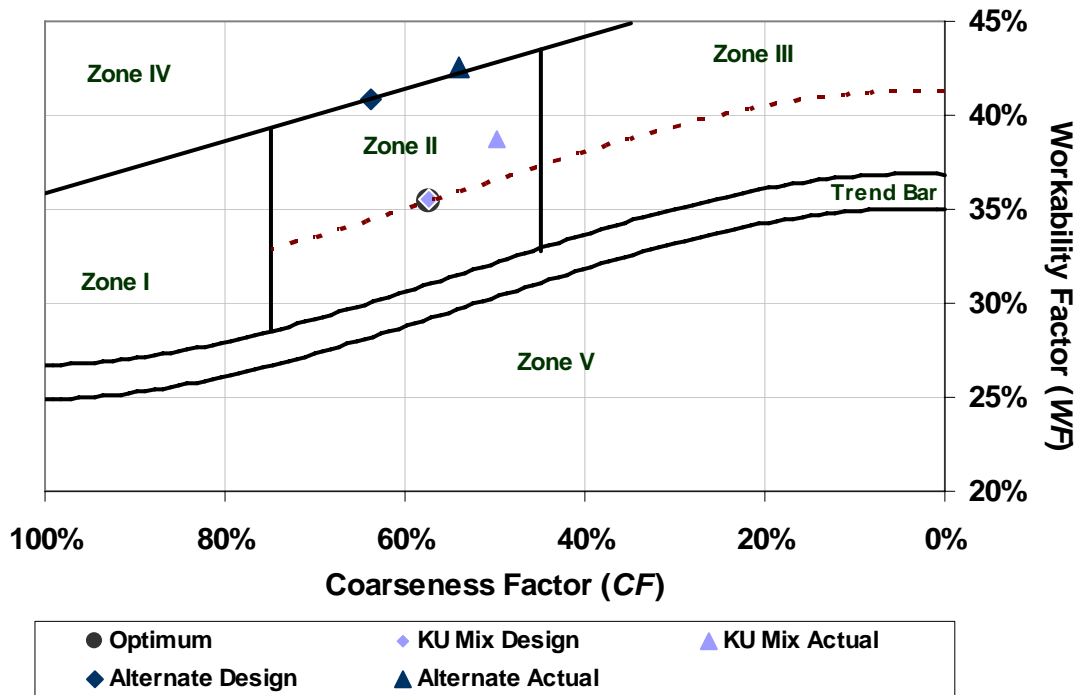


Fig. 5.17 – Combined *Design* Gradation (used for the qualification batch and slab) and Combined *Actual* Gradation (used for the LC-HPC bridges).

Unfortunately, difficulties pumping and finishing the concrete, which became apparent only after the placement of the qualification slab (some of which resulted because of changes in the pumping equipment), resulted in a number of changes to the mixture throughout the project to provide more workability and pumpability. Part of these difficulties resulted from the angular manufactured sand and from over-estimated free-surface moistures (F.S.M.) of the manufactured sand. The ready-mix supplier stockpiled the manufactured sand next to a lightweight aggregate bin that was continuously saturated. As a result, it was difficult (or impossible) to both accurately measure the moisture content and ensure uniformity throughout the stockpile. The reported free-surface moisture for the manufactured sand varied from a 3.9% all the way to 7.1% throughout the placement of these decks. In retrospect, most of the readings were considered to be overestimates of the true moisture content. The mixture designed using KU Mix was affected the most by over-estimated free surface moistures due to the relatively high percentage included in the mixture. Details of the mixtures used for each placement are provided in Table 5.19. The complete concrete mixture designs, aggregate gradations, plastic concrete test results, and compressive strength test results are provided in Appendix D.

Table 5.19 – Construction Dates for LC-HPC-3 through 6

Item Constructed	Mixture Design	W/C Ratio	Manufactured Sand F.S.M.	Water Reducer
Qualification Batch	Both	0.42	--	Mid-Range [†]
Qualification Slab	Both	0.42	--	Mid-Range [†]
LC-HPC-4 Placement 1	KU Mix	0.42	6.5 – 7.1%	Mid-Range [†]
LC-HPC-4 Placement 2	Alternate	0.42	4.0%	Mid-Range [†]
LC-HPC-6	Alternate	0.45	5.8%	High-Range [‡]
LC-HPC-3	Alternate	0.45	3.9 – 4.5%	High-Range [‡]
LC-HPC-5	Alternate	0.42 – 0.45	4.5%	High-Range [‡]

[†]Type A/F lignosulfonate-based mid-range water reducer.

[‡]Type A/F polycarboxylate-based high-range water reducer.

Qualification Batch – The KU Mix mixture design and the alternative mixture design were batched and evaluated on June 7, 2007. A 49% replacement of water with ice [65 kg/m^3 (110 lb/yd^3)] was used with chilled water to control the concrete temperature. A summary of the plastic concrete properties after a 27 minute simulated haul is shown in Table 5.20. The KU Mix had a temperature of 21.7° C (71° F), an air content of 9.6%, and a slump of 100 mm (4 in.). The slump actually increased from 90 mm (3.5 in.) to 100 mm (4 in.) during the simulated haul as the ice melted. The batch exceeded the maximum allowable air content of 9.5%, but despite this fact, the batch was accepted in order “to limit the amount of concrete wasted.” The supplier and transportation officials were satisfied with the mixture and deemed it suitable for use in the qualification slab.

In addition to the KU Mix, the supplier batched the alternate mixture in an attempt to quantify the effect of the manufactured sand on the workability of the two proposed mixtures. The KU mixture contained 33.1% manufactured sand (by weight) compared to only 13.0% for the alternate mixture. The alternate mixture was batched with the same air entraining agent and mid-range water reducer dosage as the qualified KU Mix. The air content was nearly identical, but the slump was 25 mm (1 in.) greater. The slump for this batch clearly did not meet the concrete specification although once again, the results were accepted. This comparison appeared to indicate that the increased percentage of the angular manufactured sand reduced the workability of the mixtures, but the difference was not significant enough to distinguish between the two mixtures in a practical sense, and the decision was made to again test both mixtures at the qualification slab.

Qualification Slab – The qualification slab was completed successfully on September 14, 2007. No significant construction-related issues arose during the placement, finishing, or covering operations, and following examination of several cores taken from the slab to assess consolidation, the contractor was given permission

Table 5.20 –Summary of Plastic Concrete Properties for the Qualification Batch of LC-HPC-3 through 6

Qualification Batch	Plastic Property [†]			
	Temperature, °C (°F)	Air Content, %	Slump, mm (in.)	Unit Weight, kg/m ³ (lb/ft ³)
KU Mix	21.7° (71°)	9.6	100 (4)	2175 (135.8)
Alternate Mix	22.2° (72°)	9.5	125 (5)	2207 (137.8)

[†]Test results are from samples taken directly from the ready-mix truck after a 27 min. simulated haul.

to proceed with the bridge deck placements. As discussed previously, the qualification slab was placed using two mixtures: the KU Mix containing 33.1% manufactured sand and an alternate mixture containing only 13.0% manufactured sand. The mixtures were evaluated side-by-side for pumpability and finishability and the KU Mix was selected for use in the bridge deck placements. The increased percentage of manufactured sand did not appear to adversely affect the concrete's plastic properties.

The first two ready-mix trucks contained the alternate mixture and the remaining two trucks contained the mixture designed using KU Mix. Concrete was placed using a relatively small pump without a fixture attached to the discharge hose to limit air loss (e.g. bladder valve or "S-Hook"). The plastic concrete test results for the four trucks are provided in Table 5.21. The first and third trucks were tested before and after placement through the pump to determine the effect of pumping on the air content, and in both cases, the air content actually increased by 1% for the alternate mixture and 0.1% for the mixture designed using KU Mix. The slumps, measured before placement in the slab, were 70 and 55 mm (2.75 and 2.25 in.) for the alternate mixture and 40 and 35 mm (1.5 in.) for the KU Mix. Concrete temperatures were controlled using ice and chilled water and did not exceed 19.4° C (67° F). The different slumps of the two mixtures made a direct comparison difficult; however, both of the mixtures pumped and finished well, and in the judgment of the contractor,

KDOT officials, and KU personnel, the mixture designed using KU Mix was more than suited for use in the upcoming bridge decks.

Table 5.21 –Summary of Plastic Concrete Properties for the Qualification Slab of LC-HPC-3 through 6

Qualification Slab	Plastic Property [†]			
	Temperature, °C (°F)	Air Content, %	Slump, mm (in.)	Unit Weight, kg/m ³ (lb/ft ³)
Truck #1: Alternate Mix, Out of Truck	18.5° (65°)	7.0	70 (2.75)	2220 (138.6)
Truck #1: Alternate Mix, After Pump	18.0° (64°)	8.0	70 (2.75)	2222 (138.7)
Truck #2: Alternate Mix, Out of Truck	17.0° (63°)	7.0	55 (2.25)	2226 (139.0)
Truck #3: KU Mix, Out of Truck	17.0° (63°)	6.9	40 (1.5)	2232 (139.3)
Truck #3: KU Mix, After Pump	19.5° (67°)	7.0	45 (1.75)	2218 (138.5)
Truck #4: KU Mix, Out of Truck	16.5° (62°)	5.6	35 (1.5)	2274 (142.0)

LC-HPC-4 Bridge Deck – The first bridge cast in this four bridge series was originally planned as one placement scheduled for September 29, 2007. The placement began as scheduled, but an electrical outage at the ready-mix plant halted construction approximately one-third of the way through the placement. While this outage ultimately stopped the placement, the ready-mix producer was not able to consistently supply concrete that met the specifications, and the contractor was not able to effectively pump the LC-HPC. Just prior to the electrical outage, the contractor and ready-mix supplier made the decision to switch from the KU Mix to the alternate mixture to reduce the quantity of manufactured sand – which they deemed the problem.

A number of factors contributed to the difficulties that occurred during the first LC-HPC-4 placement. First, a different and much larger pump was used for the bridge placement than was used for the qualification slab. For conventional concrete with relatively high paste contents and slumps, switching between pumps is generally not a concern; this is not the case for the low paste volume LC-HPC. Smaller pumps operate at higher pressures with smaller stroke lengths compared to larger pumps.

The KU Mix pumped adequately with the high pressure smaller pump used for the qualification slab, but when a much larger pump was used to reach the elevated bridge placement, the mixture pumped poorly. The contractor was allowed to proceed with the bridge placement and the mixture designed using KU Mix (containing 33.1% manufactured sand) was selected based on the successful completion of the qualification slab. A clear lesson is that any changes to approved and qualified materials or equipment should have been tested and reapproved prior to any bridge placements.

In addition to using a different pump, the ready-mix supplier consistently had a difficult time meeting the specifications for slump and air content. The first two trucks were delivered to the site with slumps of 30 and 18 mm (1.25 and 0.75 in.) and air contents of 7.8 and 6.8% measured directly from the truck. These two batches pumped and finished poorly. The admixture dosages were adjusted for the third truck which arrived with a slump of 100 mm (4 in.) and an air content of 10.4%, well above the maximum allowable air content of 9.5%. This truck was rejected, and problems continued throughout the placement. The ready-mix supplier found that as the slump was increased to between 75 and 100 mm (3 and 4 in.) by adding more mid-range water reducer, the air content also increased – often above the maximum allowed. After struggling with the mixture designed using KU Mix, the decision was made to switch to the alternate mixture containing only 13.0% manufactured sand. Before this mixture could be batched, however, a power outage occurred at the ready-mix plant forcing the end of placement operations. Two trucks with air contents of 11.6 and 10.6% were accepted before shutting down to reach a header placed in the negative moment region.

Part of the problem in obtaining consistent plastic concrete properties likely resulted from an over-estimated free-surface moisture of the manufactured sand. The ready-mix supplier stockpiled the sand next to a lightweight aggregate pile that was

continuously saturated. The reported free-surface moisture for the manufactured sand appears to have been over-estimated at 7.1% for the first truck, which was reduced slightly to 6.5% for the remaining 16 trucks. This moisture content was reduced further to 4.0% for the second LC-HPC-4 placement cast only three days later. If the correct moisture content of the manufactured sand had been only 4.0% on the first placement, the actual w/c ratio for the first placement would have been 0.37 compared to the design w/c ratio of 0.42.

The average plastic properties for samples taken directly from the ready-mix truck prior to placement on the deck for the first LC-HPC-4 placement are presented in Table 5.22. The first truck was tested before and after pumping to establish the slump and air content changes through the pump. The slump was unchanged while the air content dropped by 0.8%. A bladder valve (similar to the one shown in Fig. 5.8) was used to limit air loss. Air contents ranged from 6.8% to 11.6% with an average of 8.7% (7.9% with the 0.8% air loss removed), and slump values ranged from 20 to 105 mm (0.75 to 4.25 in.) with an average of 50 mm (2 in.). Concrete temperatures were controlled using chilled water and ice.

Table 5.22 –Summary of Plastic Concrete Properties for LC-HPC-4 Placement 1

Bridge		Plastic Property [†]			
		Temperature, °C (°F)	Air Content, %	Slump, mm (in.)	Unit Weight, kg/m ³ (lb/ft ³)
46-339 LC-HPC-4	Average	--	8.7	50 (2)	2202 (137.4)
Placement 1	Minimum	--	6.8	20 (0.75)	2116 (132.1)
	Maximum	--	11.6	105 (4.25)	2255 (140.8)

[†]Test results are from samples taken directly from the ready-mix truck prior to placement on the deck. One load was tested before and after placement through the pump and a 0.8% reduction in the air content was observed.

The bridge deck was completed with a second placement on 10/2/07 – three days after the first placement was halted. For this placement, the contractor did not use a bladder valve to limit air loss through the pump. Prior to moving forward with

the second placement, 3.1 m³ (4 yd³) of the alternate mixture was pumped with the same type and size of pump required to complete the bridge deck. The concrete used to test the pump arrived with a slump of 100 mm (4 in.) and an air content of 11.4%. The concrete pumped well and gave the contractor and ready-mix supplier confidence to move forward with the deck placement despite the high air content and slump values. The actual deck placement went smoothly with only a few small delays at the beginning and end of the deck. The concrete pumped well for the entire placement, and the ready-mix supplier was able to consistently produce concrete that met the specifications for nearly the entire deck.

The first truck was tested before and after placement on the deck, indicating a 2.0% air was loss through the pump. This was significantly higher than occurred for the first placement, where only 0.8% air was lost, due to the absence of any measures used to restrict concrete flow and limit air loss. Acceptance testing for the remaining concrete occurred prior to placement on the deck. All of the slumps met the specifications, but three trucks with slightly elevated air contents (9.6, 9.8, and 10.4%) were placed in the deck because it was assumed that the concrete would lose 2.0% air through the pump. There was some confusion among the inspectors as to whether or not these trucks should be accepted, and no attention was given to trucks with concrete near the low end of the specification.

A summary of the plastic properties for the second LC-HPC-4 placement is presented in Table 5.23. Slumps ranged from 135 to 100 mm (1.5 to 4 in.) with an average of 80 mm (3 in.), and air contents ranged from 7.2% to 10.4% with an average of 8.8%. The average air content decreases to 6.8% when the 2.0% air loss is subtracted. Concrete temperatures were again controlled using chilled water and ice. Temperatures ranged from 15.0° to 21.7° C (64° to 71° F) with an average temperature of 17.5° C (64° F). A 28% replacement of mix water with ice [48 kg/m³

(80 lb/yd³) was used for the first several trucks, which was reduced to 21% [36 kg/m³ (60 lb/yd³)] and finally to 14% [24 kg/m³ (40 lb/yd³)].

Table 5.23 –Summary of Plastic Concrete Properties for LC-HPC-4 Placement 2

Bridge		Plastic Property [†]			
		Temperature, °C (°F)	Air Content, %	Slump, mm (in.)	Unit Weight, kg/m ³ (lb/ft ³)
46-339 LC-HPC-4	Average	17.5° (64°)	8.8	80 (3)	2210 (137.9)
Placement 2	Minimum	15.0° (59°)	7.2	35 (1.5)	2164 (135.1)
	Maximum	21.7° (71°)	10.4	100 (4)	2260 (141.1)

[†]Test results are from samples taken directly from the ready-mix truck prior to placement on the deck. One load was tested before and after the pump and a 2.0% reduction in the air content was observed.

LC-HPC-6 Bridge Deck – The second bridge in this project was constructed in early November when no measures were needed to limit the plastic concrete temperatures, but the deck and girders were covered and heated to ensure that their temperatures never fell below 4.4° C (40° F) during the 14-day curing period. The alternate concrete mixture was used for the placement with two significant changes: First, the *w/c* ratio was increased from 0.42 to 0.45, and second, a Type A/F high-range water reducer (polycarboxylate-based) replaced the mid-range water reducer (lignosulfonate-based). The free-surface moisture content of the manufactured sand was set at 5.8% for the entire placement, compared to 6.5% and 4.0% for the first and second LC-HPC-4 placements, respectively. These changes did not appear to improve the plastic properties of the concrete.

The majority of concrete testing was performed on concrete taken directly from the ready-mix truck prior to placement on the deck. Concrete from two ready-mix trucks was tested before and after placement on the deck to establish the amount of air lost through the pump. A bladder valve was attached to the discharge hose and limited air loss to 0.6% and 1.4% when measured on the deck, but when the pump boom was positioned straight up and down, the air loss increased to 2.9%. Of the tests performed directly from the ready-mix trucks, 12 of the 27 slump tests and 9 of

the 15 air tests did not meet the specifications. All of these tests exceeded the maximum allowable limits [100 mm (4 in.) slump and 9.5% air]. Many of these loads were placed in the deck, but a few were set aside for several minutes and then placed in the deck without retesting.

The plastic concrete properties for LC-HPC-6 are summarized in Table 5.24. Slumps ranged from 60 to 140 mm (2.25 to 5.5 in.) with an average of 95 mm (3.75 in.), and air contents measured directly at the truck ranged from 7.5 to 11.5% with an average value of 9.5%. Concrete temperatures ranged from 15.3° to 17.8° C (52° to 64° F) with an average of 15.3° C (60° F). When the average air loss through the pump is subtracted from the average air content, the expected “as-placed” air content reduces to 8.5%.

Table 5.24 –Summary of Plastic Concrete Properties for LC-HPC-6

Bridge		Plastic Property [†]			
		Temperature, °C (°F)	Air Content, %	Slump, mm (in.)	Unit Weight, kg/m ³ (lb/ft ³)
46-340 LC-HPC-6	Average	15.3° (60°)	9.5	95 (3.75)	--
Unit 2	Minimum	11.1° (52°)	7.5	60 (2.25)	--
	Maximum	17.8° (64°)	11.5	140 (5.5)	--

[†]Test results are from samples taken directly from the ready-mix truck prior to placement on the deck. Two loads were tested before and after the pump, and on average, a 1.0% reduction in the air content was observed.

LC-HPC-3 Bridge Deck – The third LC-HPC deck in this project was cast on 11/13/07 with clear guidelines for concrete testing and acceptance. The rule was simple: no concrete with a slump greater than 100 mm (4 in.) or an air content greater than 9.5% would be placed in the deck. All concrete was sampled from the ready-mix truck prior to placement on the deck to ensure that no out-of-specification concrete was placed in the deck. Concrete that did not meet the specifications for slump would be rejected or set aside and retested prior to placement. Concrete with an air content that exceeded 9.5% was either tested on the deck after pumping or set

aside and retested after several minutes. A total of five trucks with either a high air content, high slump, or both were set aside, retested, and subsequently placed into the deck. The establishment of these guidelines eliminated the ambiguity that existed on the three previous placements and gave inspectors a clear procedure to follow.

The alternate concrete mixture used for the LC-HPC-6 placement, with a w/c ratio of 0.45, was also used for this placement. The concrete surface was somewhat difficult to finish and required considerable work with a bullfloat to remove surface irregularities. Air loss through the pump was limited to 1.6%, 1.1%, and 1.5% using a bladder valve for three trucks tested before and after placement.

The average plastic concrete properties for LC-HPC-3 are shown in Table 5.25. All of the concrete placed in the deck met the specifications for slump with values ranging from 45 to 100 mm (1.75 to 4 in.). Four trucks with slumps greater than 100 mm (4 in.) were set aside for 10 to 20 minutes and retested prior to placement in the deck. Air content values ranged from 6.5% to 10.5% with an average of 8.7% (7.3% when the average air loss through the pump is subtracted). One truck with an air content of 12.0% was allowed to sit for 10 minutes and retested. The air content dropped 2.8% to 9.2%, and the concrete was placed in the deck. The last two ready-mix trucks tested had air contents of 10.5% and 10.0% and were allowed to be placed in the deck. The concrete load with an air content of 10.5% was retested on the deck and found to be 9.0%. The second truck was assumed to behave similarly and was not retested.

LC-HPC-5 Bridge Deck – The last bridge in this project, LC-HPC-5, was cast one day following LC-HPC-3. No measures were taken to control the concrete temperature, although as with LC-HPC-3 and 6, the deck and girders were covered and periodically heated to ensure that their temperatures never dropped below 4.4° C (40° F) during the 14-day curing period. The concrete mixture initially selected for this placement was the same as the concrete used for the LC-HPC-4 Placement 2

Table 5.25 –Summary of Plastic Concrete Properties for LC-HPC-3

Bridge			Plastic Property [†]			
			Temperature, °C (°F)	Air Content, %	Slump, mm (in.)	Unit Weight, kg/m ³ (lb/ft ³)
46-338	LC-HPC-3	Average	14.3° (58°)	8.7	85 (3.25)	--
Deck		Minimum	11.1° (52°)	6.5	45 (1.75)	--
		Maximum	16.7° (62°)	10.5	100 (4)	--

[†]Test results are from samples taken directly from the ready-mix truck prior to placement on the deck. Three loads were tested before and after the pump, and on average, a 1.4% reduction in the air content was observed reducing the average air content expected on the deck to 7.3%.

except that a polycarboxylate-based high-range water reducer was used instead of a lignosulfonate-based mid-range water reducer. For this placement, the alternate mixture was used in conjunction with a *w/c* ratio of 0.42, but the *w/c* ratio was increased from 0.42 to 0.45 during the placement due to problems pumping the lower *w/c* ratio mixture. The free-surface moisture content of the manufactured sand was set at 4.5% for the entire placement.

Concrete was tested at the ready-mix truck prior to placement on the deck. As with many of the other placements, the first truck was tested before and after pumping to establish the air content lost during placement. Air loss for concrete taken from the first truck was limited to 0.6% with the use of a bladder valve. The plastic concrete test results met the specifications for all but three of the ready-mix trucks. The plastic concrete properties are summarized in Table 5.26. Slumps ranged from 50 to 100 mm (2 to 4 in.) with an average of 80 mm (3 in.), and air contents measured directly at the truck ranged from 6.8 to 10.3% with an average value of 8.7%. When the 0.6% air loss is subtracted from the average air content, the approximate air content expected in the deck is decreased to 8.1%. Concrete temperatures ranged from 13.9° to 17.8° C (57° to 71° F) with an average of 15.9° C (61° F).

Table 5.26 –Summary of Plastic Concrete Properties for LC-HPC-5

Bridge			Plastic Property [†]			
			Temperature, °C (°F)	Air Content, %	Slump, mm (in.)	Unit Weight, kg/m ³ (lb/ft ³)
46-340	LC-HPC-5	Average	17.5° (61°)	8.7	80 (3)	2236 (139.6)
Unit 1		Minimum	15.0° (57°)	6.8	50 (2)	2181 (136.1)
		Maximum	17.8° (64°)	10.3	100 (4)	2294 (143.2)

[†]Test results are from samples taken directly from the ready-mix truck prior to placement on the deck. One load was tested before and after the pump, and a 0.6% reduction in the air content was observed, reducing the average air content expected on the deck to 8.1%.

The plastic concrete test results were consistent throughout the placement; however, the contractor continued to have difficulties pumping the LC-HPC with a w/c ratio of 0.42. The pump seized on three separate occasions while the first seven trucks were being unloaded. These problems resulted in several delays that, at one point, resulted in ready-mix trucks waiting to begin discharge for 45 minutes or more. The supplier began to add 2.5 kg/m³ (0.5 gal/yd³) of water to the next seven trucks in an effort to improve the pumpability and avoid any additional delays. Shortly thereafter, the design w/c ratio was increased 0.42 to 0.43 to provide a clear record of the mixtures used in the deck. The 0.43 w/c ratio mixture did not appear to pump any easier, and the design w/c ratio was again increased to 0.45 – matching the w/c ratio of LC-HPC-3 and 6. Increasing the w/c ratio from 0.42 to 0.45 increased the paste content from 23.4% to 24.4%, and made the concrete more pumpable. The paste content and w/c ratio are plotted for each ready-mix truck in Fig. 5.18.

Summary – Several challenges related to the LC-HPC were faced during the construction of LC-HPC-3 through 6. Adjustments were made throughout the project to address these issues, and in the process, several important lessons were learned. For these bridges, the most critical aspect was the ability, or inability, to adequately pump the mixture. These issues should be addressed during the qualification slab; however, for this project, a different pump was used for the qualification slab than for

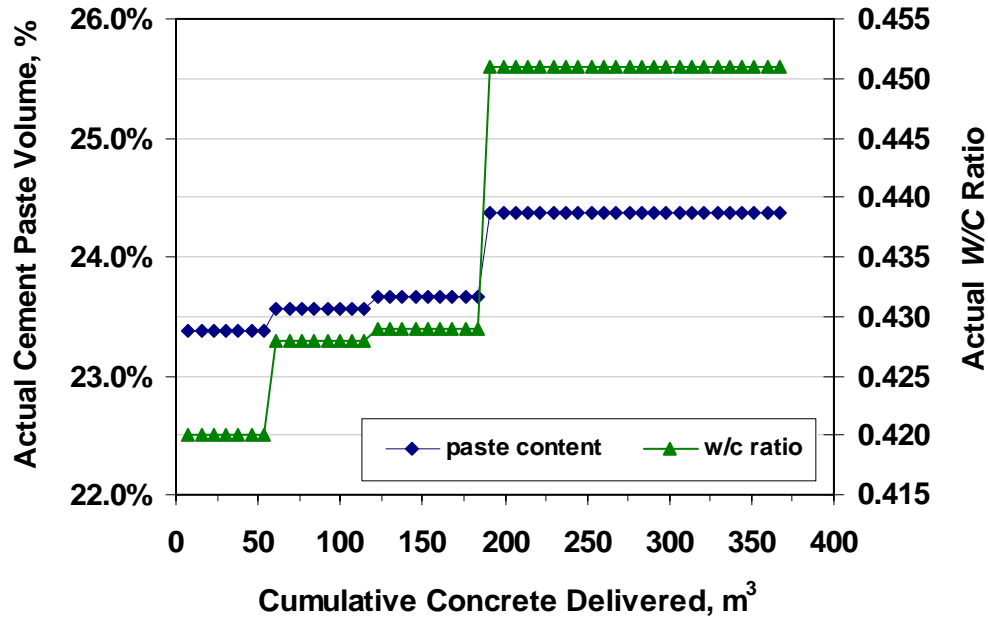


Fig. 5.18 – Cement paste volume and w/c ratio versus the cumulative volume of concrete delivered for LC-HPC-5. Each data point represents one ready-mix truck.

the bridge placements. A small pump, which operates at much higher pressures, pumped the concrete without any problem during the qualification slab. A much larger pump that operates at lower pressures was required to reach the elevated bridge decks. The large pump had a difficult time pumping the mixture originally planned for this series of LC-HPC decks.

The original mixture, with a w/c ratio of 0.42 designed using KU Mix, relied on a large percentage of manufactured sand (crushed granite) to fill in the middle aggregate sizes. This angular sand increased particle interference and reduced both the workability and pumpability of the mixture. Overestimated free-surface moistures of the manufactured sand compounded the difficulties – especially for the mixture designed using KU Mix that contained a much larger proportion of the manufactured sand. After the first placement, the ready-mix supplier switched to an alternate mixture with a w/c ratio of 0.42 that less than half the quantity of manufactured sand. The alternate mixture pumped adequately, but the decision was

made to increase the w/c ratio to 0.45 and replace the lignosulfonate-based mid-range water reducer with a more efficient polycarboxylate high-range water reducer. These two changes improved both the workability and pumpability of the mixture for LC-HPC-6 and LC-HPC-3. The w/c ratio was briefly dropped to 0.42 for the last bridge, LC-HPC-5, but the mixture again pumped poorly, and the w/c ratio was increased back to 0.45.

The 28-day compressive strengths for the four LC-HPC bridges are shown in Fig. 5.19. The cylinders cast for LC-HPC-4 (Placement 2) and LC-HPC-5 have w/c ratios of 0.42. A mid-range water reducer (MRWR) was used for LC-HPC-4 and a high-range water reducer (HRWR) was used for LC-HPC-5. The HRWR more efficiently deflocculates cement particles, which results in increased compressive strengths compared to concretes containing a MRWR. The difference in water reducers accounts for at least part of the 10.9 MPa (1580 psi) difference in strength observed for the two concrete mixtures. The remaining two bridge decks, LC-HPC-3 and 6, were cast with a 0.45 w/c ratio and a HRWR. The compressive strengths for these decks were 40.3 and 41.3 MPa (5850 and 5990 psi), respectively. These strengths are higher than the strengths observed for the three LC-HPC-1 and 2 placements, also cast with a w/c ratio of 0.45 and a MRWR. Compressive strengths for the earlier placements ranged from 31.7 to 35.9 MPa (4600 to 5210 psi).

5.3.6 LC-HPC Bridge 14: Metcalf over Indian Creek

The final LC-HPC bridge let to date is located in Overland Park, KS on Metcalf Ave. over Indian Creek and is a city project rather than a Kansas Department of Transportation (KDOT) project. Pyramid Construction was awarded the project and Fordyce provided the concrete. By the end of the project, Fordyce Concrete had provided the ready-mix concrete for seven of the 14 LC-HPC bridges. Fordyce concrete is located approximately 29 km (18.0 mi) from the bridge location. The individual aggregate gradations, combined gradation, plastic concrete test results, and

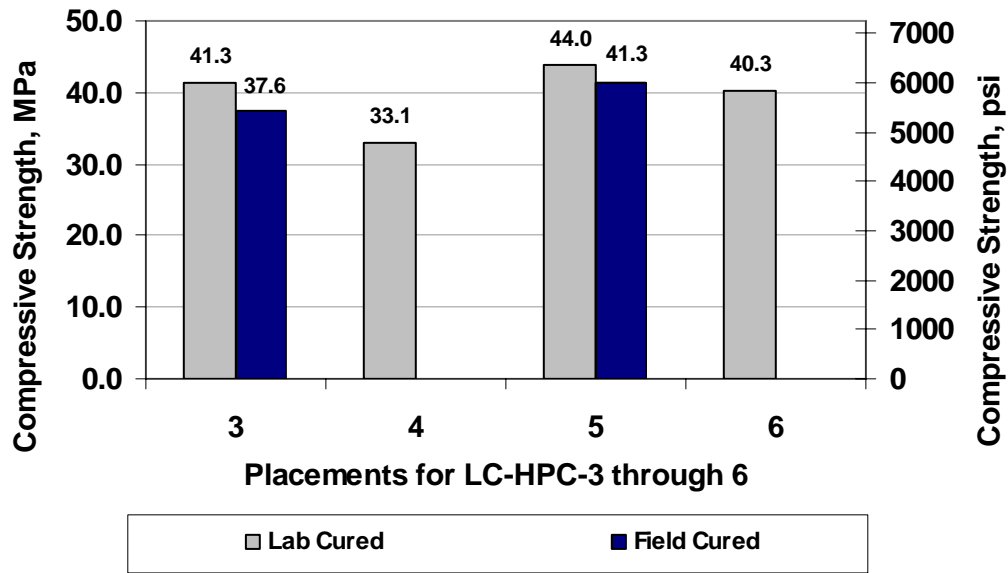


Fig. 5.19 – Compressive Strengths for LC-HPC-3 through 6

compressive strength test results are provided in Appendix D. A summary of the completion dates for the qualification batch, qualification slab, and the three bridge placements are shown in Table 5.27.

Table 5.27 – Construction Dates for LC-HPC-14

Item Constructed	Date Completed
Qualification Slab	11/13/2007
LC-HPC-14 Placement 1	12/19/2007
LC-HPC-14 Placement 2	5/2/2008
LC-HPC-14 Placement 3	5/21/08

As indicated in Table 5.27, the ready-mix supplier was not required to complete a qualification batch since the same ready-mix supplier was producing concrete for LC-HPC-3 through 6 at approximately the same time. The concrete mixture originally planned for LC-HPC-14 was the alternate mixture (used for LC-HPC-4 and 5 described in Section 5.3.5) with a w/c ratio of 0.42 and a cement content

of 317 kg/m^3 (535 lb/yd^3) incorporating a Type A/F high-range water reducer (polycarboxylate-based). The same combined aggregate gradation with excess material on the 0.15-mm (No. 100) sieve (Fig. 5.16) that plots near Zone IV on the modified coarseness factor chart (Fig. 5.17) was used throughout the project. A number of the same difficulties encountered in the previous bridges were encountered in LC-HPC-14. Following suspension of a first attempted placement on 11/19/07 due to a blown gasket on the pump, the w/c ratio was increased to 0.45 and a conveyor was used for the remaining placements. A summary of the qualification slab and the three bridge placements is provided next.

Qualification Slab – The qualification slab was completed successfully on November 13, 2007. The ready-mix supplier delivered the alternate LC-HPC mixture with a w/c ratio of 0.45 rather than 0.42. The contractor was able to finish and cover the slab in a timely fashion without any difficulties. Following placement of the mixture with a w/c ratio of 0.45, additional concrete was ordered with a w/c ratio of 0.42. The slump and air content for this concrete was 75 mm (3 in.) and 7.4%, respectively. Both mixtures pumped and finished easily with no significant difference between the two. The decision was made to move forward with the first bridge placement using the mixture with a w/c ratio of 0.42.

LC-HPC-14 Deck Placements – The first attempt at the **first placement** for LC-HPC-14 occurred on November 19, 2007, but the placement was halted due to a number of problems, including out-of-specification concrete and significant difficulties pumping the concrete. These difficulties began immediately. Several ready-mix trucks arrived with air contents and slumps that exceeded the maximum values when measured from samples taken directly from the trucks. These trucks were set aside, and after 15 minutes, concrete from most of these trucks met the specifications. One truck was rejected. The accepted concrete was placed and tested on the deck where it was determined that approximately 2% air and 25 mm (1 in.) of

slump were lost through the pump. No measures (e.g. bladder valve or “S-Hook”) were taken to limit the air loss. Due to these large variations that were a function of the concrete testing location, the acceptance testing was moved to the pump discharge.

Concrete from the trucks that were allowed to sit began to become difficult to pump. The difficulties were compounded as pumping delays began to cause several trucks to lineup waiting to discharge. By the time concrete from these trucks was being placed, the concrete was not workable and eventually the pump blew a gasket. By the time the gasket was replaced, the pump lines were clogged and the placement was cancelled. As a result, the contractor removed the deck (but not the end-wall) concrete and re-placed a portion of the reinforcing steel.

The second attempt at the first placement was completed successfully on December 19, 2007 using a conveyor rather than a pump. In addition to that change, the *w/c* ratio was increased from 0.42 to 0.45 and concrete with slumps of up to 125 mm (5 in.) was accepted. The conveyor was positioned so that the concrete dropped approximately 4 m (13.1 ft), which resulted in an air loss of between 2 and 2.5%. In general, the placement went smoothly with the exception of two problems that may result in increased cracking. First, the contractor spent a considerable amount of time finishing the concrete surface with a bullfloat. This increased the amount of time before the surface was covered with wet burlap by at least 10 minutes throughout most of the placement. In addition, the contractor used water from the fogging system to aid finishing the deck surface. The second problem involved over-heating the supporting girders during the curing period. Several heaters were placed beneath the deck to ensure that both the concrete deck and the steel girder temperatures were maintained between 12.8° and 21.1° C (55° and 70° F) throughout the curing period (as required by the specifications). These requirements were met for the entire curing

period, except for the day of placement when air temperatures measured under the deck, next to the girders, rose as high as 29.4° C (85° F).

A summary of the plastic concrete properties is presented in Table 5.28. Slumps ranged from 45 to 135 mm (1.75 to 5.25 in.) with an average of 95 mm (3.75 in.), and air contents measured directly at the truck ranged from 7.8 to 9.7% with an average value of 8.7%. When the 2 to 2.5% air loss is subtracted from the average air content, the estimated average air content for concrete in the deck is between 6.2 and 6.7%. No measures were necessary to control concrete temperatures, which ranged from 15.6° to 20.6° C (60° to 69° F) with an average of 18.1° C (65° F). Twenty-eight day compressive strengths measured for 12 lab-cured cylinders varied from 27.3 to 34.7 MPa (3960 to 5030 psi) with an average of 30.6 MPa (4440 psi).

Table 5.28 – Summary of Plastic Concrete Properties for LC-HPC-14 Placement 1

Bridge		Plastic Property [†]			
		Temperature, °C (°F)	Air Content, %	Slump, mm (in.)	Unit Weight, kg/m ³ (lb/ft ³)
LC-HPC-14	Average	18.1° (65°)	8.7	95 (3.75)	2237 (139.7)
Placement 1	Minimum	15.6° (60°)	7.8	45 (1.75)	2188 (136.6)
	Maximum	20.6° (69°)	9.7	135 (5.25)	2274 (142.0)

[†]Test results are from samples taken directly from the ready-mix truck prior to placement on the deck. Air loss resulting from the conveyor drop was estimated at 2 to 2.5%, making the average air content 6.2 to 6.7%.

The **second placement** was completed the following May, again using a conveyor for placement. The first placement (adjacent to the second placement) was completely closed to traffic for slightly under 72 hours due to concerns that increased settlement cracking would result due to traffic vibrations. For this placement, a double-drum (rather than single-drum) roller screed, metal-pan drag, and a burlap drag were used to finish the concrete surface. Bullfloating was mainly limited to the north end of the deck where the finishing operations were delayed due to an

insufficient quantity of concrete early in the placement. In general, the finished deck was covered more quickly than for the first placement.

It was clear from the second placement that Overland Park officials were influenced by the contractor to accept concrete with slumps that exceeded the maximum slump of 100 mm (4 in.). The contractor used the first failed attempt at the first placement as justification for the need to use elevated slumps [which often exceeded 100 mm (4 in.)]. All of the LC-HPC-14 placements will be monitored closely for increased settlement cracking compared to the other placement due to the increased potential resulting from high slumps.

A summary of the plastic concrete properties is presented in Table 5.29. The concrete was sampled directly from the ready-mix trucks. Two samples were tested at the truck and after placement on the deck, and the resulting air loss was 1.4% and 2.4%. For the samples taken directly from the truck, slumps ranged from 65 to 150 mm (2.5 to 6 in.) with an average of 110 mm (4.25 in.), and air contents ranged from 7.0 to 11.0% with an average value of 9.8%. When the 1.9% average air loss is subtracted from the average air content, the estimated average air content for concrete in the deck is 7.9%. A partial replacement of mix water with ice and chilled water was used to control concrete temperatures. The temperature ranged from 17.2° to 18.3° C (63° to 65° F) with an average of 18.1° C (65° F). Twenty-eight day compressive strengths measured for eight lab-cured cylinders varied from 19.2 to 33.1 MPa (2790 to 4800 psi) with an average of 25.6 MPa (3710 psi).

The **third and final placement** was completed on May 21, 2008. A conveyor was used to place the concrete and a double-drum roller screed, followed by a metal-pan drag and a bullfloat or burlap drag, was used to finish the concrete surface. Initially, a bullfloat was used to finish the surface but was later replaced with a burlap drag. The concrete surface finished easily, although this was attributed to slumps which were never measured below 110 mm (4.25 in.).

Table 5.29 –Summary of Plastic Concrete Properties for LC-HPC-14 Placement 2

Bridge		Plastic Property [†]			
		Temperature, °C (°F)	Air Content, %	Slump, mm (in.)	Unit Weight, kg/m ³ (lb/ft ³)
LC-HPC-14	Average	17.9° (64°)	9.8	110 (4.25)	2213 (138.1)
Placement 2	Minimum	17.2° (63°)	7.0	65 (2.5)	2157 (134.7)
	Maximum	18.3° (65°)	11.0	150 (6)	2284 (142.6)

[†]Test results are from samples taken directly from the ready-mix truck prior to placement on the deck. The average air loss resulting from the conveyor drop was measured at 1.9%, making the average air content 7.9%.

A portion of the mix water [5 L/m³ (1 gal/yd³)] was initially withheld from the mixture, although in nearly every case, the water was added back to the truck prior to discharge. For this placement, the ready-mix trucks were required to use extended chutes to reach the conveyor hopper. Only half of this length was used for the other LC-HPC bridge placements. As a result, the chute angle was shallow which required high-slump concrete to adequately discharge the concrete. An elevated approach (as shown in Fig. 5.4) would have provided the necessary chute angle, but the contractor was more interested in using high-slump concrete. Elevated slumps are of particular concern for this bridge deck because the reinforcement was not firmly supported on the formwork. This could potentially result in increased settlement cracking as the reinforcing shifts during placement.

A summary of the plastic concrete properties is presented in Table 5.30. As with the other placements, concrete testing was performed prior to placement on the deck and two samples were tested to establish the air loss resulting from placement. The air losses for these two samples were 0.5% and 1.2%. For the samples taken directly from the truck, slumps ranged from 110 to 165 mm (4.25 to 6.5 in.) with an average of 130 mm (5.25 in.), and air contents ranged from 9.5 to 10.5% with an average value of 9.9%. When the average air loss of 0.9% is subtracted from the average air content, the estimated average air content for concrete in the deck is 9.0%. Ice and chilled water was used to control concrete temperatures, which ranged from

16.7° to 19.4° C (62° to 67° F) with an average of 18.3° C (65° F). Twenty-eight day compressive strengths measured for eight lab-cured cylinders varied from 25.4 to 28.3 MPa (3680 to 4100 psi) with an average of 26.4 MPa (3830 psi).

Table 5.30 –Summary of Plastic Concrete Properties for LC-HPC-14 Placement 3

Bridge		Plastic Property [†]			
		Temperature, °C (°F)	Air Content, %	Slump, mm (in.)	Unit Weight, kg/m ³ (lb/ft ³)
LC-HPC-14	Average	18.3° (65°)	9.9	130 (5.25)	2195 (137.1)
Placement 3	Minimum	16.7° (62°)	9.5	110 (4.25)	2165 (135.1)
	Maximum	19.4° (67°)	10.5	165 (6.5)	2215 (138.3)

[†]Test results are from samples taken directly from the ready-mix truck prior to placement on the deck. The average air loss resulting from the conveyor drop was measured at 0.9%, making the average air content 9.0%.

5.3.7 LC-HPC Bridge 12: K-130 over Neosho River Unit 2

The twelfth LC-HPC bridge let (and constructed) is located southeast of Emporia near Hartford, KS on K-130 over the Neosho River. A. M. Cohron Construction was awarded the project and Builder's Choice Concrete, a subsidiary of Concrete Supply of Topeka (CST), provided the concrete. Concrete Supply of Topeka provided the concrete for LC-HPC-7 (discussed in Section 5.3.2). Builder's Choice is located in Emporia, KS approximately 31 km (19.3 mi) from the bridge location. The individual aggregate gradations, combined gradation, plastic concrete test results, and compressive strength test results are provided in Appendix D. This bridge, in addition to Control-12, is being constructed in two phases. The first phase was completed on April 4, 2008, and phase two is anticipated for spring 2009. A summary of the completion dates for the qualification batch, qualification slab, and phase one of the bridge construction are given in Table 5.31.

Based on the concrete specifications governing the construction of this bridge, the maximum *w/c* ratio and cement content was specified as 0.42 and 317 kg/m³ (535 lb/yd³), respectively. At times, this mixture has been difficult to place and finish,

Table 5.31 – Construction Dates for LC-HPC-12

Item Constructed	Date Completed
Qualification Batch	3/24/2008
Qualification Slab	3/28/2008
Bridge Deck – Phase I	4/4/2008
Bridge Deck – Phase II	--

especially compared to mixtures with a w/c ratio of 0.45 and a cement content of 320 kg/m^3 (540 lb/yd^3). For this reason, the cement content and w/c ratio for LC-HPC-12 were increased to 320 kg/m^3 (540 lb/yd^3) and 0.44, respectively. A Type A mid-range water reducer (lignosulfonate-based) was selected by the ready-mix supplier to obtain the desired workability. Adjustments to the slump were made by adjusting the water reducer dosage, and no water was withheld from the mixture. A total of three aggregates (two crushed granite coarse aggregates and natural sand) were required to meet the combined aggregate gradation requirements.

Qualification Batch – The qualification batch was completed successfully with one batch on March 24, 2008. Plastic concrete tests were performed before and after the 45-minute simulated haul. Initially the slump, air content, and concrete temperature were 115 mm (4.5 in.), 10.5%, and 17.2° C (63° F), respectively. Following the simulated haul, the slump and air content dropped to 100 mm (4 in.) and 8%, respectively, and the concrete temperature increased slightly to 18.3° C (65° F). Performing tests on the concrete before the simulated haul gives the ready-mix supplier an indication of how the haul time affects the concrete and what the target values for slump, air content, and temperature should be immediately after batching. In addition to testing the plastic concrete, the contractor placed the concrete in a small form to test the workability and finishability of the mixture. This provided the

contractor one additional opportunity to work with the concrete and provide feedback to the ready-mix supplier prior to construction of the qualification slab.

Qualification Slab – Two concrete buckets were used to place the qualification slab, unlike any of the previous LC-HPC placements, which utilized either a conveyor or a pump. No special measures were needed to control concrete temperatures, which ranged from 13.3° to 14.8° C (56° to 59° F) for the four trucks required to complete the placement. The ready-mix supplier had no troubles providing concrete that met the specifications for air content, but three of the four trucks arrived with elevated slumps. Concrete from the first three trucks arrived with slumps of 110, 135, and 150 mm (4.25, 5.25, and 6 in.). These trucks were set aside for 15 to 30 minutes and retested, but the slump values decreased by no more than 15 mm (½ in.) due to the low concrete temperatures. Concrete from the first truck was placed in the deck with a slump 95 mm (3.75 in.), but the second and third trucks were rejected. Concrete from the second truck was later accepted to keep construction moving, and the last two trucks met the specifications with slumps of 70 and 85 mm (2.75 and 3.25 in.), respectively. No entrained air was lost during the placement process, and air contents at the time of placement ranged from 7.5 to 8.5% with an average of 7.9%.

It is necessary and prudent to reject ready-mix trucks that do not meet the specifications – especially for batches performed prior to the bridge deck placement. Based on experiences with contractors, ready-mix suppliers, and inspectors, it is clear that concrete is rarely rejected. This is mainly due to the wide range of acceptable values for slump and air content and the limited number of tests that are performed on the plastic concrete. For this placement, however, one out of the two trucks that arrived with elevated slumps was rejected and the other was allowed into the deck. This strategy sends a clear message to the supplier, and at the same time, does not significantly impede construction.

LC-HPC Bridge Deck – A summary of the plastic concrete test results is shown in Table 5.32. The first two trucks were adjusted in the field to meet the specifications, but concrete from the remaining trucks met the requirements for slump, air content, and concrete temperature. The average values for slump, air content, and concrete temperature were 70 mm (2.75 in.), 7.4%, and 14.5° C (58° F). Concrete samples for these tests were taken from the back of the ready-mix truck, but as mentioned previously, no air was lost during placement with the bucket. A metal pan attached to the back of the single-roller screed finished the concrete surface without any trouble. This simple operation allowed the contractor to quickly cover the concrete surface after strike-off. The average compressive strength based on two sets of three cylinders each was 31.5 MPa (4570 psi).

Table 5.32 –Summary of Plastic Concrete Properties for LC-HPC-12

Bridge		Plastic Property [†]			
		Temperature, °C (°F)	Air Content, %	Slump, mm (in.)	Unit Weight, kg/m ³ (lb/ft ³)
56-57 LC-HPC-12	Average	14.5° (58°)	7.4	70 (2.75)	2259 (141.0)
Deck	Minimum	11.9° (53°)	6.2	45 (1.75)	2235 (139.5)
	Maximum	19.6° (67°)	8.1	90 (3.5)	2299 (143.5)

[†]Test results are from samples taken directly from the ready-mix truck prior to placement on the deck. No loss in the air content was observed after placement on the deck.

5.3.8 LC-HPC Bridge 13: Northbound US-69 over BNSF Railway

The thirteenth LC-HPC bridge is located on US-69 in Linn County, KS. Koss Construction was awarded the project and subcontracted with Beachner Construction to construct the bridge and O'Brien Ready-Mix to supply the concrete. The construction dates for the qualification slab and the bridge deck are shown in Table 5.33. A qualification batch was not required due to the considerable experience of O'Brien Ready Mix on LC-HPC-8 and 10. The individual aggregate gradations,

combined gradation, plastic concrete test results, and compressive strength test results are provided in Appendix D.

Table 5.33 – Construction Dates for LC-HPC-13

Item Constructed	Date Completed
Qualification Batch	--
Qualification Slab	4/16/08
Bridge Deck	4/29/08

The mixture design was based on the LC-HPC-12 mixture with a design w/c ratio of 0.44 and a cement content of 320 kg/m^3 (540 lb/yd^3). The cement content was later reduced to 317 kg/m^3 (535 lb/yd^3) following completion of the qualification slab to help limit the concrete slump. Additional details are provided with the discussion of the qualification slab. A total of three aggregates [crushed granite coarse aggregate, coarse natural sand (i.e., pea gravel), and natural sand] were required to meet the combined aggregate gradation requirements.

Qualification Slab – The qualification slab was placed on April 16, 2008 using a pump fitted with a bladder valve (shown in Fig. 5.5). No measures were taken to control concrete temperatures, which ranged at the high-end of the allowable limit from 23.3° to 23.9° C (74° to 75° F) for the four trucks required to complete the placement. The ready-mix supplier had some difficulties supplying concrete that met the specifications. The first two trucks arrived with 7.5 L/m^3 (1.5 gal/yd^3) of water withheld from the mixture and a Type A mid-range water reducer (lignosulfonate based). The slump for concrete taken from these trucks met the specification, but the air contents were low (5.7 and 6.0%). For the following two trucks, no water was withheld and the water-reducer dosage was reduced to zero. Slump values for these trucks increased to over 100 mm (4 in.) while the air content remained low. The

average slump and air content values for samples taken following placement were 115 mm (4.5 in.) and 6.2%, respectively.

Following completion of the qualification slab, the ready-mix supplier was asked to modify the mixture so that the slump could be maintained below 100 mm (4 in.) with no water withheld from the mixture. The ready-mix supplier achieved this goal by cutting the cement content from 320 to 317 kg/m³ (540 to 535 lb/yd³) while maintaining the *w/c* ratio at 0.44. This was the second LC-HPC bridge (after LC-HPC-7) that did not require a water reducer to consistently maintain workable concrete with slumps between 40 and 100 mm (1.5 and 4 in.).

LC-HPC Bridge Deck – A summary of the plastic concrete test results is shown in Table 5.34. Concrete from the first three trucks were sampled and tested directly from the ready-mix truck prior to placement on the deck. Based on three samples taken before and after the pump, air loss through the pump was limited to an average of 1.1% using a bladder valve. Concrete slump values were consistent throughout the placement with only one sample exceeding 100 mm (4 in.). The average values for slump, air content, and concrete temperature were 75 mm (3 in.), 8.1%, and 20.4° C (69° F). The samples for these tests were taken from the deck after placement with the pump. Concrete for this placement finished smoothly using a single roller from a double-drum roller screed with a pan drag supplemented by a bullfloat. A bridge-wide burlap drag mounted on a work bridge was used for a portion of the deck, but was removed because it tended to work ponded water into the concrete surface. Twenty-nine day compressive strengths measured for six lab-cured cylinders varied from 23.4 to 32.5 MPa (3390 to 4710 psi) with an average of 29.5 MPa (4280 psi).

Table 5.34 –Summary of Plastic Concrete Properties for LC-HPC-13

Bridge			Plastic Property [†]			
			Temperature, °C (°F)	Air Content, %	Slump, mm (in.)	Unit Weight, kg/m ³ (lb/ft ³)
54-66	LC-HPC-13	Average	20.4° (69°)	8.1	75 (3)	2266 (141.5)
Deck		Minimum	15.9° (61°)	6.8	45 (1.75)	2195 (137.0)
		Maximum	22.1° (72°)	9.5	125 (5)	2317 (144.6)

[†]Test results are from samples taken directly from the ready-mix truck prior to placement on the deck. Samples from three trucks were tested before and after the pump, and an average air content reduction of 1.1% was observed.

5.3.9 Summary of Lessons Learned

This section presents a summary of the lessons learned during the construction of LC-HPC-1 through 14, and in many cases, indicated how these lessons will be incorporated into future versions of the specifications to further improve bridge performance. As described in Sections 5.3.1 through 5.3.8, the majority of these experiences were positive, resulting in the successful completion of 12 LC-HPC bridge decks. The long-term performance of these decks will be measured over a period of several years; however, as described in the next section, the early-age cracking results indicate clearly that these specifications have reduced the level of cracking. The focus of this report is limited specifically to experiences with the concrete and aggregate. A complete discussion of the construction experiences and the associated lessons learned is provided by McLeod et al. (2009).

The construction of the LC-HPC decks generally begins with the selection of aggregates. This crucial step is necessary to ensure that the low paste volume LC-HPC is pumpable, placeable, and finishable. KU Mix has been used successfully on a number of occasions to both select and optimize the aggregate required to meet the combined gradation specifications. Natural fine and coarse sands selected to meet these requirements greatly aid the pumpability of these mixtures. On the other hand,

angular manufactured sands, in addition to excessively elongated aggregate particles, can impede the ability of the contractor to place concrete.

Careful consideration should be given to selecting and optimizing the aggregate blend so that the combined gradation meets the specification throughout the entire project. If necessary, the mixture should be re-optimized to account for “as-delivered” aggregate gradations and the mixture should be tested to ensure, at a minimum, that the mixture is placeable. In addition to changing aggregate gradations, special attention must be given to determining the free surface moisture contents of the aggregate before and during concrete placement. Aggregate stockpiles should be protected from radical changes in moisture contents and properly mixed to ensure reasonable uniformity. The quality control plan, required by the specifications, should include provisions to account for these important factors.

Concrete mixtures with design w/c ratios of 0.44 and 0.45 with cement contents of 317 or 320 kg/m^3 (535 or 540 lb/yd^3) have consistently pumped and finished well, while some of the placements cast with a design w/c ratio of 0.42 and a cement content of 317 kg/m^3 (535 lb/yd^3) have been difficult to place. A number of factors have contributed to these difficulties, including withholding a portion of the design mix water and overestimating the aggregate free surface moisture. Based on these experiences, future LC-HPC specifications will require as-batched w/c ratios of 0.43 to 0.45 and all of the design water to be added at the plant. Reduced w/c ratios increase concrete strengths with a concurrent reduction in the tensile creep capacity.

Twenty-eight day compressive strengths for the LC-HPC placements are shown in Fig. 5.20. For the lab-cured specimens, the compressive strengths vary from 28.2 MPa (4090 psi) to 44.0 MPa (6380 psi) for specimens cast with a design w/c ratio of 0.42 and from 25.6 MPa (3710 psi) to 41.3 MPa (5990 psi) for specimens cast with a design w/c ratio of 0.45. Part of these differences in compressive strengths is due to the use of different water reducers. The compressive strength of

cylinders cast during the construction of LC-HPC-4 and LC-HPC-5 highlights this difference. The LC-HPC-5 mixture, which was cast with a high-range water reducer (HRWR), had a compressive strength that was 10.9 MPa (1580 psi) greater than the LC-HPC-4 mixture, which contained a mid-range water reducer. Cylinders for both of these decks were cast with a w/c ratio of 0.42. Increased compressive strengths reduce tensile creep of concrete and increase the potential for cracking. Mixtures specified with a w/c ratio of 0.44 and a cement content of 320 kg/m^3 (540 lb/yd^3) may not require a HRWR to obtain a 75 mm (3 in.) slump.

In many cases, part of the problem with high slumps is based on requests from the contractor. Often, a slump of 100 mm (4 in.), the maximum allowed under the current specification, is set as the target slump, rather than the desired range of 40 to 75 mm (1.5 to 3 in.). Based on the experiences through the first 14 bridge however, these high slumps are not necessary to adequately place and finish LC-HPC. The maximum allowable slump for future versions of the specification will be 90 mm (3.5 in.) to help minimize settlement cracking while still maintaining placeable and finishable concrete. It is imperative that inspectors recognize the importance of limiting slump to ensure that proper enforcement is maintained throughout the placement.

A clear understanding of the testing schedule and how out-of-specification concrete will be handled should be established prior to placement of the qualification slab. Changes to the concrete properties resulting from the placement method should be considered – especially if the acceptance testing is performed on concrete taken directly from the back of the ready-mix truck. These changes are most easily accounted for by sampling concrete before and after placement. To minimize changes in concrete properties, two additional changes are planned for the upcoming specifications. First, if a pump is used for placement, a bladder valve or “S-Hook” must be fitted to the discharge hose. Typical air losses through a pump fitted with a

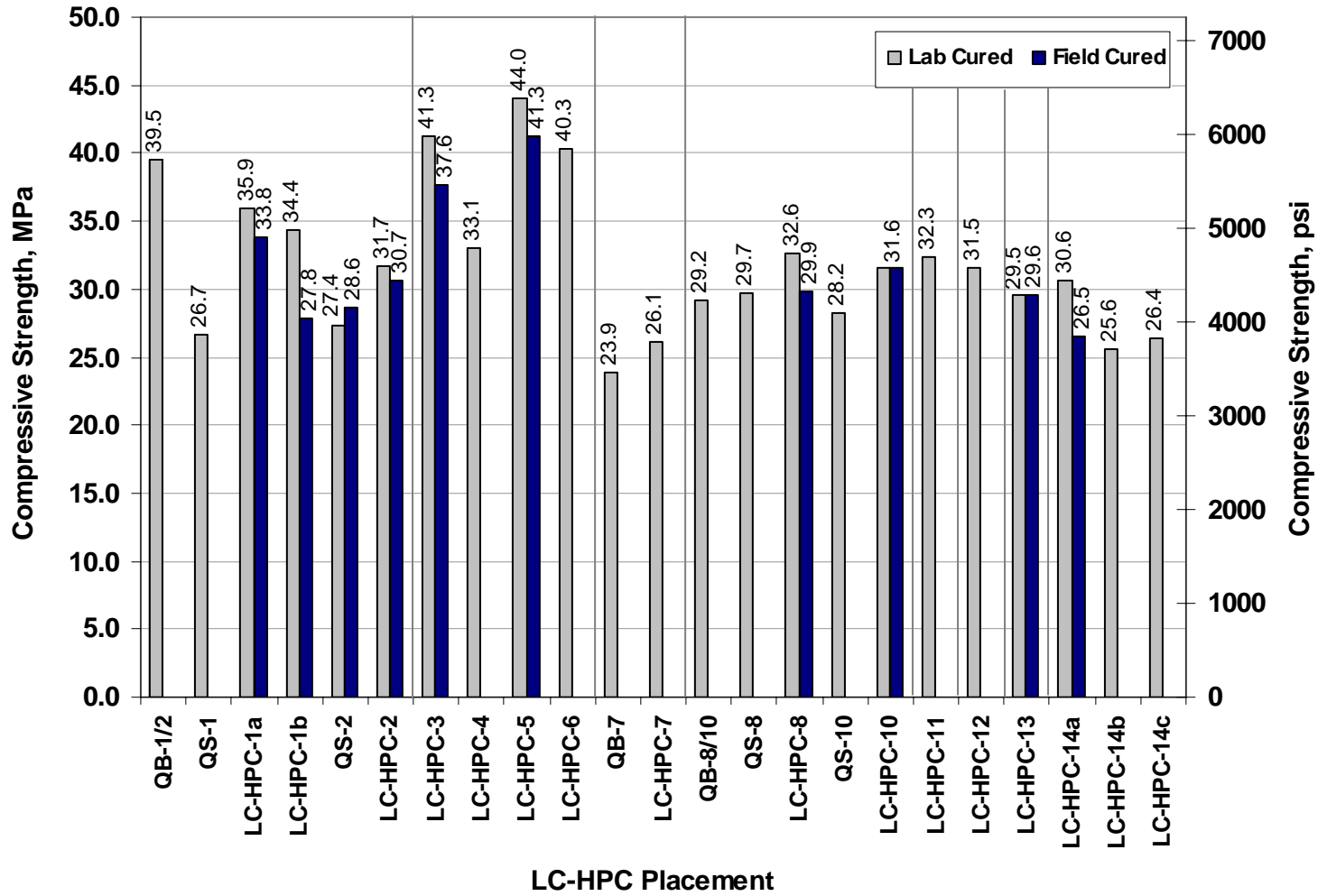


Fig. 5.20 – Twenty-eight day compressive strengths for all LC-HPC placements

bladder valve or “S-Hook” are at or below 1.5%. If a conveyor or bucket is used for placement, the maximum drop will be limited to 1.5 m (5 ft).

Finally, it is necessary that the same equipment used to place and finish the qualification slab as used to place and finish the bridge deck. This includes the same pump or conveyor and minimizes the potential for problems pumping or finishing the concrete during deck placement. Any changes to the concrete mixture design or aggregate gradations, other than re-optimizing the aggregate gradation based on the gradations of the as-delivered aggregates, should be accompanied by additional testing to ensure that the concrete remains placeable and finishable. In some cases, a qualification slab may not be necessary for experienced crews. However, the ability to adequately place and finish the concrete must be demonstrated prior to the actual deck placement.

5.4 CRACK SURVEY RESULTS AND EVALUATION

The performance of low-cracking high-performance concrete (LC-HPC) bridge decks is evaluated based on crack densities obtained in the field. These crack densities are compared to crack densities obtained for control decks surveyed as a part of this study and to data collected for other Kansas decks by Schmidt and Darwin 1995, Miller and Darwin 2000, and Lindquist et al. 2005. In addition, the influence of individual variables related to the deck age, deck type, and material properties are analyzed by comparing variables from these categories with measured crack densities from this study and previous studies. The influence of bridge design parameters and environmental conditions is covered by McLeod et al. (2009).

The balance of this section is divided into four parts. Section 5.4.1 examines the effect of age on bridge deck cracking, while Sections 5.4.2 and 5.4.3 compare the performance of LC-HPC decks with their associated control decks. Section 5.4.4 examines the influence of material properties on crack densities. The results presented in Sections 5.4.2 through 5.4.4 are presented two ways, using raw crack

density data and projected crack density data. The raw crack density data is based on the most recent crack survey for each placement, and the projected crack density represents the expected level of cracking at 78 months (6½ years). A discussion of the age-correction procedure is provided in Section 5.4.1.

A total of seven LC-HPC and seven control bridges have been surveyed to date. Results for these bridges are separated into four categories based on the type of superstructure. All seven of the monolithic LC-HPC decks are supported by steel girders, while the control decks make up the remaining three categories: five silica-fume overlay decks supported by steel girders (SFO), one monolithic deck supported by steel girders (MONO), and one monolithic deck supported by prestressed girders (MONO/PS). The crack density data and bridge data used as the basis of the comparisons that follow are presented in Table D.9.

5.4.1 Bridge Deck Cracking Versus Bridge Age

The crack density results for the 14 bridge decks surveyed to date are plotted versus bridge age in Fig. 5.21. At the time of the survey, the bridge decks varied in age from 5 to 37 months with an average age of 16 months. For bridge decks containing two separate placements, the age is calculated as the difference between the survey date and the date of the last concrete placement. Data points connected by lines indicate bridges that have been surveyed on two or three separate occasions. These results represent the crack density for the entire deck surface, with the exception of two bridges (LC-HPC-4 and Control-7), which have points plotted for each placement. The deck for LC-HPC-4 has two partial length placements with different concrete mixture designs (discussed in Section 5.3.5), and Control-7 consists of two partial-width placements that were constructed nearly six months apart. The crack densities for the eight control decks show substantial scatter with values that range from 0.000 m/m² to 0.665 m/m². The converse is true for the LC-HPC decks,

which have much lower crack density values that range from only 0.007 to 0.063 m/m^2 .

As shown in Fig. 5.21, the LC-HPC crack densities for the three decks surveyed on more than one occasion increase gradually over time. The average cracking rate for these bridge decks is 0.00111 $\text{m}/\text{m}^2/\text{month}$. For the five control decks surveyed multiple times, the crack density values increase rapidly following the first survey with an average cracking rate of 0.01373 $\text{m}/\text{m}^2/\text{month}$. For the two control decks surveyed three times, the cracking rate drops significantly following the second survey and the crack density appears to stabilize. Additional surveys are needed to fully assess the long-term performance of these decks, but surveys performed after 12 to 24 months appear to provide a better assessment of deck performance.

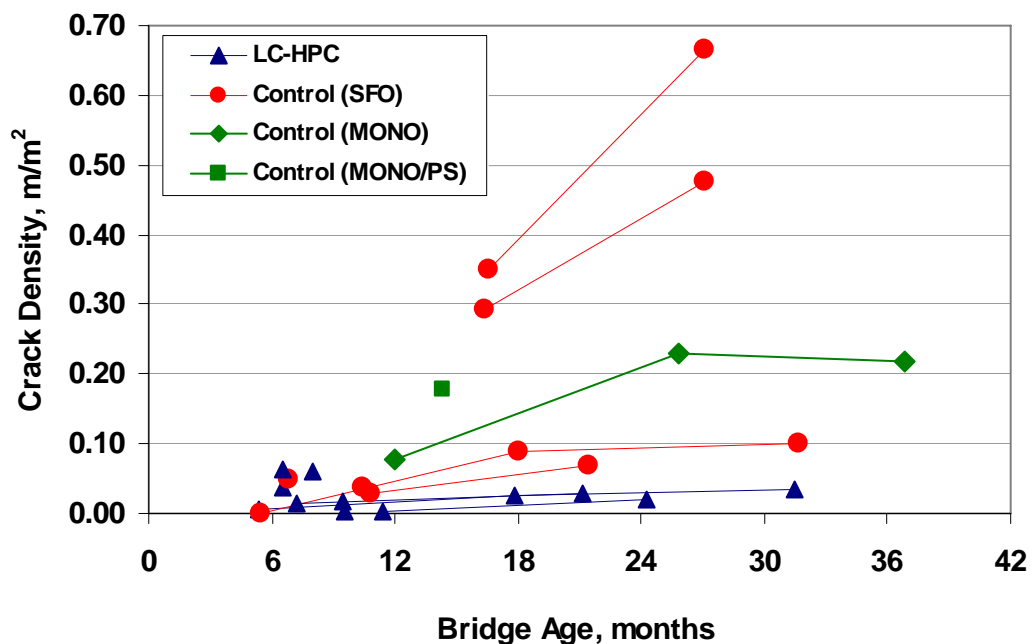


Fig. 5.21 – Crack density of bridge decks versus bridge age for all LC-HPC and control decks included in the analysis. Data points connected by lines indicate the same bridge surveyed more than once.

A summary of the individual cracking rates for the seven bridges surveyed more than once is provided in Table 5.35. These rates are compared to the cracking rates obtained by Lindquist et al. (2005) for monolithic (MONO) and silica-fume overlay (SFO) decks supported by steel-girders. The study by Lindquist et al. (2005) included a total of 14 monolithic decks and 20 silica-fume overlay decks that were surveyed two or three times. At the time of the surveys, these monolithic decks ranged in age from 12 to 220 months with an average age of 111 months, and the silica-fume overlay decks ranged in age from 4 to 142 months with an average age of 54 months. The cracking rates for these bridge types were calculated as 0.00125 and 0.00284 m/m²/month for the monolithic and silica-fume overlay bridges, respectively. As shown in Table 5.35, these rates appear to provide a good estimation of the LC-HPC decks, but significantly underestimate the cracking rate obtained for the control decks.

Table 5.35 –Summary of Cracking Rates for Bridges Surveyed Multiple Times

Bridge	Bridge Type	Cracking Rate, m/m ² /month				
		Between Surveys 1 & 2	Between Surveys 2 & 3	Average Rate [†]	Lindquist et al. (2005)	Difference, %
LC-HPC-1	MONO	0.00157	0.00054	0.00103	0.00125	18
LC-HPC-2	MONO	0.00107	--	0.00107	0.00125	14
LC-HPC-7	MONO	0.00124	--	0.00124	0.00125	1
Control-1/2	SFO	0.00709	0.00074	0.00374	0.00284	-32
Control-7 (East)	SFO	0.01714	--	0.01714	0.00284	-504
Control-7 (West)	SFO	0.00365	--	0.00365	0.00284	-29
Control-11	SFO	0.02968	--	0.02698	0.00284	-945
Control-Alt	MONO	0.01109	-0.00100	0.00595	0.00125	-374

[†]The average rate of cracking is calculated as the slope of the linear regression line calculated for each deck.

For comparison purposes, the crack density results plotted versus bridge age in Fig. 5.21 are plotted again in Fig. 5.22 along with the monolithic deck results from

Lindquist et al. (2005). It is clear that while these monolithic decks represent a much wider range in ages, the LC-HPC concrete decks are performing at a level approximately equal to or exceeding the best performing monolithic decks surveyed in Kansas.

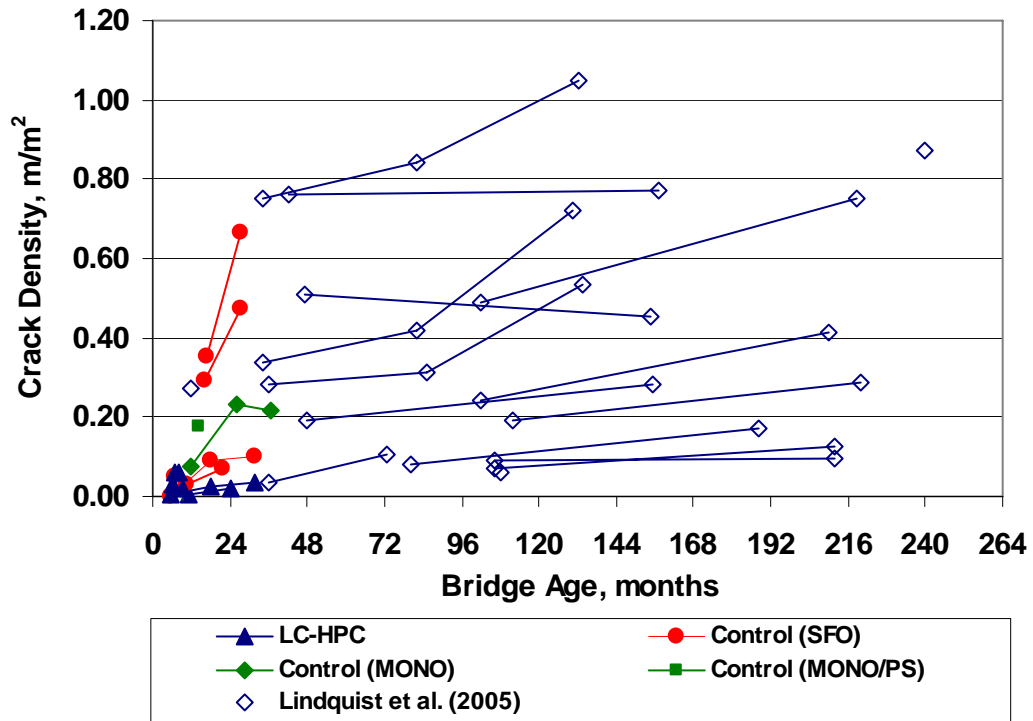


Fig. 5.22 – Crack density versus bridge age for the LC-HPC, control decks, and monolithic control decks surveyed by Lindquist et al. (2005). Observations connected by lines indicate the same bridge surveyed more than once.

5.4.2 Individual LC-HPC Crack Density Results

This section presents a bridge-by-bridge comparison of the crack densities and projected crack densities for the seven LC-HPC decks and their corresponding control decks. To do this, the individual crack densities are compared for each placement based on both the most recent survey results and the projected crack densities at 78 months (6½ years). These projected crack densities are calculated using the cracking rates obtained by Lindquist et al. (2005) and shown in Table 5.35. Using these rates, the raw crack densities are adjusted to an age of 78 months, the average age at the

time of the survey for all of bridges evaluated by Lindquist et al. (2005). These adjustments represent an age correction that helps to limit differences in deck performance due to age and provides an estimate of future performance. For bridges surveyed on more than one occasion (shown in Table 5.35), the projected crack density (or age-corrected crack density) is calculated by taking the average of the individual projected crack densities obtained for each survey.

A summary of the eleven decks included in the comparison is provided in Table 5.36. As indicated, the control decks for LC-HPC-5 and LC-HPC-6 have not been completed. These comparisons provide an initial evaluation of the LC-HPC decks, although clearly, additional surveys are needed to fully assess the long-term performance of these decks and the reliability of the cracking rates used to project crack densities. All of the control decks shown in Figs. 5.21 and 5.22 are not discussed in this section because they do not correspond to one of the LC-HPC decks for which crack data has been obtained.

Table 5.36 – LC-HPC and Corresponding Control Decks Surveyed to Date

LC-HPC Deck	Control Deck
LC-HPC-1	Control-1/2
LC-HPC-2	
LC-HPC-3	Control-3
LC-HPC-4	Control-4
LC-HPC-5	
LC-HPC-6	
LC-HPC-7	Control-7

5.4.2.1 LC-HPC-1 and 2 Crack Density Results

The crack density results for LC-HPC-1, LC-HPC-2, and Control-1/2 are shown in Figs. 5.23 through 5.25. The results for LC-HPC-1 and Control-1/2 include

three separate surveys performed over a 32-month period following construction. The results for LC-HPC-2 include two surveys performed over a 21-month period. Based on crack density results taken at similar ages (18 to 21 months), the control deck has more than three times the cracking of either of the LC-HPC decks. When the age-corrected crack densities are considered, the control deck has two times the level of cracking in the LC-HPC decks.

The crack density of LC-HPC-1 increases from 0.007 m/m^2 after only five months to 0.034 m/m^2 after 31 months (Fig. 5.23). Age-corrected values, indicated for each survey with by the vertical lines, range from 0.093 to 0.103 m/m^2 with an average of 0.098 m/m^2 . Crack densities for the two individual LC-HPC-1 placements are also given for each survey. The first placement exhibits more cracking than the second placement for all three surveys. The average age-corrected values for placements one and two are 0.109 and 0.086 m/m^2 , respectively.

The crack density results for LC-HPC-2 are shown in Fig. 5.24 and include two surveys performed 7 and 21 months after deck construction. Crack densities increase from 0.014 m/m^2 at 7 months to 0.029 m/m^2 at 21 months. The second crack density survey value (0.029 m/m^2 at 21 months) is similar to the crack density of LC-HPC-1 measured at a similar age (0.027 m/m^2 at 18 months). The individual age-corrected crack densities for the two LC-HPC-2 surveys vary by only 0.002 m/m^2 with an average age-corrected value of 0.102 m/m^2 . This age-corrected crack density is nearly identical to the age-corrected crack density for LC-HPC-1 (0.098 m/m^2).

The survey results for Control-1/2, which also consists of two separate placements, are shown in Fig. 5.25. The measured crack densities for the bridge deck increase rapidly from no cracking after five months to 0.099 m/m^2 after 31 months. This value is similar to the projected crack density value at 78 months for both LC-HPC-1 and 2. The average age-corrected crack density is 0.232 m/m^2 – more than twice the projected crack densities for LC-HPC-1 and 2.

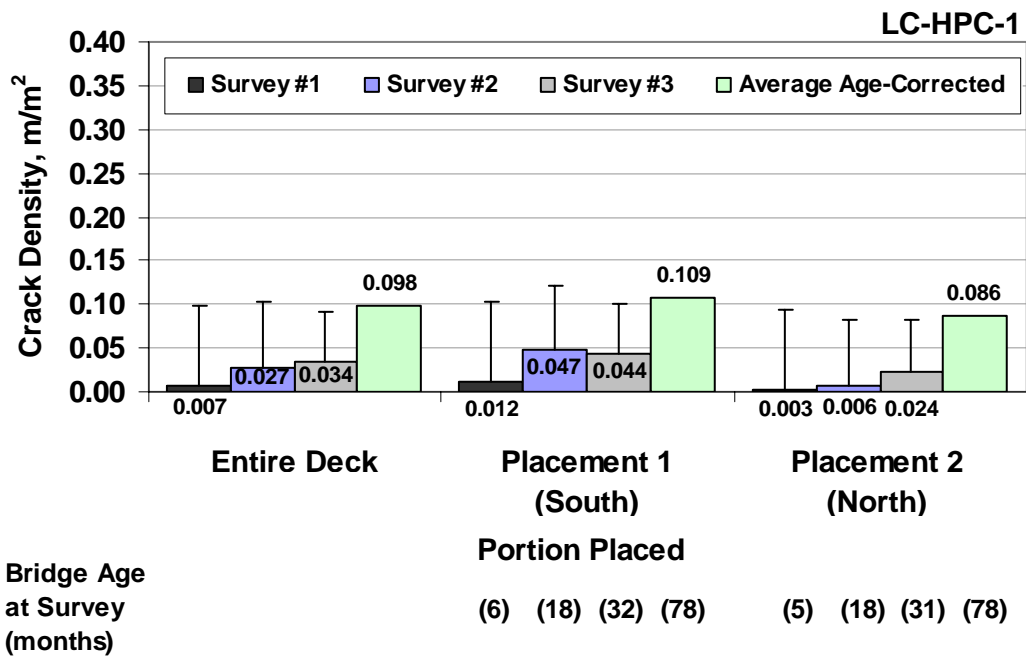


Fig. 5.23 – Crack density values for LC-HPC-1 and LC-HPC-1 placements.

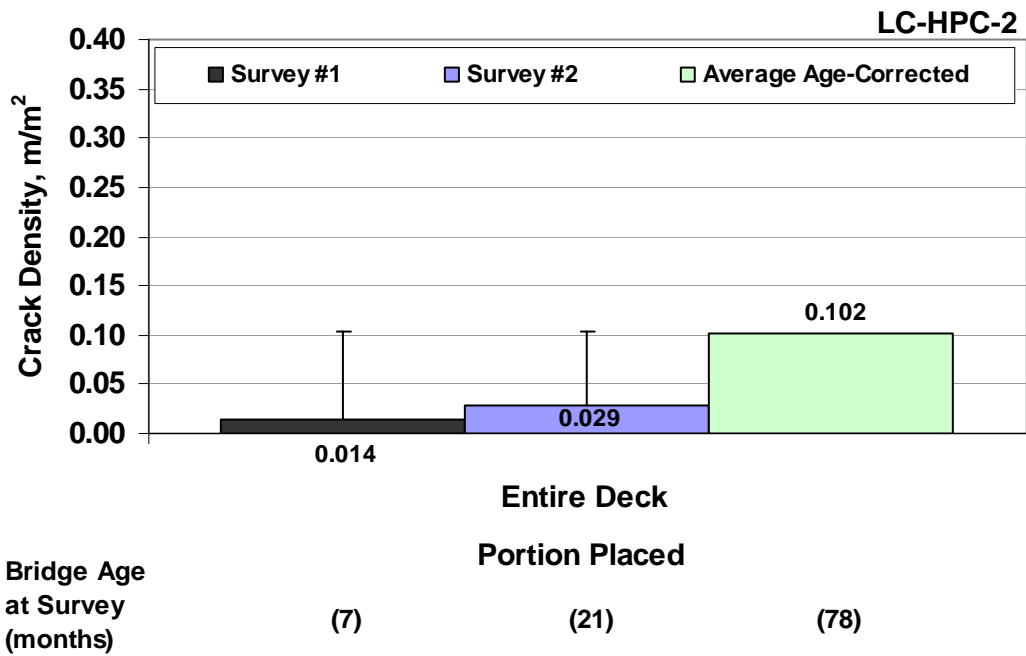


Fig. 5.24 – Age-corrected and uncorrected crack density values for LC-HPC-2

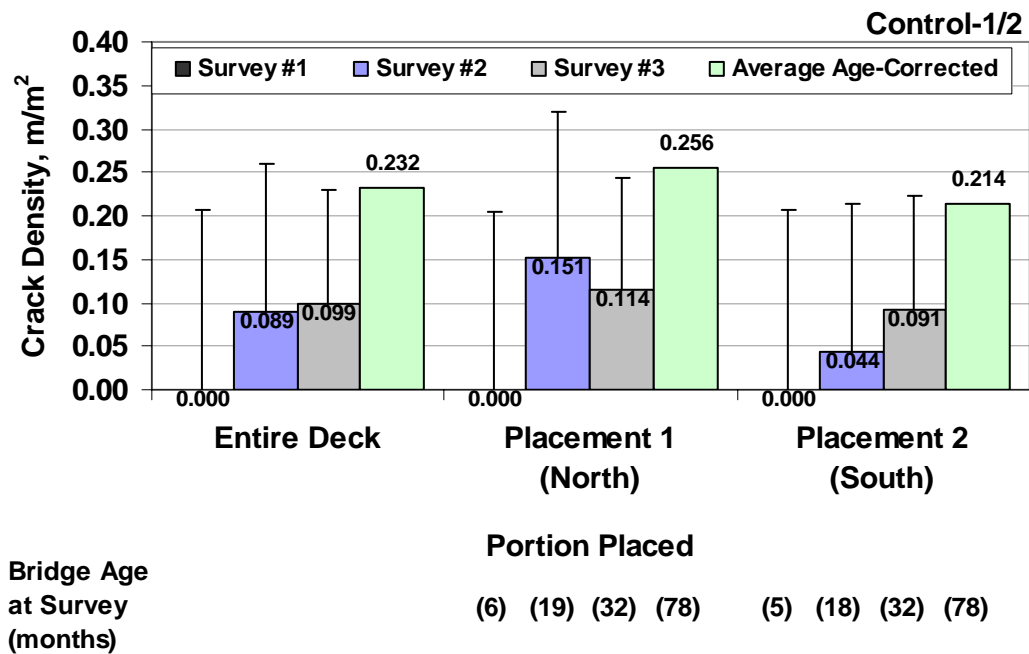


Fig. 5.25 – Age-corrected and uncorrected crack density values for Control-1/2

5.4.2.2 LC-HPC-3 through 6 Crack Density Results

The crack density results for LC-HPC-3 through 6 and Control-3 and 4 are shown in Figs. 5.26 and 5.27. These bridges have each been surveyed once between seven and 10 months after construction. The results are preliminary, especially given the rapid increase in cracking observed for Control-1/2. Construction for two of the control bridges (Control-5 and 6) is schedule for fall 2008.

As discussed in Section 5.3.5, two different w/c ratios (and paste contents) were used for the four LC-HPC bridges in this group. The first bridge, LC-HPC-4, was completed in two placements – both with w/c ratios of 0.42. The w/c ratio for the next two bridges constructed (LC-HPC-6 and 3) was increased to 0.45 due to difficulties pumping, finishing, and maintaining consistent plastic concrete properties. The w/c ratio for the last bridge (LC-HPC-5) ranged from 0.42 to 0.45. In addition to increasing the w/c ratio following the construction of LC-HPC-4, the type of water reducer was changed from a lignosulfonate-based mid-range water reducer (MRWR)

to a polycarboxylate-based high-range water reducer (HRWR). Interestingly, the concrete cast for LC-HPC-4 with a less efficient MRWR and a 0.42 w/c ratio had the lowest compressive strength compared to the other concrete placements cast with a HRWR and a 0.45 w/c ratio.

The crack density for LC-HPC-3 (shown in Fig. 5.26), measured only seven months after construction, is 0.032 m/m^2 , compared to a crack density of 0.037 m/m^2 for Control-3 at 10 months. These results do not indicate a significant difference in performance, but this difference is expected to increase over the next few years. The age-corrected crack densities are 0.122 and 0.229 m/m^2 for the LC-HPC deck and control deck, respectively.

The crack density results for LC-HPC-4 through 6 and Control-4 are shown in Fig. 5.27. The two LC-HPC-4 placements, cast with a w/c ratio of 0.42, have crack densities of 0.004 and 0.018 m/m^2 . The LC-HPC-5 placement, with w/c ratios ranging from 0.42 to 0.45, has a crack density of 0.059 m/m^2 , and LC-HPC-6, with a w/c ratio of 0.45, has a crack density of 0.063 m/m^2 . The crack density of the single control deck in this group completed to date is 0.050 m/m^2 . The projected age-corrected crack densities for the LC-HPC decks range from 0.090 to 0.153 m/m^2 compared to 0.252 for the control deck.

The difficulties involved in placing and finishing the 0.42 w/c ratio concrete used for LC-HPC-4 has not translated into more cracking. In fact, it appears that the reduced w/c ratio (and paste content) and the use of a MRWR may ultimately result in less cracking compared to the LC-HPC decks cast with a w/c ratio of 0.45 and a HRWR. The fifth and sixth LC-HPC bridges have more cracking than any of the other LC-HPC bridges surveyed to date. It is difficult to ascertain the exact cause of this increased cracking; however, some difficulties were identified during the two placements. For LC-HPC-6, the concrete slump frequently exceeded 100 mm (4 in.), and the average slump of 95 mm (3.75 in.) was near the maximum allowable slump

of 100 mm (4 in.). For LC-HPC-5, difficulties pumping the concrete and changes to the mixture design resulted in long delays in finishing and covering the deck with moist burlap.

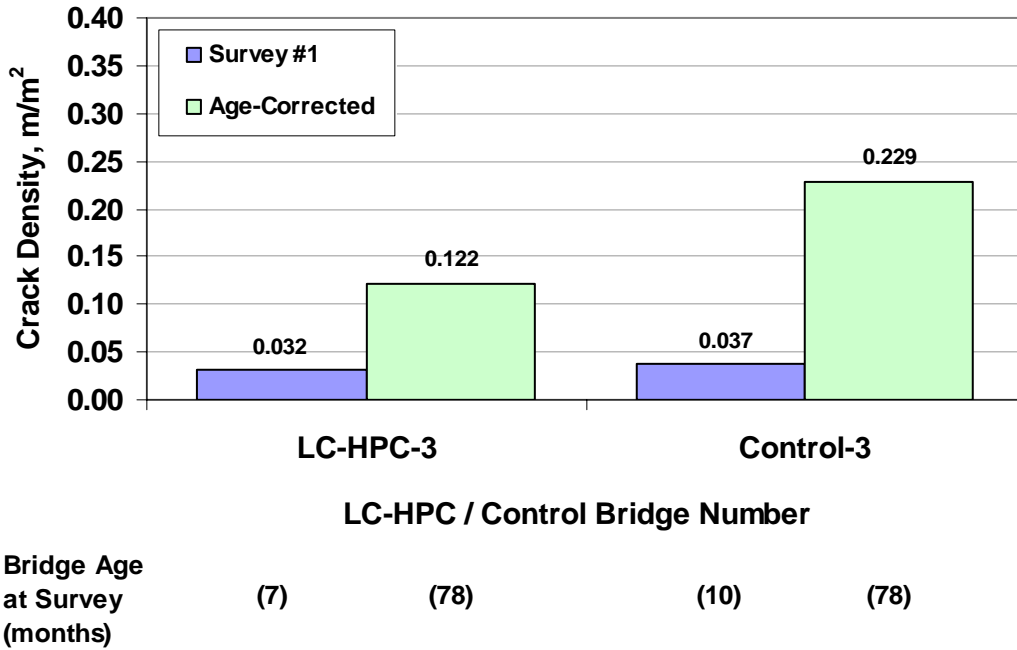


Fig. 5.26 – Crack density values for LC-HPC-3 and Control-3

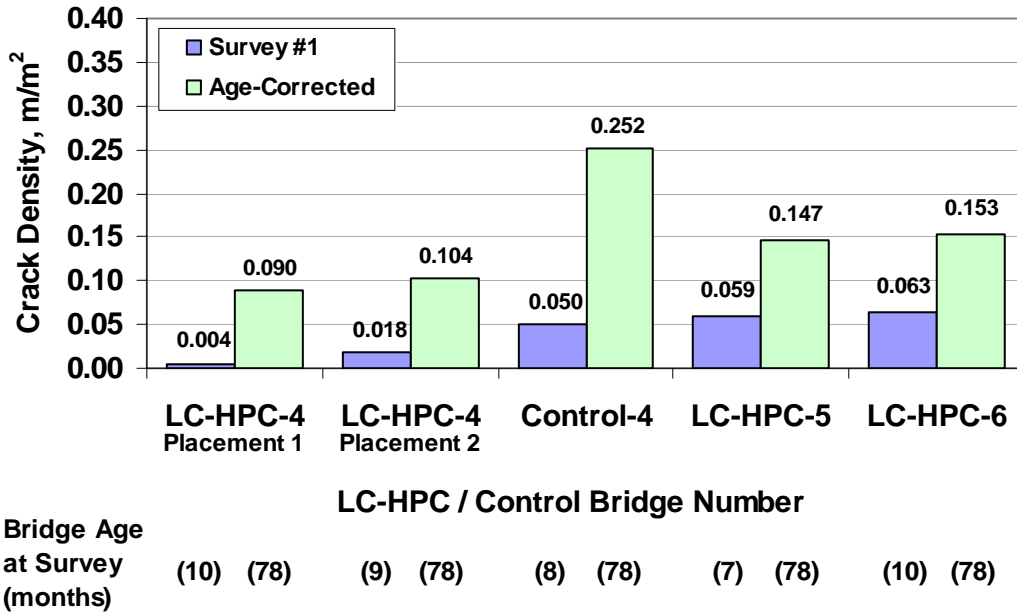


Fig. 5.27 – Crack density values for LC-HPC-4, Control 4, LC-HPC-5 and 6

5.4.2.3 LC-HPC-7 Crack Density Results

The crack density results for LC-HPC-7 and Control-7 are shown in Fig. 5.28. The results include data from two surveys performed over a 28-month period following construction. The control bridge consists of two placements, which are not presented together due to the large difference in the placement dates and crack densities. Unlike the first two group of bridges (discussed in Sections 5.4.2.1 and 5.4.2.2), the same contractor was not responsible for the construction of LC-HPC-7 and Control-7.

The crack density of LC-HPC-7 increases from 0.003 m/m^2 11 months after construction to 0.019 m/m^2 after 24 months (Fig. 5.28). The corresponding age-corrected values are 0.087 and 0.086 m/m^2 , respectively, with an average of 0.086 m/m^2 . These values are less than the crack densities obtained for LC-HPC-1 and 2. The crack density for the east Control-7 placement is much higher – increasing rapidly from 0.293 m/m^2 at 16 months to 0.476 m/m^2 at 27 months. Considerable variation exists between the age-corrected values for these two surveys due to the rapid increase in crack density that occurs between 11 and 22 months. These values vary from 0.468 to 0.621 m/m^2 for the first and second surveys, respectively. The west placement, constructed over five months after the east placement, has significantly less cracking with measured values of 0.030 and 0.069 m/m^2 at 16 and 27 months, respectively. The age-corrected crack densities for the west placement are 0.221 and 0.229 m/m^2 with an average of 0.225 m/m^2 .

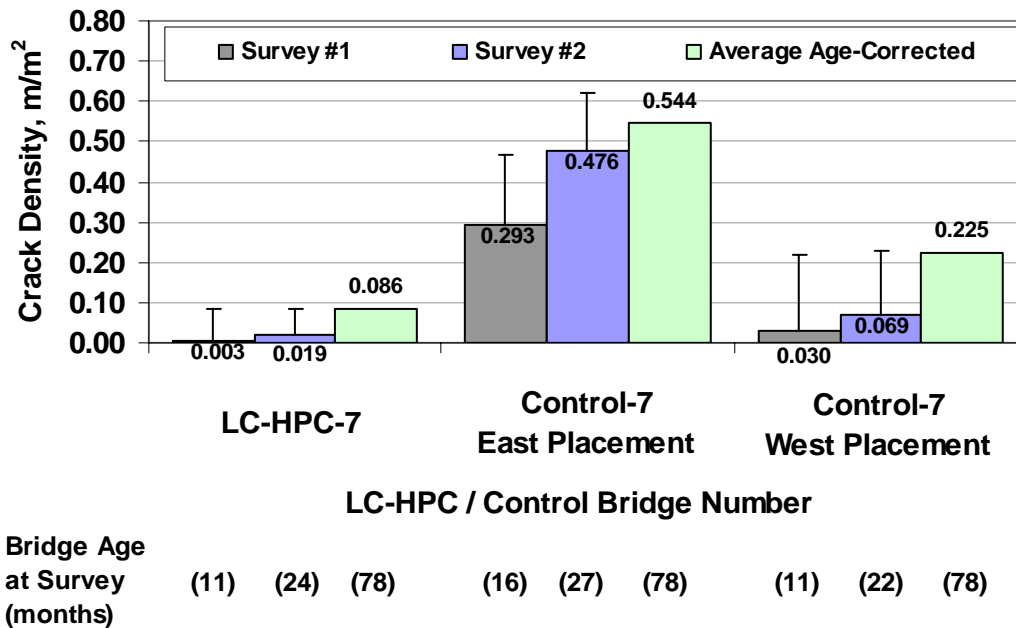


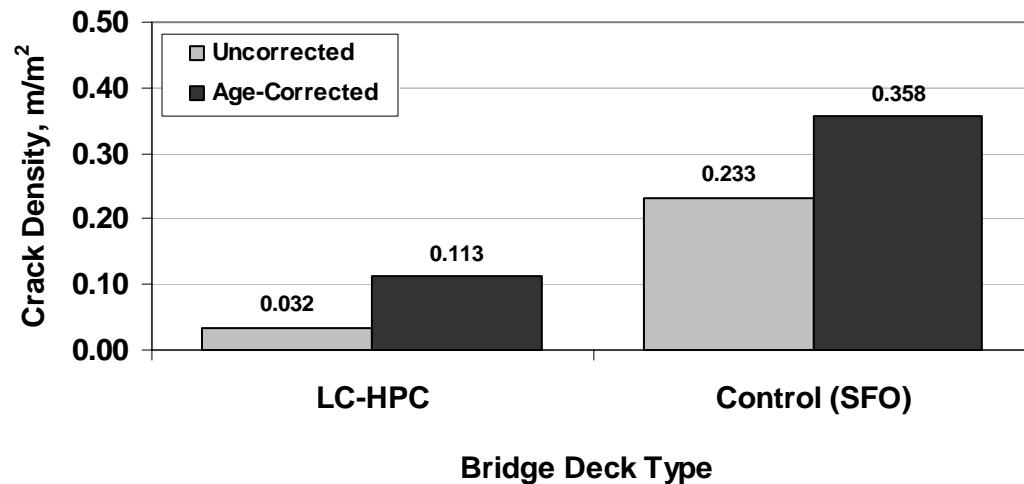
Fig. 5.28 – Crack density results for LC-HPC-7 and Control-7

5.4.3 Influence of Bridge Deck Type

Mean age-corrected and uncorrected crack densities are shown as a function of bridge deck type in Fig. 5.29. A total of four different bridge types have been surveyed to date, but only the LC-HPC decks and the control decks with a silica fume overlay (SFO) include more than one bridge. The Student’s t-test (described in Section 4.2) is used to determine whether the differences between the two samples represent actual differences between populations. The results indicate clearly that the current high-performance silica-fume overlay decks used in Kansas have significantly more cracking than the LC-HPC decks.

The mean uncorrected crack density for the LC-HPC decks is 0.032 m/m² compared to 0.233 m/m² for the silica fume overlays. The difference in crack densities for these placements is significant at $\alpha = 0.1$ (Table 5.37). This difference increases (due to the difference in cracking rates) slightly for the age-corrected crack densities, which are 0.113 and 0.358 m/m² for the LC-HPC and silica fume overlay

decks, respectively. Lindquist et al. (2005) reported a mean age-corrected crack density of 0.499 m/m² for bridges containing silica fume overlays and 0.328 m/m² for conventional monolithic decks. When the effect of cracking on corrosion is considered, these results support the use of LC-HPC decks to improve bridge deck performance and long-term durability.



	LC-HPC	Control (SFO)
Number of Bridges	(8)	(6)
Number of Surveys	(12)	(11)

Fig. 5.29 – Age-corrected and uncorrected crack density values for the entire LC-HPC-1 deck and individual placements.

Table 5.37 – Student’s t-test for average crack density versus bridge deck type [both age-corrected and uncorrected data (Fig. 5.29)]

Group 1	Group 2	Mean Crack Density (m/m ²)		Statistical Difference
		Group 1	Group 2	
LC-HPC	Control (SFO)	0.032	0.233	90
LC-HPC	Control (SFO)	0.113*	0.358*	Y

*Indicates average *age-corrected* crack density data rather than uncorrected data.

Note: For the results of the Student’s t-tests, “Y” indicates a statistical difference between the two samples at a confidence level of $\alpha = 0.02$ (98%). “N” indicates that there is no statistical difference at the lowest confidence level, $\alpha = 0.2$ (80%). Statistical differences at confidence levels at, but not exceeding $\alpha = 0.2, 0.1,$ and 0.05 are indicated by “80”, “90”, and “95,” respectively.

5.4.4 INFLUENCE OF MATERIAL PROPERTIES

Bridge deck survey data gathered for monolithic bridge decks in Kansas since the early 1990s by Schmitt and Darwin (1995), Miller and Darwin (2000), and Lindquist et al. (2005) are included with the data obtained in this study to increase the sample size and provide additional data that can be used to evaluate LC-HPC. This section examines the influence of five material-related variables on conventional monolithic decks typically used in Kansas and monolithic decks cast with LC-HPC. The variables evaluated include water content, cement content, cement-paste volume, compressive strength, and slump. Material properties for bridges in each of these categories are compared with the age-corrected crack densities and the differences between categories are tested for statistical significance using the Student's t-test. The uncorrected crack density results calculated with the most recent survey results are also included.

The results obtained from the previous surveys include a total of 16 monolithic decks, representing 35 individual placements. One conventional monolithic deck (alternate control) surveyed as a part of the current study brings the total number of conventional monolithic decks to 17. Fourteen of these bridges have been surveyed two or more times. As discussed previously, seven LC-HPC decks, representing nine individual placements have been surveyed. The number of LC-HPC placements included in the analysis of each variable is either eight or nine depending on the data available. The results show large amounts of scatter due to the myriad factors contributing to cracking, and for this reason, histograms are used (similar to the one shown in Fig. 5.29) to identify trends. Each category represents a range of values for the variable being considered and is defined by the midpoint of that range.

5.4.4.1 Water Content

The mean age-corrected crack densities (and uncorrected crack densities) are shown as a function of water content for individual monolithic placements in Fig. 5.30. Water content values for the conventional monolithic placements range from 143 to 167 kg/m³ (241 to 281 lb/yd³) with categories ranging from 147 to 165 kg/m³ (248 to 278 lb/yd³). For the LC-HPC placements, the water content values are either 133 or 144 kg/m³ (224 or 243 lb/yd³). These water contents also correspond to a reduction in the *w/c* ratio from 0.45 to 0.42. A total of eight LC-HPC placements and 34 monolithic placements are included in the comparison. The water content for the first LC-HPC-5 placement varied throughout the placement and is not included in the comparison.

The relationship between cracking and water content (Fig. 5.30) is clear: an increase in the water content results in an increase in crack density. This increase is most noticeable for mixtures with water contents that exceed the 147 kg/m³ (248 lb/yd³) category. Only a small difference in crack density (0.012 m/m²) is observed between the two LC-HPC categories, which is not statistically significant (Table 5.38). For the conventional placements, an increase in the water content from 147 to 165 kg/m³ (248 to 278 lb/yd³) increases crack density from 0.142 to 0.733 m/m². This increase is statistically significant at the highest level of confidence (Table 5.38). The uncorrected crack density data, also shown in Fig. 5.30, has an identical trend.

Due to the small number of placements in the first LC-HPC category [133 kg/m³ (224 lb/yd³)], many of the differences in crack density are not statistically significant (Table 5.38). The crack density for placements in the second LC-HPC category [144 kg/m³ (243 lb/yd³)], however, is statistically lower than the crack densities for placements in both the 156 and 165 kg/m³ (263 and 278 lb/yd³) categories (Table 5.38).

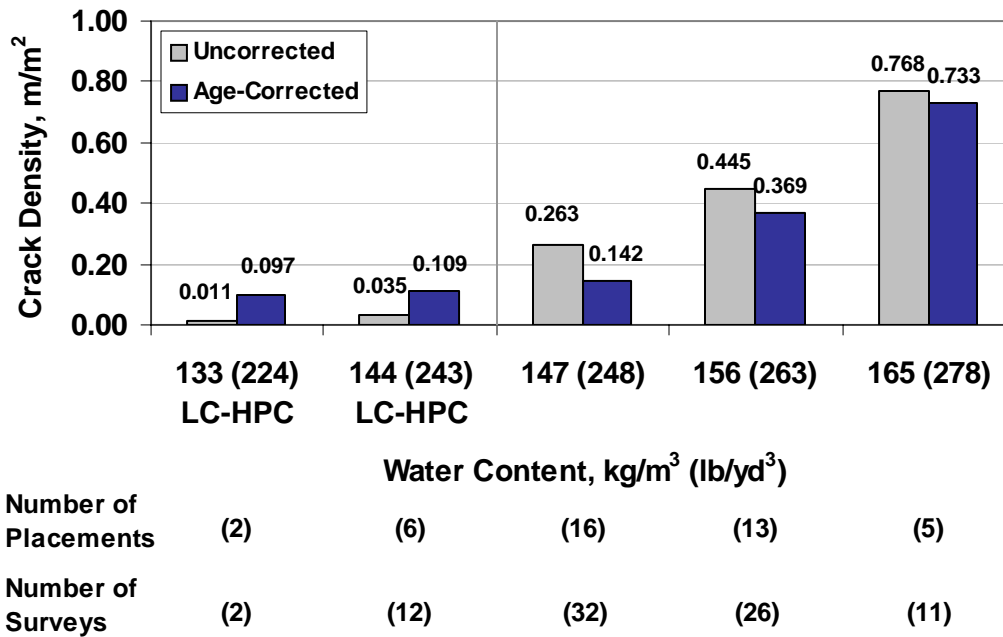


Fig. 5.30 – Mean age-corrected and uncorrected crack density values versus water content.

Table 5.38 – Student’s t-test for mean age-corrected crack density versus water content (Fig. 5.30)

Water Content, kg/m ³ (lb/yd ³)		Mean Age-Corrected Crack Density		Statistical Difference
Group 1	Group 2	Group 1	Group 2	
133 (224)*	144 (243)*	0.097	0.109	N
133 (224)*	147 (248)	0.097	0.142	N
133 (224)*	156 (263)	0.097	0.369	N
133 (224)*	165 (278)	0.097	0.733	Y
144 (243)*	147 (248)	0.109	0.142	N
144 (243)*	156 (263)	0.109	0.369	80
144 (243)*	165 (278)	0.109	0.733	Y
147 (248)	156 (263)	0.142	0.369	95
147 (248)	165 (278)	0.142	0.733	Y
156 (263)	165 (278)	0.369	0.733	90

Note: See the Table 5.37 note for an explanation of the terms “N”, “80”, “90”, “95”, and “Y”.
 *Indicates categories containing LC-HPC placements.

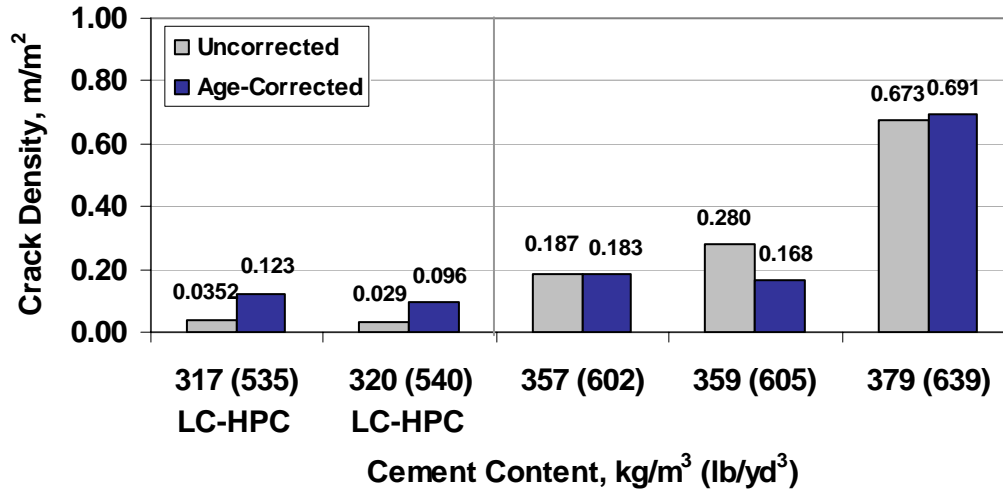
It is difficult to draw significant conclusions regarding the LC-HPC placements given the small sample size, but in terms of cracking, reducing the water content from 144 to 133 kg/m³ (243 to 224 lb/yd³) does not appear to play a significant role. In fact, the results do not indicate a significant increase in crack density until the water content is increased beyond the 147 kg/m³ (248 lb/yd³) category (Table 5.38). Based on these results, it is clear that emphasis should be placed on selecting a water content that enables the contractor to adequately place, finish, and cover the concrete in a timely fashion. Selecting a water content of 144 kg/m³ (243 lb/yd³) also enables the ready-mix supplier to use a lower water-reducer dosage. These mixtures tend to have reduced compressive strengths (due to more flocculated cement particles) leading to increased creep and reduced cracking.

5.4.4.2 Cement Content

For conventional monolithic placements, cement contents include 357 kg/m³ (602 lb/yd³), 359 kg/m³ (605 lb/yd³), and 379 kg/m³ (639 lb/yd³). The cement content for the LC-HPC placements is either 317 or 320 kg/m³ (535 or 540 lb/yd³). All nine LC-HPC placements and 33 conventional monolithic placements are included in the comparison.

The mean age-corrected crack density (and uncorrected crack density) for individual placements is shown as a function of cement content in Fig. 5.31. For the LC-HPC placements, an increase in the cement content from 317 to 320 kg/m³ (535 to 540 lb/yd³) results in a slight reduction in the crack density from 0.123 to 0.096 m/m². The reduction in crack density is statistically significant at $\alpha = 0.20$ (Table 5.39). For the conventional monolithic placements, the mean age-corrected crack density is 0.183 and 0.168 m/m² for cement contents of 357 and 359 kg/m³ (602 and 605 lb/yd³), which increases sharply to 0.691 m/m² as the cement content is increased to 379 kg/m³ (639 lb/yd³). The small difference in crack density between the 357 and 359 kg/m³ (602 and 605 lb/yd³) categories is not statistically significant, but the

increase in crack density observed for placements with cement contents of 379 kg/m³ (639 lb/yd³) is significant at the highest level of confidence (Table 5.39).



Number of Placements	(5)	(4)	(10)	(15)	(8)
Number of Surveys	(5)	(10)	(21)	(29)	(16)

Fig. 5.31 – Mean age-corrected and uncorrected crack density values versus cement content for monolithic placements.

Table 5.39 – Student’s t-test for mean age-corrected crack density versus cement content (Fig. 5.31)

Cement Content, kg/m ³ (lb/yd ³)		Mean Age-Corrected Crack Density		Statistical Difference
Group 1	Group 2	Group 1	Group 2	
317 (535)*	320 (540)*	0.123	0.096	80
317 (535)*	357 (602)	0.123	0.183	80
317 (535)*	359 (605)	0.123	0.168	N
317 (535)*	379 (639)	0.123	0.691	Y
320 (540)*	357 (602)	0.096	0.183	90
320 (540)*	359 (605)	0.096	0.168	N
320 (540)*	379 (639)	0.096	0.691	Y
357 (602)	359 (605)	0.183	0.168	N
357 (602)	379 (639)	0.183	0.691	Y
359 (605)	379 (639)	0.168	0.691	Y

Note: See the Table 5.37 note for an explanation of the terms “N”, “80”, “90”, “95”, and “Y”.

*Indicates categories containing LC-HPC placements.

The LC-HPC bridge decks with a cement content of 317 kg/m^3 (535 lb/yd^3) included in this comparison are LC-HPC-3 through 6. The concrete for these decks was difficult to pump due in part to the low cement content, but additional factors discussed in Section 5.3.5 also contributed. Three additional LC-HPC bridges were cast with a cement content of 317 kg/m^3 (535 lb/yd^3) but have yet to be surveyed. These surveys will be invaluable in further evaluating the effect of cement content on cracking for bridge cast with significantly reduced paste contents. It is clear, however, that the ability to place, finish, and cover the concrete quickly is more important than reducing the cement content from 320 to 317 kg/m^3 (540 to 535 lb/yd^3).

5.4.4.3 Percent Volume of Water and Cement

The percentage volume of water and cement in the concrete mixture is the constituent that undergoes the majority of the shrinkage so it comes as no surprise that this volume has a strong influence on the level of cracking observed in bridge decks. The mean age-corrected crack density (and uncorrected crack density) is shown as a function of paste volume in Fig. 5.32. The paste volume for the LC-HPC placements range from only 23.4 to 24.6% and are grouped together in one category. For the conventional monolithic placements, the paste volume ranges from 25.7 to 28.8% with categories of 26, 27, 28, and 29%. All nine of the LC-HPC placements surveyed to date and 34 monolithic placements are included in the comparison.

The highest crack densities occur for placements with the largest volume of cement paste. For the conventional monolithic placements, the mean age-corrected crack density is 0.684 and 0.733 m/m^2 for paste volumes of 28 and 29%, respectively. Crack densities decrease considerably to 0.192 and 0.163 m/m^2 as the paste volume decreases to 26 and 27%, respectively. As the paste volume is reduced further for the LC-HPC placements, the mean age-corrected crack density decreases to 0.111 m/m^2 .

Many of the differences observed between categories are statistically significant (Table 5.40).

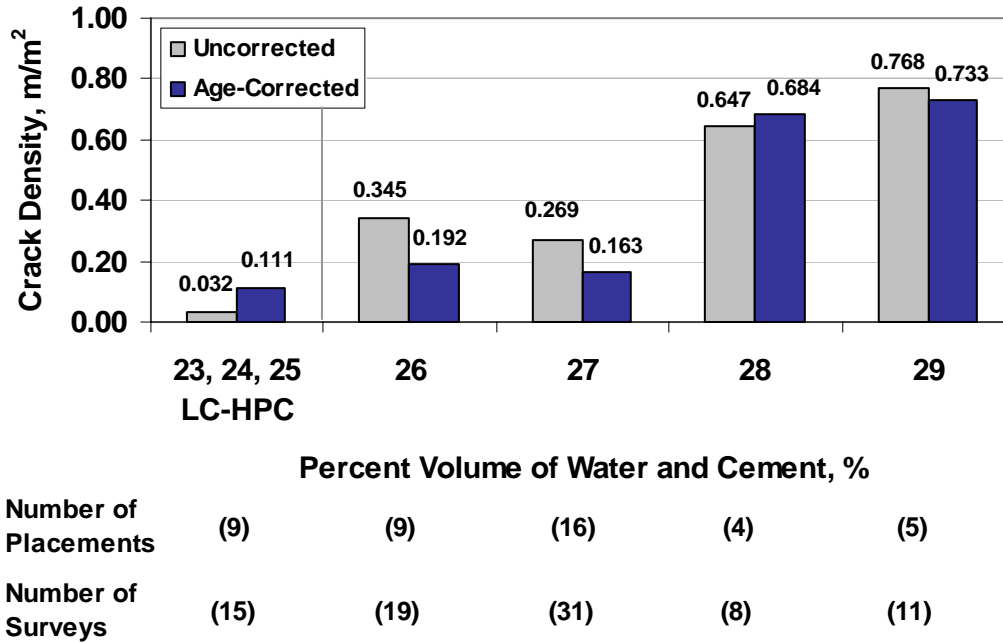


Fig. 5.32 – Mean age-corrected and uncorrected crack density values versus percent volume of water and cement for monolithic placements.

Table 5.40 – Student’s t-test for mean age-corrected crack density versus percent volume of water and cement (Fig. 5.32)

Paste Volume, %		Mean Age-Corrected Crack Density		Statistical Difference
Group 1	Group 2	Group 1	Group 2	
23, 24, 25*	26	0.111	0.192	Y
23, 24, 25*	27	0.111	0.163	N
23, 24, 25*	28	0.111	0.684	Y
23, 24, 25*	29	0.111	0.733	Y
26	27	0.192	0.163	N
26	28	0.192	0.684	Y
26	29	0.192	0.733	Y
27	28	0.163	0.684	Y
27	29	0.163	0.733	Y
28	29	0.684	0.733	N

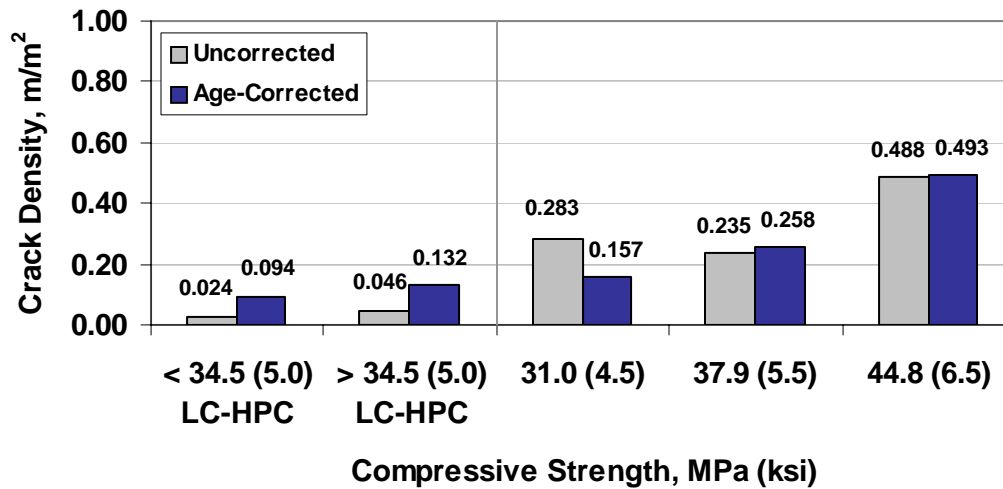
Note: See the Table 5.37 note for an explanation of the terms “N”, “80”, “90”, “95”, and “Y”.

*Indicates categories containing LC-HPC placements.

5.4.4.4 Compressive Strength

Mean age-corrected (and uncorrected) crack density for individual placements is shown as a function of compressive strength in Fig. 5.33. The compressive strengths are based on cylinders cast in the field during deck placement and cured in the laboratory for the balance of 28 days (cylinders for the first LC-HPC placement were only cured for 27 days). For the LC-HPC placements, compressive strength varies from 26.1 to 44.0 MPa (3790 to 6380 psi) with two categories: greater than or less than 31 MPa (5.0 ksi). For the conventional monolithic placements, compressive strength varies from 28.8 to 51.2 MPa (4170 to 7430 psi) with categories ranging from 31 to 45 MPa (4.5 to 6.5 ksi). A total of eight LC-HPC placements and 30 monolithic placements are included in the comparison.

The relationship between compressive strength and cracking is clear for both the LC-HPC placements and the conventional monolithic placements. For the LC-HPC placements, the mean age-corrected crack density increases from 0.094 m/m² for placements in the first category [<34.5 MPa (5.0 ksi)] to 0.132 m/m² for placements in the second category [>34.5 MPa (5.0 ksi)]. This increase in crack density is significant at $\alpha = 0.02$ (Table 5.41). An even larger difference is observed for the conventional monolithic decks, where the mean age-corrected crack density increases from 0.157 m/m² to 0.493 m/m² as the compressive strength increases from 31.0 to 44.8 MPa (4.5 to 6.5 ksi). This increase is significant at the highest level of confidence, $\alpha = 0.05$ (Table 5.41).



	Compressive Strength, MPa (ksi)				
Number of Placements	(4)	(4)	(7)	(13)	(10)
Number of Surveys	(8)	(6)	(13)	(27)	(23)

Fig. 5.33 – Mean age-corrected and uncorrected crack density values versus measured air content for monolithic placements.

Table 5.41 – Student’s t-test for mean age-corrected crack density versus compressive strength (Fig. 5.33)

Compressive Strength, MPa (ksi)		Mean Age-Corrected Crack Density		Statistical Difference
Group 1	Group 2	Group 1	Group 2	
< 34.5 (5.0)*	> 34.5 (5.0)*	0.094	0.132	Y
< 34.5 (5.0)*	31.0 (4.5)	0.094	0.157	N
< 34.5 (5.0)*	37.9 (5.5)	0.094	0.258	80
< 34.5 (5.0)*	44.8 (6.5)	0.094	0.493	95
> 34.5 (5.0)*	31.0 (4.5)	0.132	0.157	N
> 34.5 (5.0)*	37.9 (5.5)	0.132	0.258	N
> 34.5 (5.0)*	44.8 (6.5)	0.132	0.493	90
31.0 (4.5)	37.9 (5.5)	0.157	0.258	N
31.0 (4.5)	44.8 (6.5)	0.157	0.493	95
37.9 (5.5)	44.8 (6.5)	0.258	0.493	95

Note: See the Table 5.37 note for an explanation of the terms “N”, “80”, “90”, “95”, and “Y”.
 *Indicates categories containing LC-HPC placements.

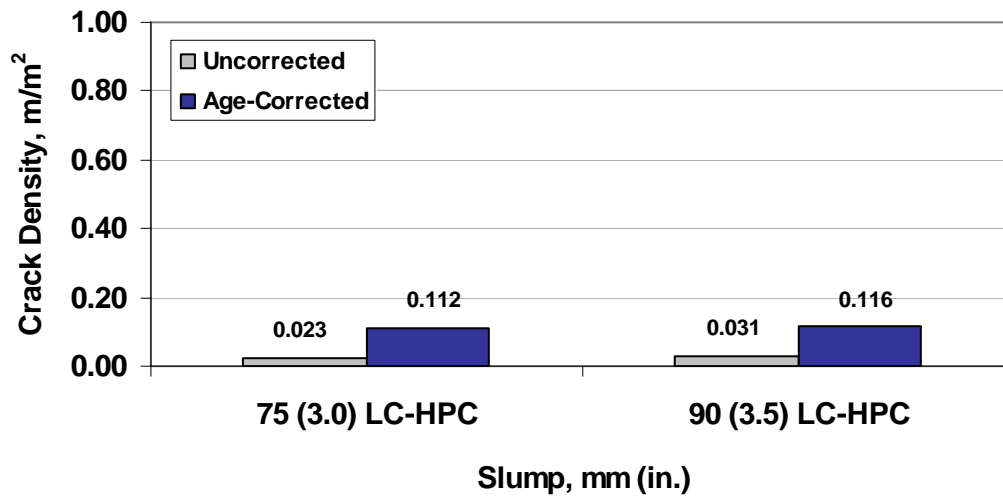
Limiting compressive strengths is recognized by many researchers as a way to limit the amount of cracking. Krauss and Rogalla recommend 28-day compressive strengths between 21 and 28 MPa (3000 and 4000 psi). Lower compressive strengths coincide with higher levels of creeps which can alleviate some of the tensile stresses that result in cracking. It should be pointed out that three of the four placements in the second category [>34.5 (5.0)] were cast with a high-range water reducer (HRWR) and a 0.45 w/c ratio. The four placements in the first category [<34.5 (5.0)] were either cast without a water reducer or with a mid-range water reducer and w/c ratios of 0.42 or 0.45. High-range water reducers should be used with caution only when absolutely necessary to achieve a slump of 75 mm (3 in.).

5.4.4.5 Slump

Concrete slump, in addition to bar size and top cover depth, has long been recognized as a key controller of settlement cracking (Dakhil, Cady, and Carrier 1975). Lindquist et al. (2005) examined 31 monolithic placements, cast primarily without water reducers, with slumps that ranged from 40 to 75 mm (1.5 to 3 in.). As a result, the slump for these placements was mainly a function of the water content – a key factor influencing crack density (Fig. 5.30). Using the technique of dummy variables, the influence of water content on crack density was removed helping to isolate the influence of slump. Crack density was found to increase from 0.11 to 0.22 m/m^2 as the slump increased from 40 to 75 mm (1.5 to 3 in.).

Due to the low paste content in LC-HPC, the majority of placements (16 of 18) in this study were cast with a water reducer to achieve the desired workability. This key difference makes a direct comparison impossible. For the LC-HPC placements, the influence of slump on crack density is shown in Fig. 5.34. The average slump values vary from 55 to 95 mm (2.25 to 3.75 in.) and are separated into three categories: 50 mm (2.5 in.), 75 mm (3 in.), and 90 mm (3.5 in.). Only one placement (LC-HPC-4 placement 1) falls into the first category and is therefore

excluded from the comparison. For the placements in the remaining two categories, there is a slight increase in crack density from 0.023 to 0.031 m/m^2 as the slump increases from 75 to 90 mm (3 to 3.5 in.) for the uncorrected data, but a significant difference is not observed for the age-corrected values, 0.112 and 0.116 m/m^2 , respectively (Table 5.42).



	75 (3.0) LC-HPC	90 (3.5) LC-HPC
Number of Placements	(5)	(3)
Number of Surveys	(8)	(6)

Fig. 5.34 – Mean age-corrected and uncorrected crack density values versus slump for monolithic placements.

Table 5.42 – Student’s t-test for mean age-corrected crack density versus slump (Fig. 5.34)

Slump, mm (in.)		Mean Age-Corrected Crack Density		Statistical Difference
Group 1	Group 2	Group 1	Group 2	
76 (3.0)	89 (3.5)	0.112	0.116	N

Note: See the Table 5.37 note for an explanation of the terms “N”, “80”, “90”, “95”, and “Y”.

5.5 LC-HPC COSTS

The relative cost of low-cracking high-performance concrete (LC-HPC) compared to similar control decks is a significant factor contributing to the feasibility of implementing future LC-HPC bridge decks. A discussion of these costs for the 14 Kansas decks and their corresponding control decks is provided in this section. The awarded contract cost for the LC-HPC and control concrete, reported on a cubic meter and a cubic yard basis for each deck, includes the concrete material costs, placement operations, and all falsework and forming that is required for elements above the beam seat. These costs include the barrier rails. The reinforcing steel and the qualification slabs (for the LC-HPC bridges) are separate bid items that are not included individually in the bridge deck concrete costs. It should be noted, however, that the reinforcing steel required for the qualification slab is included in the cost of the slab. The relative cost of the qualification slabs compared to the LC-HPC bridge decks is addressed separately.

All of the bridges (and control bridges) in this study, with the exception of LC-HPC-14, were let in larger contracts awarded to the lowest overall project bidder. The contract price awarded for each bridge is the focus of this section, but it should be noted that the lowest overall bidder did not necessarily have the lowest concrete bid. Eight of the 14 LC-HPC bridges and eight of the 12 control bridges were awarded to contractors with both the lowest overall project bid and the lowest concrete bid. The number of bids for each project varied from as many as six for the alternate control bridge to only one for LC-HPC-11. These bid metrics are provided for each of the bridges in Appendix E.

The standard high-performance bridge deck used in Kansas consists of a concrete subdeck protected by a silica-fume overlay. The subdeck and silica-fume overlay are listed as a separate bid items, but for this comparison, the two are combined to provide a reasonable cost comparison between the two protection

systems. The silica-fume overlay bid quantity, bid on a square meter or square yard basis, is converted to a volume using the overlay thickness and added to the cost of the subdeck. Two of the control bridges (Control-8/10 and Control-Alt) are monolithic decks located on low traffic-volume roads that do not have silica-fume overlays. The alternate control deck (denoted Control-Alt) is not specifically paired with a corresponding LC-HPC deck.

The bridges built in this study can be divided into two groups: those built in urban areas and those built in rural areas. Standard bridges built in urban areas are generally more expensive due to a number of factors. In the Kansas City Area, for example, union wages in addition to tighter material restrictions mandated by the Kansas City Metro Materials Board result in higher costs. Control bridges 3 through 7 and 14 fall under the jurisdiction of the Metro Materials Board, which most notably, require the use of a coarse aggregate with an absorption of less than 0.5% (compared to 0.7% in the LC-HPC specification). Granite or quartzite is imported to meet this specification, and for the control decks specific to this study, the same granite that was used for all of the LC-HPC decks (except LC-HPC-11) was used for the control decks. The rural control decks do not have a similar restriction, and as a result, are generally less expensive than their associated LC-HPC decks.

The awarded contract cost and range of bids, in dollars per cubic meter and dollars per cubic yard, are shown in Figs. 5.35 for *urban* bridges built in the Kansas City Metropolitan or Topeka areas. The first two bridges, LC-HPC-1 and 2, with concrete costs of \$1,800 and \$1,600/m³ (\$1,376 and \$1,223/yd³), respectively, are significantly more expensive than Control-1/2. The costs of these first two bridges include a large amount of speculation regarding the risk associated with these new decks. In fact, the range of bids for these two decks [\$1,303 and \$1,471/m³ (\$996 and \$1,124/yd³) for LC-HPC-1 and 2, respectively] is nearly as large as the winning bids. Interestingly, the subcontractor responsible for constructing LC-HPC-1 and 2 was

awarded the contract for LC-HPC-3 through 6 before LC-HPC-1 and 2 were constructed. For these four decks, the price varied from \$746 to \$914/m³ (\$570 to \$699/yd³) compared to \$795 to \$858/m³ (\$608 to \$656/yd³) for the control decks. The significant reduction in the cost for these LC-HPC decks and the close proximity in cost to their associated control decks indicate very little difference in cost between the two high-performance deck types. Different contractors in significantly different markets were awarded the contracts for Control-7 and LC-HPC-7. This may at least partly explain why the control deck was \$198/m³ (\$152/yd³) more expensive than the corresponding LC-HPC deck, \$750 versus \$948/m³ (\$573 versus \$725/yd³). The cost of the LC-HPC-14 deck concrete is the third highest among urban bridge at \$825/m³ (\$1,079/yd³), and LC-HPC-14 was not part of a significantly larger project. With the exception of the first two decks, the concrete costs for the LC-HPC decks compared to the control decks are very similar.

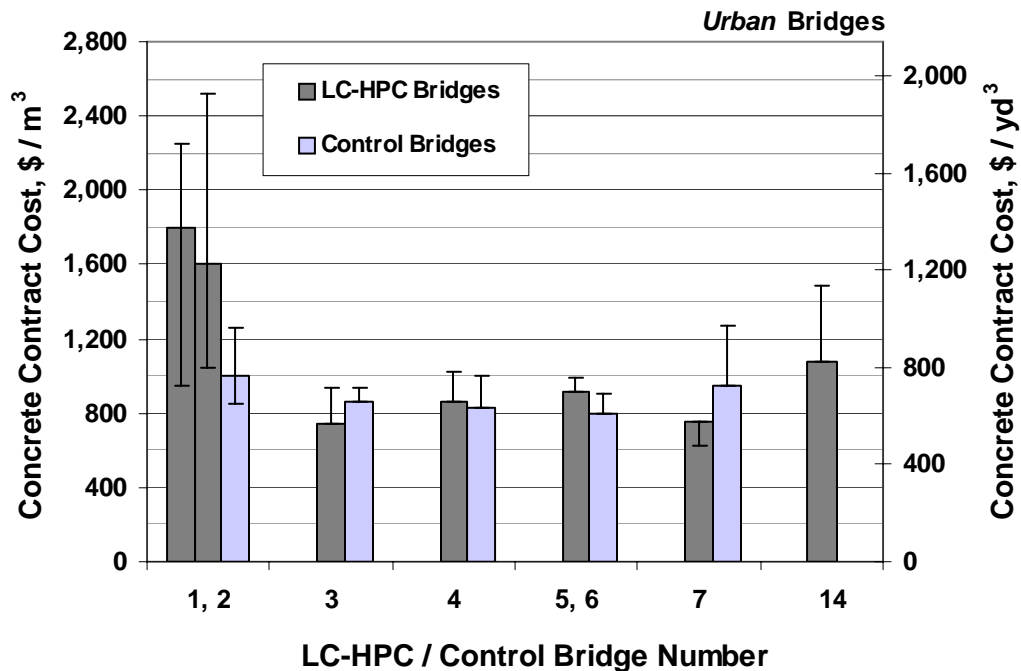
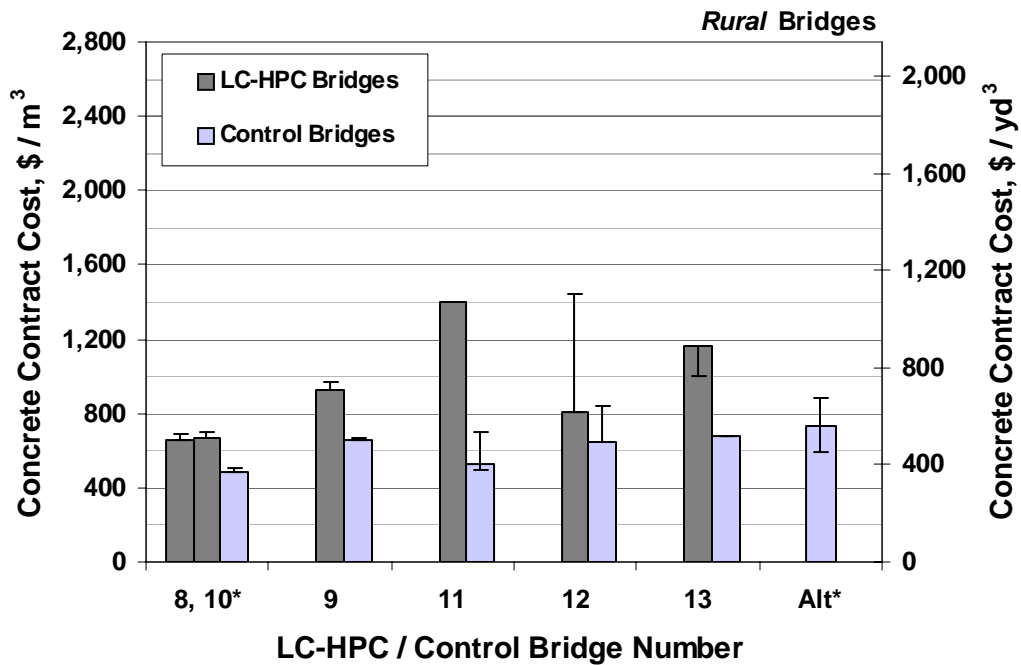


Fig. 5.35 – Awarded concrete cost and range of non-winning bids for low-cracking high-performance concrete and their associated concrete for control bridges built in the Kansas City metropolitan or Topeka areas (*urban* areas).

The cost of the LC-HPC and the associated control bridges built in *rural* areas is shown in Fig. 5.36. The control decks for this series of decks utilize locally available limestone that is less expensive than the imported granite or quartzite required for the control decks in the Kansas City Metropolitan area. As a result, all of the *rural* control decks are less expensive than their paired LC-HPC decks, which require the higher cost aggregate. In addition to the less restrictive requirements on the coarse aggregate, Control-8/10 and the alternate control are monolithic decks without silica fume overlays. LC-HPC-8 and 10, both constructed with prestressed girders, are the two least expensive LC-HPC decks in the study at \$655 and \$665/m³ (\$501 and \$508/yd³), respectively. The cost for Control-8/10 is slightly less at \$485/m³ (\$371/yd³). Bridges LC-HPC-9 and Control-9 were awarded to the same contractor under the same project as LC-HPC-8 and 10 and Control-8/10. The costs for these two decks was \$925 and \$662/m³ (\$707 and 506/yd³), respectively. Part of the reason these bridges are more expensive is due to the increased costs associated with spanning a river as compared to a highway. LC-HPC-11 and Control-11 were awarded to different contractors in different counties, and in addition, LC-HPC-11 was bid on by only one contractor. The contract containing LC-HPC-12 was awarded to the same contractor that was awarded LC-HPC-11. Interestingly, the bid for LC-HPC-12 was let prior to construction of LC-HPC-11 and was still considerably less.



*Control-8/10 and Control-Alt are monolithic decks cast without a silica-fume overlay.

Fig. 5.36 – Awarded concrete cost and range of non-winning bids for low-cracking high-performance concrete and the associated concrete for control bridges built in *rural* areas.

The qualification slab is required for LC-HPC decks to ensure that the ready-mix supplier and contractor can adequately produce, place, finish, and cure the LC-HPC and must be completed prior to placing the bridge deck. The qualification slab requirement has been waived for some bridges in multiple bridge contracts, and in the future, the slab may not be necessary for construction crews with considerable experience successfully placing LC-HPC bridge decks. For the near future, however, the qualification slab will remain an integral part of the specifications and will remain part of the cost for these decks.

The awarded contract cost and range of bids, in dollars per cubic meter and dollars per cubic yard, for the LC-HPC used in the qualification slab and the bridge deck is shown in Fig. 5.37. The unit cost of the qualification slab concrete either equals or exceeds the cost of the deck concrete. With the exception of LC-HPC-1 and

2, the difference in the awarded costs for the qualification slab and bridge concrete varies from \$0 to \$645/m³ (0 to \$493/yd³) with an average cost of \$386/m³ (\$295/yd³). Most of the difference in these costs is likely a result of the fixed mobilization costs and the cost of the reinforcing steel. As noted previously, the qualification slab cost includes the reinforcing steel while the bridge deck cost does not. Perhaps a more meaningful evaluation of the qualification slab cost is provided in Fig. 5.38, which presents the total cost of the qualification slab. The first two slabs cost nearly \$150,000 each, although this cost decreased significantly for the remaining qualification slabs, which ranged in cost from \$26,250 to \$43,453 with an average of \$33,619.

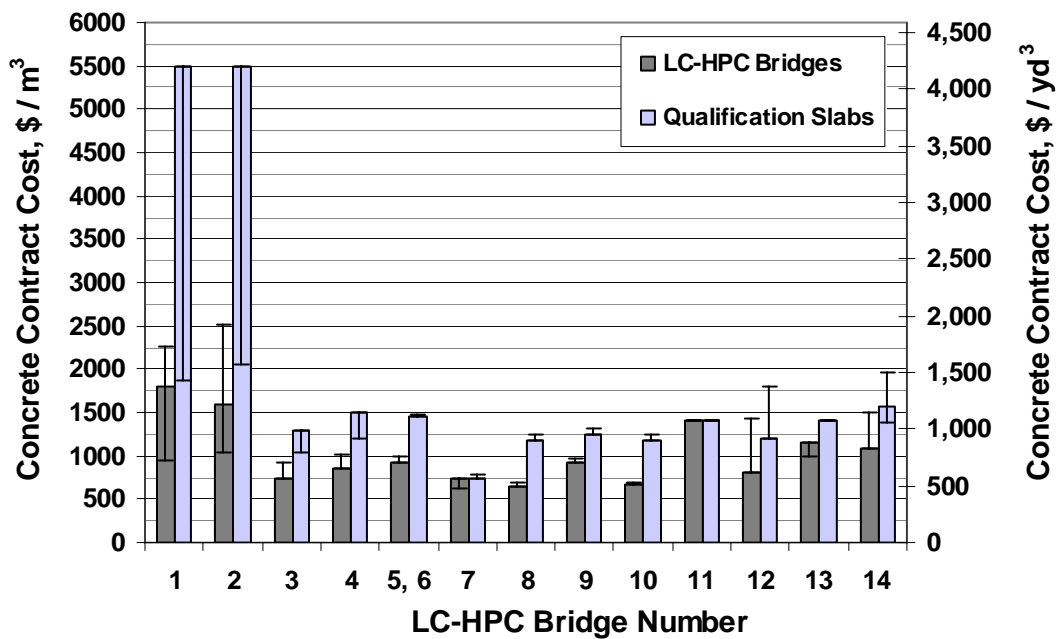


Fig. 5.37 – Unit costs of the qualification slab compared to the LC-HPC deck

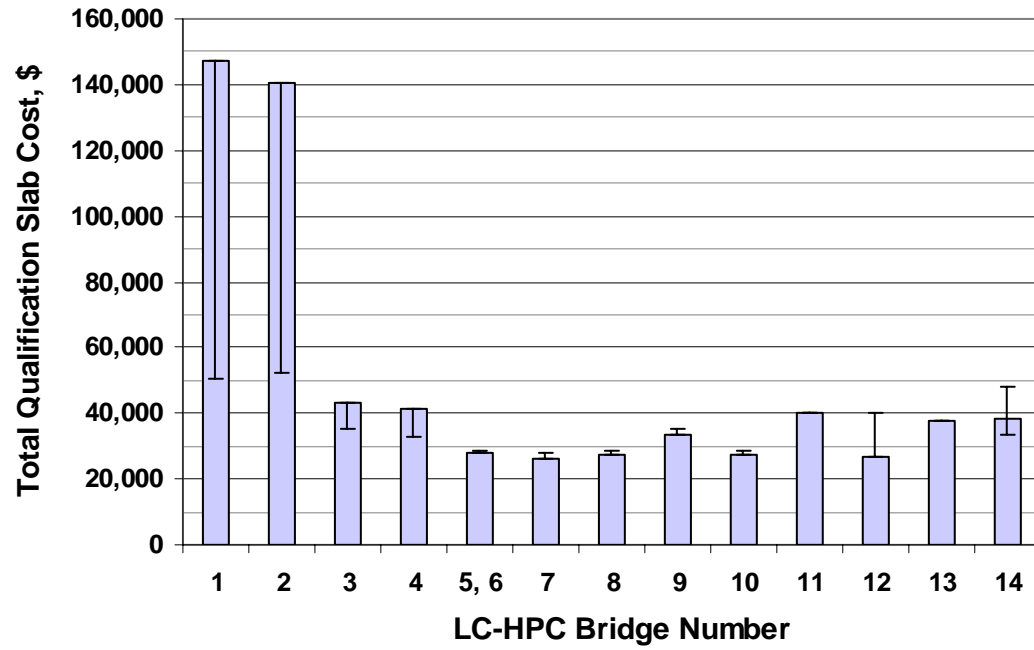


Fig. 5.38 – Total costs of the qualification slab for each LC-HPC deck

CHAPTER 6: SUMMARY, CONCLUSIONS, AND RECOMMENDATIONS

6.1 SUMMARY

Bridge deck cracking is well documented and often studied, and while there is much agreement on practices that contribute to cracking, there are still many questions that exist, especially with regard to the implementation of techniques to reduce cracking in the field. This study bridges that gap through the development and implementation of low-cracking high-performance concrete (LC-HPC). The study is divided into three parts covering (1) the development of an aggregate optimization program entitled *KU Mix*, (2) a comprehensive evaluation of the shrinkage properties of LC-HPC candidate mixtures, and (3) the development, construction, and preliminary evaluation of 14 LC-HPC bridge decks constructed in Kansas.

An optimized aggregate gradation has little or no effect on concrete shrinkage or cracking by itself, but for concrete with a low volume of cement paste, such as LC-HPC, an optimized combined gradation is essential in maintaining good characteristics in the plastic concrete. The *KU Mix* design methodology for determining an optimized combined gradation uses the percent retained chart and the Modified Coarseness Factor Chart (MCFC). The process begins by developing an *ideal gradation* that plots as a “haystack” on the percent retained chart and falls in the center of the optimum region on the MCFC. The optimum blend of a particular set of aggregates is then determined by performing a series of least-squared minimization calculations using the *ideal gradation* as a model for the actual blended gradation. A Microsoft[®] Excel spreadsheet enhanced with Visual Basic for Applications is available to perform the *KU Mix* optimization at www.iri.ku.edu.

The second portion of the study involves evaluating the effect of paste content, water-cementitious material ratio, aggregate type, mineral admixture type and content, cement type and fineness, shrinkage reducing admixture, and the

duration of curing on the free-shrinkage characteristics of concrete mixtures in the laboratory using the “Standard Test Method for Length Change of Hardened Hydraulic Cement Mortar and Concrete,” ASTM C 157. Performance is evaluated over a one-year period with special attention given to the early-age shrinkage that occurs during the first 30 days of drying. For each mixture, careful consideration was given to the aggregate gradations, cohesiveness, workability, finishability, and apparent constructability prior to casting the laboratory specimens. All of the mixtures evaluated in this study have an optimized aggregate gradation, paste volumes less than 24.4%, a design air content of $8.4 \pm 0.5\%$, and a target slump of 75 ± 25 mm (3 ± 1 in.).

The evaluation of shrinkage properties includes a total of 56 individual concrete batches, divided into six test programs. Program I evaluates mixtures with w/c ratios ranging from 0.41 to 0.45 containing either a relatively porous limestone coarse aggregate (with an absorption between 2.5 and 3.0%) or granite coarse aggregate (with an absorption below 0.7%). The specimens with limestone coarse aggregate are cast with Type I/II and coarse-ground Type II cements. For this program, a reduction in the w/c ratio is obtained by reducing the water content (and paste volume) and replacing the water with an equal volume of aggregate while maintaining workability using a high-range water reducer. The effects of paste content, w/c ratio, and curing period are evaluated in Program II. The first set in this series includes four mixtures with w/c ratios of 0.36, 0.38, 0.40, and 0.42. Unlike the specimens cast in Program I, which had different paste content values, the mixtures in Program II all have a paste content of 23.3%. A second set includes mixtures with a w/c ratio of 0.42, a paste content of either 23.3% or 21.6%, and a curing period of either 7, 14, or 21 days. Program III evaluates three coarse aggregates (granite, quartzite, and limestone) to determine their effect on free shrinkage, and Program IV examines the effect of a shrinkage reducing admixture on free shrinkage. The

influence of cement type and fineness on free shrinkage is examined in Program V. Four portland cements (one Type I/II, two Type II, and one Type III) with Blaine fineness values ranging from 323 to 549 m²/g are included in the Program V evaluation. The final test program evaluates three mineral admixtures as partial replacements for Type I/II cement. The mineral admixtures (and volume replacements examined) include silica fume (3 and 6% volume replacement), Class F fly ash (20 and 40%), and Grade 100 and 120 slag cement (30 and 60%). A minimum of two sources and two coarse aggregate types are included in the evaluation for each mineral admixture.

The third and final portion of the study details the development, construction, and preliminary performance of 14 low-cracking high-performance concrete (LC-HPC) bridge decks that are built or planned in Kansas. The evaluation is divided into four sections detailing (1) the specifications used for construction, (2) the experiences and lessons learned during the construction of the LC-HPC bridge decks, (3) the crack density results based on initial crack surveys, and (4) the cost of LC-HPC. The performance and cost of the LC-HPC bridge decks is evaluated based on comparisons with *control* decks that, where possible, are paired for their similarities. The construction experiences and crack density evaluation presented in this report is primarily limited to a discussion of the LC-HPC. A complete discussion of the bridge design and construction experiences is presented by McLeod et al. (2009).

6.2 CONCLUSIONS

The following observations and conclusions are based on the results and analyses presented in this report.

6.2.1 Aggregate Optimization Using the KU Mix Method

1. The two cubic polynomial equations used to model the *ideal* gradation [Eqs. (3.9a) and (3.9b)] for a particular set of aggregates accurately represent an optimized gradation.
2. The KU Mix design methodology is easily implemented and transferred to concrete suppliers and governing officials, and the optimized LC-HPC mixture designs developed with KU Mix are workable, placeable, and finishable.

6.2.2 Free Shrinkage of Potential LC-HPC Mixtures

1. A reduction in the w/c ratio (and paste content) obtained by reducing the water content and replacing the water with an equal volume of aggregate and using a high-range water reducer (HRWR) to maintain workability reduces concrete shrinkage.
2. For a given w/c ratio and curing period, very little difference in shrinkage is observed between specimens cast with Type I/II (Blaine fineness = 377 m^2/kg) and those cast with coarse-ground Type II (Blaine fineness = 334 m^2/kg) cement.
3. For a given paste content, a reduction in the w/c ratio from 0.42 to 0.36 reduces shrinkage from 317 to 237 $\mu\epsilon$ after 30 days of drying and from 443 to 410 $\mu\epsilon$ after one year of drying. These results represent the performance of mixtures containing relatively porous limestone coarse aggregate. The porous limestone may provide internal curing water and extend the hydration reaction longer than might occur otherwise. These results may not extend to concrete

mixtures containing a low-absorption aggregate (that does not provide internal curing water) due to the possibility of autogenous shrinkage for mixtures with w/c ratios below 0.42.

4. Longer curing periods reduce concrete shrinkage. For mixtures containing limestone coarse aggregate and no mineral admixtures, increasing the curing period from 7 to 14 days or from 14 to 21 days is approximately equal to reducing the paste content from 23.3 to 21.6%.
5. Concrete containing aggregate with a higher modulus of elasticity, as indicated by a low absorption (e.g., granite and quartzite), will shrink less in the long term than concrete containing aggregate with a lower modulus (e.g., limestone). Increasing the curing period from 7 to 14 days reduces shrinkage for mixtures containing each of the aggregate types, but the reductions for concrete containing granite or quartzite are generally small and not statistically significant. In addition, internal curing provided by the porous limestone results initially in a slower shrinkage rate for the concrete containing limestone compared to those containing granite or quartzite through the first 10 to 25 days of drying. After this initial period, the concretes containing stiffer aggregates exhibit less shrinkage.
6. The addition of a shrinkage reducing admixture (SRA) to concrete mixtures results in significantly less shrinkage as the dosage is increased from 3165 to 6330 mL/m³ (0.64 to 1.28 gal/yd³). Before these mixtures are implemented in the field, careful consideration must be given to interaction with other chemical admixtures, mixing procedures, and placing techniques to ensure a stable, properly spaced air-void system.
7. The use of Type III cement results in a significant increase in early-age shrinkage compared to mixtures containing Type I/II cement, but only a slight increase in the long-term shrinkage.

8. When concrete is cast with a high-absorption coarse aggregate (e.g., limestone with an absorption between 2.5 and 3.0%), the volume replacement of cement by 3% silica fume or 30% slag cement results in similar or slightly reduced shrinkage at all ages compared to a control mixture with 100% portland cement. Mixtures exhibit reduced shrinkage when the silica fume or slag cement content is doubled to 6 or 60%, respectively, or when the curing period is increased from 7 to 14 days. Before these mixtures are implemented in the field, scaling tests and restrained ring tests should be performed to ensure that the reduced shrinkage observed in the laboratory will translate into to increased performance in the field.
9. When concrete is cast with a low-absorption coarse aggregate (e.g., granite or quartzite with an absorption less than 0.7%) and only cured for 7 days, the volume replacement of cement by 3 or 6% silica fume or 30 or 60% slag results in increased early-age shrinkage and slightly reduced long-term shrinkage compared to a control mixture with 100% portland cement. When cured for 14 days, both the early-age and long-term shrinkage of these binary mixtures is reduced compared to the control mixture.
10. Internal curing provided by water held in the pores of limestone coarse aggregate particles reduces the free shrinkage of concrete containing silica fume or slag cement as a replacement for portland cement.
11. The addition of Class F fly ash (20 or 40%) results in significantly increased early-age shrinkage compared to the 100% portland cement control mixture for concrete cast with either a low or high-absorption coarse aggregate and cured for either 7 or 14 days. Based on the test results, the effect of fly ash on long-term shrinkage is somewhat unclear, but in no case did the addition of fly ash reduce long-term shrinkage.

12. Ternary mixtures with a paste content of 20% containing 60 or 80% slag cement and 6% silica fume have adequate workability, finishability, and cohesiveness. These mixtures have reduced shrinkage compared to control mixtures containing 100% portland cement due to a reduction in the paste content (made possible with the mineral admixtures) and the addition of slag cement, silica fume, or both.

6.2.3 Construction Experiences and Preliminary Evaluation of LC-HPC Bridge Decks

1. Natural fine and coarse sands selected to meet the combined gradation specification greatly aid the pumpability and finishability of LC-HPC. Angular manufactured sands and excessively elongated coarse aggregate particles can hinder placement (especially when pumped) and finishing.
2. Special attention must be given to accurately determining the free surface moisture of the aggregate before and during concrete placement.
3. LC-HPC mixtures with an optimized aggregate gradation and design w/c ratios of 0.44 and 0.45 with cement contents of 317 or 320 kg/m^3 (535 or 540 lb/yd^3) have consistently pumped and finished well.
4. Some of the LC-HPC placements cast with a design w/c ratio of 0.42 and a cement content of 317 kg/m^3 (535 lb/yd^3) have not pumped or finished well. A number of factors contributed to these difficulties, including withholding a portion of the design mixture water and overestimating the aggregate free surface moisture.
5. Concretes cast with high-range water reducers exhibit increased compressive strengths compared to concrete casts with a mid-range water reducers or without a water reducer.
6. A slump of 75 mm (3 in.) is adequate to place and finish properly designed LC-HPC, but a slump of 100 mm (4 in.), the maximum allowed under the

current LC-HPC specification, is often set as the target at the request of the contractor. This practice, in turn, often results in concrete slumps that regularly exceed 75 mm (3 in.) rather than slumps within the desired range of 40 to 75 mm (1.5 to 3.0 in.).

7. Based on samples taken before and after placement, air loss through the pump ranged from 0.6 to 1.6% when an “S-Hook” or bladder valve was used to limit air loss and from 2.0 to 4.5% when no measures were taken. A drop of approximately 3.7 m (12 ft) from a conveyor through an elephant trunk resulted in an average air loss of 2.4%.
8. A positive relationship between the inspectors, contractor, and ready-mix supplier is critical to the success of LC-HPC decks.
9. The crack densities for the three LC-HPC decks surveyed on more than one occasion increased gradually over time at a rate similar to that reported for monolithic decks by Lindquist et al. (2005).
10. The crack densities for the five control decks surveyed on more than one occasion increased rapidly following the first survey. Additional surveys are needed to fully assess the long-term performance of these decks, but surveys performed between 12 and 24 months appear to provide a better assessment of the deck performance than surveys performed at less than one year.
11. On average, LC-HPC decks had both a lower average cracking rate and a lower crack density than the control decks.
12. The five LC-HPC decks surveyed to date are performing at a level approximately equal to or exceeding the best performing monolithic decks in Kansas surveyed over the past 15 years.
13. A reduction in the water content from 144 to 133 kg/m³ (243 to 224 lb/yd³) does not measurably reduce the level of cracking in bridge decks. Based on these results, it is clear that emphasis should be placed on selecting a water

content within this range that enables the contractor to adequately place, finish, and cover the concrete in a timely fashion.

14. Further evaluation is required to fully evaluate the effect of cement content on cracking for the LC-HPC decks, but it is clear that the ability to place, finish, and cover the concrete quickly is more important than reducing the cement content from 320 to 317 kg/m³ (540 to 535 lb/yd³).
15. Crack density increases with increasing concrete compressive strength.
16. There is no appreciable increase in crack density as the average slump is increased from 75 to 90 mm (3.0 to 3.5 in.).
17. With the exception of the first two LC-HPC decks, the costs of control decks cast with low-absorption aggregate (as specified by the Kansas City Metro Materials Board) are similar to the costs of the LC-HPC decks.

6.3 RECOMMENDATIONS

Based on the observations and conclusions in this report, the following recommendations are made to limit concrete shrinkage and improve bridge deck performance.

1. The minimum curing time for all bridge deck placements should be 14 days to help limit concrete shrinkage.
2. For mixtures containing a low-absorption coarse aggregate, 100% portland cement should be selected. This recommendation is based on two observations: (1) concrete containing aggregate with a higher modulus of elasticity, as indicated by a low absorption (e.g., granite and quartzite), will shrink less than concrete with a lower modulus (e.g., limestone), and (2) concrete with a low-absorption coarse aggregate is pumped more easily than concrete containing a porous coarse aggregate. Concrete containing porous

coarse aggregate may lose a significant amount of workability through the pump as water is forced into the aggregate pores as the concrete is pumped.

3. Angular manufactured sands can hinder the ability of the contractor to place and finish the concrete and should not be used as a principal contributor to sieve sizes of 9.5-mm ($\frac{3}{8}$ -in.) and below. Pumping is especially hindered by angular manufactured sands.
4. Careful consideration should be given to selecting and optimizing the combined aggregate blend to meet the specifications throughout the project. The mixture should be re-optimized to account for “as-delivered” aggregate gradations to ensure that the mixture is placeable prior to construction of the deck.
5. The design w/c ratio for LC-HPC should be specified between 0.43 and 0.45, and the maximum cement content should be specified as 320 kg/m^3 (540 lb/yd^3). A somewhat reduced cement content can be used if the w/c ratio range and the specified cement content results in a slump above the desired range.
6. The use of high-range water reducers (HRWRs) should be strictly limited due to their potential to increase compressive strengths, and whenever possible, a mid-range water reducer should be used instead. Mixtures specified with a w/c ratio of 0.44 and a cement content of 320 kg/m^3 (540 lb/yd^3) may not require a water-reducer to obtain a 75 mm (3 in.) slump.
7. All of the water included in the mixture design should be added at the ready-mix plant. Slump control in the field should be accomplished through the addition of a mid-range water reducer.
8. The maximum allowable slump for future LC-HPC bridge placements should be limited to 90 mm (3.5 in.) to help minimize settlement cracking while still maintaining placeable and finishable concrete. It is imperative that inspectors

recognize the importance of limiting slump to ensure that they enforce this provision throughout the placement.

9. A clear understanding of the concrete testing schedule and how out-of-specification concrete will be handled should be established prior to placement of the qualification slab. Changes to the concrete properties resulting from the placement method should be accounted for if the samples are taken directly from the ready-mix truck.
10. If a pump is used for placement, a bladder valve or “S-Hook” should be fitted to the discharge hose, and if a conveyor or bucket is used for placement, the maximum drop should be limited to 1.5 m (5 ft).
11. The same equipment used to place and finish the qualification slab should be used to place and finish the bridge placement. Any changes to the placing or finishing equipment or to the concrete mixture design, other than re-optimizing the aggregate gradation based on the as-delivered aggregates, should be accompanied by additional testing to ensure that the concrete remains placeable and finishable.
12. Successfully completing the qualification batch and qualification slab are critical steps that should be completed prior to construction of the LC-HPC deck. In some cases, a qualification slab may not be necessary for experienced crews, but the ability to adequately place and finish the concrete must be demonstrated prior to placement.
13. The LC-HPC specifications should be adopted to replace the current concrete specifications used for monolithic decks and bridge subdecks. The LC-HPC decks constructed and surveyed to date have both a lower average crack density and a lower average cracking rate.

REFERENCES

- ACI Committee 209 (2005). *Report on Factors Affecting Shrinkage and Creep of Hardened Concrete* (ACI 209.1R-05), American Concrete Institute, Farmington Hills, MI, 12 pp.
- ACI Committee 211 (2004). *ACI 211.1 Appendix 1 – Method for Assessing Aggregate Gradings, Ballot version*, ACI Subcommittee 211A, American Concrete Institute, Farmington Hills, MI, 31 pp.
- ACI Committee 232 (2002). *Use of Fly Ash in Concrete* (ACI 232.2R-96), American Concrete Institute, Farmington Hills, MI, 34 pp.
- ACI Committee 233 (2003). *Slag Cement in Concrete and Mortar* (ACI 233R-03), American Concrete Institute, Farmington Hills, MI, 19 pp.
- ACI Committee 234 (1996). *Guide for the Use of Silica Fume in Concrete* (ACI 234R-96), American Concrete Institute, Farmington Hills, MI, 51 pp.
- Alexander, K. M. (1964). “Factors Affecting the Drying Shrinkage of Concrete,” *Construction Review*, Vol. 37, No. 3, Mar., pp. 15-23.
- Alexander, M. G. (1996). “Aggregates and the Deformation Properties of Concrete,” *ACI Materials Journal*, Vol. 93, No. 6, Nov.-Dec., pp. 569-577.
- American Society of Civil Engineers (2005). “Report Card for America’s Infrastructure,” *ASCE website: www.asce.org/reportcard/2005*
- ASTM C 157-04 (2004). “Standard Test Method for Length Change of Hardened Hydraulic-Cement Mortar and Concrete,” *2006 Annual Book of ASTM Standards*, Vol. 4.02, American Society of Testing and Materials, West Conshohocken, PA.
- ASTM C 618-05 (2005). “Standard Specification for Coal Fly Ash and Raw or Calcined Natural Pozzolan for Use in Concrete,” *2006 Annual Book of ASTM Standards*, Vol. 4.02, American Society of Testing and Materials, West Conshohocken, PA.
- ASTM C 989-06 (2006). “Standard Specification for Ground Granulated Blast-Furnace Slag for Use in Concrete and Mortars,” *2006 Annual Book of ASTM Standards*, Vol. 4.02, American Society of Testing and Materials, West Conshohocken, PA.

Atiș, C. D. (2003). "High-Volume Fly Ash Concrete with High Strength and Low Drying Shrinkage," *Journal of Materials in Civil Engineering*, ASCE, Vol. 15, No. 2, Mar.-April, pp. 153-156.

Babaei, K. and Fouladgar, A. M. (1997). "Solutions to Concrete Bridge Deck Cracking," *Concrete International*, Vol. 15, No. 7, July, pp. 34-37.

Babaei, K. and Purvis, R. L. (1996). "Prevention of Cracks in Concrete Bridge Decks Summary Report," *Report No. 233*, Wilbur Smith Associates, Falls Church, VA, 30 pp.

Bakker, R. F. M. (1980). "On the Cause of Increased Resistance of Concrete Made from Blast Furnace Cement to Alkali Reaction and to Sulfate Corrosion," *Special Publication 79*, American Concrete Institute, Farmington Hills, MI, Vol. 1, pp. 589-605.

Bissonnette, B., Pierre, P., and Pigeon, M. (1999). "Influence of Key Parameters on Drying Shrinkage of Cementitious Materials," *Cement and Concrete Research*, Oct., Vol. 29, No. 10, pp. 1655-1662.

Blanks, R. F., Vidal, E. N., Price, W. H., and Russell, F. M. (1940). "The Properties of Concrete Mixes," *ACI Journal, Proceedings* Vol. 36, April, 44 pp.

Brown, J. H. (1980). "Effect of Two Different Pulverized-Fuel Ashes Upon the Workability and Strength of Concrete," *Technical Report No. 536*, Cement and Concrete Association, Wexham Springs, 18 pp.

Brunauer, S., Emmett, P. H., and Teller, E. (1938). "Adsorption of Gases in Multimolecular Layers," *Journal of American Chemical Society*, Vol. 60, No. 2, Feb., pp. 309-319.

Cabrera, J. G. and Atiș, C. D. (1999). "ACI SP-186 Design and Properties of High Volume Fly Ash High-Performance Concrete," *Proceedings*, ACI Int. Conf. on High Performance Concrete and Performance and Quality Control Structures, American Concrete Institute, Detroit, pp. 21-37.

Carlson, R. (1938). "Drying Shrinkage of Concrete as Affected by Many Factors," *ASTM Proceedings*, Vol. 38, Part II, pp. 419-440.

Chariton, T. and Weiss, W. J. (2002). "Using Acoustic Emission to Monitor Damage Development in Mortars Restrained from Volumetric Changes," *Concrete: Material Science to Application, A Tribute to Surendra P. Shah*, SP-206, American Concrete Institute, Farmington Hills, MI, pp. 205-219.

Collins, F. and Sanjayan J. G. (1999). "Strength and Shrinkage Properties of Alkali-Activated Slag Concrete Containing Porous Coarse Aggregate," *Cement and Concrete Research*, Vol. 29, No. 4, April, pp. 607-610.

Committee on the Comparative Costs of Rock Salt and Calcium Magnesium Acetate (CMA) for Highway Deicing (1991). "Highway Deicing: Comparing Salt and Calcium Magnesium Acetate," *Transportation Research Board Special Report 235*, Transportation Research Board, National Research Council, Washington, D. C., 163 pp.

Cramer, S. M., Hall, M., and Parry J. (1995). "Effect of Optimized Total Aggregate Gradation on Portland Cement Concrete for Wisconsin Pavements," *Transportation Research Board Record* No. 1478, National Research Council, July, pp. 100-106.

Dakhil, F. H., Cady, P. D., and Carrier, R. E. (1975). "Cracking of Fresh Concrete as Related to Reinforcement," *ACI Journal, Proceedings* Vol. 72, No. 8, Aug., pp. 421-428.

Deshpande, S., Darwin, D., Browning, J. (2007). "Evaluating Free Shrinkage of Concrete for Control of Cracking in Bridge Decks," *SM Report* No. 89, University of Kansas Center for Research, Inc., Lawrence, KS, 290 pp.

Ding, J. and Li, Z. (2002). "Effects of Metakaolin and Silica Fume on Properties of Concrete," *ACI Materials Journal*, Vol. 99, No. 4, July-Aug., pp. 393-398.

Durability of Concrete Bridge Decks-A Cooperative Study, Final Report, (1970). The state highway departments of California, Illinois, Kansas, Michigan, Minnesota, Missouri, New Jersey, Ohio, Texas, and Virginia; the Bureau of Public Roads; and Portland Cement Association, 35 pp.

Easa, S. M., and Can, K. (1985). "Optimization Model for Aggregate Blending," *Journal of Construction Engineering and Management*, Vol. 111, No. 3, Sept., pp. 216-230.

Eppers, L., French, C., and Hajjar, J. F. (1998). "Transverse Cracking in Bridge Decks: Field Study," *Report*, Minnesota Department of Transportation, Saint Paul, MN, 195 pp.

Federal Highway Administration (FHWA) (2006). "FHWA Bridge Programs NBI Data," *FHWA website: www.fhwa.dot.gov/bridge/defbr06.htm*

Feldman, R. F., and Swenson, E. G. (1975). "Volume Change on First Drying of Hydrate Portland Cement with and without Admixture," *Cement and Concrete Research*, V. 5, No. 1, pp. 25-35.

Fraay, A. L. A., Bijen, J. M., and de Haan, Y. M. (1989). "The Reaction of Fly Ash in Concrete: A Critical Examination," *Cement and Concrete Research*, Vol. 19, No. 2, pp. 235-246.

Frigione, G. (1986). "Manufacture and Characteristics of Portland Blast-Furnace Slag Cements," Blended Cements, *ASTM Special Technical Publication No. 897*, G. Frohnsdorff, Ed. American Society of Testing and Materials, Philadelphia, PA, pp. 15-18.

Fujiwara, T. (1984). "Change in Length of Aggregate Due to Drying," *Bulletin of the International Association of Engineering Geology*, No. 30, pp. 225-227.

Fuller, W. B. and Thompson, S. E. (1907). "The Laws of Proportioning Concrete," *Proceedings of the American Society of Civil Engineers*, Vol. 33, No. 3, Mar., pp. 222-298.

Fulton, F. S. (1974). "The Properties of Portland Cement Containing Milled Granulated Blast-Furnace Slag," *Monograph*, Portland Cement Association, Johannesburg, pp. 4-46.

Ghosh, R. S., and Malhotra (1979). "Use of Superplasticizers as Water Reducers," *Cement, Concrete, and Aggregates*, Vol. 1, No. 2, pp. 56-63.

Goltermann, P., Johansen, V., and Palbøl, L. (1997). "Packing of Aggregates: An Alternative Tool to Determine the Optimal Aggregate Mix," *ACI Materials Journal*, Vol. 94, No. 5, Sept.-Oct., pp. 435-443.

Hobbs, D. W. (1974). "Influence of Aggregate Restraint on the Shrinkage of Concrete," *ACI Journal, Proceedings* Vol. 71, No. 9, Sept., pp. 445-450.

Hogan, F. J., and Meusel, J. W. (1981). "Evaluation for Durability and Strength Development of a Ground Granulated Blast-Furnace Slag," *Cement, Concrete, and Aggregates*, Vol. 3, No. 1, pp. 40-52.

Holland, T. C. (2005). "Silica Fume User's Manual," *FHWA-IF-05-016*, Silica Fume Association, Lovettsville, VA, April, 183 pp.

Ibragimov, A. M. (1989). "Effect of the Maximum Size of Coarse Aggregate on the Main Parameters of Concrete," *Hydrotechnical Construction*, Vol. 23, No. 3, pp. 141-144.

Imamoto, K. and Arai, M. (2005). "The Influence of Specific Surface Area of Coarse Aggregate on Drying Shrinkage of Concrete," *Creep and Shrinkage and Durability*

Mechanics of Concrete and Other Quasi-brittle Materials, presented at Concreep.7, Nantes, France, Sept., pp. 95-100.

Jardine, D. J. and Wolhuter, C. W. (1977). "Some Properties of High-Slag Concrete," *Civil Engineer in South Africa*, Vol. 19, No. 11, pp. 249-251.

Kasperkiewicz, J. (1994). "Optimization of Concrete Mix Using a Spreadsheet Package," *ACI Materials Journal*, Vol. 91, No. 6, Nov.-Dec., pp. 551-559.

Khatri, R. and Sirivivatnanon, V. (1995). "Effect of Different Supplementary Cementitious Materials on Mechanical Properties of High Performance Concrete," *Cement and Concrete Research*, Vol. 25, No. 1, Jan., pp. 209-220.

Krauss, P. D., and Rogalla, E. A. (1996). "Transverse Cracking in Newly Constructed Bridge Decks," *National Cooperative Highway Research Program Report 380*, Transportation Research Board, Washington, D.C., 126 pp.

Le, Q. T. C., French, C., and Hajjar, J. F. (1998). "Transverse Cracking in Bridge Decks: Parametric Study," *Report*, Minnesota Department of Transportation, Saint Paul, MN, 195 pp.

Lindquist, W. D., Darwin, D., and Browning, J. (2005). "Cracking and Chloride Contents in Reinforced Concrete Bridge Decks," *SM Report No. 78*, University of Kansas Center for Research, Inc., Lawrence, KS, 453 pp.

Lindquist, W. D., Darwin, D., Browning, J., and Miller, G. G. (2006). "Effect of Cracking on Chloride Content in Concrete Bridge decks," *ACI Materials Journal*, Vol. 103, No. 6, Nov.-Dec., pp. 467-473.

Lynam, C. G., (1934). *Growth and Movement in Portland Cement Concrete*, Oxford University Press, London, pp. 26-27.

McLeod, H., Darwin, D., and Browning, J. (2009). "Development and Construction of Low-Cracking High-Performance Concrete Bridge Decks: Construction Methods, Temperature Effects, and Resistance to Chloride Ion Penetration," *SM Report*, University of Kansas Center for Research, Inc., Lawrence, KS [manuscript in prep.]

Miller, G. G., and Darwin, D., (2000) "Performance and Constructability of Silica Fume Bridge Deck Overlays," *SM Report No. 57*, University of Kansas Center for Research, Inc., Lawrence, KS, Jan., 423 pp.

Mindess, S., Young, F., and Darwin, D. (2003). *Concrete*, 2nd ed., Prentice-Hall, Inc., Englewood Cliffs, NJ, 644 pp.

- Mokarem, D., Weyers, R., and Lane, D. (2005). "Development of a Shrinkage Performance Specifications and Prediction Model Analysis for Supplemental Cementitious Material Concrete Mixtures," *Cement and Concrete Research*, Vol. 35, No. 5, May, pp. 918-925.
- Ödman, S. T. A. (1968). "Effects of Variations in Volume, Surface Area Exposed to Drying, and Composition of Concrete Shrinkage," *RILEM/CEMBUREAU Intl. Colloquium on the Shrinkage of Hydraulic Concretes*, Madrid, V. 1, 1968, 20 pp.
- Papayianni, J. (1987). "An Investigation of the Pozzolanicity and Hydraulic Reactivity of High-Lime Fly Ash," *Magazine of Concrete Research*, Vol. 39, No. 138, pp. 19-28.
- Pickett, G. (1956). "Effect of Aggregate on Shrinkage of concrete and a Hypothesis Concerning Shrinkage," *ACI Journal, Proceedings* Vol. 52, No. 1, Jan., pp. 581-590.
- Powers, T. C. (1959). "Causes and Control of Volume Change," *Journal of Portland Cement Association Research and Development Laboratories*, Vol. 1, Jan., pp. 29-39.
- Rao, G. (1988). "Influence of Silica Fume Replacement of Cement on Expansion and Drying Shrinkage," *Cement and Concrete Research*, Vol. 28, No. 10, Oct., pp. 1505-1509.
- Roberts, F. L., Kandhal, P. S., Brown, E. R., Lee, H. Y., Kennedy, T. W. (1996). *Hot Mix Asphalt Materials, Mixture Design, and Construction*, 2nd Edition, NAPA Education Foundation, Lanham, Maryland, 1996, 575 pp.
- Saric-Coric, M. and Aïtcin, P. (2003). "Influence of Curing Conditions on Shrinkage of Blended Cements Containing Various Amounts of Slag," *ACI Materials Journal*, Vol. 100, No. 6, Nov.-Dec., pp. 477-484.
- Schmitt, T. R., and Darwin, D. (1995). "Cracking in Concrete Bridge Decks," *SM Report* No. 39, The University of Kansas Center for Research, Inc., Lawrence, Kansas, 151 pp.
- Schmitt, T. R., and Darwin, D. (1999). "Effect of Material Properties on Cracking in Bridge Decks," *Journal of Bridge Engineering*, ASCE, Feb., Vol. 4, No. 1, pp. 8-13.
- Shilstone, J. M., Sr. (1990). "Concrete Mixture Optimization," *Concrete International*, Vol. 12, No. 6, Jun., pp. 33-39.
- Suprenant, B., and Malisch, W. (1999). "The Fiber Factor," *Concrete Construction*, Oct., pp 43-46.

Symons, M. G., and Fleming, K. H. (1980). "Effect of Port Augusta Fly Ash on Concrete Shrinkage," *Transactions of the Institution of Engineers, Australia*, Vol. 22, No. 3, pp. 181-185.

Tazawa, E., and Miyazawa, S. (1993). "Autogenous Shrinkage of Concrete and its Importance in Concrete," Creep and Shrinkage in Concrete, *Proceedings*, 5th International RILEM Symposium, Z. P. Bazant and I. Carol, eds., E & FN Spon, London, pp. 159-168.

Tazawa, E., Yonekura A., and Tanaka, S. (1989). "Drying Shrinkage and Creep of Concrete Containing Granulated Blast Furnace Slag," ACI SP-114 Fly Ash, Silica Fume, Slag and Natural Pozzolans in Concrete, *Proceedings*, 3rd International Conference on Fly Ash, Silica Fume, and Natural Pozzolans in Concrete, V. M. Malhotra, ed., Trondheim, Norway, pp. 1325-43.

Tritsch, N. Darwin, D., and Browning, J. P. (2005). "Evaluating Shrinkage and Cracking Behavior of Concrete Using Restrained Ring and Free Shrinkage Tests," *SM Report No. 77*, University of Kansas Center for Research, Inc., Lawrence, KS, Jan., 178 pp.

Wimpenny, D. E., Ellis, C. M, and Higgins, D. D. (1989). "The Development of Strength and Elastic Properties in Slag Cement under Low Temperature Curing Conditions," ACI SP-114 Fly Ash, Silica Fume, Slag and Natural Pozzolans in Concrete, *Proceedings*, 3rd International Conference on Fly Ash, Silica Fume, and Natural Pozzolans in Concrete, V. M. Malhotra, ed., Trondheim, Norway, p. 1288.

Whiting, D. A., and Detwiler, R. (1998). "Silica Fume Concrete for Bridge Decks," *National Cooperative Highway Research Program Report 410*, Transportation Research Board, Washington, D. C., 180 pp.

Yunovich, M., Thompson, N. G., Balvanyos, T., and Lave, L. (2002). "Highway Bridges," Appendix D, *Corrosion Cost and Preventive Strategies in the United States*, by G. H. Koch, M. PO, H. Broongers, N. G. Thompson, Y. P. Virmani, and J. H. Payer, *Report No. FHWA-RD-01-156*, Federal Highway Administration, McLean, VA, 773 pp.

APPENDIX A: CONCRETE MIXTURE PROPORTIONS

A.1 GENERAL

Appendix A presents the mixture proportions, properties, and compressive strengths for the six free-shrinkage programs described in Chapters 2 and 4.

Table A.1 – Cement and mineral admixture chemical composition

Oxides	Percentages							
	Portland Cement Type							
	I/II							
Sample No.	1	2	3		4		5	
SiO₂	21.04	21.23	20.89	309	21.69	344	20.88	407
Al₂O₃	4.81	4.69	4.71	312	4.92	347	4.85	408
Fe₂O₃	3.25	3.56	3.46	317	3.38	351	3.42	409
CaO	63.24	63.31	63.17	322	61.91	354	62.91	412
MgO	2.00	1.69	1.69	323	1.70	355	1.92	414
SO₃	2.77	2.76	2.96	323	3.10	355	2.79	414
Na₂O	0.23	0.22	0.20	324	0.24	358	0.21	417
K₂O	0.46	0.53	0.47	325	0.46	363	0.52	419
TiO₂	0.29	0.28	0.30	325	0.32	363	0.30	419
P₂O₅	0.10	0.09	0.10	325	0.10	363	0.10	419
Mn₂O₃	0.10	0.13	0.13	326	0.10	364	0.11	421
SrO	0.19	0.17	0.16		0.15		0.20	
BaO	--	--	--		--		--	
LOI	1.40	1.39	1.52		1.67		1.99	
Total	99.88	100.06	99.76		99.74		100.20	
Batch Numbers	234	239	273	309	328	344	368	407
	235		274	312	330	347	369	408
			275	317	334	351	370	409
			278	322	335	354	373	412
			282	323	338	355	378	414
			290	324	340	358	392	417
			292	325	342	363	394	419
			308	326	343	364	399	421

Table A.1 (con't) – Cement and mineral admixture chemical composition

Oxides	Percentages						
	Portland Cement Type				Mineral Admixture		
	III	II			Silica Fume		F-Ash
Sample No.	1	1(a)	1(b)	2	1	2	1
SiO₂	20.42	20.85	20.83	21.16	90.87	94.49	55.67
Al₂O₃	5.46	4.79	4.80	4.63	0.48	0.07	15.42
Fe₂O₃	2.40	3.58	3.57	3.51	1.62	0.10	5.20
CaO	62.67	65.00	64.69	64.96	0.42	0.53	12.79
MgO	1.36	1.18	1.19	1.01	0.98	0.62	4.22
SO₃	3.27	1.44	2.25	2.29	0.28	0.11	0.66
Na₂O	0.15	0.50	0.51	0.46	0.43	0.09	1.99
K₂O	0.80	0.16	0.17	0.20	1.29	0.54	2.08
TiO₂	0.34	0.24	0.25	0.28	0.01	--	0.50
P₂O₅	0.12	0.07	0.07	0.08	0.08	0.07	0.12
Mn₂O₃	0.05	0.09	0.09	0.07	0.03	0.02	0.04
SrO	0.07	0.14	0.14	0.15	0.01	0.01	0.26
BaO	--	--	--	--	--	--	0.45
LOI	3.32	1.67	1.46	0.70	3.35	3.21	0.43
Total	100.43	99.73	100.03	99.50	99.85	99.86	99.83
Batch Numbers	367	240 244 246 298		300	274 275	325 326 354 355 358 392 394	419 421

Table A.1 (con't) – Cement and mineral admixture chemical composition

Oxides	Percentages							
	Mineral Admixture							
	F-Ash			Grade 120 Slag Cement		Grade 100 Slag Cement		
	2(a)	2(b)	3	1	2	1 [†]	2	3
SiO₂	64.97	64.36	57.17	32.70	38.28	--	36.35	43.36
Al₂O₃	17.47	17.47	18.65	8.58	10.69	--	9.64	8.61
Fe₂O₃	3.10	3.08	3.08	1.70	0.49	--	0.88	0.37
CaO	8.55	8.95	11.61	44.82	35.35	--	39.92	31.13
MgO	2.06	1.97	2.21	9.33	10.68	--	9.17	12.50
SO₃	0.23	0.29	2.83	1.16	2.85	--	2.21	2.24
Na₂O	0.63	0.61	0.63	0.30	0.27	--	0.23	0.21
K₂O	0.85	0.84	0.81	0.41	0.37	--	0.44	0.40
TiO₂	1.06	0.97	1.03	0.57	0.44	--	0.50	0.32
P₂O₅	0.11	0.12	0.18	0.06	0.01	--	0.02	--
Mn₂O₃	0.04	0.04	0.04	0.45	0.34	--	0.40	0.35
SrO	0.16	0.16	0.17	0.09	0.05	--	0.07	0.04
BaO	0.18	--	--	--	--	--	--	--
LOI	0.40	0.73	1.26	0.00	0.00	--	0.00	0.37
Total	99.81	99.59	99.67	100.17	99.82	--	99.83	99.90
Batch Numbers	290	363	278	309	322	328	368	
	292	364	282	312		340	369	
	399			317			407	
	403			324			408	
				351				
				354				
				355				
				358				

[†]The chemical composition of the first Grade 100 Slag Cement sample, used for Batch 322, was not analyzed.

Table A.2 (con't) – Aggregate Gradations

Sieve Size	Percent Retained on Each Sieve								
	19-mm (¾-in.) Limestone Gradations						19-mm (¾-in.) Quartzite Gradations		
	3	3(a)	3(b)	4	4(a)	4(b)	1	1(a)	1(b)
37.5-mm (1½-in.)	0	0	0	0	0	0	0	0	0
25-mm (1-in.)	0	0	0	0	0	0	0	0	0
19-mm (¾-in.)	0	0	0	0	0	0	2.3	6.9	0
12.5-mm (½-in.)	20.8	42.2	0	22.0	42.3	0	14.9	44.0	0
9.5-mm (⅜-in.)	28.6	57.8	0	30.1	57.7	0	15.5	45.6	0
4.75-mm (No. 4)	42.4	0	83.8	41.4	0	89.6	51.0	0	77.2
2.36-mm (No. 8)	6.0	0	11.8	3.1	0	6.7	10.2	0	15.4
1.18-mm (No. 16)	0	0	0	0	0	0	2.5	0	3.8
0.60-mm (No. 30)	0	0	0	0	0	0	0.7	0	1.1
0.30-mm (No. 50)	0	0	0	0	0	0	0.6	0	0.8
0.15-mm (No. 100)	0	0	0	0	0	0	0	0	0
0.075-mm (No. 200)	0	0	0	0	0	0	0	0	0
Pan	2.3	0	4.5	3.5	0	3.8	2.3	3.5	1.8
Batch Numbers	--	298 308 309 317 322 323 326 328 325 351 326 354 328 355 351 358 354 364 355 363 358 367 363 368 364 369 367 373 368 369	309 317 322 323 326 328 351 354 355 358 364 363 367 368 369 373	--	373	--	--	312 324 344	312 324 344

Table A.2 (con't) – Aggregate Gradations

Sieve Size	Percent Retained on Each Sieve								
	19-mm (¾-in.) Granite Gradations						Pea Gravel		
	1	1(a)	1(b)	2	2(a)	2(b)	A	B	1
37.5-mm (1½-in.)	0	0	0	0	0	0	0	0	0
25-mm (1-in.)	0	0	0	0	0	0	0	0	0
19-mm (¾-in.)	2.0	3.9	0	0	0	0	0	0	0
12.5-mm (½-in.)	18.2	35.7	0	15.7	34.2	0	0	0	0
9.5-mm (⅜-in.)	30.8	60.4	0	29.8	64.7	0	0	0	0
4.75-mm (No. 4)	44.4	0	90.4	39.2	0	78.5	10.1	9.5	14.7
2.36-mm (No. 8)	1.7	0	3.5	10.2	0	20.4	46.6	40.9	39.5
1.18-mm (No. 16)	2.8	0	5.7	0	0	0	28.3	35.2	29.5
0.60-mm (No. 30)	0.2	0	0.4	0	0	0	8.8	8.8	9.2
0.30-mm (No. 50)	0	0	0	0	0	0	3.8	3.4	4.6
0.15-mm (No. 100)	0	0	0	0	0	0	1.5	1.3	1.8
0.075-mm (No. 200)	0	0	0	0	0	0	0.3	0.3	0.3
Pan	0	0	0	5.1	1.2	1.1	0.4	0.6	0.4
Batch Numbers	--	340	340	--	392	392	234	244	273
		343	343		394	394	235	246	274
				399	399	239			275
				403	403	240			278
				407	407				282
				408	408				290
				409	409				292
				412	412				298
				414	414				300
				417	417				
				419	419				

Table A.3 – Program I Set 1 mixture proportions and concrete properties

Batch	234	235	239
w/c	0.41	0.43	0.45
Paste Content, %	23.1	23.7	24.4
Coarse Aggregate Content, %	34.3	34.0	33.7
Cement Content, kg/m ³ (lb/yd ³)			
Type I/II Sample 1	317 (535)	317 (535)	--
Type I/II Sample 2	--	--	317 (535)
Water content, kg/m ³ (lb/yd ³)	130 (219)	136 (230)	143 (241)
Coarse Aggregate, kg/m ³ (lb/yd ³)			
19-mm (¾-in.) Limestone Gradation A	882 (1486)	873 (1472)	865 (1458)
Pea Gravel, kg/m ³ (lb/yd ³)			
Gradation A	355 (598)	352 (593)	348 (587)
Fine Aggregate, kg/m ³ (lb/yd ³)			
Gradation A	557 (938)	558 (941)	546 (921)
Admixtures, mL/m ³ (oz/yd ³)			
Type A-F HRWR	994 (25.7)	860 (22.2)	327 (8.5)
Air-entraining agent	77 (2.0)	55 (1.4)	92 (2.4)
Batch Size, m ³ (yd ³)	0.131 (0.171)		
Slump, mm (in.)	70 (2.75)	90 (3.5)	80 (3.25)
Air Content, %	8.65	8.15	8.15
Temperature, C (F)	21° (69°)	22° (72°)	24° (75°)
Compressive Strength, MPa (psi)			
28-Day Strengths [†]			
3-Day Wet Cure	31.4 (4550)	31.6 (4580)	26.0 (3770)
7-Day Wet Cure	29.6 (4300)	31.4 (4560)	28.4 (4120)
14-Day Wet Cure	33.6 (4880)	32.1 (4660)	28.3 (4110)
28-Day Wet Cure	31.0 (4500)	31.7 (4600)	28.1 (4080)

[†]Three 100 × 200 mm (4 × 8 in.) cylinders each were cured for 3, 7, 14, or 28 days in lime-saturated water, transferred to a drying tent [22° C (73° F) and 50% RH], and tested at an age of 28 days. The compressive strengths reported represent an average of three compressive strength tests.

Table A.4 – Program I Set 2 mixture proportions and concrete properties

Batch	240	244	246
w/c	0.41	0.43	0.45
Paste Content, %	23.1	23.7	24.4
Coarse Aggregate Content, %	34.3	32.6	32.2
Cement Content, kg/m ³ (lb/yd ³) Type II Sample 1	317 (535)	317 (535)	317 (535)
Water content, kg/m ³ (lb/yd ³)	130 (219)	136 (230)	143 (241)
Coarse Aggregate, kg/m ³ (lb/yd ³) 19-mm (¾-in.) Limestone			
Gradation A	882 (1486)	--	--
Gradation B(a)	--	516 (869)	510 (860)
Gradation B(b)	--	322 (542)	318 (536)
Pea Gravel, kg/m ³ (lb/yd ³) Gradation A	355 (598)	520 (876)	514 (866)
Fine Aggregate, kg/m ³ (lb/yd ³) Gradation A	557 (938)	--	--
Gradation B	--	422 (712)	418 (704)
Admixtures, mL/m ³ (oz/yd ³) Type A-F HRWR	994 (25.7)	360 (9.3)	117 (3.0)
Air-entraining agent	72 (1.9)	120 (3.1)	172 (4.4)
Batch Size, m ³ (yd ³)	0.131 (0.171)		
Slump, mm (in.)	75 (3)	80 (3.25)	70 (2.75)
Air Content, %	8.65	8.15	7.9
Temperature, C (F)	23° (74°)	23° (74°)	21° (70°)
Compressive Strength, MPa (psi) 28-Day Strengths [†]			
3-Day Wet Cure	27.9 (4050)	23.4 (3400)	22.3 (3230)
7-Day Wet Cure	28.0 (4060)	25.1 (3640)	24.6 (3570)
14-Day Wet Cure	28.5 (4140)	26.4 (3830)	26.3 (3810)
28-Day Wet Cure	28.6 (4150)	26.5 (3840)	26.0 (3770)

[†]Three 100 × 200 mm (4 × 8 in.) cylinders were cured for 3, 7, 14, or 28 days in lime-saturated water, transferred to a drying tent [22° C (73° F) and 50% RH], and tested at an age of 28 days. The compressive strengths reported represent an average of three compressive strength tests.

Table A.5 – Program I Set 3 mixture proportions and concrete properties

Batch	412	414	417
w/c	0.41	0.43	0.45
Paste content, %	22.9	23.3	24.2
Coarse Aggregate Content, %	30.8	30.5	30.3
Cement Content, kg/m ³ (lb/yd ³) Type I/II Sample	317 (535)	317 (535)	317 (535)
Water content, kg/m ³ (lb/yd ³)	129 (218)	136 (229)	142 (240)
Coarse Aggregate, kg/m ³ (lb/yd ³) 19-mm (¾-in.) Granite Gradation 2(a) Gradation 2(b)	488 (823) 322 (542)	484 (815) 319 (538)	479 (808) 316 (533)
Pea Gravel, kg/m ³ (lb/yd ³) Gradation 5	558 (941)	553 (932)	548 (923)
Fine Aggregate, kg/m ³ (lb/yd ³) Gradation 4	444 (749)	441 (743)	437 (736)
Admixtures, mL/m ³ (oz/yd ³) Type A-F HRWR Air-entraining agent	1383 (35.8) 86 (2.2)	896 (23.2) 64 (1.7)	561 (14.5) 94 (2.4)
Batch Size, m ³ (yd ³)	0.027 (0.035)		
Slump, mm (in.)	60 (2.25)	65 (2.5)	75 (3)
Air Content, %	8.65	7.9	8.15
Temperature, C (F)	19° (67°)	22° (71°)	21° (69°)
Compressive Strength, MPa (psi) [†] 7-Day 28-Day	25.2 (3660) 40.0 (5800)	26.8 (3880) 33.5 (4860)	21.9 (3180) 33.3 (4830)

[†]Three 100 × 200 mm (4 × 8 in.) cylinders were cured for 7 or 28 days in lime-saturated water and tested immediately. The compressive strengths reported represent an average of three compressive strength tests.

Table A.6 – Program II Set 1 and Set 2[†] mixture proportions and concrete properties

Batch	330	334	335	338
w/c	0.36	0.38	0.40	0.42
Paste Content, %	23.3	23.3	23.3	23.3
Coarse Aggregate Content, %	31.8	31.9	32.0	32.1
Cement Content, kg/m ³ (lb/yd ³) Type I/II Sample 4	346 (583)	336 (566)	326 (550)	317 (535)
Water content, kg/m ³ (lb/yd ³)	123 (207)	126 (213)	129 (218)	132 (223)
Coarse Aggregate, kg/m ³ (lb/yd ³) 19-mm (¾-in.) Limestone Gradation 3(a) Gradation 3(b)	510 (860) 306 (515)	511 (862) 307 (518)	513 (865) 309 (521)	514 (867) 311 (524)
Pea Gravel, kg/m ³ (lb/yd ³) Gradation 2	714 (1203)	705 (1189)	698 (1176)	691 (1164)
Fine Aggregate, kg/m ³ (lb/yd ³) Gradation 3	255 (430)	260 (438)	265 (447)	269 (454)
Admixtures, mL/m ³ (oz/yd ³) Air-entraining agent Type A-F HRWR	64 (1.7) 2128 (55.0)	70 (1.8) 1635 (42.3)	73 (1.9) 1308 (33.8)	68 (1.8) 1079 (27.9)
Batch Size, m ³ (yd ³)	0.050 (0.066)			
Slump, mm (in.)	95 (3.75)	75 (3)	50 (2)	50 (2)
Air Content, %	8.15	8.4	8.65	8.4
Temperature, C (F)	23° (73°)	22° (72°)	22° (72°)	23° (73°)
Compressive Strength, MPa (psi) [‡] 7-Day 28-Day	45.9 (6660) 50.7 (7350)	39.0 (5650) 43.0 (6230)	30.8 (4460) 38.8 (5630)	28.8 (4170) 37.9 (5500)

[†]Program II Set 2 also includes Batch 342 (shown in Table A.7).

[‡]Two 100 × 200 mm (4 × 8 in.) cylinders were cured for 7 or 28 days in lime-saturated water and tested immediately. The compressive strengths reported represent an average of two compressive strength tests.

Table A.7 –Program III mixture proportions and concrete properties

Batch	342	343	344
w/c	0.42	0.42	0.42
Paste Content, %	21.6	21.6	21.6
Coarse Aggregate Content, %	34.7	35.1	35.3
Cement Content, kg/m ³ (lb/yd ³) Type I/II Sample 4	295 (497)	295 (497)	295 (497)
Water content, kg/m ³ (lb/yd ³)	122 (206)	122 (206)	122 (206)
Coarse Aggregate, kg/m ³ (lb/yd ³)			
19-mm (¾-in.) Limestone			
Gradation 3(a)	529 (892)	--	--
Gradation 3(b)	363 (612)	--	--
19-mm (¾-in.) Granite			
Gradation 1(a)	--	552 (931)	--
Gradation 1(b)	--	364 (613)	--
19-mm (¾-in.) Quartzite			
Gradation 1(a)	--	--	589 (993)
Gradation 1(b)	--	--	342 (576)
Pea Gravel, kg/m ³ (lb/yd ³) Gradation 3	568 (958)	557 (938)	621 (1046)
Fine Aggregate, kg/m ³ (lb/yd ³) Gradation 3	365 (616)	368 (620)	299 (504)
Admixtures, mL/m ³ (oz/yd ³)			
Air-entraining agent	82 (2.1)	82 (2.1)	78 (2.0)
Type A-F HRWR	1504 (38.9)	1700 (44.0)	1602 (41.4)
Batch Size, m ³ (yd ³)	0.031 (0.040)		
Slump, mm (in.)	70 (2.75)	95 (3.75)	70 (2.75)
Air Content, %	7.9	8.4	8.4
Temperature, C (F)	22° (72°)	23° (73°)	22° (72°)
Compressive Strength, MPa (psi) [‡]			
7-Day	29.9 (4330)	28.3 (4100)	31.1 (4510)
28-Day	35.0 (5070)	34.3 (4980)	36.5 (5300)

[‡]Three 100 × 200 mm (4 × 8 in.) cylinders were cured for 7 or 28 days in lime-saturated water and tested immediately. The compressive strengths reported represent an average of three compressive strength tests.

Table A.8 – Program IV mixture proportions and concrete properties

Batch	273	308	323
w/c	0.42	0.42	0.42
Paste Content, %	23.3	23.3	23.3
Coarse Aggregate Content, %	31.6	33.4	34.2
Cement Content, kg/m ³ (lb/yd ³) Type I/II Sample 3	317 (535)	317 (535)	317 (535)
Water content, kg/m ³ (lb/yd ³)	132 (223)	125 (212)	129 (217)
Coarse Aggregate, kg/m ³ (lb/yd ³) 19-mm (¾-in.) Limestone			
Gradation 1(b)	--	368 (620)	390 (657)
Gradation 2(a)	539 (909)	--	--
Gradation 2(b)	295 (497)	--	--
Gradation 3(a)	--	514 (866)	514 (866)
Pea Gravel, kg/m ³ (lb/yd ³)			
Gradation 1	459 (774)	--	--
Gradation 2	--	542 (914)	453 (763)
Fine Aggregate, kg/m ³ (lb/yd ³)			
Gradation 1	494 (832)	--	--
Gradation 2	--	361 (609)	428 (722)
Admixtures, mL/m ³ (oz/yd ³)			
Air-entraining agent	64 (1.7)	458 (11.8)	154 (4.0)
Type A-F HRWR	1006 (26.0)	850 (22.0)	1275 (33.0)
Shrinkage Reducing Admixture	--	3165 (0.64)	6330 (1.28)
Batch Size, m ³ (yd ³)	0.031 (0.040)		
Slump, mm (in.)	60 (2.25)	50 (2)	75 (3)
Air Content, %	8.65	7.9	7.9
Temperature, C (F)	23° (73°)	19° (66°)	20° (68°)
Compressive Strength, MPa (psi) [‡]			
7-Day	29.4 (4260)	28.1 (4070)	31.4 (4560)
28-Day	36.3 (5260)	39.9 (5780)	37.5 (5440)

[‡]Three 100 × 200 mm (4 × 8 in.) cylinders were cured for 7 or 28 days in lime-saturated water and tested immediately. The compressive strengths reported represent an average of three compressive strength tests.

Table A.9 – Program V mixture proportions and concrete properties

Batch[†]	298	300	367
w/c	0.42	0.42	0.42
Paste Content, %	23.3	23.3	23.3
Coarse Aggregate Content, %	32.1	31.9	31.3
Cement Content, kg/m ³ (lb/yd ³)			
Type II Sample 3	317 (535)	--	--
Type II Sample 2	--	317 (535)	--
Type III Sample 1	--	--	317 (535)
Water content, kg/m ³ (lb/yd ³)	132 (223)	132 (223)	132 (223)
Coarse Aggregate, kg/m ³ (lb/yd ³)			
19-mm (¾-in.) Limestone			
Gradation 1(a)	--	504 (850)	--
Gradation 1(b)	333 (562)	337 (568)	--
Gradation 3(a)	514 (867)	--	514 (866)
Gradation 3(b)	--	--	311 (524)
Pea Gravel, kg/m ³ (lb/yd ³)			
Gradation 1	430 (725)	438 (739)	--
Gradation 4	--	--	690 (1163)
Fine Aggregate, kg/m ³ (lb/yd ³)			
Gradation 2	508 (857)	506 (853)	--
Gradation 3	--	--	269 (454)
Admixtures, mL/m ³ (oz/yd ³)			
Air-entraining agent	100 (2.6)	105 (2.7)	46 (1.2)
Type A-F HRWR	1079 (27.9)	1243 (32.1)	1504 (38.9)
Batch Size, m ³ (yd ³)	0.031 (0.040)		
Slump, mm (in.)	65 (2.5)	70 (2.75)	100 (4)
Air Content, %	8.65	8.9	8.65
Temperature, C (F)	22° (72°)	22° (71°)	22° (72°)
Compressive Strength, MPa (psi) [‡]			
7-Day	29.2 (4240)	26.5 (3850)	35.2 (5110)
28-Day	35.8 (5190)	28.5 (4140)	37.9 (5500)

[†]Batch 273 is the control for Program V and is shown in Table A.8.

[‡]Three 100 × 200 mm (4 × 8 in.) cylinders were cured for 7 or 28 days in lime-saturated water and tested immediately. The compressive strengths reported represent an average of three compressive strength tests.

Table A.10 – Program VI Set 1[†] mixture proportions and concrete properties

Batch	274	275	325	326
<i>Batch Designation</i>	3% SF #1	6% SF #1	3% SF #2	6% SF #2
<i>w/cm</i>	0.42	0.42	0.42	0.42
Paste Content, %	23.3	23.3	23.3	23.3
Coarse Aggregate Content, %	32.4	32.4	35.5	35.5
Cement Content, kg/m ³ (lb/yd ³) Type I/II Sample 3	310 (522)	301 (508)	310 (522)	301 (508)
Silica Fume Content, kg/m ³ (lb/yd ³) Sample 1	6.5 (11)	13 (22)	--	--
Sample 2	--	--	6.5 (11)	13 (22)
Water content, kg/m ³ (lb/yd ³)	132 (222)	131 (221)	132 (222)	131 (221)
Coarse Aggregate, kg/m ³ (lb/yd ³) 19-mm (¾-in.) Limestone				
Gradation 2(a)	539 (908)	539 (908)	--	--
Gradation 2(b)	295 (497)	295 (497)	--	--
Gradation 3(a)	--	--	514 (866)	514 (866)
Gradation 3(b)	--	--	399 (673)	399 (673)
Pea Gravel, kg/m ³ (lb/yd ³)				
Gradation 1	460 (776)	461 (777)	--	--
Gradation 2	--	--	426 (718)	426 (718)
Fine Aggregate, kg/m ³ (lb/yd ³)				
Gradation 1	493 (831)	493 (831)	--	--
Gradation 2	--	--	446 (752)	446 (752)
Admixtures, mL/m ³ (oz/yd ³)				
Air-entraining agent	63 (1.6)	63 (1.6)	63 (1.6)	50 (1.3)
Type A-F HRWR	1160 (30.0)	1199 (31.0)	1083 (28.0)	1406 (36.4)
Batch Size, m ³ (yd ³)	0.031 (0.040)			
Slump, mm (in.)	100 (4)	50 (2)	63 (2.5)	65 (2.5)
Air Content, %	8.65	8.4	8.9	8.65
Temperature, C (F)	22° (72°)	22° (72°)	22° (71°)	21° (69°)
Compressive Strength, MPa (psi) [‡]				
7-Day	32.4 (4700)	34.1 (4940)	29.7 (4310)	34.3 (4970)
28-Day	36.0 (5220)	43.1 (6250)	40.4 (5860)	45.0 (6530)

[†]Batch 273 is the control (0% silica fume) for Program VI Set 1 and is shown in Table A.8.

[‡]Three 100 × 200 mm (4 × 8 in.) cylinders were cured for 7 or 28 days in lime-saturated water and tested immediately. The compressive strengths reported represent an average of three compressive strength tests.

Table A.11 – Program VI Set 2 mixture proportions and concrete properties

Batch	409	392	394
<i>Batch Designation</i>	control	3% SF #2	6% SF #2
<i>w/cm</i>	0.42	0.42	0.42
Paste Content, %	23.3	23.3	23.3
Coarse Aggregate Content, %	30.7	35.5	35.5
Cement Content, kg/m ³ (lb/yd ³) Type I/II Sample 5	317 (535)	310 (522)	301 (508)
Silica Fume Content, kg/m ³ (lb/yd ³) Sample 2	--	6.5 (11)	13 (22)
Water content, kg/m ³ (lb/yd ³)	132 (223)	132 (222)	131 (220)
Coarse Aggregate, kg/m ³ (lb/yd ³) 19-mm (¾-in.) Granite Gradation 2(a) Gradation 2(b)	487 (820) 320 (540)	555 (936) 379 (639)	555 (936) 379 (639)
Pea Gravel, kg/m ³ (lb/yd ³) Gradation 5	556 (937)	374 (631)	374 (631)
Fine Aggregate, kg/m ³ (lb/yd ³) Gradation 3 Gradation 4	-- 443 (747)	497 (838) --	497 (838) --
Admixtures, mL/m ³ (oz/yd ³) Air-entraining agent Type A-F HRWR	67 (1.7) 1083 (28.0)	75 (1.9) 1457 (37.7)	75 (1.9) 1682 (43.5)
Batch Size, m ³ (yd ³)	0.027 (0.035)		
Slump, mm (in.)	65 (2.5)	90 (3.5)	95 (3.75)
Air Content, %	8.65	7.9	7.9
Temperature, C (F)	21° (70°)	21° (70°)	20° (68°)
Compressive Strength, MPa (psi) [‡] 7-Day 28-Day	26.3 (3820) 36.3 (5270)	32.5 (4710) 39.5 (5730)	31.7 (4600) 39.2 (5690)

[‡]Three 100 × 200 mm (4 × 8 in.) cylinders were cured for 7 or 28 days in lime-saturated water and tested immediately. The compressive strengths reported represent an average of three compressive strength tests.

Table A.12 – Program VI Set 3[†] mixture proportions and concrete properties

Batch	363	364	290	292
<i>Batch Designation</i>	20% FA #1	40% FA #1	20% FA #2	40% FA #2
<i>w/cm</i>	0.42	0.42	0.42	0.42
Paste Content, %	23.3	23.3	23.3	23.3
Coarse Aggregate Content, %	32.1	32.0	31.5	32.1
Cement Content, kg/m ³ (lb/yd ³)				
Type I/II Sample 3	--	--	262 (441)	202 (341)
Type I/II Sample 4	257 (433)	195 (329)		
Class F Fly Ash, kg/m ³ (lb/yd ³)				
Sample 1	58 (97)	117 (197)	--	--
Sample 2	--	--	49 (83)	101 (170)
Water content, kg/m ³ (lb/yd ³)	131 (221)	130 (219)	130 (219)	127 (214)
Coarse Aggregate, kg/m ³ (lb/yd ³)				
19-mm (¾-in.) Limestone				
Gradation 1(a)	--	--	503 (848)	502 (846)
Gradation 1(b)	--	--	--	322 (543)
Gradation 2(b)	--	--	305 (514)	--
Gradation 3(a)	513 (865)	513 (864)	--	--
Gradation 3(b)	310 (523)	309 (521)	--	--
Pea Gravel, kg/m ³ (lb/yd ³)				
Gradation 1	--	--	494 (833)	468 (789)
Gradation 4	693 (1168)	697 (1174)	--	--
Fine Aggregate, kg/m ³ (lb/yd ³)				
Gradation 1	--	--	483 (814)	493 (831)
Gradation 3	268 (451)	265 (447)	--	--
Admixtures, mL/m ³ (oz/yd ³)				
Air-entraining agent	105 (2.7)	163 (4.2)	108 (2.8)	173 (4.5)
Type A-F HRWR	1144 (29.6)	981 (25.4)	654 (16.9)	490 (12.7)
Batch Size, m ³ (yd ³)	0.031 (0.040)			
Slump, mm (in.)	70 (2.75)	100 (4)	75 (3)	75 (3)
Air Content, %	8.9	8.65	8.4	7.9
Temperature, C (F)	22° (71°)	21° (70°)	22° (72°)	22° (71°)
Compressive Strength, MPa (psi) [‡]				
7-Day	25.4 (3680)	25.4 (3680)	23.5 (3410)	19.4 (2820)
28-Day	32.5 (4710)	30.6 (4440)	27.8 (4030)	28.0 (4060)

[†]Batch 338 is the control (0% Fly Ash) for Batches 363 and 364 and is shown in Table A.6. Batch 273 is the control (0% Fly Ash) for Batches 290 and 292 and is shown in Table A.8.

[‡]Three 100 × 200 mm (4 × 8 in.) cylinders were cured for 7 or 28 days in lime-saturated water and tested immediately. The compressive strengths reported represent an average of three compressive strength tests.

Table A.13 – Program VI Set 4[†] mixture proportions and concrete properties

Batch	399	403	419	421
<i>Batch Designation</i>	20% FA #2	40% FA #2	20% FA #3	40% FA #3
<i>w/cm</i>	0.42	0.42	0.42	0.42
Paste Content, %	23.3	23.3	23.3	23.3
Coarse Aggregate Content, %	31.5	32.1	30.6	30.5
Cement Content, kg/m ³ (lb/yd ³) Type I/II Sample 5	262 (441)	202 (341)	260 (438)	200 (337)
Class F Fly Ash, kg/m ³ (lb/yd ³) Sample 2	49 (83)	101 (170)	--	--
Class C Fly Ash, kg/m ³ (lb/yd ³) Sample 3	--	--	52 (87)	106 (179)
Water content, kg/m ³ (lb/yd ³)	130 (219)	127 (214)	130 (219)	128 (216)
Coarse Aggregate, kg/m ³ (lb/yd ³) 19-mm (¾-in.) Granite Gradation 2(a)	503 (848)	510 (860)	485 (818)	484 (816)
Gradation 2(b)	325 (547)	334 (563)	319 (537)	317 (534)
Pea Gravel, kg/m ³ (lb/yd ³) Gradation 5	534 (900)	510 (860)	561 (946)	567 (956)
Fine Aggregate, kg/m ³ (lb/yd ³) Gradation 4	442 (745)	450 (759)	440 (742)	437 (736)
Admixtures, mL/m ³ (oz/yd ³) Air-entraining agent	97 (2.5)	146 (3.8)	71 (1.8)	173 (4.5)
Type A-F HRWR	785 (20.3)	635 (16.4)	710 (18.4)	105 (2.7)
Batch Size, m ³ (yd ³)	0.027 (0.035)			
Slump, mm (in.)	63 (2.5)	55 (2.25)	65 (2.5)	90 (3.5)
Air Content, %	8.4	7.9	8.4	8.4
Temperature, C (F)	21° (70°)	21° (70°)	17° (63°)	18° (64°)
Compressive Strength, MPa (psi) [‡] 7-Day	21.2 (3080)	17.1 (2480)	23.3 (3380)	16.8 (2440)
28-Day	29.9 (4340)	27.2 (3940)	32.6 (4730)	19.7 (2850)

[†]Batch 409 is the control (0% Fly Ash) for Program VI Set 4 and is shown in Table A.11.

[‡]Three 100 × 200 mm (4 × 8 in.) cylinders were cured for 7 or 28 days in lime-saturated water and tested immediately. The compressive strengths reported represent an average of three compressive strength tests.

Table A.14 – Program VI Set 5[†] mixture proportions and concrete properties

Batch	278	282	309	317
<i>Batch Designation</i>	30% GGBFS #1	60% GGBFS #1	60% GGBFS #2	80% GGBFS #2
<i>w/cm</i>	0.42	0.42	0.42	0.42
Paste Content, %	23.3	23.3	23.3	23.3
Coarse Aggregate Content, %	32.3	32.1	35.5	35.5
Cement Content, kg/m ³ (lb/yd ³) Type I/II Sample 3	226 (381)	131 (221)	131 (221)	66 (112)
Grade 120 Slag, kg/m ³ (lb/yd ³) Sample 1	88 (148)	179 (301)	--	--
Sample 2	--	--	179 (301)	240 (405)
Water content, kg/m ³ (lb/yd ³)	131 (221)	129 (218)	129 (218)	128 (216)
Coarse Aggregate, kg/m ³ (lb/yd ³) 19-mm (¾-in.) Limestone				
Gradation 1(a)	--	503 (848)	--	--
Gradation 2(a)	538 (906)	--	--	--
Gradation 2(b)	293 (494)	305 (514)	--	--
Gradation 3(a)	--	--	512 (863)	512 (863)
Gradation 3(b)	--	--	400 (674)	400 (674)
Pea Gravel, kg/m ³ (lb/yd ³)				
Gradation 1	463 (780)	495 (834)	--	--
Gradation 2	--	--	426 (718)	426 (718)
Fine Aggregate, kg/m ³ (lb/yd ³)				
Gradation 1	492 (829)	483 (814)	--	--
Gradation 2	--	--	446 (752)	446 (752)
Admixtures, mL/m ³ (oz/yd ³)				
Air-entraining agent	65 (1.7)	141 (3.7)	144 (3.7)	353 (9.1)
Type A-F HRWR	916 (23.7)	878 (22.7)	902 (23.3)	817 (21.1)
Batch Size, m ³ (yd ³)	0.031 (0.040)			
Slump, mm (in.)	75 (3)	55 (2.25)	75 (3)	55 (2.25)
Air Content, %	8.15	8.4	8.4	7.9
Temperature, C (F)	22° (71°)	23° (74°)	18° (65°)	21° (69°)
Compressive Strength, MPa (psi) [‡]				
7-Day	31.9 (4620)	28.8 (4180)	31.5 (4570)	30.1 (4360)
28-Day	41.7 (6050)	38.3 (5550)	37.1 (5380)	36.6 (5310)

[†]Batch 273 is the control (0% GGBFS) for Program VI Set 5 and is shown in Table A.8.

[‡]Three 100 × 200 mm (4 × 8 in.) cylinders were cured for 7 or 28 days in lime-saturated water and tested immediately. The compressive strengths reported represent an average of three compressive strength tests.

Table A.15 – Program VI Set 6 mixture proportions and concrete properties

Batch	322	312	324
<i>Batch Designation</i>	60% GGBFS #2	60% GGBFS #2	60% GGBFS #2
<i>w/cm</i>	0.42	0.42	0.42
Paste Content, %	23.3	23.3	23.3
Coarse Aggregate Content, %	35.5	36.5	35.5
Cement Content, kg/m ³ (lb/yd ³) Type I/II Sample 3	132 (222)	131 (221)	131 (221)
Grade 120 Slag, kg/m ³ (lb/yd ³) Sample 2	177 (298)	179 (301)	179 (301)
Water content, kg/m ³ (lb/yd ³)	129 (217)	129 (218)	129 (218)
Coarse Aggregate, kg/m ³ (lb/yd ³) 19-mm (¾-in.) Limestone Gradation 3(a)	512 (863)	--	--
Gradation 3(b)	400 (674)	--	--
19-mm (¾-in.) Quartzite Gradation 1(a)	--	573 (967)	573 (967)
Gradation 1(b)	--	389 (656)	389 (656)
Pea Gravel, kg/m ³ (lb/yd ³) Gradation 2	426 (718)	448 (755)	448 (755)
Fine Aggregate, kg/m ³ (lb/yd ³) Gradation 2	446 (752)	398 (671)	398 (671)
Admixtures, mL/m ³ (oz/yd ³) Air-entraining agent Type A-F HRWR	144 (3.7) 1014 (26.2)	144 (3.7) 719 (18.6)	144 (3.7) 719 (18.6)
Batch Size, m ³ (yd ³)	0.031 (0.040)		
Slump, mm (in.)	70 (2.75)	80 (3.25)	75 (3)
Air Content, %	8.65	8.4	8.4
Temperature, C (F)	22° (72°)	22° (71°)	21° (69°)
Compressive Strength, MPa (psi) [†] 7-Day 28-Day	22.3 (3230) 36.5 (5300)	23.9 (3460) 39.6 (5750)	23.9 (3460) 36.3 (5260)

[†]Three 100 × 200 mm (4 × 8 in.) cylinders were cured for 7 or 28 days in lime-saturated water and tested immediately. The compressive strengths reported represent an average of three compressive strength tests.

Table A.16 – Program VI Set 7[†] mixture proportions and concrete properties

Batch	328	340
<i>Batch Designation</i>	60% G100 #4	60% G100 #4
<i>w/cm</i>	0.42	0.42
Paste Content, %	23.3	23.3
Coarse Aggregate Content, %	32.0	35.0
Cement Content, kg/m ³ (lb/yd ³) Type I/II Sample 4	132 (222)	132 (222)
Grade 100 Slag, kg/m ³ (lb/yd ³) Sample 4	177 (298)	177 (298)
Water content, kg/m ³ (lb/yd ³)	129 (217)	129 (217)
Coarse Aggregate, kg/m ³ (lb/yd ³) 19-mm (¾-in.) Limestone Gradation 3(a) Gradation 3(b) 19-mm (¾-in.) Granite Gradation 1(a) Gradation 1(b)	513 (864) 309 (520) -- --	-- -- 484 (815) 322 (542)
Pea Gravel, kg/m ³ (lb/yd ³) Gradation 2	700 (1180)	601 (1013)
Fine Aggregate, kg/m ³ (lb/yd ³) Gradation 2 Gradation 3	263 (444) --	-- 395 (666)
Admixtures, mL/m ³ (oz/yd ³) Air-entraining agent Type A-F HRWR	144 (3.7) 1149 (29.7)	144 (3.7) 1210 (31.3)
Batch Size, m ³ (yd ³)	0.050 (0.066)	0.031 (0.040)
Slump, mm (in.)	80 (3.25)	65 (2.5)
Air Content, %	8.9	8.9
Temperature, C (F)	20° (68°)	23° (73°)
Compressive Strength, MPa (psi) [‡] 7-Day 28-Day	26.4 (3830) 35.2 (5110)	21.6 (3140) 33.4 (4850)

[†]Batch 338 is the control (0% GGBFS and limestone coarse aggregate) for Program VI Set 7 and is shown in Table A.6.

[‡]Three 100 × 200 mm (4 × 8 in.) cylinders were cured for 7 or 28 days in lime-saturated water and tested immediately. The compressive strengths reported represent an average of three compressive strength tests.

Table A.17 – Program VI Set 8[†] mixture proportions and concrete properties

Batch	407	408
<i>Batch Designation</i>	30% G100 #3	60% G100 #3
<i>w/cm</i>	0.42	0.42
Paste Content, %	23.3	23.3
Coarse Aggregate Content, %	32.0	32.0
Cement Content, kg/m ³ (lb/yd ³) Type I/II Sample 5	226 (381)	132 (222)
Grade 100 Slag, kg/m ³ (lb/yd ³) Sample 3	87 (147)	177 (298)
Water content, kg/m ³ (lb/yd ³)	131 (220)	129 (217)
Coarse Aggregate, kg/m ³ (lb/yd ³) 19-mm (¾-in.) Granite Gradation 2(a)	503 (847)	503 (847)
Gradation 2(b)	338 (569)	338 (569)
Pea Gravel, kg/m ³ (lb/yd ³) Gradation 5	506 (853)	507 (854)
Fine Aggregate, kg/m ³ (lb/yd ³) Gradation 4	459 (773)	458 (772)
Admixtures, mL/m ³ (oz/yd ³) Air-entraining agent Type A-F HRWR	82 (2.1) 1271 (32.8)	144 (3.7) 1243 (32.1)
Batch Size, m ³ (yd ³)	0.027 (0.035)	
Slump, mm (in.)	70 (2.75)	65 (2.5)
Air Content, %	7.9	7.9
Temperature, C (F)	21° (69°)	21° (69°)
Compressive Strength, MPa (psi) 7-Day	30.1 (4360)	22.7 (3290)
28-Day	41.1 (5960)	41.3 (5990)

[†]Batch 409 is the control (0% GGBFS) for Program VI Set 8 and is shown in Table A.11.

[‡]Three 100 × 200 mm (4 × 8 in.) cylinders were cured for 7 or 28 days in lime-saturated water and tested immediately. The compressive strengths reported represent an average of three compressive strength tests.

Table A.18 – Program VI Set 9[†] mixture proportions and concrete properties

Batch	368	369	373	427
<i>Batch Designation</i>	60% GGBFS OD	60% GGBFS SSD	Control SSD	Control OD
<i>w/cm</i>	0.42	0.42	0.42	0.42
Paste Content, %	23.3	23.3	23.3	23.3
Coarse Aggregate Content, %	32.0	32.0	32.1	32.0
Cement Content, kg/m ³ (lb/yd ³) Type I/II Sample 5	132 (222)	132 (222)	317 (535)	317 (535)
Grade 100 Slag, kg/m ³ (lb/yd ³) Sample 5	177 (298)	177 (298)	--	--
Water content, kg/m ³ (lb/yd ³)	129 (217)	129 (217)	132 (223)	132 (223)
Coarse Aggregate, kg/m ³ (lb/yd ³) 19-mm (¾-in.) Limestone				
Gradation 3(a)	513 (864)	513 (864)	--	--
Gradation 3(b)	309 (520)	309 (520)	311 (524)	--
Gradation 4(a)	--	--	515 (868)	--
Gradation 5(a)	--	--	--	541 (912)
Gradation 5(b)	--	--	--	281 (473)
Pea Gravel, kg/m ³ (lb/yd ³)				
Gradation 4	700 (1180)	700 (1180)	689 (1162)	--
Gradation 5	--	--	--	594 (1001)
Fine Aggregate, kg/m ³ (lb/yd ³)				
Gradation 3	263 (444)	263 (444)	270 (455)	--
Gradation 4	--	--	--	370 (623)
Admixtures, mL/m ³ (oz/yd ³)				
Air-entraining agent	131 (3.4)	131 (3.4)	43 (1.1)	75 (1.9)
Type A-F HRWR	1014 (26.2)	1014 (26.2)	916 (23.7)	747 (19.3)
Batch Size, m ³ (yd ³)	0.050 (0.066)			0.027 (0.035)
Slump, mm (in.)	75 (3)	65 (2.5)	70 (2.75)	90 (3.5)
Air Content, %	8.4	8.15	8.15	8.4
Temperature, C (F)	23° (73°)	19° (67°)	23° (73°)	18° (65°)
Compressive Strength, MPa (psi)				
7-Day	24.5 (3560)	27.6 (4000)	29.5 (4280)	26.8 (3890)
28-Day	31.7 (4600)	39.3 (5700)	36.3 (5260)	35.1 (5090)

[†]Batches 369 and 373 were cast with aggregate in the saturated-surface-dry (SSD) condition, and batches 368 and 427 were cast with oven-dried aggregate.

[‡]Three 100 × 200 mm (4 × 8 in.) cylinders were cured for 7 or 28 days in lime-saturated water and tested immediately. The compressive strengths reported represent an average of three compressive strength tests.

Table A.19 – Program VI Set 10[†] mixture proportions and concrete properties

Batch	351	354	355	358
<i>Batch Designation</i>	497 – 60% G120 #2	497 – 60% G120 #2 6% SF #2	460 – 60% G120 #2 6% SF #2	460 – 80% G120 #2 6% SF #2
<i>w/cm</i>	0.42	0.42	0.42	0.42
Paste Content, %	21.6	21.6	20.5	20.5
Coarse Aggregate Content, %	32.0	33.1	33.7	33.7
Cement Content, kg/m ³ (lb/yd ³) Type I/II Sample 4	132 (222)	104 (175)	98 (166)	41 (69)
Grade 120 Slag, kg/m ³ (lb/yd ³) Sample 2	177 (298)	170 (287)	161 (272)	217 (366)
Silica Fume, kg/m ³ (lb/yd ³) Sample 2	--	12 (21)	12 (20)	12 (20)
Water content, kg/m ³ (lb/yd ³)	120 (203)	119 (201)	112 (189)	112 (188)
Coarse Aggregate, kg/m ³ (lb/yd ³) 19-mm (¾-in.) Limestone Gradation 3(a) Gradation 3(b)	529 (891) 321 (541)	528 (890) 320 (540)	539 (908) 328 (553)	539 (908) 328 (552)
Pea Gravel, kg/m ³ (lb/yd ³) Gradation 3 Gradation 4	695 (1171) --	-- 697 (1175)	-- 696 (1173)	-- 698 (1176)
Fine Aggregate, kg/m ³ (lb/yd ³) Gradation 3	284 (478)	282 (475)	294 (496)	293 (494)
Admixtures, mL/m ³ (oz/yd ³) Air-entraining agent Type A-F HRWR	133 (3.4) 1031 (26.6)	121 (3.1) 1507 (39.0)	131 (3.4) 1962 (50.7)	167 (4.3) 1834 (47.4)
Batch Size, m ³ (yd ³)	0.050 (0.066)			
Slump, mm (in.)	55 (2.25)	55 (2.25)	90 (3.5)	75 (3)
Air Content, %	8.25	8.9	8.9	8.4
Temperature, C (F)	24° (75°)	22° (72°)	24° (75°)	22° (72°)
Compressive Strength, MPa (psi) [‡] 7-Day 28-Day	30.9 (4480) 36.5 (5300)	33.6 (4880) 39.8 (5770)	31.8 (4610) 39.2 (5680)	26.9 (3900) 32.5 (4710)

[†]Batch 342 is the control for Program VI Set 10 and is shown in Table A.7.

[‡]Three 100 × 200 mm (4 × 8 in.) cylinders were cured for 7 or 28 days in lime-saturated water and tested immediately. The compressive strengths reported represent an average of three compressive strength tests.

APPENDIX B: AGGREGATE OPTIMIZATION EXAMPLE PROBLEM

B.1 GENERAL

Appendix B presents an example that demonstrates the application of the optimization process described in Chapter 3. This process is iterative and requires many repetitive calculations, including regularly inverting an 8×8 matrix, and as such, does not lend itself easily to hand calculations. For this reason, Appendix B only includes calculations for one iteration. The concrete specifications used as a guide for this example are a modification of the low-cracking high-performance concrete (LC-HPC) specifications used in Kansas and described in Chapter 5. The specifications have been modified to include Grade 120 slag cement to fully illustrate the optimization process for mixtures containing mineral admixtures.

B.2 EXAMPLE CONCRETE SPECIFICATIONS

The modified LC-HPC specifications used in this example are presented in Tables B.1 – B.3.

Table B.1 – Low-cracking high-performance concrete (LC-HPC) specification

Grade of Concrete Type of Aggregate	lb. (kg) of Cement per cu yd (cu m) of Concrete, min / max	lb. (kg) of Slag Cement per cu yd (cu m) of Concrete, min / max*	lb. (kg) of Water per lb. (kg) of Cementitious Material, max	Designated Air Content Percent by Volume**
Grade 3.5 (AE) (LC-HPC) (Grade 24 (AE) (LC-HPC))				
MA-4	400 (237) / 435(258)	100 (59) / 135 (80)	0.42	8.0 ± 1.0

*Meets the requirement for Grade 120 Slag (ASTM C 989).

**Concrete with an air content less than 6.5% or greater than 9.5% shall be rejected.

Table B.2 – LC-HPC slump requirements

Type of Work	Designated Slump in. (mm)	Maximum Allowable Slump in. (mm)
Grade 3.5 (AE) (LC-HPC) (Grade 24 (AE) (LC-HPC))	1 ½ - 3 (36-75)	4 (100)

Table B.3 – Grading requirements for combined aggregates for LC-HPC

Type	Percent Retained Per Sieve - Square Mesh Sieves										
	1½" (37.5 mm)	1" (25.0 mm)	¾" (19.0 mm)	½" (12.5 mm)	3/8" (9.5 mm)	No. 4 (4.75 mm)	No. 8 (2.36 mm)	No. 16 (1.18 mm)	No. 30 (600 µm)	No. 50 (300 µm)	No. 100 (150 µm)
MA-4	0	2-6	5-18	8-18	8-18	8-18	8-18	8-18	8-15	5-15	0-5

*Use a proven optimization method, such as the Shilstone Method or the KU Mix Method.

**Maximum allowed percent passing the No. 200 sieve is 2.5% by weight.

B.3 MATERIALS SELECTED

The following concrete properties and material quantities are selected based on the LC-HPC specifications presented in Section B.2:

Table B.4 – Cementitious material quantities selected based on the specifications

	Variable	Quantity, lb/yd ³	SG
Portland Cement	M_C	400	3.20
G120 Slag Cement	M_I	135	2.90

1. Cement content: $M_C = 400$ lb/yd³
2. Grade 120 slag cement content: $M_I = 135$ lb/yd³
3. w/cm ratio: 0.42
4. Air content: 8.0%
5. Slump: 2.5 in.
6. MSA: 1 in.

At this point in the optimization process it is necessary to select a trial set of aggregates. These aggregates should include at least one aggregate that contains material retained on the desired maximum size sieve (1 in. in this case), and the remaining aggregates should contain material on all of the other size fractions. Selecting aggregates that meet these criteria is the most critical step in the process and will ensure that a well-graded blend is attainable. Three aggregates have been selected as possible candidates for use in the mixture design. The aggregate properties are shown in Table B.5, and the aggregate gradations are shown in Table B.6 and plotted in Fig. B.1.

Table B.5 – Aggregate Properties

	Aggregate No.	BSG_{SSD}	F.M.
1 in. Granite	1	2.64	7.21
½ in. Granite	2	2.64	6.44
Sand	3	2.63	3.32

Table B.6 – Percent Retained on Each Sieve for the Trial Set of Aggregates

Sieve	1 in. Granite Aggregate 1	½ in. Granite Aggregate 2	Sand Aggregate 3
1½-in. (37.5 mm)	0.0	0.0	0.0
1-in. (25 mm)	16.1	0.0	0.0
¾-in. (19 mm)	27.1	0.0	0.0
½-in. (12.5 mm)	27.8	26.0	0.0
⅜-in. (9.5 mm)	13.2	25.8	0.0
No. 4 (4.75 mm)	14.9	45.1	3.1
No. 8 (2.36 mm)	0.0	2.2	19.8
No. 16 (1.18 mm)	0.0	0.0	25.9
No. 30 (0.60 mm)	0.0	0.0	20.3
No. 50 (0.30 mm)	0.0	0.0	21.0
No. 100 (0.15 mm)	0.0	0.0	7.8
No. 200 (0.075 mm)	0.0	0.0	2.1
Pan	0.9	0.9	0.0

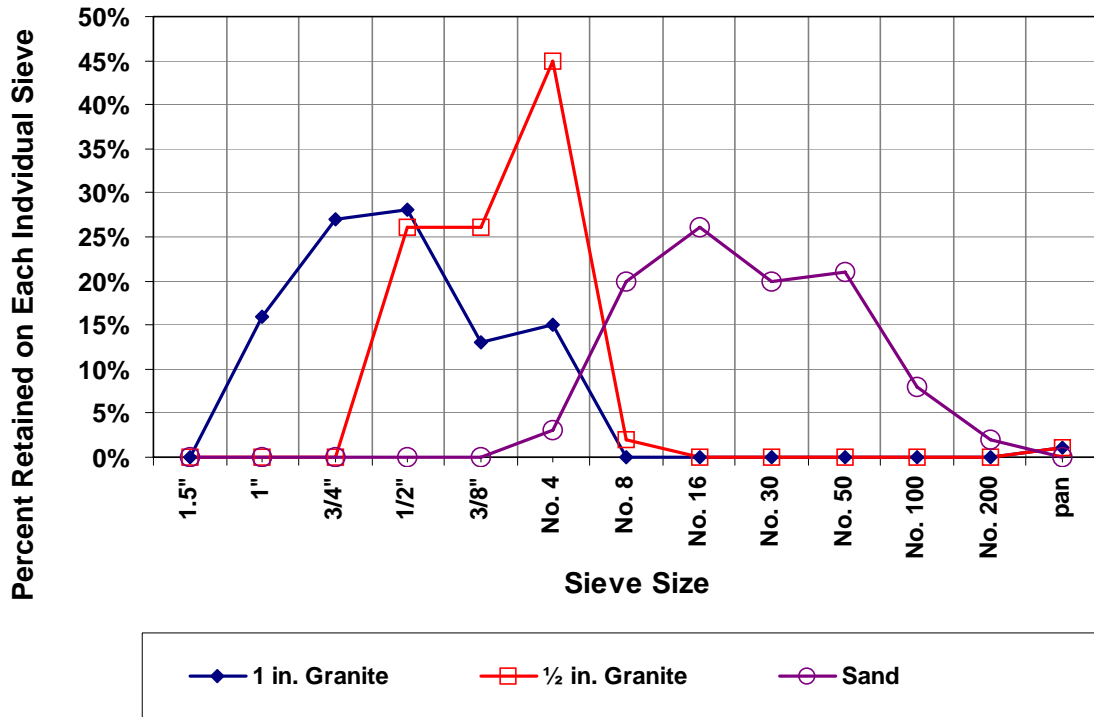


Fig. B.1 – Percents retained on each sieve for the trial set of aggregates

B.4 CALCULATE THE IDEAL GRADATION

As described in Section 3.2, the mathematical model chosen to describe the *ideal* gradation on a percent retained chart, entitled the *Cubic-Cubic Model*, consists of two overlapping cubic polynomial equations that are each defined for specific sieves:

$$y(x_n) = A(\log x_n)^3 + B(\log x_n)^2 + C(\log x_n) + D \quad (3.9a)$$

$$z(x_n) = A'(\log x_n)^3 + B'(\log x_n)^2 + C'(\log x_n) + D' \quad (3.9b)$$

where $y(x)$ and $z(x)$ represent the percent of total aggregate retained on sieve n with opening size x_n , $\log x_n$ represents the sieve opening in millimeters plotted on a logarithmic scale, and A , B , C , and D are the coefficients for the first equation, and A' , B' , C' , and D' are the coefficients for the second equation. Values of the sieve opening x_n , $\log x_n$, $\log x_n$ squared, and $\log x_n$ cubed are shown in Table B.7.

Table B.7 – Sieve openings and related log calculations

Sieve	Sieve opening (mm), x_n	$\log(x_n)$	$\log(x_n)^2$	$\log(x_n)^3$
1½-in. (37.5 mm)	37.5	1.574	2.478	3.900
1-in. (25 mm)	25	1.398	1.954	2.732
¾-in. (19 mm)	19	1.279	1.635	2.091
½-in. (12.5 mm)	12.5	1.097	1.203	1.320
⅜-in. (9.5 mm)	9.5	0.978	0.956	0.935
No. 4 (4.75 mm)	4.75	0.677	0.458	0.310
No. 8 (2.36 mm)	2.36	0.373	0.139	0.052
No. 16 (1.18 mm)	1.18	0.072	0.005	0.000
No. 30 (0.60 mm)	0.6	-0.222	0.049	-0.011
No. 50 (0.30 mm)	0.3	-0.523	0.273	-0.143
No. 100 (0.15 mm)	0.15	-0.824	0.679	-0.560
No. 200 (0.075 mm)	0.075	-1.125	1.265	-1.424

The eight equations required to determine the *ideal* gradation using the concrete specifications and selected materials outlined in Sections B.1 and B.2 are described next.

Criterion 1. The percentage of aggregate retained on the top sieve in the *ideal* gradation model is equal to the quantity retained on the top sieve of the actual aggregate gradation. The quantity retained on the top sieve of the actual aggregate gradation is initially unknown, and as a result, the user is required to select a range of percentages for the top sieve (defined by a desired minimum and maximum percent retained on the top sieve that is commonly specified in aggregate specifications) and the midpoint of that range is used for the first iteration.

The following information is identified from the specifications shown in Table B.3:

- The top sieve is the 1 in. (25 mm) sieve.
- The minimum desired percent retained on the top sieve is 2% and the maximum is 6%. Therefore, the target percent retained is 4%.

$$2.732 \cdot A + 1.954 \cdot B + 1.398 \cdot C + D = 4 \quad (\text{B.1})$$

Criterion 2. The quantity retained on the 0.075-mm (No. 200) sieve of the *ideal* gradation is set equal to the quantity retained on the 0.075-mm (No. 200) sieve of the optimized gradation. The percent retained is assumed to be 2% for the first iteration.

Using Eq. (3.11),

$$-1.424 \cdot A' + 1.265 \cdot B' - 1.125 \cdot C' + D' = 2 \quad (\text{B.2})$$

Criterion 3. The quantity retained on the 2.36-mm (No. 8) sieve must be equal for both of the cubic equations that define the *ideal* gradation.

Using Eq. (3.12),

$$0.052 \cdot A + 0.139 \cdot B + 0.373 \cdot C + D = 0.052 \cdot A' + 0.139 \cdot B' + 0.373 \cdot C' + D' \quad (\text{B.3})$$

Criterion 4. The quantity retained on the 4.75-mm (No. 4) sieve must be equal for both of the cubic equations that define the *ideal* gradation.

Using Eq. (3.13),

$$0.310 \cdot A + 0.458 \cdot B + 0.677 \cdot C + D = 0.310 \cdot A' + 0.458 \cdot B' + 0.677 \cdot C' + D' \quad (\text{B.4})$$

Criterion 5. The quantity retained on the 9.5-mm ($\frac{3}{8}$ -in.) sieve must be equal for both of the cubic equations that define the *ideal* gradation.

Using Eq. (3.14),

$$0.935 \cdot A + 0.956 \cdot B + 0.978 \cdot C + D = 0.935 \cdot A' + 0.956 \cdot B' + 0.978 \cdot C' + D' \quad (\text{B.5})$$

Criteria 6 – 8. The final three criteria required to solve for the eight coefficients that define the *Cubic-Cubic Model* are based on WF_{ideal} and CF_{ideal} , which are used to calculate Q_{ideal} , I_{ideal} , and W_{ideal} . The initial CF_{ideal} value used for the *ideal* gradation model is assumed to be 60, resulting in a WF_{ideal} of 35.0 [calculated using Eq. (3.18)].

$$WF(60.0) = 2.17 \times 10^{-5}(60.0)^3 - 0.00340(60.0)^2 + 0.0216(60.0) + 41.3 \quad (\text{B.6})$$

$$WF(60.0) = 35.0$$

The percent passing the 0.075-mm (No. 200) sieve is included in the W particles and must also be included in the *ideal* gradation model. The initial percent retained on the 0.075-mm (No. 200) sieve for the *ideal* gradation model is assumed to be 2%. Given CF_{ideal} and WF_{ideal} , the next step is to calculate W_{ideal} , Q_{ideal} , and I_{ideal} .

Solve Eq. (3.7) for W_{ideal} ,

$$WF_{ideal} = \frac{W_{ideal}}{Q_{ideal} + I_{ideal} + W_{ideal}} \times 100 = \frac{W_{ideal}}{100} \times 100 = 35 \quad (\text{B.7})$$

giving $W_{ideal} = 35$

Solve Eq. (3.4) for $Q_{ideal} + I_{ideal}$,

$$Q_{ideal} + I_{ideal} = 100 - W_{ideal} = 100 - 35 = 65 \quad (\text{B.8})$$

Solve Eq. (3.5) for Q_{ideal} ,

$$CF_{ideal} = \frac{Q_{ideal}}{Q_{ideal} + I_{ideal}} \times 100 = \frac{Q_{ideal}}{65} \times 100 = 60 \quad (\text{B.9})$$

giving $Q_{ideal} = \frac{60 \times 65}{100} = 39$

Finally, using Eq. (3.4) again, solve for I_{ideal} ,

$$I_{ideal} = 100 - Q_{ideal} - W_{ideal} = 100 - 39 - 35 = 26 \quad (\text{B.10})$$

The final three equations defining the *ideal* gradation are based on these three target gradation fractions. The first criterion is that the quality filler Q for the *ideal* gradation model is set equal to Q_{ideal} using Eq. (3.15).

$$Q_{ideal} = \begin{aligned} & 2.732 \cdot A + 1.954 \cdot B + 1.398 \cdot C + D + \\ & 2.091 \cdot A + 1.635 \cdot B + 1.279 \cdot C + D + \\ & 1.320 \cdot A + 1.203 \cdot B + 1.097 \cdot C + D + \\ & 0.935 \cdot A + 0.956 \cdot B + 0.978 \cdot C + D \end{aligned} \quad (\text{B.11a})$$

$$Q_{ideal} = 7.078 \cdot A + 5.748 \cdot B + 4.752 \cdot C + 4 \cdot D = 39 \quad (\text{B.11b})$$

Second, set I for the *ideal* gradation model equal to I_{ideal} following Eq. (3.16).

$$I_{ideal} = A[0.310 + 0.052] + B[0.458 + 0.139] + C[0.677 + 0.373] + 2D \quad (\text{B.12a})$$

$$I_{ideal} = 0.362 \cdot A + 0.597 \cdot B + 1.050 \cdot C + 2 \cdot D = 26 \quad (\text{B.12b})$$

Third, set W for the *ideal* gradation model equal to W_{ideal} following Eq. (3.17).

The percent retained on the pan must be subtracted from W_{ideal} because the percent retained on the pan is not included in the *Cubic-Cubic Model* but should be accounted for in W particles.

$$W_{ideal} - \bar{R}_{pan} = A'[0.000 - 0.011 - 0.143 - 0.559 - 1.424] + B'[0.005 + 0.049 + 0.273 + 0.679 + 1.265] + C'[0.072 - 0.222 - 0.523 - 0.824 - 1.125] + 5D' \quad (\text{B.13a})$$

$$W_{ideal} - \bar{R}_{pan} = -2.137 \cdot A' + 2.271 \cdot B' - 2.622 \cdot C' + 5 \cdot D' = 35 - 2 = 33 \quad (\text{B.13b})$$

Solve equations (B.1) through (B.5) and (B.11) through (B.13) simultaneously to determine the eight coefficients that define the *Cubic-Cubic Model*. These eight linear equations are easily solved using linear algebra as shown next.

$$\begin{bmatrix} 2.732 & 1.954 & 1.398 & 1 & 0 & 0 & 0 & 0 \\ 0 & 0 & 0 & 0 & -1.424 & 1.265 & -1.125 & 1 \\ 0.052 & 0.139 & 0.373 & 1 & -0.052 & -0.139 & -0.373 & -1 \\ 0.310 & 0.458 & 0.677 & 1 & -0.310 & -0.458 & -0.677 & -1 \\ 0.935 & 0.956 & 0.978 & 1 & -0.935 & -0.956 & -0.978 & -1 \\ 7.078 & 5.748 & 4.752 & 4 & 0 & 0 & 0 & 0 \\ 0.362 & 0.597 & 1.050 & 2 & 0 & 0 & 0 & 0 \\ 0 & 0 & 0 & 0 & -2.137 & 2.271 & -2.622 & 5 \end{bmatrix} \begin{bmatrix} A \\ B \\ C \\ D \\ A' \\ B' \\ C' \\ D' \end{bmatrix} = \begin{bmatrix} 4 \\ 2 \\ 0 \\ 0 \\ 0 \\ 39 \\ 26 \\ 33 \end{bmatrix} \quad (\text{B.14})$$

$$\begin{bmatrix} A \\ B \\ C \\ D \\ A' \\ B' \\ C' \\ D' \end{bmatrix} = \begin{bmatrix} -28.77 \\ 54.33 \\ -29.29 \\ 17.36 \\ -0.92 \\ -2.12 \\ 6.32 \\ 10.48 \end{bmatrix} \quad (\text{B.15})$$

Therefore the two cubic equations are:

$$1. \ y(x_n) = -28.77(\log x_n)^3 + 54.33(\log x_n)^2 - 29.29(\log x_n) + 17.36$$

$$2. \ z(x_n) = -0.92(\log x_n)^3 - 2.12(\log x_n)^2 + 6.32(\log x_n) + 10.48$$

While these two equations define the *Cubic-Cubic Model* with parameters and assumptions defined in this section (namely, $CF=60$ and $WF=35$), the model must be updated as CF_{ideal} and WF_{ideal} are updated and as the actual percentages retained on the top sieve, No. 200 sieve, and the pan are determined.

Table B.8 – Percents retained for both cubic equations and the *Cubic-Cubic Model* prior to optimizing the *CF* and *WF* using notation defined in Table 3.2

Sieve	Sieve Designation, n	Eq. (3.9a), $y(x_n)$	Eq. (3.9b), $z(x_n)$	<i>Cubic-Cubic Model (Ideal Gradation)</i> , \bar{R}_n
1½-in. (37.5 mm)	a	–6.32	11.58	0.00
1-in. (25 mm)	b	4.00	12.65	4.00
¾-in. (19 mm)	c	8.59	13.17	8.59
½-in. (12.5 mm)	d	12.63	13.64	12.63
⅜-in. (9.5 mm)	e	13.77	13.77	13.77
No. 4 (4.75 mm)	f	13.50	13.50	13.50
No. 8 (2.36 mm)	g	12.50	12.50	12.50
No. 16 (1.18 mm)	h	15.52	10.93	10.93
No. 30 (0.60 mm)	i	26.84	8.99	8.99
No. 50 (0.30 mm)	j	51.64	6.73	6.73
No. 100 (0.15 mm)	k	94.46	4.35	4.35
No. 200 (0.075 mm)	l	160.01	2.00	2.00
Pan	m	--	--	2.00

B.5 DETERMINE CF_{ideal} AND WF_{ideal}

The target CF and WF depend on the top sieve and the percent retained on the top sieve and are obtained by minimizing Eq. (3.19). The relationship between WF_{ideal} and CF_{ideal} is defined by Eq. (3.18). A spreadsheet solver routine is a simple tool that can be used to identify the optimum CF (and WF) that minimizes Eq. (3.19). In addition to minimizing Eq. (3.19), the solver routine must continuously update the *Cubic-Cubic Model* (by solving for the eight coefficients) each time the CF (and WF) is changed. The initial calculation for Eq. (3.19) is shown next, where values for \bar{R}_e , \bar{R}_f , and \bar{R}_g are taken from Table B.8.

$$\text{Minimize } \left\{ |\bar{R}_f - \bar{R}_g| + |\bar{R}_e - \bar{R}_f| + |\bar{R}_e - \bar{R}_g| \right\} \text{ by changing the } CF \quad (3.19)$$

With $CF=60$ and $WF=35$ prior to determining the CF_{ideal} and WF_{ideal} (B.16)

$$|13.50 - 12.50| + |13.77 - 13.50| + |13.77 - 12.50| = 2.54\%$$

The CF_{ideal} and WF_{ideal} for the *ideal* gradation determined by minimizing Eq. (3.19) while imposing the relationship between CF and WF [Eq. (3.8)] are 57.7 and 35.4, respectively. The updated *ideal* gradation for these new values of CF_{ideal} and WF_{ideal} is shown in Table B.9.

Equation (3.19) obtained during the minimization process (based on values for \bar{R}_e , \bar{R}_f , and \bar{R}_g shown in Table B.9) is

$$|14.04 - 13.31| + |13.31 - 14.04| + |13.31 - 13.31| = 1.46\% \quad (\text{B.17})$$

Table B.9 – Percents retained for both cubic equations and the *Cubic-Cubic Model* with the optimized CF_{ideal} and WF_{ideal}

Sieve	Sieve Designation, n	Eq. (3.9a), $y(x_n)$	Eq. (3.9b), $z(x_n)$	<i>Cubic-Cubic Model (Ideal Gradation)</i> , \bar{R}_n
1½-in. (37.5 mm)	<i>a</i>	-4.58	6.14	0.00
1-in. (25 mm)	<i>b</i>	4.00	9.18	4.00
¾-in. (19 mm)	<i>c</i>	8.04	10.77	8.04
½-in. (12.5 mm)	<i>d</i>	11.94	12.55	11.94
⅜-in. (9.5 mm)	<i>e</i>	13.31	13.31	13.31
No. 4 (4.75 mm)	<i>f</i>	14.04	14.04	14.04
No. 8 (2.36 mm)	<i>g</i>	13.31	13.31	13.31
No. 16 (1.18 mm)	<i>h</i>	14.31	11.56	11.56
No. 30 (0.60 mm)	<i>i</i>	19.90	9.22	9.22
No. 50 (0.30 mm)	<i>j</i>	33.43	6.56	6.56
No. 100 (0.15 mm)	<i>k</i>	57.95	4.02	4.02
No. 200 (0.075 mm)	<i>l</i>	96.58	2.00	2.00
Pan	<i>m</i>	--	--	2.00

The updated *ideal* gradation coefficients are

$$\begin{bmatrix} A \\ B \\ C \\ D \\ A' \\ B' \\ C' \\ D' \end{bmatrix} = \begin{bmatrix} -19.05 \\ 30.74 \\ -13.71 \\ 15.14 \\ -2.38 \\ -3.05 \\ 7.60 \\ 11.03 \end{bmatrix} \quad (\text{B.18})$$

The initial *ideal* gradation, shown in Table B.8 and based on $CF=60$ and $WF=35$, is plotted with the updated *ideal* gradation, shown in Table B.9 and based on $CF=57.7$ and $WF=35.4$, in Fig. B.2. As shown in the figure, the small change in the CF and WF resulted in only a small change in the *ideal* gradation.

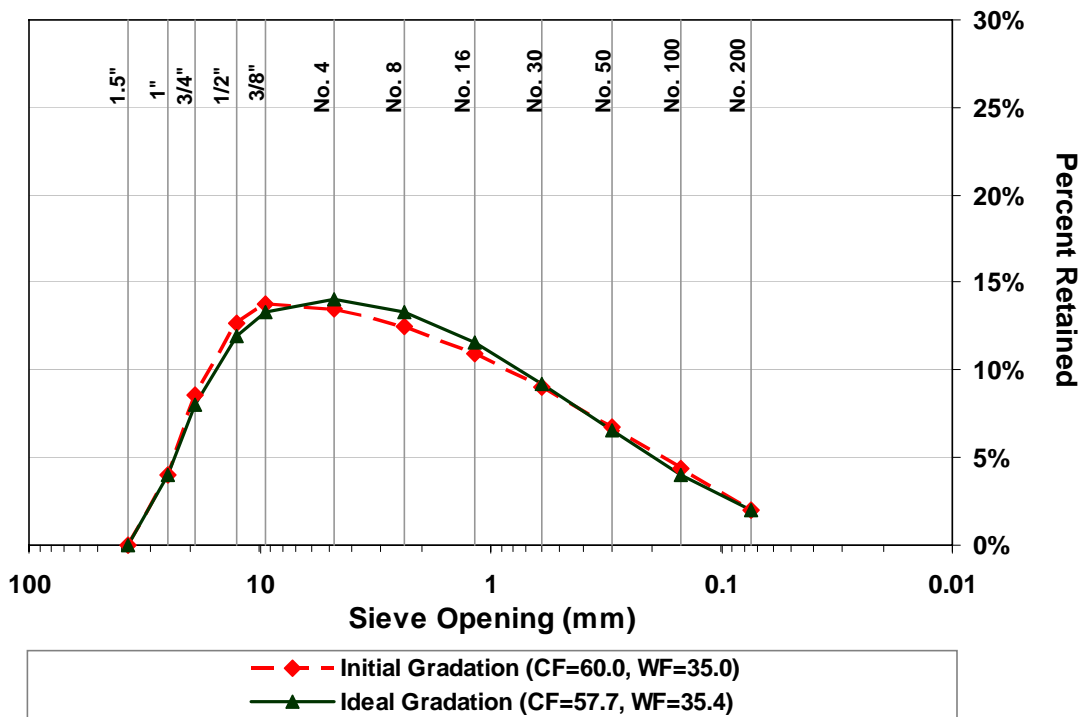


Fig. B.2 – Percents retained for the initial *Cubic-Cubic Model* prior to optimizing CF and WF and for the *ideal* gradation after optimizing CF and WF

B.6 ADJUSTING THE *IDEAL* GRADATION TO ACCOUNT FOR CHANGES IN THE CEMENTITIOUS MATERIAL CONTENT

The following eight-step procedure modifies the *ideal* gradation to account for the influence of the cementitious material content on the workability of the concrete mixture.

Step 1. The first step is to calculate the deviation, by volume, from a U.S. six-sack mixture using Eq. (3.19). The specific gravity and quantity of the cement and the slag cement used in this example are shown in Table B.4.

$$V_{dev} = \frac{M_C}{SG_C \times UW_W} + \sum_n \left(\frac{M_n}{SG_n \times UW_W} \right) - \frac{6 \cdot S}{SG_C \times UW_W} \quad (3.20)$$

$$V_{dev} = \frac{400}{3.20 \times 62.4} + \frac{135}{2.90 \times 62.4} - \frac{6 \times 94}{3.20 \times 62.4} = -0.075 \text{ ft}^3 \quad (B.19)$$

Step 2. Convert V_{dev} to an equivalent weight of fine aggregate by volume using Eq. (3.20). The bulk specific gravity SSD for the fine aggregate (the aggregate with the lowest fineness modulus) is 2.63 as shown in Table B.5.

$$M_{dev} = V_{dev} \times SG_{FA} \times UW_W \quad (3.21)$$

$$M_{dev} = -0.075 \times 2.63 \times 62.4 = -12.3 \text{ lb.} \quad (B.20)$$

Step 3. Calculate the percent retained on each sieve for the combined aggregate gradation. Since the actual aggregate blend is unknown at this point in the process, it will be assumed that each of the three aggregates comprise one third of the weight fraction. The combined aggregate gradation is shown in Table B.10.

Table B.10 – Blended Aggregate Gradation

Sieve	% Retained, $r_{n,t}$			Blended % Retained, R_n
	$MF_1=33.3\%$	$MF_2=33.3\%$	$MF_3=33.4\%$	
	Aggregate 1	Aggregate 2	Aggregate 3	
1½-in. (37.5 mm)	0.0	0.0	0.0	0.0
1-in. (25 mm)	16.1	0.0	0.0	5.4
¾-in. (19 mm)	27.1	0.0	0.0	9.0
½-in. (12.5 mm)	27.8	26.0	0.0	17.9
⅜-in. (9.5 mm)	13.2	25.8	0.0	13.0
No. 4 (4.75 mm)	14.9	45.1	3.1	21.0
No. 8 (2.36 mm)	0.0	2.2	19.8	7.3
No. 16 (1.18 mm)	0.0	0.0	25.9	8.7
No. 30 (0.60 mm)	0.0	0.0	20.3	6.8
No. 50 (0.30 mm)	0.0	0.0	21.0	7.0
No. 100 (0.15 mm)	0.0	0.0	7.8	2.6
No. 200 (0.075 mm)	0.0	0.0	2.1	0.7
Pan	0.9	0.9	0.0	0.6
Total	100.0	100.0	100.0	100.0

Step 4. Convert the percent retained on each sieve R_n to an aggregate weight retained (on a yd^3 basis) on each sieve. The first step for this calculation is to determine the total volume of aggregate. This is accomplished by calculating the volume of the other constituents and then determining the volume of aggregate using Eq. (3.22).

$$V_{paste} = \frac{400}{3.20 \times 62.4} + \frac{135}{2.90 \times 62.4} + \frac{0.42(400 + 135)}{1 \times 62.4} = 6.35 \text{ ft}^3$$

$$V_{air} = 8\% \times 27 = 2.16 \text{ ft}^3$$

$$V_{agg} = UV - V_{paste} - V_{air} \quad (3.22)$$

$$V_{agg} = 27 - 6.35 - 2.16 = 18.49 \text{ ft}^3$$

The total weight of aggregate is calculated using the effective specific gravity [calculated with Eq. (3.23)] and the total volume of aggregate using Eq. (3.24).

$$SG_{Eff} = \frac{100}{\frac{MF_1}{SG_{A_1}} + \frac{MF_2}{SG_{A_2}} + \frac{MF_3}{SG_{A_3}}} \quad (3.23)$$

$$SG_{Eff} = \frac{100}{\frac{33.3}{2.64} + \frac{33.3}{2.64} + \frac{33.4}{2.63}} = 2.637$$

$$M_{agg} = V_{agg} \times SG_{Eff} \times UW_w \quad (3.24)$$

$$M_{agg} = 18.49 \times 2.637 \times 62.4 = 3042.5 \text{ lb.}$$

The aggregate weight retained on each sieve is calculated by multiplying the percent retained on each sieve of the combined aggregate gradation (Table B.10) by the total aggregate weight. To illustrate this calculation for the weight retained on the pan:

$$M_{pan} = M_{agg} \times R_{pan}$$

$$M_{pan} = 3042.5 \times 0.6\% = 18.3 \text{ lb.}$$

Step 5. Add M_{dev} to the weight retained on the pan M_{pan} of the combined aggregate gradation calculated.

$$M'_{pan} = M_{pan} + M_{dev}$$

$$M'_{pan} = 18.3 - 12.3 = 6.0 \text{ lb.}$$

Step 6. Recalculate the percent retained on each sieve for the combined gradation (see *Step 3* for an example) using the adjusted percentage retained on the pan M'_{pan} calculated in *Step 5*. The results for *Steps 3* through *6* are summarized in Table B.11.

Table B.11 – Summary Results for *Steps 3* through *6*

Sieve	Blended % Retained, R_n	Blended Wt. Retained (lb.), M_n	Adjusted Blended Wt. Retained (lb.), M'_n	Adjusted Blended % Retained, R'_n
	<i>Step 3</i>	<i>Step 4</i>	<i>Step 5</i>	<i>Step 6</i>
1½-in. (37.5 mm)	0.0	0.0	0.0	0.0
1-in. (25 mm)	5.4	164.3	164.3	5.4
¾-in. (19 mm)	9.0	273.8	273.8	9.0
½-in. (12.5 mm)	17.9	544.6	544.6	18.0
⅜-in. (9.5 mm)	13.0	395.5	395.5	13.1
No. 4 (4.75 mm)	21.0	638.9	638.9	21.1
No. 8 (2.36 mm)	7.3	222.1	222.1	7.3
No. 16 (1.18 mm)	8.7	264.7	264.7	8.7
No. 30 (0.60 mm)	6.8	206.9	206.9	6.8
No. 50 (0.30 mm)	7.0	213.0	213.0	7.0
No. 100 (0.15 mm)	2.6	79.1	79.1	2.6
No. 200 (0.075 mm)	0.7	21.3	21.3	0.7
Pan	0.6	18.3	18.3-12.3=6.0	0.2
Total	100.0	3042.5	3030.2	100.0

Step 7. Calculate the change in the workability particles ΔW [Eq. (3.28)] resulting from the deviation in cementitious materials from a U.S. six-sack mix.

$$\Delta W = W_{adj} - W \quad (3.27)$$

$$\Delta W = (8.7 + 6.8 + 7.0 + 2.6 + 0.7 + 0.2) - (8.7 + 6.8 + 7.0 + 2.6 + 0.7 + 0.6) = -0.4\%$$

The adjusted workability particles for the *ideal* gradation W_{ideal} is calculated using Eq. (3.29).

$$W'_{ideal} = W_{ideal} - \Delta W \quad (3.29)$$

$$W'_{ideal} = 35.3 + 0.4 = 35.7$$

Step 8. Recalculate Q_{ideal} , I_{ideal} using W_{ideal} , WF_{target} , and CF_{target} .

Solve Eq. (3.4) for $Q_{ideal} + I_{ideal}$,

$$Q_{ideal} + I_{ideal} = 100 - W_{ideal} = 100 - 35.7 = 64.3$$

Solve Eq. (1.1) for Q_{ideal} ,

$$CF = \frac{Q_{ideal}}{Q_{ideal} + I_{ideal}} \times 100 = \frac{Q_{ideal}}{64.3} \times 100 = 57.7$$

giving

$$Q_{ideal} = \frac{57.7 \times 64.3}{100} = 37.1$$

Finally, solve Eq. (3.4) again for I_{ideal} ,

$$I_{ideal} = 100 - W_{ideal} - Q_{ideal} = 100 - 35.7 - 37.1 = 27.2$$

The updated *ideal* gradation is calculated following the steps in Section B.3 and B.4 and is shown in Fig. B.3 (in addition to the initial aggregate blend). The *ideal* gradation is tabulated in Table B.12.

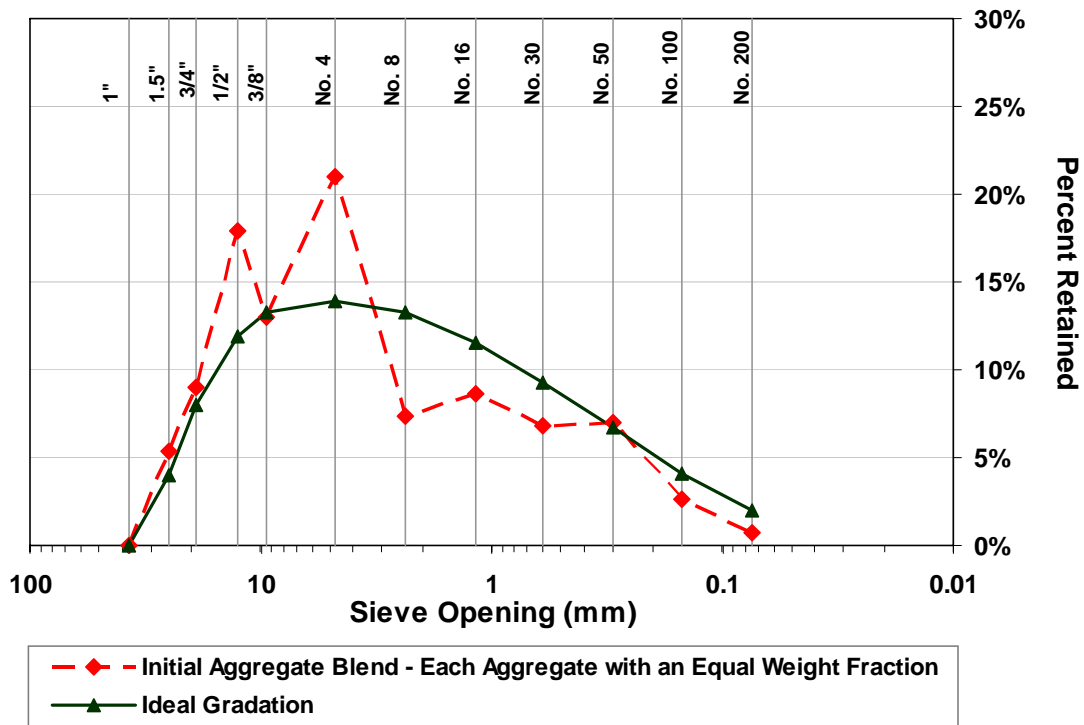


Fig. B.3 – Percent retained for the initial aggregate blend (based on the assumption that each aggregate is 33% of the total blend) and for the *ideal* gradation

Table B.12 – Percents retained for both cubic equations and the *Ideal* Gradation

Sieve	Sieve Designation, n	Cubic Eq. 1	Cubic Eq. 2	<i>Ideal</i> Gradation
1½-in. (37.5 mm)	a	-4.57	6.40	0.00
1-in. (25 mm)	b	4.00	9.30	4.00
¾-in. (19 mm)	c	8.02	10.83	8.02
½-in. (12.5 mm)	d	11.91	12.52	11.91
⅜-in. (9.5 mm)	e	13.26	13.26	13.26
No. 4 (4.75 mm)	f	13.95	13.95	13.95
No. 8 (2.36 mm)	g	13.26	13.26	13.26
No. 16 (1.18 mm)	h	14.38	11.56	11.56
No. 30 (0.60 mm)	i	20.22	9.28	9.28
No. 50 (0.30 mm)	j	34.19	6.66	6.66
No. 100 (0.15 mm)	k	59.35	4.11	4.11
No. 200 (0.075 mm)	l	98.88	2.00	2.00
Pan	m	--	--	2.00

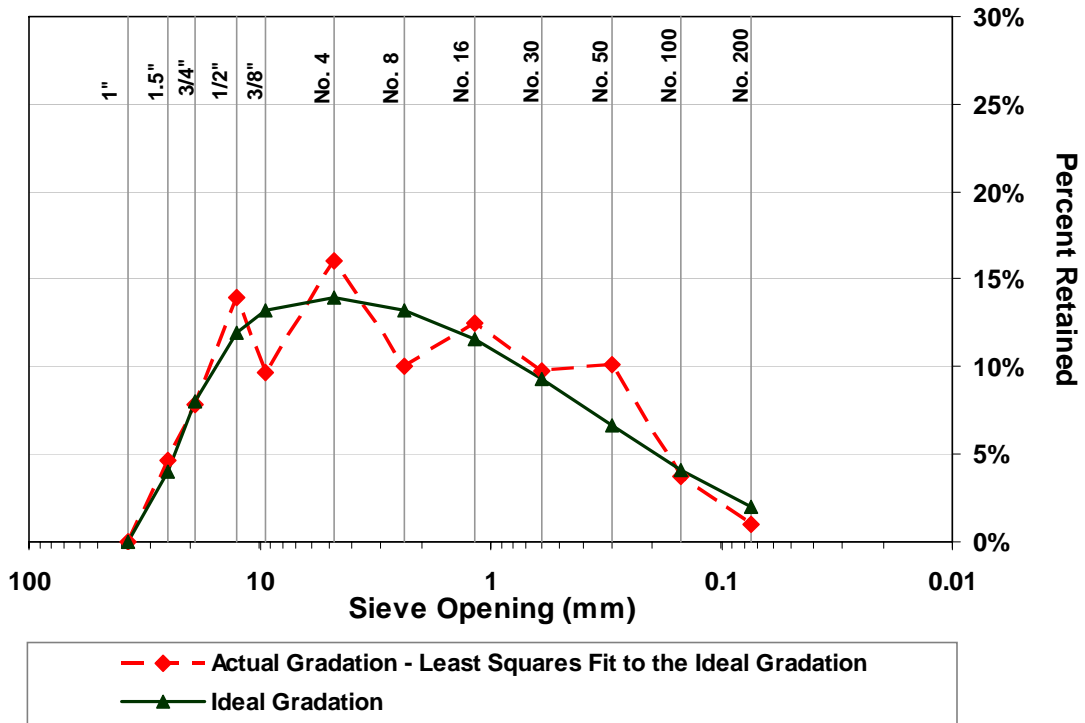


Fig. B.4 – Percent Retained Chart of the aggregate blend (after a least squared fit) and the *ideal* gradation.

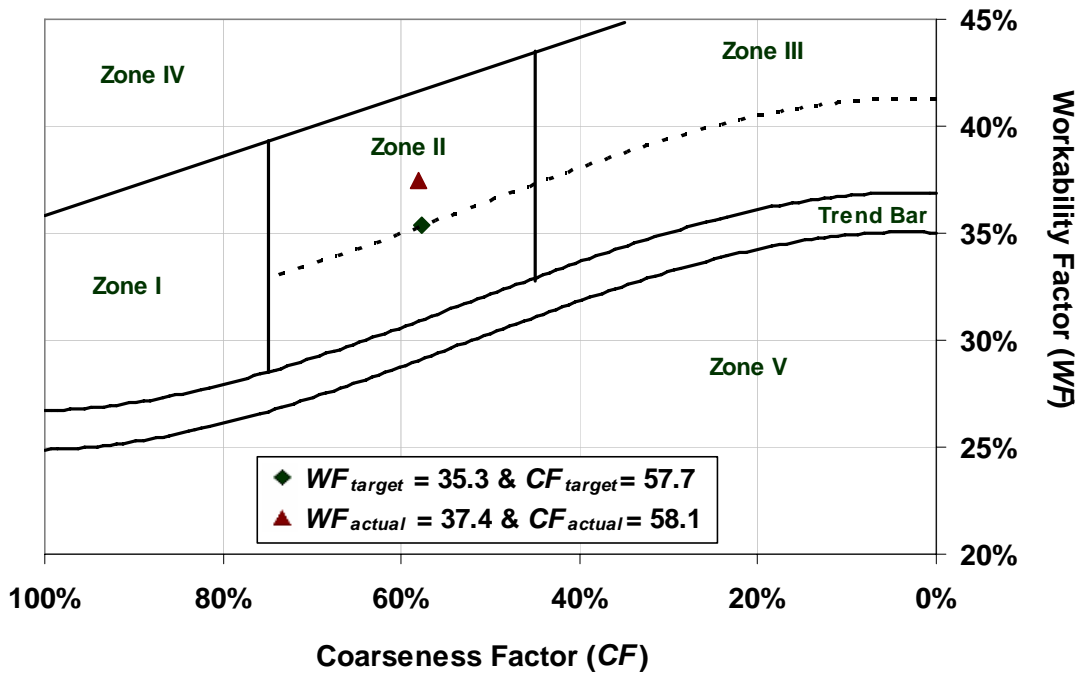


Fig. B.5 – MCFC for the *ideal* gradation and the actual aggregate gradation (after a least squared fit)

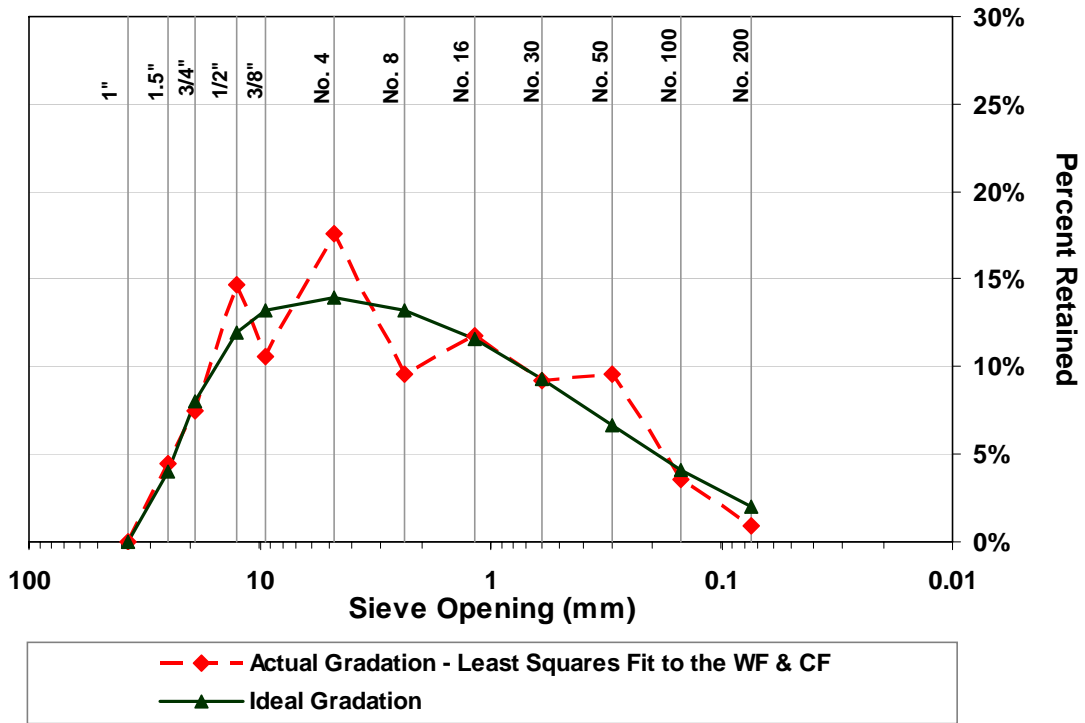


Fig. B.6 – Percent Retained Chart of the combined aggregate gradation (after a least squared fit of the *WFs* and *CFs*) and the *ideal* gradation

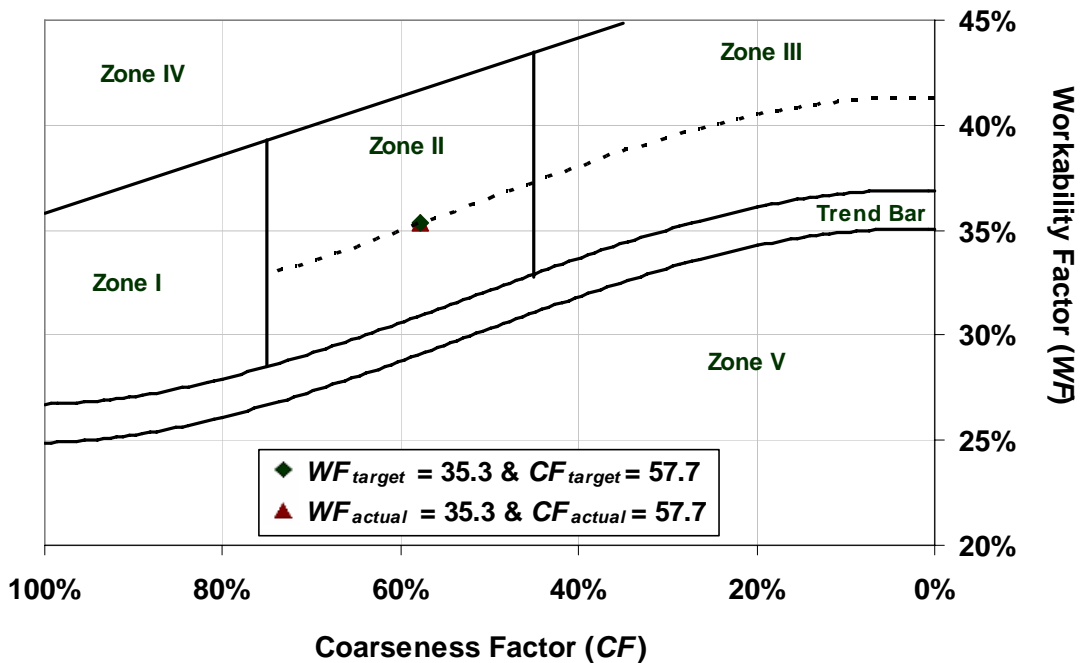


Fig. B.7 – MCFC for the *ideal* gradation and the actual aggregate gradation (after a least squared fit of the *WFs* and *CFs*)

Step 3. Check to determine whether or not an additional iteration is required. Iterations should be repeated until the sum of the absolute differences between the percent retained on the pan, 0.075-mm (No. 200) sieve, and the top sieve [1-in. (25-mm)] for the actual blended gradation and the *ideal* gradation is less than 0.1%.

$$|4.46 - 4.00| + |0.96 - 2.00| + |0.49 - 2.00| = 3.01\% > 0.1\%$$

The total difference for the first iteration is larger than 0.1%, and thus, at least one additional iteration is required. For the second iteration, the percent retained on the pan, No. 200 (0.075-mm) sieve, and the 1-in. (25-mm) sieve of the actual blended gradation shown in Table B.15 are used to determine the updated *ideal* gradation. After the updated *ideal* gradation is determined, the optimization process proceeds as previously described.

B.8 COMPLETE MIX DESIGN

The final optimized combined gradation and the final *ideal* gradation are presented in Table B.16. These two combined gradations, in addition to the gradation limits specifications shown in Table B.3, are shown in Fig. B.8. The combined gradation falls within the specified gradation limits, and while some deficiencies are present, in each case an adjacent sieve has excess material to balance the deficiency. The CF and WF for the actual gradation are equal to CF_{target} and WF_{target} , as shown in the MCFC (Fig. B.9).

Table B.15 – Final Optimized Aggregate Gradation

Sieve	% Retained, $r_{n,t}$			Actual % Retained, R_n	Ideal % Retained, \bar{R}_n	Difference Squared
	$MF_1=30.6\%$	$MF_2=24.2\%$	$MF_3=45.2\%$			
	Aggregate 1	Aggregate 2	Aggregate 3			
1½-in. (37.5 mm)	0.0	0.0	0.0	0.00	0.00	0.00
1-in. (25 mm)	16.1	0.0	0.0	4.92	4.92	0.00
¾-in. (19 mm)	27.1	0.0	0.0	8.28	8.51	0.05
½-in. (12.5 mm)	27.8	26.0	0.0	14.78	11.86	8.53
⅜-in. (9.5 mm)	13.2	25.8	0.0	10.27	12.96	7.24
No. 4 (4.75 mm)	14.9	45.1	3.1	16.86	13.38	12.11
No. 8 (2.36 mm)	0.0	2.2	19.8	9.49	12.98	12.18
No. 16 (1.18 mm)	0.0	0.0	25.9	11.72	11.82	0.01
No. 30 (0.60 mm)	0.0	0.0	20.3	9.19	10.03	0.71
No. 50 (0.30 mm)	0.0	0.0	21.0	9.50	7.57	3.72
No. 100 (0.15 mm)	0.0	0.0	7.8	3.53	4.52	0.98
No. 200 (0.075 mm)	0.0	0.0	2.1	0.95	0.95	0.00
Pan	0.9	0.9	0.0	0.49	0.49	0.00
Total	100.0	100.0	100.0	100.0	100.0	45.54

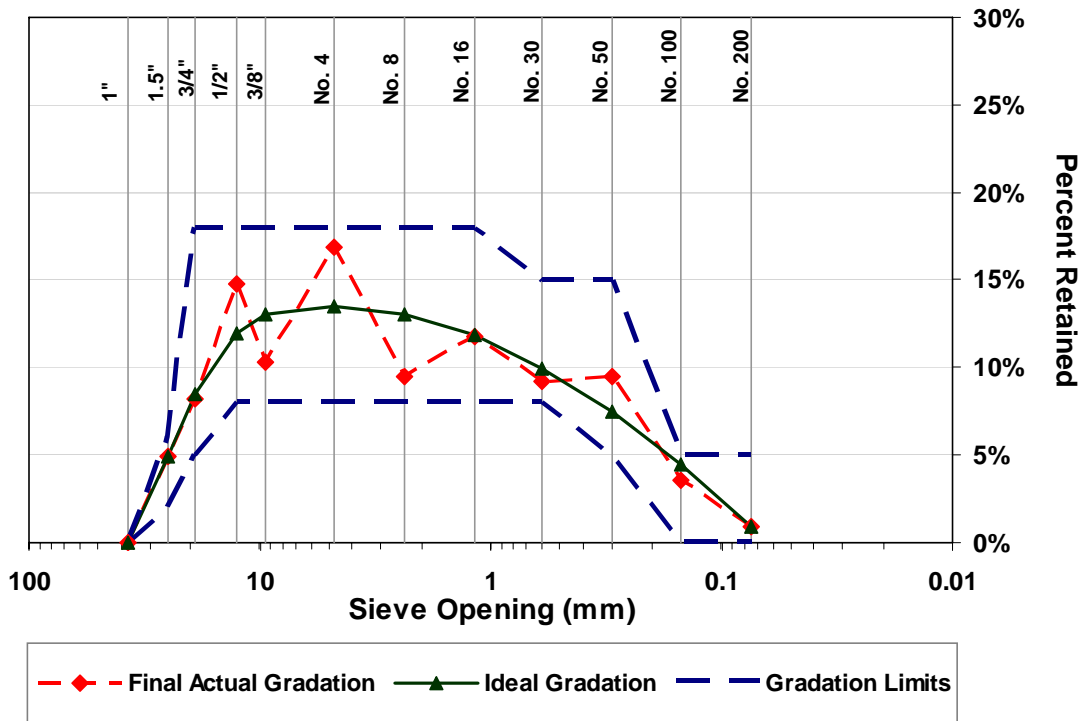


Fig. B.8 – Percent Retained Chart for the optimized combined gradation and for the *ideal* gradation – the gradation limits are identified in Table B.3

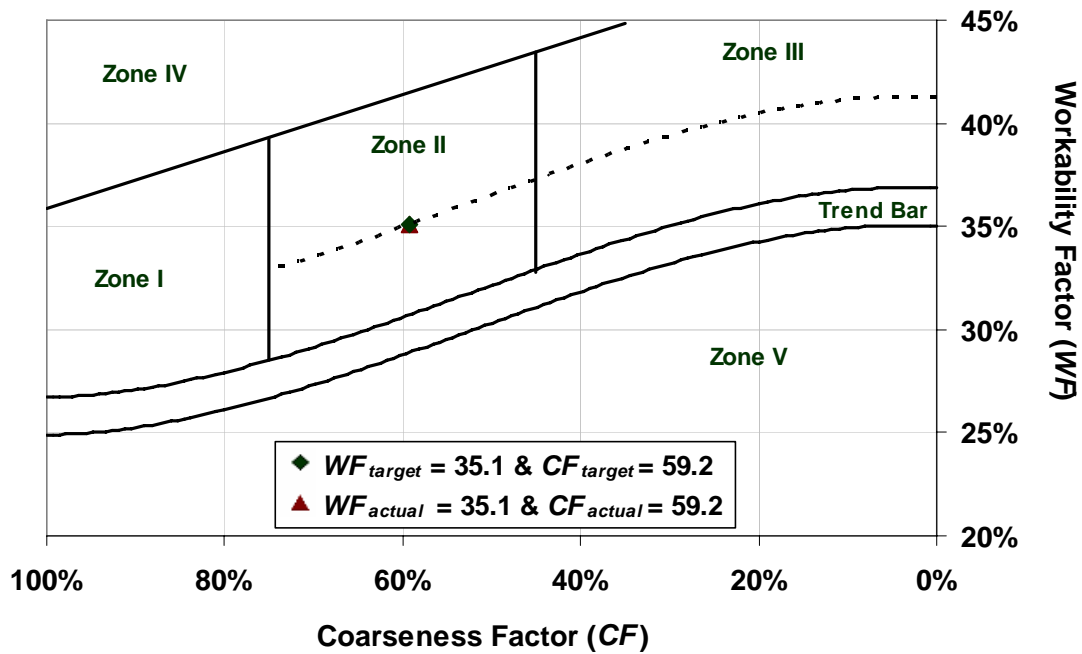


Fig. B.9 – Modified Coarseness Factor Chart for the optimized combined gradation and the *ideal* gradation

The total weight of aggregate calculated using Eqs. (3.23) and (3.24) is shown next for completeness, although this calculation was already required to complete the aggregate optimization process.

$$SG_{Eff} = \frac{100}{\frac{30.6}{2.64} + \frac{24.2}{2.64} + \frac{45.2}{2.63}} = 2.635$$

$$M_{agg} = 18.49 \times 2.635 \times 62.4 = 3040.2 \text{ lb.}$$

The weights of the individual aggregates are then calculated by multiplying the individual aggregate weight fractions by the total aggregate weight [Eq. (3.31)].

$$W_1 = \frac{30.6}{100} \times 3040.2 = 930 \text{ lb.}$$

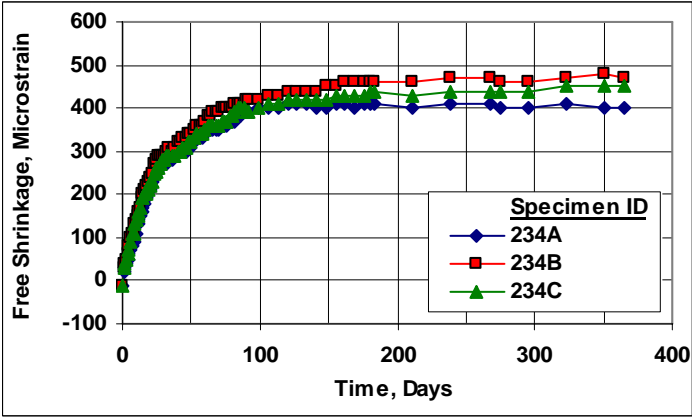
$$W_2 = \frac{24.2}{100} \times 3040.2 = 736 \text{ lb.}$$

$$W_3 = \frac{45.2}{100} \times 3040.2 = 1374 \text{ lb.}$$

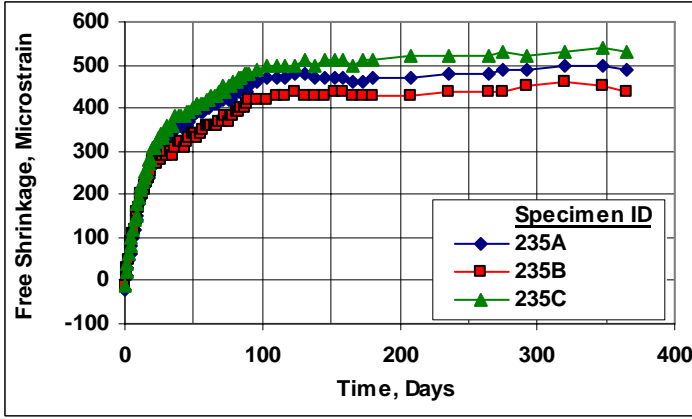
The quantities of chemical admixtures generally depend on the quantity of cement in the batch proportions and must be selected based on past experience and trial batches. While the use of these admixtures is required to meet the requirements outlined in Table B.1 and B.2, they are not included in this example. When admixtures are incorporated into the mixture, the design water content should be adjusted to account for water contained in the admixtures (see Section 3.1.2).

Table B.16 – Final Mix Proportions

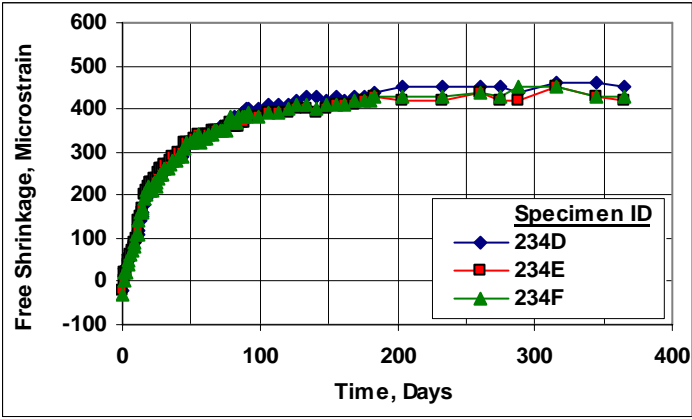
Material / Blend	Quantity, SSD	S.G.	Yield, ft³
portland cement	400 lb.	3.20	2.00
slag cement	135 lb.	2.90	0.75
water	225 lb.	1.00	3.61
1 in. Granite 1 / 30.4%	930 lb.	2.64	5.65
½ in. Granite 2 / 24.3%	736 lb.	2.64	4.47
River Sand 3 / 45.3%	1374 lb.	2.63	8.37
Total Air, percent	8	--	2.16
Total	--	--	27.01



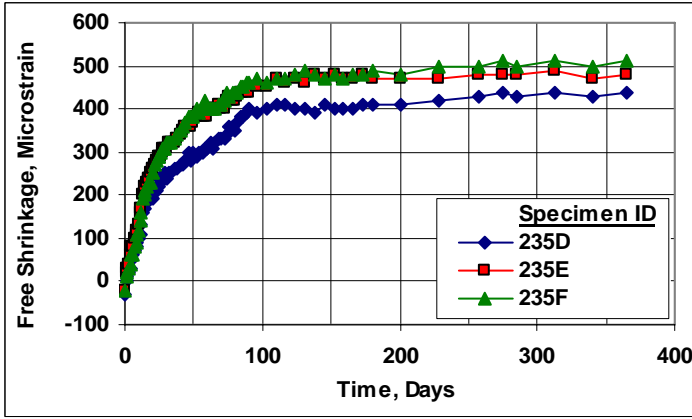
(a)



(a)



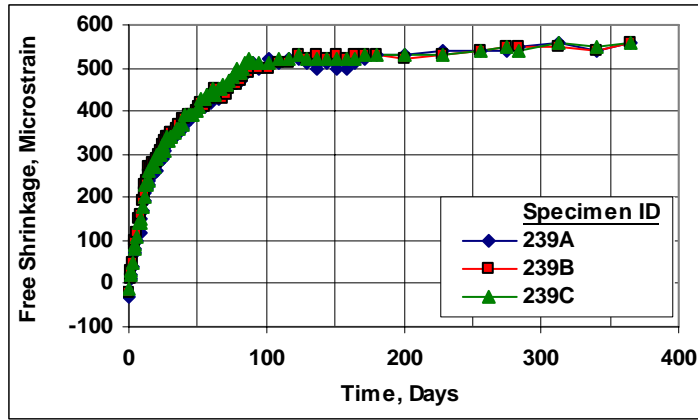
(b)



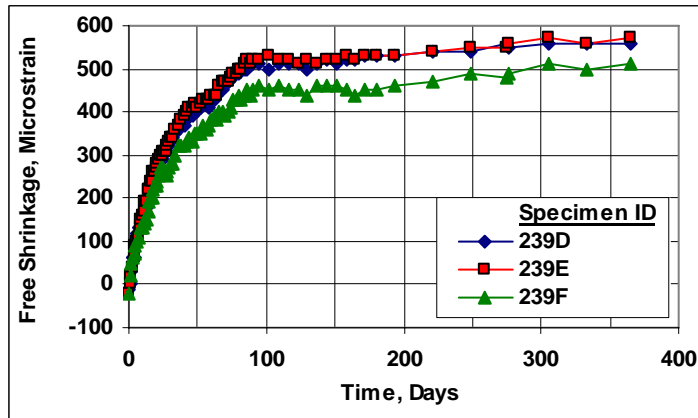
(b)

Fig. C.1 – Free Shrinkage, Batch 234. Program I Set 1. Type I/II Cement, Limestone CA, 0.41 w/c ratio, (a) 7-day cure and (b) 14-day cure.

Fig. C.2 – Free Shrinkage, Batch 235. Program I Set 1. Type I/II Cement, Limestone CA, 0.43 w/c ratio, (a) 7-day cure and (b) 14-day cure.

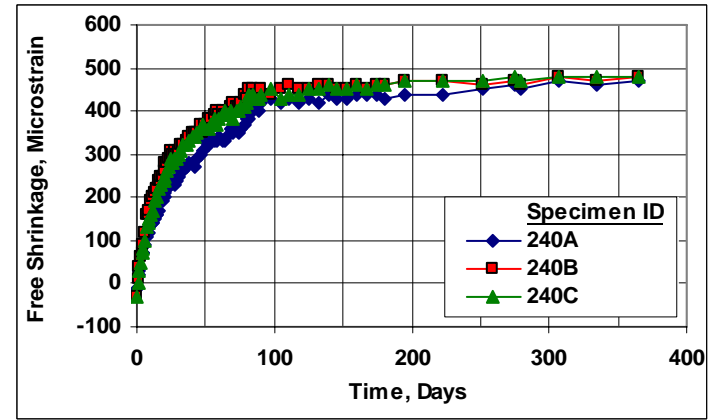


(a)

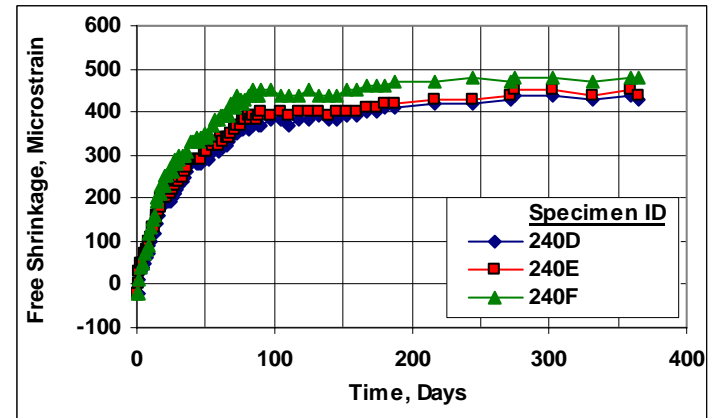


(b)

Fig. C.3 – Free Shrinkage, Batch 239. Program I Set 1. Type I/II Cement, Limestone CA, 0.45 w/c ratio, (a) 7-day cure and (b) 14-day cure.

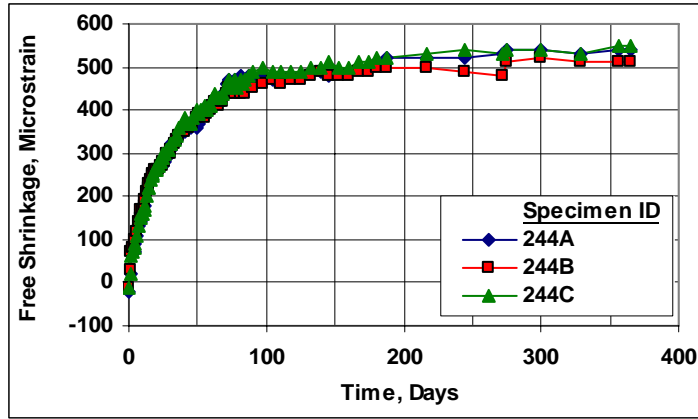


(a)

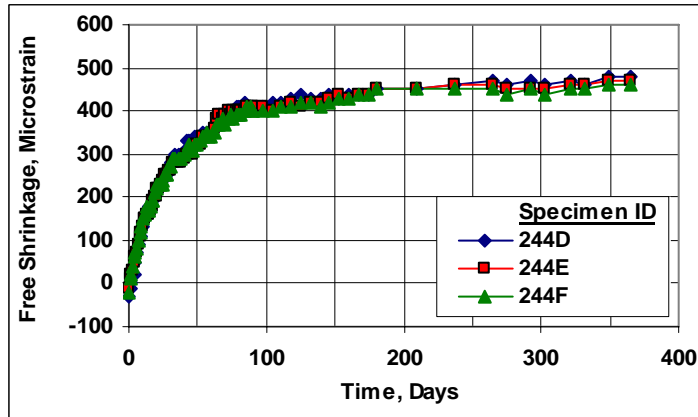


(b)

Fig. C.4 – Free Shrinkage, Batch 240. Program I Set 2. Type II Cement, Limestone CA, 0.41 w/c ratio, (a) 7-day cure and (b) 14-day cure.

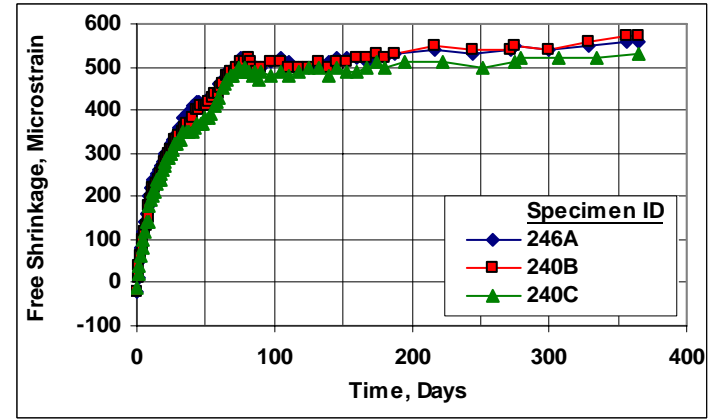


(a)

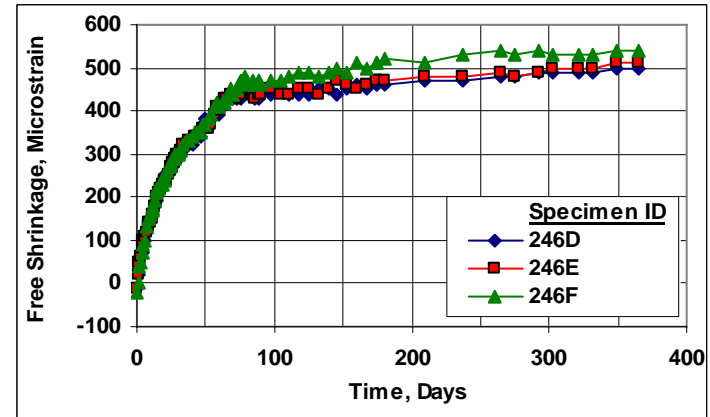


(b)

Fig. C.5 – Free Shrinkage, Batch 244. Program I Set 2. Type II Cement, Limestone CA, 0.43 w/c ratio, (a) 7-day cure and (b) 14-day cure.

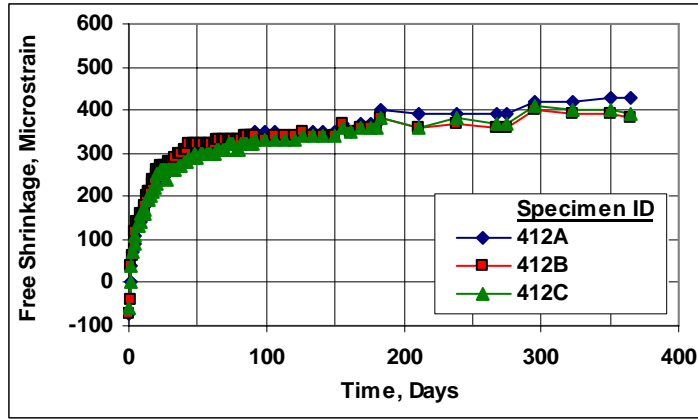


(a)

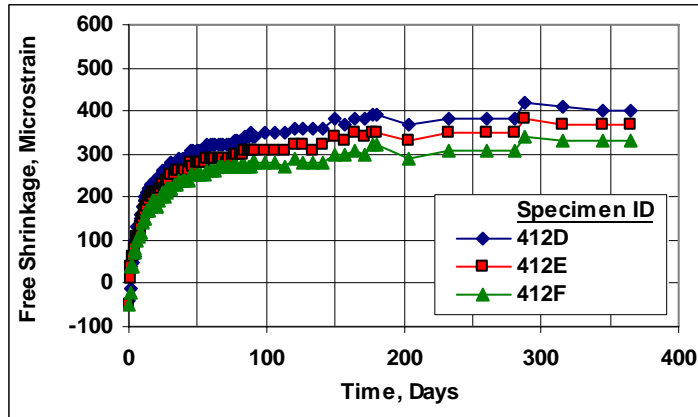


(b)

Fig. C.6 – Free Shrinkage, Batch 246. Program I Set 2. Type II Cement, Limestone CA, 0.45 w/c ratio, (a) 7-day cure and (b) 14-day cure.

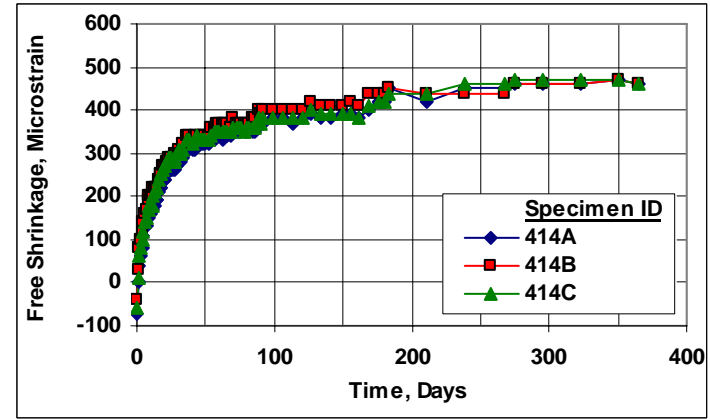


(a)

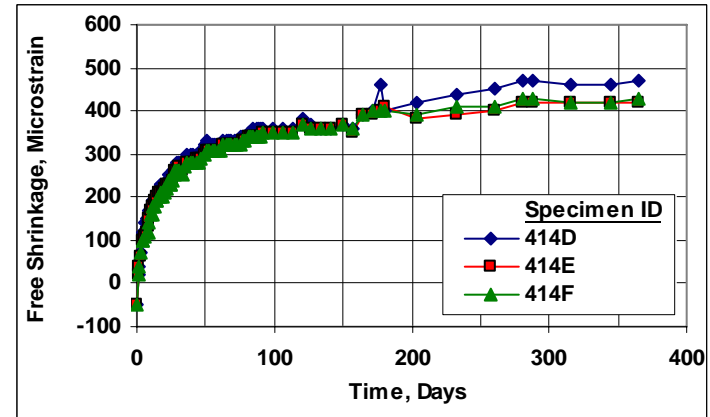


(b)

Fig. C.7 – Free Shrinkage, Batch 412. Program I Set 3. Type I/II Cement, Granite CA, 0.41 w/c ratio, (a) 7-day cure and (b) 14-day cure.

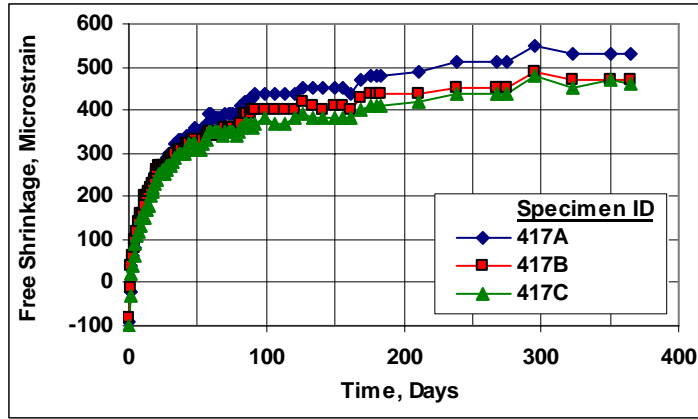


(a)

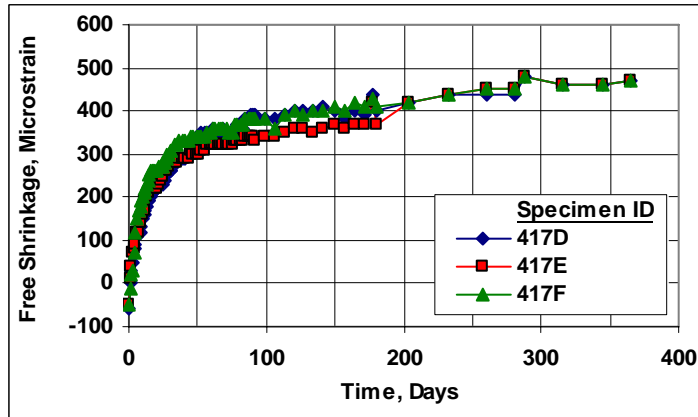


(b)

Fig. C.8 – Free Shrinkage, Batch 414. Program I Set 3. Type I/II Cement, Granite CA, 0.43 w/c ratio, (a) 7-day cure and (b) 14-day cure.

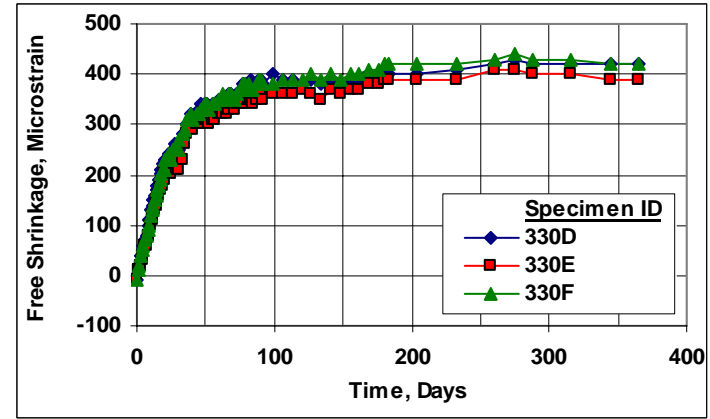


(a)

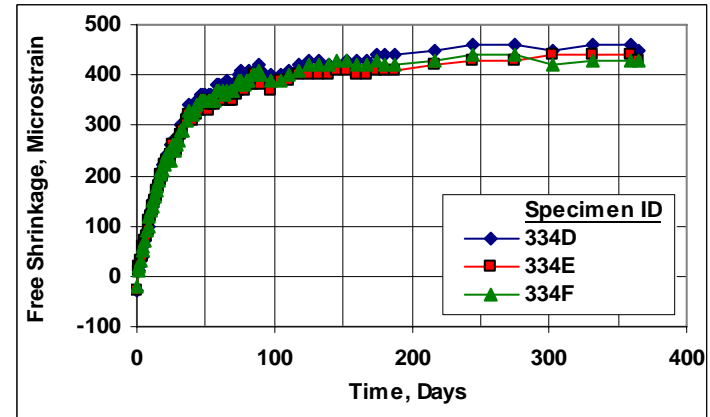


(b)

Fig. C.9 – Free Shrinkage, Batch 417. Program I Set 3. Type I/II Cement, Granite CA, 0.45 w/c ratio, (a) 7-day cure and (b) 14-day cure.

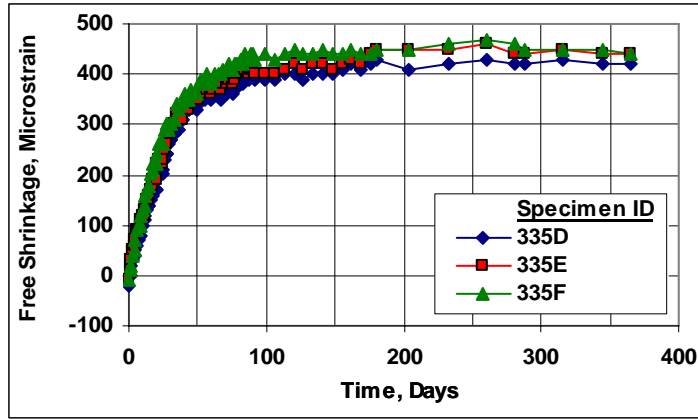


(a)

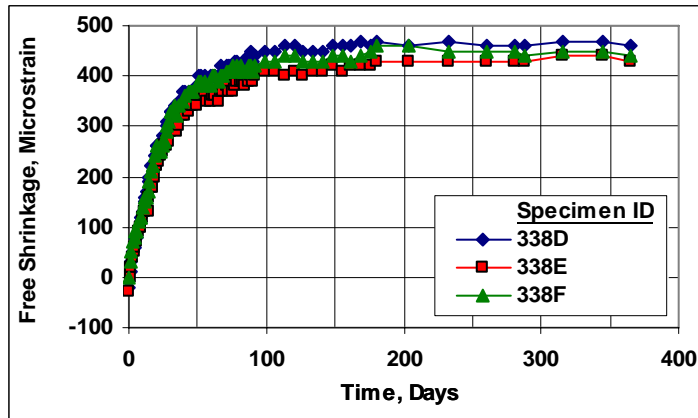


(b)

Fig. C.10 – Free Shrinkage, Batch 330 and 334. Program II Set 1. Type I/II Cement, Limestone CA, 14-day cure, (a) 0.36 w/c ratio and (b) 0.38 w/c ratio.



(a)



(b)

Fig. C.11 – Free Shrinkage, Batch 335 and 338. Program II Sets 1 and 2. Type I/II Cement, Limestone CA, 14-day cure, (a) 0.40 w/c ratio and (b) 0.42 w/c ratio.

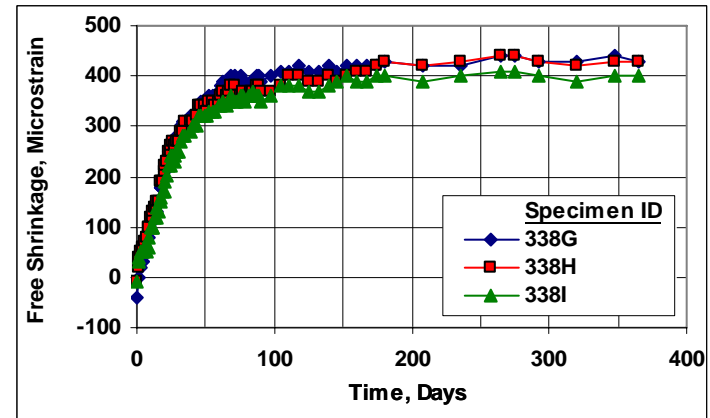
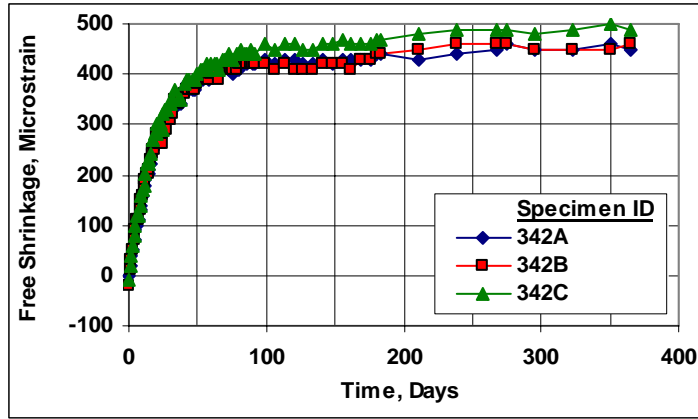
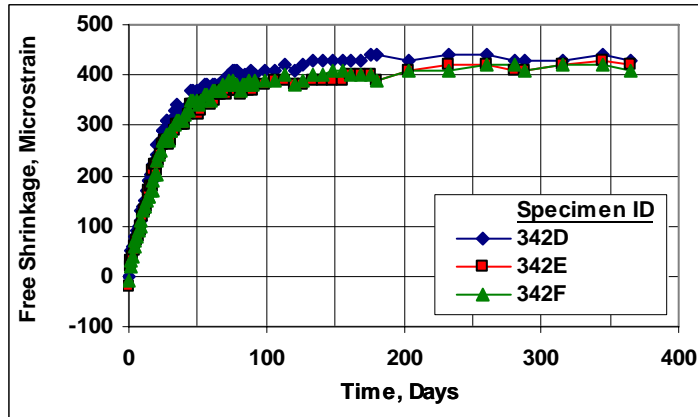


Fig. C.12 – Free Shrinkage, Batch 338. Program II Set 2. Type I/II Cement, Limestone CA, 21-day cure, 0.42 w/c ratio.

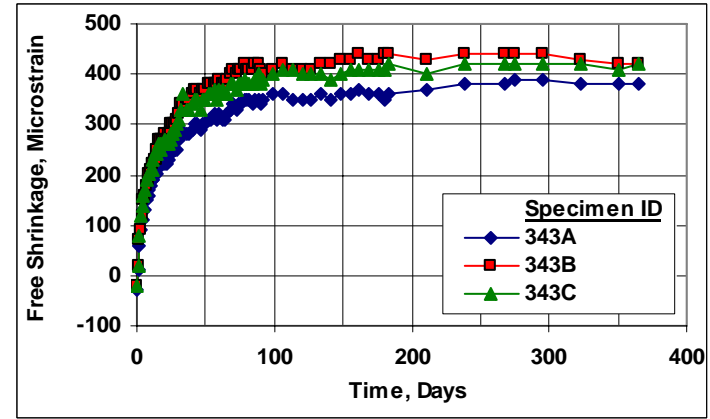


(a)

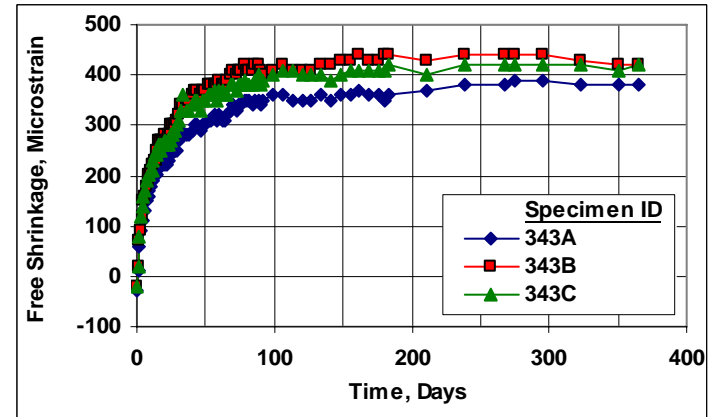


(b)

Fig. C.13 – Free Shrinkage, Batch 342. Program II Set 2 and Program III. Type I/II Cement, Limestone CA, 21.6% Paste, 0.42 w/c ratio, (a) 7-day cure and (b) 14-day cure.

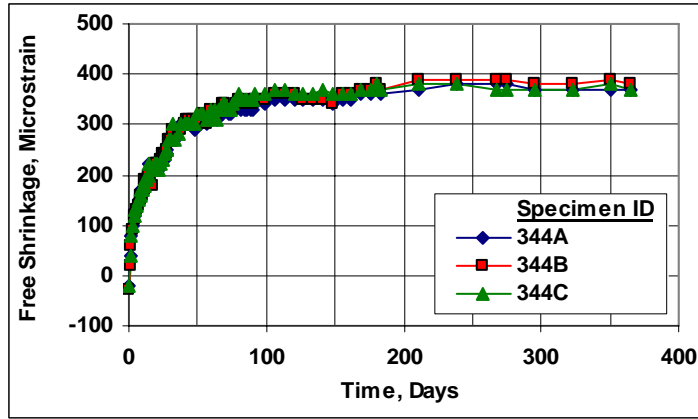


(a)

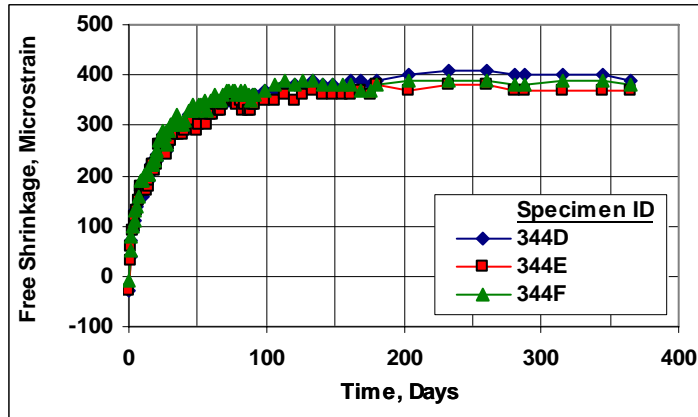


(b)

Fig. C.14 – Free Shrinkage, Batch 343. Program III. Type I/II Cement, Granite CA, 21.6% Paste, 0.42 w/c ratio, (a) 7-day cure and (b) 14-day cure.

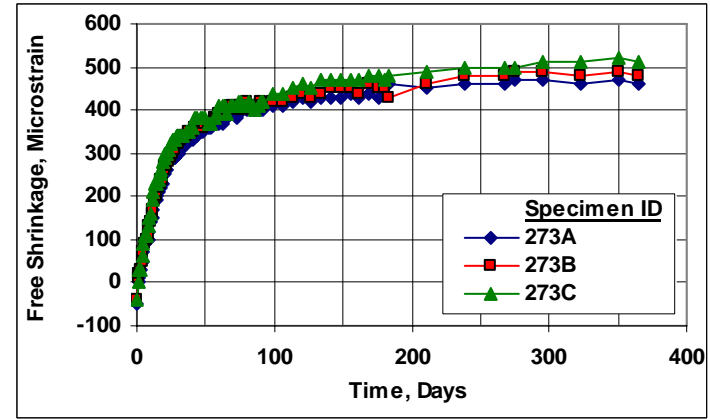


(a)

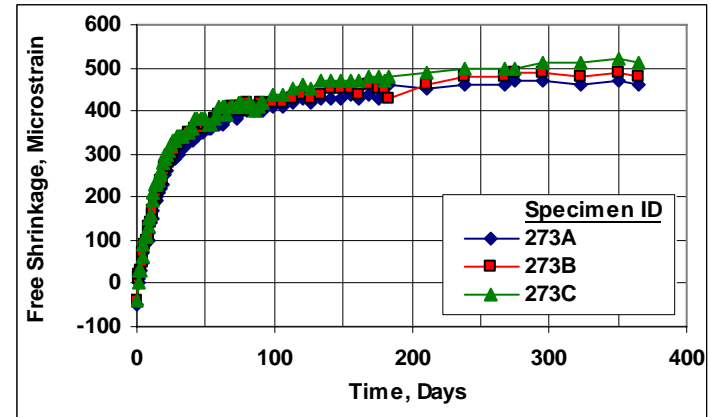


(b)

Fig. C.15 – Free Shrinkage, Batch 344. Program III. Type I/II Cement, Quartzite CA, 21.6% Paste, 0.42 w/c ratio, (a) 7-day cure and (b) 14-day cure.

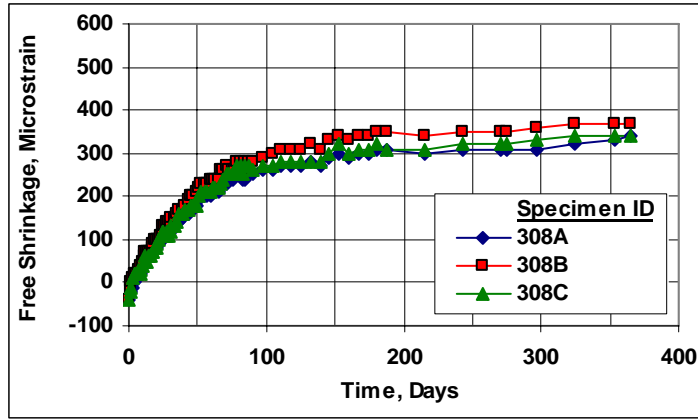


(a)

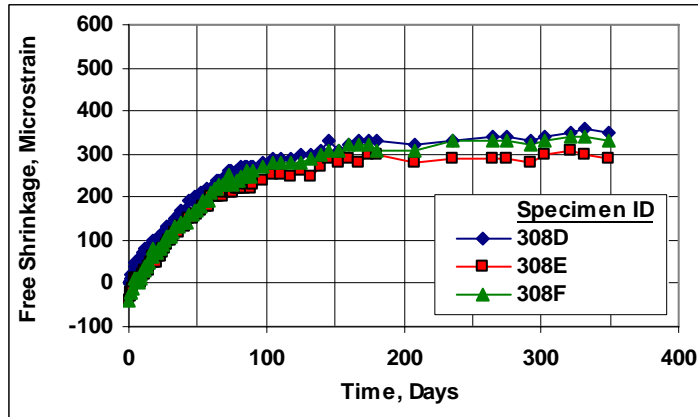


(b)

Fig. C.16 – Free Shrinkage, Batch 273. Program IV. Type I/II Cement, Limestone CA, 0% SRA, 0.42 w/c ratio, (a) 7-day cure and (b) 14-day cure.

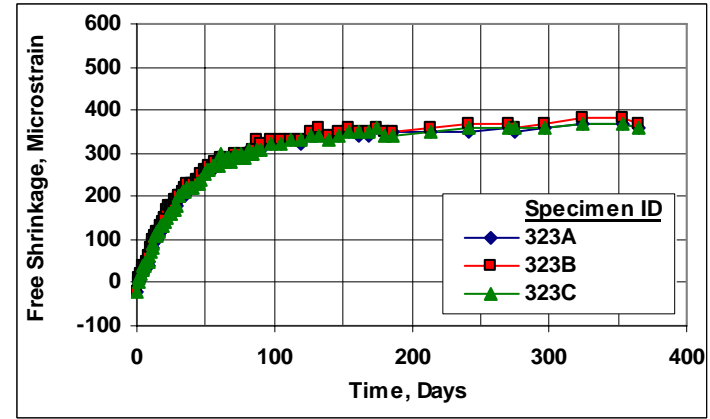


(a)

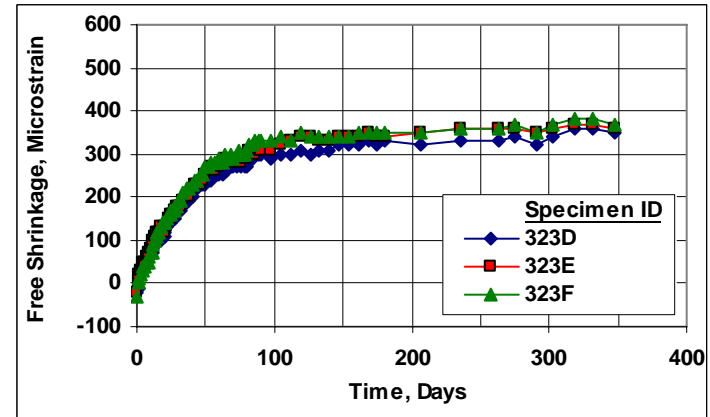


(b)

Fig. C.17 – Free Shrinkage, Batch 323. Program IV. Type I/II Cement, Limestone CA, 1% SRA, 0.42 w/c ratio, (a) 7-day cure and (b) 14-day cure.

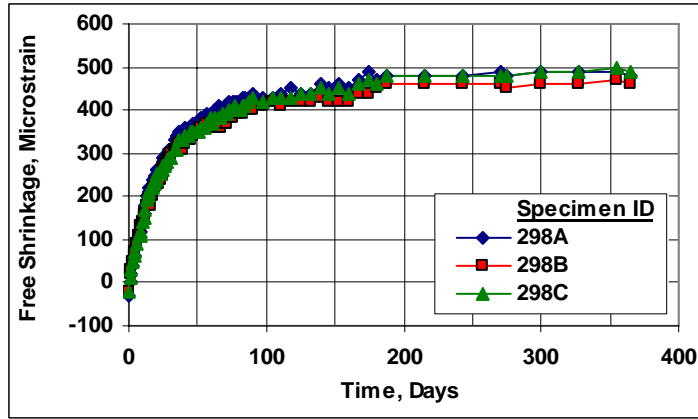


(a)

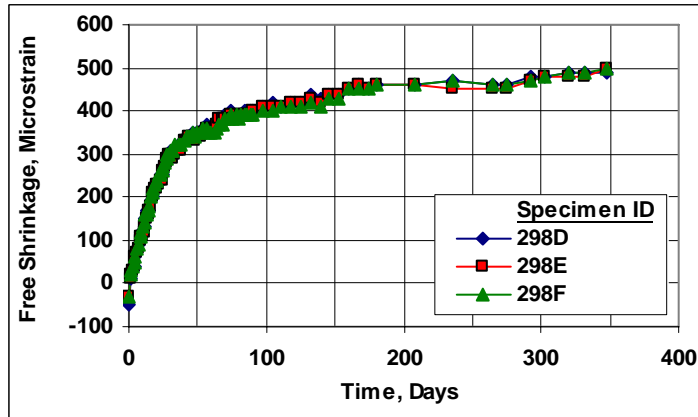


(b)

Fig. C.18 – Free Shrinkage, Batch 308. Program IV. Type I/II Cement, Limestone CA, 2% SRA, 0.42 w/c ratio, (a) 7-day cure and (b) 14-day cure.

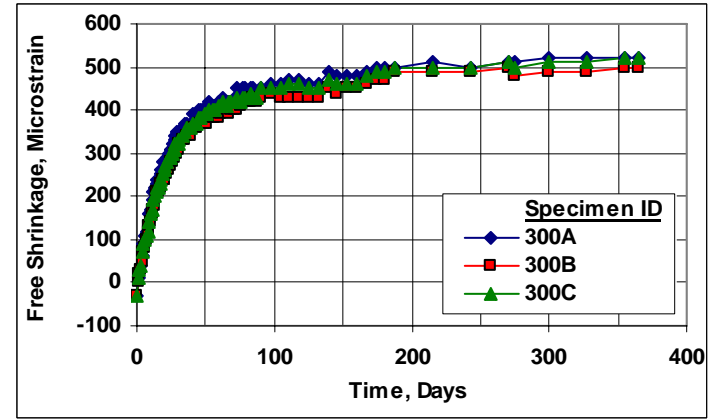


(a)

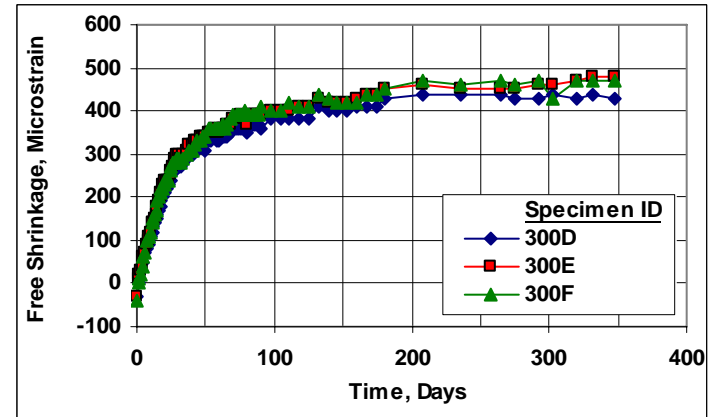


(b)

Fig. C.19 – Free Shrinkage, Batch 298. Program V. Type II Cement Sample 3, Limestone CA, 0.42 w/c ratio, (a) 7-day cure and (b) 14-day cure.

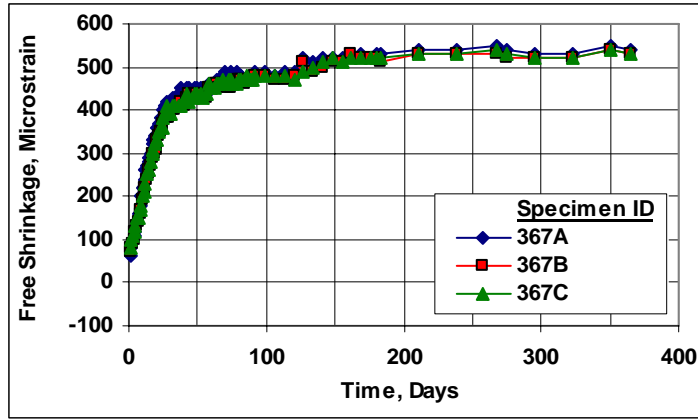


(a)

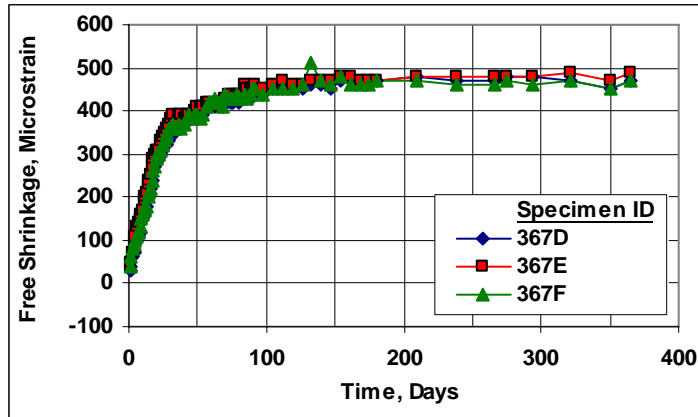


(b)

Fig. C.20 – Free Shrinkage, Batch 300. Program V. Type II Cement Sample 2, Limestone CA, 0.42 w/c ratio, (a) 7-day cure and (b) 14-day cure.

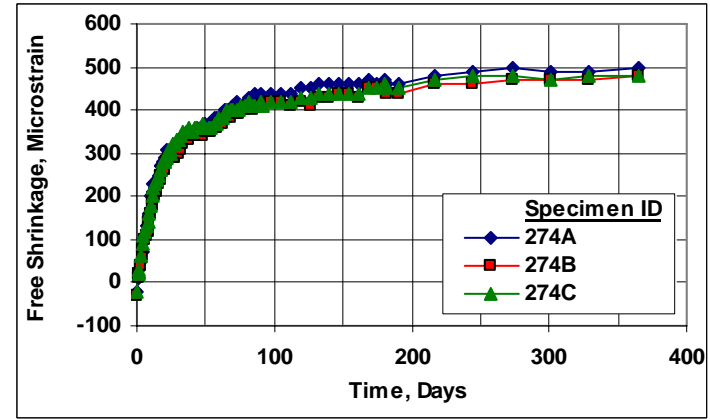


(a)

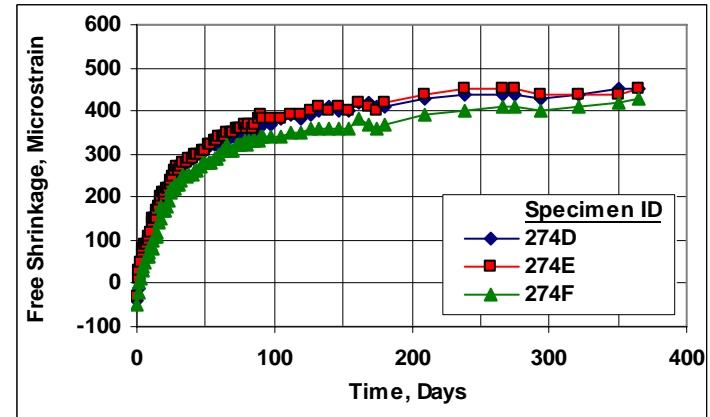


(b)

Fig. C.21 – Free Shrinkage, Batch 367. Program V. Type III Cement, Limestone CA, 0.42 w/c ratio, (a) 7-day cure and (b) 14-day cure.

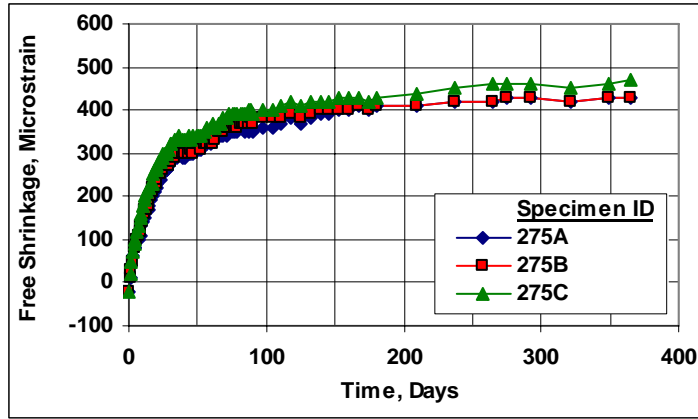


(a)

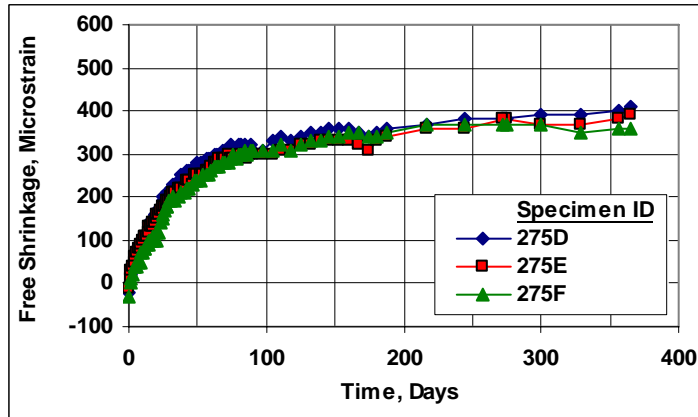


(b)

Fig. C.22 – Free Shrinkage, Batch 274. Program VI Set 1a. Type I/II Cement, Limestone CA, 0.42 w/c ratio, 3% SF Sample 1, (a) 7-day cure and (b) 14-day cure.

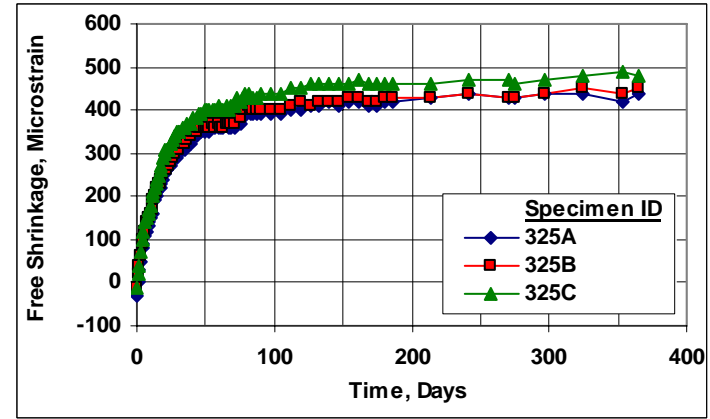


(a)

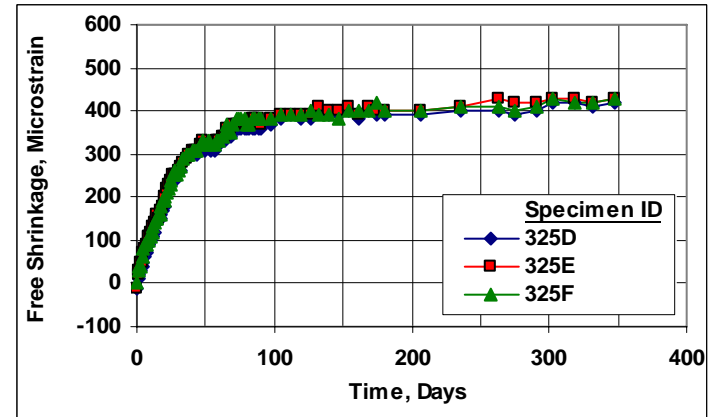


(b)

Fig. C.23 – Free Shrinkage, Batch 275. Program VI Set 1a. Type I/II Cement, Limestone CA, 0.42 w/c ratio, 6% SF Sample 1, (a) 7-day cure and (b) 14-day cure.

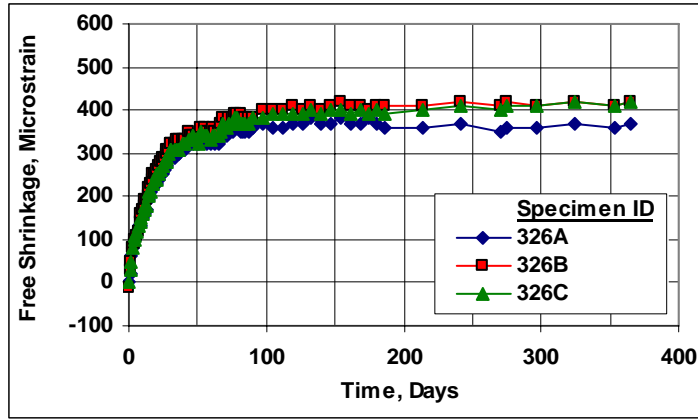


(a)

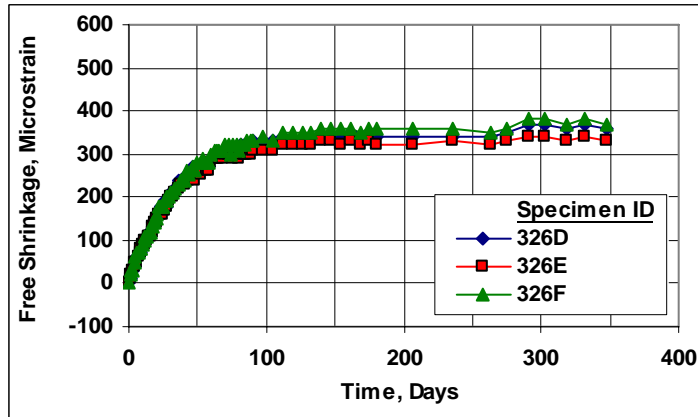


(b)

Fig. C.24 – Free Shrinkage, Batch 325. Program VI Set 1b. Type I/II Cement, Limestone CA, 0.42 w/c ratio, 3% SF Sample 2, (a) 7-day cure and (b) 14-day cure.

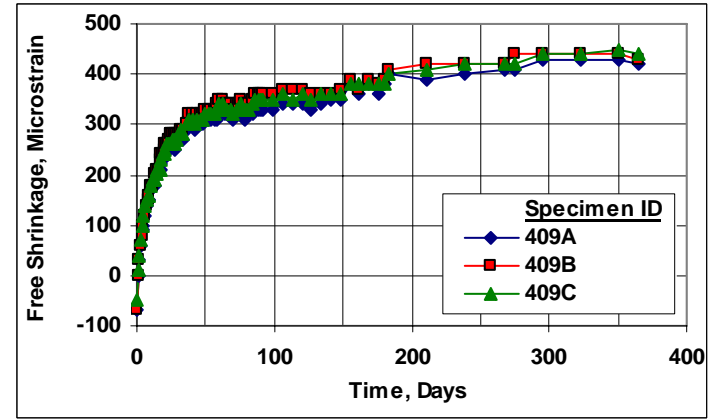


(a)

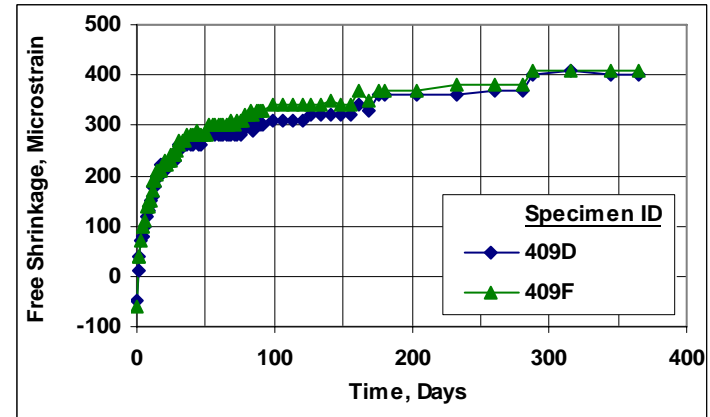


(b)

Fig. C.25 – Free Shrinkage, Batch 326. Program VI Set 1b. Type I/II Cement, Limestone CA, 0.42 w/c ratio, 6% SF Sample 2, (a) 7-day cure and (b) 14-day cure.

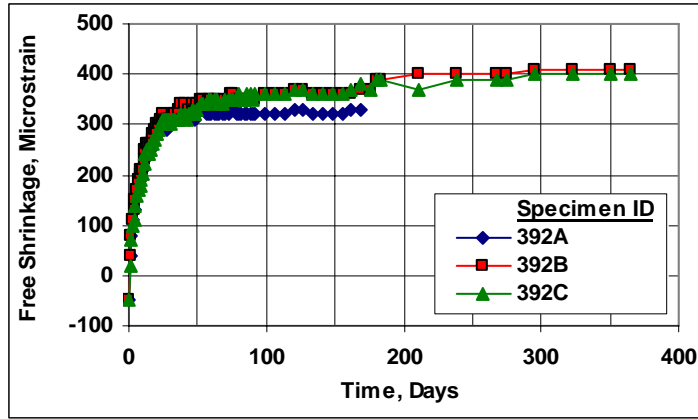


(a)

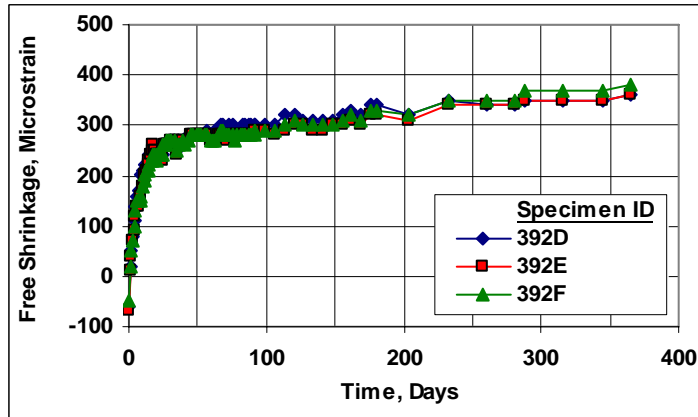


(b)

Fig. C.26 – Free Shrinkage, Batch 409. Program VI Set 2. Type I/II Cement, Granite CA, 0.42 w/c ratio, 0% SF, (a) 7-day cure and (b) 14-day cure.

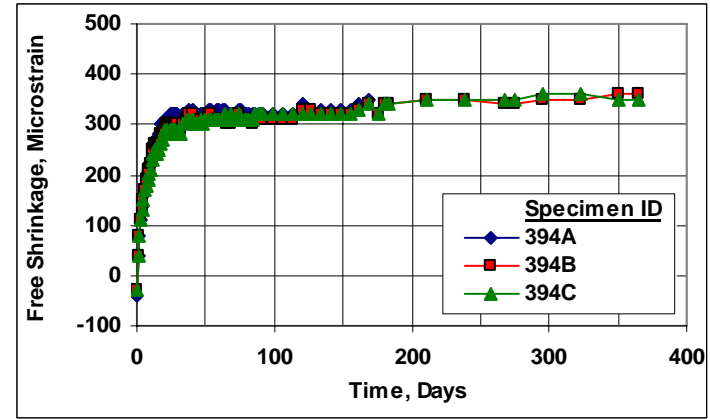


(a)

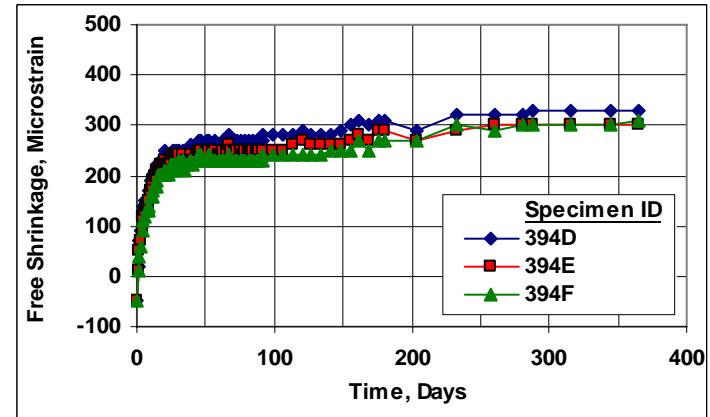


(b)

Fig. C.27 – Free Shrinkage, Batch 392. Program VI Set 2. Type I/II Cement, Granite CA, 0.42 w/c ratio, 3% SF Sample 2, (a) 7-day cure and (b) 14-day cure.

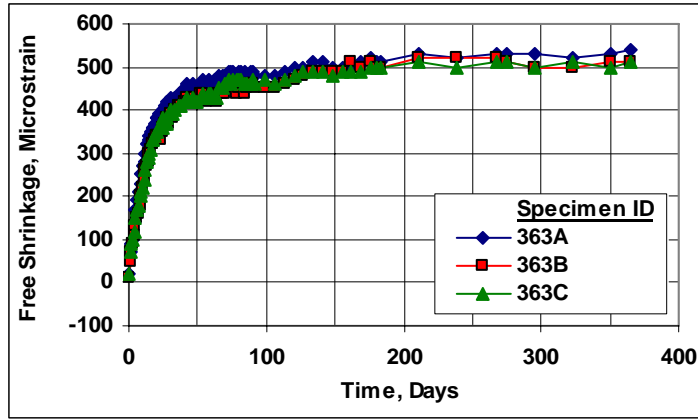


(a)

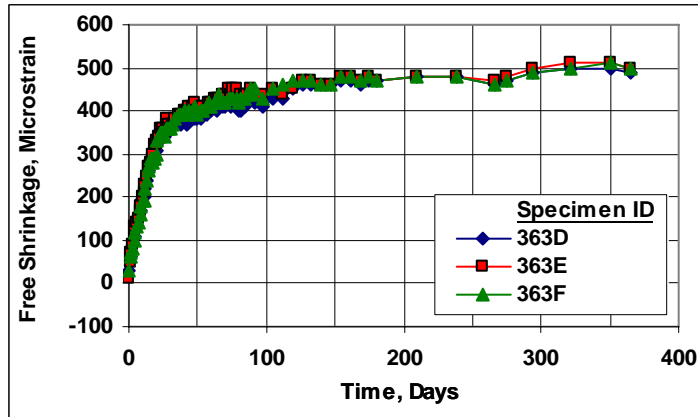


(b)

Fig. C.28 – Free Shrinkage, Batch 394. Program VI Set 2. Type I/II Cement, Granite CA, 0.42 w/c ratio, 6% SF Sample 2, (a) 7-day cure and (b) 14-day cure.

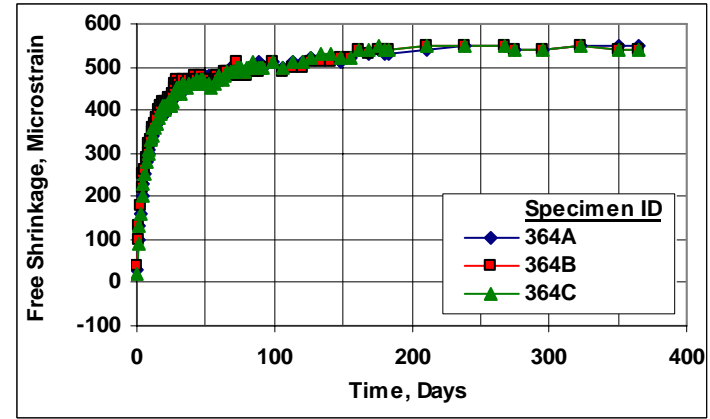


(a)

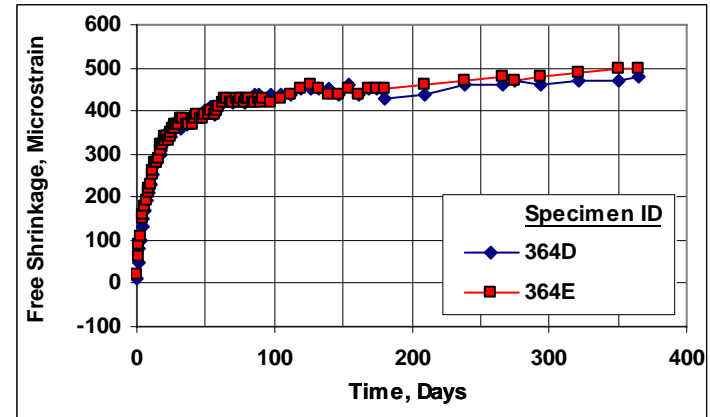


(b)

Fig. C.29 – Free Shrinkage, Batch 363. Program VI Set 3. Type I/II Cement, Limestone CA, 0.42 w/c ratio, 20% FA Sample 1, (a) 7-day cure and (b) 14-day cure.

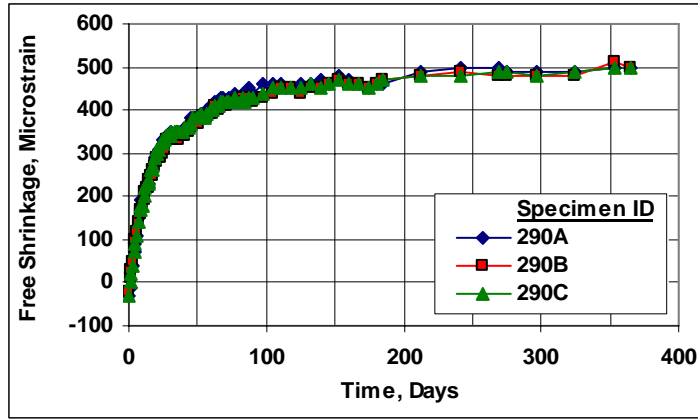


(a)

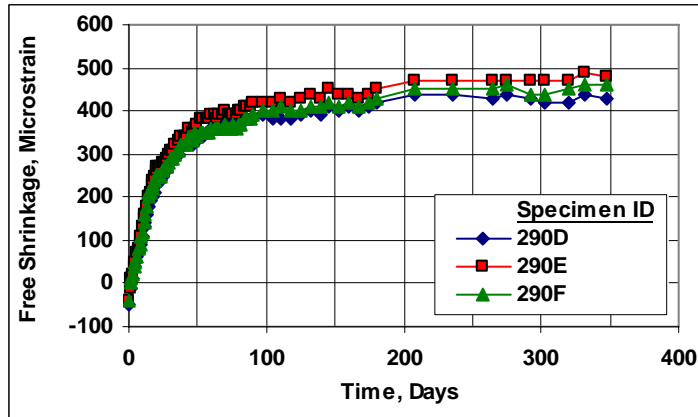


(b)

Fig. C.30 – Free Shrinkage, Batch 364. Program VI Set 3. Type I/II Cement, Limestone CA, 0.42 w/c ratio, 40% FA Sample 1, (a) 7-day cure and (b) 14-day cure.

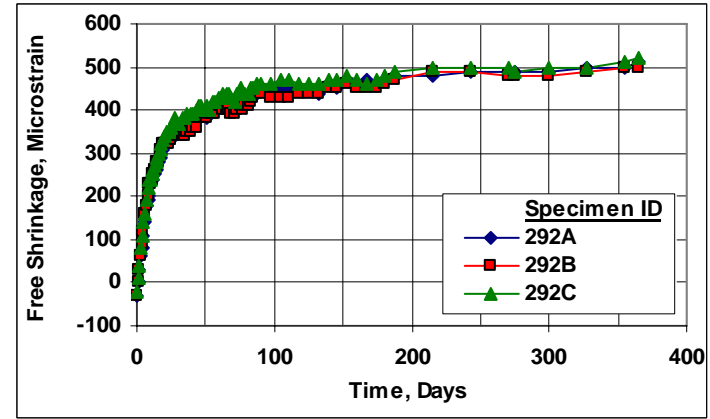


(a)

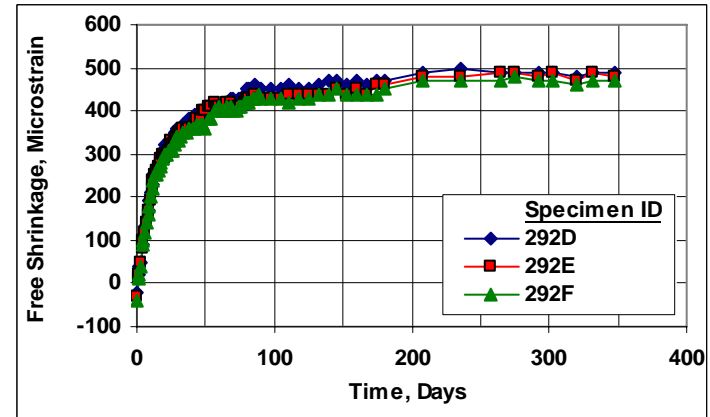


(b)

Fig. C.31 – Free Shrinkage, Batch 290. Program VI Set 3. Type I/II Cement, Limestone CA, 0.42 w/c ratio, 20% FA Sample 2, (a) 7-day cure and (b) 14-day cure.

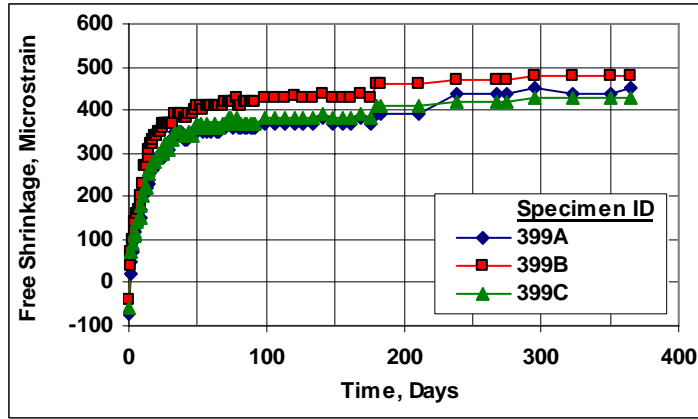


(a)

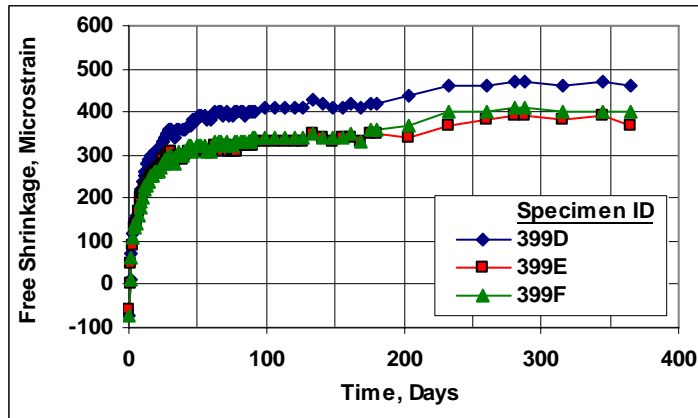


(b)

Fig. C.32 – Free Shrinkage, Batch 292. Program VI Set 3. Type I/II Cement, Limestone CA, 0.42 w/c ratio, 40% FA Sample 2, (a) 7-day cure and (b) 14-day cure.

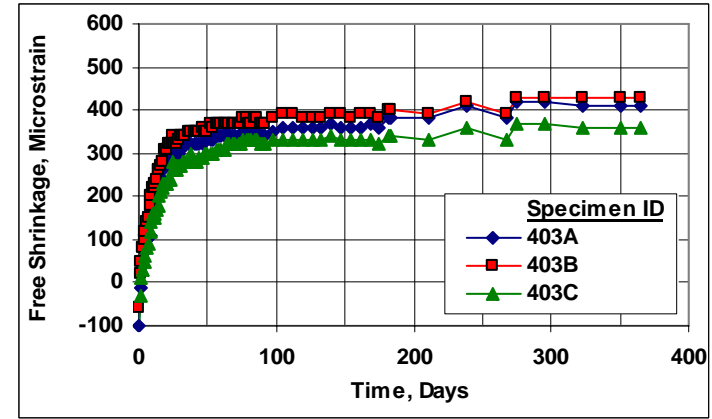


(a)

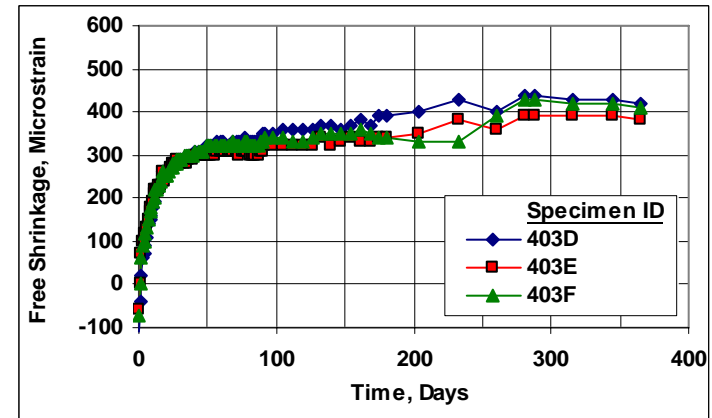


(b)

Fig. C.33 – Free Shrinkage, Batch 399. Program VI Set 4. Type I/II Cement, Granite CA, 0.42 w/c ratio, 20% FA Sample 2, (a) 7-day cure and (b) 14-day cure.

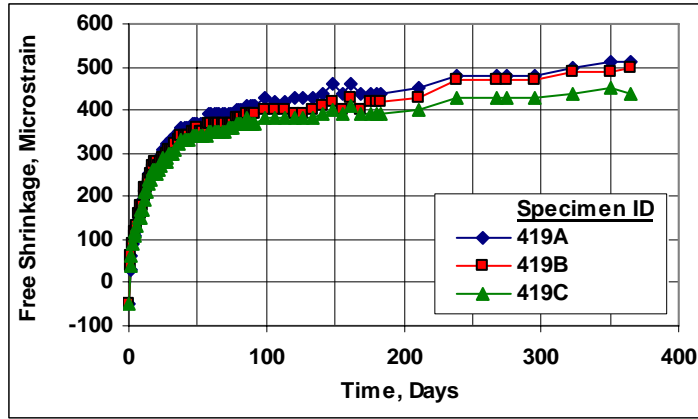


(a)

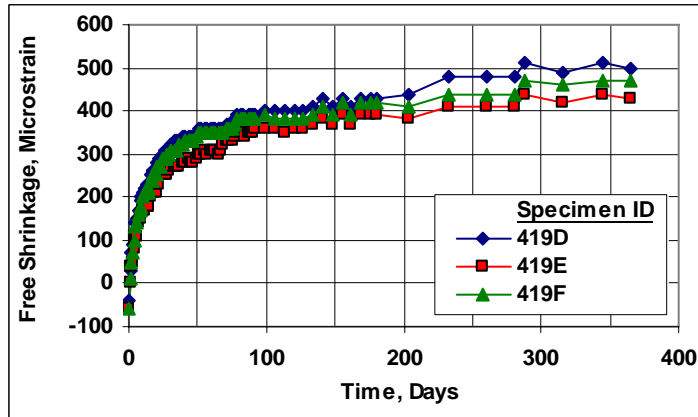


(b)

Fig. C.34 – Free Shrinkage, Batch 403. Program VI Set 4. Type I/II Cement, Granite CA, 0.42 w/c ratio, 40% FA Sample 2, (a) 7-day cure and (b) 14-day cure.

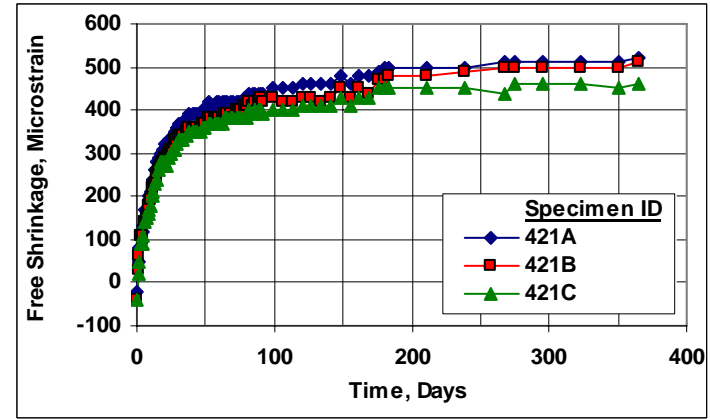


(a)

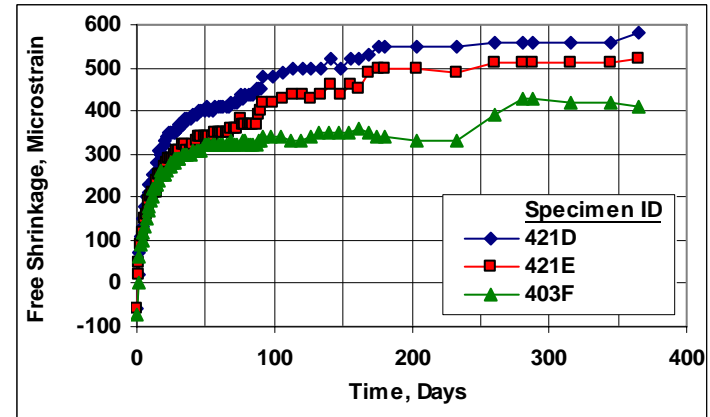


(b)

Fig. C.35 – Free Shrinkage, Batch 419. Program VI Set 4. Type I/II Cement, Granite CA, 0.42 w/c ratio, 20% FA Sample 3, (a) 7-day cure and (b) 14-day cure.

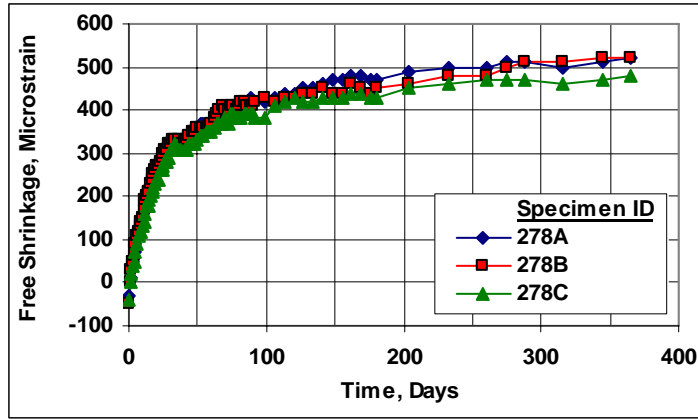


(a)

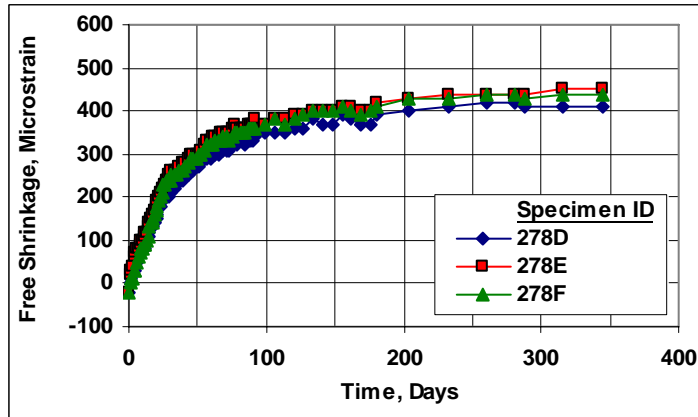


(b)

Fig. C.36 – Free Shrinkage, Batch 421. Program VI Set 4. Type I/II Cement, Granite CA, 0.42 w/c ratio, 40% FA Sample 3, (a) 7-day cure and (b) 14-day cure.

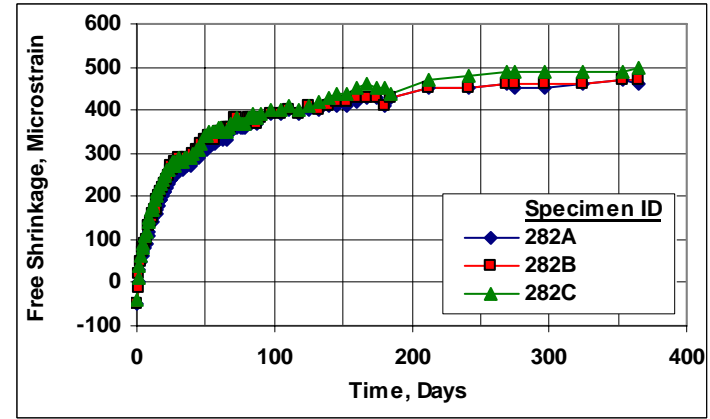


(a)

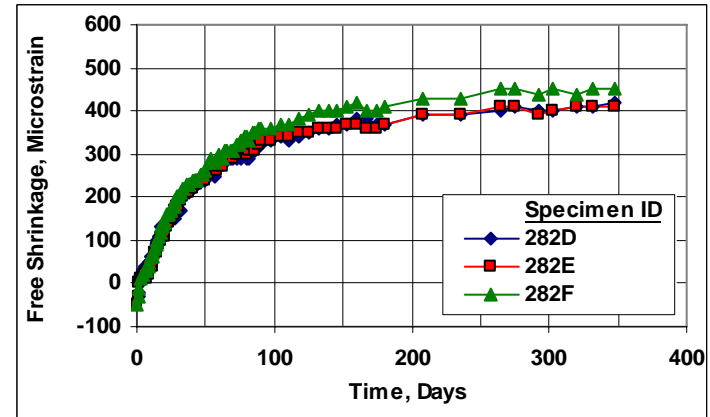


(b)

Fig. C.37 – Free Shrinkage, Batch 278. Program VI Set 5. Type I/II Cement, Limestone CA, 0.42 w/c ratio, 30% GGBFS Sample 1, (a) 7-day cure and (b) 14-day cure.

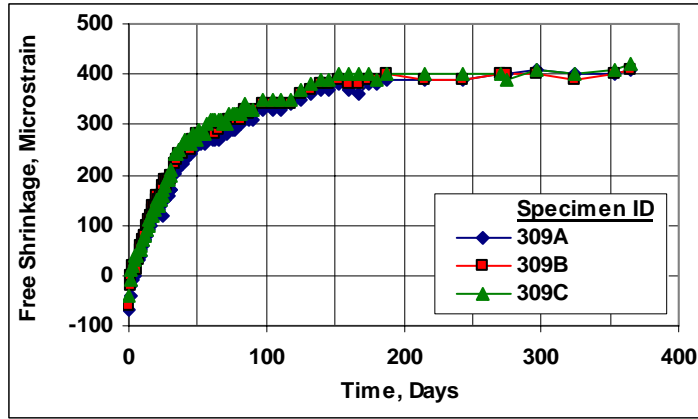


(a)

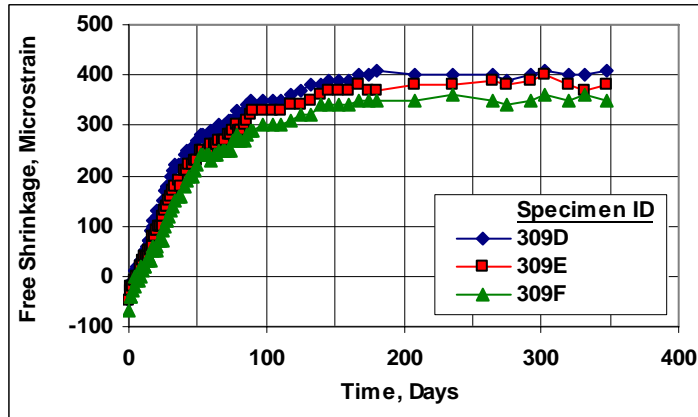


(b)

Fig. C.38 – Free Shrinkage, Batch 282. Program VI Set 5. Type I/II Cement, Limestone CA, 0.42 w/c ratio, 60% GGBFS Sample 1, (a) 7-day cure and (b) 14-day cure.

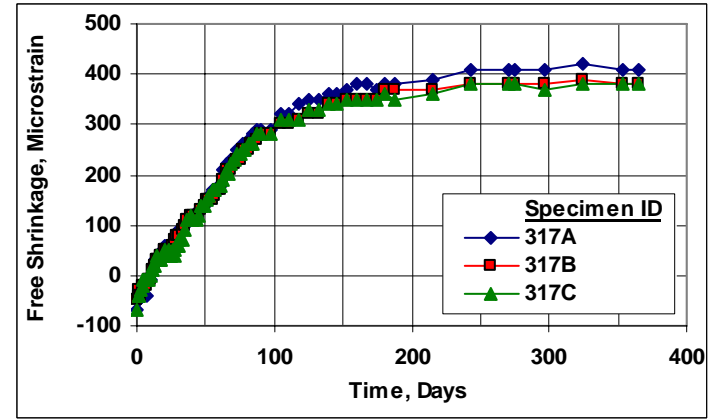


(a)

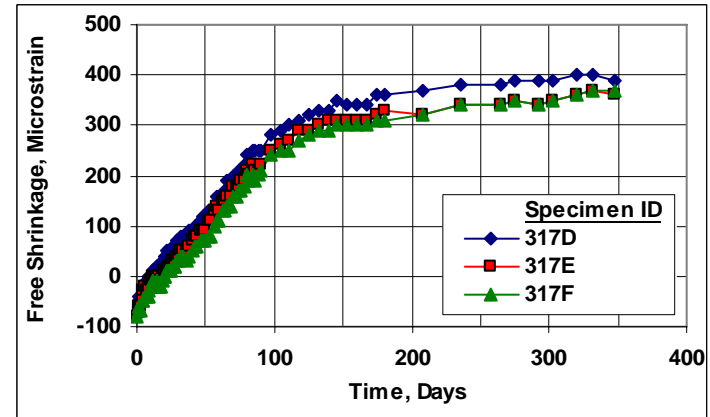


(b)

Fig. C.39 – Free Shrinkage, Batch 309. Program VI Set 5. Type I/II Cement, Limestone CA, 0.42 w/c ratio, 60% GGBFS Sample 2, (a) 7-day cure and (b) 14-day cure.

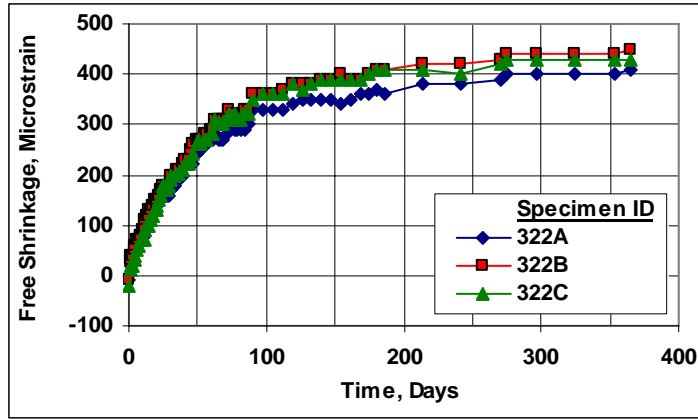


(a)

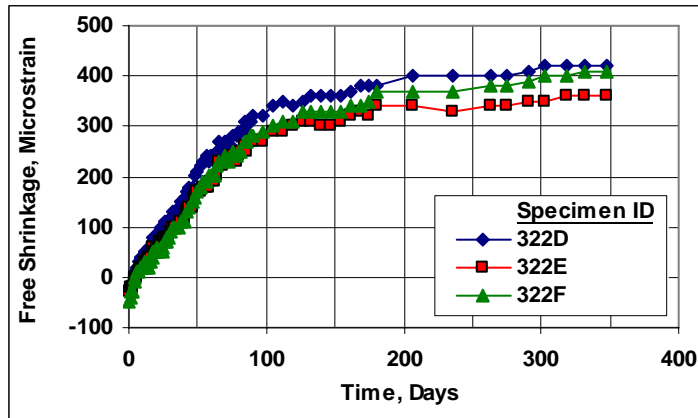


(b)

Fig. C.40 – Free Shrinkage, Batch 317. Program VI Set 5. Type I/II Cement, Limestone CA, 0.42 w/c ratio, 80% GGBFS Sample 2, (a) 7-day cure and (b) 14-day cure.

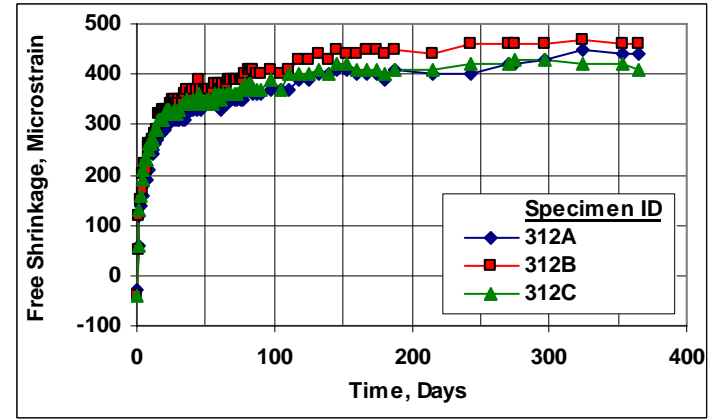


(a)

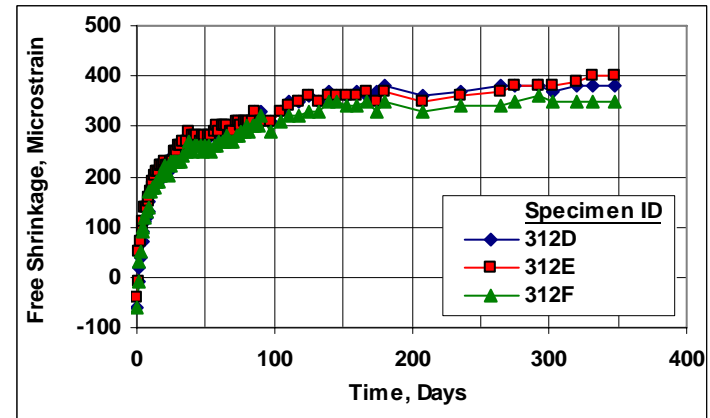


(b)

Fig. C.41 – Free Shrinkage, Batch 322. Program VI Set 6. Type I/II Cement, Limestone CA, 0.42 w/c ratio, 60% GGBFS Sample 2, (a) 7-day cure and (b) 14-day cure.

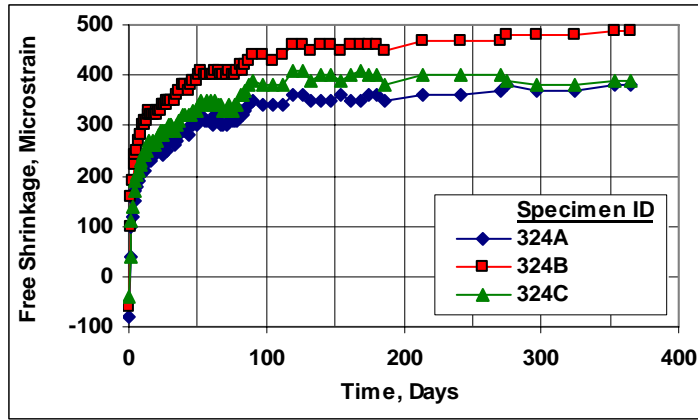


(a)

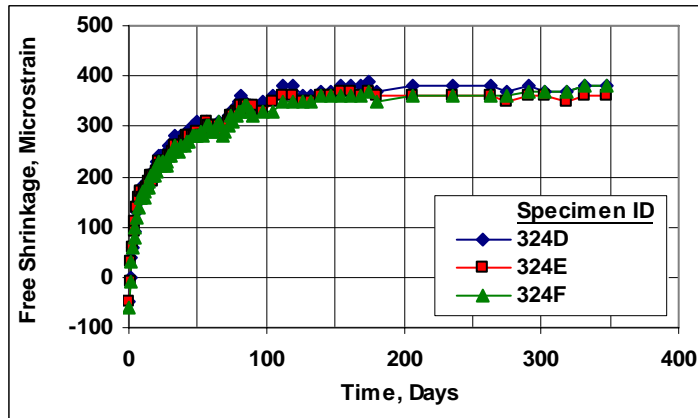


(b)

Fig. C.42 – Free Shrinkage, Batch 312. Program VI Set 6. Type I/II Cement, Quartzite CA, 0.42 w/c ratio, 60% GGBFS Sample 2, (a) 7-day cure and (b) 14-day cure.



(a)



(b)

Fig. C.43 – Free Shrinkage, Batch 324. Program VI Set 6. Type I/II Cement, Quartzite CA, 0.42 w/c ratio, 60% GGBFS Sample 2, (a) 7-day cure and (b) 14-day cure.

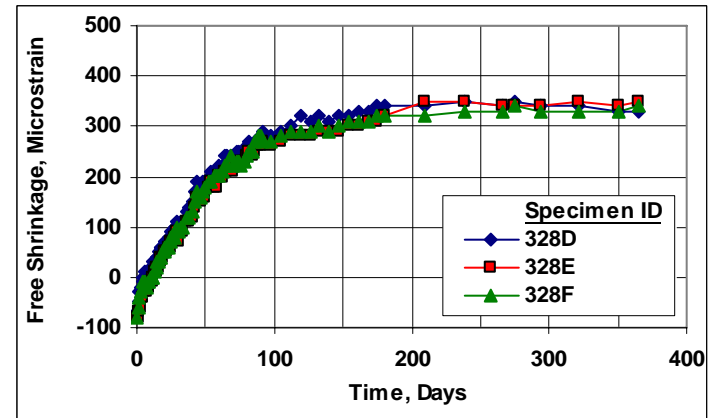
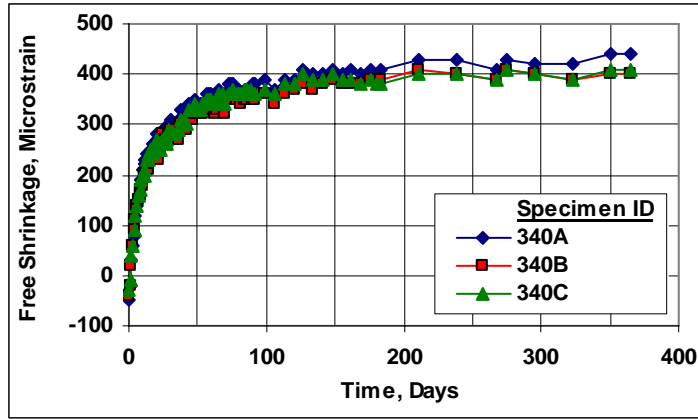
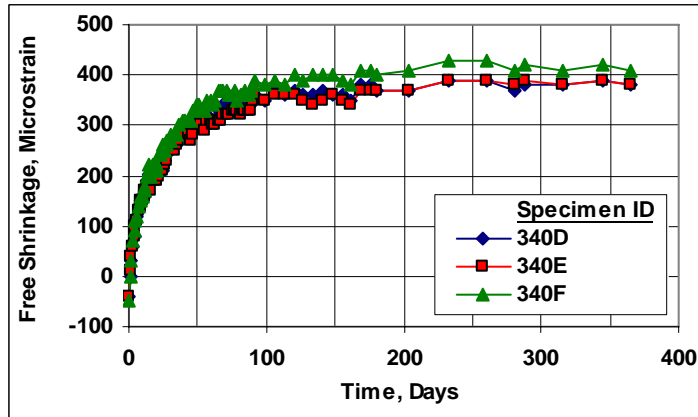


Fig. C.44 – Free Shrinkage, Batch 328. Program VI Set 7. Type I/II Cement, Limestone CA, 0.42 w/c ratio, 60% GGBFS Sample 4, 14-day cure.

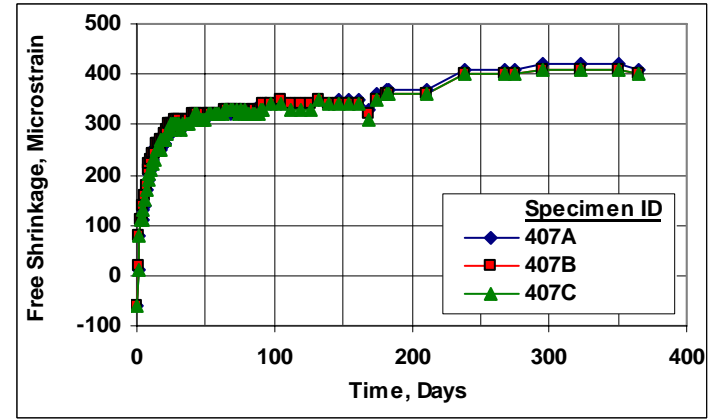


(a)

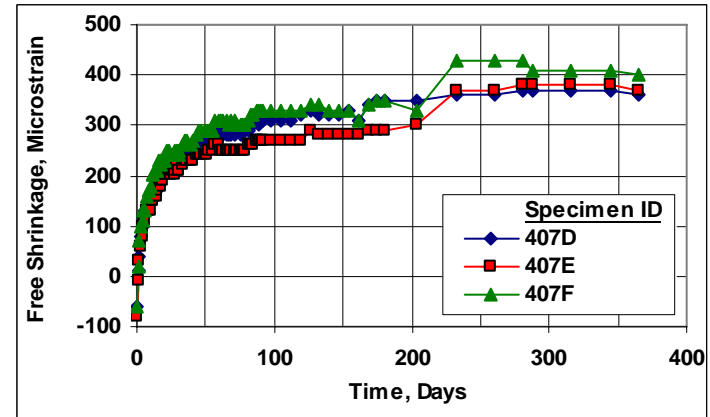


(b)

Fig. C.45 – Free Shrinkage, Batch 340. Program VI Set 7. Type I/II Cement, Granite CA, 0.42 w/c ratio, 60% GGBFS Sample 4, (a) 7-day cure and (b) 14-day cure.

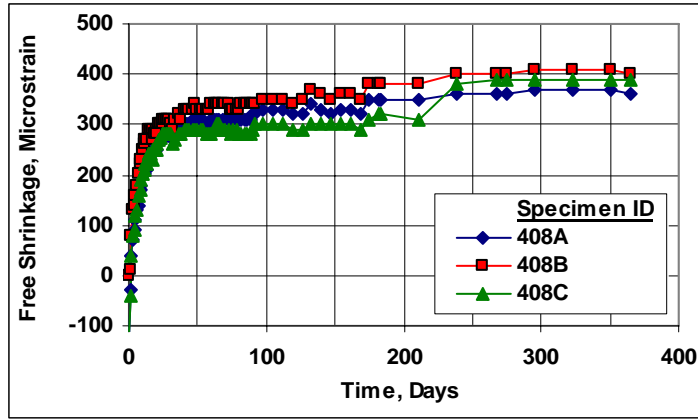


(a)

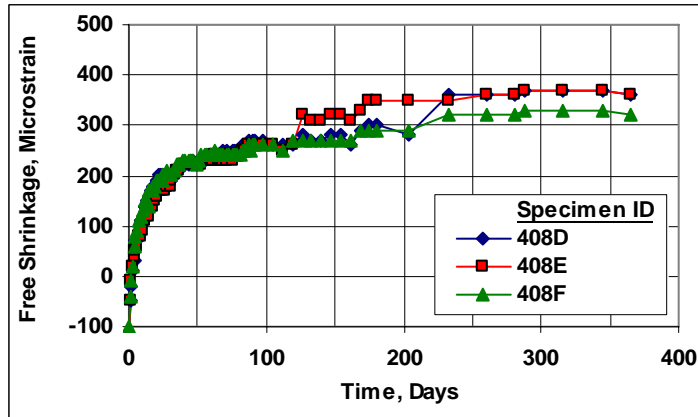


(b)

Fig. C.46 – Free Shrinkage, Batch 407. Program VI Set 8. Type I/II Cement, Granite CA, 0.42 w/c ratio, 30% GGBFS Sample 3, (a) 7-day cure and (b) 14-day cure.

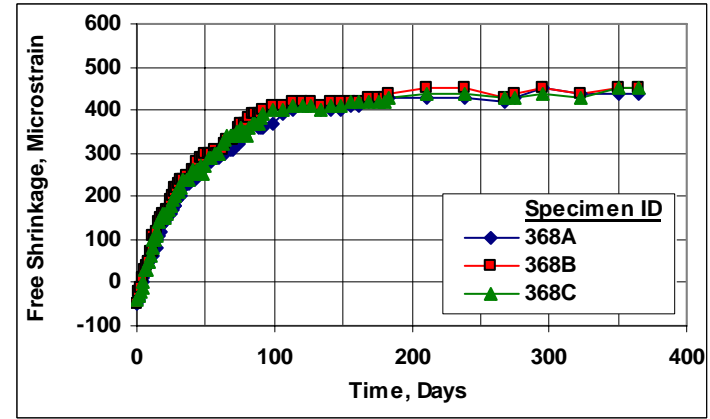


(a)

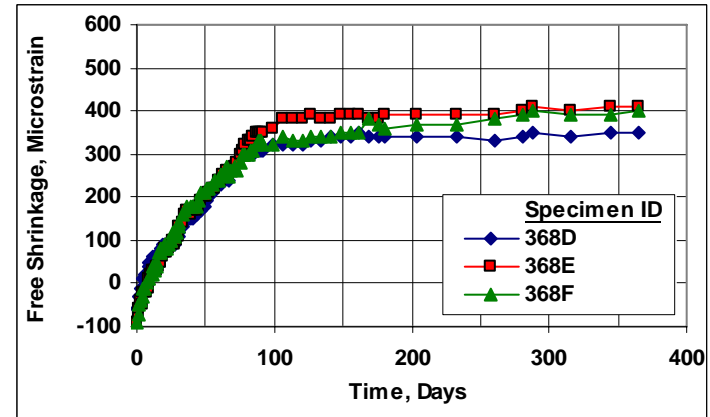


(b)

Fig. C.47 – Free Shrinkage, Batch 408. Program VI Set 8. Type I/II Cement, Granite CA, 0.42 w/c ratio, 60% GGBFS Sample 3, (a) 7-day cure and (b) 14-day cure.

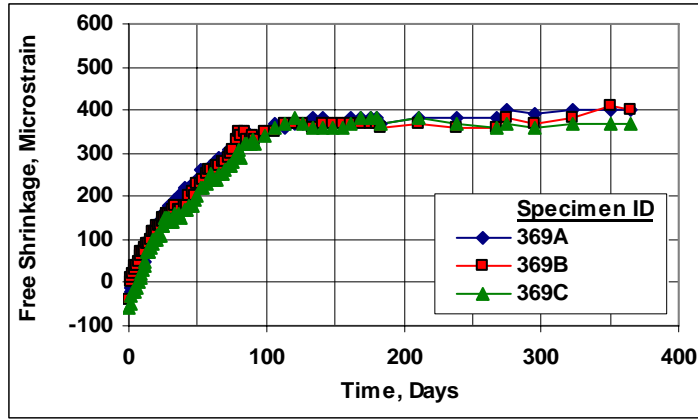


(a)

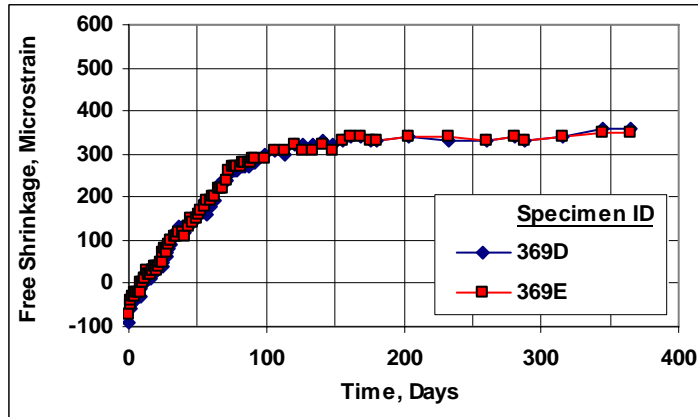


(b)

Fig. C.48 – Free Shrinkage, Batch 368. Program VI Set 9. Type I/II Cement, OD Limestone CA, 0.42 w/c ratio, 60% GGBFS Sample 5, (a) 7-day cure and (b) 14-day cure.

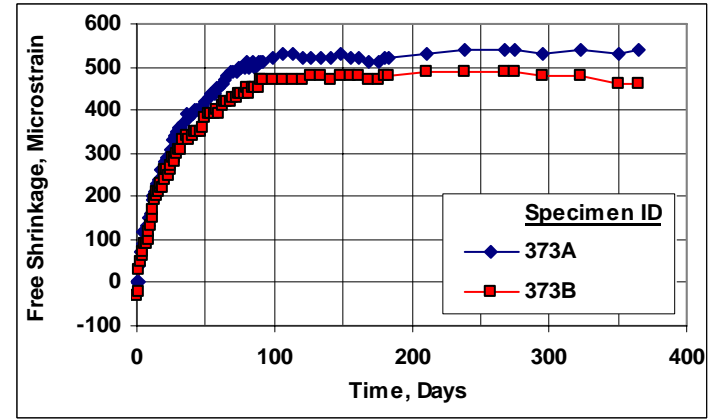


(a)

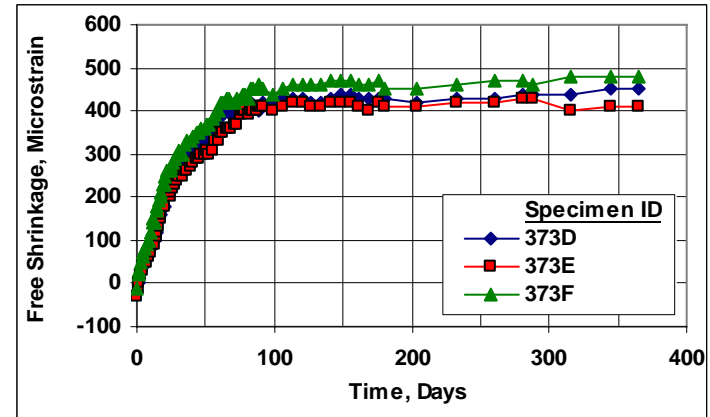


(b)

Fig. C.49 – Free Shrinkage, Batch 369. Program VI Set 9. Type I/II Cement, SSD Limestone CA, 0.42 w/c ratio, 60% GGBFS Sample 5, (a) 7-day cure and (b) 14-day cure.

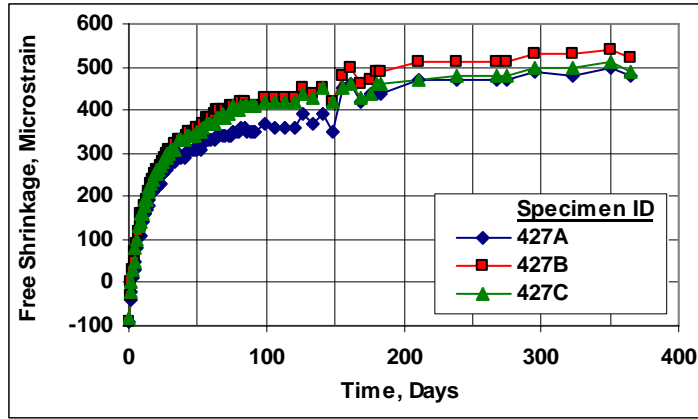


(a)

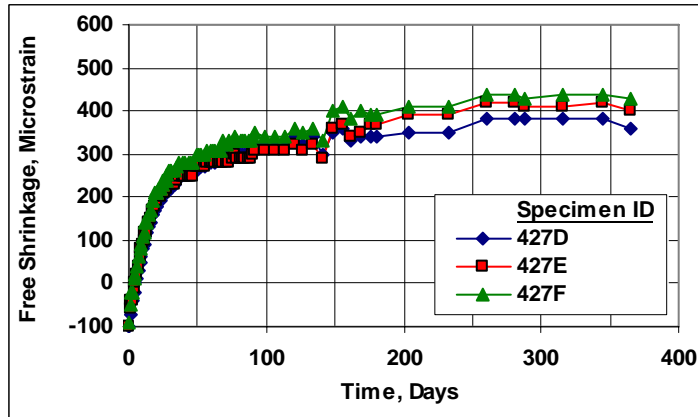


(b)

Fig. C.50 – Free Shrinkage, Batch 373. Program VI Set 9. Type I/II Cement, SSD Limestone CA, 0.42 w/c ratio, 0% GGBFS, (a) 7-day cure and (b) 14-day cure.

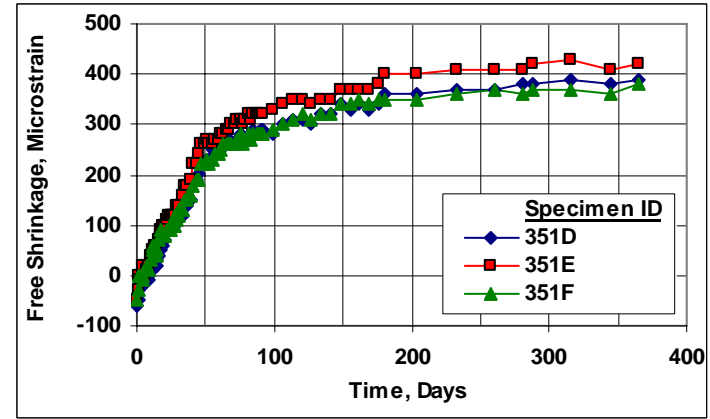


(a)

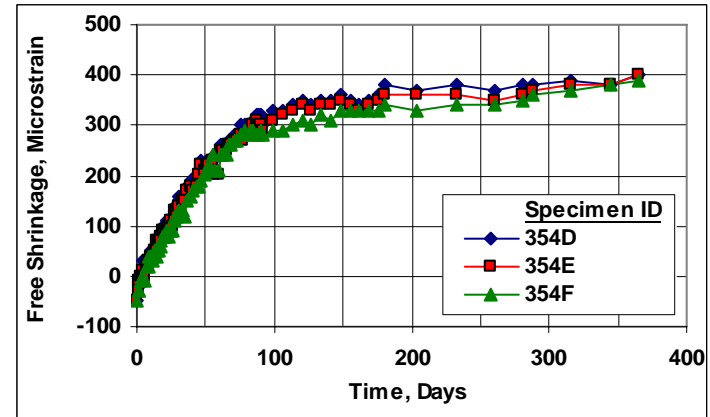


(b)

Fig. C.51 – Free Shrinkage, Batch 427. Program VI Set 9. Type I/II Cement, OD Limestone CA, 0.42 w/c ratio, 0% GGBFS, (a) 7-day cure and (b) 14-day cure.

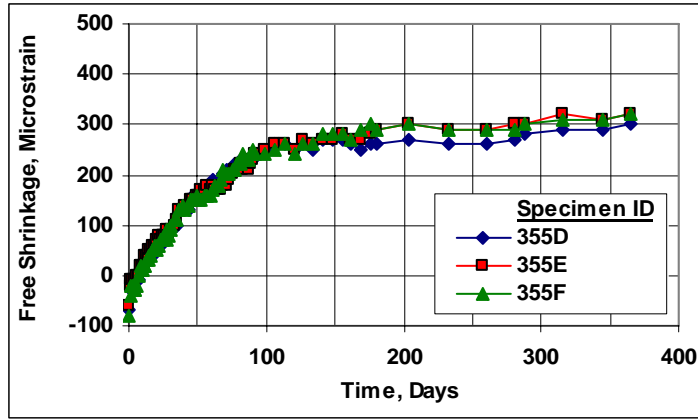


(a)

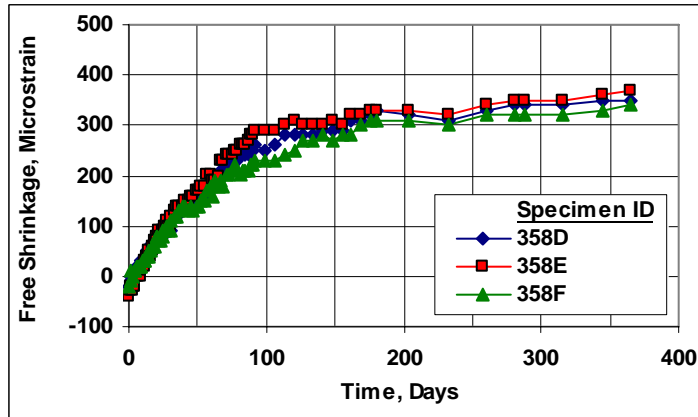


(b)

Fig. C.52 – Free Shrinkage, Batch 351 and 354. Program VI Set 10. Type I/II Cement, Limestone CA, 497 CF, (a) 60% GGBFS #2 and (b) 0% GGBFS # 2 and 6% SF #2.



(a)



(b)

Fig. C.53 – Free Shrinkage, Batch 355 and 358. Program VI Set 10. Type I/II Cement, Limestone CA, 460 CF, **(a)** 60% GGBFS #2 and 6% SF #2 and **(b)** 80% GGBFS #2 and 6% SF #2.

Table D.1 – Low-Cracking High-Performance Concrete (LC-HPC) Mix Design Information

County and Serial Number	Bridge Description	LC-HPC Number	Portion Placed	Date of Placement	Design Air Content	Water Content		Cement Content [†]	
						(kg/m ³)	(lb/yd ³)	(kg/m ³)	(lb/yd ³)
105-304	EB Parallel over I-635	1	South	10/14/05	8.0	144	243	320	539
			North	11/02/05	8.0	144	243	320	539
105-310	34th St. over I-635	2	Deck	09/13/06	8.0	144	243	320	539
46-338	WB 103rd over US-69	3	Deck	11/13/07	8.0	143	241	317	534
46-339 Unit 1	SB US-69 to I-435 Rp over 103rd St to SB US-69 Rp	4	Deck - South	09/29/07	8.0	133	224	317	534
			Deck - North	10/02/07	8.0	133	224	317	534
46-340 Unit 1	SB US-69 to WB I-435 Rp over WB I-435 to Quivera Rp	5	Deck	11/14/07	8.0	133	224	317	534
				11/14/07	8.0	135	228	317	534
				11/14/07	8.0	136	229	317	534
				11/14/07	8.0	143	241	317	534
46-340 Unit 2	SB US-69 to WB I-435 Rp over WB I-435 to Quivera Rp	6	Deck	11/03/07	8.0	143	241	317	534
43-33	Co Rd 150 over US-75	7	Deck	06/24/06	8.0	144	243	320	539
54-33	E 1350 Rd over US-69	8	Deck	10/03/07	8.0	133	224	317	534
54-60	E 1800 Rd over US-69	10	Deck	05/17/07	8.0	133	224	317	534
78-119	EB US-50 over K&O RR	11	Deck	06/09/07	8.0	133	224	317	534
56-57 Unit 2	K-130 over Neosho River	12	Deck	04/04/08	8.0	141	238	320	540
54-66	NB US-69 over BNSF RR	13	Deck	04/29/08	8.0	140	235	317	535
46-363	Metcalf Ave. over Indian Creek	14	Deck - Center	12/19/07	8.0	140	235	317	535
			Deck - West	05/02/08	8.0	140	235	317	535
			Deck - East	05/21/08	8.0	140	235	317	535

[†]The design cement content for the LC-HPC decks was 535 or 540 lb/yd³ – equivalent to 317 or 320 kg/m³. When the metric equivalents are rounded to the nearest whole number and converted back to English units, the values are 534 or 539 lb/yd³, respectively.

Table D.1 (continued) – Low-Cracking High-Performance Concrete (LC-HPC) Mix Design Information

LC-HPC Number	Portion Placed	Date of Placement	Cement Specific Gravity	W/C Ratio	Design Volume of Paste (%)	Concrete Temperature Control	Aggregate Used [†]	Types of Admixtures [‡]
1	South	10/14/05	3.15	0.45	24.6%	None	1, 2, 3, 4	AEA, Type A-F MRWR
	North	11/02/05	3.15	0.45	24.6%	None	1, 2, 3, 4	AEA, Type A-F MRWR
2	Deck	09/13/06	3.15	0.45	24.6%	Chilled Water, Ice	1, 2, 3, 4	AEA, Type A-F MRWR
3	Deck	11/13/07	3.15	0.45	24.4%	None	5, 6, 7, 8	AEA, Type A-F HRWR
4	Deck - South	09/29/07	3.15	0.42	23.4%	Chilled Water, Ice	9, 10, 11, 12	AEA, Type A-F MRWR
	Deck - North	10/02/07	3.15	0.42	23.4%	Chilled Water, Ice	5, 6, 7, 8	AEA, Type A-F MRWR
5	Deck	11/14/07	3.15	0.42	23.4%	None	5, 6, 7, 8	AEA, Type A-F HRWR
		11/14/07	3.15	0.43	23.5%	None	5, 6, 7, 8	AEA, Type A-F HRWR
		11/14/07	3.15	0.43	23.7%	None	5, 6, 7, 8	AEA, Type A-F HRWR
		11/14/07	3.15	0.45	24.4%	None	5, 6, 7, 8	AEA, Type A-F HRWR
6	Deck	11/03/07	3.15	0.45	24.4%	None	5, 6, 7, 8	AEA, Type A-F HRWR
2	Deck	06/24/06	3.15	0.45	24.6%	Ice	13, 14, 15	AEA
8	Deck	10/03/07	3.15	0.42	23.3%	Ice	16, 17, 18, 19	AEA, Type A WR
10	Deck	05/17/07	3.15	0.42	23.3%	Ice	16, 17, 18, 19	AEA, Type A WR
11	Deck	06/09/07	3.17	0.42	23.3%	Ice	20, 21, 22, 23	AEA, Type A-F MRWR
12	Deck	04/04/08	3.15	0.44	24.3%	None	24, 25, 26	AEA, Type A WR
13	Deck	04/29/08	3.15	0.44	24.0%	None	27, 28, 29	AEA
14	Deck - Center	12/19/07	3.15	0.45	24.0%	None	5, 6, 7, 8	AEA, Type A-F MRWR
	Deck - West	05/02/08	3.15	0.45	24.0%	Chilled Water, Ice	5, 6, 7, 8	AEA, Type A-F MRWR
	Deck - East	05/21/08	3.15	0.45	24.0%	Chilled Water, Ice	5, 6, 7, 8	AEA, Type A-F MRWR

[†]The aggregate gradations are shown in Table D.2.

[‡]MRWR – mid-range water reducer, HRWR – high-range water reducer, WR – water reducer

Table D.2 – LC-HPC Aggregate Gradations

Sieve Size	Percent Retained on Each Sieve							
	LC-HPC-1 and 2				LC-HPC-3, 4 (Placements 2, 5, 6), and 14			
<i>Identification</i> [†]	1	2	3	4	5	6	7	8
<i>Blend, %</i>	30.0	19.0	9.0	42.0	22.0	29.0	13.0	36.0
<i>Designation</i>	CA-6	CA-5	CA-7	FA-A	CA-6	CA-5	M.S. [‡]	FA-A
<i>S.G. SSD</i>	2.63	2.63	2.63	2.61	2.61	2.61	2.61	2.61
37.5-mm (1½-in.)	0	0	0	0	0	0	0	0
25-mm (1-in.)	12.0	8.0	0	0	10.0	0	0	0
19-mm (¾-in.)	13.0	26.0	0	0	21.0	7.0	0	0
12.5-mm (½-in.)	26.0	38.0	0	0	20.0	24.0	0	0
9.5-mm (⅜-in.)	20.0	25.0	6.0	0	19.0	22.0	0	0
4.75-mm (No. 4)	25.0	1.0	85.0	0	23.0	37.0	6.0	1.0
2.36-mm (No. 8)	1.0	0	6.0	12.0	4.0	6.0	29.0	8.0
1.18-mm (No. 16)	0	0	0	21.0	0	1.0	25.0	17.0
0.60-mm (No. 30)	0	0	0	29.0	1.0	1.0	16.0	23.0
0.30-mm (No. 50)	0	0	0	27.0	0	0	12.0	31.0
0.15-mm (No. 100)	0	0	0	10.0	1.0	0	6.0	17.0
0.075-mm (No. 200)	0	0	0	1.0	0	1.0	2.0	2.0
Pan	0	0	0	0	2.0	1.0	4.0	1.0

[†]Aggregate Identification number shown in Table D.1

[‡]Manufactured (crushed granite) Coarse Sand

Table D.2 (continued) – LC-HPC Aggregate Gradations

Sieve Size	Percent Retained on Each Sieve						
	LC-HPC-4 (Placement 1)				LC-HPC-7		
<i>Identification</i> [†]	9	10	11	12	13	14	15
<i>Blend, %</i>	23.9	25.6	33.1	17.4	33.0	20.0	47.0
<i>Designation</i>	CA-6	CA-5	M.S. [‡]	FA-A	CA-6	CA-5	MA-2
<i>S.G. SSD</i>	2.61	2.61	2.61	2.61	2.64	2.64	2.63
37.5-mm (1½-in.)	0	0	0	0	0	0	0
25-mm (1-in.)	10.0	0	0	0	7.4	0	0
19-mm (¾-in.)	21.0	7.0	0	0	15.4	0	0
12.5-mm (½-in.)	20.0	24.0	0	0	35.8	27.9	0
9.5-mm (⅜-in.)	19.0	22.0	0	0	16.9	25.3	0
4.75-mm (No. 4)	23.0	37.0	6.0	1.0	21.4	40.2	3.9
2.36-mm (No. 8)	4.0	6.0	29.0	8.0	1.7	4.3	18.5
1.18-mm (No. 16)	0	1.0	25.0	17.0	0.3	1.0	24.7
0.60-mm (No. 30)	1.0	1.0	16.0	23.0	0.2	0.4	24.1
0.30-mm (No. 50)	0	0	12.0	31.0	0.4	0.3	17.6
0.15-mm (No. 100)	1.0	0	6.0	17.0	0.1	0.3	9.3
0.075-mm (No. 200)	0	1.0	2.0	2.0	0.2	0.2	1.6
Pan	2.0	1.0	4.0	1.0	0.2	0.1	0.3

[†]Aggregate Identification number shown in Table D.1

[‡]Manufactured (crushed granite) Coarse Sand

Table D.2 (continued) – LC-HPC Aggregate Gradations

Sieve Size	Percent Retained on Each Sieve							
	LC-HPC-8, 10				LC-HPC-11			
<i>Identification</i> [†]	16	17	18	19	20	21	22	23
<i>Blend, %</i>	23.3	24.5	36.9	15.3	10.0	10.0	33.0	47
<i>Designation</i>	CA-6	CA-5	MA-1	BD-2	CA-1	CA-6	CA-7	MA-3
<i>S.D. SSD</i>	2.59	2.59	2.64	2.62	2.78	2.78	2.78	2.61
37.5-mm (1½-in.)	0	0	0	0	1.0	0	0	0
25-mm (1-in.)	15.8	0	0	0	56.0	1.0	0	0
19-mm (¾-in.)	26.2	0	0	0	30.0	20.0	0	0
12.5-mm (½-in.)	29.6	27.0	0	0	9.0	48.0	25.6	2.0
9.5-mm (⅜-in.)	11.3	25.6	2.0	3.0	2.0	11.0	21.1	1.5
4.75-mm (No. 4)	15.1	43.7	6.0	11.0	1.0	12.0	35.8	8.0
2.36-mm (No. 8)	0	1.9	16.0	28.0	0	3.0	9.6	18.5
1.18-mm (No. 16)	0	0	23.0	29.0	0	1.0	2.5	26.5
0.60-mm (No. 30)	0	0	22.0	16.0	0	2.0	1.1	18.5
0.30-mm (No. 50)	0	0	19.0	10.0	0	1.0	0.8	16.5
0.15-mm (No. 100)	0	0	10.0	2.0	0	0.0	0.6	7.5
0.075-mm (No. 200)	0	0	0	0.0	0.4	0.8	0.6	0.6
Pan	2.0	1.8	2.0	1.0	0	0	0	0

[†]Aggregate Identification number shown in Table D.1

Table D.2 (continued) – LC-HPC Aggregate Gradations

Sieve Size	Percent Retained on Each Sieve					
	LC-HPC-12			LC-HPC-13		
<i>Identification</i> [†]	24	25	26	27	28	29
<i>Blend, %</i>	40.0	12.0	48.0	50.6	35.5	13.9
<i>Designation</i>	CA-6	CA-5	MA-2	CA-1	MA-1	FA-A
<i>S.G. SSD</i>	2.64	2.64	2.63	2.59	2.62	2.62
37.5-mm (1½-in.)	0	0	0	0	0	0
25-mm (1-in.)	8.2	0	0	11.8	0	0
19-mm (¾-in.)	15.3	10.8	0	20.3	0	0
12.5-mm (½-in.)	30.9	44.7	0.2	21.8	0.7	0
9.5-mm (⅜-in.)	13.6	19.3	1.2	17.9	3.7	0
4.75-mm (No. 4)	23.7	21.3	6.8	24.1	15.5	0.8
2.36-mm (No. 8)	3.3	0.9	19.8	1.7	18.8	9.2
1.18-mm (No. 16)	0.8	0.5	27.5	0.4	20.0	17.7
0.60-mm (No. 30)	0.6	0.4	21.3	0.3	17.2	20.8
0.30-mm (No. 50)	0.5	0.3	16.1	0.2	16.1	29.9
0.15-mm (No. 100)	0.6	0.2	6.1	0.2	6.3	18.7
0.075-mm (No. 200)	0.5	0.3	0.8	0	0	0
Pan	2.0	1.3	0.2	0	0	0

[†]Aggregate Identification number shown in Table D.1

Table D.3 – Average Concrete Properties for LC-HPC Bridge Decks

LC-HPC Number	Portion Placed	Date of Placement	Average Air Content	Average Slump		Average Concrete Temperature		Average Unit Weight		Average Compressive Strength [†]	
				(mm)	(in.)	(°C)	(°F)	(kg/m ³)	(lb/yd ³)	(MPa)	(psi)
1	South	10/14/05	7.9	95	3.75	19.8	68	2251	140.5	35.9	5210
	North	11/02/05	7.8	85	3.25	20.1	68	2238	139.7	34.4	4980
2	Deck	09/13/06	7.7	75	3.00	19.2	67	--	--	31.7	4600
3	Deck	11/13/07	8.7	85	3.25	14.3	58	--	--	41.3	5990
4	Deck - South	09/29/07	8.7	50	2.00	--	--	2202	137.4	--	--
	Deck - North	10/02/07	8.8	80	3.00	17.5	64	2210	137.9	33.1	4790
5	Deck - 0.420 w/c	11/14/07	8.3	70	2.75	16.7	62	2249	140.4	44.0	6380
	Deck - 0.428 w/c	11/14/07	9.0	60	2.50	16.4	62	2242	140.0	--	--
	Deck - 0.429 w/c	11/14/07	9.1	90	3.50	15.2	59	2230	139.2	--	--
	Deck - 0.451 w/c	11/14/07	8.7	80	3.25	15.7	60	2228	139.1	--	--
Average Values		11/14/07	8.7	80	3.00	15.9	61	2236	139.6	--	--
6	Deck	11/03/07	9.5	95	3.75	15.3	60	--	--	40.3	5840
7	Deck	06/24/06	8.0	95	3.75	21.9	71	2221	138.6	26.1	3790
8	Deck	10/03/07	7.9	50	2.00	19.5	67	2264	141.3	32.6	4730
10	Deck	05/17/07	7.3	80	3.25	18.6	66	2212	138.1	31.6	4580
11	Deck	06/09/07	7.8	80	3.00	15.8	60	2278	142.2	32.3	4680
12	Deck	04/04/08	7.4	70	2.75	14.5	58	2259	141.0	31.5	4570
13	Deck	04/29/08	8.1	75	3.00	20.4	69	2266	141.5	29.5	4280
14	Deck - Center	12/19/07	8.7	95	3.75	18.1	65	2237	139.7	30.6	4440
	Deck - West	05/02/08	9.8	110	4.25	17.9	64	2213	138.1	25.6	3710
	Deck - East	05/21/08	9.9	130	5.25	18.3	65	2195	137.1	26.4	3830

[†]Average 28-day compressive strength for lab-cured specimens. Strengths were taken at 27 days for the first LC-HPC-1 placement and LC-HPC-11, and 31 days for LC-HPC-7.

Table D.4 – Average Compressive Strength Results for All LC-HPC Placements

Bridge No.	Placement	Age	Lab Cured	Sample Size	Field Cured	Sample Size
		Days	MPa (psi)		MPa (psi)	
1, 2	Qualification Batch – 1/2	28	39.5 (5730)	3	--	--
	Qualification Slab – 1	28	26.7 (3870)	4	--	--
	LC-HPC-1 Placement 1	27	35.9 (5210)	3	33.8 (4900)	2
	LC-HPC-1 Placement 2	28	34.4 (4980)	3	27.8 (4030)	2
	Qualification Slab – 2	28	27.4 (3970)	3	28.6 (4150)	2
	LC-HPC-2	28	31.7 (4600)	3	30.7 (4450)	2
3 – 6	LC-HPC-3	28	41.3 (5990)	3	37.6 (5450)	2
	LC-HPC-4	28	33.1 (4790)	3	--	--
	LC-HPC-5	28	44.0 (6380)	3	41.3 (5990)	2
	LC-HPC-6	28	40.3 (5840)	2	--	--
7	Test Batch	6	17.0 (2470)	3	--	--
	Qualification Batch – 7	28	23.9 (3470)	3	--	--
	Qualification Slab – 7	5	22.4 (3250)	3	--	--
	LC-HPC-7	31	26.1 (3790)	3	--	--
8, 10	Qualification Batch – 8/10	28	29.2 (4240)	3	--	--
	Qualification Slab – 8	28	29.7 (4310)	3	--	--
	LC-HPC-8	28	32.6 (4730)	6	29.9 (4340)	4
	Qualification Slab – 10	28	28.2 (4090)	3	--	--
	LC-HPC-10	28	31.6 (4580)	6	31.6 (4580)	4
11	Qualification Slab - 11	6	35.2 (5110)	3	--	--
	LC-HPC-11	9	23.9 (3460)	3	--	--
		16	27.1 (3920)	2	--	--
		27	32.3 (4680)	3	--	--
12	LC-HPC-12	28	31.5 (4570)	6	--	--
13	LC-HPC-13	29	29.5 (4280)	6	29.6 (4300)	4
14	LC-HPC-14 Placement 1	7	25.2 (3660)	6	--	--
		14	25.9 (3760)	6	23.9 (3470)	3
		28	30.6 (4440)	12	26.5 (3850)	4
	LC-HPC-14 Placement 2	2	--	--	11.4 (1660)	3
		3	--	--	12.1 (1750)	7
		7	18.6 (2700)	14	--	--
		14	21.7 (3150)	14	--	--
		28	25.6 (3710)	7	--	--
	LC-HPC-14 Placement 3	41	26.7 (3870)	6	26.5 (3840)	3
		2	--	--	11.6 (1680)	2
7		19.4 (2810)	8	--	--	
14		23.4 (3390)	8	22.3 (3230)	3	
	28	26.4 (3830)	8	--	--	

Table D.5 – Individual Plastic Concrete Test Results for LC-HPC Bridge Placements

Truck	Air Content	Slump		Concrete Temperature [†]		Unit Weight		Water Withheld		Actual w/c ratio	Actual Paste Content	Notes
		(mm)	(in.)	(°C)	(°F)	(kg/m ³)	(lb/yd ³)	(L/m ³)	(gal/yd ³)			
LC-HPC-1 (105-304) Placement 1, Cast on 10/14/05												
1	7.5	95	3.75	18.9	66	2258	141.0	0	0	0.45	24.6%	18° C using ASTM C 1064
2	6.2	85	3.25	19.2	67	2276	142.1	0	0	0.45	24.6%	16° C using ASTM C 1064
3	8.0	65	2.50	20.0	68	2250	140.5	0	0	0.45	24.6%	22° C using ASTM C 1064
4	--	--	--	18.3	65	--	--	0	0	0.45	24.6%	
5	--	--	--	18.9	66	--	--	0	0	0.45	24.6%	
6	--	--	--	20.0	68	--	--	0	0	0.45	24.6%	
7	9.0	95	3.75	17.2	63	2188	136.6	0	0	0.45	24.6%	19° C using ASTM C 1064
8	--	--	--	16.1	61	--	--	0	0	0.45	24.6%	
9	--	--	--	18.3	65	--	--	0	0	0.45	24.6%	
10	11.5	165	6.50	19.4	67	2260	141.1	0	0	0.45	24.6%	19° C using ASTM C 1064
11	6.0	90	3.50	20.0	68	2273	141.9	0	0	0.45	24.6%	20° C using ASTM C 1064
12	--	--	--	17.2	63	--	--	0	0	0.45	24.6%	
13	--	--	--	18.3	65	--	--	0	0	0.45	24.6%	
14	--	--	--	20.6	69	--	--	0	0	0.45	24.6%	
15	7.5	90	3.50	20.0	68	2250	140.5	0	0	0.45	24.6%	22° C using ASTM C 1064
16	--	--	--	19.7	68	--	--	0	0	0.45	24.6%	
17	--	--	--	20.0	68	--	--	0	0	0.45	24.6%	
18	--	--	--	18.6	66	--	--	0	0	0.45	24.6%	
19	--	--	--	18.3	65	--	--	0	0	0.45	24.6%	
20	--	--	--	19.4	67	--	--	0	0	0.45	24.6%	
21	7.4	85	3.25	20.3	69	2253	140.6	0	0	0.45	24.6%	22° C using ASTM C 1064
LC-HPC-1 (105-304) Placement 2, Cast on 11/2/05												
1	7.0	110	4.25	18.9	66	2261	141.1	0	0	0.45	24.6%	19° C using ASTM C 1064
2	6.5	75	3.00	19.7	68	2281	142.4	0	0	0.45	24.6%	20° C using ASTM C 1064
3	3.0	65	2.50	19.2	67	2354	146.9	0	0	0.45	24.6%	20° C using ASTM C 1064
4	9.0	95	3.75	15.6	60	2227	139.0	0	0	0.45	24.6%	19° C using ASTM C 1064

Table D.5 (continued) – Individual Plastic Concrete Test Results for LC-HPC Bridge Placements

Truck	Air Content	Slump		Concrete Temperature [†]		Unit Weight		Water Withheld		Actual w/c ratio	Actual Paste Content	Notes
		(mm)	(in.)	(°C)	(°F)	(kg/m ³)	(lb/yd ³)	(L/m ³)	(gal/yd ³)			
LC-HPC-1 (105-304) Placement 2, Cast on 11/2/05 (continued)												
5	--	--	--	17.8	64	--	--	0	0	0.45	24.6%	
6	--	--	--	17.5	64	--	--	0	0	0.45	24.6%	
7	--	--	--	17.2	63	--	--	0	0	0.45	24.6%	
8	9.0	90	3.50	18.1	65	2213	138.1	0	0	0.45	24.6%	21° C using ASTM C 1064
9	--	--	--	19.2	67	--	--	0	0	0.45	24.6%	
10	--	--	--	19.7	68	--	--	0	0	0.45	24.6%	
11	--	--	--	19.2	67	--	--	0	0	0.45	24.6%	
12	8.0	65	2.50	18.3	65	2222	138.7	0	0	0.45	24.6%	19° C using ASTM C 1064
13	--	--	--	19.2	67	--	--	0	0	0.45	24.6%	
14	--	--	--	19.2	67	--	--	0	0	0.45	24.6%	
15	--	--	--	18.1	65	--	--	0	0	0.45	24.6%	
16	8.5	100	4.00	21.1	70	2193	136.9	0	0	0.45	24.6%	20° C using ASTM C 1064
17	--	--	--	20.6	69	--	--	0	0	0.45	24.6%	
18	--	--	--	19.4	67	--	--	0	0	0.45	24.6%	
19	--	--	--	19.4	67	--	--	0	0	0.45	24.6%	
20	9.0	90	3.50	18.3	65	2227	139.0	0	0	0.45	24.6%	19° C using ASTM C 1064
21	--	--	--	19.7	68	--	--	0	0	0.45	24.6%	
22	--	--	--	18.3	65	--	--	0	0	0.45	24.6%	
23	--	--	--	19.7	68	--	--	0	0	0.45	24.6%	
24	9.0	70	2.75	19.2	67	2213	138.1	0	0	0.45	24.6%	21° C using ASTM C 1064
25	--	--	--	19.2	67	--	--	0	0	0.45	24.6%	
26	8.5	90	3.50	19.2	67	2193	136.9	0	0	0.45	24.6%	20° C using ASTM C 1064
LC-HPC-2 (105-310), Cast on 11/13/06												
1	7.0	100	4.00	18.9	66	--	--	0	0	0.45	24.6%	18.9° C using ASTM C 1064
2	8.5	95	3.75	20.6	69	--	--	0	0	0.45	24.6%	19.4° C using ASTM C 1064
3	7.2	80	3.25	19.4	67	--	--	0	0	0.45	24.6%	20° C using ASTM C 1064

Table D.5 (continued) – Individual Plastic Concrete Test Results for LC-HPC Bridge Placements

Truck	Air Content	Slump		Concrete Temperature [†]		Unit Weight		Water Withheld		Actual w/c ratio	Actual Paste Content	Notes
		(mm)	(in.)	(°C)	(°F)	(kg/m ³)	(lb/yd ³)	(L/m ³)	(gal/yd ³)			
LC-HPC-2 (105-310), Cast on 11/13/06 (continued)												
4	--	--	--	18.9	66	--	--	0	0	0.45	24.6%	
5	--	--	--	18.9	66	--	--	0	0	0.45	24.6%	
6	--	--	--	18.9	66	--	--	0	0	0.45	24.6%	
7	--	--	--	15.6	60	--	--	0	0	0.45	24.6%	
8	7.2	85	3.25	18.3	65	--	--	0	0	0.45	24.6%	16.1° C using ASTM C 1064
9	--	--	--	17.2	63	--	--	0	0	0.45	24.6%	
10	--	--	--	17.8	64	--	--	0	0	0.45	24.6%	
11	--	--	--	17.2	63	--	--	0	0	0.45	24.6%	
12	--	--	--	17.8	64	--	--	0	0	0.45	24.6%	
13	--	--	--	18.9	66	--	--	0	0	0.45	24.6%	
14	7.5	80	3.25	17.5	64	--	--	0	0	0.45	24.6%	20.6° C using ASTM C 1064
15	--	--	--	17.5	64	--	--	0	0	0.45	24.6%	
16	--	--	--	17.5	64	--	--	0	0	0.45	24.6%	
17	--	--	--	18.3	65	--	--	0	0	0.45	24.6%	
18	8.0	65	2.50	20.3	69	--	--	0	0	0.45	24.6%	18.9° C using ASTM C 1064
19	--	--	--	20.8	70	--	--	0	0	0.45	24.6%	
20	--	--	--	20.0	68	--	--	0	0	0.45	24.6%	
21	--	--	--	19.7	68	--	--	0	0	0.45	24.6%	
22	8.5	35	1.50	18.9	66	--	--	0	0	0.45	24.6%	20.6° C using ASTM C 1064
LC-HPC-3 (46-338), Cast on 11/13/07												
1	9.1	65	2.50	15.0	59	--	--	0	0	0.45	24.4%	Retested - Originally 135 mm slump
2	7.8	45	1.75	13.3	56	--	--	0	0	0.45	24.4%	6% after pump - 1.8% loss
3	8.2	52	2.00	15.6	60	--	--	0	0	0.45	24.4%	
4	--	--	--	16.7	62	--	--	0	0	0.45	24.4%	
5	--	78	3.00	15.0	59	--	--	0	0	0.45	24.4%	

Table D.5 (continued) – Individual Plastic Concrete Test Results for LC-HPC Bridge Placements

Truck	Air Content	Slump		Concrete Temperature [†]		Unit Weight		Water Withheld		Actual w/c ratio	Actual Paste Content	Notes
		(mm)	(in.)	(°C)	(°F)	(kg/m ³)	(lb/yd ³)	(L/m ³)	(gal/yd ³)			
LC-HPC-3 (46-338), Cast on 11/13/07 (continued)												
6	--	--	--	13.9	57	--	--	0	0	0.45	24.4%	
7	9.1	65	2.50	16.1	61	--	--	0	0	0.45	24.4%	
8	--	--	--	11.1	52	--	--	0	0	0.45	24.4%	
9	--	82	3.25	16.1	61	--	--	0	0	0.45	24.4%	
10	--	--	--	12.2	54	--	--	0	0	0.45	24.4%	
11	7.0	71	2.75	15.0	59	--	--	0	0	0.45	24.4%	
12	--	--	--	11.1	52	--	--	0	0	0.45	24.4%	
13	--	70	2.75	15.0	59	--	--	0	0	0.45	24.4%	
14	--	--	--	12.2	54	--	--	0	0	0.45	24.4%	
15	9.2	--	--	12.8	55	--	--	0	0	0.45	24.4%	Retested - Originally 12.0% air & 100 mm slump
16	9.0	--	--	15.6	60	--	--	0	0	0.45	24.4%	
17	--	85	3.25	15.0	59	--	--	0	0	0.45	24.4%	
18	--	--	--	11.7	53	--	--	0	0	0.45	24.4%	
19	6.5	60	2.25	15.0	59	--	--	0	0	0.45	24.4%	
20	--	--	--	11.1	52	--	--	0	0	0.45	24.4%	
21	--	--	--	13.9	57	--	--	0	0	0.45	24.4%	
22	--	--	--	14.4	58	--	--	0	0	0.45	24.4%	
23	9.5	100	4.00	13.3	56	--	--	0	0	0.45	24.4%	8.4% after pump - 1.1% loss
24	--	--	--	14.4	58	--	--	0	0	0.45	24.4%	
25	--	100	4.00	14.4	58	--	--	0	0	0.45	24.4%	
26	--	--	--	15.6	60	--	--	0	0	0.45	24.4%	
27	--	93	3.75	15.0	59	--	--	0	0	0.45	24.4%	Retested - Originally 9% air & 120 mm slump
28	--	--	--	14.4	58	--	--	0	0	0.45	24.4%	
29	--	100	4.00	12.8	55	--	--	0	0	0.45	24.4%	

Table D.5 (continued) – Individual Plastic Concrete Test Results for LC-HPC Bridge Placements

Truck	Air Content	Slump		Concrete Temperature [†]		Unit Weight		Water Withheld		Actual w/c ratio	Actual Paste Content	Notes
		(mm)	(in.)	(°C)	(°F)	(kg/m ³)	(lb/yd ³)	(L/m ³)	(gal/yd ³)			
LC-HPC-3 (46-338), Cast on 11/13/07 (continued)												
30	--	--	--	13.9	57	--	--	0	0	0.45	24.4%	
31	8.0	70	2.75	13.3	56	--	--	0	0	0.45	24.4%	
32	--	--	--	15.0	59	--	--	0	0	0.45	24.4%	
33	--	97	3.75	13.9	57	--	--	0	0	0.45	24.4%	
34	--	--	--	13.3	56	--	--	0	0	0.45	24.4%	
35	7.8	90	3.50	15.6	60	--	--	0	0	0.45	24.4%	
36	--	--	--	16.1	61	--	--	0	0	0.45	24.4%	
37	--	92	3.50	15.6	60	--	--	0	0	0.45	24.4%	Retested - Originally 160 mm slump
38	--	--	--	14.4	58	--	--	0	0	0.45	24.4%	
39	--	100	4.00	15.6	60	--	--	0	0	0.45	24.4%	Retested - Originally 8.2% air & 135 mm slump
40	--	100	4.00	14.4	58	--	--	0	0	0.45	24.4%	
41	--	89	3.50	15.0	59	--	--	0	0	0.45	24.4%	
42	--	--	--	13.3	56	--	--	0	0	0.45	24.4%	
43	9.5	89	3.50	15.6	60	--	--	0	0	0.45	24.4%	
44	--	--	--	14.4	58	--	--	0	0	0.45	24.4%	
45	--	85	3.25	13.9	57	--	--	0	0	0.45	24.4%	
46	--	--	--	15.0	59	--	--	0	0	0.45	24.4%	
47	10.5	82	3.25	15.6	60	--	--	0	0	0.45	24.4%	8.4% after pump - 1.5% loss
48	--	--	--	16.1	61	--	--	0	0	0.45	24.4%	
49	--	88	3.50	14.4	58	--	--	0	0	0.45	24.4%	
50	--	--	--	13.9	57	--	--	0	0	0.45	24.4%	
51	10.0	98	3.75	15.6	60	--	--	0	0	0.45	24.4%	
LC-HPC-4 (46-339) Placement 1, Cast on 9/29/07												
1	7.8	30	1.25	--	--	2226	139.0	0	0	0.42	23.4%	7.0% after pump - 0.8% loss

Table D.5 (continued) – Individual Plastic Concrete Test Results for LC-HPC Bridge Placements

Truck	Air Content	Slump		Concrete Temperature [†]		Unit Weight		Water Withheld		Actual w/c ratio	Actual Paste Content	Notes
		(mm)	(in.)	(°C)	(°F)	(kg/m ³)	(lb/yd ³)	(L/m ³)	(gal/yd ³)			
LC-HPC-4 (46-339) Placement 1, Cast on 9/29/07 (continued)												
2	6.8	20	0.75	--	--	2255	140.8	0	0	0.42	23.4%	
3	10.4	100	4.00	--	--	2142	133.7	0	0	0.42	23.4%	Rejected
4	7.6	55	2.25	--	--	2212	138.1	0	0	0.42	23.4%	MR Added originally 48 mm & 6.8 slump & 2240
5	--	--	--	--	--	--	--	0	0	0.42	23.4%	
6	--	35	1.50	--	--	--	--	0	0	0.42	23.4%	
7	--	--	--	--	--	--	--	0	0	0.42	23.4%	
8	7.4	20	0.75	--	--	2255	140.8	0	0	0.42	23.4%	
9	--	--	--	--	--	--	--	0	0	0.42	23.4%	
10	--	20	0.75	--	--	--	--	0	0	0.42	23.4%	
11	--	--	--	--	--	--	--	0	0	0.42	23.4%	
12	11.4	95	3.75	--	--	2127	132.8	0	0	0.42	23.4%	Rejected
13	--	--	--	--	--	--	--	0	0	0.42	23.4%	
14	--	--	--	--	--	--	--	0	0	0.42	23.4%	
15	--	60	2.25	--	--	--	--	0	0	0.42	23.4%	
16	--	--	--	--	--	--	--	0	0	0.42	23.4%	
17	11.6	105	4.25	--	--	2116	132.1	0	0	0.42	23.4%	Retested - Originally 11.8% air & 120 mm
18	8.8	--	--	--	--	2198	137.2	0	0	0.42	23.4%	
19	10.6	90	3.50	--	--	2150	134.2	0	0	0.42	23.4%	
LC-HPC-4 (46-339) Placement 2, Cast on 10/2/07												
1	8.8	65	2.50	18.3	65	2198	137.2	0	0	0.42	23.4%	6.8% after pump - 2.0% loss
2	7.2	40	1.50	16.7	62	2260	141.1	0	0	0.42	23.4%	
3	7.8	45	1.75	17.2	63	2246	140.2	0	0	0.42	23.4%	
4	--	--	--	--	--	--	--	0	0	0.42	23.4%	
5	--	35	1.50	18.9	66	--	--	0	0	0.42	23.4%	

Table D.5 (continued) – Individual Plastic Concrete Test Results for LC-HPC Bridge Placements

Truck	Air Content	Slump		Concrete Temperature [†]		Unit Weight		Water Withheld		Actual w/c ratio	Actual Paste Content	Notes
		(mm)	(in.)	(°C)	(°F)	(kg/m ³)	(lb/yd ³)	(L/m ³)	(gal/yd ³)			
LC-HPC-4 (46-339) Placement 2, Cast on 10/2/07 (continued)												
6	--	--	--	17.2	63	--	--	0	0	0.42	23.4%	
7	10.4	80	3.25	19.4	67	2164	135.1	0	0	0.42	23.4%	
8	--	--	--	17.8	64	--	--	0	0	0.42	23.4%	
9	--	90	3.50	16.7	62	--	--	0	0	0.42	23.4%	
10	--	--	--	17.8	64	--	--	0	0	0.42	23.4%	
11	9.5	100	4.00	15.0	59	2195	137.0	0	0	0.42	23.4%	
12	--	--	--	16.1	61	--	--	0	0	0.42	23.4%	
13	--	100	4.00	16.7	62	--	--	0	0	0.42	23.4%	
14	--	--	--	16.7	62	--	--	0	0	0.42	23.4%	
15	9.8	90	3.50	16.7	62	2173	135.7	0	0	0.42	23.4%	
16	--	--	--	16.7	62	--	--	0	0	0.42	23.4%	
17	--	55	2.25	16.7	62	--	--	0	0	0.42	23.4%	
18	--	--	--	15.6	60	--	--	0	0	0.42	23.4%	
19	9.6	100	4.00	15.6	60	2187	136.5	0	0	0.42	23.4%	
20	--	--	--	17.2	63	--	--	0	0	0.42	23.4%	
21	--	100	4.00	17.2	63	--	--	0	0	0.42	23.4%	
22	--	--	--	17.8	64	--	--	0	0	0.42	23.4%	
23	8.8	88	3.50	18.3	65	2209	137.9	0	0	0.42	23.4%	
24	--	--	--	17.8	64	--	--	0	0	0.42	23.4%	
25	--	75	3.00	17.8	64	--	--	0	0	0.42	23.4%	
26	--	--	--	20.0	68	--	--	0	0	0.42	23.4%	
27	7.9	95	3.75	18.9	66	2238	139.7	0	0	0.42	23.4%	
28	--	--	--	17.2	63	--	--	0	0	0.42	23.4%	
29	--	--	--	17.2	63	--	--	0	0	0.42	23.4%	

Table D.5 (continued) – Individual Plastic Concrete Test Results for LC-HPC Bridge Placements

Truck	Air Content	Slump		Concrete Temperature [†]		Unit Weight		Water Withheld		Actual w/c ratio	Actual Paste Content	Notes
		(mm)	(in.)	(°C)	(°F)	(kg/m ³)	(lb/yd ³)	(L/m ³)	(gal/yd ³)			
LC-HPC-4 (46-339) Placement 2, Cast on 10/2/07 (continued)												
30	--	100	4.00	17.8	64	--	--	0	0	0.42	23.4%	
31	9.3	90	3.50	18.9	66	2198	137.2	0	0	0.42	23.4%	
32	--	--	--	18.3	65	--	--	0	0	0.42	23.4%	
33	--	95	3.75	15.6	60	--	--	0	0	0.42	23.4%	
34	--	--	--	18.3	65	--	--	0	0	0.42	23.4%	
35	8.0	35	1.50	21.7	71	2240	139.8	0	0	0.42	23.4%	
LC-HPC-5 (46-340 Unit 1), Cast on 11/14/07												
1	8.0	70	2.75	17.8	64	2263	141.3	0	0	0.42	23.4%	Out of Pump: 7.4% air, 60 mm slump
2	7.0	92	3.50	15.0	59	2294	143.2	0	0	0.42	23.4%	
3	9.5	75	3.00	16.1	61	2201	137.4	0	0	0.42	23.4%	
4	--	--	--	--	62	--	--	0	0	0.42	23.4%	
5	--	60	2.25	17.2	63	--	--	0	0	0.42	23.4%	
6	--	--	--	--	61	--	--	0	0	0.42	23.4%	
7	8.7	50	2.00	17.8	64	2238	139.7	0	0	0.42	23.4%	
8	--	--	--	--	62	--	--	+2.48	+0.5	0.43	23.6%	
9	--	65	2.50	16.1	61	--	--	+2.48	+0.5	0.43	23.6%	
10	--	--	--	--	64	--	--	+2.48	+0.5	0.43	23.6%	
11	9.0	60	2.25	17.2	63	2246	140.2	+2.48	+0.5	0.43	23.6%	
12	--	--	--	--	61	--	--	+2.48	+0.5	0.43	23.6%	
13	--	60	2.25	16.7	62	--	--	+2.48	+0.5	0.43	23.6%	
14	--	--	--	--	57	--	--	+2.48	+0.5	0.43	23.6%	
15	--	60	2.25	16.7	62	--	--	+2.48	+0.5	0.43	23.6%	
16	8.5	65	2.50	15.6	60	2257	140.9	0	0	0.43	23.7%	
17	--	100	4.00	14.4	58	--	--	0	0	0.43	23.7%	

Table D.5 (continued) – Individual Plastic Concrete Test Results for LC-HPC Bridge Placements

Truck	Air Content	Slump		Concrete Temperature [†]		Unit Weight		Water Withheld		Actual w/c ratio	Actual Paste Content	Notes
		(mm)	(in.)	(°C)	(°F)	(kg/m ³)	(lb/yd ³)	(L/m ³)	(gal/yd ³)			
LC-HPC-5 (46-340 Unit 1), Cast on 11/14/07 (continued)												
18	--	--	--	--	58	--	--	0	0	0.43	23.7%	
19	10.3	100	4.00	16.1	61	2192	136.8	0	0	0.43	23.7%	
20	--	--	--	--	59	--	--	0	0	0.43	23.7%	
21	8.5	100	4.00	16.1	61	2240	139.8	0	0	0.43	23.7%	Retested: original slump 140 mm
22	--	95	3.75	16.1	61	--	--	0	0	0.43	23.7%	
23	--	--	--	--	57	--	--	0	0	0.43	23.7%	
24	--	--	--	--	59	--	--	0	0	0.43	23.7%	
25	--	65	2.50	16.1	61	--	--	0	0	0.45	24.4%	
26	--	--	--	--	57	--	--	0	0	0.45	24.4%	
27	6.8	60	2.25	16.1	61	2277	142.1	0	0	0.45	24.4%	
28	--	--	--	--	59	--	--	0	0	0.45	24.4%	
29	--	80	3.25	16.7	62	--	--	0	0	0.45	24.4%	
30	--	--	--	--	61	--	--	0	0	0.45	24.4%	
31	9.0	100	4.00	16.7	62	2221	138.6	0	0	0.45	24.4%	
32	--	--	--	--	59	--	--	0	0	0.45	24.4%	
33	--	80	3.25	13.9	57	--	--	0	0	0.45	24.4%	
34	--	--	--	--	60	--	--	0	0	0.45	24.4%	
35	8.8	75	3.00	16.1	61	2238	139.7	0	0	0.45	24.4%	
36	--	--	--	--	60	--	--	0	0	0.45	24.4%	
37	--	95	3.75	16.1	61	--	--	0	0	0.45	24.4%	
38	--	--	--	--	59	--	--	0	0	0.45	24.4%	
39	9.0	85	3.25	15.6	60	2215	138.3	0	0	0.45	24.4%	
40	--	--	--	--	58	--	--	0	0	0.45	24.4%	
41	--	95	3.75	16.1	61	--	--	0	0	0.45	24.4%	

Table D.5 (continued) – Individual Plastic Concrete Test Results for LC-HPC Bridge Placements

Truck	Air Content	Slump		Concrete Temperature [†]		Unit Weight		Water Withheld		Actual w/c ratio	Actual Paste Content	Notes
		(mm)	(in.)	(°C)	(°F)	(kg/m ³)	(lb/yd ³)	(L/m ³)	(gal/yd ³)			
LC-HPC-5 (46-340 Unit 1), Cast on 11/14/07 (continued)												
42	--	--	--	--	62	--	--	0	0	0.45	24.4%	
43	8.5	80	3.25	14.4	58	2238	139.7	0	0	0.45	24.4%	
44	--	--	--	--	59	--	--	0	0	0.45	24.4%	
45	--	75	3.00	16.7	62	--	--	0	0	0.45	24.4%	
46	--	--	--	--	60	--	--	0	0	0.45	24.4%	
47	10.2	85	3.25	17.2	63	2181	136.1	0	0	0.45	24.4%	
48	--	75	3.00	17.2	63	--	--	0	0	0.45	24.4%	
LC-HPC-6 (46-340 Unit 2), Cast on 11/3/07												
1	9.9	105	4.25	12.8	55	--	--	0	0	0.45	24.4%	
2	11.5	120	4.75	11.1	52	--	--	0	0	0.45	24.4%	
3	--	--	--	11.7	53	--	--	0	0	0.45	24.4%	
4	--	--	--	12.2	54	--	--	0	0	0.45	24.4%	
5	--	80	3.25	15.6	60	--	--	0	0	0.45	24.4%	
6	--	--	--	12.8	55	--	--	0	0	0.45	24.4%	
7	8.4	75	3.00	13.3	56	--	--	0	0	0.45	24.4%	7.0% after pump - 1.4% loss
8	--	--	--	12.8	55	--	--	0	0	0.45	24.4%	
9	--	60	2.25	12.8	55	--	--	0	0	0.45	24.4%	
10	--	--	--	14.4	58	--	--	0	0	0.45	24.4%	
11	9.1	70	2.75	13.9	57	--	--	0	0	0.45	24.4%	
12	--	--	--	14.4	58	--	--	0	0	0.45	24.4%	
13	--	70	2.75	15.6	60	--	--	0	0	0.45	24.4%	
14	--	--	--	15.0	59	--	--	0	0	0.45	24.4%	
15	10.5	100	4.00	14.4	58	--	--	0	0	0.45	24.4%	
16	--	--	--	15.6	60	--	--	0	0	0.45	24.4%	

Table D.5 (continued) – Individual Plastic Concrete Test Results for LC-HPC Bridge Placements

Truck	Air Content	Slump		Concrete Temperature [†]		Unit Weight		Water Withheld		Actual w/c ratio	Actual Paste Content	Notes
		(mm)	(in.)	(°C)	(°F)	(kg/m ³)	(lb/yd ³)	(L/m ³)	(gal/yd ³)			
LC-HPC-6 (46-340 Unit 2), Cast on 11/3/07 (Continued)												
17	--	105	4.25	12.2	54	--	--	0	0	0.45	24.4%	
18	--	--	--	16.1	61	--	--	0	0	0.45	24.4%	
19	10.2	105	4.25	16.1	61	--	--	0	0	0.45	24.4%	
20	--	--	--	15.6	60	--	--	0	0	0.45	24.4%	
21	--	80	3.25	16.7	62	--	--	0	0	0.45	24.4%	
22	--	--	--	15.6	60	--	--	0	0	0.45	24.4%	
23	7.5	90	3.50	16.7	62	--	--	0	0	0.45	24.4%	
24	--	--	--	16.7	62	--	--	0	0	0.45	24.4%	
25	--	110	4.25	17.2	63	--	--	0	0	0.45	24.4%	
26	--	--	--	16.1	61	--	--	0	0	0.45	24.4%	
27	9.3	80	3.25	15.6	60	--	--	0	0	0.45	24.4%	
28	--	--	--	16.7	62	--	--	0	0	0.45	24.4%	
29	--	105	4.25	17.2	63	--	--	0	0	0.45	24.4%	
30	--	--	--	16.7	62	--	--	0	0	0.45	24.4%	
31	10.1	100	4.00	16.1	61	--	--	0	0	0.45	24.4%	
32	--	--	--	16.7	62	--	--	0	0	0.45	24.4%	
33	--	105	4.25	15.6	60	--	--	0	0	0.45	24.4%	
34	--	--	--	16.1	61	--	--	0	0	0.45	24.4%	
35	10.5	125	5.00	16.1	61	--	--	0	0	0.45	24.4%	
36	--	--	--	15.0	59	--	--	0	0	0.45	24.4%	
37	--	120	4.75	16.7	62	--	--	0	0	0.45	24.4%	
38	--	--	--	15.6	60	--	--	0	0	0.45	24.4%	
39	12.5	130	5.00	16.7	62	--	--	0	0	0.45	24.4%	Rejected
40	8.4	90	3.50	16.1	61	--	--	0	0	0.45	24.4%	

Table D.5 (continued) – Individual Plastic Concrete Test Results for LC-HPC Bridge Placements

Truck	Air Content	Slump		Concrete Temperature [†]		Unit Weight		Water Withheld		Actual w/c ratio	Actual Paste Content	Notes
		(mm)	(in.)	(°C)	(°F)	(kg/m ³)	(lb/yd ³)	(L/m ³)	(gal/yd ³)			
LC-HPC-6 (46-340 Unit 2), Cast on 11/3/07 (Continued)												
41	--	140	5.50	15.0	59	--	--	0	0	0.45	24.4%	
42	--	--	--	16.1	61	--	--	0	0	0.45	24.4%	
43	9.6	85	3.25	15.6	60	--	--	0	0	0.45	24.4%	9.0% after pump - 0.6% loss
44	--	--	--	16.1	61	--	--	0	0	0.45	24.4%	
45	--	105	4.25	15.6	60	--	--	0	0	0.45	24.4%	
46	--	--	--	16.1	61	--	--	0	0	0.45	24.4%	
47	8.5	95	3.75	16.7	62	--	--	0	0	0.45	24.4%	
48	--	--	--	16.1	61	--	--	0	0	0.45	24.4%	
49	--	95	3.75	16.7	62	--	--	0	0	0.45	24.4%	
50	--	--	--	16.7	62	--	--	0	0	0.45	24.4%	
51	--	95	3.75	17.2	63	--	--	0	0	0.45	24.4%	
52	--	--	--	17.8	64	--	--	0	0	0.45	24.4%	
LC-HPC-7 (43-33), Cast on 6/24/06												
--	7.5	70	2.75	22.8	73	2292	143.1	0	0	0.45	24.6%	
--	9.0	100	4.00	23.9	75	2174	135.7	0	0	0.45	24.6%	
--	8.0	125	5.00	23.9	75	2177	135.9	0	0	0.45	24.6%	
--	7.5	135	5.25	22.8	73	2212	138.1	0	0	0.45	24.6%	
--	6.5	65	2.50	22.8	73	2245	140.1	0	0	0.45	24.6%	
--	--	75	3.00	23.3	74	--	--	0	0	0.45	24.6%	
--	6.5	70	2.75	21.7	71	2274	142.0	0	0	0.45	24.6%	
--	--	90	3.50	22.8	73	--	--	0	0	0.45	24.6%	
--	8.5	90	3.50	21.7	71	2224	138.8	0	0	0.45	24.6%	
--	--	65	2.50	22.2	72	--	--	0	0	0.45	24.6%	
--	8.5	100	4.00	22.2	72	2214	138.2	0	0	0.45	24.6%	

Table D.5 (continued) – Individual Plastic Concrete Test Results for LC-HPC Bridge Placements

Truck	Air Content	Slump		Concrete Temperature [†]		Unit Weight		Water Withheld		Actual w/c ratio	Actual Paste Content	Notes
		(mm)	(in.)	(°C)	(°F)	(kg/m ³)	(lb/yd ³)	(L/m ³)	(gal/yd ³)			
LC-HPC-7 (43-33), Cast on 6/24/06 (Continued)												
--	--	65	2.50	20.6	69	--	--	0	0	0.45	24.6%	
--	8.5	100	4.00	20.6	69	2205	137.6	0	0	0.45	24.6%	
--	--	100	4.00	21.7	71	--	--	0	0	0.45	24.6%	
--	8.5	150	6.00	21.1	70	2199	137.3	0	0	0.45	24.6%	
--	--	65	2.50	22.8	73	--	--	0	0	0.45	24.6%	
--	7.0	65	2.50	22.8	73	2279	142.3	0	0	0.45	24.6%	
--	--	55	2.25	20.6	69	--	--	0	0	0.45	24.6%	
--	9.0	100	4.00	20.6	69	2199	137.3	0	0	0.45	24.6%	
--	--	100	4.00	21.7	71	--	--	0	0	0.45	24.6%	
--	--	100	4.00	21.1	70	--	--	0	0	0.45	24.6%	
--	10.5	135	5.25	20.0	68	2148	134.1	0	0	0.45	24.6%	
--	7.0	150	6.00	20.6	69	2250	140.5	0	0	0.45	24.6%	
LC-HPC-8 (54-53), Cast on 10/3/07												
1	7.5	70	2.75	15.0	59	2257	140.9	9.90	2.00	0.39	22.6%	8.1% air before the pump - 0.6% loss
2	6.9	45	1.75	17.8	64	2270	141.7	9.90	2.00	0.39	22.6%	
3	5.7	40	1.50	17.2	63	2308	144.1	9.90	2.00	0.39	22.6%	
4	--	--	--	--	--	--	--	9.90	2.00	0.39	22.6%	
5	9.0	50	2.00	15.6	60	2241	139.9	9.90	2.00	0.39	22.6%	Held at Truck - 7.7% air when pumped
6	--	--	--	--	--	--	--	9.90	2.00	0.39	22.6%	
7	7.7	55	2.25	15.6	60	2275	142.0	9.90	2.00	0.39	22.6%	
8	--	--	--	--	--	--	--	9.90	2.00	0.39	22.6%	
9	7.3	45	1.75	20.6	69	2275	142.0	9.90	2.00	0.39	22.6%	
10	--	--	--	--	--	--	--	9.90	2.00	0.39	22.6%	
11	7.7	45	1.75	18.9	66	2277	142.1	9.90	2.00	0.39	22.6%	

Table D.5 (continued) – Individual Plastic Concrete Test Results for LC-HPC Bridge Placements

Truck	Air Content	Slump		Concrete Temperature [†]		Unit Weight		Water Withheld		Actual w/c ratio	Actual Paste Content	Notes
		(mm)	(in.)	(°C)	(°F)	(kg/m ³)	(lb/yd ³)	(L/m ³)	(gal/yd ³)			
LC-HPC-8 (54-53), Cast on 10/3/07 (Continued)												
12	--	--	--	--	--	--	--	9.90	2.00	0.39	22.6%	
13	9.0	45	1.75	17.8	64	2227	139.0	9.90	2.00	0.39	22.6%	
14	--	--	--	--	--	--	--	7.43	1.50	0.40	22.8%	
15	8.2	50	2.00	21.1	70	2279	142.3	7.43	1.50	0.40	22.8%	
16	--	--	--	--	--	--	--	7.43	1.50	0.40	22.8%	
17	9.0	60	2.25	18.3	65	2240	139.8	4.95	1.00	0.40	23.0%	
18	--	--	--	--	--	--	--	4.95	1.00	0.40	23.0%	
19	8.7	40	1.50	18.9	66	2258	141.0	7.43	1.50	0.40	22.8%	
20	--	--	--	--	--	--	--	7.43	1.50	0.40	22.8%	
21	8.2	40	1.50	20.6	69	2266	141.5	7.43	1.50	0.40	23.0%	
22	--	--	--	--	--	--	--	4.95	1.00	0.40	23.0%	
23	8.2	50	2.00	22.2	72	2254	140.7	4.95	1.00	0.40	23.0%	
24	--	--	--	--	--	--	--	4.95	1.00	0.40	23.0%	
25	8.7	65	2.50	20.6	69	2242	140.0	4.95	1.00	0.40	23.0%	
26	--	--	--	--	--	--	--	4.95	1.00	0.40	23.0%	
27	7.0	40	1.50	20.0	68	2286	142.7	4.95	1.00	0.40	23.0%	
28	--	--	--	--	--	--	--	4.95	1.00	0.40	23.0%	
29	7.2	40	1.50	20.6	69	2292	143.1	4.95	1.00	0.40	23.0%	
30	--	--	--	--	--	--	--	4.95	1.00	0.40	23.0%	
31	7.2	40	1.50	21.7	71	2283	142.5	4.95	1.00	0.40	23.0%	
32	--	--	--	--	--	--	--	4.95	1.00	0.40	23.0%	
33	7.9	35	1.50	20.6	69	2267	141.5	4.95	1.00	0.40	23.0%	
34	--	--	--	--	--	--	--	4.95	1.00	0.40	23.0%	
35	6.9	55	2.25	22.2	72	2295	143.3	2.48	0.50	0.41	23.2%	

Table D.5 (continued) – Individual Plastic Concrete Test Results for LC-HPC Bridge Placements

Truck	Air Content	Slump		Concrete Temperature [†]		Unit Weight		Water Withheld		Actual w/c ratio	Actual Paste Content	Notes
		(mm)	(in.)	(°C)	(°F)	(kg/m ³)	(lb/yd ³)	(L/m ³)	(gal/yd ³)			
LC-HPC-8 (54-53), Cast on 10/3/07 (Continued)												
36	--	--	--	--	--	--	--	2.48	0.50	0.41	23.2%	
37	9.8	70	2.75	21.7	71	2217	138.4	4.95	1.00	0.40	23.0%	Tested out of the Truck
38	8.2	--	--	--	66	--	--	4.95	1.00	0.40	23.0%	Tested out of the Truck
39	--	--	--	--	--	--	--	4.95	1.00	0.40	23.0%	
40	--	75	3.00	21.7	71	--	--	4.95	1.00	0.40	23.0%	
41	8.8	65	2.50	18.9	66	2247	140.3	4.95	1.00	0.40	23.0%	
42	--	--	--	--	--	--	--	4.95	1.00	0.40	23.0%	
43	--	--	--	--	--	--	--	4.95	1.00	0.40	23.0%	
44	--	--	--	--	--	--	--	4.95	1.00	0.40	23.0%	
45	--	--	--	--	--	--	--	2.48	0.50	0.41	23.2%	
46	6.2	25	1.00	22.8	73	2321	144.9	2.48	0.50	0.41	23.2%	
47	--	85	3.25	19.4	67	--	--	1.86	0.38	0.41	23.2%	Tested out of the Truck
48	8.2	55	2.25	19.4	67	2242	140.0	3.71	0.75	0.41	23.1%	
49	--	--	--	--	--	--	--	2.48	0.50	0.41	23.2%	
50	7.7	70	2.75	20.0	68	2265	141.4	2.48	0.50	0.41	23.2%	
51	--	--	--	--	--	--	--	2.48	0.50	0.41	23.2%	
52	--	--	--	--	--	--	--	2.48	0.50	0.41	23.2%	
53	10.2	75	3.00	17.8	64	2194	137.0	2.48	0.50	0.41	23.2%	
54	--	--	--	--	--	--	--	2.48	0.50	0.41	23.2%	
55	9.7	--	--	17.2	63	2221	138.6	2.48	0.50	0.41	23.2%	
56	--	--	--	--	--	--	--	2.48	0.50	0.41	23.2%	
LC-HPC-10 (54-60), Cast on 5/17/07												
1	5.5	70	2.75	16.1	61	2261.6	141.2	0.00	0.00	0.42	23.4%	
2	4.9	55	2.25	18.3	65	2275.7	142.1	0.00	0.00	0.42	23.4%	Added Air and Retested

Table D.5 (continued) – Individual Plastic Concrete Test Results for LC-HPC Bridge Placements

Truck	Air Content	Slump		Concrete Temperature [†]		Unit Weight		Water Withheld		Actual w/c ratio	Actual Paste Content	Notes
		(mm)	(in.)	(°C)	(°F)	(kg/m ³)	(lb/yd ³)	(L/m ³)	(gal/yd ³)			
LC-HPC-10 (54-60), Cast on 5/17/07 (Continued)												
2R	5.1	45	1.75	18.1	65	2275.7	142.1	--	--	--	--	
3	11.1	125	5.00	15.6	60	--	--	0.00	0.00	0.42	23.4%	Sat our for 20 min.
3R	7.7	95	3.75	15.6	60	--	--	--	--	--	--	
4	7.2	95	3.75	18.3	65	2205	137.6	0.62	0.13	0.42	23.3%	
5	--	85	3.25	18.3	65	--	--	0.00	0.00	0.42	23.4%	
6	--	--	--	--	--	--	--	1.86	0.38	0.41	23.2%	
7	6.1	100	4.00	18.3	65	2233	139.4	1.86	0.38	0.41	23.2%	
8	--	--	--	--	--	--	--	4.95	1.00	0.40	23.0%	
9	--	55	2.25	17.5	64	--	--	0.00	0.00	0.42	23.4%	
10	--	--	--	--	--	--	--	0.00	0.00	0.42	23.4%	
11	6.5	65	2.50	19.8	68	2247	140.3	0.00	0.00	0.42	23.4%	
12	--	--	--	--	--	--	--	1.24	0.25	0.42	23.3%	
13	--	--	--	--	--	--	--	1.24	0.25	0.42	23.3%	
14	--	--	--	--	--	--	--	1.24	0.25	0.42	23.3%	
15	6.7	70	2.75	18.9	66	2219	138.5	1.86	0.38	0.41	23.2%	
16	--	60	2.25	18.3	65	--	--	1.86	0.38	0.41	23.2%	
17	7.7	90	3.50	18.3	65	2191	136.8	1.86	0.38	0.41	23.2%	
18	6.3	80	3.25	18.3	65	2233	139.4	1.86	0.38	0.41	23.2%	
19	--	75	3.00	18.3	65	--	--	1.86	0.38	0.41	23.2%	
20	7.7	75	3.00	18.3	65	2191	136.8	0.62	0.13	0.42	23.3%	
21	--	--	--	--	--	--	--	0.00	0.00	0.42	23.4%	
22	--	--	--	--	--	--	--	0.00	0.00	0.42	23.4%	
23	--	85	3.25	18.9	66	--	--	2.48	0.50	0.41	23.2%	
24	--	--	--	--	--	--	--	2.48	0.50	0.41	23.2%	

Table D.5 (continued) – Individual Plastic Concrete Test Results for LC-HPC Bridge Placements

Truck	Air Content	Slump		Concrete Temperature [†]		Unit Weight		Water Withheld		Actual w/c ratio	Actual Paste Content	Notes
		(mm)	(in.)	(°C)	(°F)	(kg/m ³)	(lb/yd ³)	(L/m ³)	(gal/yd ³)			
LC-HPC-10 (54-60), Cast on 5/17/07 (Continued)												
25	7.7	80	3.25	18.3	65	2191	136.8	4.33	0.88	0.41	23.0%	
26	--	--	--	--	--	--	--	4.33	0.88	0.41	23.0%	
27	--	80	3.25	17.8	64	--	--	4.95	1.00	0.40	23.0%	
28	--	--	--	--	--	--	--	3.71	0.75	0.41	23.1%	
29	7.7	90	3.50	18.3	65	2205	137.6	3.09	0.63	0.41	23.1%	
30	--	--	--	--	--	--	--	1.24	0.25	0.42	23.3%	
31	--	100	4.00	--	--	--	--	2.48	0.50	0.41	23.2%	
32	--	--	--	--	--	--	--	4.33	0.88	0.41	23.0%	
33	7.5	80	3.25	18.3	65	2205	137.6	5.57	1.13	0.42	23.3%	
34	--	--	--	--	--	--	--	5.57	1.13	0.42	23.3%	
35	--	75	3.00	18.3	65	--	--	3.71	0.75	0.41	23.1%	
36	--	--	--	--	--	--	--	5.57	1.13	0.42	23.3%	
37	9.2	125	5.00	18.3	65	2149	134.2	5.57	1.13	0.42	23.3%	Held 15 minutes and then used
38	--	--	--	--	--	--	--	3.71	0.75	0.41	23.1%	
39	8.5	85	3.25	18.3	65	2177	135.9	3.09	0.63	0.41	23.1%	
40	--	90	3.50	17.2	63	--	--	2.48	0.50	0.41	23.2%	
41	--	--	--	--	--	--	--	1.86	0.38	0.41	23.2%	
42	7.8	75	3.00	18.9	66	2205	137.6	3.71	0.75	0.41	23.1%	
43	--	--	--	--	--	--	--	3.09	0.63	0.41	23.1%	
44	8.2	75	3.00	19.4	67	2219	138.5	3.71	0.75	0.41	23.1%	
45	--	--	--	--	--	--	--	3.09	0.63	0.41	23.1%	
46	7.3	55	2.25	20.6	69	2205	137.6	3.09	0.63	0.41	23.1%	
47	--	--	--	--	--	--	--	2.48	0.50	0.41	23.2%	
48	--	105	4.25	21.1	70	--	--	0.62	0.13	0.42	23.3%	

Table D.5 (continued) – Individual Plastic Concrete Test Results for LC-HPC Bridge Placements

Truck	Air Content	Slump		Concrete Temperature†		Unit Weight		Water Withheld		Actual w/c ratio	Actual Paste Content	Notes
		(mm)	(in.)	(°C)	(°F)	(kg/m ³)	(lb/yd ³)	(L/m ³)	(gal/yd ³)			
LC-HPC-10 (54-60), Cast on 5/17/07 (Continued)												
49	--	--	--	--	--	--	--	0.00	0.00	0.42	23.4%	
50	7.7	85	3.25	21.1	70	2205	137.6	1.86	0.38	0.41	23.2%	
51	--	--	--	--	--	--	--	1.86	0.38	0.41	23.2%	
52	--	--	--	--	--	--	--	4.33	0.88	0.41	23.0%	
53	--	--	--	--	--	--	--	1.86	0.38	0.41	23.2%	
54	--	--	--	--	--	--	--	3.71	0.75	0.41	23.1%	
55	--	--	--	--	--	--	--	3.09	0.63	0.41	23.1%	
56	--	--	--	--	--	--	--	3.09	0.63	0.41	23.1%	
57	--	--	--	--	--	--	--	2.48	0.50	0.41	23.2%	
58	--	--	--	--	--	--	--	0.62	0.13	0.42	23.3%	
59	--	90	3.50	22.2	72	--	--	2.48	0.50	0.41	23.2%	
LC-HPC-11 (78-119), Cast on 6/9/07												
1	7.0	55	2.25	15.4	60	2300	143.6	0	0	0.42	23.3%	
2	7.6	75	3.00	14.7	59	2269	141.6	+2.48	+0.5	0.43	23.7%	
3	6.0	60	2.25	15.6	60	2317	144.6	+2.48	+0.5	0.43	23.7%	
4	5.4	45	1.75	16.3	61	2356	147.1	+2.48	+0.5	0.43	23.7%	Rejected
5	6.8	70	2.75	14.9	59	2303	143.8	+4.96	+1.0	0.44	23.7%	
6	--	--	--	--	--	--	--	0	0	0.42	23.3%	
7	7.0	100	4.00	15.0	59	2311	144.3	0	0	0.42	23.3%	
8	--	--	--	--	--	--	--	0	0	0.42	23.3%	
9	7.8	75	3.00	16.0	61	2269	141.6	0	0	0.42	23.3%	
10	--	--	--	--	--	--	--	0	0	0.42	23.3%	
11	8.6	140	5.50	15.4	60	2249	140.4	0	0	0.42	23.3%	
11	--	120	4.75	--	--	--	--	0	0	0.42	23.3%	

Table D.5 (continued) – Individual Plastic Concrete Test Results for LC-HPC Bridge Placements

Truck	Air Content	Slump		Concrete Temperature [†]		Unit Weight		Water Withheld		Actual w/c ratio	Actual Paste Content	Notes
		(mm)	(in.)	(°C)	(°F)	(kg/m ³)	(lb/yd ³)	(L/m ³)	(gal/yd ³)			
LC-HPC-11 (78-119), Cast on 6/9/07 (Continued)												
11	--	100	4.00	--	--	--	--	0	0	0.42	23.3%	
12	--	--	--	--	--	--	--	0	0	0.42	23.3%	
13	8.5	60	2.25	15.5	60	2266	141.5	0	0	0.42	23.3%	
14	--	--	--	--	--	--	--	0	0	0.42	23.3%	
15	7.8	60	2.25	17.1	63	2280	142.3	0	0	0.42	23.3%	
16	--	--	--	--	--	--	--	0	0	0.42	23.3%	
17	8.4	95	3.75	15.6	60	2255	140.8	0	0	0.42	23.3%	
18	--	--	--	--	--	--	--	0	0	0.42	23.3%	
19	9.0	100	4.00	15.4	60	2235	139.5	0	0	0.42	23.3%	6.6% after conveyor - 2.4% loss
20	--	--	--	--	--	--	--	0	0	0.42	23.3%	
21	9.2	100	4.00	17.0	63	2238	139.7	0	0	0.42	23.3%	
22	--	--	--	--	--	--	--	0	0	0.42	23.3%	
23	--	80	3.25	18.0	64	2294	143.2	0	0	0.42	23.3%	
23	7.5	--	--	--	--	2305	143.9	0	0	0.42	23.3%	Retested after 25 minutes
LC-HPC-12 (78-119), Cast on 4/4/08												
1	6.1	40	1.5	13.3	56	2292	143.1	--	--	0.42	23.6%	Initially a 0.42 w/c ratio
1	6.2	45	1.75	--	--	2299	143.5	--	--	0.44	24.3%	Water added to bring up to 0.44 w/c ratio
2	5.7	40	1.5	13.9	57	2302	143.7	0	0	0.44	24.3%	
2	6.8	45	1.75	--	--	2289	142.9	0	0	0.44	24.3%	MRWR added and retested
3	8.1	85	3.25	13.1	56	2251	140.5	0	0	0.44	24.3%	
4	7.3	70	2.75	13.6	56	2270	141.7	0	0	0.44	24.3%	
5	--	--	--	13.6	57	--	--	0	0	0.44	24.3%	
6	7.9	65	2.5	12.3	54	2251	140.5	0	0	0.44	24.3%	
7	--	--	--	13.8	57	--	--	0	0	0.44	24.3%	

Table D.5 (continued) – Individual Plastic Concrete Test Results for LC-HPC Bridge Placements

Truck	Air Content	Slump		Concrete Temperature [†]		Unit Weight		Water Withheld		Actual w/c ratio	Actual Paste Content	Notes
		(mm)	(in.)	(°C)	(°F)	(kg/m ³)	(lb/yd ³)	(L/m ³)	(gal/yd ³)			
LC-HPC-12 (78-119), Cast on 4/4/08 (Continued)												
8	--	65	2.5	13.9	57	--	--	0	0	0.44	24.3%	
9	7.2	70	2.75	11.9	53	2257	140.9	0	0	0.44	24.3%	
10	--	85	3.25	14.1	57	--	--	0	0	0.44	24.3%	
11	--	85	3.25	13.9	57	--	--	0	0	0.44	24.3%	
12	--	--	--	14.1	57	--	--	0	0	0.44	24.3%	
13	7.6	75	3	14.6	58	2251	140.5	0	0	0.44	24.3%	
14	--	--	--	14.7	59	--	--	0	0	0.44	24.3%	
15	--	70	2.75	13.8	57	--	--	0	0	0.44	24.3%	
16	7.9	85	3.25	15.4	60	2241	139.9	0	0	0.44	24.3%	
17	--	--	--	14.2	58	--	--	0	0	0.44	24.3%	
18	--	--	--	14.5	58	--	--	0	0	0.44	24.3%	
19	--	70	2.75	14.7	58	--	--	0	0	0.44	24.3%	
20	--	--	--	14.4	58	--	--	0	0	0.44	24.3%	
21	8.0	90	3.5	14.9	59	2235	139.5	0	0	0.44	24.3%	
22	--	--	--	14.8	59	--	--	0	0	0.44	24.3%	
23	--	75	3	16.0	61	--	--	0	0	0.44	24.3%	
24	--	--	--	16.0	61	--	--	0	0	0.44	24.3%	
25	7.4	70	2.75	15.6	60	2251	140.5	0	0	0.44	24.3%	
26	--	--	--	15.9	61	--	--	0	0	0.44	24.3%	
27	--	--	--	19.6	67	--	--	0	0	0.44	24.3%	
28	--	--	--	16.0	61	--	--	0	0	0.44	24.3%	
LC-HPC-13 (54-66), Cast on 4/29/08												
1	8.3	75	3.00	15.9	61	2257	140.9	7.43	1.5	0.41	23.4%	
1	7.5	85	3.25	--	--	--	--	--	--	--	--	Taken after the pump - 0.8% loss

Table D.5 (continued) – Individual Plastic Concrete Test Results for LC-HPC Bridge Placements

Truck	Air Content	Slump		Concrete Temperature [†]		Unit Weight		Water Withheld		Actual w/c ratio	Actual Paste Content	Notes
		(mm)	(in.)	(°C)	(°F)	(kg/m ³)	(lb/yd ³)	(L/m ³)	(gal/yd ³)			
LC-HPC-13 (54-66), Cast on 4/29/08 (Continued)												
2	11.0	100	4.00	16.4	62	2192	136.8	0	0	0.44	24.0%	AEA added at the truck
2	9.0	75	3.00	--	--	--	--	0	0	0.44	24.0%	Taken after the pump - 2.0% loss
3	10.0	100	4.00	16.9	62	2180	136.1	0	0	0.44	24.0%	
3	9.5	75	3.00	19.0	66	2232	139.3	0	0	0.44	24.0%	Taken after the pump - 0.5% loss
4	--	--	--	--	--	--	--	0	0	0.44	24.0%	
5	--	55	2.25	20.0	68	--	--	0	0	0.44	24.0%	
8	6.8	50	2.00	21.1	70	2289	142.9	0	0	0.44	24.0%	
9	--	75	3.00	--	--	--	--	0	0	0.44	24.0%	
12	7.0	75	3.00	20.0	68	2303	143.8	0	0	0.44	24.0%	
14	7.3	95	3.75	21.1	70	2294	143.2	0	0	0.44	24.0%	
16	--	65	2.50	21.6	71	--	--	0	0	0.44	24.0%	
18	8.0	100	4.00	21.4	71	2260	141.1	0	0	0.44	24.0%	
20	--	100	4.00	21.2	70	--	--	0	0	0.44	24.0%	
22	6.8	45	1.75	21.4	71	2317	144.6	0	0	0.44	24.0%	
24	--	65	2.50	22.1	72	--	--	0	0	0.44	24.0%	
26	7.0	65	2.50	20.8	70	2294	143.2	0	0	0.44	24.0%	
28		50	2.00	21.8	71	--	--	0	0	0.44	24.0%	
30	7.7	75	3.00	21.3	70	2289	142.9	0	0	0.44	24.0%	
32		65	2.50	20.9	70	--	--	0	0	0.44	24.0%	
34	8.7	70	2.75	21.3	70	2255	140.8	0	0	0.44	24.0%	
36		100	4.00	20.4	69	--	--	0	0	0.44	24.0%	
38	9.2	110	4.25	20.6	69	2195	137.0	0	0	0.44	24.0%	
40		100	4.00	21.3	70	--	--	0	0	0.44	24.0%	
42	9.2	75	3.00	20.8	69	2221	138.6	0	0	0.44	24.0%	

Table D.5 (continued) – Individual Plastic Concrete Test Results for LC-HPC Bridge Placements

Truck	Air Content	Slump		Concrete Temperature [†]		Unit Weight		Water Withheld		Actual w/c ratio	Actual Paste Content	Notes
		(mm)	(in.)	(°C)	(°F)	(kg/m ³)	(lb/yd ³)	(L/m ³)	(gal/yd ³)			
LC-HPC-13 (54-66), Cast on 4/29/08 (Continued)												
44		125	5.00	20.4	69	--	--	0	0	0.44	24.0%	
45		70	2.75	--	--	--	--	0	0	0.44	24.0%	Taken from the truck
46	8.7	75	3.00	21.1	70	2252	140.6	0	0	0.44	24.0%	
48		75	3.00	20.6	69	--	--	0	0	0.44	24.0%	
50	9.2	95	3.75	20.4	69	2241	139.9	0	0	0.44	24.0%	
52		70	2.75	20.2	68	--	--	0	0	0.44	24.0%	
54	7.9	70	2.75	19.6	67	2272	141.8	0	0	0.44	24.0%	
56		45	1.75	20.3	69	--	--	0	0	0.44	24.0%	
58	7.5	55	2.25	22.0	72	2275	142.0	0	0	0.44	24.0%	
60		70	2.75	21.1	70	--	--	0	0	0.44	24.0%	
LC-HPC-14 (46-363) Placement 1, Cast on 12/19/07												
1	8.8	65	2.5	18.3	65	2218	138.4	0	0	0.45	24.4%	
3	7.9	45	1.75	17.8	64	2274	142.0	0	0	0.45	24.4%	
--	--	50	2	18.9	66	--	--	0	0	0.45	24.4%	
--	7.8	100	4	20.6	69	2259	141.0	--	--	--	--	A small amount of water was added
--	7.8	95	3.75	18.3	65	2260	141.1	0	0	0.45	24.4%	
--	9.0	90	3.5	18.3	65	2229	139.2	0	0	0.45	24.4%	
--	9.1	135	5.25	18.9	66	2231	139.3	0	0	0.45	24.4%	
--	8.7	100	4	19.4	67	2274	142.0	0	0	0.45	24.4%	Originally tested at 145 mm
--	--	--	--	--	--	--	--	0	0	0.45	24.4%	
--	--	125	5	--	--	--	--	0	0	0.45	24.4%	
--	9.0	95	3.75	17.2	63	2224	138.8	0	0	0.45	24.4%	
--	9.1	100	4	15.6	60	2216	138.4	0	0	0.45	24.4%	
--	9.7	110	4.25	16.7	62	2188	136.6	0	0	0.45	24.4%	

Table D.5 (continued) – Individual Plastic Concrete Test Results for LC-HPC Bridge Placements

Truck	Air Content	Slump		Concrete Temperature [†]		Unit Weight		Water Withheld		Actual w/c ratio	Actual Paste Content	Notes
		(mm)	(in.)	(°C)	(°F)	(kg/m ³)	(lb/yd ³)	(L/m ³)	(gal/yd ³)			
LC-HPC-14 (46-363) Placement 2, Cast on 5/2/08												
1	11.0	110	4.25	18.3	65	2193	136.9	0	0	0.45	24.4%	
2	10.4	125	5	17.2	63	2177	135.9	0	0	0.45	24.4%	
3	10.9	150	6	17.8	64	2157	134.7	0	0	0.45	24.4%	
4	8.1	135	5.25	17.8	64	2250	140.5	0	0	0.45	24.4%	
4	6.7	115	4.5	--	--			0	0	0.45	24.4%	Tested on deck following placement
5	--	--	--	--	--			0	0	0.45	24.4%	
6	--	--	--	--	--			0	0	0.45	24.4%	
7	--	--	--	--	--			0	0	0.45	24.4%	
8	12.0	100	4	18.3	65	2155	134.5	0	0	0.45	24.4%	
8	10.7	--	--	--	--			0	0	0.45	24.4%	Retested
9	--	--	--	--	--			0	0	0.45	24.4%	
10	--	--	--	--	--			0	0	0.45	24.4%	
11	--	--	--	--	--			0	0	0.45	24.4%	
12	--	--	--	--	--			0	0	0.45	24.4%	
13	10.5	110	4.25	17.8	64	2199	137.3	0	0	0.45	24.4%	
14	--	--	--	--	--			0	0	0.45	24.4%	
15	--	--	--	--	--			0	0	0.45	24.4%	
16	10.4	90	3.5	--	--	2201	137.4	0	0	0.45	24.4%	
17	10.5	100	4	18.3	65	2206	137.7	0	0	0.45	24.4%	
18	--	--	--	--	--			0	0	0.45	24.4%	
19	--	--	--	--	--			0	0	0.45	24.4%	
20	--	--	--	--	--			0	0	0.45	24.4%	
21	--	--	--	--	--			0	0	0.45	24.4%	
22	10.4	115	4.5	18.3	65	2199	137.3	0	0	0.45	24.4%	

Table D.5 (continued) – Individual Plastic Concrete Test Results for LC-HPC Bridge Placements

Truck	Air Content	Slump		Concrete Temperature [†]		Unit Weight		Water Withheld		Actual w/c ratio	Actual Paste Content	Notes
		(mm)	(in.)	(°C)	(°F)	(kg/m ³)	(lb/yd ³)	(L/m ³)	(gal/yd ³)			
LC-HPC-14 (46-363) Placement 2, Cast on 5/2/08 (Continued)												
22	8.0	100	4	--	--	2259	141.0	0	0	0.45	24.4%	Tested on deck following placement
23	--	--	--	--	--			0	0	0.45	24.4%	
24	--	--	--	--	--			0	0	0.45	24.4%	
25	--	--	--	--	--			0	0	0.45	24.4%	
26	--	--	--	--	--			0	0	0.45	24.4%	
27	--	--	--	--	--			0	0	0.45	24.4%	
28	7.0	65	2.5	17.8	64	2284	142.6	0	0	0.45	24.4%	
29	--	--	--	--	--			0	0	0.45	24.4%	
30	--	--	--	--	--			0	0	0.45	24.4%	
31	8.1	90	3.5	17.8	64	2259	141.0	0	0	0.45	24.4%	
32	--	--	--	--	--			0	0	0.45	24.4%	
33	--	--	--	--	--			0	0	0.45	24.4%	
34	--	--	--	--	--			0	0	0.45	24.4%	
35	--	--	--	--	--			0	0	0.45	24.4%	
LC-HPC-14 (46-363) Placement 3, Cast on 5/21/08												
1	10.5	135	5.25	19.4	67	2165	135.1	1.30	0.26	0.45	24.3%	
2	10.5	165	6.5	18.3	65	2185	136.4	1.18	0.24	0.45	24.3%	
3	9.9	150	6	17.8	64	2210	138.0	1.79	0.36	0.44	24.3%	
4	--	--	--	--	--	--	--	1.14	+0.23	0.45	24.3%	
5	--	--	--	--	--	--	--	3.76	0.76	0.44	24.1%	
6	9.5	115	4.5	16.7	62	2205	137.6	1.44	0.29	0.45	24.3%	
6	9.0	50	2	18.9	66	2219	138.5	--	--	--	--	Taken after placement - 0.5% loss
7	--	--	--	--	--	--	--	0.99	0.20	0.45	24.3%	
8	--	--	--	--	--	--	--	1.19	0.24	0.45	24.3%	

Table D.5 (continued) – Individual Plastic Concrete Test Results for LC-HPC Bridge Placements

Truck	Air Content	Slump		Concrete Temperature [†]		Unit Weight		Water Withheld		Actual w/c ratio	Actual Paste Content	Notes
		(mm)	(in.)	(°C)	(°F)	(kg/m ³)	(lb/yd ³)	(L/m ³)	(gal/yd ³)			
LC-HPC-14 (46-363) Placement 3, Cast on 5/21/08 (Continued)												
9	--	--	--	--	--	--	--	1.19	0.24	0.45	24.3%	
10	--	--	--	--	--	--	--	2.33	+0.47	0.46	24.6%	
11	8.0	85	3.25	19.4	67	2239	139.8	1.09	0.22	0.45	24.3%	
11	9.6	125	5	19.4	67	2192	136.8	3.86	+0.78	0.46	24.7%	1 gal/yd ³ water added and retested
12	--	--	--	--	--	--	--	0.79	0.16	0.45	24.3%	
13	--	--	--	--	--	--	--	0.30	0.06	0.45	24.4%	
14	--	--	--	--	--	--	--	1.63	0.33	0.45	24.3%	
15	--	--	--	--	--	--	--	0.05	0.01	0.45	24.4%	
16	9.8	125	5	18.9	66	2196	137.1	0.84	+0.17	0.45	24.5%	
16	8.6	75	3	18.9	66	2212	138.1	--	--	--	--	Taken after placement - 1.2% loss
17	--	--	--	--	--	--	--	0.30	+0.06	0.45	24.4%	
18	--	--	--	--	--	--	--	0.89	+0.18	0.45	24.3%	
19	--	--	--	--	--	--	--	2.77	0.56	0.44	24.2%	
20	--	--	--	--	--	--	--	4.70	0.95	0.44	24.0%	
21	9.5	110	4.25	17.2	63	2215	138.3	3.86	0.78	0.44	24.1%	
22	--	--	--	--	--	--	--	3.81	0.77	0.44	24.1%	
23	--	--	--	--	--	--	--	4.16	0.84	0.44	24.1%	

[†]Unless noted the temperatures are taken at the truck discharge using an infrared thermometer.

Table D.6 – Mix Design Information for Control Bridge Decks

County and Serial Number	Bridge Description	Control Number	Portion Placed	Date of Placement	Design Air Content
105-311	EB Parallel over I-635	1 / 2	North 1/2 - Subdeck	09/30/05	6.5
			North 1/2 - Overlay	10/10/05	6.5
			South 1/2 - Subdeck	10/18/05	6.5
			South 1/2 - Overlay	10/28/05	6.5
46-337	EB 103rd St. over US-69	3	Subdeck	07/06/07	6.5
			Overlay	07/17/07	6.5
46-347	US-69/Rp/WB I-435 to NB US-69 Rp	4	Subdeck	10/20/07	6.5
			Overlay	11/16/07	6.5
46-340 Unit 3	SB US-69 to EB I-435 Rp over US-69 Hwy and I-435	5	Subdeck - Seq. 1 & 2	11/08/08	6.5
			Subdeck Seq. 3, 5, & 6	11/13/08	6.5
			Subdeck - Seq. 4 & 7	11/17/08	6.5
			Overlay - West Half	11/22/08	6.5
			Overlay - East Half	11/25/08	6.5
			6	Subdeck - Seq. 1 & 2	09/16/08
46-340 Unit 4	SB US-69 to EB I-435 Rp over US-69 Hwy and I-435	6	Subdeck Seq. 3	09/18/08	6.5
			Subdeck - Seq. 5 & 6	09/23/05	6.5
			Subdeck Seq. 4	09/26/08	6.5
			Subdeck - Seq. 7	09/30/08	6.5
			Overlay - West 2/3	10/16/08	6.5
			Overlay - East 1/3	10/20/08	6.5
46-334	NB Antioch over I-435	7	East - Subdeck	03/15/06	6.5
			East - Overlay	03/29/06	6.5
			West - Subdeck	08/16/06	6.5
			West - Overlay	09/15/06	6.5
54-59	K-52 over US-69	8 / 10	Deck	04/16/07	6.5
54-58	SB US-69 over Marair Des Cyğ	9	Subdeck	11/03/07	6.5
			West - Overlay	05/21/08	6.5
			East - Overlay	05/28/08	6.5
56-155	US-50 over BNSF RR	11	North 1/2 - Subdeck	02/03/06	6.5
			South 1/2 - Subdeck	02/14/06	6.5
			Overlay	03/28/06	6.5
56-57 Unit 1	K-130 over Neosho Rv Phase I	12	Subdeck	03/11/08	6.5
			Overlay	04/01/08	6.5
54-67	SB US-69 over BNSF RR	13	Subdeck	07/11/08	6.5
			Overlay	07/25/08	6.5
56-49	K-52 over US-69	Alt	Deck	04/16/07	6.5

Table D.6 (continued) – Mix Design Information for Control Bridge Decks

Control Number	Portion Placed	Water Content		Cement Content		Cement Specific Gravity	Silica Fume Content	
		(kg/m ³)	(lb/yd ³)	(kg/m ³)	(lb/yd ³)		(kg/m ³)	(lb/yd ³)
1 / 2	North 1/2 - Subdeck	143	241	357	602	3.15	0	0
	North 1/2 - Overlay	138	233	346	583	3.15	26	44
	South 1/2 - Subdeck	143	241	359	605	3.15	0	0
	South 1/2 - Overlay	138	233	346	583	3.15	26	44
3	Subdeck	159	268	318	536	3.15	0	0
	Overlay	138	233	346	583	3.15	26	44
4	Subdeck	159	268	318	536	3.15	0	0
	Overlay	138	233	346	583	3.15	26	44
5	Subdeck - Seq. 1 & 2	159	268	318	536	3.15	0	0
	Subdeck Seq. 3, 5, & 6	159	268	318	536	3.15	0	0
	Subdeck - Seq. 4 & 7	159	268	318	536	3.15	0	0
	Overlay - West Half	138	233	346	583	3.15	26	44
	Overlay - East Half	138	233	346	583	3.15	26	44
6	Subdeck - Seq. 1 & 2	159	268	318	536	3.15	0	0
	Subdeck Seq. 3	159	268	318	536	3.15	0	0
	Subdeck - Seq. 5 & 6	159	268	318	536	3.15	0	0
	Subdeck Seq. 4	159	268	318	536	3.15	0	0
	Subdeck - Seq. 7	159	268	318	536	3.15	0	0
	Overlay - West 2/3	138	233	346	583	3.15	26	44
	Overlay - East 1/3	138	233	346	583	3.15	26	44
7	East - Subdeck	159	268	318	536	3.15	0	0
	East - Overlay	138	233	346	583	3.15	26	44
	West - Subdeck	159	268	318	536	3.15	0	0
	West - Overlay	138	233	346	583	3.15	26	44
8 / 10	Deck	145	244	363	612	3.15	0	0
9	Subdeck	145	244	363	612	3.15	0	0
	West - Overlay	139	234	350	590	3.15	26	44
	East - Overlay	139	234	350	590	3.15	26	44
11	North 1/2 - Subdeck	143	241	357	602	3.15	0	0
	South 1/2 - Subdeck	143	241	357	602	3.15	0	0
	Overlay	138	233	346	583	3.15	26	44
12	Subdeck	157	265	357	602	3.15	0	0
	Overlay	137	231	345	581	3.15	26	44
13	Subdeck	145	244	363	612	3.15	0	0
	Overlay	139	234	350	590	3.15	26	44
Alt	Deck	143	241	357	602	3.15	0	0

Table D.6 (continued) – Mix Design Information for Control Bridge Decks

Control Number	Portion Placed	Silica Fume Specific Gravity	Class F Fly Ash Content		Fly Ash Specific Gravity	W/C Ratio	Design Volume of Paste (%)
			(kg/m ³)	(lb/yd ³)			
1 / 2	North 1/2 - Subdeck	--	0	0	--	0.40	25.6%
	North 1/2 - Overlay	2.22	0	0	--	0.37	26.0%
	South 1/2 - Subdeck	--	0	0	--	0.40	25.7%
	South 1/2 - Overlay	2.22	0	0	--	0.37	26.0%
3	Subdeck	--	79	133	2.60	0.40	29.0%
	Overlay	2.22	0	0	--	0.37	26.0%
4	Subdeck	--	79	133	2.60	0.40	29.0%
	Overlay	2.22	0	0	--	0.37	26.0%
5	Subdeck - Seq. 1 & 2	--	79	133	2.60	0.40	29.0%
	Subdeck Seq. 3, 5, & 6	--	79	133	2.60	0.40	29.0%
	Subdeck - Seq. 4 & 7	--	79	133	2.60	0.40	29.0%
	Overlay - West Half	2.22	0	0	--	0.37	26.0%
	Overlay - East Half	2.22	0	0	--	0.37	26.0%
6	Subdeck - Seq. 1 & 2	--	79	133	2.60	0.40	29.0%
	Subdeck Seq. 3	--	79	133	2.60	0.40	29.0%
	Subdeck - Seq. 5 & 6	--	79	133	2.60	0.40	29.0%
	Subdeck Seq. 4	--	79	133	2.60	0.40	29.0%
	Subdeck - Seq. 7	--	79	133	2.60	0.40	29.0%
	Overlay - West 2/3	2.22	0	0	--	0.37	26.0%
	Overlay - East 1/3	2.22	0	0	--	0.37	26.0%
7	East - Subdeck	--	79	133	2.60	0.40	29.0%
	East - Overlay	2.22	0	0	--	0.37	26.0%
	West - Subdeck	--	79	133	2.60	0.40	29.0%
	West - Overlay	2.22	0	0	--	0.37	26.0%
8 / 10	Deck	--	0	0	--	0.40	26.0%
9	Subdeck	--	0	0	--	0.40	26.0%
	West - Overlay	2.20	0	0	--	0.37	26.2%
	East - Overlay	2.20	0	0	--	0.37	26.2%
11	North 1/2 - Subdeck	--	0	0	--	0.40	25.6%
	South 1/2 - Subdeck	--	0	0	--	0.40	25.6%
	Overlay	2.20	0	0	--	0.37	26.0%
12	Subdeck	--	0	0	--	0.44	27.1%
	Overlay	2.20	0	0	--	0.37	25.8%
13	Subdeck	--	0	0	--	0.40	26.0%
	Overlay	2.20	0	0	--	0.37	26.2%
Alt	Deck	--	0	0	--	0.40	25.6%

Table D.6 (continued) – Mix Design Information for Control Bridge Decks

Cement Content	Portion Placed	Coarse Aggregate Type	Types of Admixtures[†]
1 / 2	North 1/2 - Subdeck	Limestone	AEA, Type A-F HRWR
	North 1/2 - Overlay	Granite	AEA, Type A-F MRWR and HRWR
	South 1/2 - Subdeck	Limestone	AEA, Type A-F HRWR and Type A-D WR
	South 1/2 - Overlay	Granite	AEA, Type A-F MRWR and HRWR
3	Subdeck	Granite	--
	Overlay	Granite	AEA, Type A-F HRWR
4	Subdeck	Granite	--
	Overlay	Granite	AEA, Type A-F HRWR
5	Subdeck - Seq. 1 & 2	Granite	--
	Subdeck Seq. 3, 5, & 6	Granite	--
	Subdeck - Seq. 4 & 7	Granite	--
	Overlay - West Half	Granite	AEA, Type A-F HRWR
	Overlay - East Half	Granite	AEA, Type A-F HRWR
6	Subdeck - Seq. 1 & 2	Granite	--
	Subdeck Seq. 3	Granite	--
	Subdeck - Seq. 5 & 6	Granite	--
	Subdeck Seq. 4	Granite	--
	Subdeck - Seq. 7	Granite	--
	Overlay - West 2/3	Granite	AEA, Type A-F HRWR
	Overlay - East 1/3	Granite	AEA, Type A-F HRWR
7	East - Subdeck	Granite	--
	East - Overlay	Granite	AEA, Type A-F HRWR
	West - Subdeck	Granite	--
	West - Overlay	Granite	AEA, Type A-F HRWR
8 / 10	Deck	Limestone	AEA, Type A-D WR
9	Subdeck	Limestone	AEA, Type F HRWR
	West - Overlay	Quartzite	AEA, Type F HRWR
	East - Overlay	Quartzite	AEA, Type F HRWR
11	North 1/2 - Subdeck	Limestone	AEA, Type A WR
	South 1/2 - Subdeck	Limestone	AEA, Type A WR
	Overlay	Quartzite	AEA, Type F HRWR
12	Subdeck	Limestone	AEA, Type A WR
	Overlay	Quartzite	AEA, Type F HRWR
13	Subdeck	Limestone	Type A-D WR, Type D Retarder
	Overlay	Quartzite	Type F HRWR
Alt	Deck	Limestone	AEA, Type A WR

[†]MRWR – mid-range water reducer, HRWR – high-range water reducer, WR – water reducer

Table D.7 – Average Properties for Control Bridge Decks

County and Serial Number	Control Number	Portion Placed	Date of Placement	Average Air Content	Average Slump	
					(mm)	(in.)
105-311	1 / 2	North 1/2 - Subdeck	09/30/05	5.3	110	4.25
		North 1/2 - Overlay	10/10/05	5.5	125	5.00
		South 1/2 - Subdeck	10/18/05	6.5	80	3.25
		South 1/2 - Overlay	10/28/05	7.0	115	4.50
46-337	3	Subdeck	07/06/07	5.8	170	6.75
		Overlay	07/17/07	7.3	185	7.25
46-347	4	Subdeck	10/20/07	7.3	195	7.75
		Overlay	11/16/07	6.9	145	5.75
46-340 Unit 3	5	Subdeck - Seq. 1 & 2	11/08/08	5.6	200	7.75
		Subdeck Seq. 3, 5, & 6	11/13/08	6.8	230	9.25
		Subdeck - Seq. 4 & 7	11/17/08	5.5	205	8.00
		Overlay - West Half	11/22/08	7.6	150	6.00
		Overlay - East Half	11/25/08	6.6	230	9.00
46-340 Unit 4	6	Subdeck - Seq. 1 & 2	09/16/08	7.4	205	8.00
		Subdeck Seq. 3	09/18/08	7.3	180	7.00
		Subdeck - Seq. 5 & 6	09/23/05	6.4	175	6.75
		Subdeck Seq. 4	09/26/08	6.6	160	6.25
		Subdeck - Seq. 7	09/30/08	5.5	225	8.75
		Overlay - West 2/3	10/16/08	7.7	175	7.00
		Overlay - East 1/3	10/20/08	8.1	210	8.25
46-334	7	East - Subdeck	03/15/06	5.9	235	9.25
		East - Overlay	03/29/06	7.4	190	7.50
		West - Subdeck	08/16/06	7.3	195	7.75
		West - Overlay	09/15/06	6.4	175	7.00
54-59	8 / 10	Deck	04/16/07	7.4	130	5.00
54-58	9	Subdeck	11/03/07	6.2	65	2.75
		West - Overlay	05/21/08	5.6	90	3.50
		East - Overlay	05/28/08	6.2	130	5.00
56-155	11	North 1/2 - Subdeck	02/03/06	6.8	90	3.50
		South 1/2 - Subdeck	02/14/06	7.0	135	5.25
		Overlay	03/28/06	6.0	80	3.00
56-57 Unit 1	12	Subdeck	03/11/08	6.9	110	4.25
		Overlay	04/01/08	6.8	95	3.75
54-67	13	Subdeck	07/11/08	5.8	90	3.50
		Overlay	07/25/08	6.3	135	5.25
56-49	Alt	Deck	06/02/05	5.9	85	3.00

Table D.7 (continued) – Average Properties for Control Bridge Decks

Control Number	Portion Placed	Average Concrete Temperature		Average Unit Weight		Average Compressive Strength [†]	
		(°C)	(°F)	(kg/m ³)	(lb/yd ³)	(MPa)	(psi)
1 / 2	North 1/2 - Subdeck	19.0	66	2318	144.7	39.1	5670
	North 1/2 - Overlay	18.0	64	2281	142.4	40.1	5810
	South 1/2 - Subdeck	24.7	76	2274	142.4	35.1	5090
	South 1/2 - Overlay	20.0	68	2254	140.7	55.6	8060
3	Subdeck	27.1	81	2251	140.5	39.2	5690
	Overlay	29.9	86	2249	140.4	57.6	8350
4	Subdeck	22.8	73	2240	139.9	43.7	6340
	Overlay	20.0	68	2239	140	53	7700
5	Subdeck - Seq. 1 & 2	19.0	66	2278	142.2	--	--
	Subdeck Seq. 3, 5, & 6	20.0	68	2245	140.1	--	--
	Subdeck - Seq. 4 & 7	17.0	63	2275	142.0	--	--
	Overlay - West Half	18.0	64	2250	140.5	--	--
	Overlay - East Half	17.0	63	2262	141.2	--	--
6	Subdeck - Seq. 1 & 2	24.0	75	2238	139.7	34.1	4950
	Subdeck Seq. 3	21.0	70	2246	140.2	--	--
	Subdeck - Seq. 5 & 6	31.0	88	2261	141.1	--	--
	Subdeck Seq. 4	30.0	86	2254	140.7	--	--
	Subdeck - Seq. 7	26.0	79	2269	141.6	--	--
	Overlay - West 2/3	22.0	72	2258	141.0	--	--
	Overlay - East 1/3	22.0	72	2231	139.3	53.1	7700
7	East - Subdeck	26.5	80	2239	139.8	38.2	5540
	East - Overlay	23.0	73	2239	139.8	--	--
	West - Subdeck	21.3	70	2226	139.0	37.9	5500
	West - Overlay	18.0	64	2252	140.6	50.8	7370
8 / 10	Deck	21.2	70	2234	139.4	33.3	4830
9	Subdeck	19.0	66	2286	142.7	33.5	4850
	West - Overlay	24.7	77	2282	142.4	44.0	6380
	East - Overlay	21.7	71	2262	141.2	42.6	6170
11	North 1/2 - Subdeck	22.0	72	2263	141.3	40.6	5890
	South 1/2 - Subdeck	23.0	73	2252	140.6	37.5	5440
	Overlay	15.5	60	2277	142.1	52.7	7640
12	Subdeck	21.9	72	2250	140.5	36.4	5270
	Overlay	14.8	59	2254	140.7	43.0	6240
13	Subdeck	31.7	89	2271	141.7	--	--
	Overlay	33.0	91	2269	141.6	57.1	8280
Alt	Deck	--	--	2255	140.8	38.0	5510

[†]Average 28-day compressive strength for lab-cured specimens. Strengths were taken at 31 days for the second overlay placement for Control-1/2.

Table D.8 – Crack Densities for Individual Bridge Placements

Bridge Number	County and Serial Number	Portion Placed	Date of Placement	Survey #1				Survey #2	
				Date of Survey	Age (months)	Crack Density (m/m ²)	Age-Corrected Crack Density (m/m ²)	Date of Survey	Age (months)
LC-HPC-1	105-304	South	10/14/2005	04/13/06	5.9	0.012	0.102	4/30/2007	18.5
		North	11/2/2005	04/13/06	5.3	0.003	0.094	4/30/2007	17.9
		Entire Deck	--	04/13/06	--	0.007	0.098	4/30/2007	--
LC-HPC-2	105-310	Deck	9/13/2006	04/20/07	7.2	0.014	0.103	6/18/2008	21.2
Control-1/2	105-311	North	10/10/2005	04/13/06	6.1	0.000	0.204	4/30/2007	18.6
		South	10/28/2005	04/13/06	5.5	0.000	0.206	4/30/2007	18.0
		Entire Deck	--	04/13/06	--	0.000	0.206	4/30/2007	--
LC-HPC-3	46-338	Deck	11/13/2007	05/29/08	6.5	0.032	0.122	--	--
Control-3	46-337	Deck	7/17/2007	05/29/08	10.4	0.037	0.229	--	--
LC-HPC-4	46-339	South	9/29/2007	07/15/08	9.5	0.004	0.090	--	--
		North	10/2/2007	07/15/08	9.4	0.018	0.104	--	--
Control-4	46-347	Deck	11/16/2007	06/10/08	6.8	0.050	0.252	--	--
LC-HPC-5	46-340 Unit 1	Deck	11/14/2007	07/15/08	8.0	0.059	0.147	--	--
LC-HPC-6	46-340 Unit 2	Deck	11/3/2007	05/20/08	6.5	0.063	0.153	--	--
LC-HPC-7	43-33	Deck	6/24/2006	06/05/07	11.4	0.003	0.087	7/1/2008	24.2
Control-7	46-334	East	9/15/2006	08/10/07	10.8	0.293	0.484	6/30/2008	21.5
		West	3/29/2006	08/10/07	16.4	0.030	0.205	6/30/2008	27.1
Control-8/10	54-59	Deck	4/16/2007	06/26/08	14.4	0.177	0.257	--	--
Control-11	56-155	Deck	3/28/2006	08/13/07	16.5	0.351	0.526	6/30/2008	27.1
Control Alt	56-49	Deck	6/2/2005	06/02/06	12.0	0.077	0.160	7/27/2007	25.8

Table D.8 (continued) – Crack Densities for Individual Bridge Placements

Bridge Number	Survey #2		Survey #3				All Surveys
	Crack Density (m/m ²)	Age-Corrected Crack Density (m/m ²)	Date of Survey	Age (months)	Crack Density (m/m ²)	Age-Corrected Crack Density (m/m ²)	Mean Age-Corrected Crack Density (m/m ²)
LC-HPC-1	0.047	0.122	6/17/2008	32.1	0.044	0.102	0.109
	0.006	0.081	6/17/2008	31.5	0.024	0.082	0.086
	0.027	0.102	6/17/2008	--	0.034	0.092	0.098
LC-HPC-2	0.029	0.100	--	--	--	--	0.102
Control-1/2	0.151	0.320	6/17/2008	32.2	0.114	0.244	0.256
	0.044	0.214	6/17/2008	31.6	0.091	0.223	0.214
	0.089	0.259	6/17/2008	--	0.099	0.231	0.232
LC-HPC-3	--	--	--	--	--	--	0.229
Control-3	--	--	--	--	--	--	0.229
LC-HPC-4	--	--	--	--	--	--	0.090
	--	--	--	--	--	--	0.104
Control-4	--	--	--	--	--	--	0.252
LC-HPC-5	--	--	--	--	--	--	0.147
LC-HPC-6	--	--	--	--	--	--	0.153
LC-HPC-7	0.019	0.086	--	--	--	--	0.086
Control-7	0.476	0.636	--	--	--	--	0.560
	0.069	0.214	--	--	--	--	0.209
Control-8/10	--	--	--	--	--	--	0.257
Control-11	0.665	0.810	--	--	--	--	0.668
Control-Alt	0.230	0.295	6/26/2008	36.8	0.219	0.271	0.242

Table D.9 – LC-HPC / Control Bridge Deck Bid Quantities and Costs

LC-HPC / Control Number	Bid Number†	Subdeck or LC-HPC Bid Quantity		Subdeck or LC-HPC Bid		Silica-Fume Overlay Bid Quantity		Silica-Fume Overlay Cost		Total Deck Concrete Cost		Qualification Slab Bid Quantity		Qualification Slab Cost		Qualification Slab Cost
		(m ³)	(yd ³)	(\$/m ³)	(\$/yd ³)	(m ²)	(yd ²)	(\$/m ²)	(\$/yd ²)	(\$/m ³)	(\$/yd ³)	(m ³)	(yd ³)	(\$/m ³)	(\$/yd ³)	(\$)
LC-HPC-1	1	309.2	404.4	1,800	1,376	--	--	--	--	1,800	1,376	26.8	35.1	5,500	4,205	147,400
	2	309.2	404.4	953	729	--	--	--	--	953	729	26.8	35.1	1,876	1,434	50,277
	3	309.2	404.4	1,479	1,131	--	--	--	--	1,479	1,131	26.8	35.1	2,609	1,995	69,921
	4	309.2	404.4	2,256	1,725	--	--	--	--	2,256	1,725	26.8	35.1	3,739	2,859	100,204
LC-HPC-2	1	226.8	296.6	1,600	1,223	--	--	--	--	1,600	1,223	25.6	33.5	5,500	4,205	140,800
	2	226.8	296.6	1,045	799	--	--	--	--	1,045	799	25.6	33.5	2,050	1,567	52,480
	3	226.8	296.6	1,755	1,342	--	--	--	--	1,755	1,342	25.6	33.5	2,631	2,012	67,354
	4	226.8	296.6	2,516	1,923	--	--	--	--	2,516	1,923	25.6	33.5	3,781	2,891	96,792
1/2 Control	1	246.4	322.3	1,000	765	970.0	1160.1	42	35	1,007	770	--	--	--	--	--
	2	246.4	322.3	800	612	970.0	1160.1	46	38	848	648	--	--	--	--	--
	3	246.4	322.3	900	688	970.0	1160.1	48	40	941	719	--	--	--	--	--
	4	246.4	322.3	1,201	919	970.0	1160.1	65	54	1,258	962	--	--	--	--	--
LC-HPC-3	1	394.4	515.9	746	570	--	--	--	--	746	570	33.4	43.7	1,301	995	43,453
	2	394.4	515.9	934	714	--	--	--	--	934	714	33.4	43.7	1,048	801	35,014
3 Control	1	420.8	550.4	840	642	1375.0	1644.5	40	33	858	656	--	--	--	--	--
	2	420.8	550.4	943	721	1375.0	1644.5	36	30	939	718	--	--	--	--	--
LC-HPC-4	1	349.9	457.7	865	661	--	--	--	--	865	661	27.3	35.7	1,510	1,154	41,223
	2	349.9	457.7	1,023	782	--	--	--	--	1,023	782	27.3	35.7	1,193	912	32,578
4 Control	1	607.4	794.4	820	627	2459.0	2940.9	34	28	824	630	--	--	--	--	--
	2	607.4	794.4	993	759	2459.0	2940.9	41	35	999	764	0.0	0.0	0	0	0
LC-HPC-5 and 6	1	705.7	923.0	914	699	--	--	--	--	914	699	19.2	25.1	1,456	1,113	27,955
	2	705.7	923.0	990	757	--	--	--	--	990	757	19.2	25.1	1,478	1,130	28,373
5 and 6 Control	1	1592.1	2082.4	772	590	5952.0	7118.5	38	32	795	608	--	--	--	--	--
	2	1592.1	2082.4	904	691	5952.0	7118.5	36	30	904	691	--	--	--	--	--

Table D.9 (continued) – LC-HPC / Control Bridge Deck Bid Quantities and Costs

LC-HPC / Control Number	Bid Number [†]	Subdeck or LC-HPC Bid Quantity		Subdeck or LC-HPC Bid		Silica-Fume Overlay Bid Quantity		Silica-Fume Overlay Cost		Total Deck Concrete Cost		Qualification Slab Bid Quantity		Qualification Slab Cost		Qualification Slab Cost
		(m ³)	(yd ³)	(\$/m ³)	(\$/yd ³)	(m ²)	(yd ²)	(\$/m ²)	(\$/yd ²)	(\$/m ³)	(\$/yd ³)	(m ³)	(yd ³)	(\$/m ³)	(\$/yd ³)	(\$)
LC-HPC-7	1	404.8	529.5	750	573	--	--	--	--	750	573	35.0	45.8	750	573	26,250
	2	404.8	529.5	750	573	--	--	--	--	750	573	35.0	45.8	750	573	26,250
	3	404.8	529.5	750	573	--	--	--	--	750	573	35.0	45.8	750	573	26,250
	4	404.8	529.5	625	478	--	--	--	--	625	478	35.0	45.8	795	608	27,825
	5	404.8	529.5	750	573	--	--	--	--	750	573	35.0	45.8	750	573	26,250
7 Control	1	302.3	395.4	963	736	925.0	1106.3	33	28	948	725	--	--	--	--	--
	2	302.3	395.4	1,314	1,005	925.0	1106.3	38	32	1,275	975	0.0	0.0	0	0	0
LC-HPC-8	1	307.6	402.3	655	501	--	--	--	--	655	501	23.1	30.2	1,185	906	27,374
	2	307.6	402.3	686	525	--	--	--	--	686	525	23.1	30.2	1,242	949	28,682
	3	307.6	402.3	675	516	--	--	--	--	675	516	23.1	30.2	1,221	933	28,195
LC-HPC-9	1	385.6	504.3	925	707	--	--	--	--	925	707	26.8	35.1	1,250	956	33,500
	2	385.6	504.3	969	741	--	--	--	--	969	741	26.8	35.1	1,310	1,001	35,102
	3	385.6	504.3	953	728	0.0	0.0	0	0	953	728	26.8	35.1	1,288	984	34,505
9 Control	1	367.9	481.2	575	440	1652.0	1975.8	46	38	662	506	--	--	--	--	--
	2	367.9	481.2	576	441	1652.0	1975.8	48	40	672	513	--	--	--	--	--
	3	367.9	481.2	567	433	1652.0	1975.8	47	40	660	505	--	--	--	--	--
LC-HPC-10	1	343.3	449.0	665	508	--	--	--	--	665	508	23.1	30.2	1,185	906	27,374
	2	343.3	449.0	697	533	--	--	--	--	697	533	23.1	30.2	1,242	949	28,682
	3	343.3	449.0	685	524	--	--	--	--	685	524	23.1	30.2	1,221	933	28,195
8/10 Control	1	398.8	521.6	485	371	--	--	--	--	485	371	--	--	--	--	--
	2	398.8	521.6	508	389	--	--	--	--	508	389	--	--	--	--	--
	3	398.8	521.6	500	382	--	--	--	--	500	382	--	--	--	--	--
LC-HPC-11	1	149.2	195.1	1,400	1,070	--	--	--	--	1,400	1,070	28.5	37.3	1,400	1,070	39,900
11 Control	1	436.7	571.2	490	375	1389.0	1661.2	32	27	525	401	--	--	--	--	--
	2	436.7	571.2	650	497	1389.0	1661.2	45	38	704	538	--	--	--	--	--

Table D.9 (continued) – LC-HPC / Control Bridge Deck Bid Quantities and Costs

LC-HPC / Control Number	Bid Number [†]	Subdeck or LC-HPC Bid Quantity		Subdeck or LC-HPC Bid		Silica-Fume Overlay Bid Quantity		Silica-Fume Overlay Cost		Total Deck Concrete Cost		Qualification Slab Bid Quantity		Qualification Slab Cost		Qualification Slab Cost
		(m ³)	(yd ³)	(\$/m ³)	(\$/yd ³)	(m ²)	(yd ²)	(\$/m ²)	(\$/yd ²)	(\$/m ³)	(\$/yd ³)	(m ³)	(yd ³)	(\$/m ³)	(\$/yd ³)	(\$)
11 Control	3	436.7	571.2	395	302	1389.0	1661.2	50	42	492	376	--	--	--	--	--
	4	436.7	571.2	518	396	1389.0	1661.2	34	28	555	424	--	--	--	--	--
LC-HPC-12	1	410.9	537.4	804	615	--	--	--	--	804	615	22.2	29.1	1,207	923	26,859
	2	410.9	537.4	1,229	940	--	--	--	--	1,229	940	22.2	29.1	1,805	1,380	40,158
	3	410.9	537.4	1,439	1,100	--	--	--	--	1,439	1,100	22.2	29.1	1,700	1,300	37,830
12 Control	1	356.3	466.0	595	455	1429.8	1710.0	38	32	649	496	--	--	--	--	--
	2	356.3	466.0	785	600	1429.8	1710.0	45	38	839	641	--	--	--	--	--
	3	356.3	466.0	654	500	1429.8	1710.0	45	38	725	555	--	--	--	--	--
LC-HPC-13	1	306.0	400.2	1,161	888	--	--	--	--	1,161	888	26.8	35.1	1,400	1,070	37,520
	2	306.0	400.2	1,161	888	--	--	--	--	1,161	888	26.8	35.1	1,400	1,070	37,520
	3	306.0	400.2	1,000	765	--	--	--	--	1,000	765	26.8	35.1	1,400	1,070	37,520
13 Control	1	267.4	349.7	603	461	1095.0	1309.6	45	38	676	517	--	--	--	--	--
	2	267.4	349.7	603	461	1095.0	1309.6	45	38	676	517	--	--	--	--	--
	3	267.4	349.7	603	461	1095.0	1309.6	45	38	676	517	--	--	--	--	--
LC-HPC-14	1	573.4	750.0	1,079	825	--	--	--	--	1,079	825	24.5	32.0	1,570	1,200	38,400
	2	573.4	750.0	1,491	1,140	--	--	--	--	1,491	1,140	24.5	32.0	1,373	1,050	33,600
	3	573.4	750.0	1,144	875	--	--	--	--	1,144	875	24.5	32.0	1,570	1,200	38,400
	4	573.4	750.0	1,282	980	--	--	--	--	1,282	980	24.5	32.0	1,962	1,500	48,000
Alt Control	1	173.3	226.7	732	560	--	--	--	--	732	560	--	--	--	--	--
	2	173.3	226.7	759	580	--	--	--	--	759	580	--	--	--	--	--
	3	173.3	226.7	589	450	--	--	--	--	589	450	--	--	--	--	--
	4	173.3	226.7	746	570	--	--	--	--	746	570	--	--	--	--	--
	5	173.3	226.7	888	679	--	--	--	--	888	679	--	--	--	--	--

[†]The first bid listed for each bridge deck was awarded the contract.

